AFWAL-TR-82-2082

AD-A134 765

ANALYSIS OF AIRCR[illegible]ELS AND RELATED MATERIALS

F. Neil Hodgson, Edward A. Steinmetz, John D. Tobias, Billy B. Bowles, and Charlotte D. Fritsch

MONSANTO RESEARCH CORPORATION
DAYTON LABORATORY
DAYTON, OHIO 45407

SEPTEMBER 1982

FINAL REPORT FOR PERIOD 15 APRIL 1978—31 DECEMBER 1981

Approved for public release; distribution unlimited

AERO PROPULSION LABORATORY
AIR FORCE WRIGHT AERONAUTICAL LABORATORIES
AIR FORCE SYSTEMS COMMAND
WRIGHT-PATTERSON AIR FORCE BASE, OHIO 45433

NOTICE

When Government drawings, specifications, or other data are used for any purpose other than in connection with a definitely related Government procurement operation, the United States Government thereby incurs no responsibility nor any obligation whatsoever; and the fact that the government may have formulated, furnished, or in any way supplied the said drawings, specifications, or other data, is not to be regarded by implication or otherwise as in any manner licensing the holder or any other person or corporation, or conveying any rights or permission to manufacture, use, or sell any patented invention that may in any way be related thereto.

This report has been reviewed by the Office of Public Affairs (ASD/PA) and is releaseable to the National Technical Information Service (NTIS). At NTIS, it will be available to the general public, including foreign nations.

This technical report has been reviewed and is approved for publication.

Donald D. Potter

DONALD D. POTTER, Major, USAF
Fuels Branch, Fuels and Lubr. Div.
Aero Propulsion Laboratory

Arthur V. Churchill

ARTHUR V. CHURCHILL
Chief, Fuels Branch
Fuels and Lubrication Division
Aero Propulsion Laboratory

Robert D. Sherrill

ROBERT D. SHERRILL
Chief, Fuels and Lubrication Division
Aero Propulsion Laboratory

"If your address has changed, if you wish to be removed from our mailing list, or if the addressee is no longer employed by your organization please notify AFWAL/POSF, W-PAFB OH 45433 to help us maintain a current mailing list".

Copies of this report should not be returned unless return is required by security considerations, contractual obligations, or notice on a specific document.

UNCLASSIFIED

SECURITY CLASSIFICATION OF THIS PAGE (When Data Entered)

REPORT DOCUMENTATION PAGE		READ INSTRUCTIONS BEFORE COMPLETING FORM
1. REPORT NUMBER AFWAL-TR-82-2082	2. GOVT ACCESSION NO. A134768	3. RECIPIENT'S CATALOG NUMBER
4. TITLE (and Subtitle) ANALYSIS OF AIRCRAFT FUELS AND RELATED MATERIALS		5. TYPE OF REPORT & PERIOD COVERED Final Report for Period 15 Apr 78 - 31 Dec 81 6. PERFORMING ORG. REPORT NUMBER
7. AUTHOR(s) F. N. Hodgson, E. A. Steinmetz, J. D. Tobias, B. B. Bowles, and C. D. Fritsch		8. CONTRACT OR GRANT NUMBER(s) F33615-78-C-2004
9. PERFORMING ORGANIZATION NAME AND ADDRESS Monsanto Research Corporation, Dayton Laboratory Station B, Box 8 Dayton, OH 45407		10. PROGRAM ELEMENT, PROJECT, TASK AREA & WORK UNIT NUMBERS 30480593
11. CONTROLLING OFFICE NAME AND ADDRESS Aero Propulsion Laboratory (AFWAL/POSF) AF Wright Aeronautical Laboratories (AFSC) Wright-Patterson Air Force Base, OH 45433		12. REPORT DATE September 1982 13. NUMBER OF PAGES 583
14. MONITORING AGENCY NAME & ADDRESS(if different from Controlling Office)		15. SECURITY CLASS. (of this report) UNCLASSIFIED 15a. DECLASSIFICATION/DOWNGRADING SCHEDULE None

16. DISTRIBUTION STATEMENT (of this Report)

Approved for public release; distribution unlimited.

17. DISTRIBUTION STATEMENT (of the abstract entered in Block 20, if different from Report)

18. SUPPLEMENTARY NOTES

19. KEY WORDS (Continue on reverse side if necessary and identify by block number)

Jet fuels	Fuel vapors	Fuel charging tendency
Fuel properties	Hydrocarbon type analyses	Fuel tank sealants
High density fuels	Modified fuels	Antistatic additives
Fuel contaminants	Fuel composition	Water separometers

20. ABSTRACT (Continue on reverse side if necessary and identify by block number)

Fuel tests, analyses, and analytical method development were conducted on a number of fuels of an experimental nature in conjunction with ongoing Air Force programs for studying fuel combustion behavior, turbine engine design, and other fuel related technologies. Fuels from conventional and alternate sources were studied, as were fuels of the high density missile propellant type. A wide variety of both physical and chemical properties of the fuels were measured and are tabulated. Studies conducted to aid in the solution of operational problems are also reported.

DD FORM 1 JAN 73 1473 EDITION OF 1 NOV 68 IS OBSOLETE

UNCLASSIFIED

SECURITY CLASSIFICATION OF THIS PAGE (When Data Entered)

FOREWORD

This final report was submitted by Monsanto Research Corporation under Contract F33615-78-C-2004. The effort was sponsored by the Air Force Aero Propulsion Laboratory, Air Force Systems Command, Wright-Patterson Air Force Base, Ohio under Project 3048, Task 304805, and Work Unit 30480593, with Dr. Ronald D. Butler as Contract Monitor through May 1979 and with Major Donald D. Potter as Contract Monitor from June 1979 through the conclusion of the efforts. Mr. F. Neil Hodgson of Monsanto Research Corporation was technically responsible for the work, which was performed during the period 15 April 1978 to 31 December 1981.

Much of the work performed during the course of this program was planned in coordination with a number of other related fuel technology studies being conducted at, or under the sponsorship of, the Air Force Aero Propulsion Laboratory. Such efforts include research on turbine engine combustor design, fuel combustion behavior, improved fuel characterization methodology, high density missile fuel development, and alternate fossil fuel source development. The experimental results presented in this report are intended to be used in the context of those research programs, and it is expected that the significance of the data will become apparent as the technical aspects of the related programs are published. In particular, many of the fuel specimens examined during this program were experimental in nature, and the various chemical and physical properties tabulated herein should not necessarily be regarded as characteristic of particular fuel types.

The authors wish to gratefully acknowledge the excellent guidance provided by Major Donald D. Potter during the course of this work. Special gratitude is also expressed to members of the Monsanto Research Corporation staff: J. V. Pustinger for his technical consultation and advice, and D. Q. Douglas, M. K. Hershey, E. M. Hughes, L. Metcalfe, J. F. Moon, L. Parts, J. E. Strobel, and G. L. Thomas for their technical contributions. H. W. Luebke and O. P. Tanner, Monsanto Company, St. Louis, are also recognized for the special data they have provided.

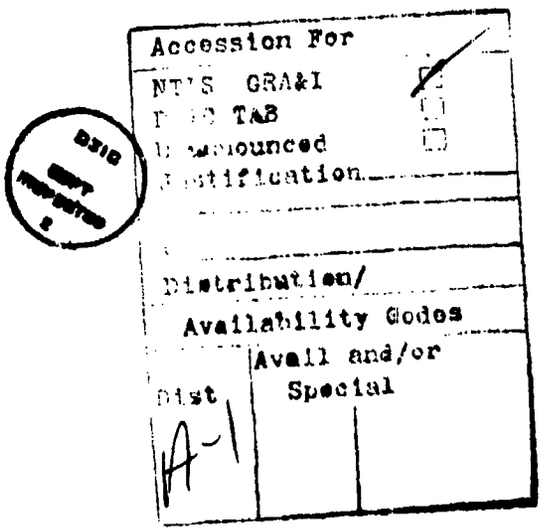

TABLE OF CONTENTS

TABLE OF CONTENTS (continued)

TABLE OF CONTENTS (continued)

TABLE OF CONTENTS (continued)

TABLE OF CONTENTS (continued)

TABLE OF CONTENTS (continued)

TABLE OF CONTENTS (continued)

TABLE OF CONTENTS (continued)

LIST OF ILLUSTRATIONS

LIST OF ILLUSTRATIONS (continued)

LIST OF ILLUSTRATIONS (continued)

LIST OF ILLUSTRATIONS (continued)

LIST OF ILLUSTRATIONS (continued)

LIST OF ILLUSTRATIONS (continued)

LIST OF ILLUSTRATIONS (continued)

LIST OF ILLUSTRATIONS (continued)

LIST OF ILLUSTRATIONS (continued)

LIST OF ILLUSTRATIONS (continued)

LIST OF ILLUSTRATIONS (continued)

LIST OF ILLUSTRATIONS (continued)

LIST OF ILLUSTRATIONS (continued)

LIST OF ILLUSTRATIONS (continued)

LIST OF ILLUSTRATIONS (continued)

LIST OF TABLES

LIST OF TABLES (continued)

LIST OF TABLES (continued)

LIST OF TABLES (continued)

LIST OF TABLES (continued)

LIST OF TABLES (continued)

LIST OF TABLES (continued)

LIST OF TABLES (continued)

LIST OF TABLES (continued)

LIST OF TABLES (continued)

LIST OF TABLES (continued)

SECTION I

INTRODUCTION AND SUMMARY

The Fuels and Lubrication Division of the Air Force Aero Propulsion Laboratory conducts in-house and contractual programs in all aspects of aircraft and missile fuels technology. These programs are designed to ensure an adequate supply of dependable fuels for operational use. The concerns encompassed in that goal cover every aspect of fuel technology: production, availability, properties, and quality; fuel storage, transportation, distribution, handling, and contamination; fuel additive effects and synthetic fuels for particular weapons systems; and combustion behavior, combustor design, and engine exhaust emissions. Work performed under this contract during the past four years has supported these efforts.

A large number of fuel specimens were physically and chemically characterized in connection with Air Force contractual programs to study the combustion properties of modified or experimental fuels. This work involved characterization of fuels after modification with aromatic stocks or a hydrocarbon stock consisting largely of relatively high boiling paraffins. Analyses and property measurements were continued throughout the course of the program to determine changes in the fuels resulting from the various combustion tests.

A number of investigations and analyses were conducted on high density fuels and fuel blends. The fuels included RJ-5 and RJ-5 blends, RJ-6, JP-9, and JP-10. Tests included IR analyses for identification of particulate contamination, GC analyses of degradation products, detailed measurements of a number of physical and chemical properties, and compositional analyses by gas chromatography.

Various special investigations were conducted. The effectiveness of two antistatic fuel additives in minimizing the buildup of static electrical charges in various JP-4 and JP-8 fuels was determined. The problem of polysulfide sealant chalking in F-16 aircraft fuel tanks was investigated in a special study to define the effects trace metals, mercaptan sulfur, and peroxide content have on the process. The Microsep II Water Separometer was evaluated against the Minisonic system for measuring the ease with which fuels release entrained or emulsified water. Gas specimens were analyzed to determine if they contained hydrazine-type propellants. Various JP-4 type fuels were analyzed for metals content to determine the amount of dissolved metal that had been transferred from water lying in the bottom of the fuel tanks. A series of chemical analyses were conducted for the main engine filters to determine the cause of plugging in certain aircraft. The ball-on-cylinder fuel lubricity tester at AFWAL/POSF was modified and evaluated for significance of test data. Troublesome sulfur compounds present in shale derived JP-4 fuels were identified by gas chromatography/mass spectrometry (GC/MS) after application of unique concentration techniques.

These and other studies required for research support or problem solving are described in the sections that follow.

SECTION II

SPECIAL INVESTIGATIONS

A number of special investigations were conducted either to provide solutions for operational problems, to improve existing test methodology, to respond to particular unanticipated needs as they arose, or to make measurements of a nonroutine nature. These tasks encompassed a wide range of activities including fabrication and modification of test apparatus, identification of fuel contaminant and filter deposits, studies of sealant and elastomer degradation, and a variety of other specialized investigations.

1. CHARGING TENDENCY OF FUELS CONTAINING ANTISTATIC ADDITIVES

Static electrical charges can be generated when fuel is added to aircraft fuel tanks containing reticulated polyurethane foam. On several occasions electrical discharges are known to have caused low-grade explosions during aircraft refueling. This problem can be minimized by the use of an antistatic additive in the fuel. The purpose of this investigation was to generate data to compare the effectiveness of two such antistatic fuel additives, Stadis® 450 (Du Pont Petroleum Products) and ASA-3 (Shell). Comparisons were conducted using two different fuel tank foams, specifically the blue polyether urethane and the red polyester urethane. Tests were conducted at room temperature (70°F) and in a cold chamber (20°F). The concentration of additive in the fuel was prepared to bracket an electrical conductivity value of 200 picosiemens per meter (pS/m) at 70°F, or 100 pS/m at 20°F. A variation of the Exxon ministatic tester (MST) was constructed for these measurements. The fuels used in this investigation were selected to include a variety of fuel types. Two of the fuels, a JP-4 from Tinker AFB and a JP-4 from Richards Gebaur AFB, had exhibited electrostatic charge problems in actual usage. This subsection describes the apparatus, procedure and results.

Apparatus

The Exxon ministatic tester consists essentially of a cell to hold the test foam specimen and a syringe drive to force fuel through the foam specimen. A schematic diagram of the modified test unit constructed for these studies is shown in Figure 1. The unit has the essential features of the Exxon MS tester; however, rather than using a syringe drive to pass fuel through the test cell, a Teflon gear pump was employed for that purpose. The entire unit was constructed in an upright freezer cabinet so that tests could be conducted at reduced temperatures, as well as at room temperature.

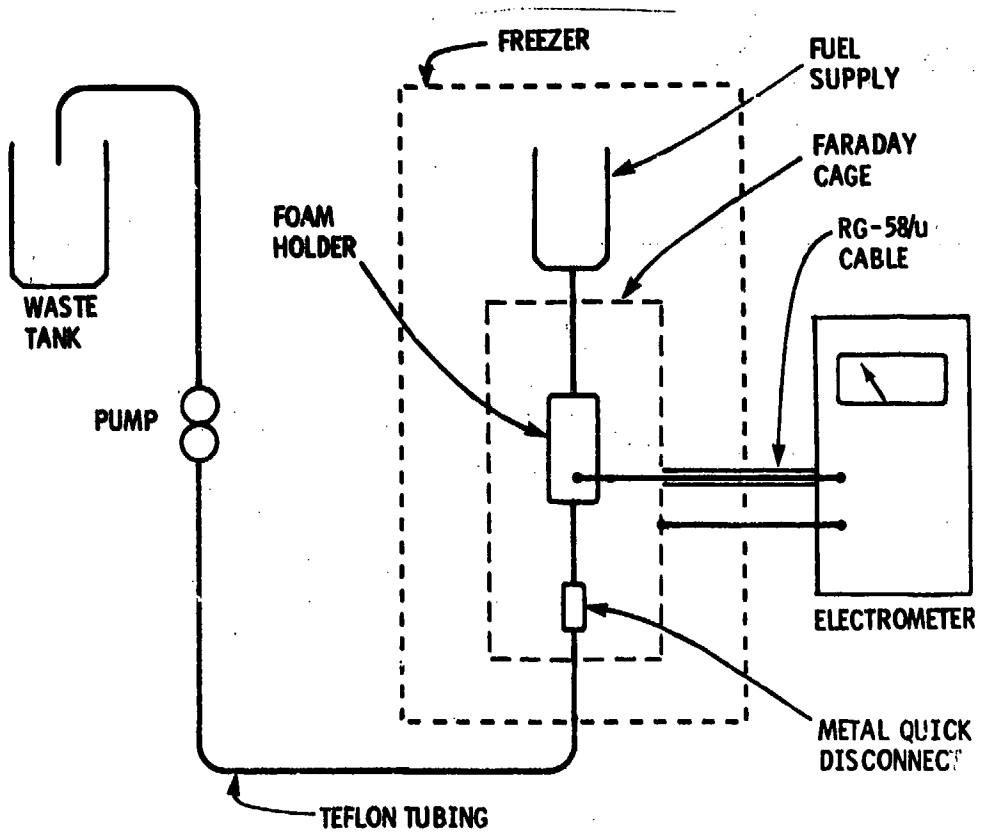

Figure 1. Schematic of test apparatus for fuel charge measurements.

Originally the test cell was constructed to accommodate a foam specimen 3 inches in length and 1 inch in diameter. The cell size was later reduced so that specimens 3 inches x 1/2 inch diameter could be used.

A foam specimen cutter was designed and constructed as a piece of auxiliary equipment for these tests. The device employed an electrically heated wire to cut either 1/2 inch or 1 inch diameter specimens. Rectangular blocks of foam are mounted on a rotating mandrel. The hot wire, which is mounted parallel to the axis of rotation of the foam, can be adjusted to give a cylindrical foam specimen of the desired diameter. This technique for cutting foam specimens was selected because of the smooth cut given by the hot wire and the resulting excellent reproducibility of specimen dimensions.

The principal objective in designing the apparatus was to produce a tester in which as many parameters as possible were controlled. The test cell, shown in Figure 2 in its 1 inch diameter configuration, was constructed of stainless steel. The cell position, relative to the other components in the freezer cabinet, is shown in Figure 3. To prevent formation of a flammable fuel vapor/air mixture in the freezer enclosure, the unit was continuously flushed with a slow flow of nitrogen.

A Teflon gear pump is located on the left outside wall of the freezer and is shown at close range in Figure 4. All connections are made with polytetrafluoroethylene tubing. The pumping rate as a function of pump voltage was recorded. The voltage required to produce the desired flow of exactly 400 ml per minute through the device was determined. A controlled power supply to accurately produce the required voltage was employed to drive the pump.

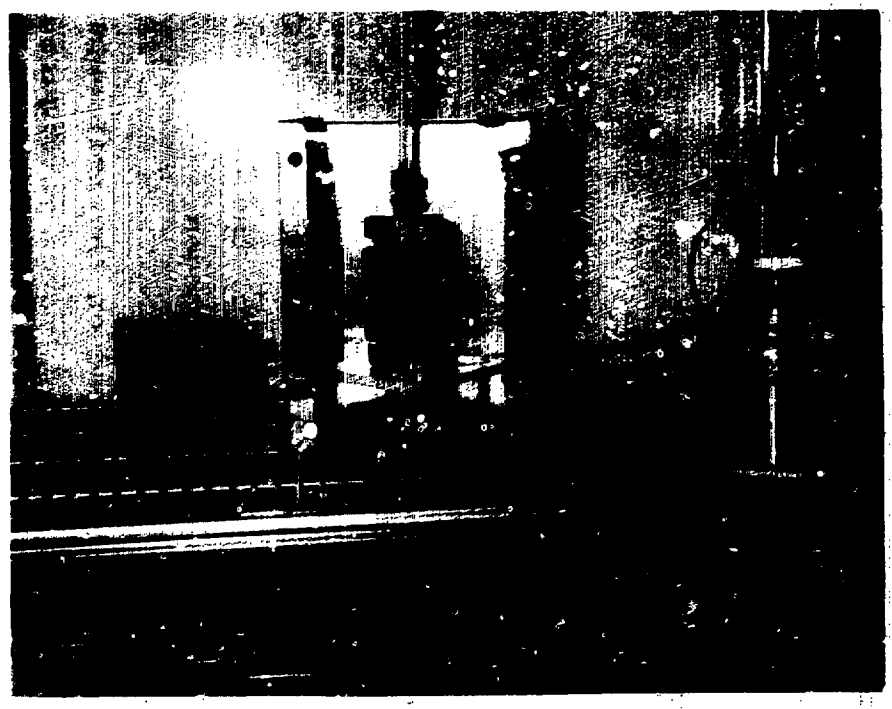

Figure 2. Cell designed to hold foam test specimen for static charge measurement.

Figure 3. Freezer containing static charge test apparatus.

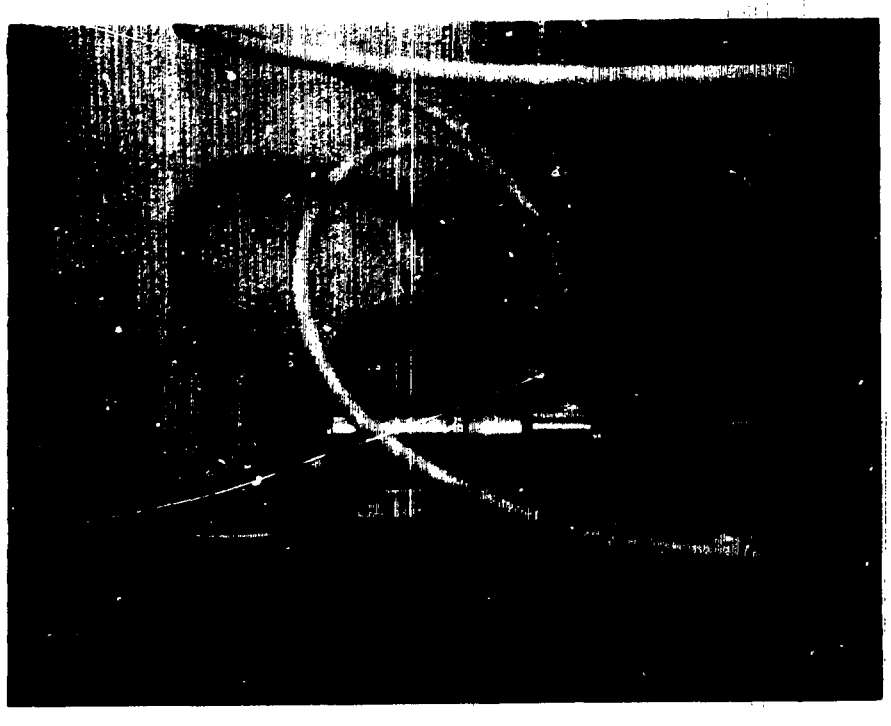

Figure 4. Teflon® gear pump used in static charge test apparatus.

A Keithly Model 600B electrometer was used for the charge measurements as well as for preliminary electrical conductivity measurements.

Procedure

ASTM test method D 3114-72, "DC Electrical Conductivity of Hydrocarbon Fuels," was used to measure electrical conductivities of the test fuels after addition of the antistatic additives. In order to correlate additive concentrations with fuel conductivity, blends having various additive levels were prepared. By plotting additive concentration versus conductivity, the additive levels corresponding to conductivities of 200 pS/m at 70°F and 100 pS/m at 20°F were determined for each fuel. These additive concentrations, which were used for the evaluations, are presented in Table 1. The conductivity test apparatus, consisting of a Keithly Model 600B electrometer and conductivity cell, is shown in Figure 5. Conductivity-additive concentration plots for some of the fuels included in this study are presented in Figures 6 through 14.

TABLE 1. ADDITIVE CONCENTRATIONS REQUIRED TO OBTAIN FUEL ELECTRICAL CONDUCTIVITY VALUES OF 200 pS/m[a] AT 70°F AND 100 pS/m[a] AT 20°F

	Concentration, ppm			
	ASA-3		S-450	
Fuel	70°F (22°C)	20°F (-6.7°C)	70°F (22°C)	20°F (-6.7°C)
JP-4, AFFB 13-69	0.5	0.4	0.9	0.5
JP-8	1.0	0.9	1.2	0.7
JP-4, AFFB 14-70	1.0	0.7	1.0	0.7
Clay Treated JP-4	0.5	0.5	0.4	0.3
JP-4, Tinker AFB	0.6	0.4	0.5	0.4
JP-4, Richards Gebaur AFB	0.5	0.4	0.5	0.4

[a]Picosiemens per meter

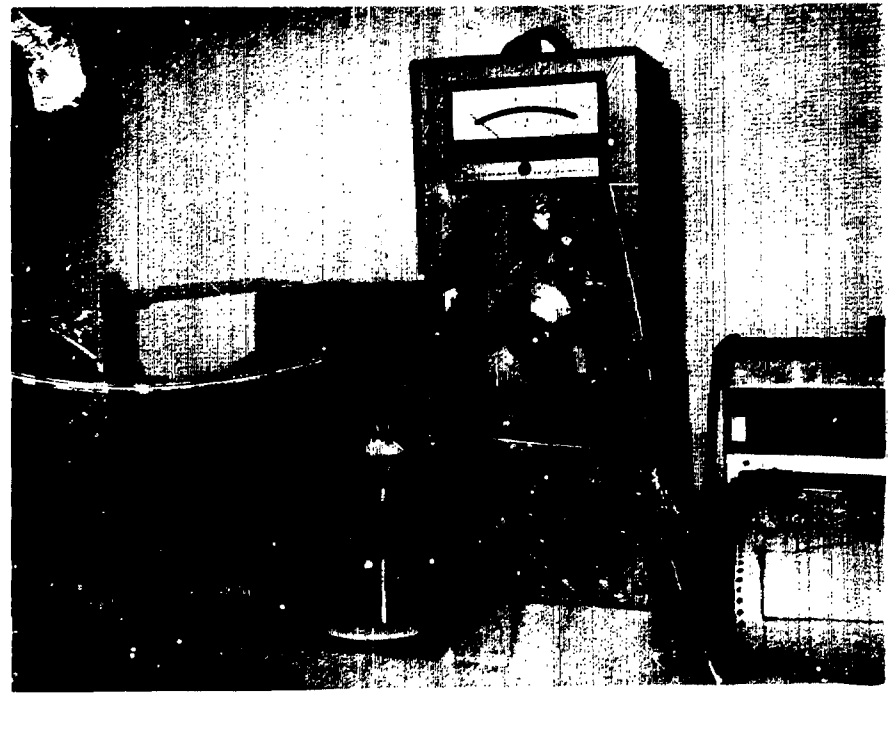

Figure 5. Fuel electrical conductivity test apparatus.

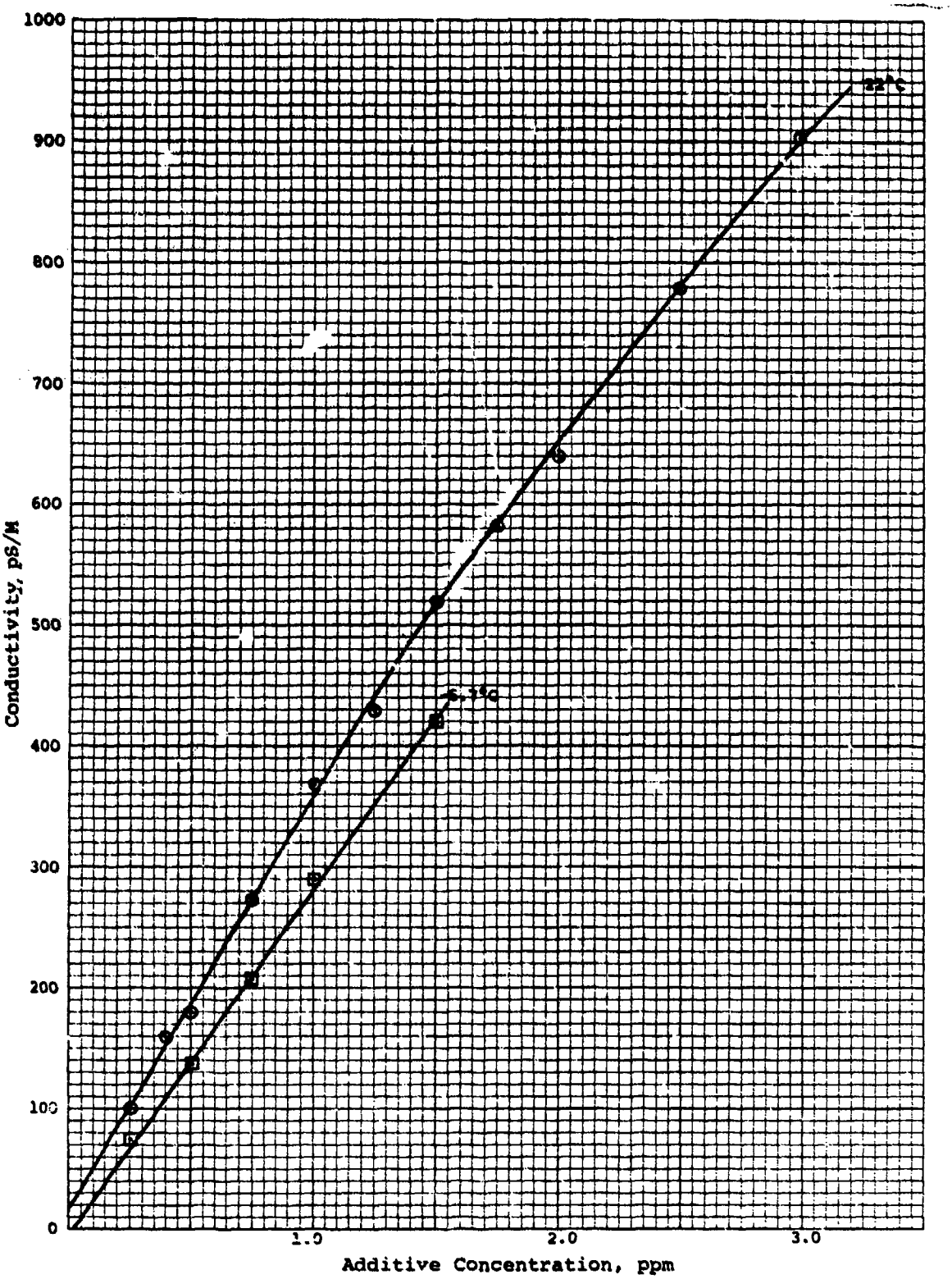

Figure 6. Fuel conductivity/additive concentration plots for fuel AFFB 13-69 with ASA-3 additive.

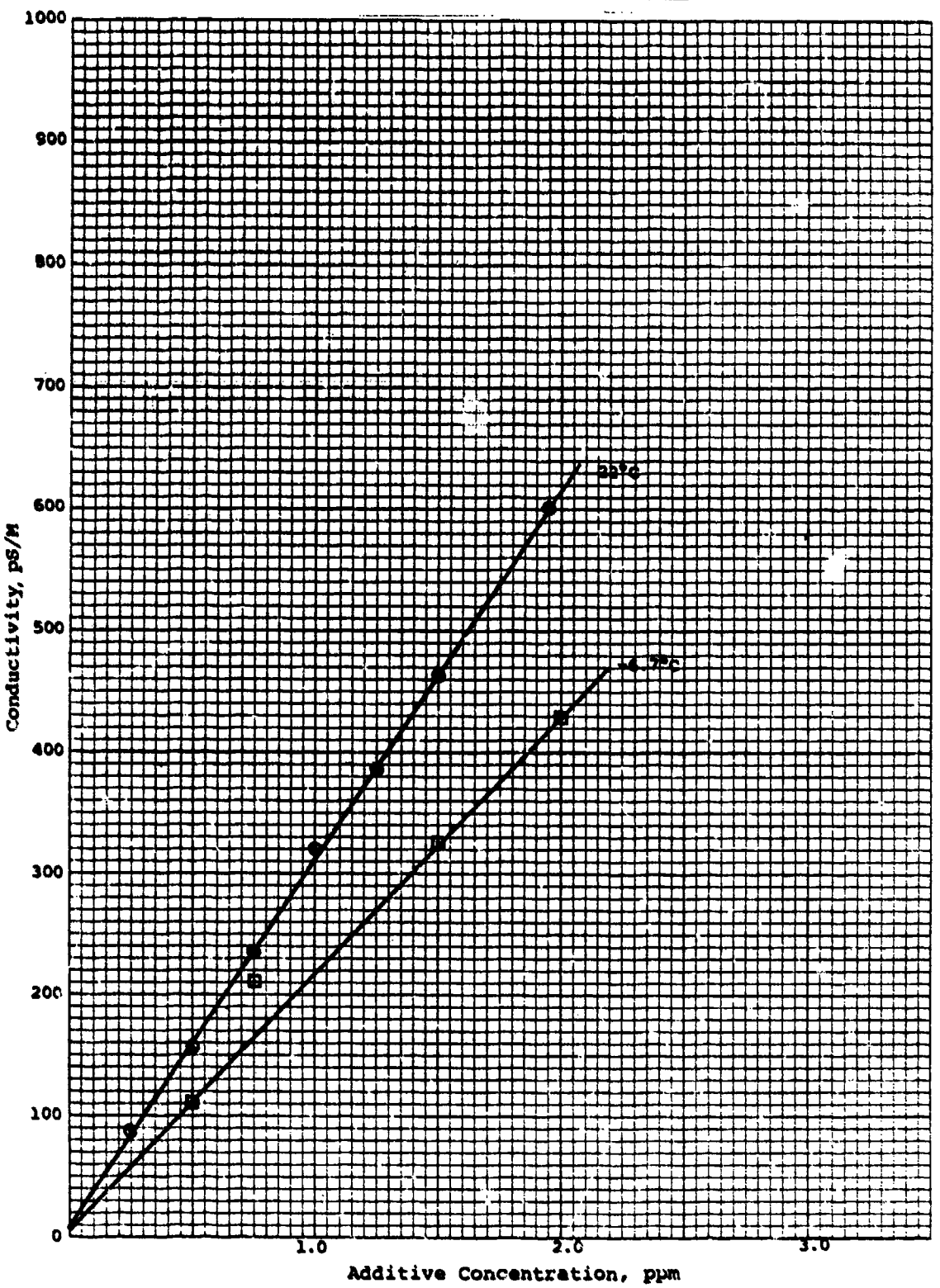

Figure 7. Fuel conductivity/additive concentration plots for fuel AFFB 13-69 with S-450 additive.

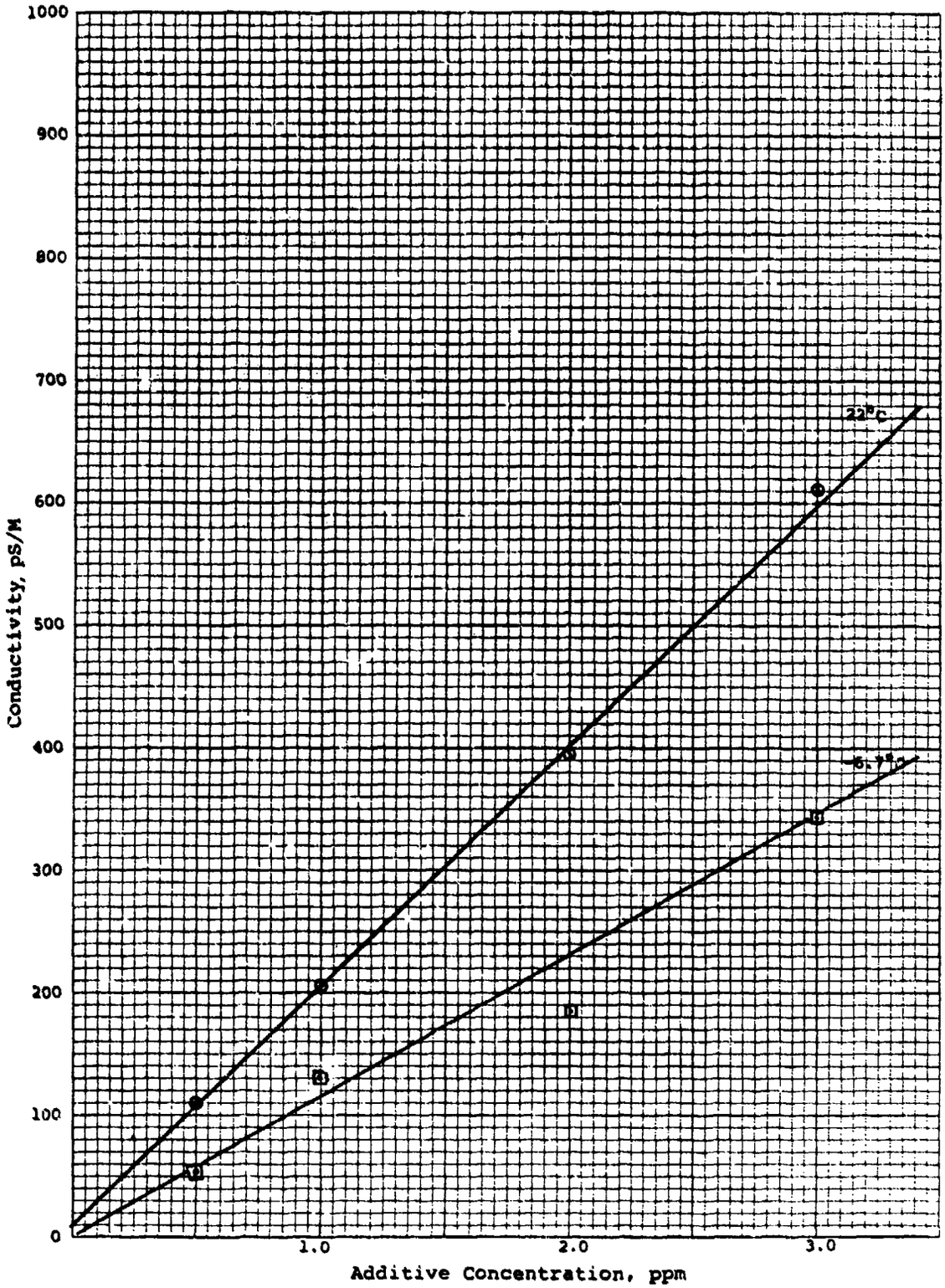

Figure 8. Fuel conductivity/additive concentration plots for JP-8 with ASA-3 additive.

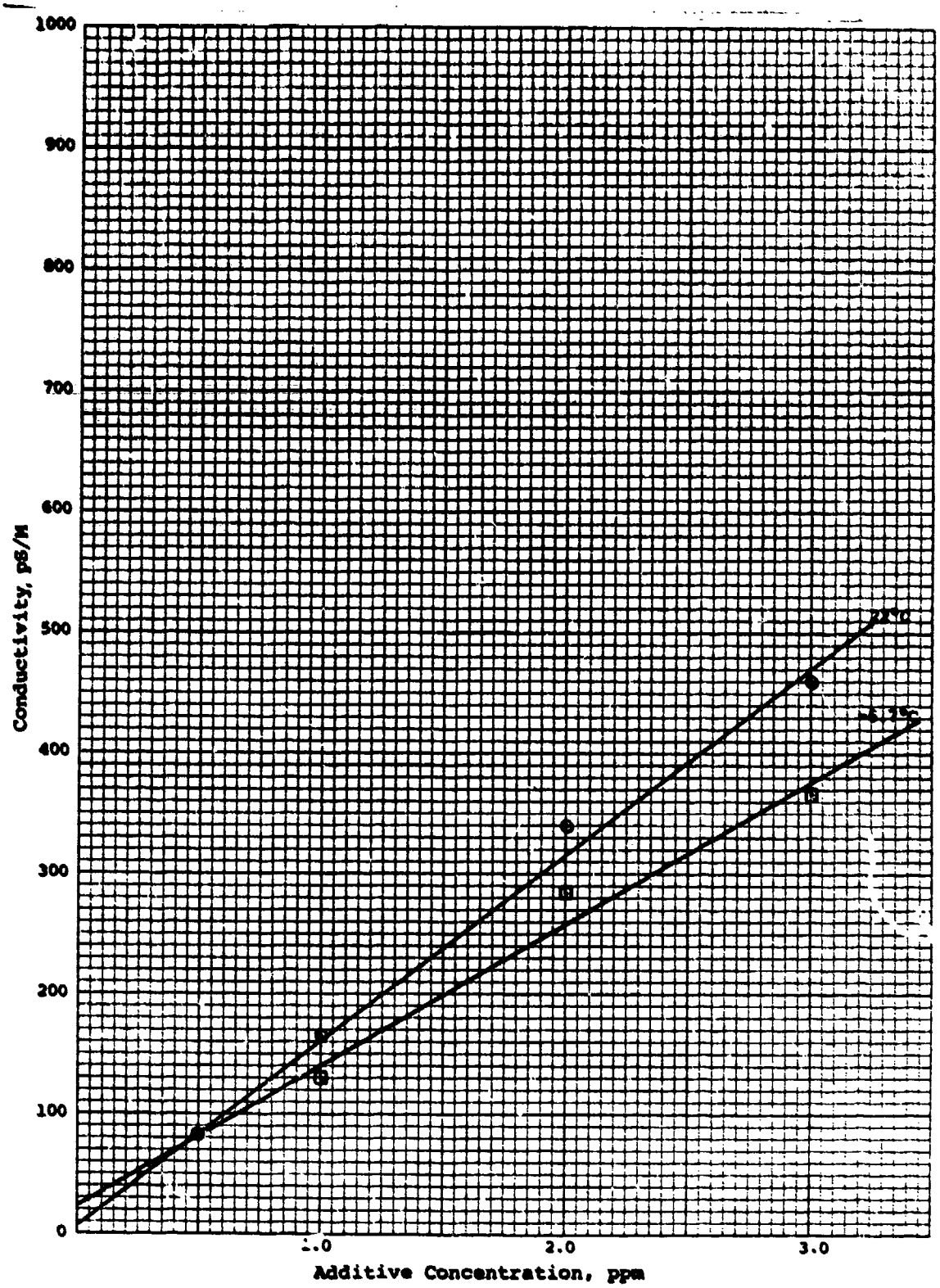

Figure 9. Fuel conductivity/additive concentration plots for JP-8 with S-450 additive.

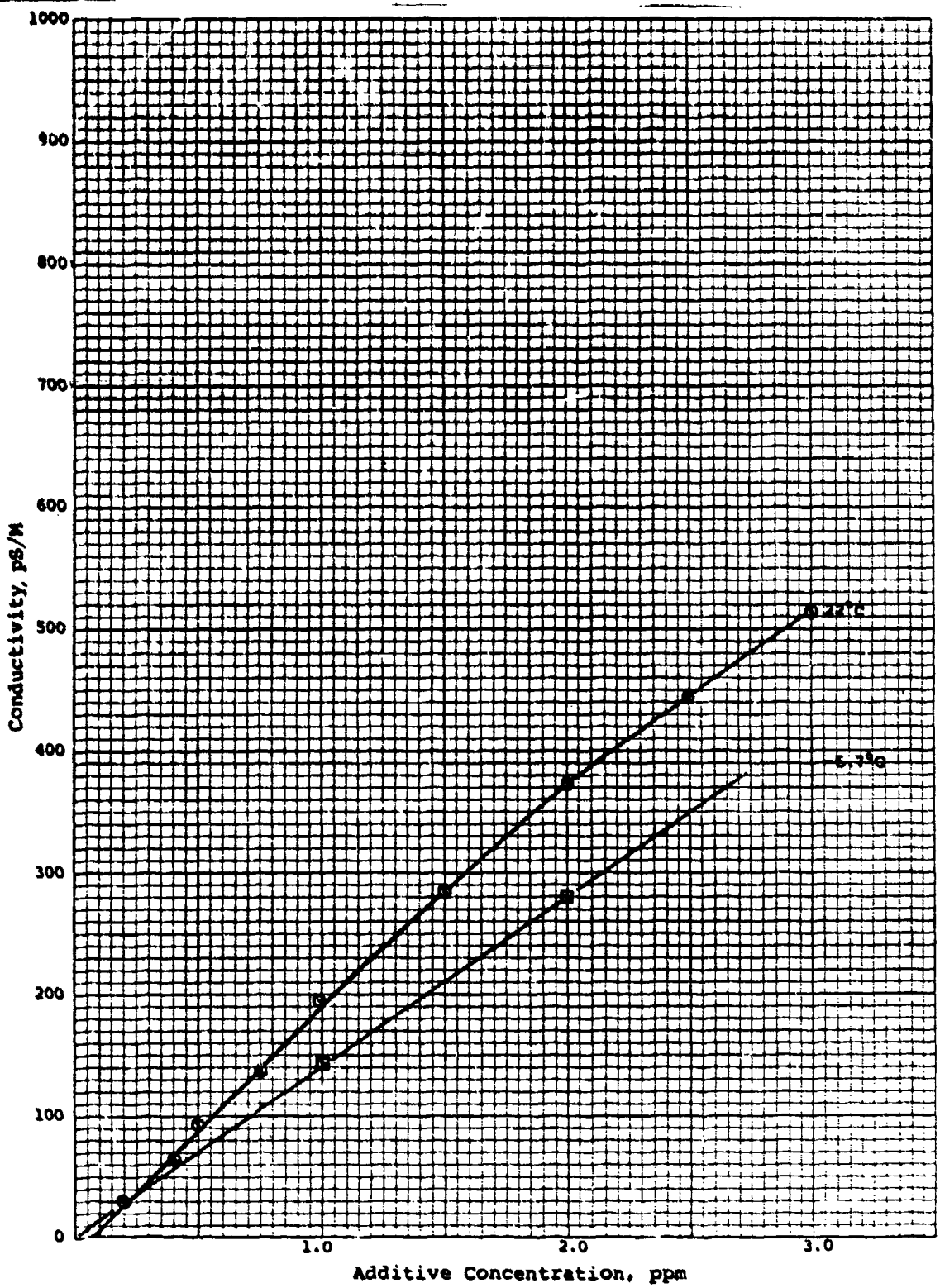

Figure 10. Fuel conductivity/additive concentration plots for fuel AFFB 14-70 with ASA-3 additive.

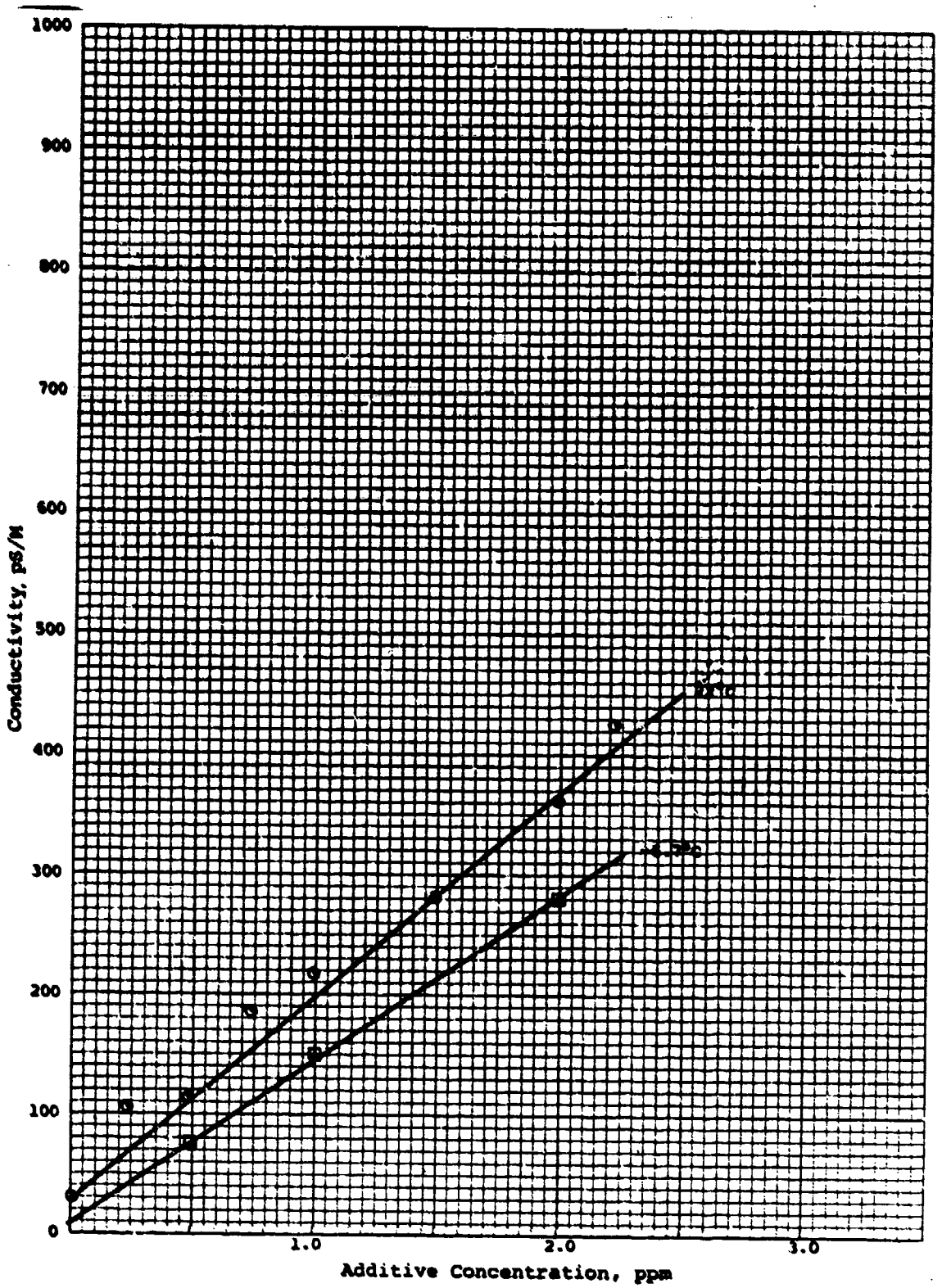

Figure 11. Fuel conductivity/additive concentration plots for fuel AFFB 14-70 with S-450 additive.

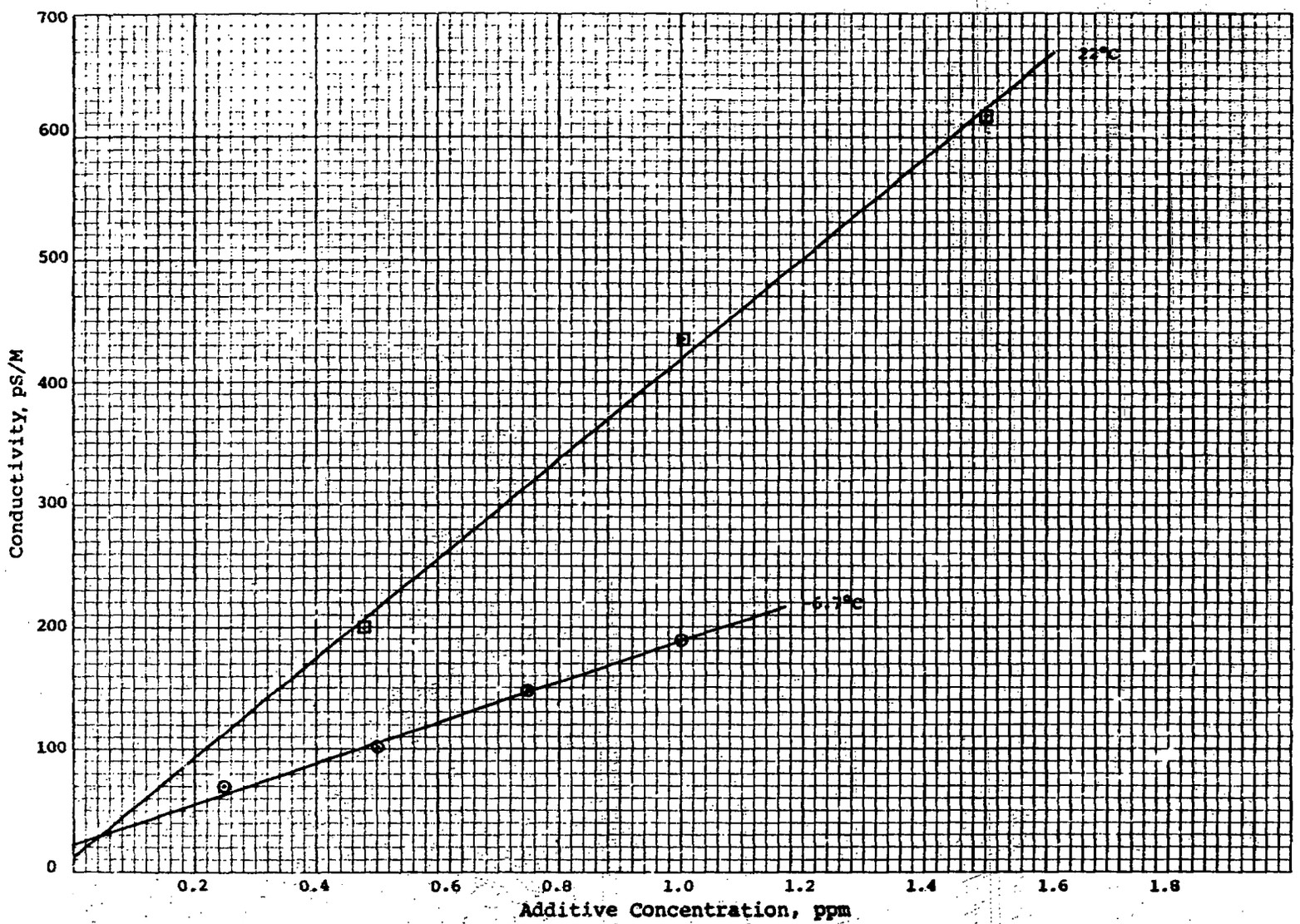

Figure 12. Fuel conductivity/additive concentration plots for clay treated JP-4 with ASA-3 additive.

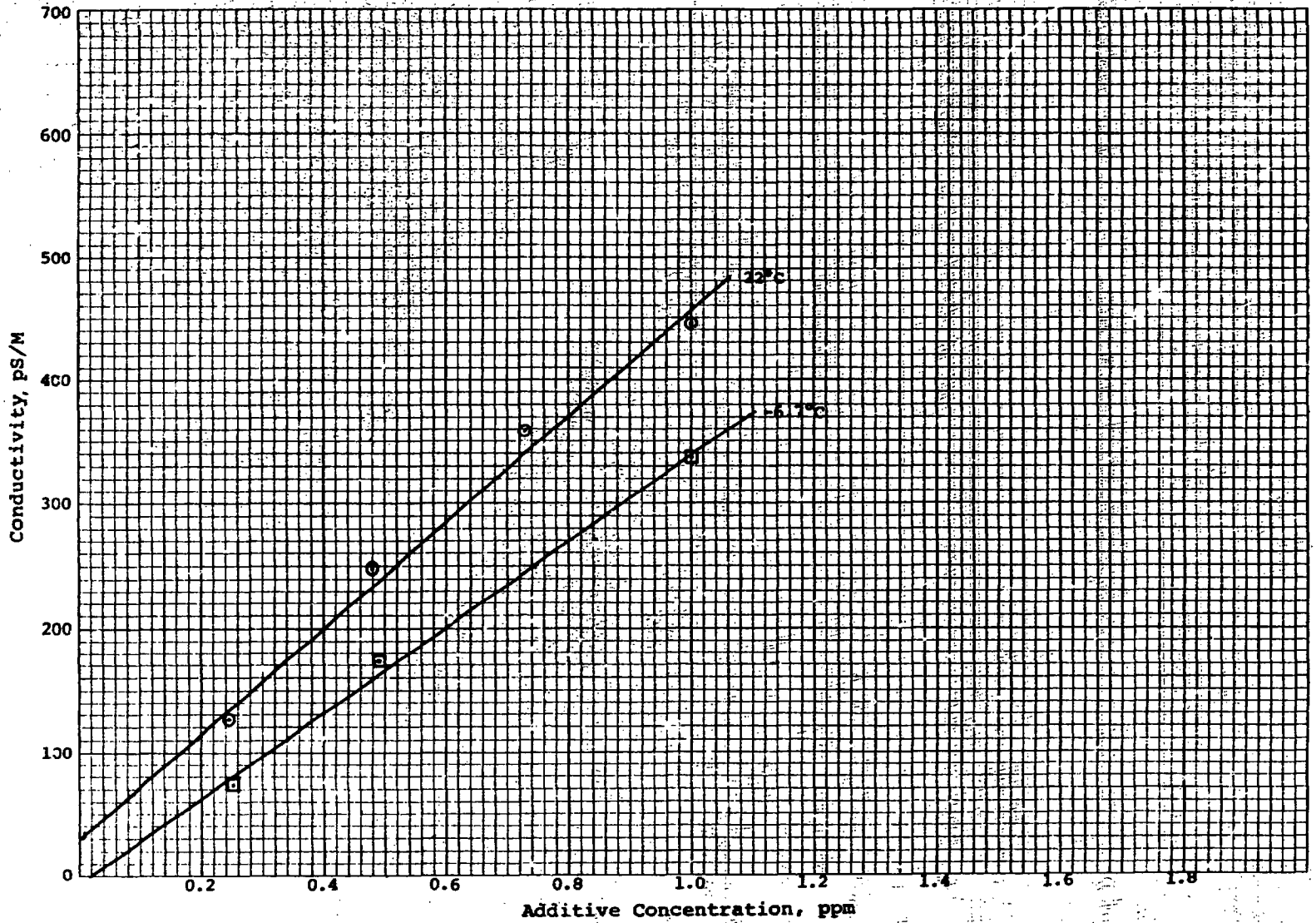

Figure 13. Fuel conductivity/additive concentration plots for clay treated JP-4 with S-450 additive.

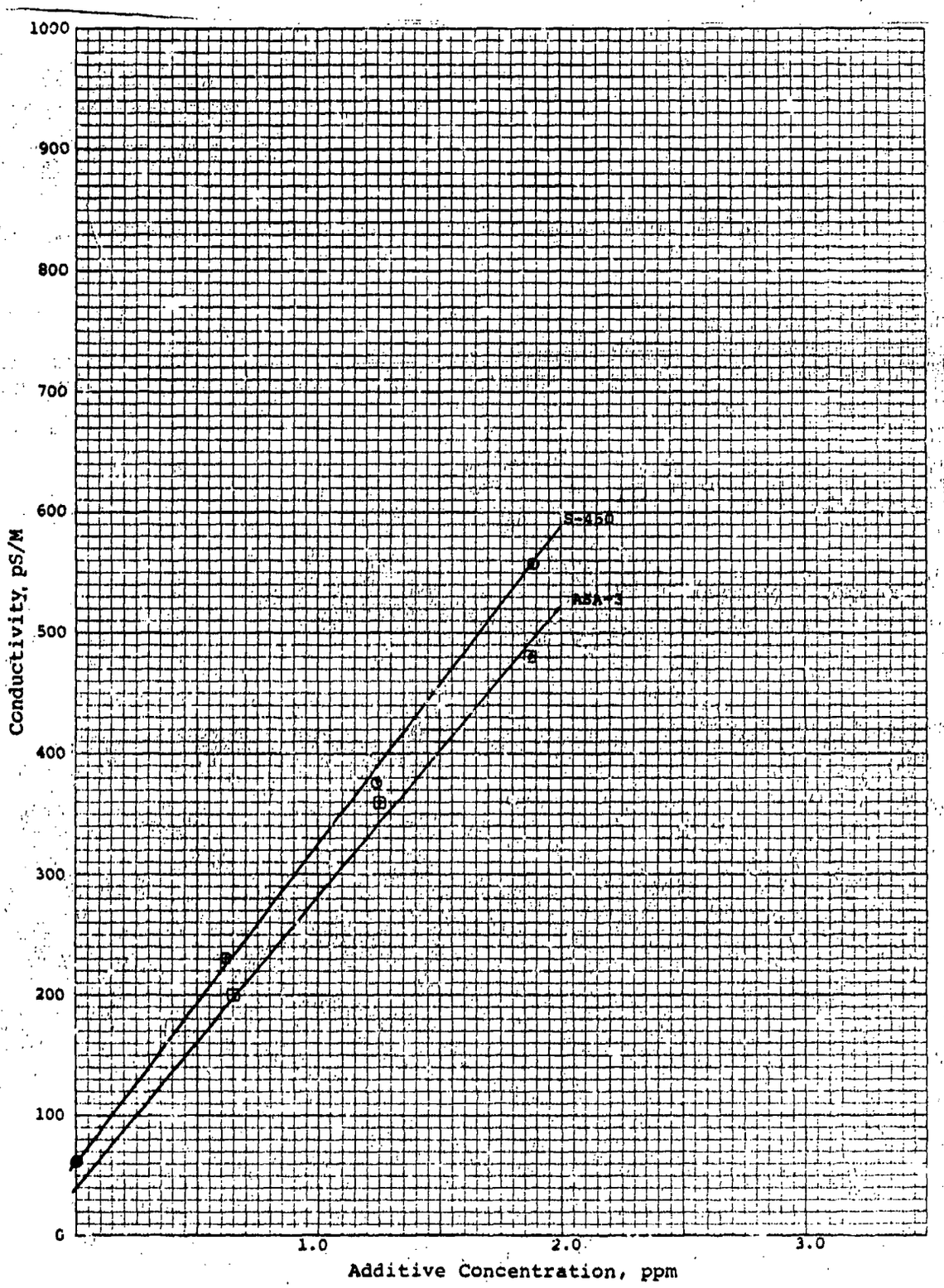

Figure 14. Fuel conductivity/additive concentration plots for Tinker AFB JP-4 with ASA-3 and S-450 additives.

Charging tendency measurements were conducted for each fuel at 70°F and 20°F, using both red and blue fuel tank foams. Fuel flow was exactly 400 ml/min, and a new foam specimen was employed for each test. To facilitate evaluation of the effect of the additives, measurements were conducted over a range of additive concentrations. For many fuel/foam/additive combinations, the sign of the accumulated charge changed as the concentration of additive was increased. Comparable tests were conducted with each additive and these were completed within the same test period. This precaution was felt to be important so that uncontrolled factors such as relative humidity or foam storage conditions would not bias the evaluation.

In order to determine the influence of corrosion inhibitor on charging tendency, two different corrosion inhibitors were added to clay-treated JP-4 at the concentration specified for that additive. Unicor J and DCI-4a were added at the level of 15.2 ppm in the fuel. Using this fuel, charging tendency measurements were conducted at 70°F with both antistatic additives and with both foams.

Results and Discussion

Results of the tests are presented in Tables 2 through 7 and are plotted in Figures 15-24. Values are given in microcoulombs per cubic meter of fuel. It should be noted that data for the first three fuels, presented in Tables 2-4, were obtained under slightly different conditions than for subsequent fuels. It was discovered that previous similar tests (ref. 1) had been conducted using foam specimens having a 0.5 inch diameter rather than a 1 inch diameter. To make the current tests comparable to those in the referenced report, either the foam specimen volume needed to be decreased or the fuel flow scaled up proportionately. The first option was selected, that of modifying the sample cell to accept a 0.5 inch foam sample.

TABLE 2. CHARGING TENDENCY OF JP-8 ON POLYURETHANE FOAMS WITH ASA-3 AND S-450 FUEL ADDITIVES

Foam type	Additive conc., ppm	Charge, $\mu C/m^3$ 70°F S-450	70°F ASA-3	20°F S-450	20°F ASA-3
Red polyester	0	+12	+11	+27	+24
	0.5	-11	-7	-22	-13.5
	1.0	-7	-3	-16	-7.5
	1.5	-5	-1.5	-13	-7.5
	2.0	-3	-0.5	-8	-3.5
	2.5	-1.5	-	-	-
Blue polyether	0	+46	+44	+57	+55
	0.5	-28	-15	-38	-21
	1	-13.5	-8	-27	-15
	1.5	-3	-3	-21	-8
	2	-1.5	-1.5	-15	-7
	2.5	-	-	-7	-4

TABLE 3. CHARGING TENDENCY OF FUEL AFFB 13-69 ON POLYURETHANE FOAMS WITH ASA-3 AND S-450 FUEL ADDITIVES

Foam type	Additive conc., ppm	Charge, $\mu C/m^3$ 70°F S-450	70°F ASA-3	20°F S-450	20°F ASA-3
Red foam	0	-29	-28	-31	-32
	0.5	-22	-4	-16	-13
	1.0	-12	-2.5	-8	-6
	1.5	-3	-2.5	-5	-3
	2.0	-0.8	-0.8	-3	-0.7
Blue foam	0	-36	-36	-45	-46
	0.5	-8	-7	-29	-11.5
	1.0	-2	-5	-13.5	-6
	1.5	-0.8	-2	-6	-2
	2.0	-0.8	-0.8	-4.5	-0.7
	2.5	-	-	-1.5	-

TABLE 4. CHARGING TENDENCY OF FUEL AFFB 14-70 ON POLYURETHANE FOAMS WITH ASA-3 AND S-450 FUEL ADDITIVES

Foam type	Additive conc., ppm	Charge, $\mu C/m^3$ 70°F S-450	70°F ASA-3	20°F S-450	20°F ASA-3
Red foam	0	+11	+11	+32	+32
	0.5	-8	-3	-15	-2.3
	1.0	-7	-1.2	-12	-1.1
	1.5	-5	-1.1	-7	-1.1
	2.0	-3	-0.8	-4.5	-0.5
				-3.8	
Blue foam	0	+50	+50	+68	+68
	0.5	-13	-4.5	-17	-4.5
	1.0	-8	-1.8	-8.5	-1.5
	1.5	-5	-1.3	-6	-1.4
	2.0	-3	-0.8	-4	-1.1
	2.5	-2	-	-3	-0.8

TABLE 5. CHARGING TENDENCY OF JP-4 (Richards Gebaur AFB) ON POLYURETHANE FOAMS WITH ASA-3 AND S-450 FUEL ADDITIVES

Foam type	Additive conc., ppm	Charge, $\mu C/m^3$ 70°F S-450	70°F ASA-3	20°F S-450	20°F ASA-3
Red foam	0	+39	+39	+44	+43
	0.15	-	-9	-	-6
	0.25	-11	-4.5	-7.5	-4
	0.50	-8	-3	-2.2	-4
	0.75	-1.5	-3	-1.5	-4
	1.0	-1.5	-3	-0.7	-3.5
Blue foam	0	+30	+33	+33	+33
	0.25	-18	-18	-9.0	-6.7
	0.50	-10.5	-11	-7.5	-2.2
	0.75	-1.8	-1.8	-2.9	-1.8
	1.0	-0.9	-0.9	-1.6	-0.9

TABLE 6. CHARGING TENDENCY OF JP-4 (Tinker AFB) ON POLYURETHANE FOAMS WITH ASA-3 AND S-450 FUEL ADDITIVES

Foam type	Additive conc., ppm	Charge, $\mu C/m^3$ 70°F S-450	70°F ASA-3	20°F S-450	20°F ASA-3
Red foam	0	+35	+35	+40	+42
	0.15	+15	+9.0	-	+13.5
	0.25	+11	+4.5	+6.7	+6
	0.50	+7	+3.0	+5	+4.5
	0.75	+1.5	+3.0	+2	+3.8
	1.0	+1.3	+3.0	+2	+3.8
Blue foam	0	+30	30	37	38
	0.15	18	-	-	-
	0.25	11	4.5	9	7.5
	0.50	1.8	3.0	6.8	5
	0.75	0.9	1.5	4	3
	1.0	-	-	0.7	0.9

TABLE 7. CHARGING TENDENCY OF CLAY TREATED JP-4 ON POLYURETHANE FOAMS WITH ANTISTATIC ADDITIVE AND CORROSION INHIBITORS

Foam type	Additive conc., ppm	Charge, ($\mu C/m^3$) at 70°F Unicor J 15.2 ppm S-450	Unicor J 15.2 ppm ASA-3	DCI-4A 15.2 ppm S-450	DCI-4A 15.2 ppm ASA-3
Red polyester	0	+45	45	45	44
	0.17	33	12.5	8.5	14
	0.34	8.1	11	5.5	7
	0.50	4.2	10	2.8	5
	0.67	2.2	4.8	2.0	3
	1.0	0.7	1.1	0.8	0.9
Blue polyether	0	+58	58	60	60
	0.17	40	33	42	45
	0.34	31	29	29	33
	0.50	9	12	15	10
	0.67	5	7	4	6
	1.0	3	4	2	3

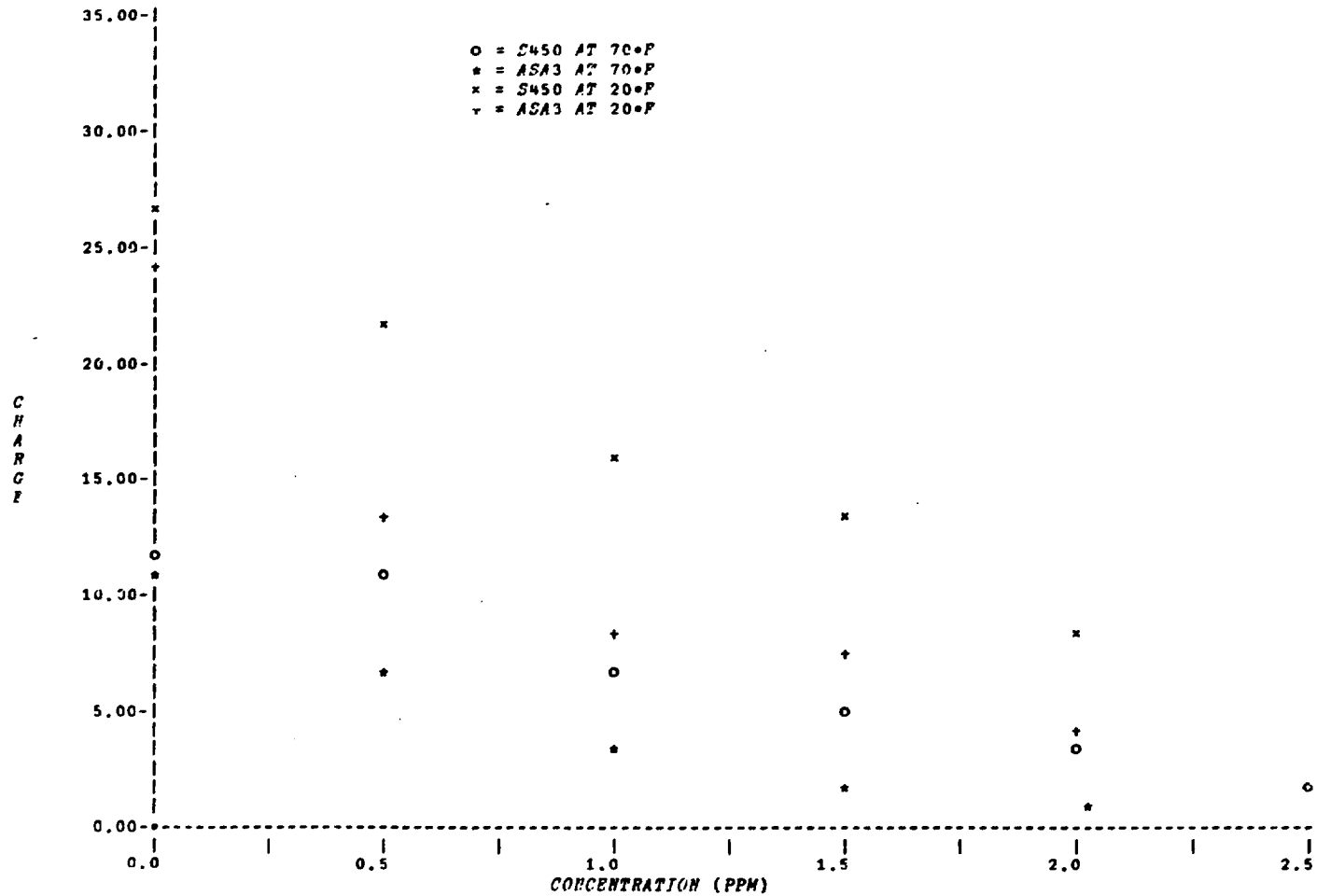

Figure 15. Accumulated charge ($\mu C/m^3$) versus additive concentration for JP-8 fuel with red foam.

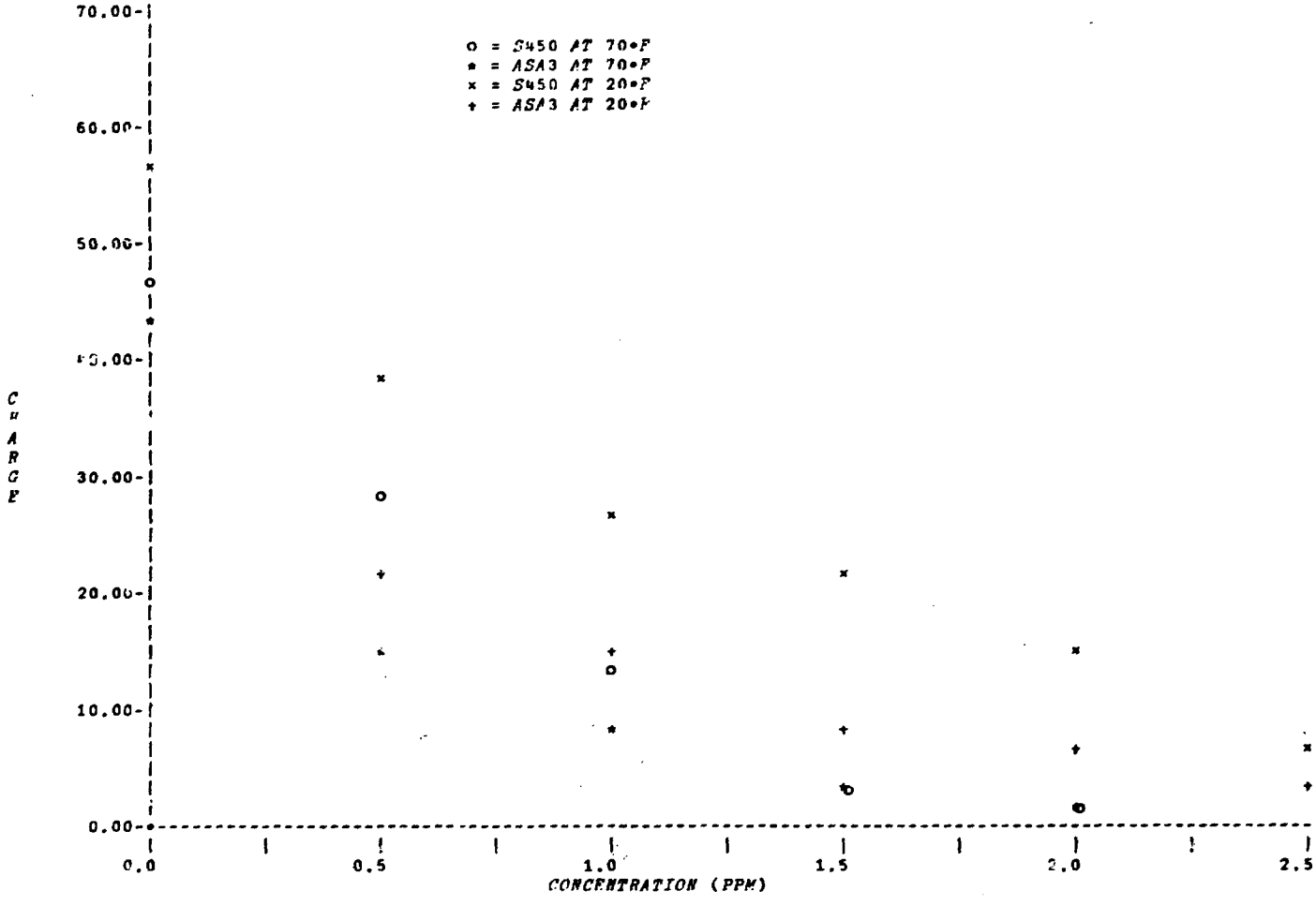

Figure 16. Accumulated charge ($\mu C/m^3$) versus additive concentration for JP-8 fuel with blue foam.

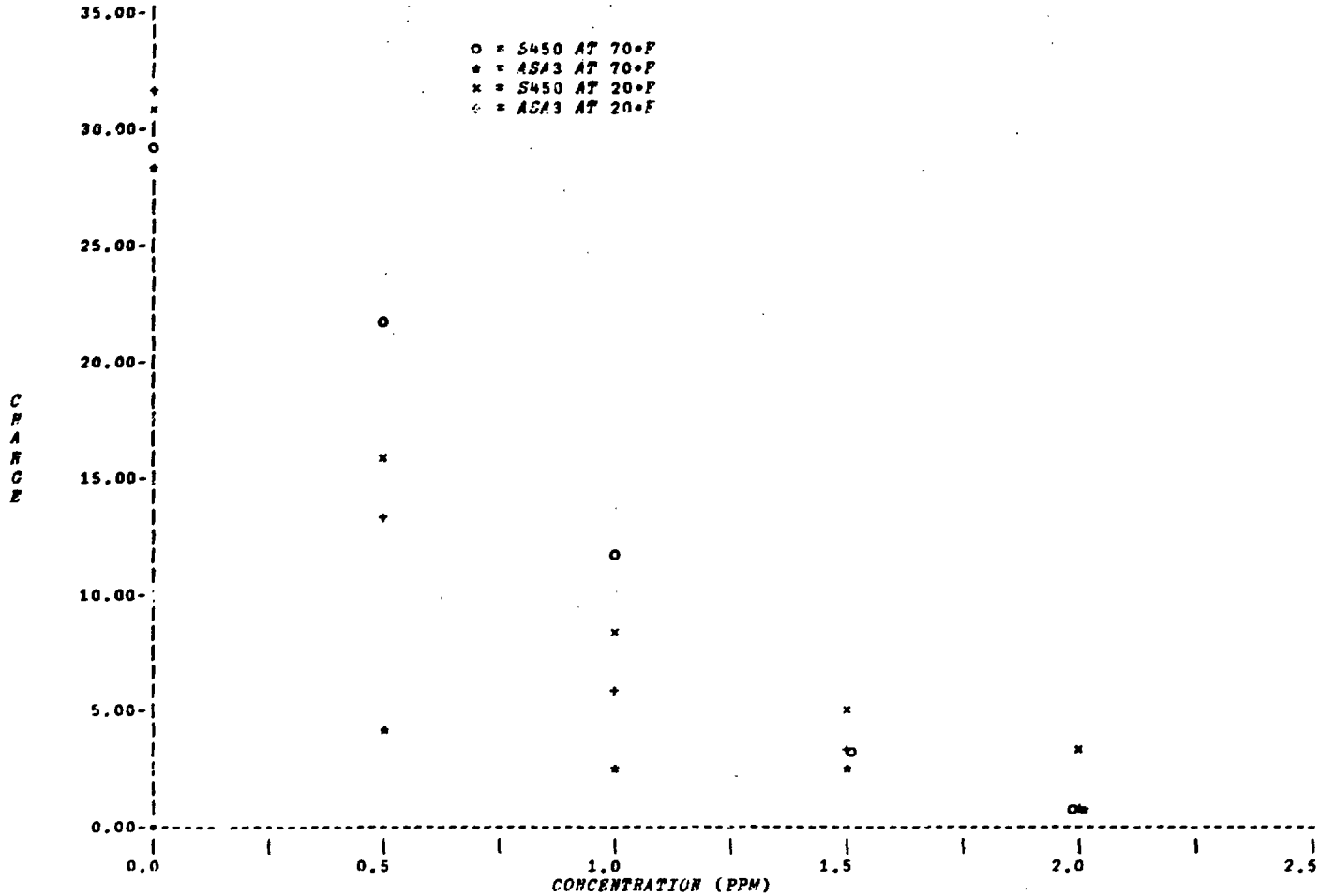

Figure 17. Accumulated charge ($\mu C/m^3$) versus additive concentration for AFFB 13-69 fuel with red foam.

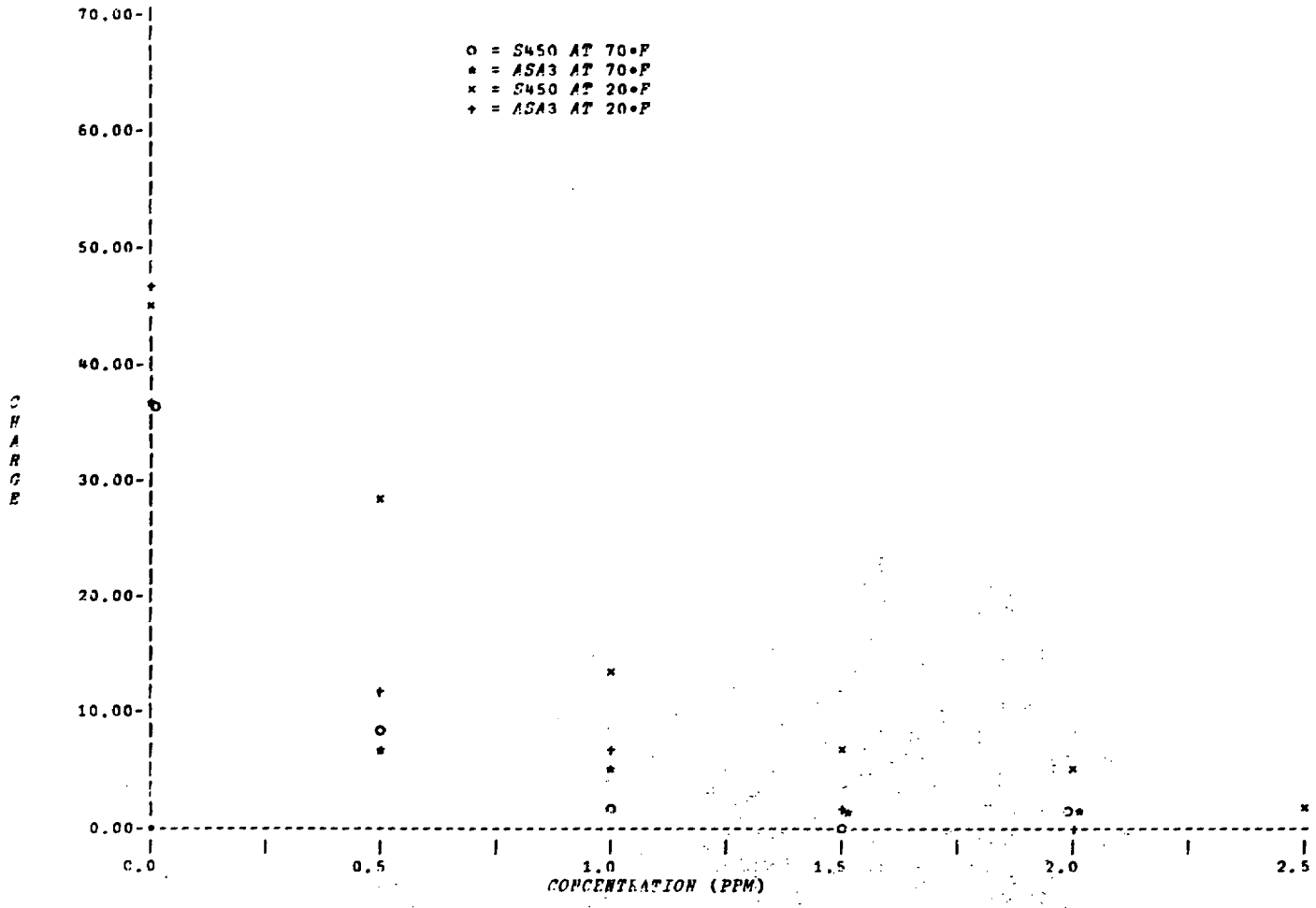

Figure 18. Accumulated charge ($\mu C/m^3$) versus additive concentration for AFFB 13-69 fuel with blue foam.

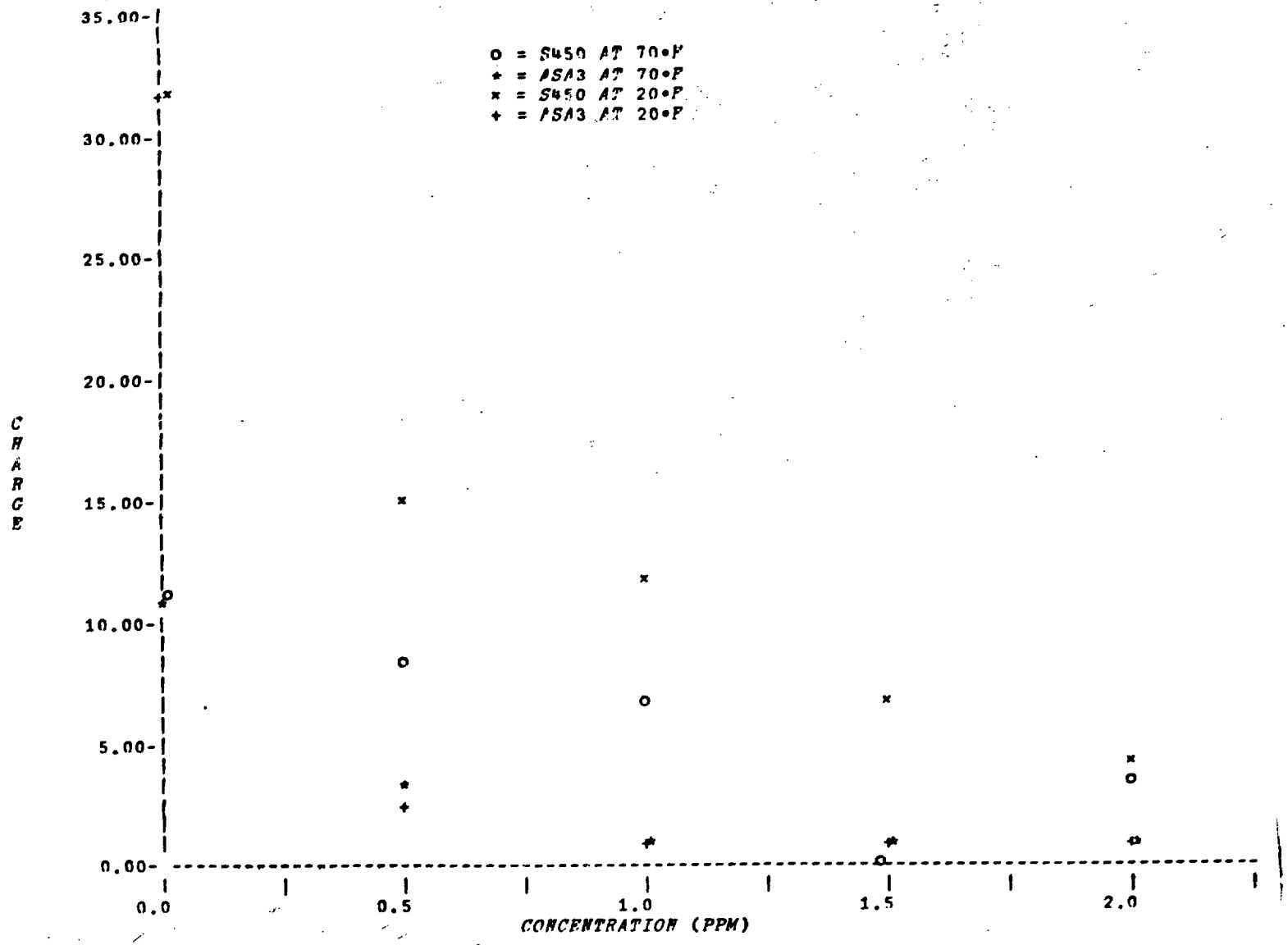

Figure 19. Accumulated charge ($\mu C/m^3$) versus additive concentration for AFFB 14-70 fuel with red foam.

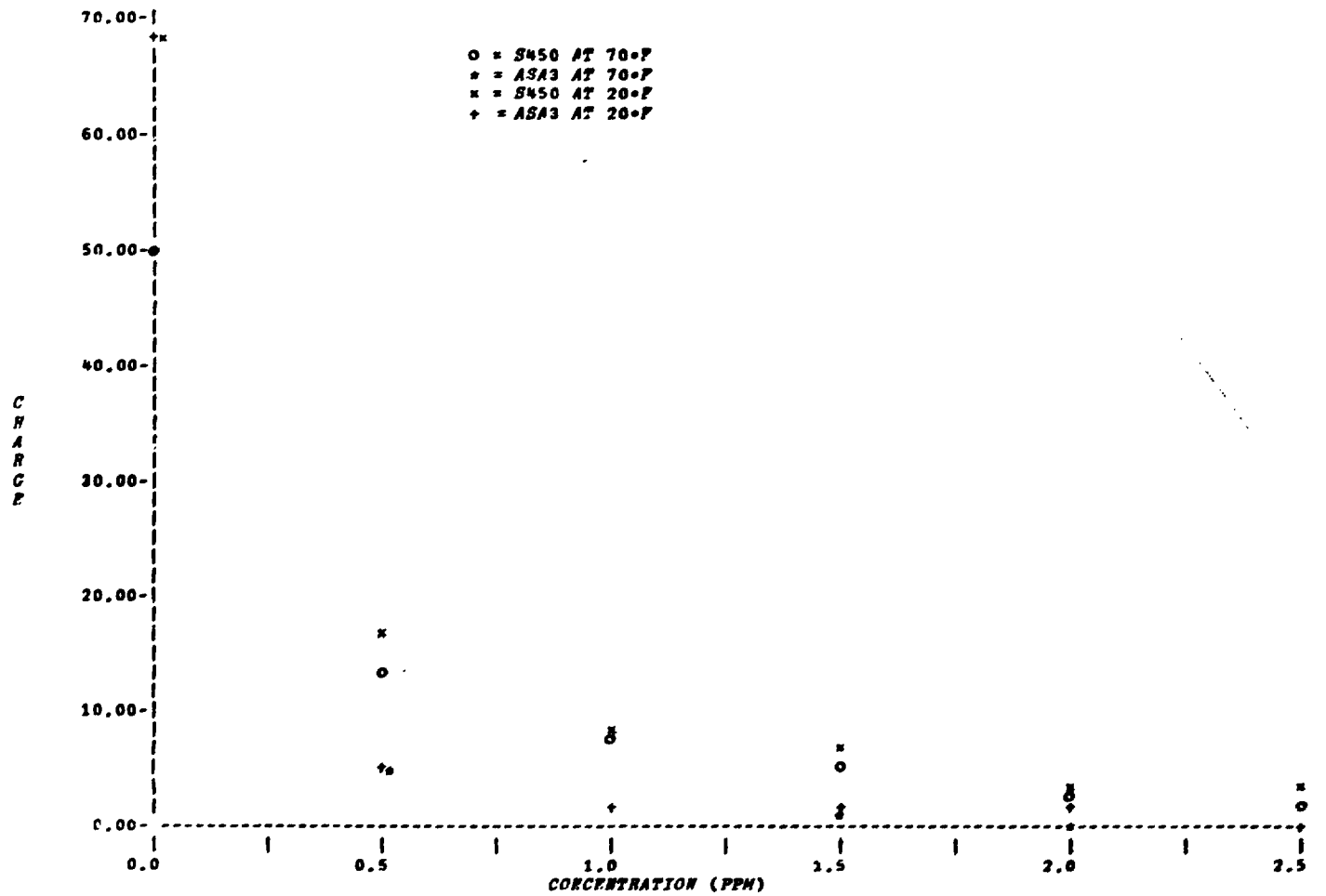

Figure 20. Accumulated charge ($\mu C/m^3$) versus additive concentration for AFFB 14-70 fuel with blue foam.

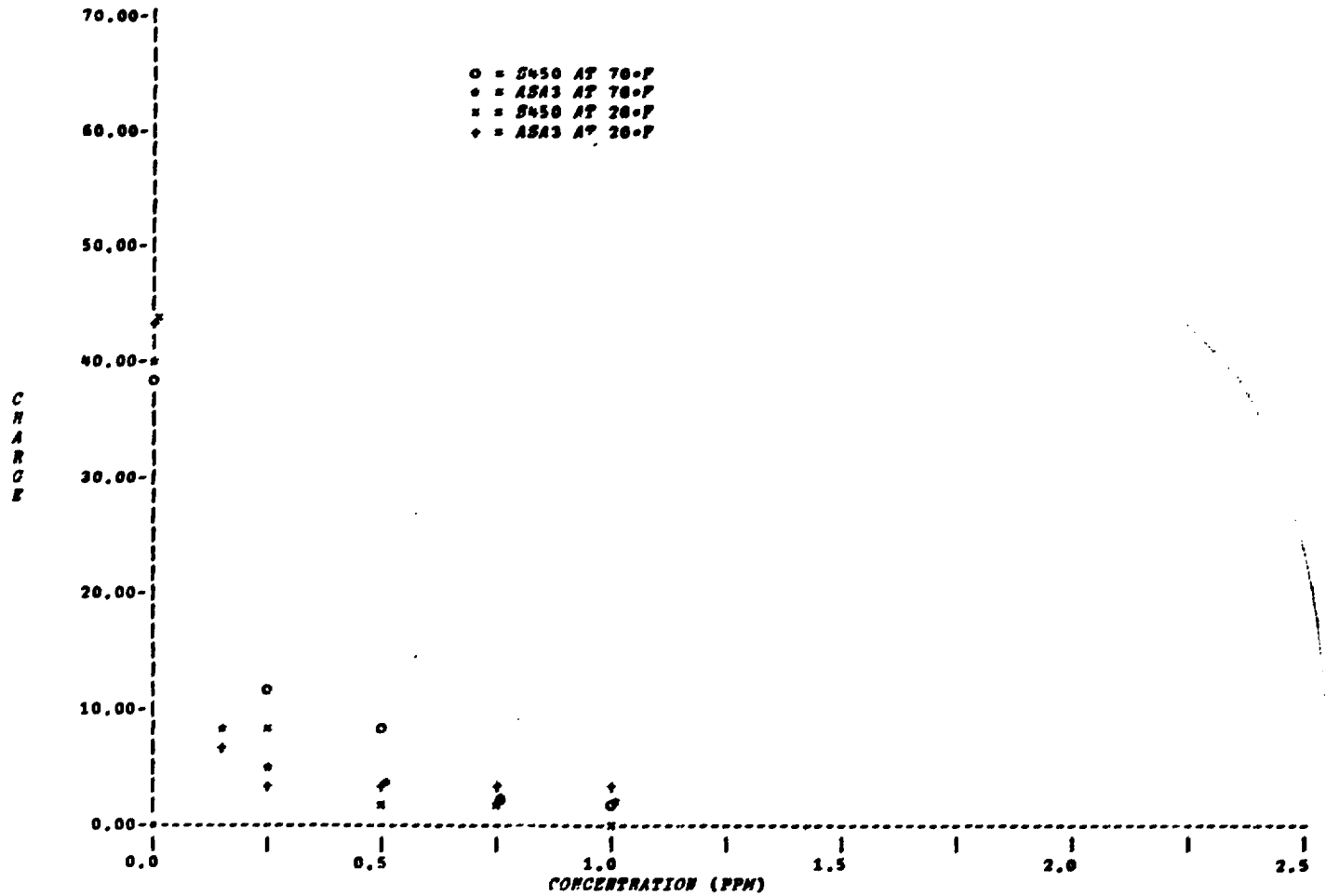

Figure 21. Accumulated charge ($\mu C/m^3$) versus additive concentration for JP-4, Richards Gebaur AFB, fuel with red foam.

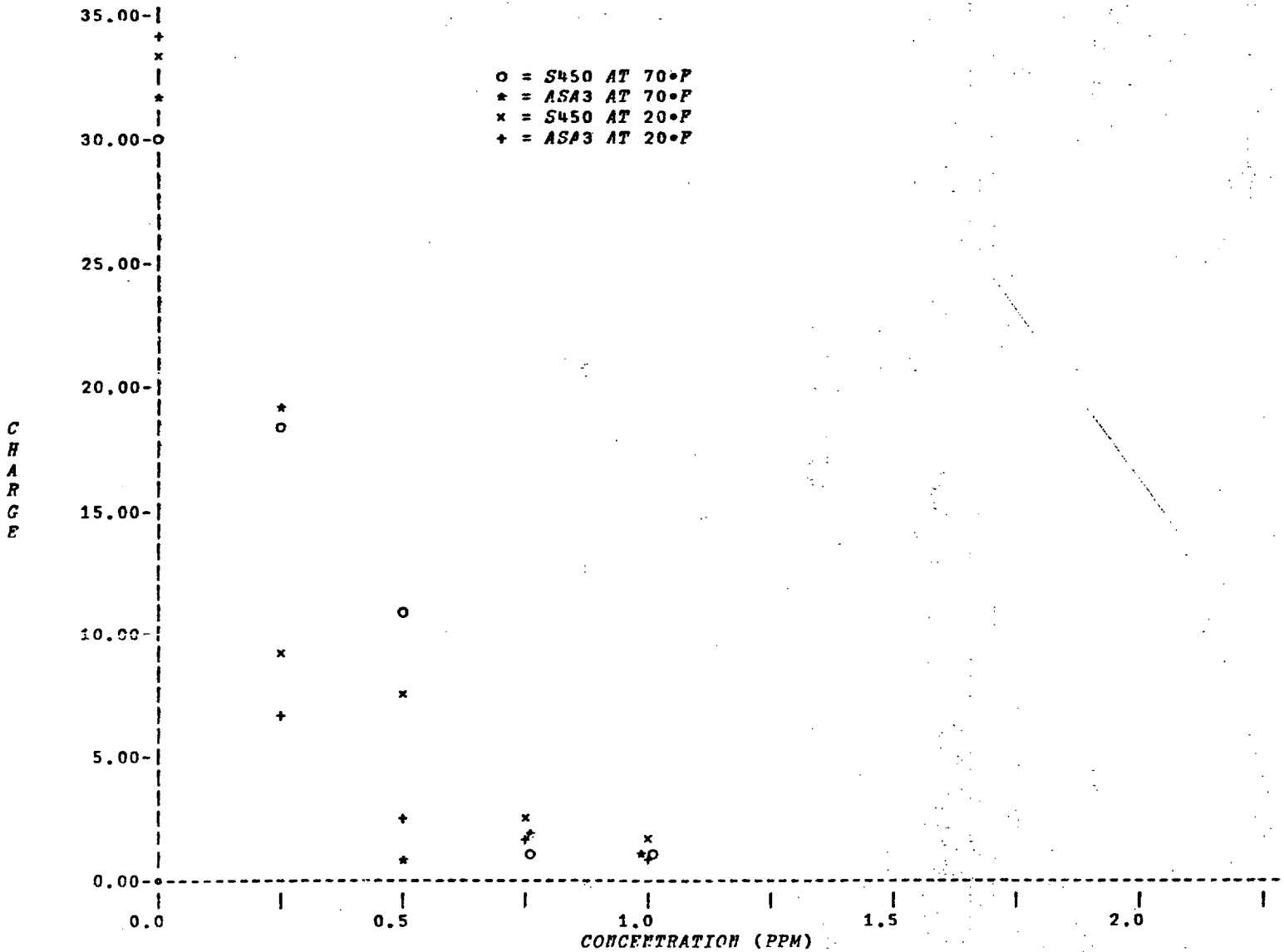

Figure 22. Accumulated charge ($\mu C/m^3$) versus additive concentration for JP-4, Richards Gebaur AFB, fuel with blue foam.

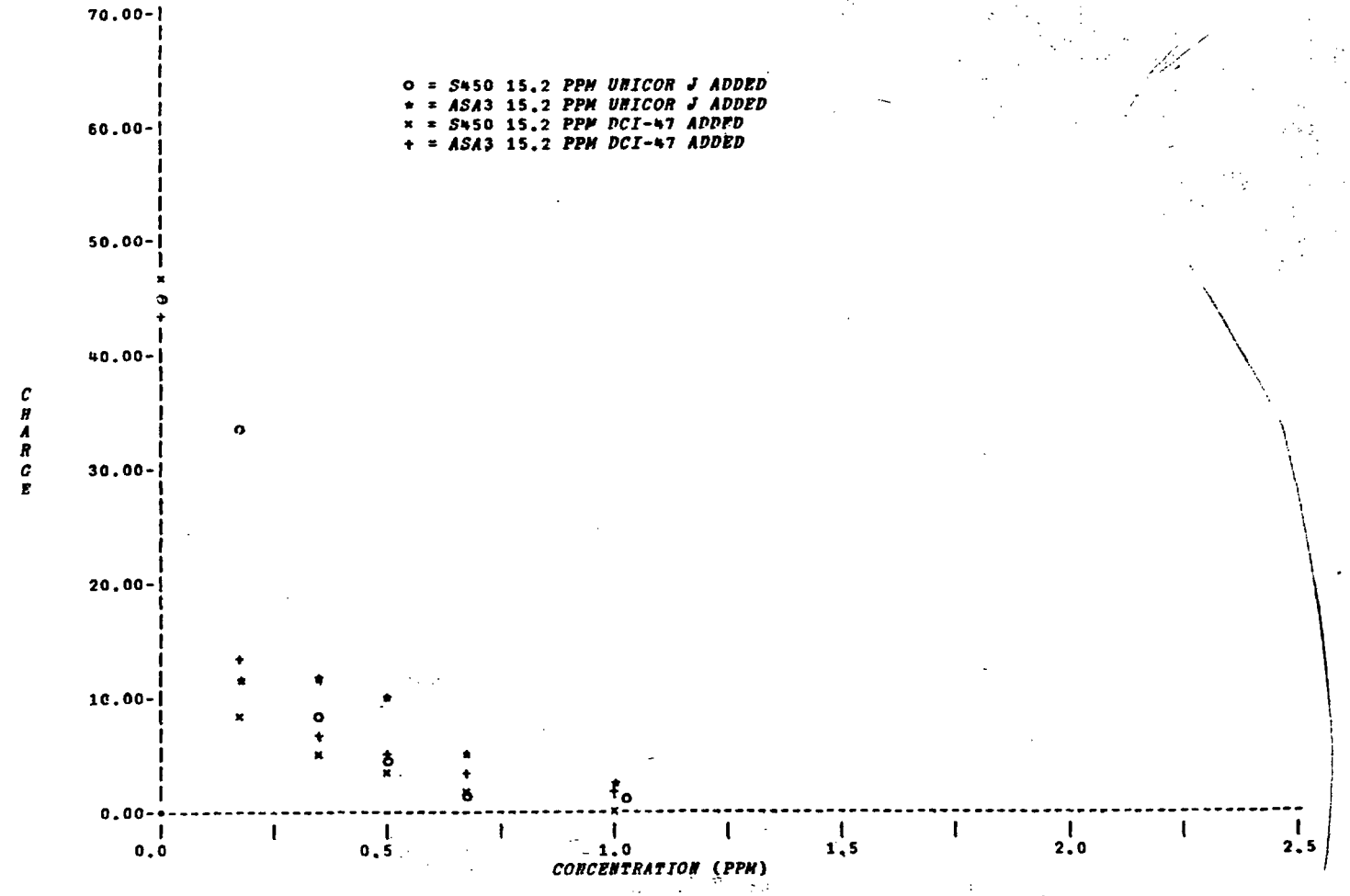

Figure 23. Accumulated charge ($\mu C/m^3$) versus additive concentration for clay treated JP-4 fuel at 70°F with red foam.

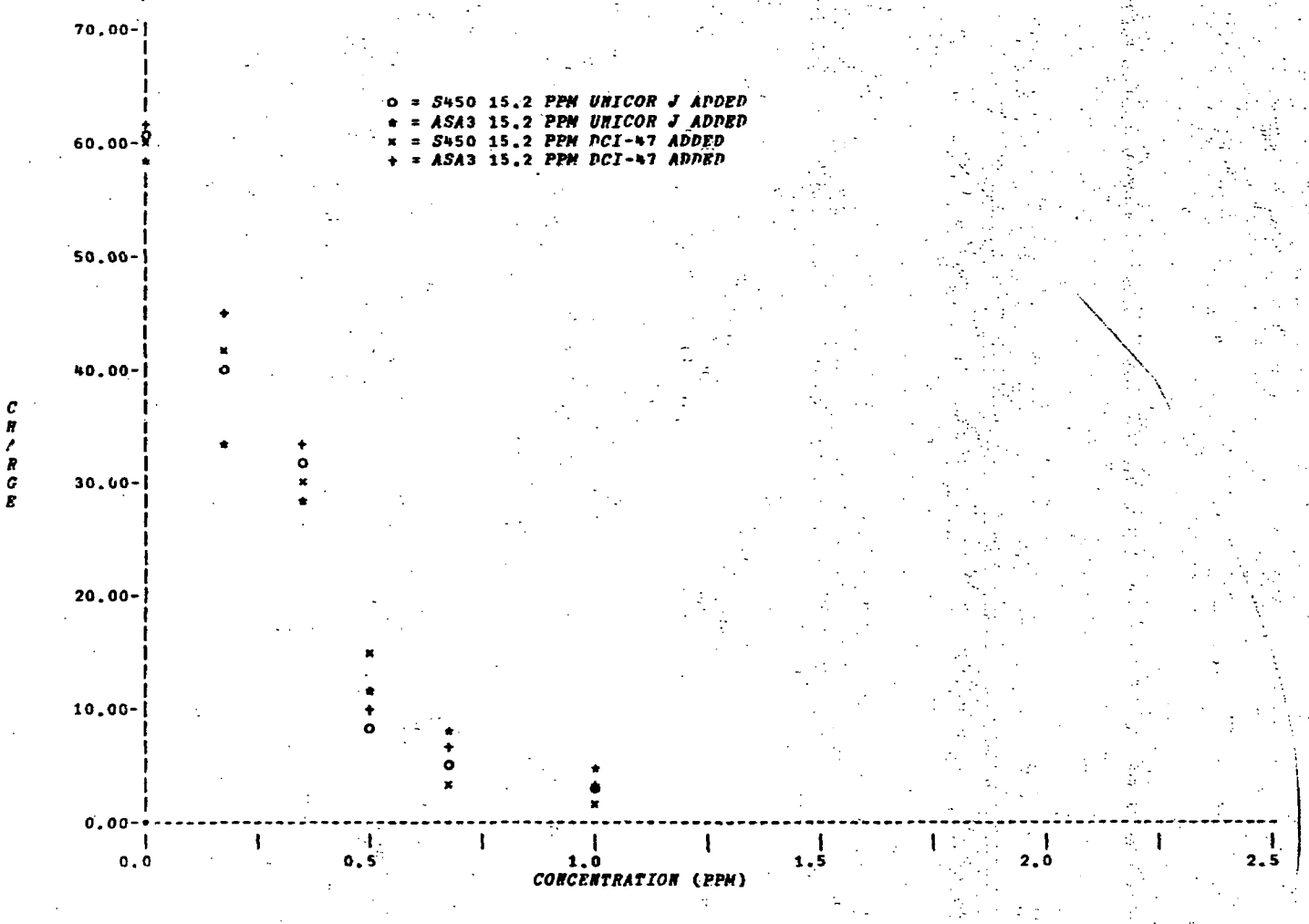

Figure 24. Accumulated charge ($\mu C/m^3$) versus additive concentration for clay treated JP-4 fuel at 70°F with blue foam.

Although the apparatus for measurement of static charging tendency was similar in all ways to the Exxon MS tester, data generally differed from that reported from the MS tester in one aspect. Samples in current tests gave a high charge value when no antistatic additive had been added. Charge generally decreased with additive concentration. MS tester data, however, have shown low charge values for the baseline fuel and higher values with the addition of antistatic additives. This discrepancy was never completely resolved. Data presented in this report, however, are felt to reflect the behavior of the additive, despite this difference from previous work.

In sampling the foam materials, an effort was made to obtain identical specimens for the comparative tests. Fuel flows were passed through the foam in the same direction relative to the specimen's position in the original foam block. Specimens were cut just before the test so that comparative specimens experienced the same sample history. Under these conditions, results were quite reproducible. In the case of the Tinker Air Force Base JP-4, twelve measurements were taken on the starting fuel for each foam and twelve were taken on the fuel having additive at the 200 pS/m conductivity level for each foam. In this series of measurements, foam specimens were not specifically selected on the basis of orientation in the original block, but rather were completely randomly taken from the block. Under these latter conditions, relative standard deviations of 16.2% for red foam and 16.1% for blue foam were obtained in the measurements with no antistatic additive. Relative standard deviations were recorded with ASA-3 antistatic additive at a level to give a 200 pS/m conductivity, these being 17.7% for blue foam and 24.5% for red foam.

Conclusions

While the matrix fuel had a great effect on the absolute value of the charge, no great difference between the two additives was apparent for most fuels. In the case of the Tinker AFB JP-4, S-450 showed slightly better performance than ASA-3 at 70°F for both foams. However, at 20°F ASA-3 out-performed S-450 for the red foam but not for the blue foam.

2. CHARGING TENDENCY OF A JP-4 SAMPLE CODED 81-3-CRM

About two years after the study described in subsection 1 above, electrical conductivity and charging tendency were evaluated for an operational JP-4 (coded 81-3-CRM) and for a reference fuel (AFFB 14-70). The measurements were conducted on the fuels before treatment and after the addition of the antistatic additives Stadis 450 (Du Pont Petroleum Products) and ASA-3 (Shell Corp.) to the fuels at various concentrations. Two different fuel tank foams, blue polyether urethane and red polyester urethane, were used in the study. The polyurethane foam specimens were cut into 1/2 inch diameter x 3 inch cylinders to provide a snug fit within the same cell of the test device. The tests were conducted at 70°F and 20°F in exactly the same manner as described in subsection 1.

Figures 25 and 26 illustrate the additive levels corresponding to various conductivity values, expressed in picosiemans per meter. Charging tendency was similarly measured over a range of additive concentrations, with the values being expressed in microcoulombs per cubic meter. Data are presented in Tables 8 and 9 for the various fuel/foam combinations at both 70°F and 20°F. It will be noted that the sign of the accumulated charge changed as the additive concentration was increased.

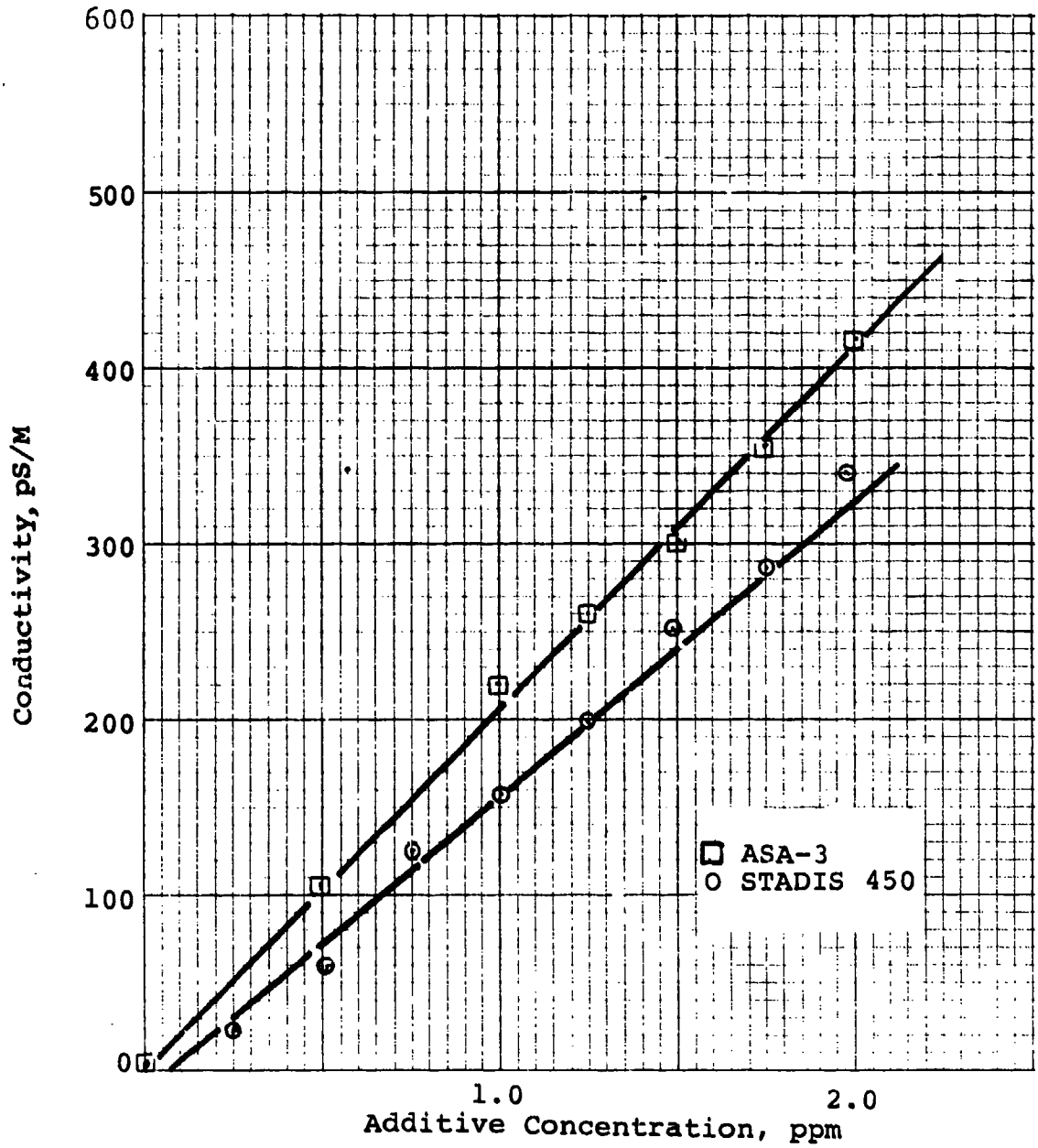

Figure 25. Fuel electrical conductivity as a function of additive concentration for reference fuel AFFB 14-70.

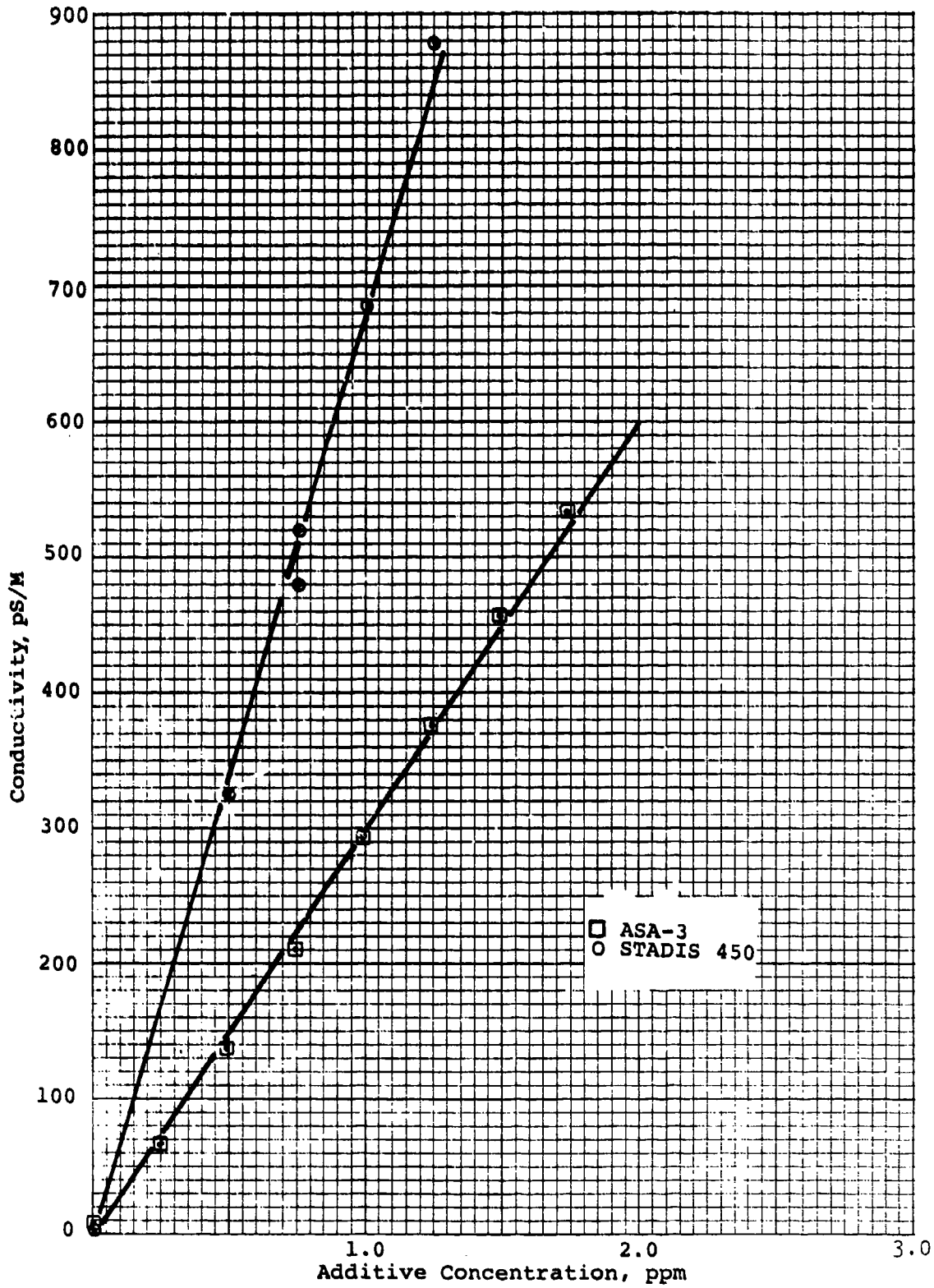

Figure 26. Fuel electrical conductivity as a function of additive concentration for fuel coded 81-3-CRM.

TABLE 8. CHARGING TENDENCY OF REFERENCE FUEL AFFB 14-70 ON POLYURETHANE FOAMS WITH ASA-3 AND S-450 FUEL ADDITIVES

Foam type	Additive conc., ppm	Charge, μC/m³ 70°F S-450	70°F ASA-3	20°F S-450	20°F ASA-3
Red foam	0	17	18	25	24
	0.5	-7	-3	-15	-3
	1.0	-5	-2.3	-9	-1.3
	1.5	-3	-1.8	-6	-1.1
	2.0	-1.5	-0.9		
Blue foam	0	+42	+44	+62	+60
	0.5	-14	-9	-18	-12
	1.0	-7	-6	-12	-5
	1.5	-2	-0.8	-6	-2
	2.0	-2	-0.8	-4	-0.8

TABLE 9. CHARGING TENDENCY OF JP-4 CODE: 81-3-CRM ON POLYURETHANE FOAMS WITH ASA-3 AND S-450 FUEL ADDITIVES

Foam type	Additive conc., ppm	Charge, μC/m³ 70°F S-450	70°F ASA-3	20°F S-450	20°F ASA-3
Red foam	0	+18	+18	24	23
	0.5	-9	+9	-15	13
	1.0	-5	-4	-4	-5
	1.5	-4	-4	-4	-5
	2.0	-4	-3	-3	-4
Blue foam	0	+78	81	95	97
	0.5	-20	24	-35	37
	1.0	-5	7	-11	-13
	1.5	-5	-5	-8	-9
	2.0	-4	-4	-5	-5

Discussion of Results

Fuel AFFB 14-70 was included in this evaluation as a reference sample since it was a part of the earlier investigation reported in subsection 1. Data for this fuel, shown in Figure 26 and Table 8 agreed quite well with that obtained previously.

The electrical conductivity plot of fuel 81-3-CRM indicates that the addition of Stadis 450 affected the conductivity of that fuel more than the addition of the same amount of ASA-3. The charging tendency of fuel 81-3-CRM, as shown in Table 9, was much higher for the blue polyurethane foam than it was for the red foam, and was higher than that of the reference fuel with blue foam. With the red foam, however, there appeared to be no substantial difference in the charging characteristics of the two fuels. The same trends observed at 70°F were also present at 20°F, except that the charging tendency was somewhat enhanced at the lower temperature.

3. POLYSULFIDE SEALANT CHALKING, INITIAL STUDY

The problem of polysulfide sealant "chalking" in F-16 aircraft fuel tanks was investigated in a special study to define the effect trace metals and mercaptan sulfur have on the process. The chalking phenomenon had been identified in previous Air Force studies as being due to exposure of the calcium carbonate filler material, presumably as a result of a process in which the sealant is rendered fuel soluble. A study was conducted to determine the extent of the chalking problem and to evaluate the effect of metal deactivators on the rate of sealant chalking.

Determination of Fuel/Metal Equilibrium Concentrations

The chalking phenomenon was known to be influenced by the type and amount of dissolved metals present in the fuel. Certain metals such as copper and cadmium are reported to induce severe chalking. A study was therefore undertaken to determine the equilibrium concentrations of various metals in jet fuels upon contact with cleaned and activated metal strips at 140°F.

Test Fuels

Jet Reference Fuel (JRF) and JP-4 were used for the tests. The JP-4 that was provided for the study was found to contain approximately 400 ppb of lead. Additional data on the JP-4 was provided[a] as follows:

Acidity, total mg KOH/gram	0.005
Corrosion	negative (1-A)
Mercaptan sulfur, wt %	0.0000
Total sulfur, wt %	0.01

The JRF fuel was prepared in glass vessels with volumetric quantities of the following materials:

cyclohexane	60 parts
toluene	30 parts
isooctane	10 parts
t-dibutyldisulfide	1 part
t-butylmercaptan	0.015 part

Test Metals and Cleaning Processes

Equilibrium studies were conducted with 3 x 3 inch coupons of copper, monel 400, cadmium, lead, mild steel, and anodized aluminum. The thickness varied slightly depending on the type of stock used. Each metal coupon was sequentially cleaned with the following solvents:

50/50 by volume methylene chloride and trichloroethylene
trichloroethylene
50/50 by volume ethanol and acetone
30/30/40 by volume ethanol, acetone and deionized water
deionized water

---

[a]Measurements performed at Det. 13 SA-ALC/SFQLA Laboratory, Wright-Patterson AFB, Ohio.

The cleaning operations were performed by rubbing the coupons with oil-free paper saturated with solvent. After all oil, grease and dirt had been removed, the coupons were immersed in deionized water and then wiped dry. Various pickling processes recommended by either the American Society for Metals or the Encyclopedia of Chemical Technology were used to activate the surfaces. These processes varied from metal to metal and generally involved acid treatment of the metal as described in Table 10.

TABLE 10. CLEANING PROCESSES FOR CHALKING STUDY TEST METALS

Copper:	• 1.5 minute immersion in 40% ACS-grade HCl at 73°F • rinse in deionized water at 73°F and blot dry
Monel 400:	• 5-second dip in bath containing 1 gallon deionized water, 1 gallon reagent grade HNO_3, and ½ lb NaCl at 73°F • rinse in deionized water at 180°F • immerse 6 minutes in 50 vol. % reagent grade HNO_3 at 73°F • immerse 1 additional minute in fresh 50% HNO_3 at 73°F (optional) • rinse in deionized water • neutralize in 2% ammonia solution at 73°F • rinse in boiling deionized water and blot dry
Cadmium:	• 3-minute immersion in 35% ACS grade HCl at 73°F • rinse in deionized water at 73°F and blot dry • repeat sequential solvent cleaning using disposable wipers and blot dry
Lead:	• 4-minute immersion in bath containing 8 vol. % reagent grade glacial acetic acid, 4.5 vol. % of reagent grade 30% hydrogen peroxide and 87.5 vol. % deionized water • repeat sequential solvent cleaning using disposable wipers and blot dry • repeat above two steps (optional)
Mild Steel:	• 5-minute immersion in 10 vol. % reagent grade sulfuric acid at 155°F • rinse in deionized water at 73°F • repeat sequential solvent cleaning using disposable wipers and blot dry • 1-minute immersion in above sulfuric acid bath at 155°F • rinse in deionized water at 73°F and blot dry • repeat sequential solvent cleaning as above and blot dry
Anodized Aluminum:	not pickled to prevent removal of anodized coating

Preparation of Glass Test Vessels and Sampling Containers

Wide-mouth quart jars with cork-backed Teflon®-lined lids were used for conducting the equilibrium studies. One-ounce French Square bottles with Polyseal-lined caps were used for taking periodic fuel samples for analysis of metal content. A rigorous cleaning procedure was employed for these containers. The glass test vessels were cleaned with a scouring type of cleanser, then rinsed with tap water followed by deionized water. They were then rinsed with 50% nitric acid, rinsed again with copious amounts of deionized water, and then dried at 110°C in an oven. The small sample bottles and all cap liners were similarly cleaned to insure that they were metals-free.

Equilibrium Test Procedure

A single 3-inch square metal coupon and 850 milliliters of either JP-4 or JRF fuel were placed in the quart vessels. The tests involved six different metal coupons in each of two fuels, along with two control vessels with no metal strips, for a total of 14 test units. The vessels were placed in an explosion-proof oven at 140°F. Samples of 25 ml each were collected after periods of 2, 5, 7, 9, 12, 19, 26, 33, 40, 47, 54, 78, and 107 days. Each 25 ml aliquot of solution was analyzed by atomic absorption spectrophotometry for the coupon metal. Iron was analyzed for the mild steel test, and copper and nickel for the test with Monel. The control solutions were analyzed for all six metals at each intervals. A total of 202 solutions was analyzed for various metals.

Results and Discussion

The results of the equilibrium studies through 107 days are shown in Table 11. Examination of these results provides the following conclusions. Nickel, iron and aluminum, if solubilized at all, are

TABLE 11. METAL CONCENTRATIONS IN JET FUELS, PARTS PER BILLION

Analysis	Jet Fuel	Metal Strip	Days Metal Strips Were Immersed in Fuel at 140°F											
			2	5	7	9	12	19	26	33	40	47	54	78	107
Cu	JP-4	None	ND[a]	ND	ND	ND	ND	ND	ND	ND	ND	ND	ND	ND	ND
		Monel	ND	ND	ND	ND	ND	ND	ND	ND	ND	ND	ND	ND	ND
		Copper	7	7	7	7	7	7	10	x[b]	x[b]	x[b]	24	24	24
	JRF	None	20	20	20	20	17	25	19	30	30	30	24	24	24
		Monel	47	47	47	47	40	43	40	50	50	50	57	59	57
		Copper	1,680	23,100	26,900	20,100	7,070	2,300	670	970	2,200	1,900	1,600	3,000	10,700
Ni	JP-4	None	ND	ND	ND	ND	ND	ND	ND	ND	ND	ND	ND	ND	ND
		Monel	ND	ND	ND	ND	ND	ND	ND	ND	ND	ND	ND	ND	ND
	JRF	None	ND	ND	ND	ND	ND	ND	ND	ND	ND	ND	ND	ND	ND
		Monel	ND	ND	ND	ND	ND	ND	ND	ND	ND	ND	ND	ND	ND
Cd	JP-4	None	ND	ND	ND	ND	ND	ND	ND	ND	ND	ND	ND	ND	ND
		Cadmium	ND	ND	ND	ND	ND	ND	ND	4	8	11	16	130	480
	JRF	None	ND	ND	ND	ND	ND	ND	ND	ND	ND	ND	ND	ND	ND
		Cadmium	4	7	7	19	21	30	35	44	46	53	55	63	170
Pb	JP-4[c]	None	395	310	310	338	268	340	480	500	400	500	330	360	220
		Lead	469	324	324	367	282	370	510	500	430	510	330	530	910
	JRF	None	ND	ND	ND	ND	ND	ND	ND	ND	ND	ND	ND	ND	ND
		Lead	ND	ND	ND	170	198	250	320	400	420	530	520	700	810
Fe	JP-4	None	ND	ND	ND	ND	ND	ND	ND	ND	ND	ND	ND	ND	ND
		Steel	ND	ND	ND	ND	ND	ND	ND	20	30	30	ND	ND	ND
	JRF	None	ND	ND	ND	ND	ND	ND	ND	30	30	40	ND	ND	ND
		Steel	ND	ND	ND	ND	ND	ND	ND	40	40	50	ND	ND	ND
Al	JP-4	None	ND	ND	ND	ND	ND	ND	ND	ND	ND	ND	ND	ND	ND
		Anod Al	ND	ND	ND	ND	ND	ND	ND	ND	ND	ND	ND	ND	ND
	JRF	None	ND	ND	ND	ND	ND	ND	ND	ND	ND	ND	ND	ND	ND
		Anod Al	ND	ND	ND	ND	ND	ND	ND	ND	ND	ND	ND	ND	ND

ND[a] - not detected at 7 ppb for copper, 40 ppb for nickel, 3 ppb for cadmium, 30 ppb for lead, 20 ppb for iron and 400 ppb for aluminum

x[b] - not detected but minimum detectability on these days was 20 ppb instead of 7 ppb

JP-4[c] - submitted fuel was known to have a high lead content

present at concentrations below detection limits of the analytical technique being used (40, 20, and 400 ppb, respectively). The copper level in JP-4 with the copper coupon is relatively low, but it appears to be increasing at a slow rate. The copper level in JRF quickly rises to an extremely high value, apparently from reaction with the mercaptan which is present as part of the JRF formulation. Wide fluctuations in copper concentration in JRF observed as a function of time may be related to a precipitate which formed on the copper and then crumbled off into the fuel. Copper build-up in the fuel containing Monel appears to be insignificant. The lead content in JRF has continued to increase at a steady rate. After 54 days the lead content began to increase in JP-4 and at a much faster rate than in JRF. A similar pattern is followed with cadmium.

The results clearly show that different metals have a widely varying range of solubility in jet fuel, and that the presence of mercaptan significantly accelerates the rate of solubility from activated metal strips.

Effect of Metals, Mercaptan, and Metal Deactivator on Sealant Chalking in Fuel

Tests similar to those used for the metal solubility studies were conducted to evaluate the sealant chalking process in various environments. These environments include JP-4 and JRF fuel with presence/absence combinations of the following: an additional 150 ppm of butyl mercaptan (50 ppm mercaptan sulfur), 5.8 ppm N,N' bis-salicylal-1,2-propane diamine metal deactivator, and 3 in. x 3 in. metal coupons of copper, Monel 40, cadmium, lead, mild steel, or anodized aluminum. The JRF fuel has as a part of its normal formulation 150 ppm butyl mercaptan, thus it contained a total of 300 ppm butyl mercaptan (100 ppm mercaptan sulfur) when additional mercaptan was added for the chalking studies.

Test Procedure

A total of 47 test vessels and metal coupons were conditioned by the solvent cleaning and acid activation procedure previously described. A 2 in. x 1/4 in. x 1/8 in. strip of sealant was vertically suspended in each test vessel and immersed in the 500 ml of jet fuel it contained. Included in the fuels were various combinations of metal coupons, mercaptan and metal deactivator. The test units were stored in a walk-in oven room maintained at 140°F and were checked daily for sealant chalking. Observations were made through the glass wall of the test vessels using strong fluorescent lighting. After 45 days, all sealant specimens were removed from the test jars and dried overnight for closer examination.

Results and Conclusions

Examinations made after the sealants had been dried showed that in most cases the chalking was more severe than was apparent when the sealants were observed through yellow-colored fuel. The times when chalking was first detected while looking through the fuels and the conditions of the dried strips are summarized in Tables 12 and 13. Photographs of the dried sealant strips are shown in Figures 27 through 33.

Generally, the presence of mercaptan caused an increase in the amount of chalking. While the presence of metal deactivator substantially decreased chalking in some tests, this was not true for all fuel/metal combinations. The overriding factor in sealant chalking was the specific fuels/metal combination. The significance of the factor is highlighted by the following observations:

(1) More chalking occurred in JP-4 than in JRF when comparing similar tests. The sealant chalking with JP-4 was more severe in the control test (neat fuel) and in tests with Monel,

TABLE 12. RESULTS OF SEALANT CHALKING STUDY AFTER 45 DAYS AT 140°F IN JRF

Metal	Additional 150 ppm Butyl-mercaptan*	5.8 ppm Metal Deactivator	Time and Description of Initial Sealant Chalking**	Final Appearance of Strips After Removal From Fuel and Overnight Drying
None	no	no	none detected	no change
None	yes	no	none detected	no change
Copper	no	no	9 days - strip yellow	thick yellow, crumbly coating
	yes	no	9 days - strip yellow	thick yellow, crumbly coating
	no	yes	10 days - strip yellow	thick yellow, crumbly coating
	yes	yes	10 days - strip yellow	thick yellow, crumbly coating
Monel	no	no	none detected	no change
	yes	no	none detected	no change
	no	yes	none detected	no change
	yes	yes	none detected	no change
Cadmium	no	no	none detected	very thin line of chalking on edges
	yes	no	none detected	light chalking, mainly on edges
	no	yes	none detected	light chalking, mainly on edges
	yes	yes	none detected	light chalking, mainly on edges
Lead	no	no	9 days - brown edges	thick brown, crumbly coating
	yes	no	9 days - strip brown	thick brown, crumbly coating
	no	yes	15 days - brown edges	thick brown, crumbly coating
	yes	yes	9 days - brown edges	thick brown, crumbly coating
Mild Steel	no	no	9 days - yellow edges	medium chalking
	yes	no	10 days - yellow edges	medium chalking
	no	yes	10 days - strip yellow	medium chalking
	yes	yes	10 days - strip yellow	medium chalking, some flaking
Anodized Aluminum	no	no	none detected	no change
	yes	no	none detected	no change
	no	yes	none detected	no change
	yes	yes	none detected	no change

* JRF contains 150 ppm mercaptan as prepared. JRF with additional mercaptan thus contains 300 ppm total, or 100 ppm total mercaptan sulfur.

** As observed through the glass test vessel and yellowish fuels, using fluorescent lighting. Only after 45 days were the sealant strips removed from solution for final observation.

TABLE 13. RESULTS OF SEALANT CHALKING STUDY AFTER 45 DAYS AT 140°F IN JP-4

Metal	Additional 150 ppm Butyl-mercaptan	5.8 ppm Metal Deactivator	Time and Description of Initial Sealant Chalking*	Final Appearance of Strips After Removal From Fuel and Overnight Drying
None	no	no	none detected	light chalking, mainly on edges
None	yes	no	none detected	light chalking, mainly on edges
Copper	no	no	34 days - yellow edges	medium chalking, some cracks
	yes	no	27 days - yellow sides	medium chalking, some cracks
	no	yes	none detected	no apparent chalking
	yes	yes	27 days - yellow edges	very light chalking
Monel	no	no	36 days - yellow edges	medium chalking, some cracks
	yes	no	27 days - yellow edges	medium chalking, some cracks
	no	yes	not detected	light chalking, some cracks
	yes	yes	31 days - yellow edges	medium chalking, some cracks
Cadmium	no	no	none detected	light chalking, mainly on edges
	no	yes	none detected	very light chalking
Lead	no	no	none detected	no change
	no	yes	none detected	no change
Mild Steel	no	no	28 days - yellow edges	heavy chalking with deep cracks
	yes	no	28 days - yellow edges	heavy chalking with deep cracks
	no	yes	38 days - yellow edges	medium chalking with no cracks
Anodized Aluminum	no	no	none detected	light chalking, mainly on edges
	yes	no	none detected	medium chalking, mainly on edges
	no	yes	none detected	very light chalking on edges
	yes	yes	none detected	medium chalking on edges

* As observed through the glass test vessel and yellowish fuels, using fluorescent lighting. Only after 45 days were the sealant strips removed from solution for final observation.

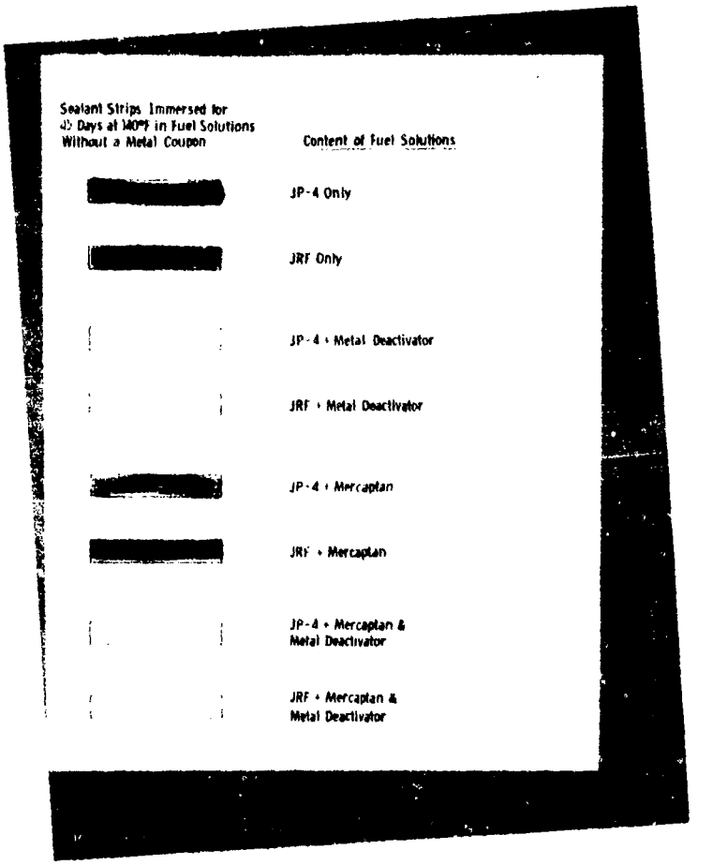

Figure 27. Control polysulfide sealant specimens for chalking tests.

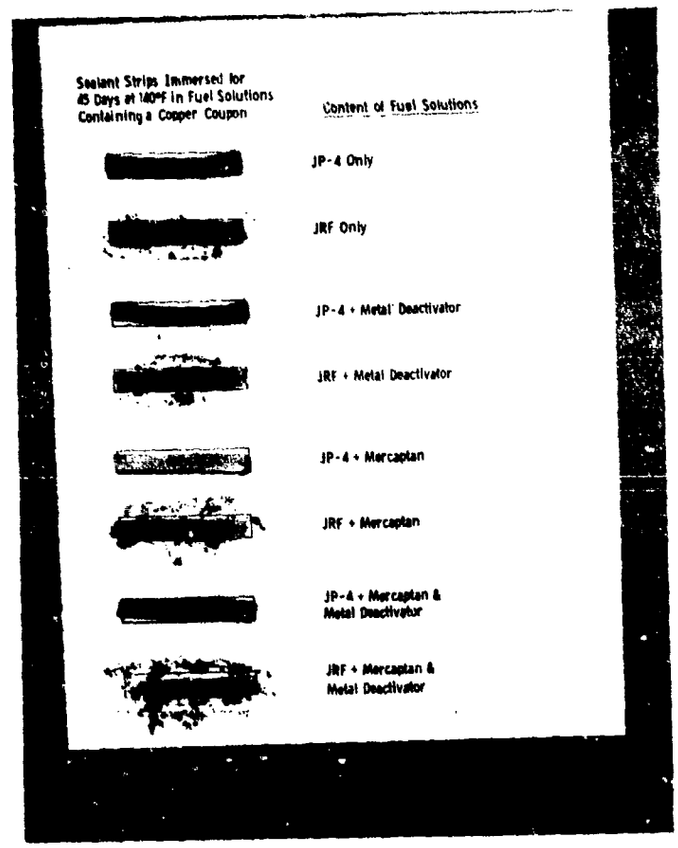

Figure 28. Polysulfide sealant chalking tests with metallic copper.

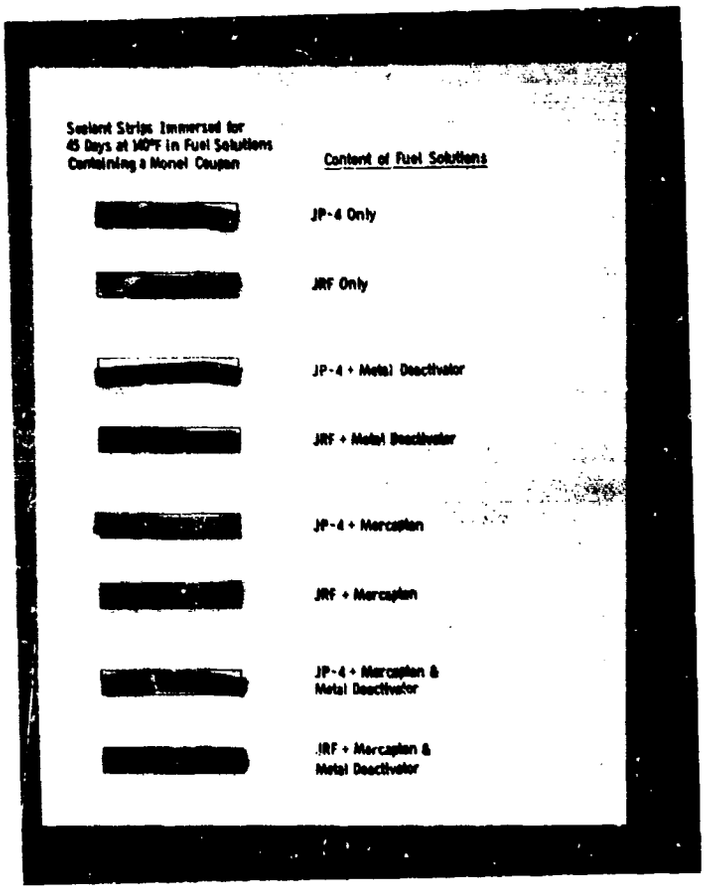

Figure 29 Polysulfide sealant chalking tests with Monel metal.

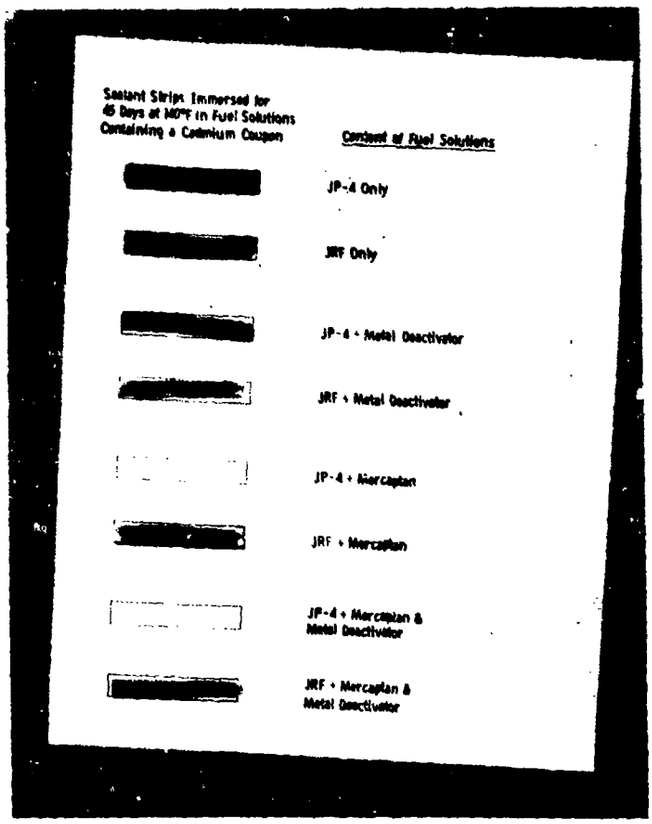

Figure 30. Polysulfide sealant chalking tests with metallic cadmium.

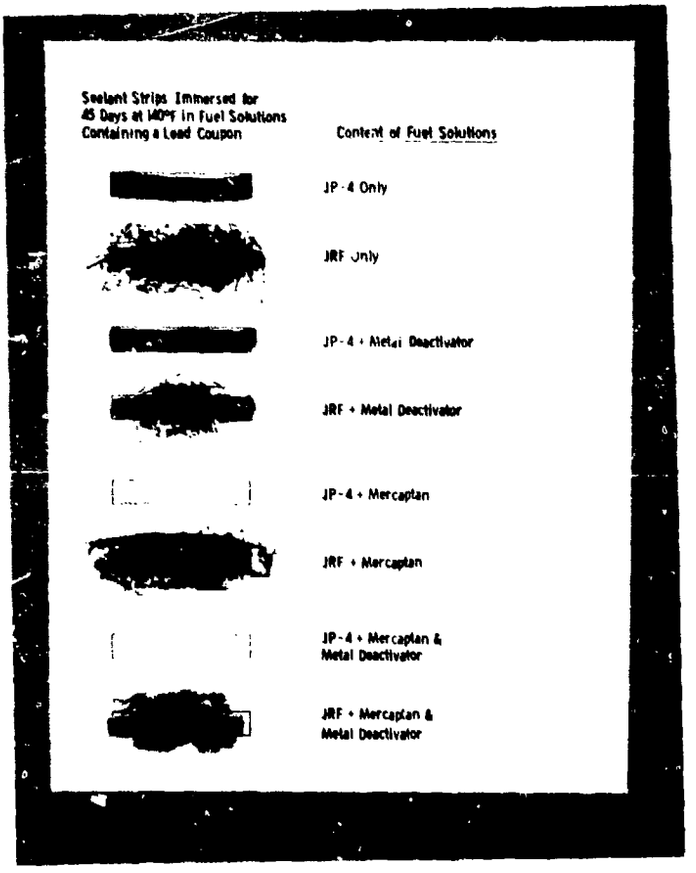

Figure 31. Polysulfide sealant chalking tests with metallic lead.

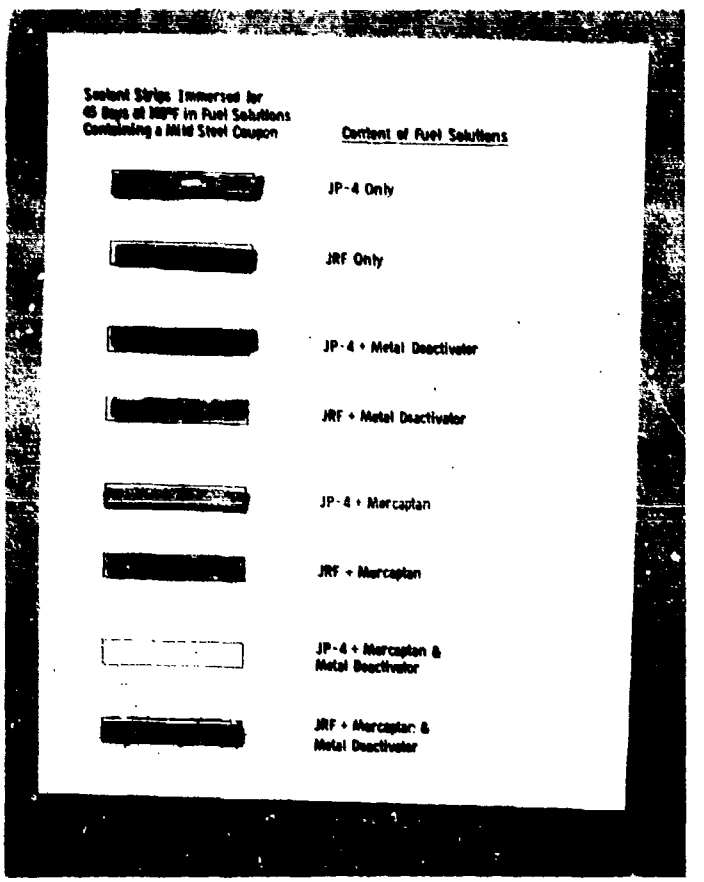

Figure 32. Polysulfide sealant chalking tests with mild steel.

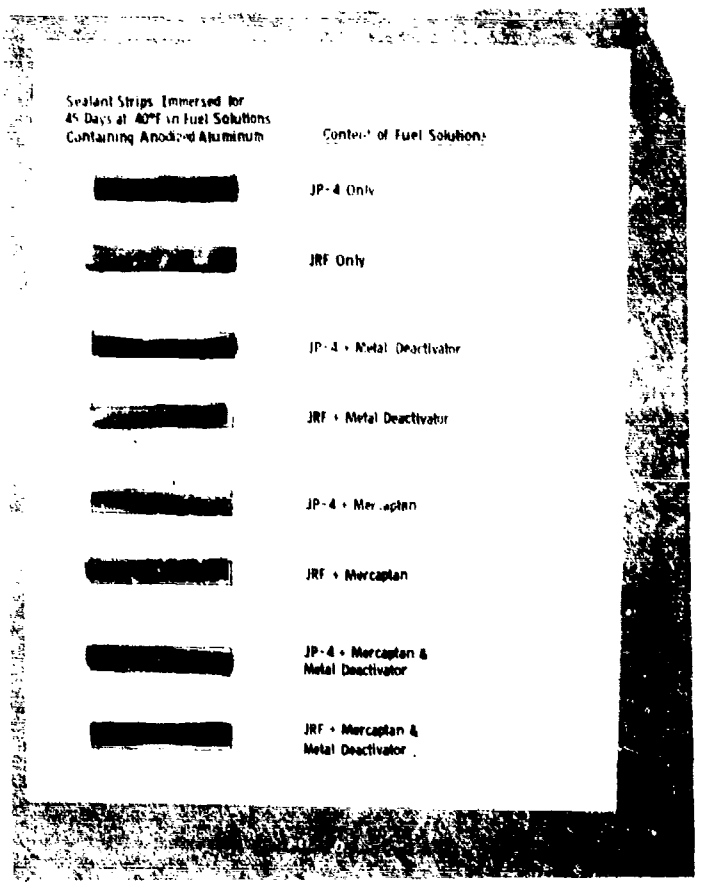

Figure 33. Polysulfide sealant chalking tests with anodized aluminum.

mild steel and aluminum; but less severe with copper and lead. Chalking with cadmium was about the same in both fuels.

(2) Sealant chalking in JP-4 occurred with all metals except lead, and it also occurred in JP-4 without metal. It is surprising that chalking occurred in the control JP-4 containing 400 ppb lead and not in JP-4 fuel with the lead coupon. The results make it appear that the presence of a lead coupon somehow acts as a chalking inhibitor. This phenomenon is probably effected by other unrecognized factors such as minor differences in sealant specimens.

(3) Sealant chalking in JRF occurred with all tests except for those containing Monel, anodized aluminum and no metal (control fuel).

Summary

The fuel/metal equilibrium studies show that steady-state concentrations would be reached only after very long periods of time. However, the results of the sealant chalking studies indicate that only small quantities of some dissolved metals are enough to initiate severe cases of polysulfide sealant chalking. The presence of mercaptan accelerates the rate of chalking while the presence of the tested metal deactivator decreases chalking at a rate dependent upon the specific fuel/metal combination. The major factor determining sealant chalking appears to be the combination of a particular metal with a specific fuel.

4. POLYSULFIDE SEALANT CHALKING, FOLLOW-UP STUDY

The polysulfide sealant chalking results in the initial study were much more severe than had been expected. Particularly puzzling was the fact that sealant chalking occurred in baseline JP-4 but not in JRF fuel which contains mercaptan in its formulation. Additional studies were therefore conducted with the original and different batches of JP-4 and the original and another lot of sealant. No metal coupons or mercaptan were used in this study. Peroxide and metals analyses were conducted on all three JP-4 test fuels.

Before the additional chalking studies with the baseline fuels were performed, additional studies with the metal deactivator N, N'-bis-salicylal-1,2-propane diamine were conducted. These tests were designed to show whether the deactivator was just as effective when applied to metal coupons before the chalking tests as when it was present in the jet fuel during the chalking tests.

Summary of Results

A. The original JP-4 used in the initial sealant chalking study was found to contain 54 ppm peroxides. Severe sealant chalking was again obtained with this fuel in the repeat studies with both lots of sealant, but no chalking was obtained with either sealant when two new batches of JP-4 containing little or no peroxides were used. The peroxide is strongly suspected to have caused the severe deterioration observed.

B. The only metal found in any of the JP-4 test fuels was a small amount of lead, and this appears to some extent in all three fuels.

C. The metal deactivator appears to lessen the severity of sealant chalking, as shown in the previous study. The deactivator

is not as effective when it is applied to metal coupons before the chalking tests as it is when it is present in jet fuel during the chalking tests.

Determination of Metal and Peroxide Content in Test Fuels

The original JP-4 used in the initial study, and two new batches of JP-4 labeled B-20 and F-2, were analyzed for metal content and peroxides. The metals were determined by emission spectrographic analysis and the peroxide analysis was conducted according to ASTM Method D 1563-60. Results are shown in Table 14 below.

TABLE 14. METAL AND PEROXIDE CONTENT OF FUELS

JP-4 sample	Peroxide content, ppm	Lead content, ppm	Other trace metals
Original	53.8	0.40	ND[a]
B-20	0.0	0.040	ND
F-2	0.5	0.125	ND

[a]ND = None detected in low ppb range.

No zinc, aluminum, copper, tin, or iron was detected in the fuels at the low ppb levels.

Repeat Sealant Chalking Studies with Baseline Fuels

Sealant chalking studies were conducted for 45 days at 140°F with the three batches of JP-4 fuel and two batches of polysulfide sealant. The one lot of sealant had been used in the initial study and the second lot came from another Air Force contractor (University of Dayton Research Institute). No metal coupons, mercaptan, or metal deactivator were used in the studies. One 1/8" x 1/4" x 2" strip of sealant from each batch was vertically suspended in 500 milliliters of each batch of JP-4 for a period

of 45 days at 140°F. The strips were then removed from solution, dried with a paper towel, and evaluated for sealant chalking. A photograph of the tested strips is shown in Figure 34.

Both batches of sealant showed severe chalking in the original JP-4 containing 54 ppm peroxide. Neither batch of sealant showed any chalking or deterioration in either the B-20 or the F-2 batch of JP-4. It is strongly suspected that the high peroxide level in the original test fuel is responsible for the severe sealant deterioration observed.

Other test data for the two additional batches of JP-4 were recorded within the Air Force Fuel Quality Laboratory and are presented in Table 15.

Alternate Method of Applying Metal Deactivator

The initial sealant chalking study result showed that the metal deactivator, N,N'-bis-salicylal-1,2-propane diamine, lessened the severity of chalking in many cases regardless of whether caused by the presence of peroxide or mercaptan in the fuel. The metal deactivator was dissolved in the JP-4 at a concentration of 6 ppm for this study. It was then questioned whether the deactivator might be just as effective if it were applied to the metal surface prior to the sealant chalking study.

Four comparative sealant chalking tests were run with copper coupons, JP-4, 150 ppm butyl mercaptan (50 ppm mercaptan sulfur), and the metal deactivator. In two tests the butyl mercaptan was present and in the other two it was not. In one each of these two sets of tests, the metal deactivator was present in the JP-4 at a concentration of 6 ppm. In the other two tests, the copper coupon had been dipped into a 1% metal deactivator solution in cyclohexane prior to the chalking tests. The original JP-4 was used in the study since it was not known to contain peroxide at

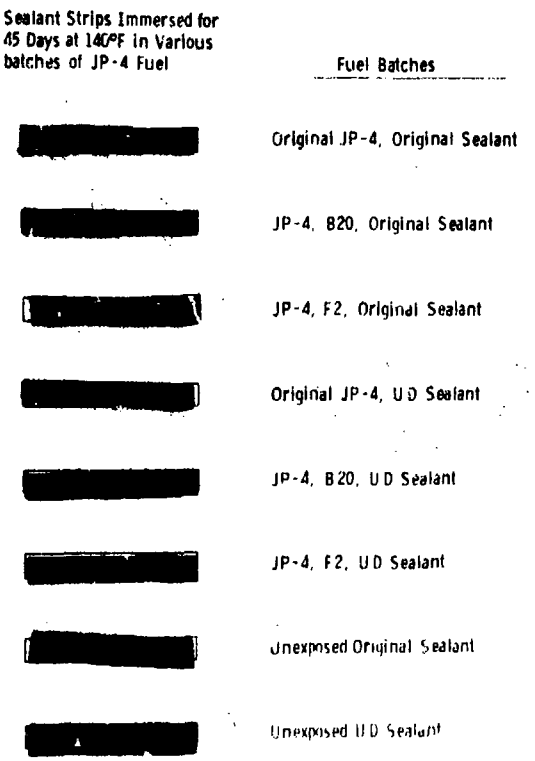

Figure 34. Polysulfide sealant chalking tests with various JP-4 specimens.

TABLE 15. ANALYTICAL TESTS ON NEW FUELS USED IN SEALANT TESTS[a]

	F-2	B-20
Total acidity, mg KOH/g	0.003	0.006
Aromatic content, vol %	10.7	9.3
Olefin content, vol %	1.6	1.9
Mercaptan sulfur, wt %	0.0000	0.0003
Total sulfur, wt %	0.04	0.02
API gravity, 60°F	54.4	55.6
Vapor pressure, psi	2.4	2.4
Freezing point, °F	-83	-82
Luminometer number	73	79
Smoke point	27.0	32.0
Copper strip, 2 hr at 212°F	1A	1A
Existent gum, mg/100 mL	1.2	1.1
Anti-icing, vol %	0.13	0.00
Distillation		
IBP	29	28
10% recovered	89	90
20% "	104	104
50% "	153	152
90% "	236	239
95% "	252	254
FBP	321	319

[a]Measurements made by laboratory, Det 13SA-ALC/SFQLA, Aerospace Fuels Laboratory, WPAFB, OH 45433.

that time. The extent of sealant chalking in these tests at 140°F was monitored for a period of 18 days by observation through the walls of the glass test vessels, and after 100 days the sealant strips were removed from solution for a final evaluation. The results of these tests are shown in Table 16.

Applying the metal deactivator to the copper coupons prior to immersing in the JP-4 did not appear as effective in reducing sealant chalking as having the deactivator present in the JP-4.

TABLE 16. SEALANT CHALKING VERSUS METHOD OF APPLYING METAL DEACTIVATOR[a]

Days immersed	6 ppm Deactivator in JP-4	1% Deactivator pre-applied	6 ppm Deactivator, 50 ppm sulfur[b] in JP-4	1% Deactivator pre-applied, 50 ppm sulfur in JP-4
4	No change	No change	No change	No change
11	No change	No change	Yellowish grey	Yellowish grey
13	No change	No change	Yellow edges	Yellow edges
18	Yellow edges	Yellow edges	Yellow edges	Light grey, cracks
100[c]	Chalked, 3 cracks more than halfway thru sealant, ∿20 other surface cracks	Chalked, 2 cracks more than halfway thru sealant, few hairline cracks, noticeably brittle	Chalked, but no cracks	Chalked, the most deteriorated strip, 1 crack almost thru entire thickness, many smaller cracks, very brittle

[a]Sealant strips immersed in JP-4 solutions containing copper coupons at 140°F. This fuel was found to contain 54 ppm peroxides and 0.40 ppm lead (only metal).

[b]As butylmercaptan.

[c]Strips were removed from JP-4, wiped dry, and then observed.

5. INVESTIGATION OF PEROXIDE COMPOUNDS FORMED IN BASELINE JP-4 USED IN CHALKING STUDIES

Introduction

The baseline JP-4 used for sealant chalking studies in the previous test program (subsection 4) was found to cause severe sealant chalking on a polysulfide sealant. Subsequent fuel analyses showed that this JP-4 contained a high concentration of peroxides and acids. The purpose of this task was to isolate and identify the peroxides present in the JP-4, and determine whether there is a correlation between peroxide concentration and acid content (acid number).

Most of the JP-4 having a high peroxide content (176 ppm after 9 months storage) was consumed during the sealant chalking studies, and none was available for peroxide identification studies. This fuel had been drawn from a 55-gallon drum and then stored six months in a clear 5-gallon glass jug on a bench top prior to initial use. A new sample of fuel drawn from the 55-gallon drum was found to contain less than 2 ppm peroxides. Consequently, 1,500 milliliter quantities of the baseline JP-4 were exposed to a variety of environmental conditions in an attempt to generate enough peroxides for identification studies and acid number correlation.

Peroxide Formation and Correlation With Acid Number

A Navy report concerning the formation of organic peroxides in JP-5 (ref. 2) indicated that high temperature and presence of oxygen and water were the key factors leading to the rapid formation of peroxides in hydrocarbon fuel. Therefore, four 2-liter flasks containing about 1,500 milliliters of baseline JP-4 were connected to water-cooled reflux condensers and exposed to variations of these parameters. All flasks were injected with

free water and bubbled with air, but each flask was heated at a different temperature.

Flask No. 1 was heated to 190°C and after four hours the fuel had turned a brown color. Flask No. 2 was heated to 150°C and after five hours the fuel had turned an amber color. Both tests were discontinued when it was learned that fuel degradation was occurring without an increase in peroxide content. Flask No. 3 was heated to 65°C for a period of about two months and was periodically monitored for peroxide content and acid number. Flask No. 4 additionally contained a strip of polysulfide sealant and mild steel and was heated to 60°C, also for a period of about 2 months. The peroxide and acid numbers gradually increased in both flasks, but not at the rate expected and required. When it became evident that moisture, oxygen, and temperature were not the key factors for rapid peroxide formation in JP-4 fuel, a quart bottle of JP-4 was then placed on a bench top in front of an east window to investigate the possibility of peroxide formation by photolysis. The sealant/JP-4 was not exposed to direct sunlight, but it was now suspected that perhaps daylight may have been responsible for the high level of peroxide formation. This suspicion was confirmed when a significant quantity of peroxide began to form in a relatively short period of time.

All analysis results for peroxides and acid number are shown in Table 17. Peroxide concentration was determined by the iodide/sodium thiosulfate method described in ASTM D 1563-60. Total acidity was determined by ASTM Method D 3242.

The test results clearly indicated that visible light was the primary cause of peroxide formation in the JP-4 used for sealant chalking studies. The test results also showed that there is some correlation between peroxide content and acid number, even though the acid number data appeared to fluctuate.

TABLE 17. PEROXIDE CONTENT AND ACID NUMBER

Exposure time	Peroxide content, ppm	Acid number	Comments
A. JP-4 Stored in clear 5-gallon Glass Jug and Used for Chalking Studies			
0	1.1	0.003	
6 months	53.8	--	
9 months	176.0	0.101, 0.097	
B. Clear Glass Bottle of JP-4 in Front of East Window			
0	2.2	--	
13 days	10.9, 10.9	0.033	
17 days	14.0	0.024	
C. Clear Glass Bottle of JP-4 in a Dark Cabinet			
0	1.1	0.003	
13 days	1.3	0.004	
40 days	1.8	0.012	
95 days	2.2	0.038	
112 days	1.3, 1.0	0.010	
D. Flask No. 1 - Exposed at 190°C to Bubbled Air and Free Water			
0	1.1	0.003	
4 hours	∿1.1	--	Fuel turned brown
E. Flask No. 2 - Exposed at 150°C to Bubbled Air and Free Water			
0	1.1	0.003	
5 hours	∿1.1	--	Fuel turned amber
F. Flask No. 3 - Exposed at 65°C to Bubbled Air and Free Water			
0	1.1	0.003	
3 days	∿1.1	--	
13 days	5.2	--	
29 days	3.9	0.038	
39 days	7.4	--	
55 days	7.2	0.013	
G. Flask No. 4 - Sealant and Mild Steel Strips, Exposed at 60°C with Air & Water			
0	1.1	0.003	
3 days	∿1.1	--	
13 days	2.9	--	
29 days	7.3	0.043	
39 days	9.3	--	
55 days	10.3	0.010	

Analytical Procedures

Because of the reactive nature of peroxides and hydroperoxides, care must be taken in the selection of an analytical method for their characterization. Mass spectrometry, for example, yields little direct information on these compounds even when low-voltage ionization techniques are employed. The Fourier-transform infrared technique provides a sensitive and flexible method of analysis, yet does nothing to promote further chemical reactions. A Digilab Model FTS-15 B/D system equipped with a General Data Nova 2/10 minicomputer was used for this work.

Fourier-transform infrared (FTIR) spectra were recorded for samples of baseline and peroxidized JP-4 fuels containing 0.8 ppm and 12 ppm of peroxide, respectively. The spectra shown in Figures 35 and 36 are the result of the co-addition of 100 scans of fuel in a 0.025 mm liquid cell, ratioed against a 50 scan reference. The spectra show that the peroxide-containing fuel had absorption bands at 3400, 1713, and 767 wave numbers (cm^{-1}), whereas the baseline fuel shows no absorption in these locations.

A computer subtraction of the spectrum of the baseline fuel from that of the peroxidized fuel is shown in Figures 37 and 38. In spectral subtraction, the larger the scaling factor (SCB), the greater the percent of the reference spectrum subtracted. The SCB is 0.8 for the spectrum in Figure 37. Figure 38, however, is a composite of 13 subtraction spectra with scaling factors ranging from 0.3 (top trace) to 1.5 (bottom trace). The persistence of certain bands even after obvious over-subtraction shows that the bands are, in fact, unique to the fuel having the high peroxide content. These bands are located at wave numbers 1713, 1126.5, 964.5, 875.8, 767.8, and 729.2. Their significance will be discussed under Results and Discussion.

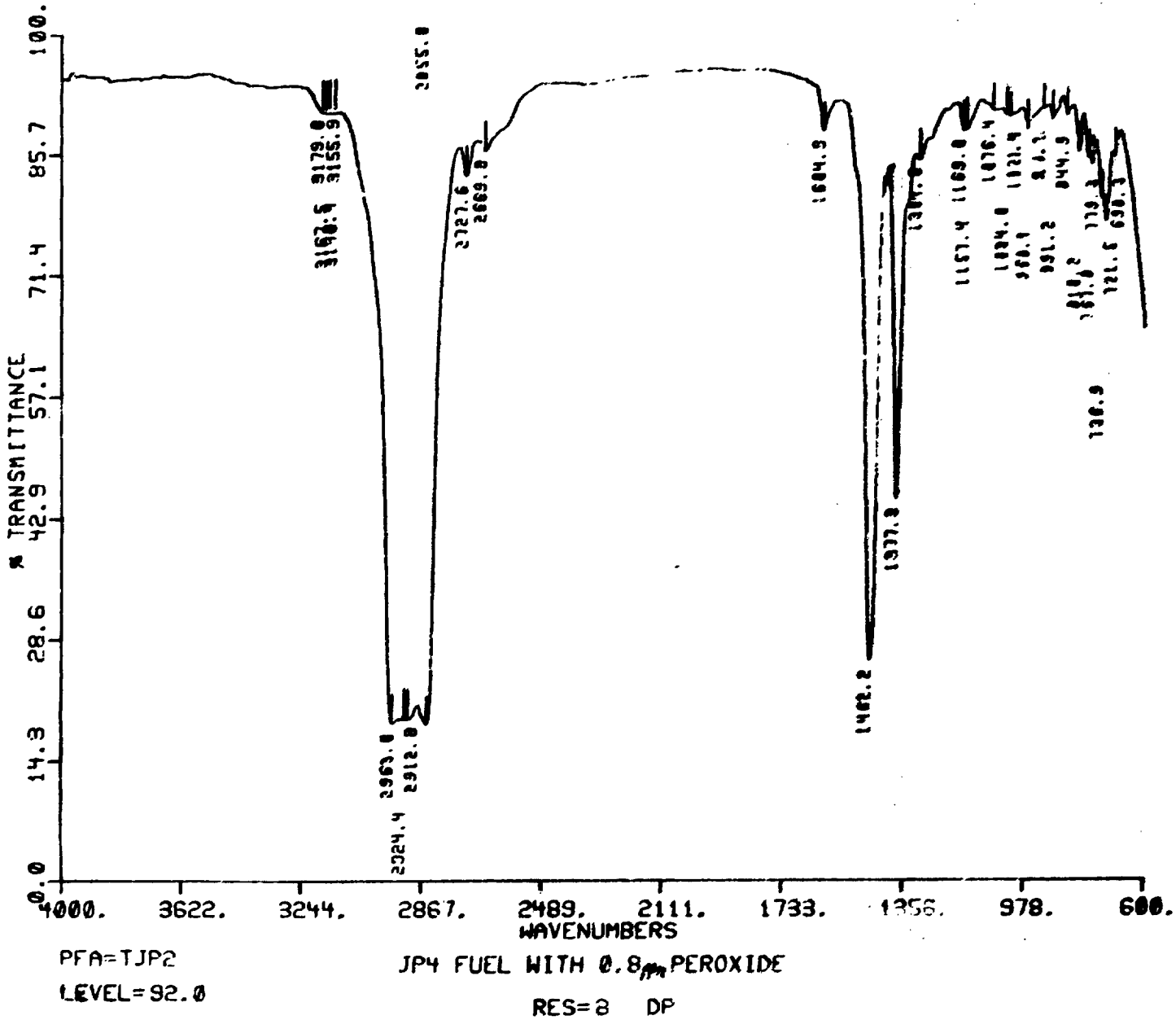

Figure 35. FTIR spectrum of JP-4 fuel containing 0.8 ppm peroxide.

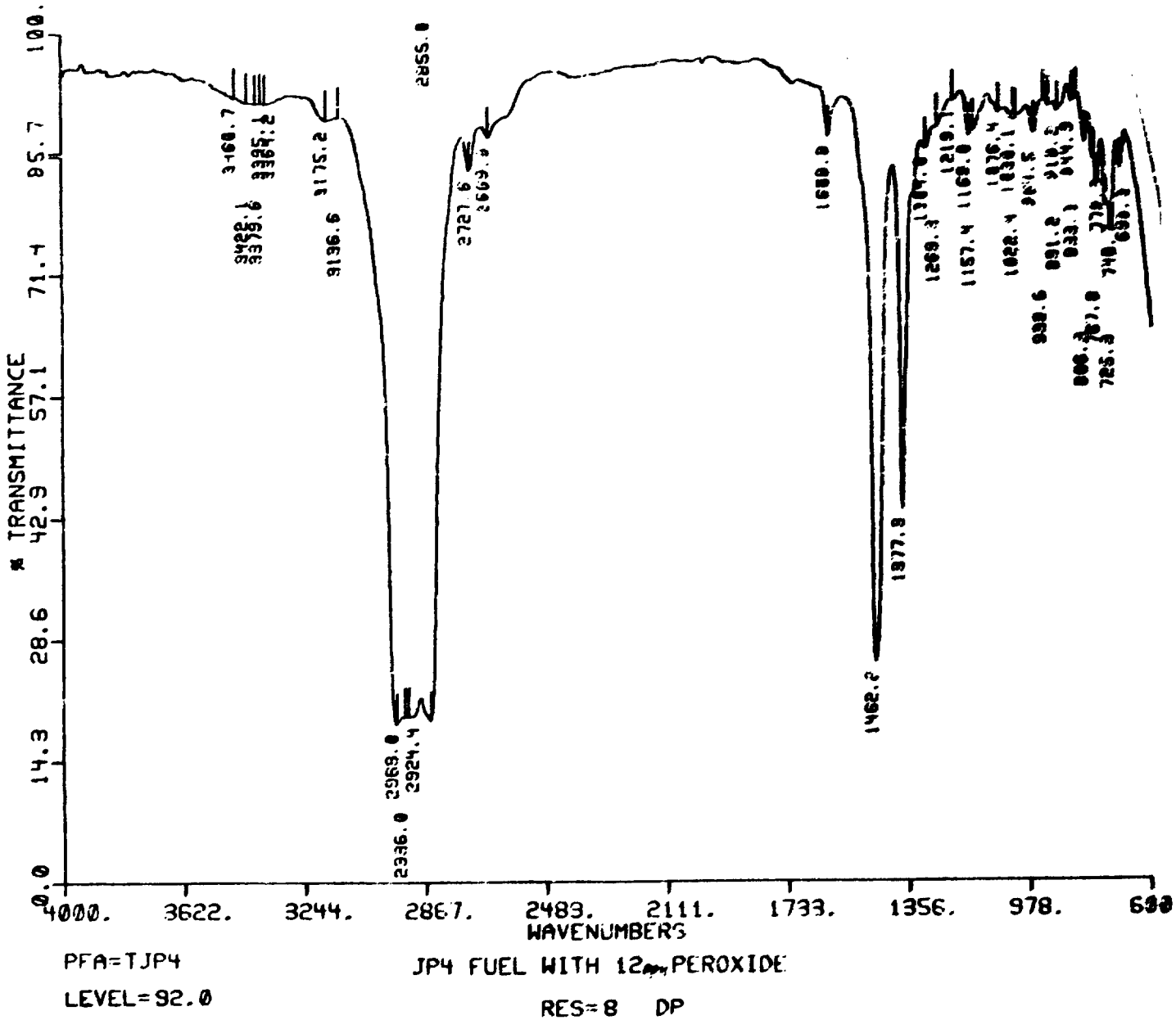

Figure 36. FTIR spectrum of JP-4 fuel containing 12 ppm peroxide.

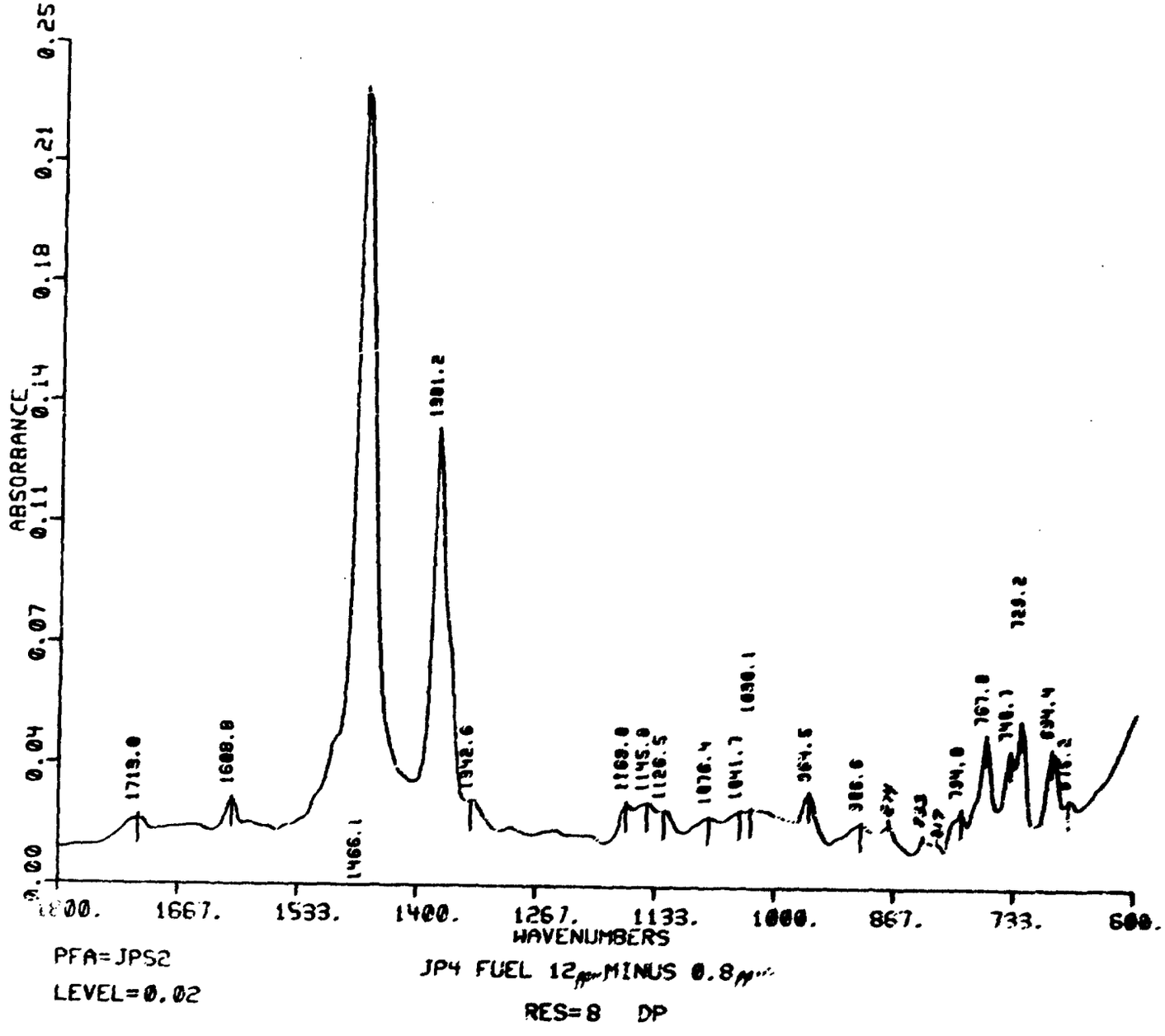

Figure 37. Computer subtracted FTIR spectrum of 0.8 ppm (peroxide) fuel from 12 ppm fuel.

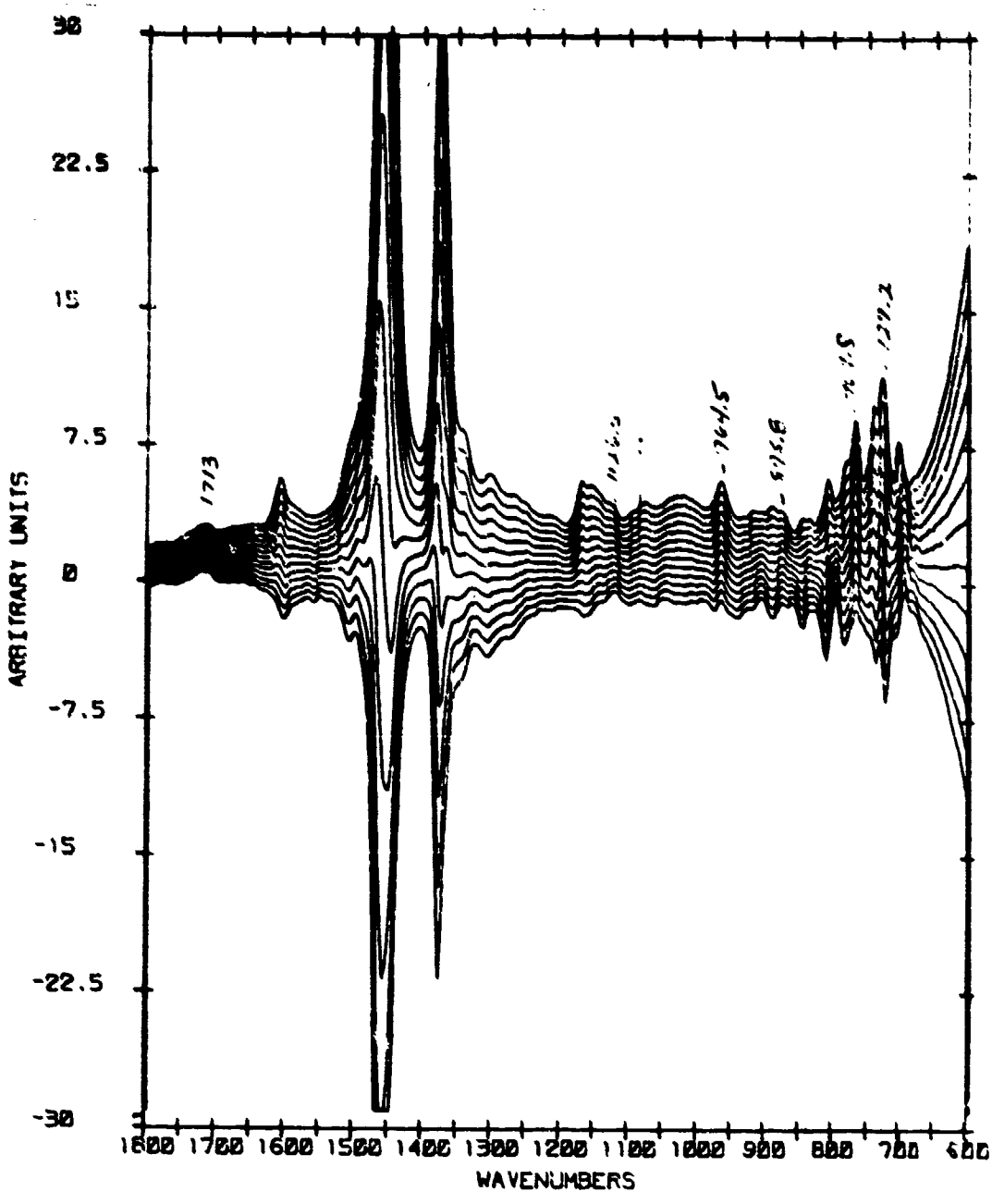

Figure 38. Composite of 13 FTIR subtraction spectra with scale factors ranging from 0.3 (top trace) to 1.5 (bottom trace).

A 200 ml portion of JP-4, containing peroxides at the 32 ppm level, was passed through a silica gel column. The fuel was the same as that used for the earlier sealant chalking study. The column was eluted with methanol and a spectrum of the residue was recorded after evaporation of the methanol. To further separate the isolated materials, 1.08 g of this residue was applied to a fresh silica gel column and sequentially eluted with solvents as shown in Table 18.

TABLE 18. SEPARATION OF RESIDUE ISOLATED FROM TEST JP-4

Fraction number	Elution solvent	Volume, ml	Weight residue, mg	Percent of total
1	Pentane - 1	50	0	0
2	Pentane - 2	50	0.3	0.03
3	Methylene chloride - 1	50	392.5	36.3
4	Methylene chloride - 2	50	51.4	4.8
5	Methylene chloride - 3	50	32.3	3.0
6	Methylene chloride - 4	20	9.3	0.9
7	Ethylether - 1	25	13.5	1.3
8	Ethylether - 2	2	146.2	13.5
9	Ethylether - 3	23	196.1	18.2
10	Acetone	50	~150	13.9
11	Methanol	50	~50	4.6
Total				~96.8

Infrared spectra were recorded for the initial residue (Figure 39) and each fraction after evaporation of solvent. The initial residue exhibited a strong carbonyl band at 1713 cm^{-1} and other bands at 1126.5 and 875.8 cm^{-1}. These bands appeared for the eluted fractions 8, 9, and 10. Their spectra are shown in Figures 40 to 42. These three fractions showed a strong positive test (red color) for peroxides using the ferrothiocyanate test for peroxide.[a]

[a]This color reaction is the basis for ASTM Method D 1022, "Peroxide Content of Light Hydrocarbons." Though the reaction has a positive interference due to unsaturated acids, the formation of these compounds is unlikely.

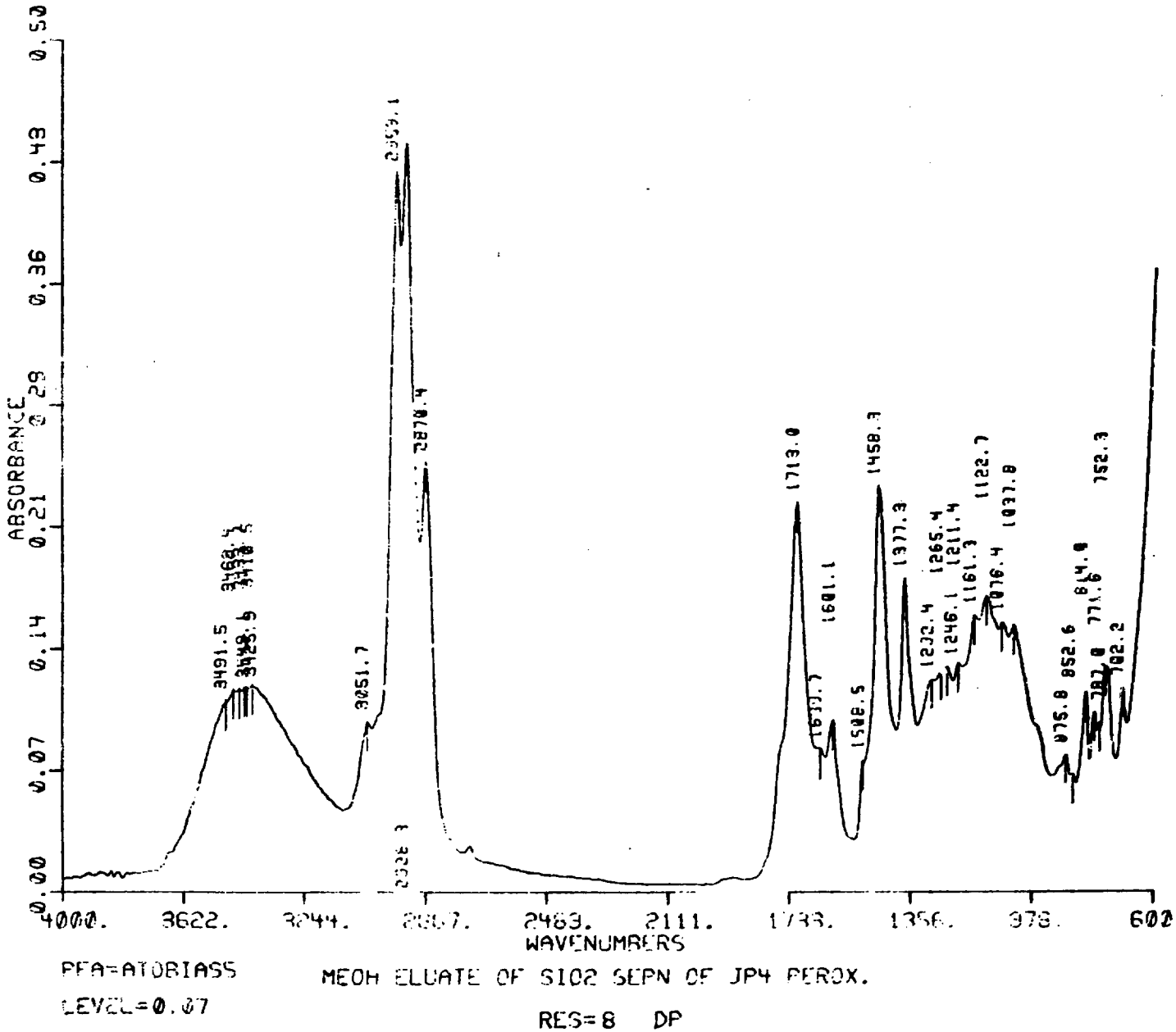

Figure 39. FTIR spectrum of residue from JP-4 containing 32 ppm peroxides, after passing through a silica gel column and being eluted with methanol.

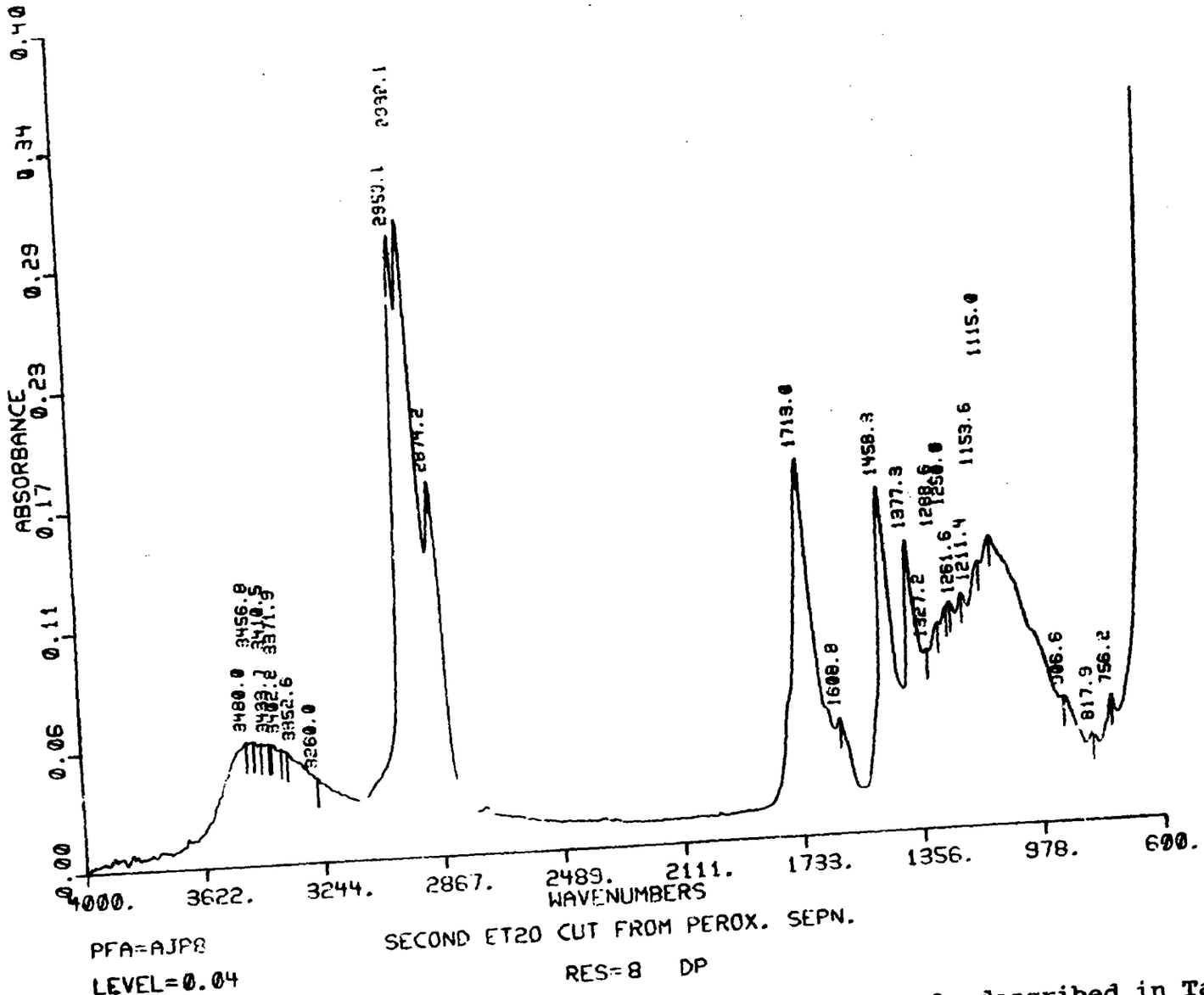

Figure 40. FTIR spectrum of ethylether elution Fraction No. 8, described in Table 2.

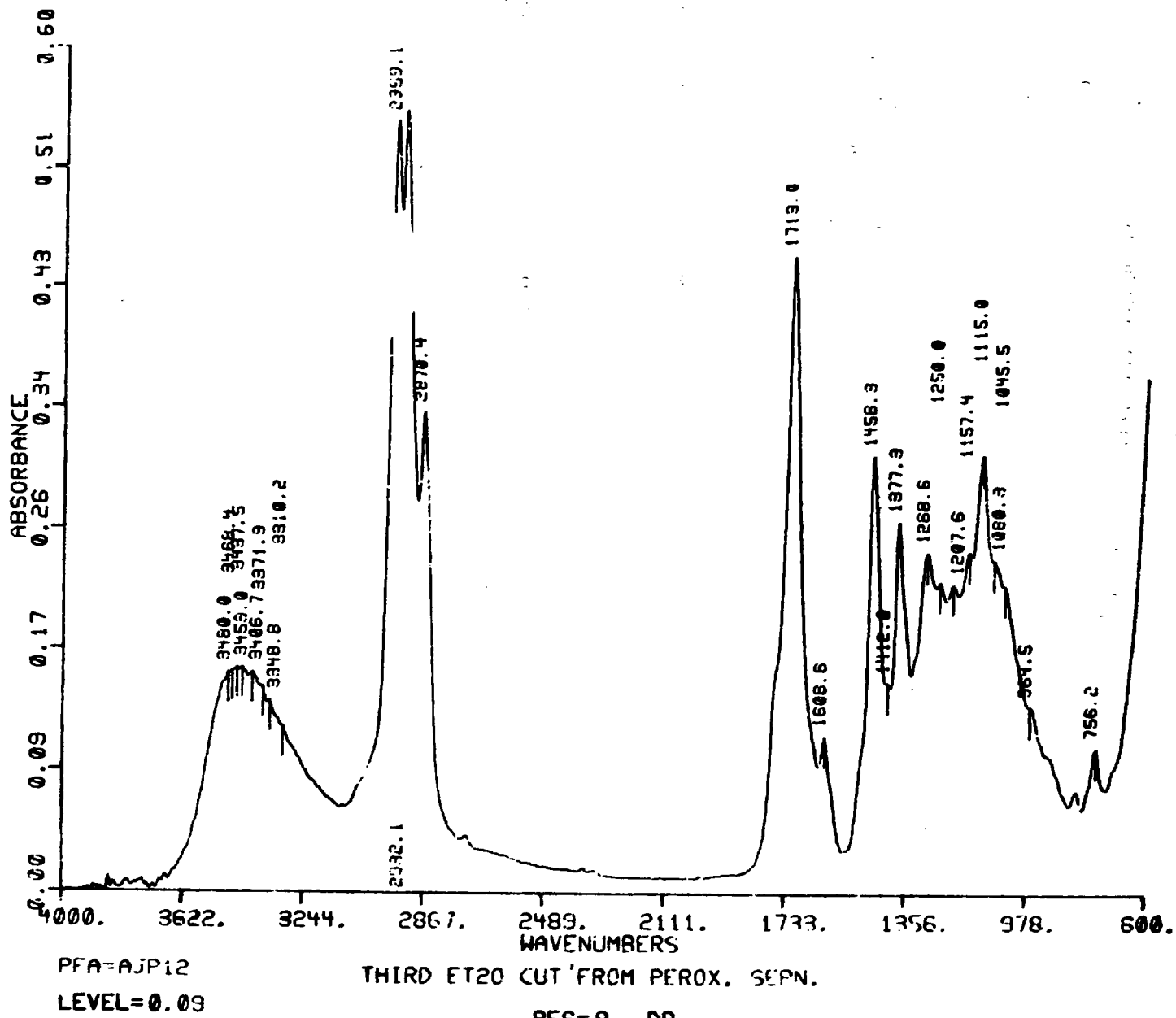

Figure 41. FTIR spectrum of ethylether elution Fraction No. 9, described in Table 2.

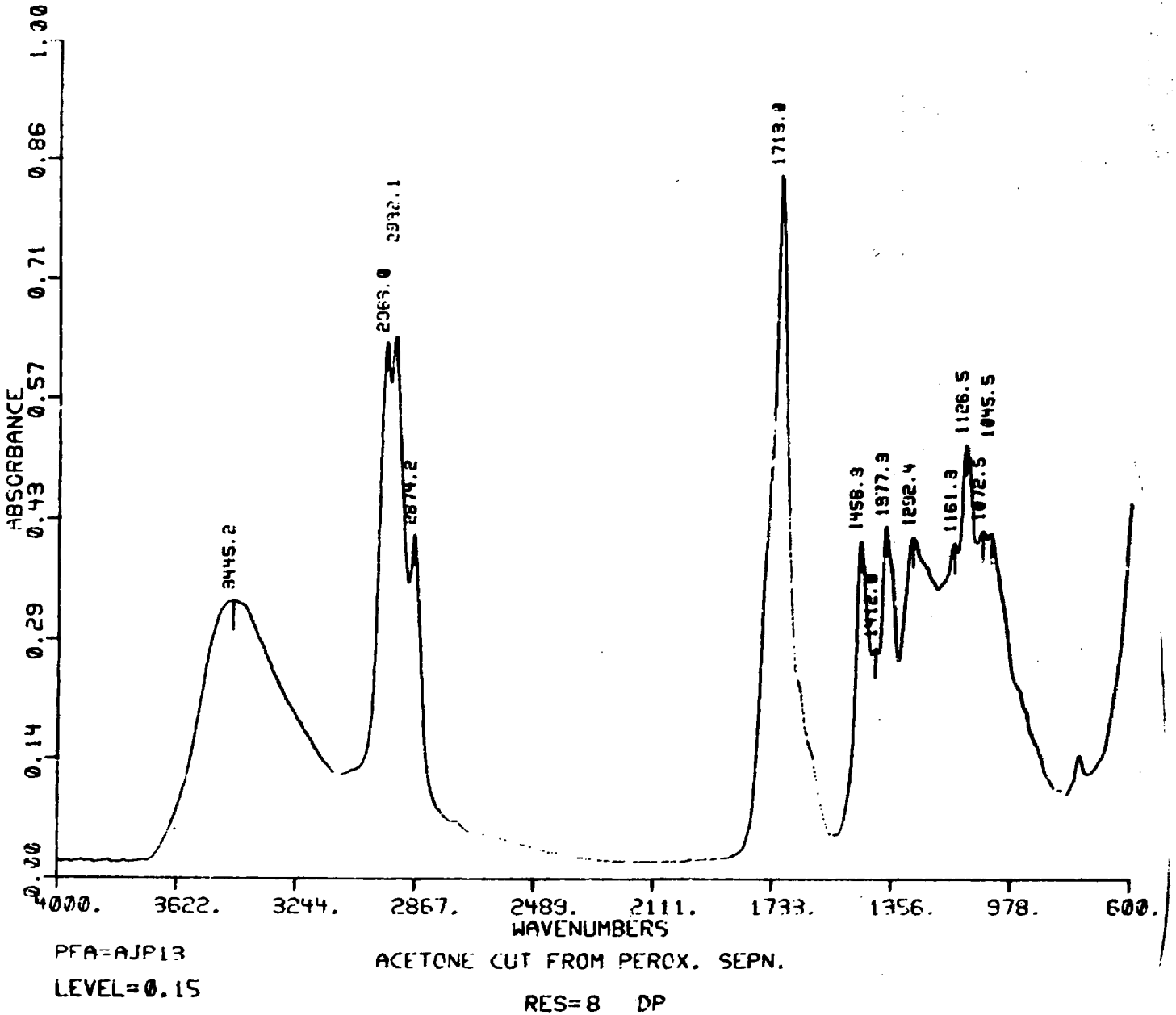

Figure 42. FTIR spectrum of acetone elution Fraction No. 10, described in Table 2.

The third ethylether fraction (No. 9) from the above separation was further separated by extraction with 3 ml of hexane, which essentially dissolved the residue. This hexane solution was extracted with 3 ml of 0.1 N NaOH solution at 0°C. The mixture was centrifuged to disperse the emulsion. The aqueous phase was separated from the hexane layer, neutralized with 0.1 N HCl, and re-extracted with 3 ml of hexane. The hexane was separated and evaporated in a flow of nitrogen to yield a 3.9 mg residue. The spectrum of the residue is shown in Figure 43.

Results and Discussion

Essentially the same spectral data were obtained for peroxide containing JP-4 samples whether the peroxides were formed accidentally, as in the previous sealant chalking study, or purposely formed by heating and bubbling with moist air. The high levels of peroxide obtained during the sealant study were never realized when deliberate peroxide generation was attempted. The techniques suggested in the Naval Air Propulsion Center report of reference 2 were employed as well as simulation of chalking test conditions, even to the point of adding a metal coupon and sealant to the fuel. Despite the Naval report suggestion that brown bottles be used for the peroxidation, it was felt that the peroxide levels achieved previously were possibly related to light intensity. Test confirmed this to be true. In a short time, fuel exposed to light from a window developed a peroxide level higher than that produced by any other technique.

Differential IR absorption bands, obtained through spectral subtraction, are localized in three of the eleven fractions from a liquid chromatograph separation of polar fuel constituents. These bands represent the compositional differences between the baseline fuel and that same fuel after being subjected to oxidizing conditions. Important features of the spectra for these three fractions are a carbonyl absorption at 1713 cm^{-1}, lack of aromatic

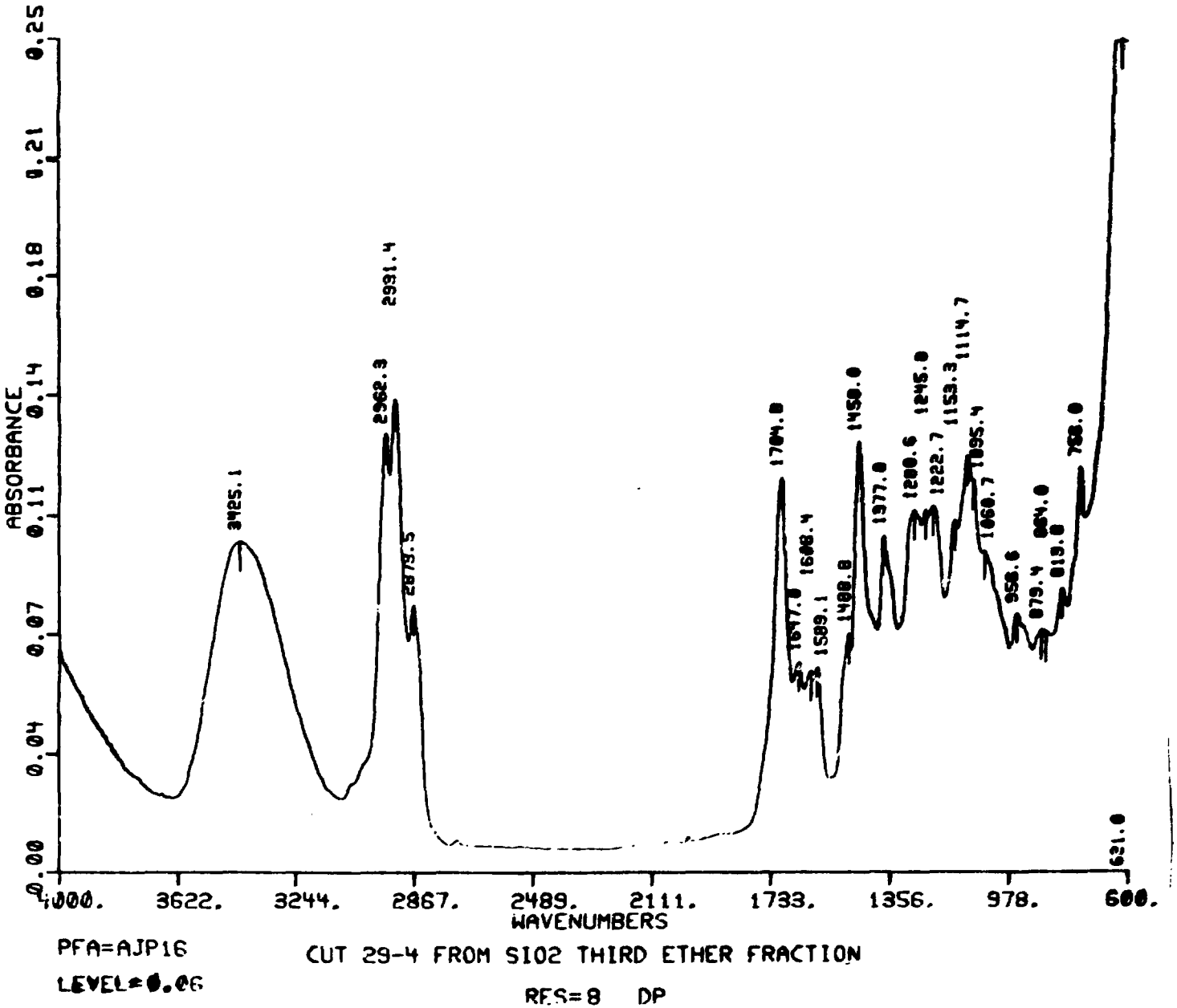

Figure 43. FTIR spectrum of ethylether Fraction No. 9 (Table 2) after extraction into 0.1 N NaOH.

character as indicated by the absence of a band at approximately 3000 cm^{-1} and the appearance of a hydroxyl (OH) band at ~3400 cm^{-1}. Other bands indicate aliphatic character. These data suggest the presence of aliphatic ketones and alcohols. The three fractions gave a strong positive color reaction for the peroxide test using the ferrothiocyanate reagent. Absorption bands for organohydroperoxides were not prominent in the spectra, suggesting that the loss of some hydroperoxide through a reduction reaction had occurred. Spectra show essentially a mixture of aliphatic alcohols and ketones. These ketones and alcohols are common products from the air oxidation of aliphatic hydrocarbons being formed both directly during the oxidation process and from the decomposition of hydroperoxides (ref. 2). The presence of a small amount of an organic acid was shown by the shift in the carbonyl band (ionized carboxyl) of the material extracted into 0.1 N NaOH. The basic extraction effectively separated the acid materials from the ketones.

Somewhat surprisingly, there was no evidence that peroxides or hydroperoxides were formed from aromatic fuel constituents, even though these constituents are generally more subject to peroxidation. The fact that a variety of materials can serve as oxidation catalysts or initiators, even though present only at trace levels, contributes to the unpredictability of the peroxidation reaction.

The significance of acid number in the peroxide forming studies was not clear. A correlation exists between acid number and peroxide content but the values were not directly proportional.

Conclusions

Peroxides and hydroperoxides were formed in the subject JP-4 fuel by a photolysis reaction. These compounds were of an aliphatic

nature, consisting largely of ketone and alcohol types. A small amount of organic acid was also found to be present. No evidence of aromatic peroxide formation was found.

6. EVALUATION OF THE MICROSEP-II WATER SEPAROMETER

All aviation turbine fuel specifications include a requirement concerning the ease with which the fuel will release entrained or emulsified water. The water separation index, modified (WSIM) test, which is described in ASTM procedure D 2550, provides a numerical rating for the fuel's water separation characteristics.

The WSIM value of a fuel is measured with a device in which a water-fuel emulsion is prepared and metered through a cell containing a standardized glass-fiber coalescer. The cell effluent turbidity, caused by entrained water, is determined by light transmission through the fuel to a photocell. The output of the photocell is measured by a meter having a 0-100 scale, thus providing a numerical rating for the fuel. The original apparatus for the test, known as ASTM-CRC Water Separometer (Emcee Electronics, Inc.), has three functions: emulsion preparation, coalescence, and analysis.

The WSIM of a fuel can also be measured by other instruments, such as the Minisonic Separometer and the Microsep Separometer. Both units are manufactured by Emcee Electronics, Inc. The ASTM-approved Minisonic Separometer is a small-scale device using the same principles as the ASTM-CRC Water Separometer. The Microsep Separometer incorporates solid-state design and a self-contained power source, but it is not yet approved by the ASTM.

The purpose of this study, which was part of a program sponsored by ASTM Committee D-2, was to evaluate the Microsep unit by comparing its results with those of the Minisonic system. Table 19 lists some differences between the two instruments.

TABLE 19. COMPARISON OF MINISONIC AND MICROSEP SEPAROMETERS

Feature	Minisonic	Microsep
Portability	Requires a.c. electric power; can be hand carried	Internal rechargeable battery; can be hand carried (lighter)
Temperature range	65°F to 85°F	65°F to 85°F
Operation	Requires external timer; about 5-10 min per test; can be used multibatch	Programmed time (internal); 3.5 min per test (after preparation)
Emulsifier	Ultrasonic adjustable (timer and intensity) prescribed by ASTM, 25 sec ±1	Stirring (high speed) motor, programmed time (set)
Syringe drive	Time adjustable (prescribed by ASTM, 45 sec ±2)	Time (programmed-set)
Settling period	1 min (prescribed by ASTM, operator timed)	1 min (programmed-set)
Turbidity	Compares (split beam) original sample to filtered sample	Compares original sample (100% transmission in memory) to filtered sample (0-100 scale reading) transmission
Calibration	Field	Factory
Small parts	Kit supplied by EMCEE	Essentially same for each

Procedure

The preparation and procedure for the Minisonic Separometer as described in ASTM D 2550-74, Section A6 was followed in detail. For the Microsep system, a procedure contained in the operation manual furnished with the apparatus by Emcee Electronics, Inc. was followed. Tests were conducted as specified in the instructions (see Table 20) provided by the ASTM program coordinator. Data for a JP-4 test fuel are presented in Tables 21 and 22.

Discussion

It was observed that if the sample vial is taken from the Microsep turbidimeter directly after reading and is placed in the Minisonic unit with the meter nulled using the appropriate blank, one gets consistently higher readings at the low end of the scale than with the Minisonic unit. This is shown in Table 23.

Several runs on each instrument were timed, and the timed operations were within the specified limits, as shown in Table 24.

Precision criteria for judging the acceptability of results are defined by a graph contained in ASTM D 2550 and shown in Figure 44. Repeatability is a measure of the variance in duplicate determinations by the same operator. For this evaluation, reproducibility is considered to be the difference in results from each of the two instruments using the same type of coalescence cell.

Reproducibility and repeatability of the data by these definitions are presented in Table 25.

Only 4 of 28 samplings failed to meet the repeatability test and 3 of these occurred with the Microsep Separometer. Three of the fourteen samplings failed the reproducibility test.

TABLE 20. TEST PROGRAM FOR MINISONIC AND MICROSEP-II SEPAROMETERS

I. TEST APPARATUS

A. D 3602-77 Mini-Sonic Separometer
B. MICROSEP-II (Modified by Emcee Electronics)

II. TEST FLUIDS

Jet A Blends			Jet B Blends		
Fuel No.	Conc. of Additive	Amt. of Concentrate Per L of Fuel	Fuel No.	Conc. of Additive	Amt. of Concentrate Per L of Fuel
1A	—	—	1B	—	—
2A	0.2 mg/L AOT	0.2 mL	2B	0.6 mg/L AOT	0.6 mL
3A	0.6 mg/L AOT	0.6 mL	3B	1.2 mg/L AOT	1.2 mL
4A	4 PTB DCI-4A	11 mL	4B	4 PTB DCI-4A	11 mL
5A	6 PTB E-515	17 mL	5B	8.5 PTB E-515	24 mL
6A	6 PTB E-515 0.5 ppm ASA-3	17 mL	6B	8.5 PTB E-515 0.7 ppm ASA-3	24 mL
7A	0.5 ppm ASA-3	0.5 mL	7B	0.7 ppm ASA-3	0.7 mL

III. PROGRAM

A. Prepare reference fuels in accordance with D 3602, Appendix A-2. If tests of Blends 2 and 3 fail to meet the criteria of D 3602, Tables 1 or 2, use a fresh reference fuel.

B. Prepare Fuel Blends in accordance with II above by adding concentrate (1000 mg/L of each additive) to reference fuel.

C. Run tests using Plasticels by both MSS and Microsep, and enter results on attached Data Sheet.

D. Repeat each Fuel Blend with the same operator on the same day in random order.

E. Run all blends using the Metal Cell to compare with plasticels. (Sufficient additive concentrate has been furnished for this purpose. Many laboratories prefer to use Metal Cells for economy reasons.)

TABLE 21. DATA SHEET FOR MICROSEP-II - MSS PROGRAM

DATA SHEET
(Complete RF Type and Blends Per Attachment I Test Fluid Table)

TESTING LABORATORY AFAPL

RKF FUEL BASE JET JP-4

COALESCER CELL TYPE METAL CELL WITH EMCEE PART# 1104-19 COALESCER DISCS

Blend

			MSS Rating		Microscope Rating	
No.	mg/l	Additive	Test 1	Test 2	Test 1	Test 2
1	-------None-------		100	99	100	100
2	0.6	AOT	75	72	62	65
3	1.2	AOT	63	67	58	55
4	12	DCI-4A	95	90	95	90
5	24	HITEC E-515	97	98	96	95
6	*	HITEC E-515	93	91	85	89
	+	ASA-3				
7	0.7	ASA-3	97	97	93	91

COMMENTS: * ADDITIVE 6 PTB-E-515 } FURNISHED
0.5 PPM ASA-3 }

24 ML/LITER FUEL WAS USED

B.B. Bowles
Signature

TABLE 22. DATA SHEET FOR MICROSEP-II - MSS PROGRAM

DATA SHEET
(Complete RF Type and Blends Per Attachment I Test Fluid Table)

TESTING LABORATORY _____

REF FUEL BASE JET JP4

COALESCER CELL TYPE PLASTICEL EMCEE PART# 5910A

Blend

			MSS Rating		Microsep Rating	
No.	mg/l.	Additive	Test 1	Test 2	Test 1	Test 2
1	---	None ---	100	99	100	99
2	0.6	AOT	82	77	64	66
3	1.2	AOT	76	67	49	50
4	11	DCI-4A	84	83	95	85
5	24	HITEC E-515	98	98	87	90
6	*	HITEC E-515	95	91	89	82
	+	ASA-3				
7	0.7	ASA-3	97	97	88	88

COMMENTS: * 6 PTB E-515 } FURNISHED
0.5 PPM ASA-3 }

2.4 mL/LITER FUEL WAS USED

B.A. Bowles
Signature

TABLE 23. TURBIDITY MEASUREMENTS ON THE SAME SAMPLE FOR EACH TEST INSTRUMENT

Sample	Microsep reading	Minisonic reading
$1B_1$	100	100
$1B_2$	99	99
$2B_1$	66	79
$2B_2$	62	72
$3B_1$	88	92
$3B_2$	50	74
$4B_1$	85	90
$4B_2$	95	96
$5B_1$	90	96
$5B_2$	96	98
$6B_1$	82	91
$6B_2$	85	91
$7B_1$	8[illegible]	93
$7B_2$	9[illegible]	97

TABLE 24. TIMING OF SEQUENTIAL EVENTS DURING SEPAROMETER OPERATION

	Time, seconds						
	Microsep runs[a]			Minisonic runs			
Event	#1	#2	#3	#1	#2	#3	(ASTM D 2550)
Emulsification (duration)	28	29	31	26	25	25	25 ± 1
Extraction (duration)	44	45	44	44	47	45	45 ± 2
Elapsed time at reading	188	189	189	180	183	190	-
Settling (duration)	60	60	60	61	60	60	60

[a]Time cycle automatically controlled.

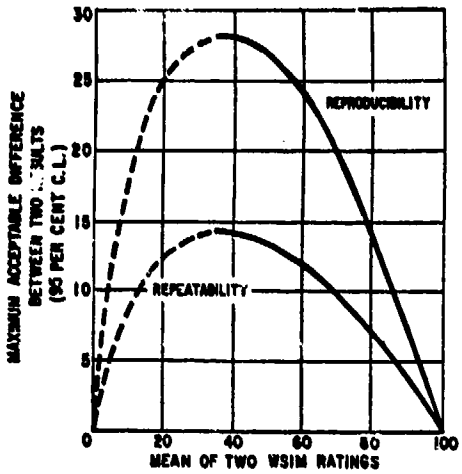

Figure 44. Variation of repeatability and reproducibility with rating level (taken from ASTM D 2550).

TABLE 25. REPRODUCIBILITY AND REPEATABILITY OF PERCENT TRANSMISSION MEASUREMENTS FOR THE TWO SEPAROMETERS

	Minisonic				Microsep				
Sample	High	Low	Avg	Repeat-ability Difference	High	Low	Avg	Repeat-ability Difference	Reproduci-bility Difference
				Plasticels					
1	100	99	99.5	1	100	99	99.5	1	1
2	82	77	79.5	5	66	64	65	2	18
3	76	67	71.5	9	50	49	49.5	1	27
4	84	83	83.5	1	95	85	90	10	12
5	98	98	98	0	90	87	88.5	3	11
6	95	91	93	4	89	82	85.5	7	13
7	97	97	97	0	88	88	88	0	9
				Metal Cells					
1	100	99	99.5	1	100	100	100	0	1
2	75	72	73.5	3	65	62	63.5	3	13
3	67	63	65	4	58	55	56.5	3	12
4	96	95	95.5	1	95	90	92.5	5	6
5	98	97	97.5	1	96	95	95.5	1	3
6	93	91	92	2	89	85	87	4	8
7	97	97	97	0	93	91	92	2	6

One of the major differences in the operation of the Minisonic and Microsep Separometers is in the emulsification cycle. In operation it appears the mixing is much more vigorous and the mixing time is slightly longer in the Microsep unit. Data show the ratings by the Microsep unit to be lower than those by the Minisonic. Table 23 indicates that the difference is in the turbidity measuring portion of the operation rather than in the emulsification step. The turbidity readings obtained from the Microsep unit are lower than those from the Minisonic.

At present there is no field method for calibrating or checking calibration of the Microsep Separometer. Section A2.2.7.2 of the Minisonic Separometer Operation Manual describes a method of calibration. A method similar to this for the Microsep unit would be useful at least to check the calibration even if there is no means of field calibration.

7. ANALYSIS OF RAMAN SPECTROSCOPY DATA FOR GOODNESS-OF-FIT TO FOUR STATISTICAL DISTRIBUTIONS

As a part of the error propagation analysis task, several sets of Coherent Antistokes Raman Spectroscopy (CARS) data have been analyzed for goodness-of-fit to four statistical distributions. This was accomplished by utilizing a goodness-of-fit program on the MRC computer. The program attempts to fit each data set to each of four theoretical distributions, namely, Weibull, normal, gamma and log-normal distributions.

Output of the computer program provides parameters that sufficiently describe the distribution, such as the mean and standard deviation for the normal distribution. Other parameters are given that describe the goodness-of-fit for a particular distribution. Some of these parameters are skewness, kurtosis, and a chi-square value. Additionally, the theoretical and actual frequencies of data groups in each class interval are provided.

Skewness is a measure of symmetry. A value of zero indicates left-to-right symmetry. A positive value indicates skewness to the right; that is, the tail of the distribution extends further to the right as the positive number becomes greater in magnitude. A negative number indicates skewness to the left in a similar fashion.

The quantity kurtosis is a measure of peakedness or thinness of a distribution. A value of three is the perfect shape of a normal distribution. Values greater than 3 indicate a tall peak and narrow width of the distribution, smaller values indicate a shorter, broader peak.

To determine how well our data fit a particular statistical distribution, a chi-square goodness-of-fit test can be used. The value of chi-square is calculated as follows:

$$\text{Chi squared, } \chi^2 = \sum_{i=1}^{k} \frac{\left[O(n_i) - E(n_i)\right]^2}{E(n_i)}$$

where $E(n_i)$ is the expected frequency, $O(n_i)$ is the observed frequency, and n_i is the number of observations in the ith cell or class interval. A "perfect fit" yields a χ^2 value of zero. As the magnitude of χ^2 increases, the likelihood that the theoretical distribution fits the data diminishes.

The procedure for using the chi-square test involves hypothesis testing. The null hypothesis H_o and its alternative H_1 are stated:

H_o - These data fit the theoretical distribution
H_1 - The data do not fit the distribution

A good fit leads to the acceptance of H_o, whereas a poor fit leads to its rejection. For this test, we must also define a level of significance, α, and a critical value, χ^2_α, from the chi-square table. The α and χ^2_α determine the critical region $\chi^2 > \chi^2_\alpha$, i.e., our calculated χ^2 exceeds the table χ^2_α. If, indeed, our chi-square value exceeds the table values, we reject the null hypothesis and conclude that our data do not fit the theoretical distribution we are considering.

An example is taken from a set of data for a still air sample at 24.5 inches. A chi-square value of 15.5 with 4 degrees of freedom is given for the normal fit. Using the chi-square distribution shown in Table 26 (ref. 3), the 0.05 column with 4 degrees of freedom gives a critical value of 9.49. We must reject the null hypothesis and repeat this test for other distributions. Now, if one traverses the table to the right, under A = 0.01, χ^2 critical = 13.28. From the example cited above of where the chi-square test value = 15.48 with 4 degrees of freedom, we can say that we reject the null hypothesis (at 5% level) but cannot reject it for the Weibull Maximum Likelihood, the gamma, or the log-normal distributions.

However, if we relax the requirement to 0.1 of making a Type II error, we see that all distributions must be rejected except the log-normal. One can then conclude that the data may be roughly log-normal. Table 27 is a summary of the results.

8. ANALYSES TO DETERMINE CAUSE OF PLUGGING IN MAIN ENGINE FILTERS

The main engine filter, designed to remove solid contaminants from jet fuel before it reaches the engine, was found to be plugging in certain aircraft. When the plugged filters were removed, it was observed that the contamination was not uniformly distributed. A small but thick mat of fiberous material was deposited near the

TABLE 26. CHI-SQUARE DISTRIBUTION

Chi-Square Distribution

A denotes the right tail area for the values of χ^2 given below. ν denotes the number of degrees of freedom (df).

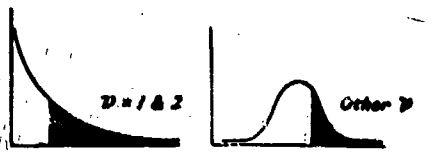

ν or df	A = 0.99	A = 0.98	A = 0.95	A = 0.90	A = 0.80	A = 0.70	A = 0.50
1	.00016	.00063	.0039	.016	.064	.15	.46
2	.02	.04	.10	.21	.45	.71	1.39
3	.12	.18	.35	.58	1.00	1.42	2.37
4	.30	.43	.71	1.06	1.65	2.20	3.36
5	.55	.75	1.14	1.61	2.34	3.00	4.35
6	.87	1.13	1.64	2.20	3.07	3.83	5.35
7	1.24	1.56	2.17	2.83	3.82	4.67	6.35
8	1.65	2.03	2.73	3.49	4.59	5.53	7.34
9	2.09	2.53	3.32	4.17	5.38	6.39	8.34
10	2.56	3.06	3.94	4.86	6.18	7.27	9.34
11	3.05	3.61	4.58	5.58	6.99	8.15	10.34
12	3.57	4.18	5.23	6.30	7.81	9.03	11.34
13	4.11	4.76	5.89	7.04	8.63	9.93	12.34
14	4.66	5.37	6.57	7.79	9.47	10.82	13.34
15	5.23	5.98	7.26	8.55	10.31	11.72	14.34
16	5.81	6.61	7.96	9.31	11.15	12.62	15.34
17	6.41	7.26	8.67	10.08	12.00	13.53	16.34
18	7.02	7.91	9.39	10.86	12.86	14.44	17.34
19	7.63	8.57	10.12	11.65	13.72	15.35	18.34
20	8.26	9.24	10.85	12.44	14.58	16.27	19.34
21	8.90	9.92	11.59	13.24	15.44	17.18	20.34
22	9.54	10.60	12.34	14.04	16.31	18.10	21.34
23	10.20	11.29	13.09	14.85	17.19	19.02	22.34
24	10.86	11.99	13.85	15.66	18.06	19.94	23.34
25	11.52	12.70	14.61	16.47	18.94	20.87	24.34
26	12.20	13.41	15.38	17.29	19.82	21.79	25.34
27	12.88	14.12	16.15	18.11	20.70	22.72	26.34
28	13.56	14.85	16.93	18.94	21.59	23.65	27.34
29	14.26	15.57	17.71	19.77	22.48	24.58	28.34
30	14.95	16.31	18.49	20.60	23.36	25.51	29.34

(continued)

TABLE 26 (continued)

Chi-Square Distribution

ν or df	A = 0.30	A = 0.20	A = 0.10	A = 0.05	A = 0.02	A = 0.01	A = 0.001
1	1.07	1.64	2.71	3.84	5.41	6.64	10.83
2	2.41	3.22	4.60	5.99	7.82	9.21	13.82
3	3.66	4.64	6.25	7.82	9.84	11.34	16.27
4	4.88	5.99	7.78	9.49	11.67	13.28	18.46
5	6.06	7.29	9.24	11.07	13.39	15.09	20.52
6	7.23	8.56	10.64	12.59	15.03	16.81	22.46
7	8.38	9.80	12.02	14.07	16.62	18.48	24.32
8	9.52	11.03	13.36	15.51	18.17	20.09	26.12
9	10.66	12.24	14.68	16.92	19.68	21.67	27.88
10	11.78	13.44	15.99	18.31	21.16	23.21	29.59
11	12.90	14.63	17.28	19.68	22.62	24.72	31.26
12	14.01	15.81	18.55	21.03	24.05	26.22	32.91
13	15.12	16.98	19.81	22.36	25.47	27.69	34.53
14	16.22	18.15	21.06	23.68	26.87	29.14	36.12
15	17.32	19.31	22.31	25.00	28.26	30.58	37.70
16	18.42	20.46	23.54	26.30	29.63	32.00	39.25
17	19.51	21.62	24.77	27.59	31.00	33.41	40.79
18	20.60	22.76	25.99	28.87	32.35	34.80	42.31
19	21.69	23.90	27.20	30.14	33.69	36.19	43.82
20	22.78	25.04	28.41	31.41	35.02	37.57	45.32
21	23.86	26.17	29.62	32.67	36.34	38.93	46.80
22	24.94	27.30	30.81	33.92	37.66	30.29	48.27
23	26.02	28.43	32.01	35.17	38.97	41.64	49.73
24	27.10	29.55	33.20	36.42	40.27	42.98	51.18
25	28.17	30.68	34.38	37.6_	41.57	44.31	52.62
26	29.25	31.80	35.56	38.88	42.86	45.64	54.05
27	30.32	32.91	36.74	40.11	44.14	46.96	55.48
28	31.39	34.03	37.92	41.34	45.42	48.28	56.89
29	32.46	35.14	39.09	42.56	46.69	49.59	58.30
30	33.53	36.25	40.26	43.77	47.96	50.89	59.70

TABLE 27. CALCULATED CHI-SQUARE VALUES

Data Set	Weibull Maximum Likelihood	Weibull Least Squares, γ	Normal, γ	Gamma, γ	Log Normal, γ
Still Air Sample 24.5	7.94, 4	11.68, 4	15.48, 4	7.66, 4	3.9, 3
Still Air Ref. 24.5	5.48, 4	4.94, 4	5.29, 4	4.75, 4	5.92, 3
Still Air Ratio 24.5	5.41, 3	5.6, 3	9.0, 2	3.94, 3	2.67, 3
Flame Sample 24.5	4.51, 1	6.96, 1	5.91, 2	5.37, 1	2.4, 2
Flame Ref. 24.5	3.89, 1	1.26, 0	4.1, 1	1.34, 0	0.91, 1
Flame Ratio 24.5	1.4, 1	0.35, 0	5.1, 1	1.2, 1	0.43, 1
Vacuum Sample 24.5	5.5, 3	5.4, 3	10.3, 3	4.36, 4	3.6, 4
Vacuum Ref. 24.5	4.2, 3	4.4, 3	4.7, 3	7.6, 3	7.9, 4
Vacuum Ration 24.5	6.7, 4	7.2, 3	13.0, 3	4.4, 4	2.4, 4
Air Flow 1.16 at 2.75	3.2, 1	2.5, 1	2.8, 1	2.3, 0	3.8, 0
Air Flow Ref. at 2.75	0.9, 1	0.8, 1	0.9, 1	0.2, 1	0.6, 1
Air Flow Ratio at 2.75	5.6, 1	6.5, 1	5.5, 1	4.4, 1	2.9, 1
Flame at 2.75	1.5, 1	2.0, 1	1.2, 1	2.6, 1	2.5, 1
Flame Ref. at 2.75	0.12, 1	0.13, 0	0.21, 0	0.1, 0	0.6, 0
Flame Ratio at 2.75	2.5, 1	2.2, 1	2.3, 1	3.2, 1	2.7, 1
Flame at 8.4	1.9, 0	1.73, 0	1.5, 0	1.4, 0	1.4, 0
Flame Ref. 8.4	2.2, 1	3.9, 1	2.5, 1	-	2.6, 1
Flame Ratio 8.4	5.2, 0	5.1, 0	4.1, 0	4.7, 0	1.9, 0
Air at 14.5	3.3, 2	2.5, 2	3.7, 2	0.85, 1	1.75, 2
Air Ref. 14.5	1.0, 2	1.0, 1	1.0, 2	0.46, 1	1.87, 2
Air Ratio 14.5	8.4, 0	7.1, 0	6.3, 0	5.7, 0	6.1, 0
Flame at 14.5	0.1, 0	0.02, 0	0.96, 0	0, 0	0.57, 1
Flame Ref. 14.5	1.85, 1	1.2, 0	1.7, 1	0.76, 1	1.2, 1
Flame Ratio 14.5	-	-	-	-	1.4, 1
Vacuum at 19.5	4.5, 3	4.6, 3	5.5, 3	4.3, 3	4.2, 4
Vacuum Ref. 19.5	4.1, 4	3.5, 4	4.6, 4	7.7, 4	9.0, 4
Vacuum Ratio 19.5	1.9, 3	1.7, 3	4.8, 3	1.5, 4	4.5, 4
Still Air 19.5	9.2, 3	8.2, 3	6.2, 2	6.1, 3	2.7, 4
Still Air Ref. 19.5	2.7, 4	3.6, 4	3.4, 4	2.5, 4	2.8, 4
Still Air Ratio 19.5	0.33, 2	1.28, 2	3.1, 2	0.48, 2	4.2, 3

inner corners of the filter pleats and a fine particulate layer was spread over much of the paper surface. The large debris appeared to be a mixture of cellulose and synthetic fibers plus pieces of fuel tank foam. These materials, however, were not specifically characterized. The composition of the fine particulate residue was unknown, but it appeared to be responsible for the filter plugging that resulted in a high pressure drop. The main purpose of this work was to identify the fine particulate contaminate on these submitted filters labeled 77-0262, 77-0248, and 77-0270.

Analysis of Fine Particulate Residue

The fine particulate residue was scraped from the surface of the three filters and analyzed by emission and infrared absorption spectral techniques. The results for the semiquantitative emission spectrographic analyses are shown in Table 28, while a typical infrared absorption spectrum for the sample is shown in Figure 45.

The emission spectrographic analyses suggest that much of the particulate contamination may be characterized as terrestrial dust or dirt. This is indicated by the presence of significant quantities of aluminum, silicon, calcium, magnesium, and iron. The significance of the presence of cadmium and zinc is not known.

The IR absorption spectra indicate the presence of oxygen-containing compounds and low levels of hydrocarbons. The hydrocarbon bands are probably due to residual fuel, while the main oxygen species are probably metal oxides. The presence of inorganic carbonate is also suggested by a weak band at approximately 7 microns. The presence of some cellulose from scraping the filter paper is indicated at a low concentration. These spectral features are consistent with the characterization of the contaminants as entrapped ambient dust.

TABLE 28. EMISSION SPECTROGRAPHIC ANALYSIS RESULTS FOR FILTER PAPER RESIDUES

Element	Percent Concentrations for Following Samples		
	77-0262	77-0248	77-0270
Aluminum	>10	>10	>10
Silica	1-10	1-10	1-10
Calcium	1-10	1-10	1-10
Magnesium	0.5	0.3	1-10
Iron	0.5	1-10	1-10
Cadmium	ND*	0.4	1-10
Zinc	0.5	0.5	1-10
Chromium	0.1	0.2	0.5
Sodium	0.03	0.04	0.4
Manganese	0.05	0.05	0.2
Copper	0.3	0.1	0.2
Lead	0.05	0.05	0.2
Nickel	0.005	0.2	0.03
Titanium	0.05	0.4	0.1
Molybdenum	0.05	0.05	0.04

ND* - not detected

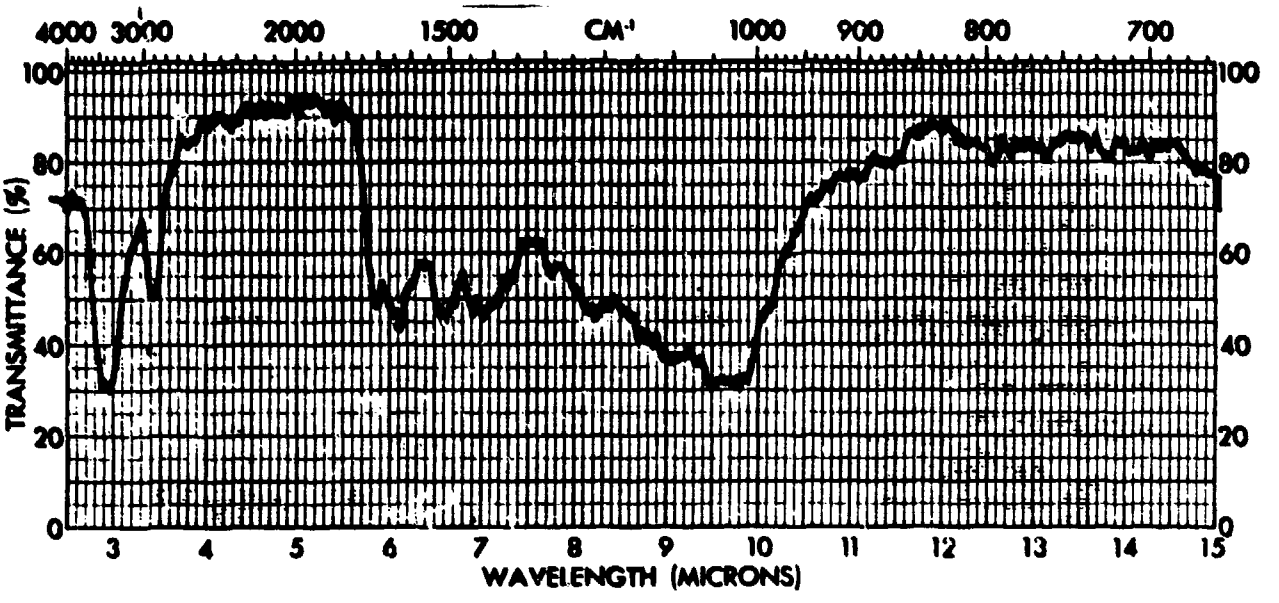

Figure 45. Infrared absorption spectrum of fine particulate residue.

Analysis of Filters for Impregnated Organic Material

It was suggested that organic material impregnated in the filter, rather than matter coated on its surface, might be responsible for the increased resistance to flow. To test this theory, the filters were extracted with a chlorinated solvent which was then analyzed for organic content.

The filter paper segments used for the previous analyses were extracted with methylene chloride at room temperature. The paper was cut into irregular shaped pieces for this purpose, with dimensions being roughly 1 x 1/2 inches. The methylene chloride extract was allowed to evaporate to near dryness in an evaporating dish and then the last several milliliters were transferred dropwise to a rock-salt plate where the remaining solvent was removed by further evaporation. An infrared (IR) adsorption spectrum of the residue was recorded.

Methylene chloride extractions were conducted on two different filters with approximately twice as much filter paper being used for the second extraction. No residue was visually observed on the rock-salt plate from either of the extractions, and no organic compounds were detected by the IR analyses. The IR spectrum for the extracts showed only the presence of water as indicated by bands at approximately 3 and 6 microns. This doubtlessly resulted from condensation during the cooling that was associated with the evaporation of solvent. Considering the high sensitivity of the infrared spectrophotometric technique for organic analysis and the excellent solvent properties of methylene chloride for most organic compounds, it can be concluded that no significant amount of organic material was contained on the filter as received.

9. TRACE METAL ANALYSES AND IDENTIFICATION OF PARTICULATE MATTER FORMED IN FUELS

Fuels used in an Air Force-sponsored test program were found to have decreased in their thermal stability, and the lowered thermal stability manifested itself by the formation of particulates in the fuel. An investigation to identify the fuel particulates and fuel contaminants responsible for particulate formation was conducted.

A study was also conducted to determine the effects of thermally stressing two test fuels, both while they were in contact with one of several metals and in the absence of metals.

Experimental and Results

Particulate Analysis

Two of the specimens examined during the course of this study consisted of particulate material contained on filters. In one case, a 1- to 2-mm spot of material was contained on a Millipore® membrane filter. The second particulate deposit was contained on a paper filter. Both residues were formed during the JFTOT testing of special test fuels. The deposits were found to be insoluble in common organic solvents. Examination of both deposits by the energy dispersive x-ray fluorescence technique showed that they contained no significant quantities of metals. The Millipore filter deposit was washed with a small quantity of methylene chloride, and the resulting rinse was analyzed by gas chromatography/mass spectrometry (GC/MS). The only materials detected were traces of di- and tricyclic aromatics. These compounds are likely due to nonvolatile traces of fuel which remained on the filter.

The bulk of the particulate deposit still remained on the Millipore filter and the spot was not noticeably lightened by the solvent rinse. An infrared attenuated total reflectance (ATR) spectrum was recorded of the filter spot after the previous solvent rinse. Only the spectrum of the filter material, polyvinyl acetate, was obtained. It was concluded that the deposit was carbonaceous and had very little organic character.

Fuel Contaminant Analysis

Several experimental fuel blends which had failed the JFTOT test, with resultant filter plugging, were examined to determine the nature of their contaminants. Two GE/TJ test fuels, coded 8AR-12% and 8XY-13%, were compared to earlier samples of the same fuels that had shown satisfactory thermal stability. Differential spectrometric techniques (GC/MS, IR, and UV absorption) were employed to find compositional differences between the fuels, but no organic contamination was detected in the test fuels by these techniques.

Emission spectrographic analyses of the fuels were conducted to determine any difference in metals content. For semiquantitative results, the fuels were extracted with dilute UltraR metals-free hydrochloric acid. This approach allows metals to be concentrated in the acid layer, a portion of which is then evaporated in the cup of a spectrographic electrode. Most metals are efficiently extracted in this manner. A few, such as silicon and aluminum, are not. Any significant amount of these metals tends to form a scum at the fuel/acid interface. In conducting the analyses, therefore, a specimen taken from the fuel/acid boundary was also analyzed. Analytical results are presented in Table 29.

Trace metals were determined in the same way in two fuels which were presumed to be identical, but which produced significantly different thermal stability test results. The two fuels were

TABLE 29. SPECTROGRAPHIC ANALYSIS OF FUEL EXTRACTS AND EXTRACTION INTERFACES

Analysis Request No.:	78015		78015		78015		78015		78026		78026	
Type Sample:	Control		Test		Control		Test		Test		Test	
JP-8 Fuel Designation:	GE/TJ-78-8AR-12%		GE/TJ-78-8AR-12.0-06		GE/TJ-78-8XY-13%		GE/TJ-78-8XY-13.0-06		Sple 2, cell 304% Round Can (A)		Sple 2, cell 304% Rectangular Can (B)	
Metal	**Fuel**	**Surface**	**Fuel**	**Surface**	**Fuel**	**Surface**	**Fuel**	**Surface**	**Fuel**	**Surface**	**Fuel**	**Surface**
Fe		trace	110	trace	4	trace	9	trace		trace		trace
Cu	5	trace	8	trace	4	trace	4	trace	4	trace	8	trace
Mn			3	trace	0.1-1.0	trace	0.1-1.0	trace		trace	0.1-1.0	trace
Pb	5		15		4		13		12		25	
Sn	0.1-1.0		38	trace			44	trace			3	
Ca			4	minor		major		major				minor
Si		major		major		major		major		trace		major
Al		trace		major		trace		major		trace		trace
Na		minor		minor		minor		trace		major		trace
Mg		trace				trace		trace		trace		trace
Cr			0.1-1.0			trace		trace				
V						trace				trace		
Zn											170	
Ag			0.1-1.0									
Ni						trace						
Ti						trace						

ppb and Qualitative Amounts of Metals* Found in Following Fuels

*Most metals could be detected at levels as low as 0.2-1.0 ppb, except for zinc which can be detected only as low as 50 ppb. For the qualitative analyses of the fuel/extract interface surface, a "major" designation indicates that this metal consisted of 10-100% of the total metals detected, a "minor" designation means 1-10% of the total metals, and "trace" means less than 1%.

numbered identically, JP-8-Sple 2-cell 304-1/2, with the only visible difference between the two samples being in the containing cans. The sample called "fuel A" was contained in a round welded steel epoxy-coated can. The other, called "fuel B," was contained in a rectangular soldered tin can. The metals analyses for these fuels are also presented in Table 29.

An examination of the analytical data showed that, for GE/TJ-78 samples 8AR-12 and 8XY-13, the test fuels contained more and significantly higher levels of trace metals than the control fuels. Tin appeared at a moderately high level in both test fuels but not in the controls. Iron was high in one test fuel but not in the control. The presence of a high level of zinc (170 ppb) and increased levels of copper and lead were the major differences found between fuel A and fuel B. High concentrations of trace metals are, of course, associated with decreased thermal stability in hydrocarbon fuels.

Thermal Stressing Study

Fuels A and B, labelled JP-8-Sple 2-cell 304-1/2, were thermally stressed under conditions that simulated a JFTOT test run. These fuels were heated in 6-inch by 1/4-inch ID glass-lined bombs containing single 1-inch strips of various metals, for periods of 15 and 40 minutes at 300°C. Air was excluded from the test cells, and fuels samples without metal strips were heated as controls. The heated fuels were then filtered dropwise through one spot on a 0.45-μm Millipore filter to isolate any particulate residue. The intensity and size of the residue spot was found to be a good visual indicator of the amount of particulate formed. Residue spots were thus given relative numerical ratings based on their approximate size and intensity; these are presented in Table 30. A photograph of all filter spots is shown in Figure 46. Emission spectrographic analyses were conducted on the residues from the 40-minute heating period to determine the presence of the

TABLE 30. ANALYSIS OF RESIDUES FORMED BY HEATING FUELS AT 300°C IN CONTACT WITH SELECTED METALS

Fuel Container	Contact Metal	Time at 300°C, min	Residue Intensity Rating[a]	Metals Detected[b] in Filtered Residues				
				Al	Cu	Pb	Sn	Zn
Round (fuel A)	none	none	0	slt	no	no	no	no
	none	15	2					
	none	40	2	yes	slt	no	no	no
	Al	15	2					
	Al	40	3	yes				
	Cu	15	1					
	Cu	40	3		yes			
	Pb	15	3					
	Pb	40	2			yes		
	Sn	15	2					
	Sn	40	1				no	
	Zn	15	1					
	Zn	40	0					no
Rectangular (fuel B)	none	none	0	slt	no	no	no	no
	none	15	2					
	none	40	3	yes	slt	no	no	no
	Al	15	2					
	Al	40	2	yes				
	Cu	15	1					
	Cu	40	3		yes			
	Pb	15	3					
	Pb	40	3			yes		
	Sn	15	2					
	Sn	40	1				no	
	Zn	15	3					
	Zn	40	3					no

[a] Refers to relative quantity of residue present on filter: 0 = none apparent; 1 = gray spot about 1/8 in. diameter; 2 = black spot about 1/8 in. diameter; 3 = black spot about 1/4 in. diameter.

[b] The following approximate quantities of metals can be detected by emission spectroscopy: 0.2 µg for aluminum and copper, 1 µg for tin and lead, and 50 µg for zinc. A "no" designation means none was detected, "slt" means a slight indication of the metal near the minimum detectability level, and "yes" means a strong indication of the metal at an undetermined concentration.

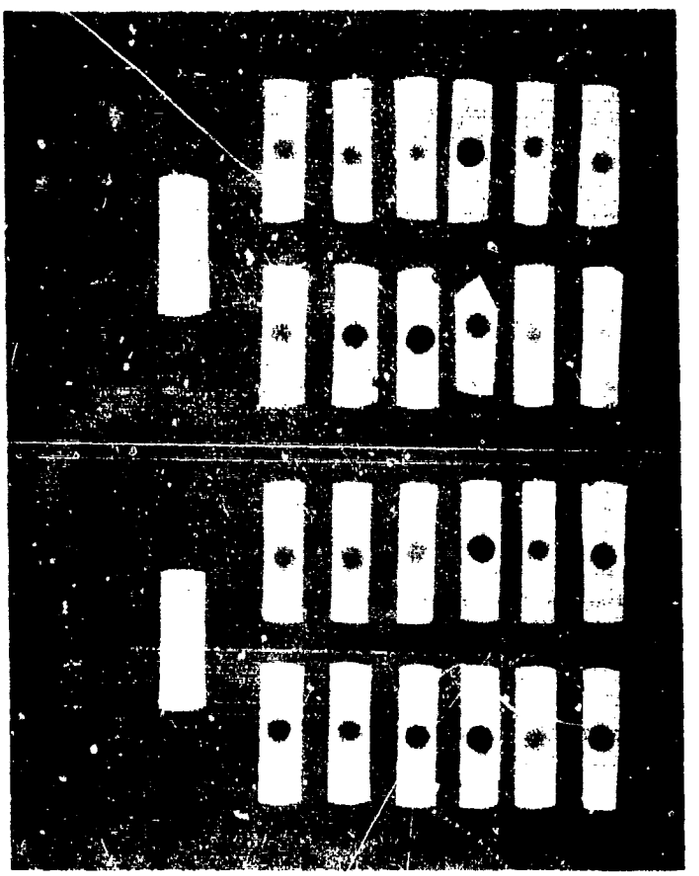

Figure 46. Photograph of residues collected on membrane filters from fuels heated at 300°C for 15- and 40-minute periods.

individual contact metals in the particulate matter. These data are included in Table 30. Aluminum, copper, and lead were detected in residues obtained from both fuel A and fuel B after heating them in the presence of the respective metals. Aluminum and copper, however, were found in the particulates after heating the fuels without contact metals.

Discussion and Conclusions

The thermal stressing studies showed some unexpected results. In several cases, with tin as the contact metal for example, the amount of particulate matter formed in 40 minutes appears to be less than that formed in 15 minutes. The particulate material formed in the fuel is extremely difficult to remove from a glass vessel surface after it has settled. The static nature of the test may have allowed greater settling of the material over the longer period of time. Thus the low observed amounts may represent poor recovery of the particulate rather than a lower rate of formation.

The two JP-8 fuels, A and B, reportedly give greatly differing results in JFTOT tests. Though not consistent for all metals, the particulate residue appeared to be generally heavier in fuel B. The difference found in trace metals content was sufficient to account for the poor thermal stability in JP-8, B.

A high trace metals content similarly appeared to be the likely cause of JFTOT failure by the modified JP-8 (8AR-12 and 8XY-13) fuels.

10. PCB ANALYSIS OF UNKNOWN WASTE FLUID

Several drums of a waste fluid material having unknown identification, composition, and history were received at AFAPL. Analytical data were required on its PCB content, if any, in

order to facilitate proper disposal of the material. A single sample was submitted for analysis to determine approximate PCB concentration.

Analytical Procedure

The oil-like fluid was diluted 1:9 with hexane and then analyzed on an HP5830A gas chromatograph fitted with an electron capture detector:

Column - 1% SP 2250 on 100/120 mesh Supelcoport in 6 foot x 1/4 inch glass
Col. Temperature - 190°C
Carrier Gas - 95% argon/5% methane at 30 ml/minute

The sample chromatogram was compared with those for standard Aroclors 1242 and 1254 which had also been diluted 1:9 with hexane prior to analysis.

Results

A trace (0.91 ppm) of PCB was detected in the sample labeled A-79008. This is much below the current EPA action level of 500 ppm. These results were reported by telephone to the request initiator.

11. ANALYSIS OF DEPOSITS ON JFTOT PREFILTERS

Deposits were formed on the prefilters (0.45-μm porosity Millipore) for the Jet Fuel Thermal Oxidation Tester during the testing of two diesel fuels. Two prefilter samples submitted for analysis of deposits were labeled:

Sample 1 - prefilter diesel fuel #2, Run 1, J79, 12/4/79
Sample 2 - prefilter diesel fuel #2, Run 1, J79, 12/6/79

Chemical analyses were conducted to determine the nature of these deposits. Both iron oxide and organic deposits were suspected. A control filter with residue and a filter blank were also analyzed to aid in the interpretation of results.

Emission Spectrographic Analyses

Deposits from the two sample prefilters and the control filter (labeled clean DF-2) were subjected to emission spectrographic analysis. Prior to analysis, the deposits were removed from the filters with a spatula using gentle abrasion in the presence of lithium carbonate. The latter material was used as a matrix diluent for analysis. The analytical results showed a number of elements to be common to both the control and sample filter deposits at nearly the same levels. These elements included major amounts of iron, aluminum, and sodium; moderate amounts of silicon, tin, copper, and lead; and small amounts of magnesium, manganese, and titanium. The only significant difference between the control and sample deposits were: (a) run 1 sample contained a major amount of nickel and (b) both run 1 and run 2 samples contained trace amounts of silver.

Infrared (IR) Spectrographic Analyses

Deposits were removed from the sample and control filters by gently rubbing a spatula across the filter surfaces in the presence of potassium bromide (KBr). The KBr/deposit mixtures were then compressed into pellets for standard IR analyses. A piece of the blank filter disk was analyzed in order to determine major absorption bands characteristic of the filter materials.

Infrared spectra for sample run 1, the control, and the blank filter are shown in Figures 47-49. The spectrum for sample run 2 was identical to that of run 1 and is not included with the

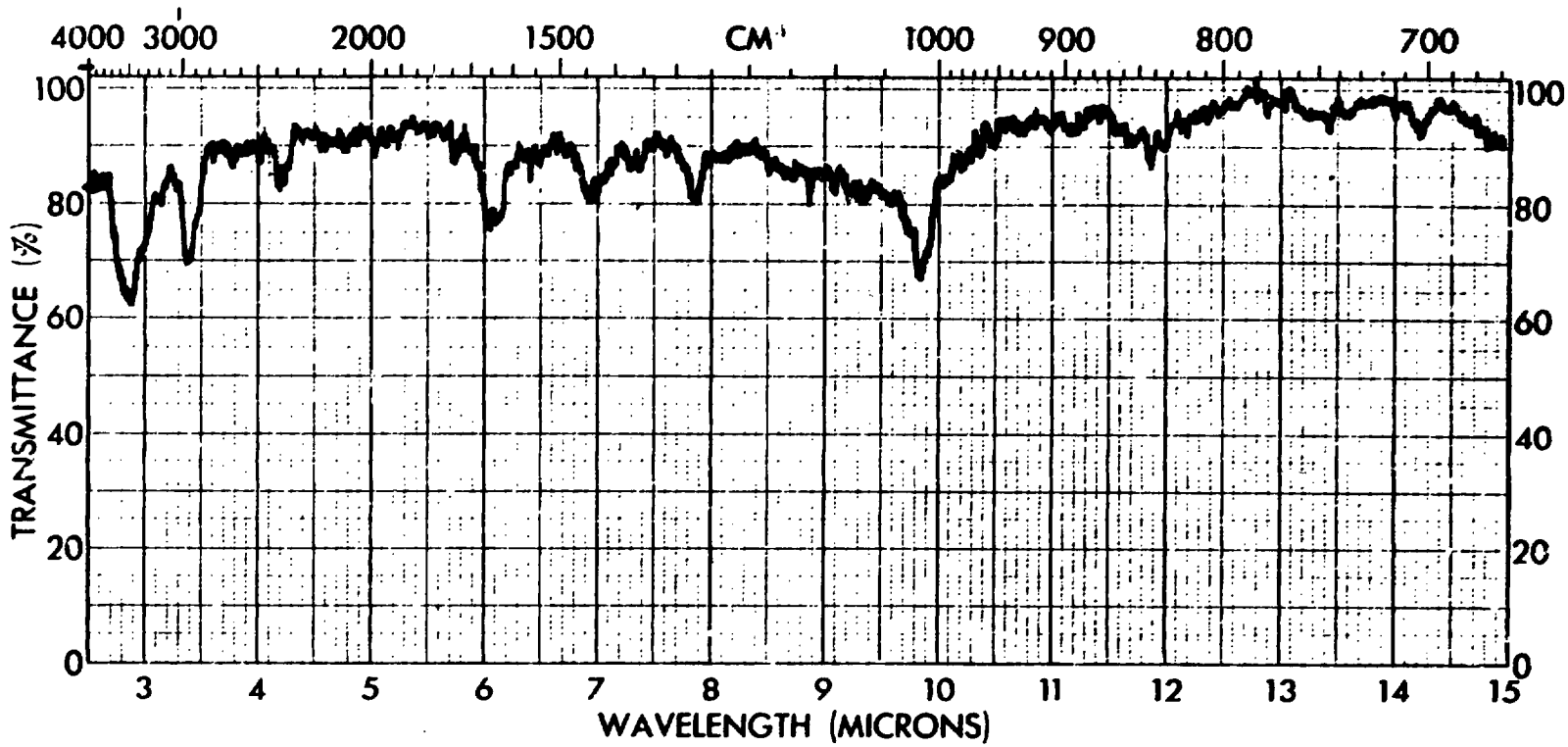

Figure 47. IR spectrum for prefilter deposit from sample run #1.

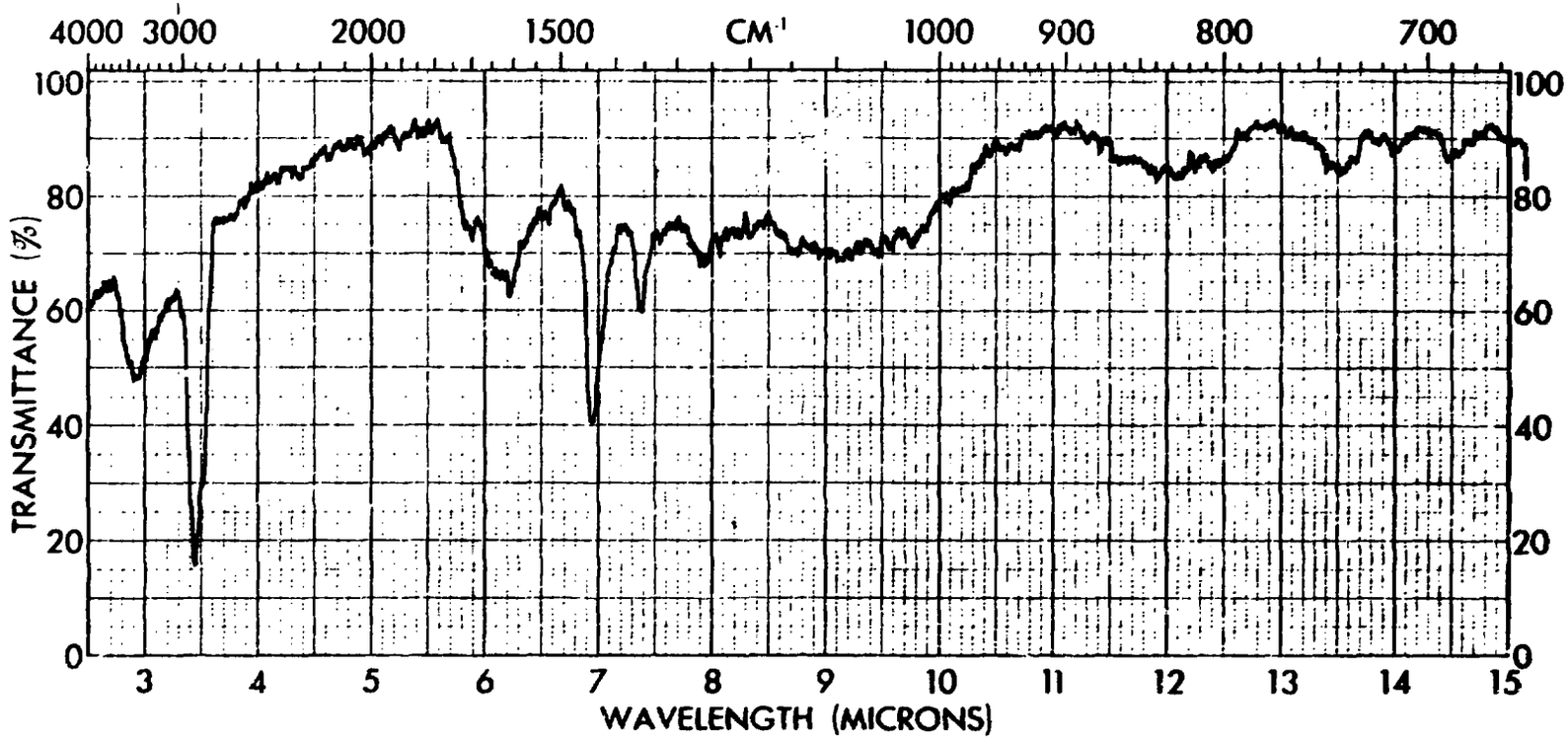

Figure 48. IR spectrum for prefilter deposit from control run with clean DF-2.

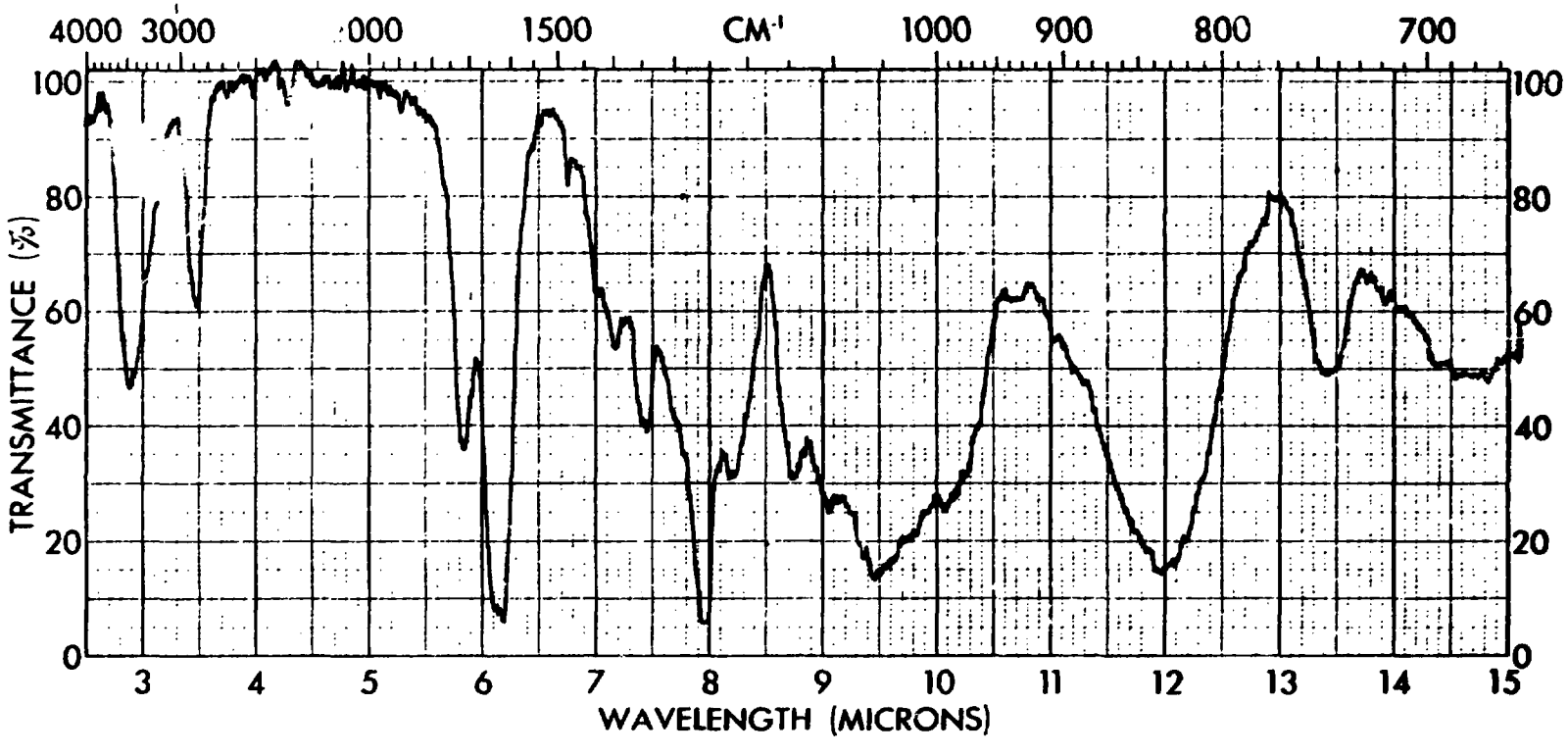

Figure 49. IR spectrum of Millipore filter.

figures. The spectrum of the Millipore filter indicates that it was a mixture of cellulose nitrate and acetate. Spectra for the control and both sample deposits show the presence of cellulose from the Millipore filter, and aliphatic hydrocarbons which were probably diesel fuel components. An additional absorption band at approximately 9.85 microns wavelength is observed for the sample deposits but not for the control deposit. This band is usually characteristic of low molecular weight oxides, although sulfates also show a similar band. The amount of sample available for analysis was insufficient for precise identification.

The absence of significant absorption bands not found in the control indicates that the sample deposits were largely inorganic in nature. Based on the emission spectrographic results and the limited infrared spectral data, the deposit appears to have consisted largely of metal oxides.

12. HPLC ANALYSIS OF MIL-L-7808 FLUID SAMPLES FOR OIL ADDITIVES

Five Air Force fluids, coded TEL-0032 through TEL-0036, were analyzed for oil additives by a high pressure liquid chromatography (HPLC) method developed on a previous Monsanto Research Corporation contract. This method is described in Report AFAPL-TR-78-50, "Reclamation of Synthetic Turbine Engine Oil Mixtures." The analyses were required because the Air Force had identified a production batch of MIL-L-7808 fluid which was suspect with respect to the concentration of additives in the oil.

Analysis Procedure

The HPLC analyses were performed using a Waters instrument having a Model 660 Solvent Programmer, an ultraviolet detector and an HP-3380A integrator. The following analytical conditions were utilized:

Column:	Partisil PX5 10/25 PAC
Sample Concentration:	10 µl of 10% sample in cyclohexane
Elution Solvent:	Programmed from isooctane to 30/70 iso-octane/methylene chloride over a 20 minute period
Flow Rate:	2 ml/minute
Detector Wavelength:	254 nm

Results and Discussion

The five MIL-L-7808 fluids were analyzed for five oil additives having the elution times shown in Table 31. The analytical results, shown as weight percents in Table 32, were calculated using peak area values obtained from the integrator for both the samples and standards. Individual additive standards were prepared in either cyclohexane or methylene chloride. A sample density value of 0.94 g/ml was used for all calculations. A typical sample chromatogram is shown in Figure 50.

Since the elution times for PANA and DOPTA were very close, there was some initial concern that the indicated PANA peaks in the samples may actually be a combination of both additives. However, the analysis of a mixed standard showed that the Partisil column would resolve the two additives if they were both present in a sample. The elution times for the single component in all samples in the 11-13 minute range matched well with that for PANA.

TABLE 31. HPLC ELUTION TIMES FOR MIL-L-7808G OIL ADDITIVES

Oil additive	Abbreviation	Minutes
4,4'-Dioctyldiphenylamine	DODPA	9.62
3,7-Dioctylphenothiazine	DOPTA	11.84
N-phenyl-α-naphthylamine	PANA	12.01
Phenothiazine	PTA	15.31
Tricresyl phosphate	TCP	23.59, 24.06, 24.32, 25.70

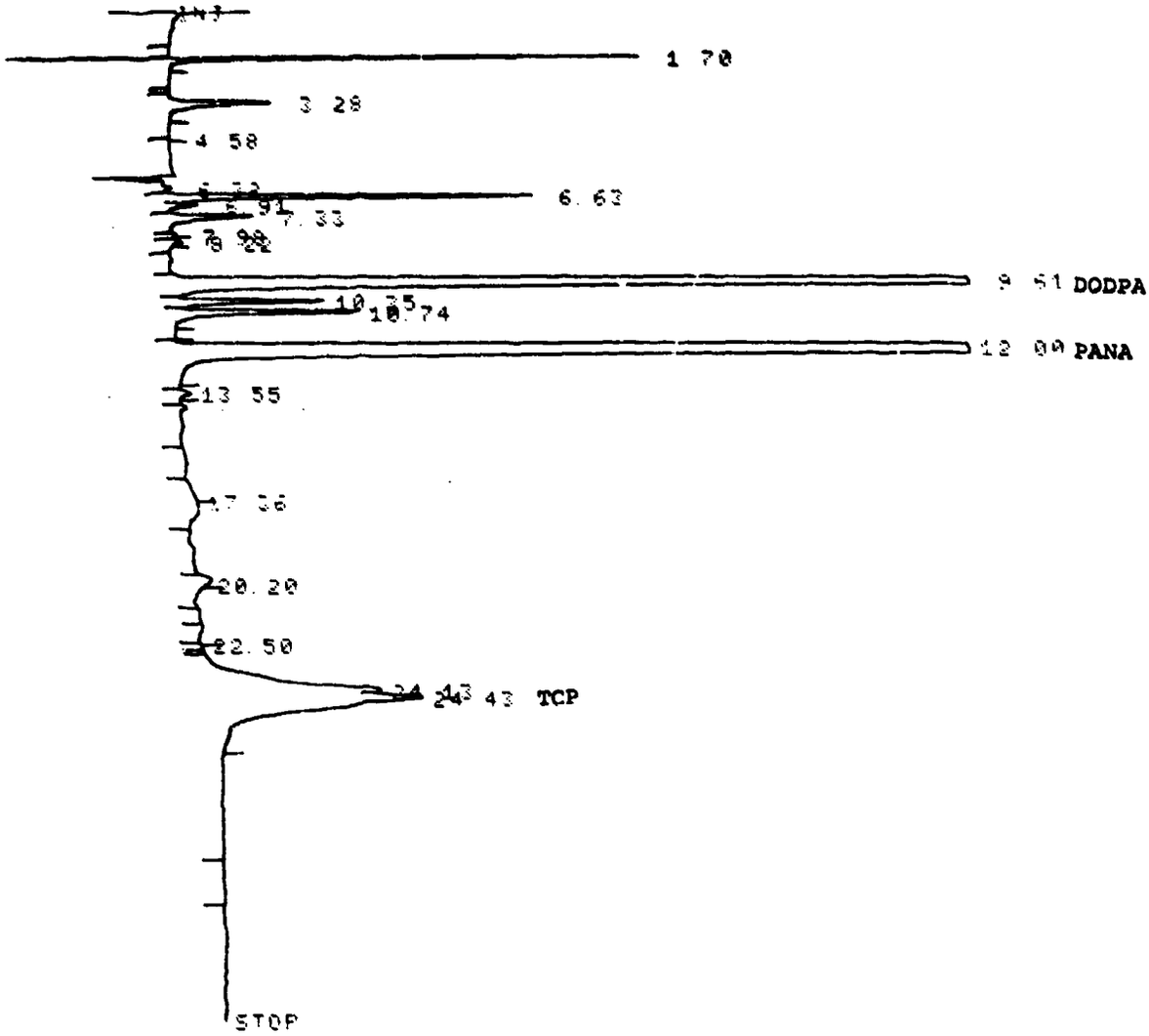

AREA %

	PT	TYPE	AREA	
1	70		135747	7.022
			11644	.602 3
			11883	.614 7
		M	30325	1 569
	91	M	7650	.395 7
		M	12882	.666 4
			567691	29 37
		T	11992	.620 3
	74	TM	16352	.845 9
	00		1002385	51 85
	55		1049	.054 26
	20		2069	.107
			44449	2 299
		M	76996	3 983

Figure 50. Typical HPLC chromatogram for a MIL-L-7808G fluid.

TABLE 32. ADDITIVE CONCENTRATIONS IN MIL-L-7808G FLUIDS

	Weight percents of additives				
Fluid	DODPA	DOPTA	PANA	PTA	TCP
TEL-0032	1.14	ND[a]	0.43	ND	2.17
TEL-0033	1.17	ND	0.83	ND	0.55
TEL-0034	1.14	ND	0.43	ND	2.41
TEL-0035	1.10	ND	0.43	ND	2.43
TEL-0036	1.15	ND	0.85	ND	0.36

[a]ND - not detected at the low ppm levels.

13. PERFORMANCE OF COMBUSTIBLE GAS MONITORS IN DETECTING JP-9, JP-10, AND RJ-6 VAPORS

Fuel vapor monitors currently in use by the Air Force were designed and calibrated primarily for the detection of JP-4 vapors in air. The Air Force also has a need to monitor workplace environments in which vapors of high density fuels (JP-9, JP-10, and RJ-6) may be encountered.

Chemical composition, diffusivity, and thermal conductivity are the properties of fuel vapors that have the greatest effect on the response characteristics of fuel vapor monitors commonly used at Air Force facilities. These properties differ for JP-4 and high density fuel vapors. Therefore, the Aero Propulsion Laboratory sought to determine some response characteristics of selected fuel vapor monitors to high density fuel/air mixtures.

The response of the following monitors to high density fuel/air mixtures was investigated in this work:

Combustible Gas Indicator, Model TBA5100-1, from Beckman Instruments, Inc.

Portable Combustible Gas Alarm, Model 100S, from Mine Safety Appliances Company

Hydrocarbon Super Surveyor, Model 1314 (GasTechtor), from GasTech, Inc.

Two units of the Beckman instrument were included in this investigation. The instrument from GasTech, Inc., was included as a reference monitor since a significant data base had been developed for its response to mixtures of low vapor pressure jet fuels with air (ref. 4). A flame ionization detector, in a Varian Model 1440 chromatographic analyzer, served as a reference sensor for hydrocarbon vapors.

Experimental

The JP-9, JP-10, and RJ-6 fuel samples used in this investigation were supplied by the Fuels Branch of the Aero Propulsion Laboratory. They carried the following identifications:

JP-9: drawn on 12 May 1980 from a 55-gallon drum, Batch 39.

JP-10: drawn on 8 April 1980 from a 55-gallon drum (No. 31) manufactured in November 1979 by Ashland Chemical Company; Batch 9317, 9335-01-048-5295.

RJ-6: drawn on 14 May 1980 from a 55-gallon drum (No. 11) manufactured in October 1979 by Ashland Chemical Company, Batch 9289.

The apparatus used in this work was designed and built with the following objectives:

1. To generate hydrocarbon/air mixtures, from fuel having different volatilities, in a continuous manner in the laboratory;
2. To monitor hydrocarbon concentrations with the instruments whose performance was to be characterized; and
3. To determine hydrocarbon concentrations simultaneously with the reference instrument.

The system used for performance characterization of combustible gas monitors is shown in Figures 51 and 52. The hydrocarbon vapor/air mixtures were generated by bubbling air at a predetermined rate through liquid hydrocarbon contained in the sparger. The hydrocarbon content of the vapor/air mixture was regulated by maintaining a desired sparger temperature with a surrounding constant temperature bath, by controlling the air flow rate through the sparger, and also by diluting the fuel/air mixture with a diluent air stream.

The hydrocarbon/air blend was thoroughly mixed. Samples were drawn into the instruments through probes that extended into the sampling manifold.

A Varian Model 1440 chromatographic analyzer incorporating a flame ionization detector (FID) was used as the reference instrument. This type of detector was selected because its response is known to be nearly linearly related to carbon (in the form of CH_n) concentration in gaseous samples (ref. 5). The lower explosive limit (LEL) of aliphatic hydrocarbon vapors of different compositions can also be expressed as a function of carbon (or CH_n) content (~75,000 ppm). Zabetakis has reported that the vapors of JP-4 and similar fuels contain approximately 48 mg/l of the fuel in air at the lower flammability limit (ref. 6).

Monitor responses, including those of the flame ionization detector, were recorded at the 1-minute time point after stable gas flow conditions had been established, and at 2-minute intervals thereafter. Under each set of selected flow conditions, monitor responses were recorded for at least a 10-minute period. For quantified comparison of response data, the concentrations indicated by the instruments at the 5-minute time points were used. As indicated in Figure 53, no significant hydrocarbon vapor

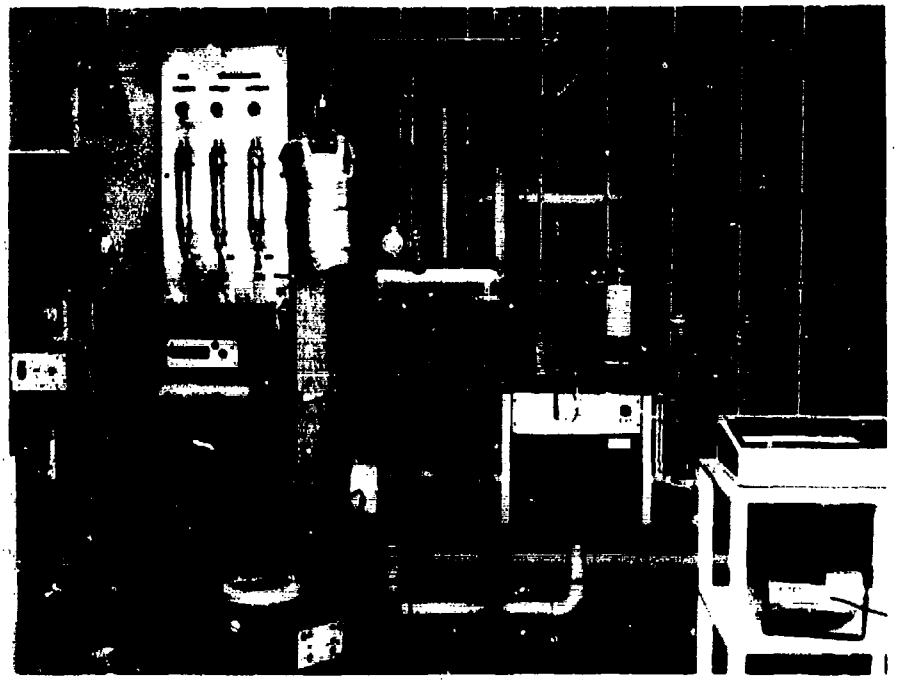

Figure 51. Apparatus for generating and monitoring fuel vapor/air mixtures.

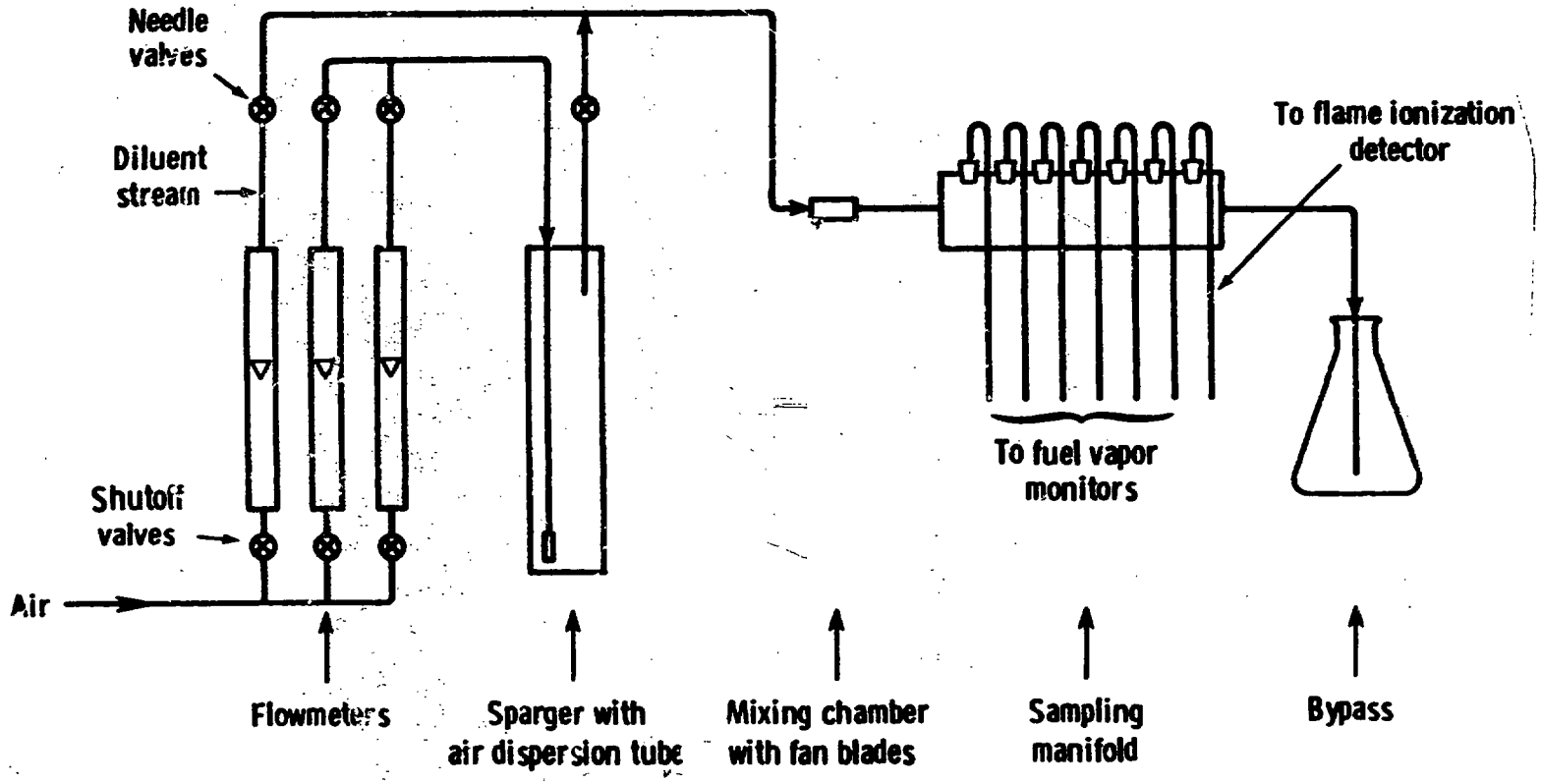

Figure 52. Schematic of apparatus used to generate and monitor fuel vapors.

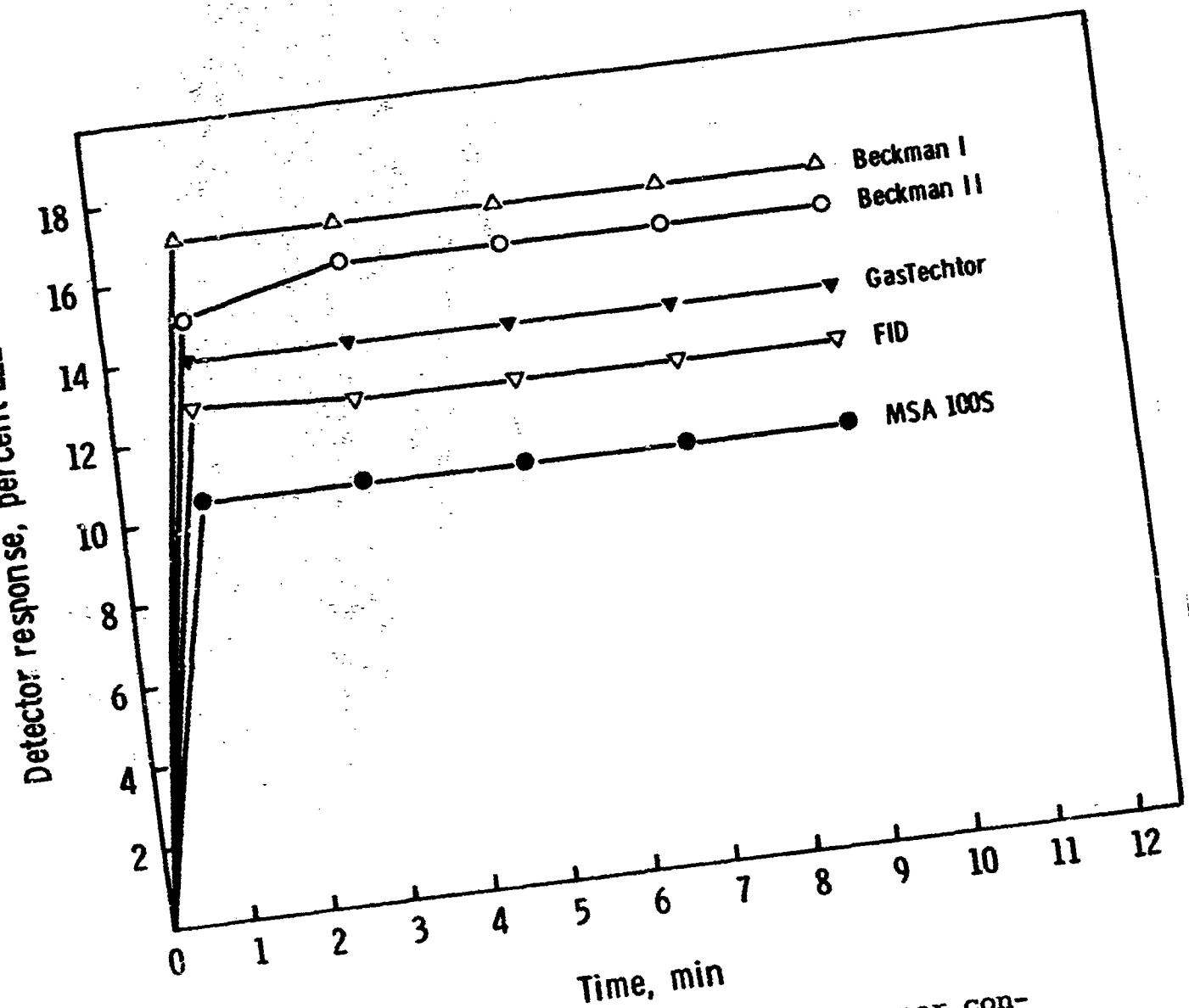

Figure 53. Monitoring of n-heptane vapor concentration in Experiment 77-1.

concentration change was observable after a 5-minute flow of the vapor/air mixture through the system, when heptane was used as the combustible hydrocarbon.

Additional details regarding the apparatus, and its calibration and operation, may be found in a recent report on performance characterization of combustible gas monitors in detecting jet fuel vapors (ref. 4).

Results and Discussion

Figure 54 depicts combustible gas monitor responses in the course of an experiment on JP-9 vapor detection. If fuels contain components of different volatilities, lowering of fuel concentration with time is observed if the temperature of the fuel remains constant.

n-Heptane was included among the combustible materials tested in this investigation because it is a frequently used calibration substance for the monitors, and its vapor pressure and concentration remain constant during an experiment.

The results of the individual experiments with the four combustible substances are listed in Tables 33 through 36. The results for each experiment are listed in the order of diminishing monitor response intensity. The conditions used during the experiments are shown in Table 37.

To facilitate data analysis, the response values of each instrument in sensing a specific combustible gas were averaged. Thus, a single number characterizing the performance of each instrument in sensing each gas was obtained (see Table 38). Normalized responses of instruments with respect to the concentration determined with the flame ionization detector were also calculated. These are presented in Table 39 and Figure 55.

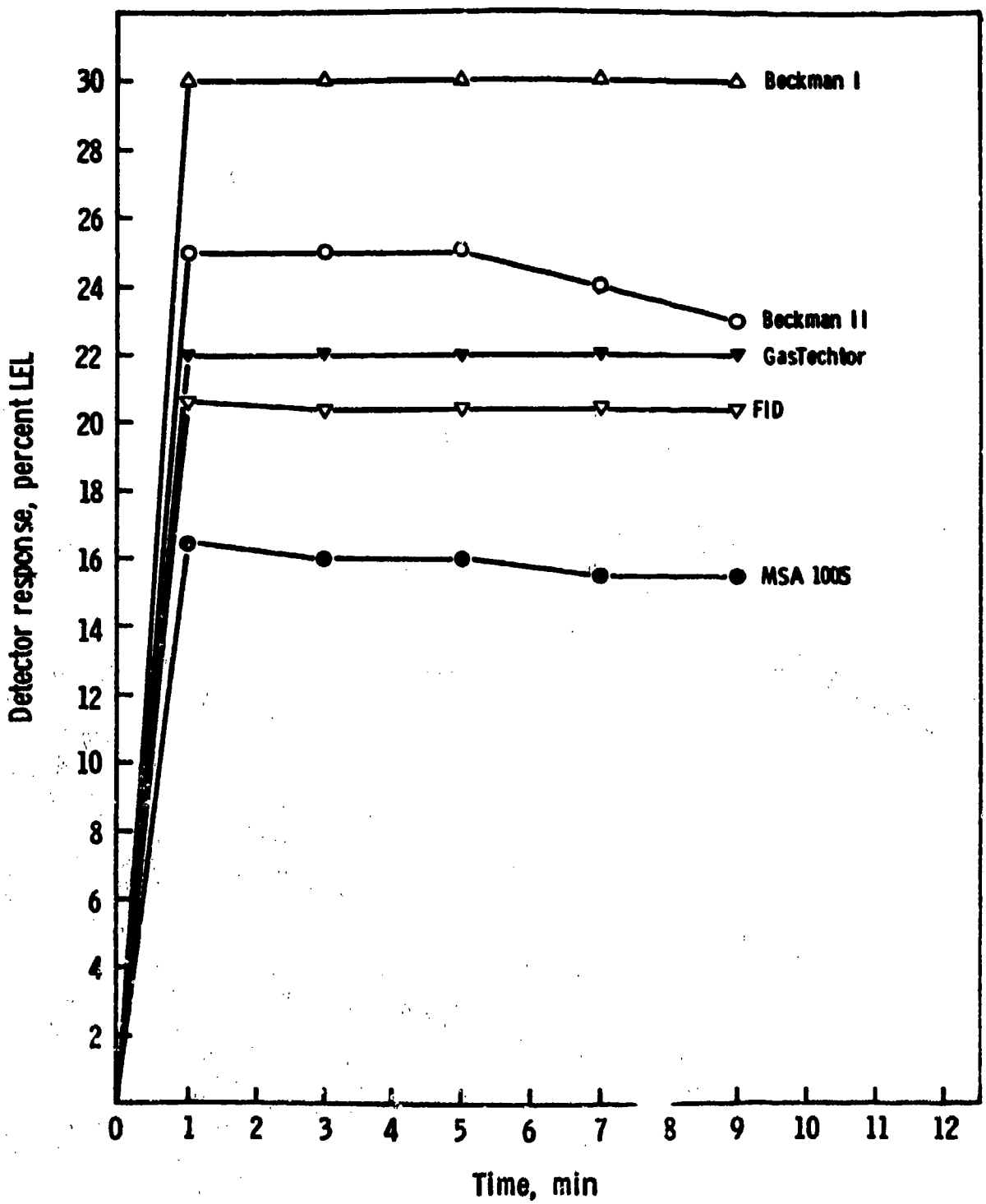

Figure 54. Monitoring of JP-9 vapor concentration in Experiment 81-2.

TABLE 33. MONITORING OF n-HEPTANE VAPOR CONCENTRATIONS, DETECTOR RESPONSES AT 5-MINUTE TIME POINTS

Exp. 74-1		Exp. 74-2		Exp. 77-1		Exp. 77-2	
Beckman I	18	Beckman I	60	Beckman I	17	Beckman I	60
Beckman II	16	Beckman II	58	Beckman II	16	Beckman II	58
GasTechtor	14	GasTechtor	46	GasTechtor	14	Gastechtor	46
FID	11.7	FID	41.1	FID	12.6	FID	42.5
				MSA 100S	10.5	MSA 100S	34.5

TABLE 34. MONITORING OF JP-9 VAPOR CONCENTRATIONS, DETECTOR RESPONSES AT 5-MINUTE TIME POINTS

Exp. 81-1		Exp. 81-2		Exp. 82-1		Exp. 82-2		Exp. 83-1		Exp. 83-2		Exp. 83-3	
		Beckman I	30			Beckman I	30	Beckman I	45	Beckman I	23	Beckman I	16
Beckman I	50	Beckman II	25	Beckman I	50	Beckman II	28	Beckman II	38	Beckman II	20	Beckman II	11
Beckman II	43	GasTechtor	23	Beckman II	48	GasTechtor	23	GasTechtor	33	GasTechtor	15	GasTechtor	8
FID	38.3	FID	20.4	FID	41.1	FID	21.2	FID	32.3	FID	13.6	FID	6.8
GasTechtor	38	MSA 100S	16	GasTechtor	41	MSA 100S	17	MSA 100S	24.5	MSA 100S	12	MSA 100S	6.5
MSA 100S	28			MSA 100S	31.5								

TABLE 35. MONITORING OF JP-10 VAPOR CONCENTRATIONS, DETECTOR RESPONSES AT 10-MINUTE TIME POINTS

Exp. 73-1	Exp. 73-2	Exp. 73-3	Exp. 79-1	Exp. 79-2	Exp. 79-3	Exp. 80-1	Exp. 80-2	Exp. 80-3
Beckman I 8	Beckman I 15	Beckman I 25		Beckman I 15	Beckman I 11		Beckman I 7	Beckman I 6
Beckman II 6	Beckman II 10	GasTechtor 15	Beckman I 23	GasTechtor 8	Beckman II 6		Beckman II 5	Beckman II 3
GasTechtor 4	GasTechtor 7	Beckman II 13	GasTechtor 20	Beckman II 7	GasTechtor 4	Beckman I 10	GasTechtor 4	Gastechtor 2
				MSA 100S 6.5	MSA 100S 3.5	GasTechtor 8	MSA 100S 2.5	MSA 100S 1.5
FID 2.9	FID 5.6	FID 12.6	FID 14.8	FID 6.0	FID 3.1	FID 6.1	FID 2.1	FID 1.0
			MSA 100S 14.5			MSA 100S 6		
			Beckman II 11			Beckman II 5		

TABLE 36. MONITORING OF RJ-6 VAPOR CONCENTRATIONS, DETECTOR RESPONSES AT 5-MINUTE TIME POINTS

Exp. 84-1	Exp. 84-2	Exp. 84-3	Exp. 85-1	Exp. 85-2	Exp. 85-3	Exp. 86-1	Exp. 86-2	Exp. 86-3
			Beckman I 11	Beckman I 5	GasTechtor 3			
GasTechtor 8	GasTechtor 4	MSA 100S 2.5	GasTechtor 10	GasTechtor 4	MSA 100S 2.5	MSA 100S 4.5	MSA 100S 3	MSA 100S 2
MSA 100S 7.5	MSA 100S 4	GasTechtor 2	MSA 100S 8.5	MSA 100S 4	Beckman 1 2	GasTechtor 4	GasTechtor 2	GasTechtor 1
FID 7.0	FID 3.2	FID 1.8	FID 7.6	FID 3.3	FID 1.7	FID 3.0	FID 1.4	FID 0.7
Beckman I 3	Beckman II 2	Beckman II 1	Beckman II 5	Beckman II 3	Beckman II 1	Beckman I 1	Beckman I 0	Beckman I 0
Beckman II 3	Beckman I 0	Beckman I 0				Beckman II 1	Beckman II 0	Beckman II 0

TABLE 37. EXPERIMENTAL CONDITIONS DURING PERFORMANCE CHARACTERIZATION OF COMBUSTIBLE GAS MONITORS

HC/fuel[a]	Experiment number	T,[b] °C	R_a,[c] l/min	R_{da},[d] l/min
n-Heptane	74-1	0	1.0	11.0
	74-2	0	3.9	8.1
	75-1	0	1.0	11.0
	75-2	0	3.9	8.1
	76-1	0	1.0	11.0
	76-2	0	3.9	8.1
	77-1	0	1.0	11.0
	77-2	0	3.9	8.1
JP-9	81-1	21.1	3.0	3.0
	81-2	21.1	1.5	4.5
	82-1	21.1	3.0	3.0
	82-2	21.1	1.5	4.5
	83-1	0	6.0	-
	83-2	0	3.0	3.0
	83-3	0	1.5	4.5
JP-10	73-1	21.1	3.0	9.0
	73-2	21.1	6.0	6.0
	73-3	21.1	6.0	-
	79-1	21.1	6.0	-
	79-2	21.1	3.0	3.0
	79-3	21.1	1.5	4.5
	80-1	0	6.0	-
	80-2	0	3.0	3.0
	80-3	0	1.5	4.5
RJ-6	84-1	21.1	6.0	-
	84-2	21.1	3.0	3.0
	84-3	21.1	1.5	4.5
	85-1	21.1	6.0	-
	85-2	21.1	3.0	3.0
	85-3	21.1	1.5	4.5
	86-1	0	6.0	-
	86-2	0	3.0	3.0
	86-3	0	1.5	4.5

[a] HC/fuel - single hydrocarbon or fuel.

[b] Temperature of the single hydrocarbon or fuel in the sparger.

[c] Flow rate of air through liquid hydrocarbon in sparger.

[d] Flow rate of air in diluent stream.

TABLE 38. SUMMARY OF AVERAGED DETECTOR RESPONSES

Instrument	n-Heptane	JP-9	JP-10	RJ-6
Beckman I	38.7	34.9	13.3	2.4
Beckman II	37.0	30.4	7.3	1.8
GasTechtor	33.0[a]	25.7	8.0	4.2
MSA 100S	22.5	19.4	5.7	4.3
FID	27.0	24.8	6.0	3.3

[a]The averaged value of experimentally determined detector responses for the GasTechtor monitor (30% LEL) was multiplied by 1.11 to correct for calibration of this instrument with hexane.

TABLE 39. SUMMARY OF NORMALIZED DETECTOR RESPONSES

Instrument	n-Heptane	JP-9	JP-10	RJ-6
Beckman I	143	141	221	74
Beckman II	137	123	122	54
GasTechtor	122	104	133	127
FID	100	100	100	100
MSA 100S	83	78	96	130

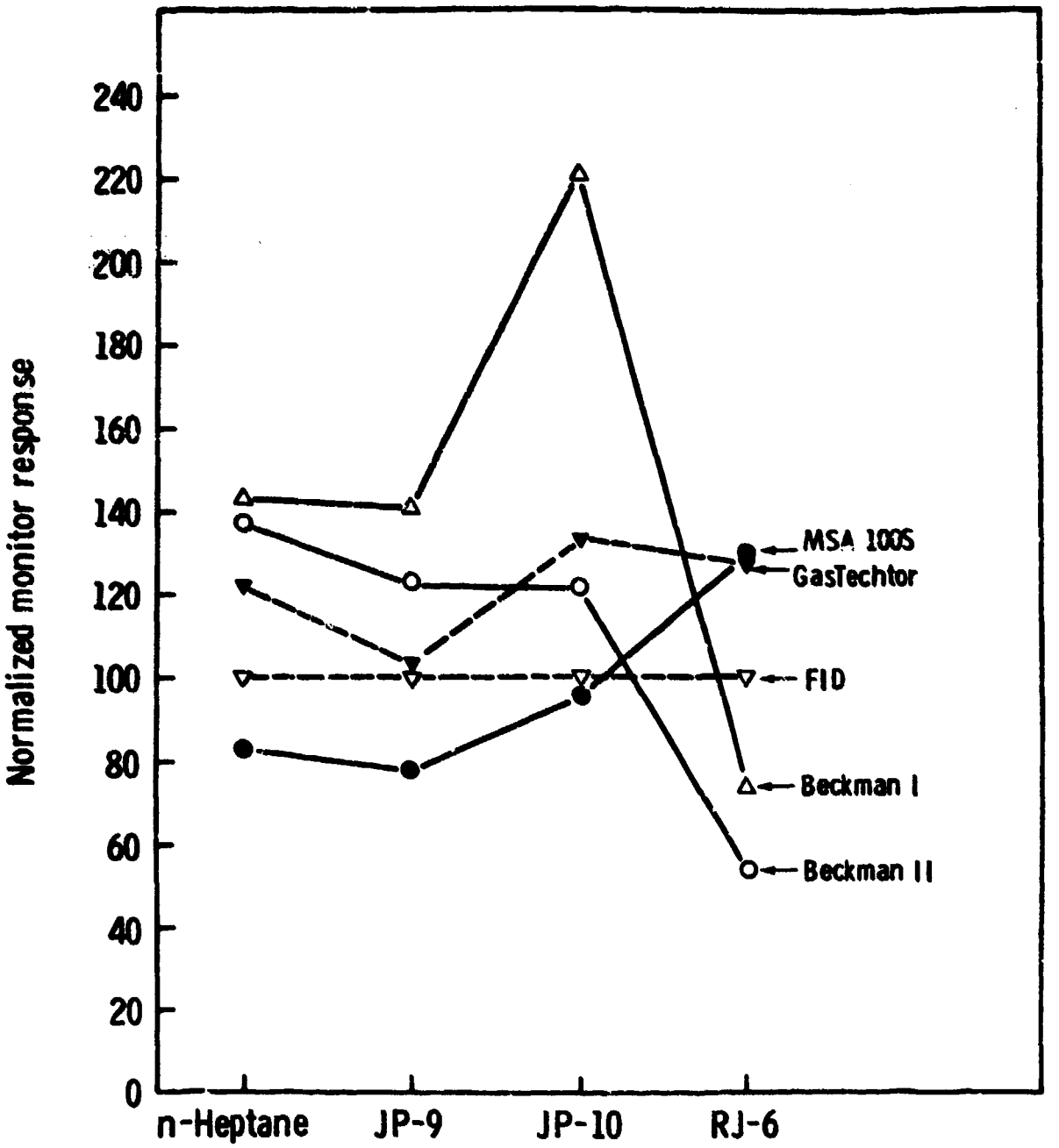

Figure 55. Combustible gas monitor responses normalized to the flame ionization detector response.

All instruments detected combustible vapors emanating from JP-9, JP-10, and RJ-6 in undiluted fuel vapor/air mixtures even when the fuels in the sparger were maintained at 0°C (32°F). Upon three-to-one dilution with air, vapors of JP-9 and JP-10 were still detected. However, the vapors of the lowest vapor pressure fuel included in this investigation, RJ-6, were not always detected upon dilution of the initially equilibrated vapor/air mixture.

The large differences in measured combustible gas concentrations, as determined with the different instruments, were attributed mainly to electronic drifts. Large drifts of the meter zero reading had been experienced in earlier work with short warm-up time (ref. 4). Upon that observation, a minimum warm-up time of 0.5 hr was used in all experiments. Despite this precaution, zero drifts ranging up to 10% LEL were experienced with the Beckman I monitor in the course of a sequence of experiments. At low combustible vapor concentration, such an error has a large effect on the value of the measured concentration, and also on the normalized response (see Table 39 and Figure 55).

Conclusions

1. The response characteristics of instruments included in this investigation were such that, despite a lack of accuracy, they would provide adequate warning when the workplace atmosphere becomes contaminated with JP-9, JP-10, or RJ-6 vapors. (This conclusion was based upon the presumption that the monitor alarms are set to provide audible or visible warning signals when the flammable vapor concentration in air reaches 25% of the LEL value.)

2. The combustible gas monitors did not enable accurate flammable vapor concentration measurements in air (see ref. 7).

3. The differences in results obtained with instruments produced by the same manufacturer, and carrying identical model designations, can be great.

4. Electronic instability was a major reason for the inaccuracy of concentration values determined with the Combustible Gas Indicator, Model TBA5100-1, manufactured by Beckman Instruments, Inc.

5. The concentrations of combustible vapors above JP-9, JP-10, and RJ-6 were 41%, 15%, and 8% LEL, respectively, when these fuels were equilibrated with air at 21°C (70°F).

Recommendations

1. Combustible gas monitors should be turned on and operated in standby mode for at least half an hour before use to stabilize the functioning of their electronic components.

2. For operation at temperatures above 32°C (90°F), an octane-air mixture is recommended as the calibration gas. A pre-mixed supply is most suitable for monitors that use small amounts of calibration gas, such as those included in this investigation.

14. ANALYSIS OF DEPOSITS ON A-10 AIRCRAFT AND SUPPLY TRUCK FUEL FILTERS

An investigation was conducted to determine the cause of fuel filter plugging in an A-10 aircraft. The investigation involved a detailed examination of the subject filter as well as the filter from a fuel supply truck. The techniques used for analysis were infrared spectrophotometry, emission spectroscopy and light microscopy.

Procedure and Results

The plastic ends were cut away from the A-10 and supply truck filters and sections of each filter were removed. The sections were then cut into small pieces and extracted with methylene chloride. The solvent from each extraction was carefully reduced in volume to a fraction of a milliliter. These small amounts of extract were then placed on rock salt plates and allowed to completely evaporate. Infrared absorption spectra of the residues showed weak bands characteristic of hydrocarbons. From the obviously small amount of material giving rise to the bands, and the nature of the overall absorption spectrum, it was concluded that the hydrocarbons were traces of jet fuel. Approximately the same amount was obtained from each filter.

The supply truck filter contained no residue and was generally very clean. The aircraft filter, however, had relatively large amounts of readily removable residue which was light and partially fibrous in nature. An emission spectrographic analysis of this residue was conducted to determine its metals content. Results are presented in Table 40.

TABLE 40. EMISSION SPECTROGRAPHIC ANALYSIS OF RESIDUE FROM A-10 AIRCRAFT FUEL FILTER

Element	Weight percent
Silicon	5
Calcium	3
Iron	2
Aluminum	2
Magnesium	0.8
Silver	0.7
Cadmium	0.6
Copper	0.6
Chromium	0.4
Tin	0.3
Sodium	0.3
Titanium	0.2
Manganese	0.1
Nickel	0.08

A portion of the A-10 filter residue was ground with potassium bromide (KBr) which was then used to press a pellet for infrared absorption analysis. Due to the nature of the material, the KBr pellet lacked the necessary transparency for a satisfactory spectrum to be obtained. Another KBr/sample pellet was prepared for analysis using Fourier Transform Infrared (FTIR) Spectroscopy. For this purpose, a Digilab FTS-15B Spectrometer was used. The general infrared pattern obtained and shown in Figure 56 is characteristic of a polyurethane prepared from a polyalkoxy alcohol. Absorption bands observed in the region (1730-1530 cm^{-1}) are characteristic of Amide I and II functional groups for polyurethanes. The strong broad band at 1111 cm^{-1} results from the polyether (aliphatic) moiety.

The IR pattern is not a simple, clean spectrum and may contain spectral data for polyurethane degradation products or for poorly formed polymer. The general region (1730-1300 cm^{-1}) contains many weak and overlapping bands which can be related to other amide type groupings. The unidentified, weak absorption at ca 2250-2260 cm^{-1} may have been due to nitrile (possibly isocyanate) residues.

The residue obtained from the aircraft fuel filter was obviously not a homogeneous material. It was approximately 70-80% consumed when ignited in a flame. The non-combustible part of the residue doubtless contained some terrestrial dust as suggested by the first five elements in Table 40. The major part of the residue was organic and a major part of the organic material appeared to have originated from the reticulated polyurethane foam used in fuel tanks for fire suppression. Polyurethanes of either the polyester or polyether type are used for that purpose, though the IR data indicated that the polyether type was used in the A-10 aircraft.

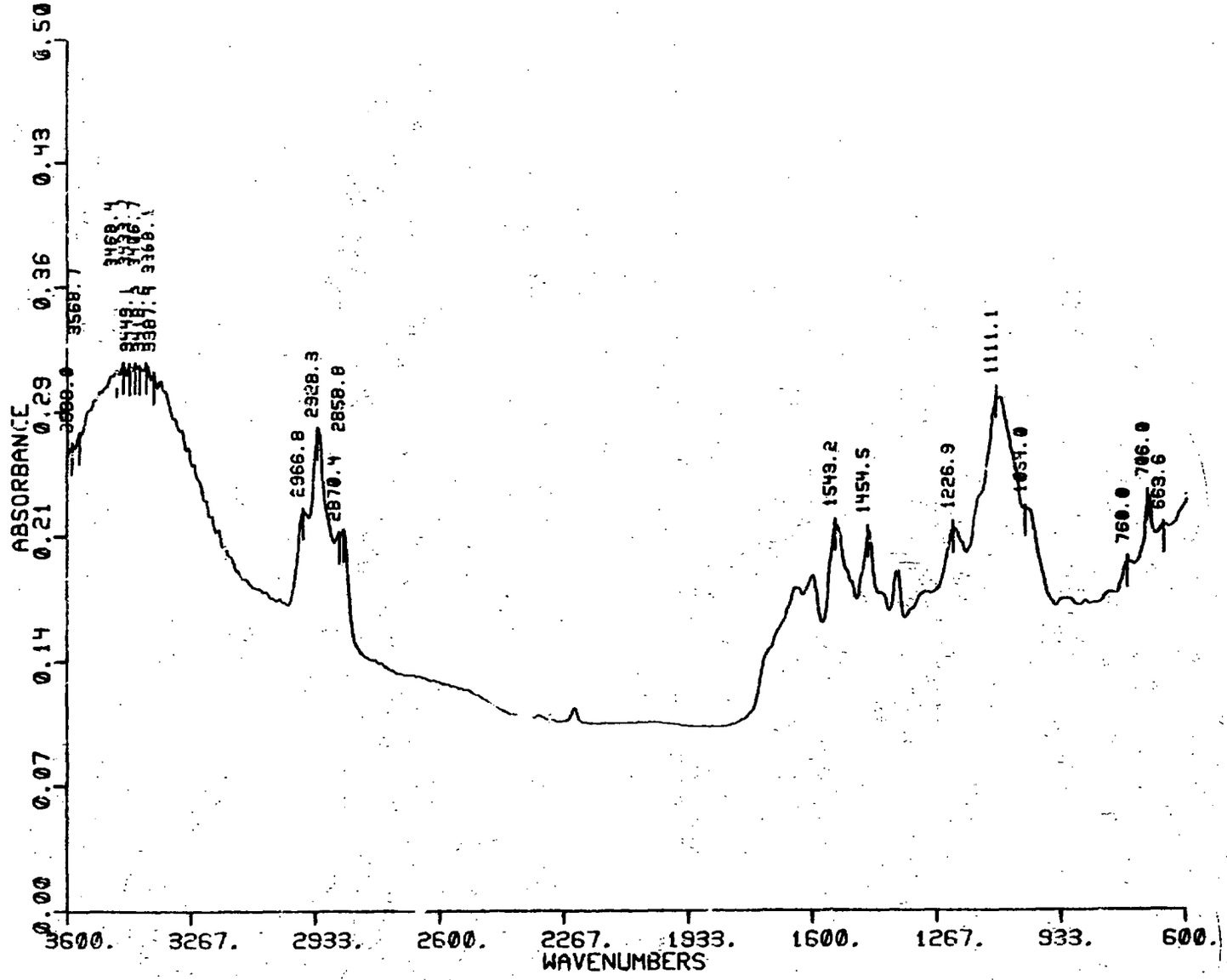

Figure 56. Fourier transform infrared spectrum of material from A-10 fuel-line filter.

Polyurethanes are known to be attacked by high humidity or water in the bottom of the fuel tank. Additionally, it has been shown that lead and/or tin at the ppm level in the anti-icing additive, ethylene glycol monomethyl ether (EGME), can cause foam degradation (ref. 8). Particles of degraded foam can be readily dislocated from the bulk block and become suspended in the fuel.

A portion of the A-10 fuel filter residue was further examined using light microscopy. By this means, the non-homogeniety of the residue became quite obvious. One puzzling feature of the residue was the presence of some fibers which did not appear to be polyurethane foam related. These appeared to be of a textile nature and in white, red, and blue colors. The IR data does not show the presence of cellulose (cotton), though for low levels of cellulose the major band could be obscured by the multitude of other overlapping bands. It could not be determined from the IR data whether the fibers were nylon because the amide bands from the polyurethane would obscure the polyamide (nylon) bands in the spectrum.

Conclusions

The residue which appeared on the A-10 aircraft filter did not appear on the filter from the supply truck and there was no evidence to suggest that the residue originated from that source. Rather, the residue appeared to be a collection of material consisting of dust (dirt) particles, degradation products from fuel tank foam, and fibers with a color and twist which suggested they were of a textile origin. The composition of the textile-type fibers was not established. They could have originated from clothes, or similar sources, but not from the filter itself since the colors did not match that of the filter.

15. MODIFICATION AND EVALUATION OF BALL-ON-CYLINDER FUEL LUBRICITY TESTER

Scope of Work to be Performed

The ball-on-cylinder (BOC) tester is the property of the Aero-propulsion Laboratory at Wright-Patterson Air Force Base. MRC was requested to investigate certain test variables as outlined by the Task Force Leader on the BOC Machine Operations' Task Force Committee. This committee was attempting to improve the precision and significance of the lubricity test. MRC work under this program encompassed three tasks:

(1) Upgrade the current flow system in the BOC; fill the cracks, crevices, and joints in the BOC test chamber with an epoxy sealant and then smooth the surfaces; and replace the bearings on the shaft rotating the test cylinder.

(2) Analyze the metallurgy of three test cylinders (numbers 108, 127, and 147) from a previous BOC round robin study to determine significant differences that might explain test results variations.

(3) Determine the repeatibility of the test method after upgrading the BOC tester.

Experimental

BOC Upgrading

The cracks, crevices, and joints in the BOC test chamber were filled with "EPOXY-PATCH" from Hysol Division of Dexter Corporation. This adhesive had been tested for fuel compatibility by bonding two pieces of glass together and then immersing the bond in JP-4 fuel for 72 hours. No discoloration of the fuel or

softening of the epoxy was observed. Additionally, new bearings for the shaft rotating the test cylinder were purchased and then installed to eliminate a chattering noise and excessive wear.

The BOC flow system was upgraded by recalibrating the flow meter for the wet and dry air inputs used to control relative humidity. The flow meters were calibrated with a Model 63115 Precision Scientific wet test meter having the range of 68-680 liters per hour flow rate. The flow rates at various rotameter settings were determined from the following equation:

$$V_s = \frac{P_m}{P_s} \times \frac{T_s}{T_m} \times V_m$$

where V_s = flow rate in liters per minute, corrected to standard atmospheric conditions

P_m = barometric pressure, mm Hg, corrected for water vapor pressure at temperature inside wet test meter

P_s = the standard barometric pressure, 760 mm

T_s = the standard temperature in degrees Kelvin, 273.16°K

T_m = the temperature measured inside the wet test meter, °K

V_m = measured gas flow in liters per minute, determined from the time it takes for a 3-liter volume of air to move through the wet test meter at ambient atmospheric conditions

The flow meter calibrations were conducted over a 3-day period. The barometric pressures, instrument temperatures, and pressure/temperature constants for those days are shown in Table 41.

TABLE 41. PRESSURE AND TEMPERATURE CONSTANTS FOR CALCULATING V_m ON A PARTICULAR DAY

Date	Instrument temp., °C	Barometric pressure, mm	$\frac{P_m}{P_s} \times \frac{T_s}{T_m}$
4/9/80	21.0	736.6	0.8772
4/10/80	23.5	735.9	0.8653
4/11/80	22.5	742.3	0.8775

The calibrated flow rates at various rotameter settings, before and after correction to standard atmospheric conditions, are represented in Table 42 (on the following page) along with the various test data used in the calculations. Significantly, the various values obtained for these rotameter calibrations were considerably different from those which had been used in all preceding tests on this device.

Metallurgy of Tested Cylinders

Test cylinders 108, 127, and 147 from a previous round robin study were tested for surface finish and Rockwell-C hardness. Test results are shown in Table 43.

Cylinder 108 was out of specification on surface finish because there was insufficient unused surface to obtain a proper measurement. Therefore, it was suggested either that future profilometer measurements be made on cylinders before the BOC test or that at least 1/4 inch of unused surface be reserved for subsequent measurements. Cylinder 127 did not meet hardness specifications. Consequently data from this cylinder were invalid.

Cylinders 108 and 127 were then sent to The Dayton Casting Company for chemical and metallography examinations. The chemical composition of both specimens met the specifications of low alloy AISI 52100 steel. Cylinder 108 had a Brinell hardness of 207 while Cylinder 127 had a Brinell hardness of 217. These readings showed both cylinders to be in the annealed condition. The cylinders were then sectioned and one section each was normalized. Sections in both the annealed and normalized conditions were examined under the microscope at 100 and 500 magnifications, but no defects or processing flaws were detected. The specimens in the annealed condition showed a fine dispersion of carbide in a ferrite matrix; this is normal for the annealed condition. The normalized condition showed that the matrix for both cylinders was comprised of

TABLE 42. FLOWMETER CALIBRATION

Test Date	Air Leg	Rotameter Reading	Flow Times for 3-Liters* of Air in Wet Test Meter — Minutes for Replicate Measurements	Average	V_m, liters per minute	V_s, liters per minute
4-9-80	Dry	6.0	0.9675; 0.9675; 0.970; 0.970; 0.970	0.969	3.096	2.716
4-9-80	Dry	7.0	0.775; 0.7725; 0.770; 0.770; 0.7725	0.772	3.886	3.409
4-9-80	Dry	8.0	0.635; 0.645; 0.645; 0.650; 0.645	0.644	4.658	4.086
4-9-80	Dry	9.0	0.560; 0.565; 0.5625; 0.565; 0.5625	0.563	5.329	4.675
4-9-80	Dry	10.0	0.505; 0.505; 0.505; 0.505; 0.500	0.504	5.952	5.221
4-9-80	Dry	11.0	0.455; 0.450; 0.450; 0.450; 0.445	0.450	6.667	5.848
4-9-80	Dry	12.0	0.410; 0.400; 0.405; 0.405; 0.400	0.404	7.427	6.515
4-9-80	Wet	2.5	5.295; 5.48; 5.25; 5.12; 5.17	5.263	0.095	0.083
4-9-80	Wet	3.0	3.74; 3.805; 3.78; 3.725; 3.68	3.746	0.133	0.117
4-9-80	Wet	3.5	2.54; 2.47; 2.50; 2.565; 2.535	2.522	0.198	0.174
4-9-80	Wet	4.0	1.94; 2.00; 1.955; 1.97; 2.00	1.973	0.253	0.222
4-9-80	Wet	4.5	1.545; 1.545; 1.495; 1.51; 1.52	1.523	0.328	0.288
4-9-80	Wet	5.0	1.25; 1.17; 1.25; 1.25; 1.16	1.216	0.410	0.360
4-9-80	Wet	5.5	1.065; 0.99; 1.05; 1.06; 0.99	1.031	0.484	0.425
4-9-80	Wet	6.0	0.915; 0.91; 0.91; 0.92; 0.91	0.913	0.547	0.480
4-9-80	Wet	6.5	0.81; 0.815; 0.81; 0.815; 0.81	0.812	0.613	0.538
4-10-80	Wet	7.0	4.54; 4.56; 4.51	4.537	0.661	0.572
4-10-80	Wet	7.5	4.07; 4.11; 4.07	4.083	0.735	0.636
4-10-80	Wet	8.0	3.76; 3.75; 3.75	3.753	0.799	0.691
4-10-80	Wet	8.5	3.63; 3.64; 3.64	3.637	0.825	0.714
4-10-80	Wet	9.0	3.31; 3.36; 3.35	3.340	0.898	0.777
4-11-80	7.0 Dry + 5.1 Wet		0.70; 0.70; 0.695; 0.70; 0.70	0.699	4.286	3.761
4-11-80	6.5 Dry + 8.75 Wet		0.705; 0.7025; 0.700; 0.700; 0.705	0.7025	4.270	3.747

*The times for only 0.5 liters of air were measured for Wet Leg Rotameter Readings of 2.5 through 6.5. These times were then multiplied by six to calculate V_m.

TABLE 43. SURFACE FINISH AND HARDNESS OF TEST CYLINDERS

Cylinder number	Surface finish, μ-in.	Rockwell-C hardness
108	5-12	20
127	4-9	16
147	4-9	21
Specification:	4-9	20-22

ferrite, pearlite, and iron carbide. Cylinder 108 showed carbides not as evenly dispersed as in 127 but more large areas of ferrite. Cylinder 127 showed more carbide than did Cylinder 108.

BOC Evaluation Study

A total of 26 BOC test runs were conducted on clay treated JP-4 to evaluate the general repeatability of the test method. Three different test cylinders, 25 different test balls, and two different percent relative humidity conditions were used in the study. The test cylinders and balls were thoroughly cleaned in alcohol, acetone, and hexane; dried in a vacuum oven in the presence of silica gel; and then stored in a desiccator prior to use. The shaft supporting the test cylinders was thoroughly cleaned and dried between test runs to eliminate the possibility of contamination from one run to the next. The test results are shown in Table 44. A statistical analysis of the test data is shown in Table 45.

Examination of the test data presented in Tables 44 and 45 leads to the following observations and conclusions:

TABLE 44. TEST DATA FROM REPLICATED BOC RUNS

Run Sequence	Date	Cylinder Number	Ball Number	%RH	Test Temp., °F		Wear Scar Diameters, mm		
					Room	Bath	Major Axis	Minor Axis	Average
1	4-14-80	88	105A	10	69.5	73	1.07	0.94	1.01
4	4-14-80	88	105D	10	67	73	0.94	0.83	0.89
5	4-14-80	88	105E	10	67	73	1.02	0.89	0.96
8	4-15-80	88	106C	10	66	77	0.84	0.57	0.71
9	4-15-80	88	106D	10	66	76	0.61	0.53	0.57
2	4-14-80	88	105B	20	70.5	73.5	0.81	0.72	0.77
3	4-14-80	88	105C	20	68	73	0.72	0.65	0.69
6	4-15-80	88	106A	20	66.5	72	0.86	0.77	0.82
7	4-15-80	88	106B	20	66	76	0.86	0.76	0.81
10	4-15-80	88	106E	20	66	78.5	0.76	0.67	0.72
11	4-16-80	202	107A	10	71.5	75.5	0.85	0.75	0.80
14	4-18-80	202	109A	10	69.5	78.5	0.71	0.62	0.67
15	4-18-20	202	109B	10	69	78.5	0.69	0.61	0.65
16	4-18-20	202	109C	10	69	78.5	0.64	0.57	0.61
17	4-18-20	202	109D	10	69.5	78	0.63	0.54	0.59
18	4-21-80	202	112A	10	69.5	79.5	0.60	0.51	0.56
12	4-16-80	202	107A	20	72	77	0.92	0.81	0.87
13	4-16-80	202	107B	20	74	77	0.69	0.61	0.65
19	4-21-80	202	112B	20	70.5	78.5	0.62	0.55	0.59
20	4-21-80	202	112C	20	70.5	78	0.78	0.68	0.73
21	4-21-80	202	112D	20	70.5	78	0.86	0.76	0.81
22	4-22-80	202	113A	20	70.5	76	0.60	0.51	0.56
23	4-22-80	202	113B	20	70.5	75.5	0.73	0.65	0.69
24	4-22-80	184	113C	20	71	77	0.73	0.66	0.70
25	4-22-80	184	113D	20	71	76	0.82	0.72	0.77
26	4-22-80	184	113E	20	71	76.5	0.64	0.55	0.60

TABLE 45. PRECISION CALCULATIONS FOR BOC TEST DATA

Test parameters compared				Average wear	σ Of
Cylinder number	% RH	Runs	Days	diameter, mm	average
88	10	5	2	0.83	0.18
88	20	5	2	0.76	0.06
202	10	6	3	0.65	0.09
202	20	7	4	0.70	0.11
184	20	3	1	0.69	0.09
88	10, 20	10	2	0.80	0.13
202	10, 20	13	4	0.68	0.10
88, 202	10	11	5	0.73	0.16
88, 202, 184	20	15	5	0.72	0.09
All	10, 20	26	6	0.72	0.12

(a) The percent relative standard deviation for the average of all 26 runs was ±17%. This precision was approximately the same whether only one or multiple test cylinders were used.

(b) The overall precision for the runs at 20% RH (0.09 σ) was significantly better than the precision at 10% RH (0.16 σ).

(c) It was suspected that a major part of the precision problem may have been due to nonhomogeneity of the test balls. This may explain the lack of a consistent difference in ball wear between the major and minor axis.

(d) More test data should be generated to evaluate the effects of relative humidity and ball variation on test precision.

16. DETERMINATION OF PRECISION FOR THE SIMULATED DISTILLATION ANALYSIS, ASTM D 2887

Background

Simulated distillation analyses by gas chromatography were conducted on 19 blind repeat fuel samples which had been analyzed earlier at times that varied from 3 to 10 months. The repeat

samples were not the same samples analyzed earlier but were fresh samples taken from the same drums of fuel. Since significant differences occurred in some of the replicated test results, the data were evaluated to determine whether specific trends and causes could be identified.

Evaluation of Test Data

The test data for nineteen pairs of duplicate samples are compared in Table 46. Table 47 shows differences in selected percent recovery values for the second set of data as compared to the first. This is essentially a measure of reproducibility since different samples were analyzed at different times against different calibration curves. The chromatograms and computer data processing charts were evaluated to insure there were no obvious errors in any of the analyses and then the data in Tables 46 and 47 were studied to enable some conclusions to be drawn about the test result variations. The ASTM method allows the following reproducibility values: 8.3°C for initial boiling point, 3.3°C for 5% recovered, 3.9°C for 10% recovered, 4.5°C for 50% recovered, 5.6°C for 95% recovered, and 13.4°C for final boiling point.

Conclusions

(a) With the exception of initial boiling point, most of the test data (particularly final boiling points) fell within the acceptable ASTM guidelines for reproducibility.

(b) Because of the extended length of time between repeat analyses, the variations in our test results would be expected to be larger than those encountered by a single laboratory conducting duplicate analyses of the same fuel.

TABLE 46. DUPLICATE SIMULATED DISTILLATIONS OVER VARIOUS TIME SPANS

Pair Number:	1		2		3		4		5		6		7		8		9		10		11	
Hrs.Between Runs:	1 3/4		1 3/4		1 3/4		1 3/4		1 3/4		1 3/4		7		8 5½		9 7		10 5½		11 7	
Sample Numbers:	S3A	80-1	S4A	80-2	S8A	80-3	S9A	80-4	S56A	80-5	S57A	80-6	800	80-7	RG0	80-8	8X0	80-9	X40	80-10	4X0	80-11
Percents	°C at Which Indicated Percents Were Recovered																					
0.5 (IBP)	139	140	139	145	21	29	77	93	104	118	98	116	128	140	128	142	80	86	31	38	32	40
1	151	151	151	157	28	37	92	111	127	136	120	133	144	150	145	151	97	99	44	57	40	57
5	184	182	184	188	64	68	156	162	170	170	167	169	176	174	177	178	144	141	91	89	82	83
10	199	197	199	204	87	88	178	178	184	183	182	184	190	186	189	190	156	152	106	106	101	98
20	219	218	219	226	106	103	195	195	198	197	197	197	203	199	203	204	165	160	140	135	123	118
30	236	232	236	241	120	119	206	205	209	209	208	209	214	210	213	216	167	164	157	151	145	139
40	251	248	251	255	140	134	216	216	218	216	217	218	222	219	222	226	171	168	166	161	161	153
50	263	260	263	269	161	151	223	222	225	225	224	228	231	226	232	236	177	176	168	93	166	161
60	276	273	275	283	182	173	232	231	236	234	233	236	239	236	240	244	197	194	170	169	170	168
70	290	286	289	299	201	193	240	240	242	244	240	246	249	245	253	259	216	213	174	172	178	180
80	305	304	305	315	219	215	252	250	254	255	253	251	259	256	266	275	232	232	181	189	203	203
90	325	329	328	340	238	236	263	263	266	270	265	272	272	271	289	303	254	256	221	221	232	232
95	344	347	343	360	254	253	271	270	274	285	273	285	282	283	310	323	-	273	246	247	-	252
99	375	371	373	386	271	271	286	279	295	304	292	301	300	299	343	350	291	296	292	282	278	280
99.5 (FBP)	380	375	379	391	279	276	290	280	302	307	299	305	306	301	355	354	301	300	305	289	289	285

Pair Number:	12		13		14		15		16		17		18		19	
Hrs.Between Runs:	7		7		4		4		4		2		2		2	
Sample Numbers:	4GX	8-12	DF2	8-13	13B	BRF13	14B	BRF14	9B	BRF9	8C	CRF8	13C	CRF13	14C	CRF14
Percents	°C at Which Indicated Percents Were Recovered															
0.5 (IBP)	28	34	132	146	121	138	122	140	25	30	40	38	139	147	124	150
1	36	42	147	159	141	151	153	154	36	40	53	50	150	162	152	164
5	78	76	180	186	177	181	178	182	71	69	67	62	194	193	188	190
10	98	92	197	199	196	199	196	196	89	89	90	82	211	211	204	203
20	121	117	216	218	222	221	216	218	105	101	166	142	236	234	227	225
30	143	133	231	234	240	241	231	230	126	120	189	179	254	253	232	234
40	164	154	24[illegible]	247	255	256	242	246	150	143	206	195	269	268	250	250
50	178	171	256	259	271	271	255	258	174	167	218	211	282	282	262	262
60	204	192	271	272	287	287	271	273	198	189	230	225	296	295	278	276
70	230	216	284	287	302	304	287	291	218	210	234	232	308	308	295	291
80	264	244	300	304	318	319	306	312	232	230	250	247	322	324	311	308
90	301	288	318	329	340	344	331	338	253	253	264	263	342	347	332	328
95	318	313	333	349	362	363	351	360	267	273	281	278	359	366	348	343
99	342	344	343	375	400	392	393	396	294	302	322	302	399	394	381	362
99.5 (FBP)	346	352	373	379	409	397	404	404	301	307	330	306	407	399	388	364

TABLE 47. DIFFERENCES IN RESULTS BETWEEN DUPLICATED SIMULATED DISTILLATIONS

	°C Change in Second Result Compared to the First Result																			Average Net Change[a]	Average Deviation[b]	ASTM Deviation Limits[c]
Pair Number:	1	2	3	4	5	6	7	8	9	10	11	12	13	14	15	16	17	18	19			
Time Span, Mos:	1 3/4	1 3/4	1 3/4	1 3/4	1 3/4	1 3/4	7	5½	7	5½	7	7	7	4	4	4	2	2	2			
% Recovered																						
0.5 (IBP)	+1	+6	+8	+16	+14	+18	+12	+14	+6	+7	+8	+6	+14	+17	+18	+5	-2	+17	+26	+11.1	‡11.3	‡8.3
1.0	0	+6	+9	+19	+9	+13	+6	+6	+2	+13	+17	+6	+12	+10	+1	+4	-3	+12	+12	+8.1	‡8.4	-
5.0	-2	+4	+4	+6	0	+2	-2	+1	-3	-2	+1	-2	+6	+4	+4	-2	-5	-1	+2	-0.8	‡2.8	‡3.3
10.0	-2	+5	+1	0	-1	+2	-4	+1	-4	0	-3	-6	+2	+3	0	0	-8	0	-1	-0.8	‡2.2	‡3.9
50.0	-3	+6	-10	-1	0	+4	-5	+4	-1	-5	-5	-6	+3	0	+3	-7	-7	0	0	-1.6	‡3.7	‡4.5
95	+3	+17	-1	-1	+11	+12	+1	+13	xx	+1	xx	-5	+15	+1	+9	+6	-3	+7	-5	+4.8	‡6.6	‡5.6
99.5 (FBP)	-5	+12	-7	-10	+ 5	+6	-5	-1	-1	-16	-4	+6	+6	-12	0	+6	-24	-8	-24	-4.3	‡8.1	‡13.4

[a] Useful for determining randomness of deviations.
[b] Without regard to sign.
[c] Reproducibility values from ASTM D 2887.

(c) The fact that the initial boiling points were almost always higher for the second analysis strongly suggests that small amounts of the low boiling compounds may have been lost from the fuels during the time period between analyses.

(d) An examination of the chromatograms for repeat analyses did not reveal gross differences. Most of the deviations in test results with the exception of initial boiling point can be attributed to normal instrumental and experimental variations. However, exceptionally poor reproducibility was obtained for sample pairs 17 and 19. For these pairs, final boiling points differed by 24 degrees centigrade. Examination of chromatograms and raw data for pair 19 shows that the samples exhibited substantial tailing after the final chromatographic peak. In such cases, accurate determination of final boiling point is more subject to error because of the extremely flat count-rate plot (counts accrued versus retention time).

Recommendations

It was recommended that better controlled experiments be conducted if additional information is required regarding the precision of the simulated distillation analysis. Replicate analyses of the same sample should be conducted at one time to determine method repeatability. Then, several days later the same sample should be reanalyzed against a new set of standards to determine method reproducibility.

Because of the indicated loss of volatiles from the test fuels during storage, as indicated by initial boiling point data, it was recommended that improved methods for long-term storage of fuels should be investigated.

17. CHARACTERIZATION OF BLENDED ERBS FUELS FROM NASA

A large number of physical and chemical properties were determined for four samples of blended ERBS fuels being used by NASA-Lewis Research Center, in tests to evaluate broad specification fuels.

Vapor Pressure, Surface Tension, and Kinematic Viscosity

Vapor pressure, surface tension, and kinematic viscosity were determined as a function of temperature, and these properties are presented in Table 48. Vapor pressure was determined by use of the micro-vapor pressure apparatus and procedure described in (ref. 9). Surface tension was determined by the capillary rise method. Kinematic viscosity was determined by ASTM Method D 445, and the viscosity/temperature plots are presented in Figures 57-60.

Hydrocarbon-Type Analyses by Three Methods

Hydrocarbon type analyses were conducted by three mass spectrometric methods. The first consisted of a separation into paraffinic and aromatic fractions using the procedure described in ASTM D 2549, followed by the mass spectrometric analysis described in ASTM D 2425. The second method used a modification of ASTM D 2789. The third method, Monsanto Method 21-PQ-38-63, was developed for hydrocarbon feed stocks.

The results of all three analyses are presented in Table 49.

TABLE 48. VAPOR PRESSURE, SURFACE TENSION, AND KINEMATIC VISCOSITY

Property	Temp., °F	Test fuels 3S	3B	3B-11.8	3B-12.3
Vapor Pressure, mm mercury	32	9.0	8.0	8.0	4.0
	70	18.0	12.5	14.5	8.0
	100	28.5	16.5	22.5	13.5
Surface Tension, dynes/cm	-20[a]	34.86	32.60	33.02	32.95
	32	32.10	29.79	30.47	30.25
	70	30.05	27.71	28.59	28.27
	100	28.47	26.07	27.13	26.71
Kinematic Viscosity, centistokes	-4	4.626	8.187	6.037	6.920
	32	2.649	4.186	3.305	3.668
	104	1.286	1.789	1.509	1.633
	140	0.9955	1.331	1.152	1.232

[a]Values at this temperature were obtained by extrapolation of data from the higher temperatures.

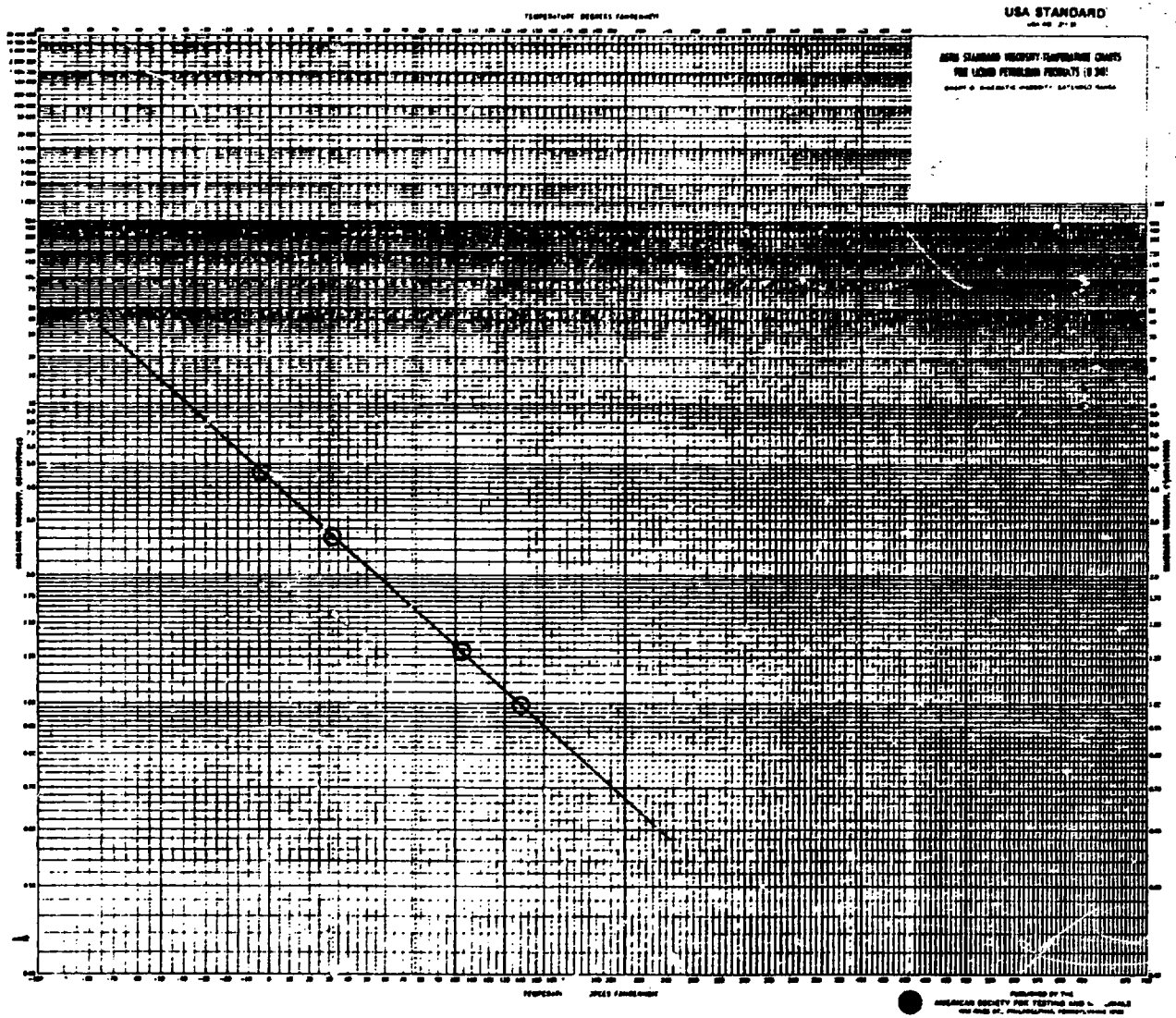

Figure 57. Viscosity/temperature plot for ERBS fuel 3S.

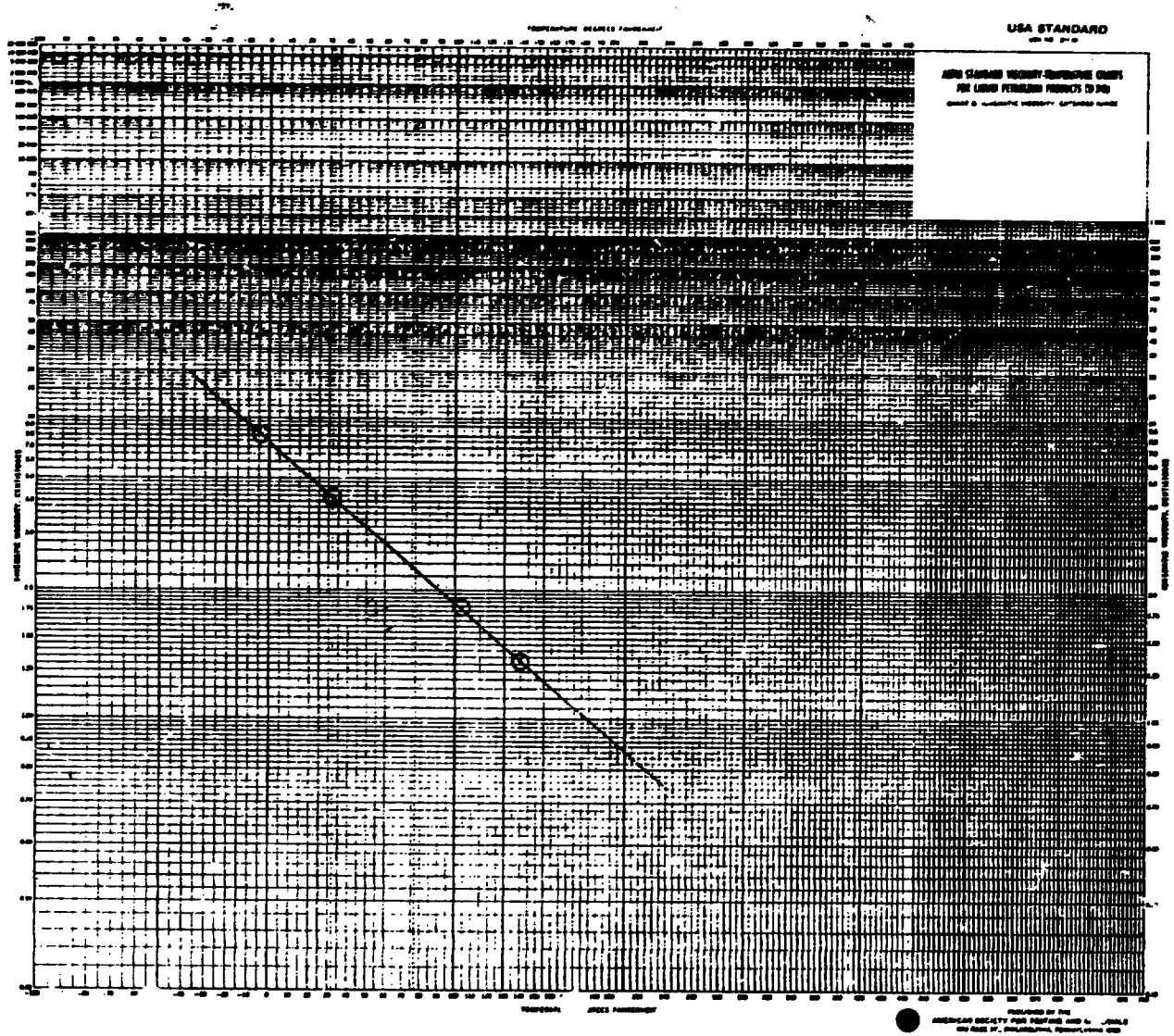

Figure 58. Viscosity/temperature plot for ERBS fuel 3B.

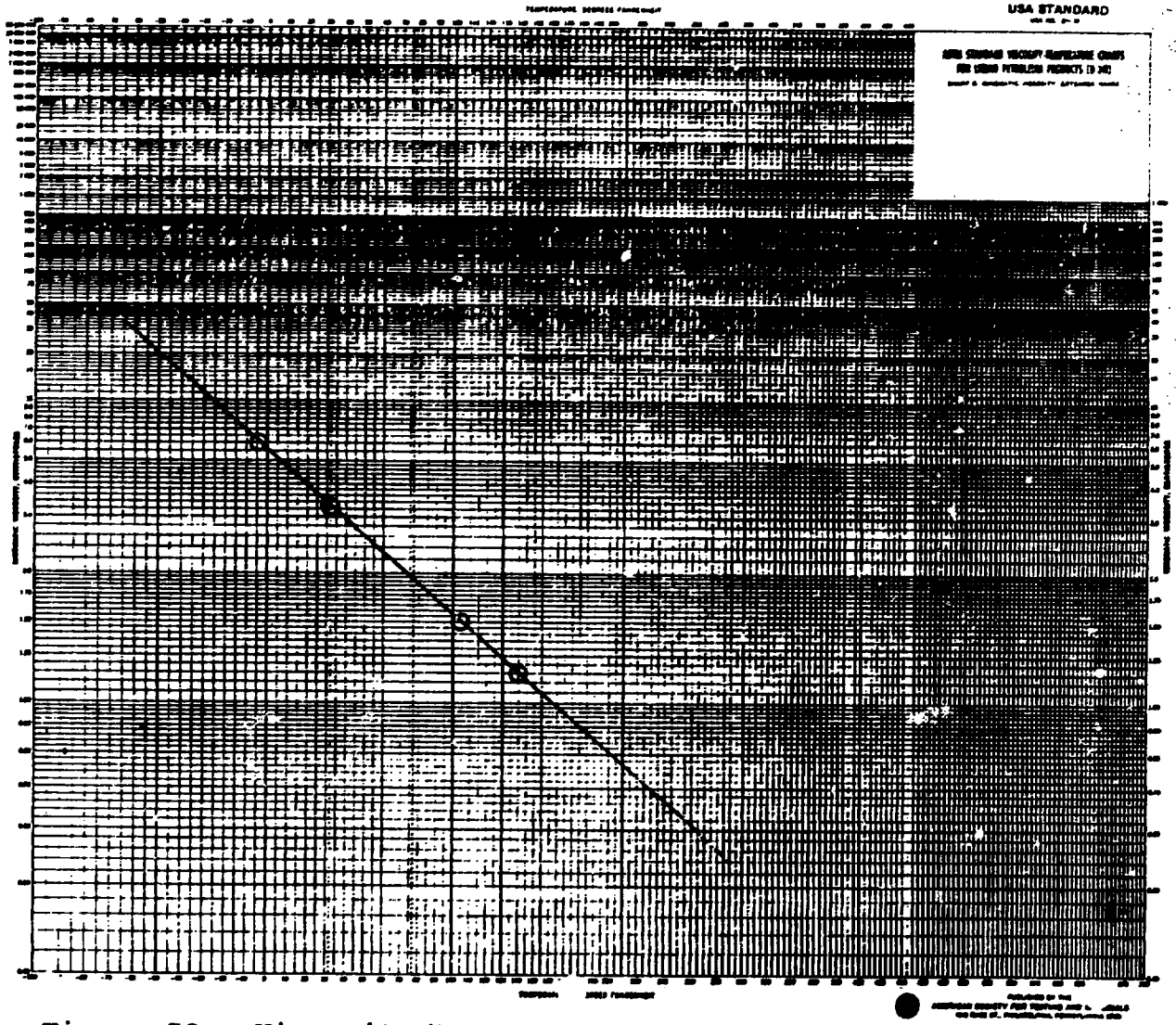

Figure 59. Viscosity/temperature plot for ERBS fuel 3B-11.8.

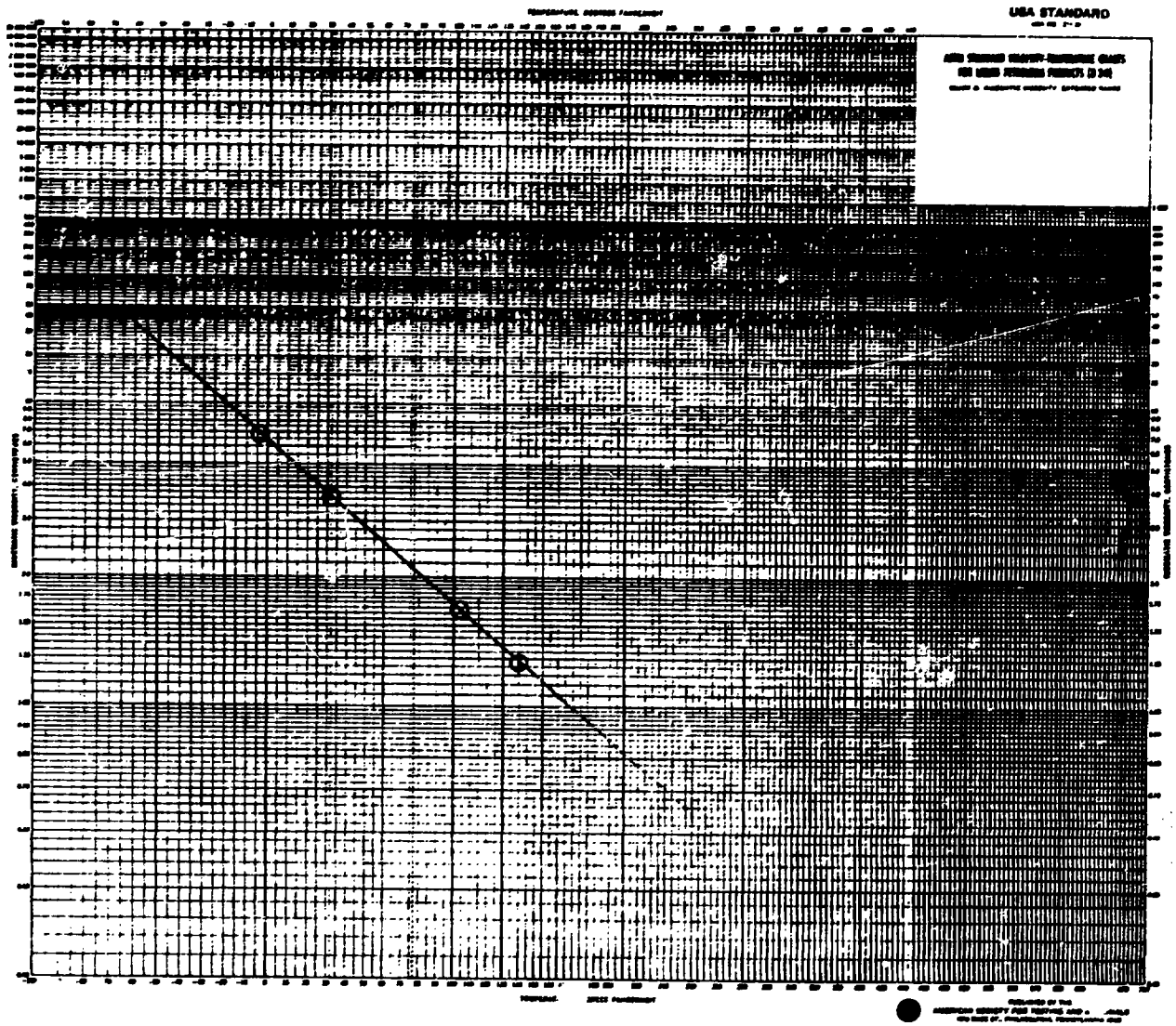

Figure 60. Viscosity/temperature plot for ERBS fuel 3B-12.3.

TABLE 49. HYDROCARBON TYPE ANALYSIS OF THE ERBS FUELS BY THREE METHODS, IN WEIGHT PERCENTS

Fuel Number:	3S			3B			3B-11.8			3B-12.3		
Analytical Method:[a]	D2425	D2789	MONS	D2425	D2789	MONS	D2425	D2789	MONS	D2425	D2789	MONS
Compound												
Paraffins	17.0	16.6	13.9	38.7	43.4	42.1	30.0	32.9	30.0	37.7	37.4	35.1
Monocycloparaffins	3.7	6.4		14.6	27.5		10.3	19.5		14.1	22.9	
Dicycloparaffins	2.9	1.0		7.2	2.8		5.3	2.2		6.9	2.7	
Tricycloparaffins	0.9			2.1			1.5			1.9		
Total-Cycloparaffins[b]	7.5	7.4	6.7	23.9	30.3	29.3	17.1	21.7	19.8	22.9	25.6	24.1
Alkyl benzenes	35.3	54.5	55.1	9.8	8.0	9.7	21.6	26.3	29.5	13.0	17.9	20.8
Indans/tetralins	5.8	5.2	5.1	7.9	9.4	7.5	7.1	7.6	6.3	7.0	8.8	7.0
Indenes	-[c]		-	1.2		-	0.5		-	0.5		-
Naphthalene	-			-			-			-		
Naphthalenes	22.3	16.3	19.2	12.2	8.9	11.4	15.9	11.5	14.4	12.4	10.3	13.0
Acenaphthenes	5.3			3.0			3.6			3.1		
Acenaphthylenes	3.9			2.0			2.6			2.1		
Tricyclic aromatics	2.9			1.3			1.6			1.3		
ASTM D2549 Fractionation												
wt % aliphatics:	29.8			62.2			53.5			60.2		
wt % aromatics:	70.2			37.8			46.6			39.8		

[a] For analytical methods, D 2425 designation indicates that fuel was first fractionated according to ASTM D 2549 and then analyzed by ASTM D 2426; D 2789 designation indicates that the fuel was analyzed by a modification of ASTM D 2789 and MONS designation indicates that Monsanto Method 21-PQ-38-63 was used.

[b] Total of mono-, di-, and tri- cycloparaffins listed above.

[c] A dash indicates that the compound was included in the analysis but none was detected. A blank space in the table indicates that the compound was not included in the analysis.

Although the results for ASTM Method D 2789 were determined in volume percent, the values in Table 49 are presented in weight percents for the purpose of comparison with the other two methods. The determined volume percents and density values used to calculate weight percents are provided in Table 52 (see the next topic).

For the ASTM D 2425 analysis of Sample 3S, 6.2% of the 35.5% alkylbenzenes appeared in the aliphatic fraction. This fact indicates that there was some breakthrough of aromatics into the aliphatic fraction during the elution chromatographic separation described in ASTM D 2549. Only 0.3% alkylbenzenes appeared in the aliphatic fractions of the other three samples.

Determination of Fuel Aromaticity by NMR and Mass Spectrometry

Scope of Data Provided

Carbon-13 NMR analyses were conducted to determine carbon aromaticity, which is a ratio of aromatic carbon in the fuel to the total carbon. Proton NMR analyses were conducted to determine hydrogen aromaticity, which is a ratio of aromatic hydrogen in the fuel to the total hydrogen. Using these aromaticity values and the ratio of total hydrogen to total carbon (obtained from elemental hydrogen analyses by a wide-line NMR method conducted at AFWAL/POSF), the ratio of aromatic hydrogen to aromatic carbon was then calculated for the four fuels. The total areas under peaks in specified spectral regions of the proton NMR curves are also provided for use in the AFWAL/POSF computer program, if desired.

Carbon aromaticity was then calculated from the ASTM D 2789 hydrocarbon type analysis data in order to compare with the NMR results. An average compound structure was formulated for each fuel constituent using an average carbon number determined from simulated distillation analyses. The percent of aromatic and aliphatic carbon in each fuel constituent was calculated from

the weight percentages and average compound structures. The carbon aromaticity of the entire fuel was then calculated from the ratio of total aromatic carbon to total carbon in the fuel.

Aromaticity by NMR Analyses

The NMR analyses were conducted on a Varian CFT-20 Fourier transform spectrometer containing a Varian 602L computer for data acquisition, data reduction, and system control. The spectrometer was operated at 20 megahertz for the ^{13}C analyses and 79.54 megahertz for the proton NMR analyses. The following instrument conditions were utilized for the two analyses:

Type NMR Analysis:		Carbon-13	Proton (^{1}H)
Sample probe		8 mm	5 mm
Sweep width		4,000 Hz	1,000 Hz
Number of transients		1,000	50
Acquisition time		1.023 s	4.095 s
Pulse width 90°		17 μ/s	24 μ/s
Pulse delay		5 s	8 s
Homo-spoil time[a]		Not on	4 m/s
Data points		8,192	8,192
Decoupler mode		3[b]	--
Chemical shift regions for integral data	Aromatics	~150-110 ppm	8.3-6.5 ppm
	Aliphatics	~70-4 ppm	4.0-0.2 ppm

[a]Homo-spoil was on during pulse delay.

[b]The gated proton decoupler was on during acquisition and off during delay.

The analytical samples were prepared for carbon-13 analysis by mixing the following components:

Jet fuel sample - 1 ml

NMR lock solvent - 0.5 ml deuterated chloroform ("100%" $CDCl_3$)

Chemical shift reference - 50 µl hexamethyl disiloxane
Relaxation agent - ~25 mg 2,4-pentanedione chromium III derivative

For the proton NMR analysis, a 20 µl quantity of the above mixture was added to 0.5 ml additional $CDCl_3$.

The carbon aromaticity values were obtained by integrating the peak areas in the aromatic region of the ^{13}C spectra relative to the total peak area in the spectra. The hydrogen aromaticities were obtained in the same manner from peak areas in the proton NMR spectra. The ratio of aromatic hydrogen to aromatic carbon was obtained from the following equation:

$$\frac{H_{ar}}{C_{ar}} = \underset{I}{\frac{C_T}{C_{ar}}} \times \underset{II}{\frac{H_{ar}}{H_T}} \times \underset{III}{\frac{H_T}{C_T}}$$

where I = the inverse of carbon aromaticity determined by ^{13}C NMR

II = the hydrogen aromaticity determined by proton NMR

III = total hydrogen/carbon ratio determined from percent hydrogen data provided by AFWAL/POSF

The aromaticity values for the four fuels and their aromatic and total hydrogen/carbon ratios are presented in Table 50. The integrated areas for the specified spectral regions of the proton NMR spectra are listed in Table 51.

Carbon Aromaticity from Mass Spectrometric Analysis Data

Carbon aromaticity was calculated from the ASTM D 2789 hydrocarbon-type analysis data presented in Table 49. Volume percents obtained by this method were re-computed to weight percents using average density values, and an average compound structure was

TABLE 50. AROMATICITY VALUES AND HYDROGEN/CARBON RATIOS

Sample designation	Carbon aromaticity,[a] C_{ar}/C_T	Hydrogen aromaticity,[a] H_{ar}/H_T	Weight percent[b] H_T	Mole ratio[c] H_T/C_T	Mole ratio H_{ar}/C_{ar}
ERBS-3S	0.542±0.009	0.244±0.003	10.34	1.37	0.617
ERBS-3B	0.194±0.006	0.072±0.007	12.95	1.77	0.657
3B-11.8	0.355±0.015	0.135±0.008	11.85	1.60	0.608
3B-12.3	0.273±0.010	0.110±0.003	12.38	1.68	0.677

[a]The reported values represent the average of three integrations per sample.

[b]Data from AFWAL/POSF.

[c]Total carbon data were obtained by subtracting the $\%H_T$ from 100.

TABLE 51. INTEGRATED AREAS[a] OF SPECIFIED PROTON NMR SPECTRAL REGIONS

Samples	HMONO 6.6-7.3, ppm	HDI 7.3-7.8, ppm	HTRI 7.8-8.3, ppm	HALP-1 2.3-4.0, ppm	HALP-2 1.9-2.3, ppm	H BETA 1.9-1.0, ppm	H GAMA 1.0-0.5, ppm	H BETH 1.90-1.65, ppm
3S	16	3	ND[b]	8	18	22	10	3
3B	5	2	ND	6	4	45	30	2
3B-11.8	9	3	ND	5	10	37	22	3
3B-12.3	8	2	ND	3	7	40	27	2

[a]The listed integral areas are accurate to ±0.5. Fractional values are rounded to the nearest whole number by the data system.

[b]ND shows a value less than 0.5.

formulated for each fuel constituent using the average carbon number from a GC simulated distillation analysis. The percents of aromatic and aliphatic carbon in each fuel constituent were calculated from the weight percentages and compound structures. The carbon aromaticity of the entire fuel was then calculated from the ratio of total aromatic carbon to total carbon in the fuel. These results and all data used in the calculations are shown in Table 52. A comparison of carbon aromaticities from the NMR analyses is also provided in this table.

TABLE 52. CARBON AROMATICITY FROM HYDROCARBON-TYPE ANALYSIS DATA

Fuel Constituents	Density, g/cc	Vol., %[a]	Wt., %[b]	Carbon No.[c]	Empirical Chemical Formula	Average Structure Assigned[d]	Mass Spectrometry: Mole Percent Aromatic Carbon[e]	Mass Spectrometry: Mole Percent Aliphatic Carbon	Mass Spectrometry: Carbon Aromaticity	^{13}C NMR: Carbon Aromaticity
ERBS FUEL 3E										
				13.30						
Paraffins	0.75	19.1	16.6	13.3	C_xH_{2x+2}	$C_{13.3}H_{28.6}$	0	15.8		
Monocycloparaffins	0.81	6.8	6.4	13.3	C_xH_{2x}	$C_{13.3}H_{26.6}$	0	6.3		
Dicycloparaffins	0.81	1.1	1.0	13.3	C_xH_{2x-2}	$C_{13.3}H_{24.6}$	0	1.0		
Alkylbenzenes	0.87	54.1	54.5	13.3	$C_6H_5-C_xH_{2x+1}$	$C_{13.3}H_{19.6}$	26.6	28.0		
Indans/tetrelin	0.93	4.8	5.2	13.3	$C_6H_4-C_xH_{2x-1}$	$C_{13.3}H_{16.6}$	2.6	2.7		
Naphthalenes	1.00	14.1	16.3	13.3	$C_{10}H_7-C_xH_{2x+1}$	$C_{13.3}H_{13.6}$	13.8	3.2		
						Totals	43.0	57.0	0.43	0.54
ERBS FUEL 3B										
				13.03						
Paraffins	0.75	46.8	43.4	13.0	C_xH_{2x+2}	$C_{13}H_{28}$	0	42.4		
Monocycloparaffins	0.81	27.5	27.5	13.0	C_xH_{2x}	$C_{13}H_{26}$	0	27.2		
Dicycloparaffins	0.81	2.8	2.8	13.0	C_xH_{2x-2}	$C_{13}H_{24}$	0	2.8		
Alkylbenzenes	0.87	7.5	8.0	12.0	$C_6H_5-C_xH_{2x+1}$	$C_{12}H_{18}$	4.1	4.1		
Indans/tetrain	0.93	8.2	9.4	12.0	$C_6H_4-C_xH_{2x-1}$	$C_{12}H_{16}$	4.9	4.9		
Naphthalenes	1.00	7.2	8.9	12.0	$C_{10}H_7-C_xH_{2x+1}$	$C_{12}H_{12}$	8.0	1.6		
						Totals	17.0	83.0	0.17	0.19
ERBS FUEL 3B-11.8										
				13.03						
Paraffins	0.75	36.4	32.9	13.0	C_xH_{2x+2}	$C_{13}H_{28}$	0	31.8		
Monocycloparaffins	0.81	20.0	19.5	13.0	C_xH_{2x}	$C_{13}H_{26}$	0	19.3		
Dicycloparaffins	0.81	2.2	2.2	13.0	C_xH_{2x-2}	$C_{13}H_{24}$	0	2.1		
Alkylbenzenes	0.87	25.1	26.3	12.0	$C_6H_5-C_xH_{2x+1}$	$C_{12}H_{18}$	13.3	13.4		
Indans/tetralin	0.93	6.8	7.6	12.0	$C_6H_4-C_xH_{2x-1}$	$C_{12}H_{16}$	3.9	3.9		
Naphthalenes	1.00	9.5	11.5	12.0	$C_{10}H_7-C_xH_{2x+1}$	$C_{12}H_{12}$	10.2	2.1		
						Totals	27.4	72.6	0.27	0.35
ERBS FUEL 3B-12.3										
				13.03						
Paraffins	0.75	41.0	37.4	13.0	C_xH_{2x+2}	$C_{13}H_{28}$	0	36.5		
Monocycloparaffins	0.81	23.2	22.9	13.0	C_xH_{2x}	$C_{13}H_{26}$	0	22.5		
Dicycloparaffins	0.81	2.7	2.7	13.0	C_xH_{2x-2}	$C_{13}H_{24}$	0	2.6		
Alkylbenzenes	0.87	16.9	17.9	12.0	$C_6H_5-C_xH_{2x+1}$	$C_{12}H_{18}$	9.2	9.1		
Indans/tetralin	0.93	7.7	8.8	12.0	$C_6H_4-C_xH_{2x-1}$	$C_{12}H_{16}$	4.5	4.6		
Naphthalenes	1.00	8.5	10.3	12.0	$C_{10}H_7-C_xH_{2x+1}$	$C_{12}H_{12}$	9.2	1.8		
						Totals	22.9	77.1	0.23	0.27

[a] Volume percent is measured by ASTM D 2789 Method.

[b] Weight percent was calculated from the average density values shown in the table and the volume percents.

[c] The average carbon number shown at the top of each column was obtained from an ASTM D2887 simulated distillation analysis. The average carbon number is the number of carbons in the normal paraffin which has the GC retention time at which 50% of the fuel is eluted. These values show excellent agreement with average carbon numbers determined as a part of the ASTM D 2425 calculation.

[d] This structure was assigned based on the carbon number. It is assumed that an aromatic compound with a boiling point equivalent to that of an aliphatic compound will contain one less carbon.

[e] For the total fuel and calculated from the structure of the average compound.

Conclusions

On the average, the mass spectrometric carbon aromaticity values were 17% lower than the corresponding NMR values. This is comparable to the 15% difference in results obtained in similar analyses on other fuels. It is worthy of note that the results from both sets of analyses are proportional to each other, and the difference in results may be due to the fact that several assumptions such as carbon number, chemical structure, and average density must be made for the mass spectrometric analyses.

Latent Heat of Vaporization

Latent heat of vaporization (ΔH_v) can be routinely calculated for a pure compound using the Clausius-Clapyron equation:

$$\log \frac{P_2}{P_1} = \frac{\Delta H_v (T_2 - T_1),}{2.303\ RT_2T_1}$$

where vapor pressures determined as a function of temperature are used for this computation. Since this approach has also been used for simple mixtures, its applicability to the calculation of ΔH_v for the subject fuels was therefore investigated. A brief examination of ΔH_v literature values for a wide range of hydrocarbons showed that most values fell within the general range of 65 to 105 calories per gram. Thus it would be expected that a fuel composed of a broad range of hydrocarbons would have a ΔH_v value well within this range. Since calculations using fuel vapor pressure data produced unreasonably low ΔH_v values (typically 30 cal/gram), it was concluded that this approach was not suitable for complex mixtures such as fuels.

Direct calorimetric measurement of this property for complex mixtures is fraught with difficulties and is thus considered impractical. Consequently, heat of vaporization was calculated using literature

ΔH_v values for the various fuel components and their weight percents as determined by the hydrocarbon type analysis. A simulated distillation analysis (ASTM D 2789) was first conducted to determine the boiling range and average carbon number for each fuel. This value was used to define the compounds whose literature values should be used in the ΔH_v calculations. Fuels, of course, are composed of a number of compound classes, each having a wide carbon number range. Fortunately, the heat of vaporization changes only gradually with increasing carbon number within an homologous series. Therefore, the ΔH_v values for compounds having the average carbon number will be representative averages for all compounds present in the homologous series of each compound class. For example, ΔH_v values for n-hexane, n-decane, and n-tetradecane are 87.5, 86.3, and 85.7 cal/gram, respectively. The average carbon number in this example is C_{10} while the average ΔH_v value is 86.5 cal/gram, which is very close to the actual 86.3 value for n-decane. The average carbon number for the subject fuels was 13 for the aliphatic portion and 12 for the aromatic portion.

Heat of vaporization values for C_{13} aliphatic compounds and C_{12} aromatic compounds were used in computing ΔH_v values for each fuel. The average ΔH_v value for all listed isomers within a compound class was multiplied by the weight percent (Table 52) of that compound class in each fuel. The products for all compound classes were then summed to obtain the total ΔH_v for each fuel. Results are shown in Table 53.

The literature shows a ΔH_v value for only n-tridecane among the numerous C_{13} paraffins. Therefore, data for C_{10} isomers were utilized for calculating the average ΔH_v, since C_{10} and C_{13} normal alkanes have very similar ΔH_v values.

TABLE 53. CALCULATED LATENT HEAT OF VAPORIZATION FOR FUELS AT 25°C

Fuel Components	No. of isomers[a]	Avg ΔH_v,[b] cal/gm	g.cal/g	Fuel Component Contribution[c] and Calculated ΔH_v for Fuels at 25°C, cal/g			
				38	39	39-11.8	39-12.3
C_{12} Paraffins	37[d]	77.9	3.3	12.9	33.9	25.7	29.2
C_{12} Monocycloparaffins	8	76.8	1.7	4.9	21.2	15.0	17.6
C_{12} Dicycloparaffins	4	81.9	2.9	0.8	2.3	1.8	2.2
C_{12} Alkylbenzenes	4	81.2	1.3	45.2	6.6	21.0	14.9
C_{12} Tetralins[e]	12	89.3	1.3	4.6	8.4	6.8	7.8
C_{12} Naphthalenes	4	103.9	3.9	17.0	9.3	12.0	10.7
Total heat of vaporization for fuels				85.4±2.1[f]	81.7±2.6	83.1±2.3	82.4±2.4

[a] Number of isomers used in calculating average ΔH_v values.

[b] Average of isomer values found in "Physical Properties of Chemical Compounds," American Chemical Society, 1955.

[c] Values were obtained by multiplying the average component ΔH_v by the weight percent in the fuel.

[d] See text for explanation of compounds selected.

[e] No values for Indans were found in the literature.

[f] A weighted average standard deviation.

It was observed that, in general, the aromatic compounds have a higher ΔH_v than similar non-aromatic compounds, and that branched paraffins have a lower ΔH_v than the corresponding normal paraffins.

Thermal Conductivity

Thermal conductivity for the four ERBS fuels was measured by the transient hot wire method (ref. 10). In this procedure a constant heating current is applied abruptly to the resistance wire immersed in the fuel. The change in temperature of the wire following application of the current is obtained from the observed change of voltage across the wire and the known resistance-temperature characteristics.

Each fuel was analyzed 8-10 times at each of three temperatures, using four power levels and two time factors for each analysis. Thermal conductivity was then calculated in both SI and English units, with the results presented in Table 54. Also shown in this

TABLE 54. THERMAL CONDUCTIVITY OF ERBS FUELS

Measurement unit and Precision	Test temp., °C(°F)	Average values[a] and precision for thermal conductivity expressed in SI and English units			
		3S	3B	3B-11.8	3B-12.3
W/m·°K[b]	0(32)	0.1277	0.1229	0.1244	0.1232
Btu/ft·hr·°F[c]		0.0738	0.0710	0.0719	0.0712
% Rel., σ[d]		0.80	0.91	0.87	0.92
W/m·°K	20(68)	0.1246	0.1190	0.1219	0.1204
Btu/ft·hr·°F		0.0720	0.0688	0.0704	0.0696
% Rel., σ		1.16	0.79	0.77	0.62
W/m·°K	40(104)	0.1221	0.1164	0.1180	0.1174
Btu/ft·hr·°F		0.0705	0.0673	0.0682	0.0678
% Rel., σ		0.77	1.52	0.74	0.72

[a]Average of 8-10 analyses per sample.

[b]SI unit of measurement in Watts per meter per degrees Kelvin.

[c]Btu/ft·hr·°F is equal to 0.5778 W/m·°K.

[d]Percent relative standard deviation of individual measurements from the average.

table is the percent relative standard deviation of the individual analysis results from the averages. A plot of thermal conductivity versus temperature is presented in Figure 61 for only the SI units, which currently are the preferred units of measurement. The polynominal equation constants which can be used to calculate thermal conductivity at any temperature are presented in Figure 62.

Specific Heat

Heat capacity or specific heat was measured by a standard thermoanalytical technique, using a Perkin-Elmer DSC-1 differential scanning calorimeter and sapphire as the reference material. The fuel samples were hermetically sealed in aluminum sample pans and heated from 62 to 92°C at a rate of 10°C per minute. The amount of heat required to raise the temperature of the fuel over this

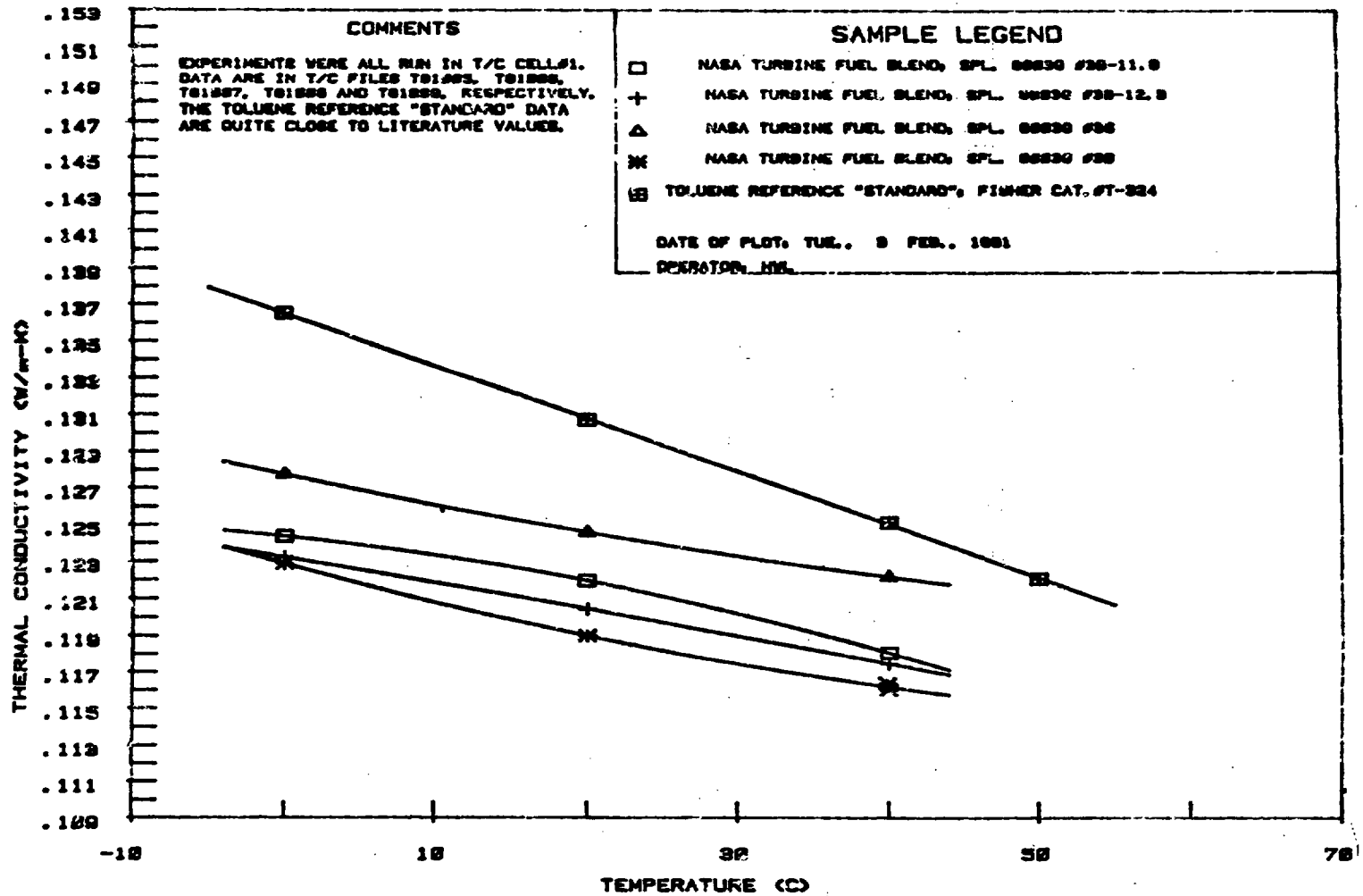

Figure 61. Thermal conductivity versus temperature.

CONSTANTS FROM CURVE FITTING DATA FROM SAMPLE(S)

$Y = A0 + A1X + A2X^2$

Y = THERMAL CONDUCTIVITY
X = TEMPERATURE

PCC = POLYNOMIAL CORRELATION COEFFICIENT

SAMPLE NAME	A0	A1	A2	PCC	95% LIMITS
MRC/NASA TURBINE FUEL BLEND; SPL. 80039 #3B-11.8	.124367	-.0000846	-.000001838	.941	.00198
MRC/NASA TURBINE FUEL BLEND; SPL. 80039 #3B-12.3	.123223	-.0001349	-.000000237	.934	.00178
MRC/NASA TURBINE FUEL BLEND; SPL. 80039 #3S	.127735	-.0001754	.0000008785	.894	.00225
MRC/NASA TURBINE FUEL BLEND; SPL. 80039 #3B	.122868	-.0002214	.0000013442	.918	.00237
TOLUENE REFERENCE "STANDARD"; FISHER CAT.#T-324	.136504	-.0002844	-.000000078	.977	.00243

********** END OF DATA **********

Figure 62. Polynomial equation coefficients and constants for thermal conductivity data.

temperature range was compared to the heat required to raise the temperature of the sapphire external standard over the same range, and specific heat of the fuel was then calculated at 5°C intervals from the known specific heats of sapphire. Specific heat was also determined for sapphire (against a sapphire reference) and reagent grade toluene to evaluate the accuracy of the instrumentation and method. Results are shown in Table 55.

Percent Carbon and Hydrogen

The ERBS fuel samples were submitted to two commercial analytical laboratories for duplicate carbon and hydrogen analyses. Both laboratories, Galbraith Laboratories, Inc. and Schwarzkopf Micro-analytical Laboratory, use the classical combustion technique for their analytical approach. Results are shown in Table 56.

TABLE 55. SPECIFIC HEAT OF ERBS FUELS AND REFERENCE MATERIALS

	Specific Heat in cal/g°C or Btu/lb°F at Following Temperatures					
Sample Tested	67°C 153°F	72°C 162°F	77°C 171°F	82°C 180°F	87°C 187°F	92°C 198°F
Fuel 3S	0.446	0.447	0.446	0.450	0.455	0.459
Fuel 3B	0.538	0.565	0.587	0.619	0.654	0.687
Fuel 3B-11.8	0.477	0.487	0.496	0.508	0.521	0.532
Fuel 3B-12.3	0.502	0.513	0.515	0.536	0.561	0.562
Sapphire[a]	0.205	0.206	0.207	0.208	0.210	0.213
Literature values	0.204	0.206	0.208	0.210	0.212	0.214
% Difference	0.5	0.0	-0.5	-0.9	-0.9	-0.5
Reagent Toluene[b]	0.446	0.446	0.455	0.466	0.474	0.483
Literature values	0.436	0.440	0.444	0.449	0.455	0.461
% Difference	2.4	1.3	2.4	3.7	4.2	4.9

[a] Sapphire in the sample pan was analyzed against sapphire in the reference pan. This was a measure of the accuracy of the instrumentation.

[b] This measurement reflected a combination of the instrumental accuracy and the purity of the toluene.

TABLE 56. PERCENT CARBON AND HYDROGEN IN ERBS FUELS

Sample Number	Percent Hydrogen Data From Galbraith	Schwartzkopf	Average	Percent Carbon Data From Galbraith	Schwartzkopf	Average
3B	9.97	10.20		89.65	89.53	
	10.09	10.41		89.58	89.42	
Avg.	10.03	10.31	10.17	89.61	89.47	89.54
3B	12.40	12.82		87.49	87.16	
	12.35	12.68		87.61	87.34	
	12.37	12.75	12.56	87.55	87.25	87.40
3B-11.8	11.79	11.95		87.73	88.17	
	11.91	11.92		87.79	88.26	
	11.85	11.93	11.89	87.76	88.21	87.99
3B-12.3	12.48	12.38		87.43	87.76	
	12.13	12.27		87.21	87.78	
	12.31	12.33	12.32	87.31	87.77	87.54

18. SULFUR ANALYSIS OF SEVEN LUBRICANT SAMPLES

Seven lubricant samples were analyzed by Schwartzkopf Microanalytical Laboratory for total sulfur. The results are shown in Table 57.

TABLE 57. SULFUR CONTENT OF LUBRICANTS

Sample number	Sulfur, ppm
OP-234-1	65
-2	556
-3	63
-4	1,100
-5	325
-6	327
-7	62

19. MERCAPTAN SULFUR, TRACE METALS, AND PEROXIDE ANALYSES OF SHALE-DERIVED AND PETROLEUM-BASED JP-4 FUELS

Two samples each of shale-derived JP-4 and petroleum-based JP-4 were analyzed for peroxide content, mercaptan sulfur, and trace metals content. These fuel samples had been in contact with

Goodyear polyurethane bladder material during six-month compatibility studies at 140°F. The complete identification of each sample is provided below.

Sample	Labeling
81002-1	82-C-39 Volume Swells 6 months at 140°F in Shale Oil JP-4; in 9/3/80, out 3/3/81
81002-2	82-C-39 Dog Bones 6 months at 140°F in Shale Oil JP-4; in 9/3/80, out 3/3/81
81002-3	82-C-39 Volume Swells 6 months at 140°F in Petroleum JP-4; in 9/3/80, out 3/3/81
81002-4	82-C-39 Dog Bones 6 months at 140°F in Petroleum JP-4 changed every 30 days, in 9/3/80, out 3/3/81

Peroxide content was determined by ASTM Method D 1563-60, in which a standardized sodium thiosulfate solution and starch indicator are used to titrate released iodine. The method has a minimum detectability of 0.1 ppm, a repeatability of 0.4 ppm, and a reproducibility of 1.3 ppm.

Mercaptan sulfur was determined by UOP Method 163-80, which utilizes a potentiometric titration with alcoholic silver nitrate. This method has a minimum detectability of 1 ppm. It has a repeatability of 0.1 ppm at the 3 ppm level and 0.5 ppm at the 10 ppm level. Analytical results for both mercaptan sulfur and peroxide are presented in Table 58.

TABLE 58. PEROXIDE AND MERCAPTAN SULFUR IN JP-4 FUELS

JP-4 sample description	Peroxide, ppm	Mercaptan sulfur, ppm
81002-1, Shale, Volume Swell	3.2	2.9
81002-2, Shale, Dog Bones	2.6	3.3
81002-3, Petroleum, Volume Swell	2.8	ND[a]
81002-4, Petroleum, Dog Bones	2.8	ND

[a]ND - not detected at 1 ppm level.

Trace metals content was determined by emission spectrographic analyses. Two gram quantities of fuel were deposited into the carbon electrodes by the dropwise addition/fuel evaporation technique. This was followed by the addition of 10 milligram quantities of lithium carbonate to simulate the matrix of the 10, 100, and 1,000 ppm metal standards used in the analysis. Each standard was a mixture of about 50 different metals. Each fuel was analyzed in duplicate, and the estimated precision of the analysis was about ±100%. Average results are shown in Table 59.

TABLE 59. EMISSION SPECTROGRAPHIC ANALYSES OF JP-4 FUELS

Metal	Approx. detection limit, ppm	Quantities of each metal in following fuels, ppm			
		81002-1 Shale	81002-2 Shale	81002-3 Petroleum	81002-4 Petroleum
Magnesium	0.1	0.2	0.2	ND[a]	ND
Silicon	0.5	0.5	0.5	0.5	0.5
Iron	0.05	0.1	0.1	0.05	ND
Aluminum	0.05	0.05	0.05	ND	ND
Copper	0.03	0.03	0.1	ND	ND
Sodium	0.01	0.01	ND	ND	ND
Chromium	0.1	ND	ND	ND	ND
Lead	0.5	ND	ND	ND	ND
Tin	0.2	ND	ND	ND	ND
Cadmium	1	ND	ND	ND	ND
Zinc	5	ND	ND	ND	ND
Nickel	0.1	ND	ND	ND	ND

[a]ND - not detected at indicated levels.

20. ANALYSIS OF SHALE-DERIVED JP-4 SAMPLE NUMBER 15B FOR PEROXIDES, TRACE METALS, AND MERCAPTAN SULFUR

A sample of shale-derived JP-4 produced in the HRI refining program and returned from the GE Evendale Plant was analyzed for peroxide content, mercaptan sulfur, and trace metals content. The sample was then placed in a soft glass quart bottle covered with aluminum foil and was stored at 140°F for a total of eight weeks. Samples were withdrawn after 1, 2, 3, 4, 6, and 8 weeks for peroxide analyses.

Peroxide content was determined by ASTM Method D 1563-60, which is a titrimetric analysis utilizing a standard sodium thiosulfate solution and starch indicator. The method has a minimum detectability of 0.1 ppm, a repeatability of 0.4 ppm, and a reproducibility of 1.3 ppm.

Mercaptan sulfur was determined by UOP Method 163-80, which utilizes a potentiometric titration with alcoholic silver nitrate. This method has a minimum detectability of 1 ppm and has a repeatability of 0.1 ppm at the 3 ppm level and 0.5 ppm at the 10 ppm level. Analytical results for both mercaptan sulfur and peroxide are presented in Table 60.

Trace metals content was determined by emission spectrographic analyses. Two gram quantities of fuel were deposited into the carbon electrodes by the dropwise addition/fuel evaporation technique. This was followed by the addition of 10 milligram quantities of lithium carbonate to simulate the matrix of the 10, 100, and 1,000 ppm metal standards used in the analysis. Each standard was a mixture of about 50 different metals. Each fuel was analyzed in duplicate, and the estimated precision of the analysis was about ±100%. Average results are shown in Table 61.

TABLE 60. PEROXIDE AND MERCAPTAN SULFUR IN SHALE-DERIVED JP-4 SAMPLE 15B-792009

Time at 140°F, weeks	Peroxides, ppm	Mercaptan sulfur, ppm
0	ND (<0.1)	4.3
1	1.1	
2	1.1	
3	0.9	
4	0.9	
6	1.2	
8	0.8	

TABLE 61. EMISSION SPECTROGRAPHIC ANALYSIS OF SHALE-DERIVED JP-4 SAMPLE 15B-792009

Metal	Amount detected (±100%), ppm
Magnesium	0.2
Silicon	2
Iron	0.1
Aluminum	3
Copper	0.03
Sodium	0.5

21. EXAMINATION OF SHALE-DERIVED JP-4 FOR COMPONENTS CAUSING ELASTOMER DETERIORATION

Introduction and Summary

A specimen of shale-derived JP-4 was found to exhibit compatibility problems with elastomeric fuel system components and bladder material during Air Force tests. The observed elastomer deterioration was initially suspected to occur because of peroxide compounds present in the fuel. Peroxide numbers, however, were determined for the fuel specimen in question, as well as for a number of related fuels, with the result that no significant peroxide levels were found.

In an effort to identify problem-causing fuel components, comparative analyses were conducted on both the problem fuels and those that presented no problems. The offending component(s) were suspected to be sulfur compounds. Analyses were, therefore, conducted by gas chromatography using a sulfur-specific Hall electrolytic conductivity detector. Additionally, wide-scan GC/MS analyses were conducted on the fuels, and fuel concentrates were prepared and analyzed. All of these analyses and their significance are discussed in the following paragraphs.

Peroxide Analysis

Peroxide numbers were measured for a total of fifteen different fuels using ASTM Method D 1563-60. In this method, the sample is diluted with carbon tetrachloride and placed in contact with an aqueous potassium iodide solution. Peroxides present are reduced by the potassium iodide with a stoichiometric release of iodine. The iodine is titrated with a standard sodium thiosulfate solution using starch as the end-point indicator. The method has a minimum detectability of 0.1 ppm, a repeatability of 0.4 ppm and reproducibility of 1.3 ppm. Results of the analyses are presented in Table 62.

In no case was the peroxide level sufficient to cause the observed elastomer deterioration.

Sulfur-Specific Gas Chromatographic Analyses

The problem component(s) of the fuel were believed to be sulfur compounds. The fuels were thus screened for the presence of sulfur-containing components using a gas chromatograph equipped with a sulfur specific detector. A Tracor Model 560 gas chromatograph with a 700A Hall electrolytic conductivity detector (HECD) and a 12-meter methylsilicone fused silica capillary column was used for these analyses. The 700A HECD, when operated in the

TABLE 62. PEROXIDE ANALYSES OF SHALE-DERIVED AND PETROLEUM-BASED JP-4 FUEL

Sample number	Description and history of fuel	Peroxide, ppm
	Shale Oil JP-4 tested 6 months at 140°F; in 8/20/80, out 2/20/81	
1	Goodyear 51956 seam adhesion	0.8
2	Pliocel seam adhesion	2.3
3	FT-136 repair adhesive	0.9
	Petroleum JP-4 (changed every 30 days) tested 6 months at 140°F; in 8/20/80, out 2/20/81	
4	Goodyear 51956 seam adhesion	1.4
5	Pliocel seam adhesion	1.9
6	Repair adhesive	1.7
	Shale Oil JP-4 tested 6 months at 140°F; in 9/3/80, out 3/31/81	
7	82C 39-A	2.7
8	82C 39-B	2.8
	Petroleum JP-4 (changed every 30 days) tested 6 months at 140°F; in 9/3/80, out 3/3/81	
9	82C 39-A	2.0
10	82C 39-B	2.5
11	Shale JP-4 from UDRI, John Dues to Charles Martel, 3/3/81	3.3
	Shale oil JP-4 fuels from Request 80007 and Report 80-18	
12	HRI-LO-2054 (80-PHJ-084A)	1.8
13	HRI-LO-2057 (80-PHJ-084B)	0.4
14	Pratt and Whitney Shale Oil JP-4, Sample ES 0001A, Previously analyzed: Request 80022, Report 80-31	ND[a] (<0.1)
15	Petroleum JP-4, sample GEC-145-400-792033, Previously analyzed: Request 79030, Report 79-45	2.0

sulfur mode, is highly selective for sulfur compounds, but also shows a small response to high levels of hydrocarbons. This small signal obtained for hydrocarbons was found to be useful in establishing the relative retention characteristics of detected compounds.

Gas chromatographic conditions used were:

Injection Port Temperature:	200°C
Detector Base Temperature:	225°C
Reactor Temperature:	850°C
Carrier:	Helium
Initial Column Temperature:	60°C for 4 min
Temperature Program Rate:	10°C/min
Final Column Temperature:	200°C

Several petroleum JP-4 fuels were included in the analyses in addition to various specimens of the shale fuel. A number of the shale fuel samples exhibited a sulfur component eluting at approximately 19 minutes. In no case was this component detected in petroleum JP-4. The fuel coded HRI-LO-2057 had the highest concentration of the sulfur compound (Figure 63-a). That fuel also contained a second sulfur component having a retention time of approximately 1.5 minutes. This retention time is close to that of dimethyl disulfide. No sulfur-containing compounds were detected in the shale JP-4 HRI-LO-2054 (Figure 63-b). The results of the evaluation are summarized in Table 63.

A number of reference blends were prepared and analyzed to determine whether standard fuel additives, or benzotriazol which is known to have been added to some lots of the fuel, are related to the sulfur-containing component. The standard additives used for test blends were DCI-4A corrosion inhibitor and the major components of ethyl antioxidant 733 (2,6-ditert-butylphenol and 2,4,6-tritert-butylphenol). Dimethyl disulfide was used in the

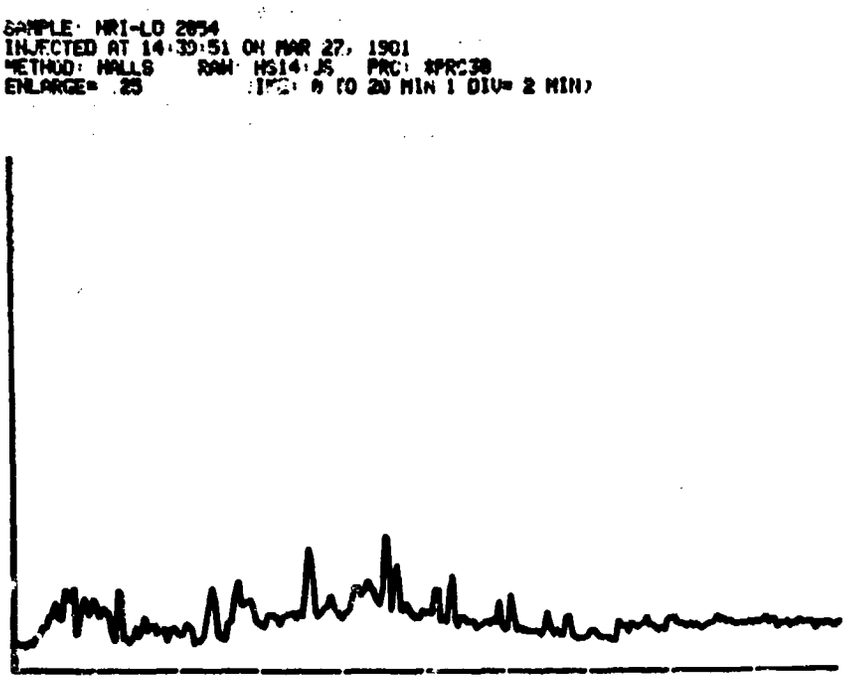

(a) Fuel HRI-LO-2054-no sulfur components.

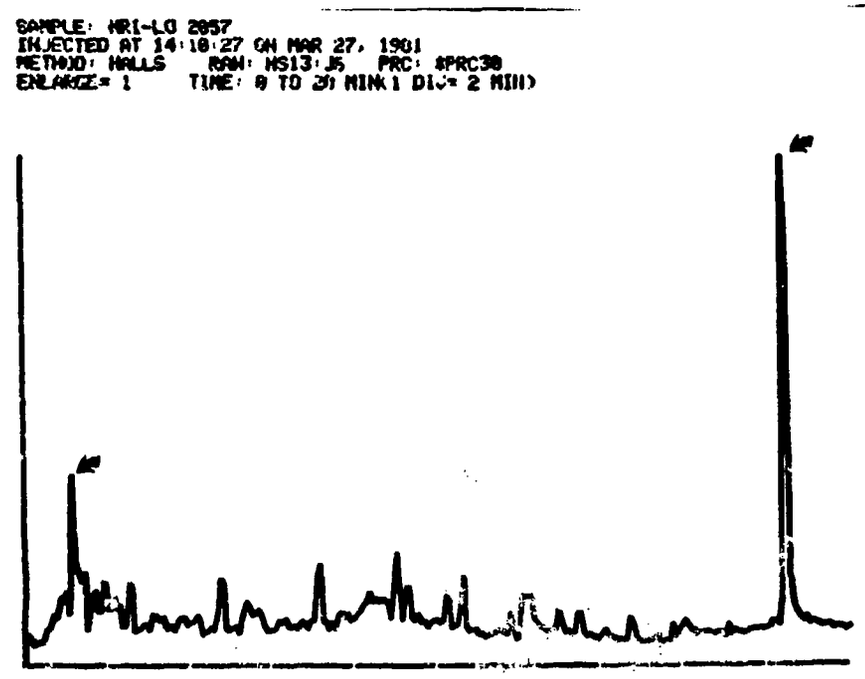

(b) Fuel HRI-LO-2057-sulfur components marked with arrows.

Figure 63. Gas chromatograms of Shale OP-4 using Hall electrolytic conductivity detector in sulfur mode.

TABLE 63. RELATIVE AMOUNT OF SULFUR COMPONENT IN FUELS TESTED[a]

Sample No. and/or Description	Relative Intensity of Peak for Sulfur Component Compared to Same Peak in Fuel HRI-LO-2057
1. HRI-LO-2057[b]	100
2. JP-4 15B	30
3. ES0001A	-[c]
4. UDRI JP-4	15
5. HRI-LO-2054	-
6. JP-4 79003	-
7. JP-4-14-70	-
8. Shale Oil 82C39A	25
9. Petroleum 82C39A	-
10. x190-64	15
11. x190-65	35
12. x190-66	25
R1 3.8 ppm Benzotriazole in EOTH	-
R2 3.8 ppm Benzotriazole in Shale Oil JP-4	30
R3 3.8 ppm Benzotriazole in Petroleum JP-4	-
R4 11 ppm DCI-4A plus 3 ppm $(CH_3)_2S_2$ in Shale Oil JP-4	31
R5 11 ppm DCI-4A plus 3 ppm $(CH_3)_2S_2$ in Petroleum JP-4	-
R6 31.6 ppm antioxidant plus 3 ppm $(CH_3)_2S_2$ in Shale Oil JP-4	28
R7 31.6 ppm antioxidant plus 3 ppm $(CH_3)_2S_2$ petroleum JP-4	-
R8 3.2 ppm benzothiazole in Shale Oil JP-4.	30
R9 3.2 ppm benzothiazole in petroleum JP-4	-
HRI-LO-2057 N_2 evaporated (spl. #1)	330
HRI-LO-2057 after further evaporation of volatiles	1180
JP-4 15B pot residue after distillation at atmospheric pressure	-
JP-4 15B tenth fraction from atmospheric pressure distillation	-
JP-4 15B pot residue solids dissolved in pentane	-

[a] Component with ~18 min. retention time, near C_{18} hydrocarbon

[b] Also contains sulfur component with ~1.5 min. retention time.

[c] Dash = non detected

fuel refining process, thus this compound was also added to determine any reactive effects. The blends were prepared using the shale JP-4 codad 15B and a petroleum JP-4. Benzothiozol was included among the additives evaluated because it is sometimes used as a corrosion inhibitor and antioxidant, and it has a name easily confused with benzotriazol. From these analyses, which are included in Table 63, it can be concluded that the presence of the various additives has no effect on the magnitude of the sulfur-component peak.

Gas Chromatography/Mass Spectrometric Analyses (GC/MS)

In order to identify the sulfur component found in some of the shale JP-4 specimens, GC/MS analyses were conducted on two fuels, one containing the unidentified component (HRI-LO-2057) and the other being free of that component (ES 0001A).

A 25-meter OV-101 fused silica capillary column was used for the separation. The unidentified component is known to fall in the boiling range of C_{18} paraffins. A hydrocarbon reference mixture was chromatographed under the same conditions as the samples in order to determine the expected location of the unknown peak. Figure 64 presents a composite of the three reconstructed total ion chromatograms. Hard copy mass spectra were obtained for each component shown in the chromatogram. The only difference found between the two fuels lies in the concentration of toluene which is substantially higher in HRI-LO-2057. That peak is marked with a star in Figure 64.

Based on the hydrocarbon reference, the sulfur component has an expected retention time of 26-28 minutes. In order to further examine the HRI-LO-2057 data for components in this area of the chromatogram, the scale was greatly expanded through a six minute retention time window from 25 to 31 minutes as shown in Figure 65. The only components detected were C_{17} paraffins at approximately

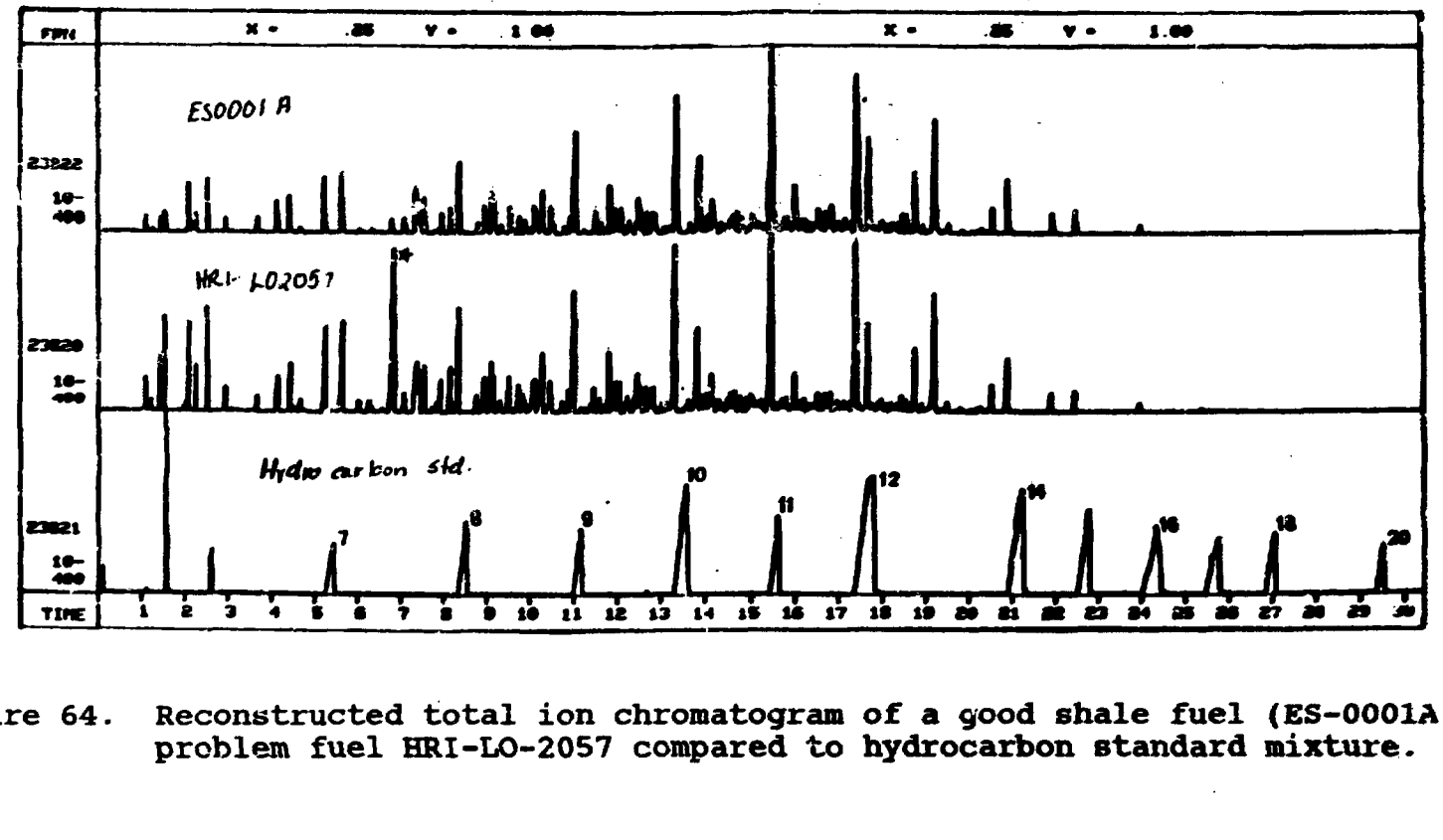

Figure 64. Reconstructed total ion chromatogram of a good shale fuel (ES-0001A) and problem fuel HRI-LO-2057 compared to hydrocarbon standard mixture.

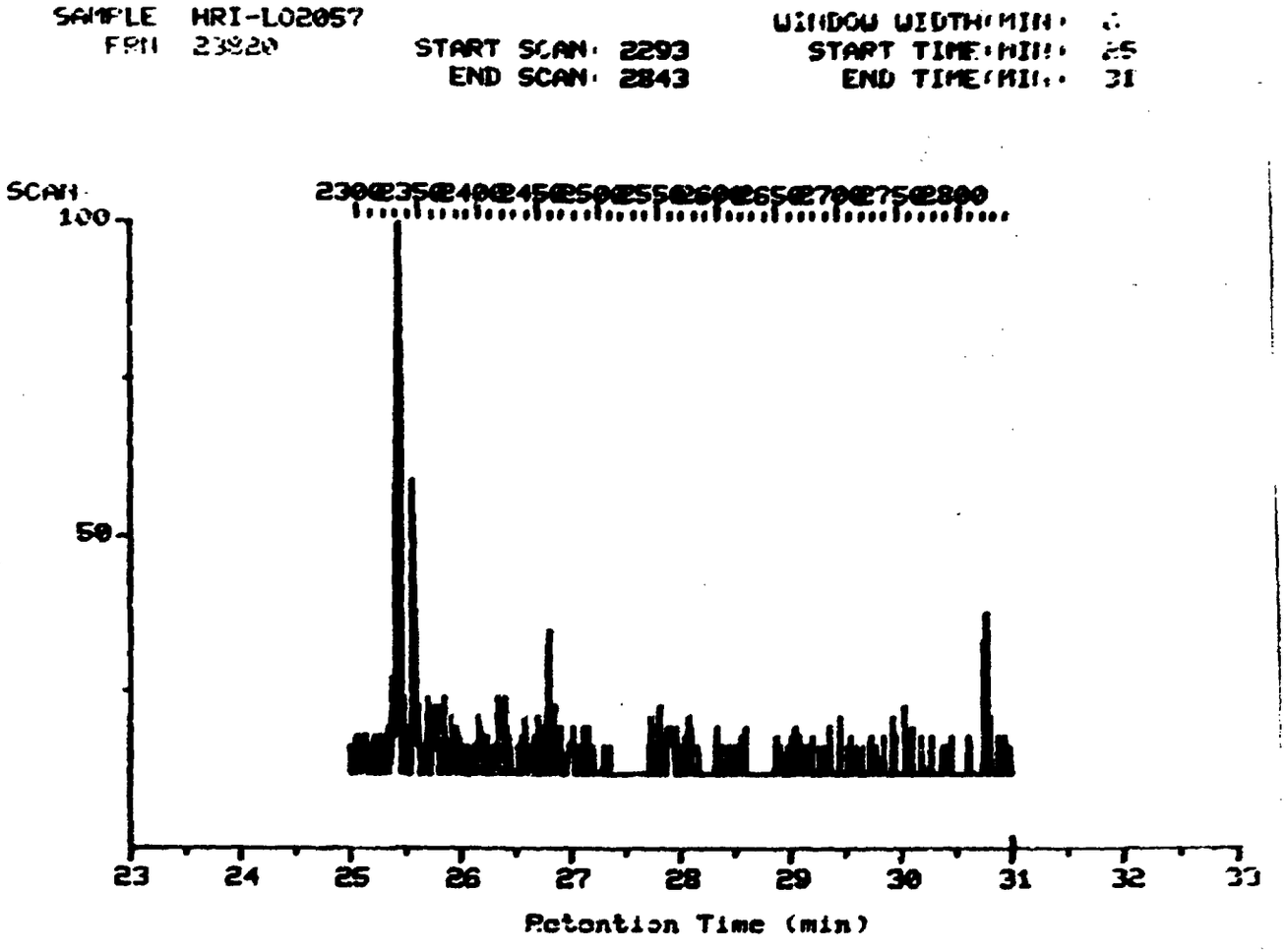

Figure 65. Examination of reconstructed total ion chromatogram of fuel HRI-LO-2057 - expanded scale, six minute window.

25.5 minutes. No other peaks were detected, with the detection limit being defined as three times baseline noise.

Concentration of Sulfur Component in Fuel

In order to concentrate the sulfur component in the fuel, a simple one-plate distillation was performed in which the fuel was separated into 10 fractions plus a small residue. The component sought was expected to be in the last fraction or in the residue. Analysis of the fraction by GC, however, showed that the sulfur component did not appear in any of the fractions or in the residue. The compound was apparently destroyed during distillation.

Several other concentration techniques were also employed. An aliquot of fuel was passed through a silica gel column where the sulfur compound was retained. The component was recovered from the gel by elution with a 50/50 chloroform-ethanol mixture. The level of the component in the solvent was approximately double its concentration in the original fuel. It was, however, readily concentrated further by evaporation of the excess solvent.

Simple evaporation of the original fuel under a nitrogen flow was also found to be a means by which a 10-fold increase in the concentration of the sulfur compound could be achieved.

Vacuum distillation was also used to obtain a more concentrated specimen of the sulfur compound. Distillation data are presented in Table 64. The component was found in the residue after vacuum distillation.

Analysis of Concentrates

GC/MS analyses were conducted on several of the concentrates. A reconstructed total-ion chromatogram of the concentrate obtained by evaporation of the fuel volatiles is presented in Figure 66.

TABLE 64. VACUUM DISTILLATION DATA FOR FUEL 15B

Fraction number	Boiling range, °C
1	29-45
2	45-60
3	60-75
4	40-48[a]
5	48-58
6	58-73
7	73-81
8	81-90
Residue	90

[a]Pressure decreased.

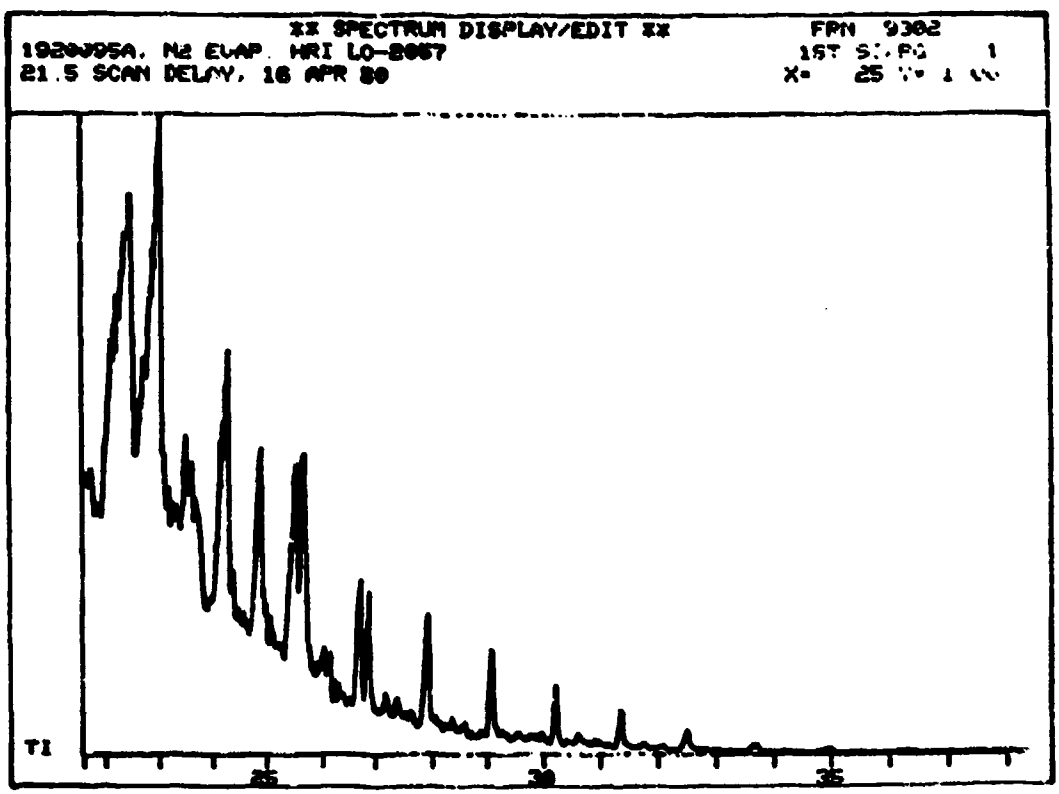

Figure 66. Reconstructed total ion chromatogram of sample HRI-LO-2057 after evaporation of volatiles.

This concentration procedure yields a sample similar to that obtained by vacuum distillation. Mass spectra of the peaks indicate that they are due to a series of paraffin hydrocarbons. No sulfur-containing or non-hydrocarbon component was detected.

A reconstructed total-ion chromatogram for the silica gel concentrate was recorded as shown in Figure 67. The portion of the chromatogram between 25 and 30 minutes was expanded as shown in Figure 68. Three components were detected as follows:

Retention time, min	Compound detected
25.9	Phenanthrene
26.6	2-Phenylbenzimidazol
27.4	Methylphenanthrene

The background was examined for evidence of the sulfur compound but none was found.

Discussion and Conclusion

The sulfur compound that was detected in a number of samples using the Hall ECD could not be confirmed or identified by GC/MS, presumably because of the instability (or high reactivity) of the component. High reactivity is, of course, expected of compounds which attack elastomers (e.g., peroxides). The other experiments demonstrated the instability of the sulfur component. Not only was the component lost during distillation at atmospheric pressure, but when attempts to evaporate fuel volatiles were carried out too vigorously (by heating) the concentration of the component was found to decrease instead of increase.

The sulfur compound was found in fuels known to be problem-causing and was absent in fuels known to be problem-free, i.e., petroleum JP-4 and certain lots of shale JP-4. Due to the apparent instability of this component, the relative amounts found may not

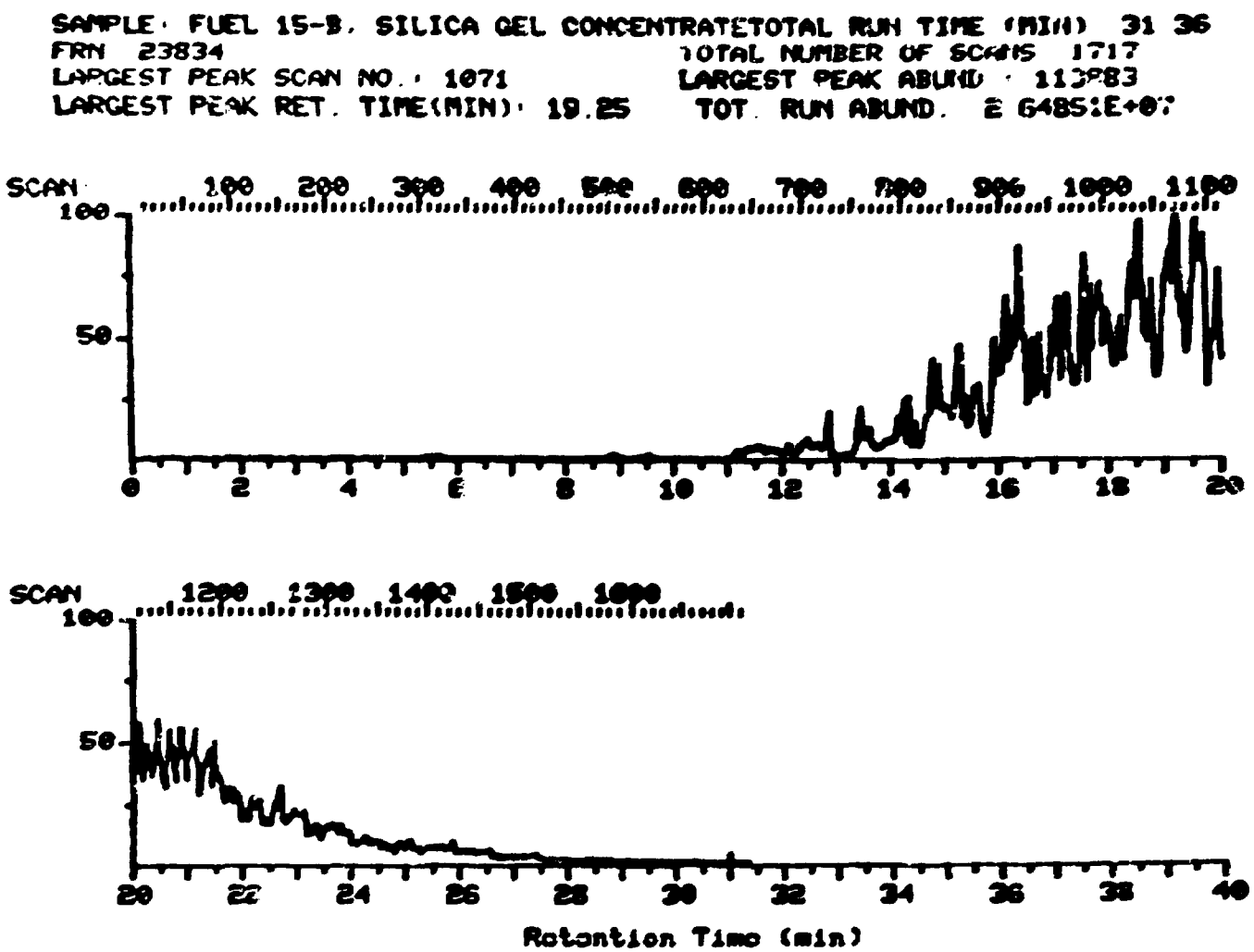

Figure 67. Reconstructed total ion chromatogram of silica gel concentrate from fuel 15B.

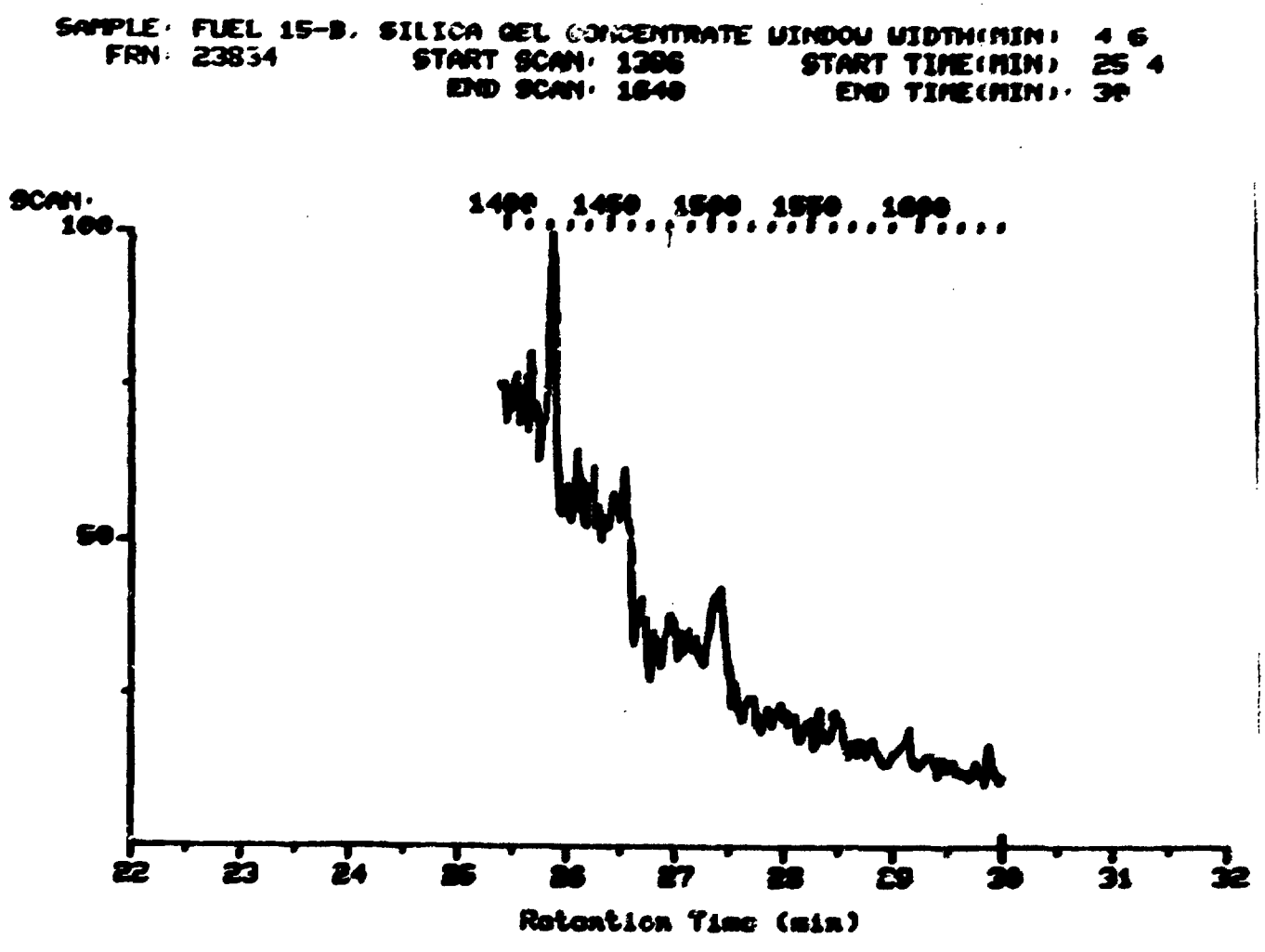

Figure 68. Portion of reconstructed total ion chromatogram of silica gel concentrate from fuel 15B.

have correlated in every case with the degree of polymer degradation. The component appeared to be unrelated to any of the normal fuel additives, or to the benzotriazol added to improve copper-strip corrosion properties.

The immediate goal of this investigation was to find differences between the good fuel and the problem fuel. Elastomer deterioration testing was not a part of the study, and differences found could not be conclusively related to elastomer deterioration. In order to directly relate the fuel or any of its fractions to elastomer attack, a small-scale accelerated test for elastomer deterioration would have been required.

22. ANALYSIS OF THREE REFERENCE GAS BLENDS FOR CARBON MONOXIDE CONCENTRATION

APL personnel had reason to suspect that three calibration gas cylinders of carbon monoxide in nitrogen did not contain the concentrations of CO specified in the containers. Each cylinder of gas was, therefore, analyzed for CO content by a method described in EPA Method 25. This method utilizes the TGNMO (total gaseous non-methane organics) apparatus which oxidizes the CO to CO_2, reduces the CO_2 to methane, and then measures the amount of methane by means of a flame ionization detector. The TGNMO apparatus had been calibrated for the range of 50-10,000 ppm CO, using standards of nominally 50, 500, and 10,000 ppm.

The calibration curve for the day on which the CO cylinders were analyzed was within 3% of the validated curve (the method specifies 5%). However, the CO cylinders were analyzed directly against the 51.1 ppm CO standard since the specified CO values were so close to this standard. Both the samples and the standard were injected four times each to improve on the accuracy of the results. Data are presented in Table 65.

TABLE 65. CARBON MONOXIDE IN NITROGEN

	51.1 ppm CO CO in air air standard	Three cylinders of CO in nitrogen		
		Tank 1	Tank 2	Tank 3
Detector response in area counts for four replicate sample injections	64,842 62,767 64,794 63,434	107,871 110,553 110,258 110,608	42,247 41,807 42,541 42,797	73,956 76,898 76,867 76,869
Mean counts	63,960	109,823	42,348	76,123
Standard deviation, σ	1,028	1,310	425	1,511
Percent relative, σ	±1.6	±1.2	±1.0	±2.0
Determined CO in N_2, ppm		87.7	33.8	60.8
Value on label, ppm		87	37	66

23. TRACE METALS ANALYSIS OF THERMALLY UNSTABLE JP-4 SAMPLES

Five samples of JP-4 coded YAH-64 were analyzed for trace metals using an ISA Model JY48P inductively coupled plasma (ICP) spectrometer. The purpose of the analyses was to determine the source of the thermal instability problem. The ICP analyses were conducted on aqueous acid extracts (ultrapure HCl) of the fuels which provided a concentration factor of 22.5 for the metals. The test results for an acid extraction blank, the fuel samples, and a reference standard are shown in Table 66.

With the exception of 183 ppb zinc in one of the fuel samples (T-I), none of the metal concentrations appears high enough to cause a thermal stability problem.

24. IDENTIFICATION OF SULFUR CONTAINING CONTAMINANT IN SHALE JP-4

A specimen of shale-derived JP-4, coded VN-81-149, was found during its routine chromatographic analysis within the Aero Propulsion Laboratory to contain an unusually high boiling component. The component, which represented approximately 0.2% of the sample, had a boiling point between those of normal C_{21} and C_{22} paraffins.

TABLE 66. TRACE METALS ANALYSIS BY INDUCTIVELY COUPLED PLASMA SPECTROMETRY

Element	Detection Limit, ppb[a]	HCl Acid Blank, ppb	Acid Extracts of JP-4 Fuels[b], ppb					Reference Standard in 3% HNO_3 (ppb)		
			A-I	F-I	P-I	S-I	T-I	Observed	True Value	% Recovery
Aluminum	4.4	ND[c]	26.0	26.7	15.9	6.0	8.2	366	330	111
Cadmium	0.6	ND	ND	2.2	ND	ND	ND	54	50	108
Iron	0.9	1.4	5.2	7.2	13.4	12.5	7.1	182	200	91
Nickel	3.2	ND	ND	ND	ND	ND	ND	185	165	112
Boron	2.5	ND	ND	ND	2.9	6.3	ND	359	360	100
Cobalt	0.4	0.5	ND	ND	ND	0.4	ND	262	235	111
Magnesium	6.7	ND	ND	ND	ND	ND	ND	-	-	-
Lead	10.0	ND	14.9	26.3	26.3	28.6	21.8	127	135	94
Chromium	1.6	ND	ND	ND	ND	ND	ND	326	315	103
Manganese	0.2	ND	1.3	0.9	1.2	ND	6.0	332	315	105
Vanadium	3.3	ND	ND	ND	ND	ND	ND	-	-	-
Beryllium	0.1	ND	ND	ND	ND	ND	ND	85	85	100
Copper	3.1	ND	ND	ND	4.0	7.1	21.7	443	430	103
Molybdenum	4.3	ND	ND	ND	ND	8.1	ND	132	120	110
Zinc	3.3	ND	11.9	17.2	21.2	4.4	182.7	329	335	98
Tin	11.1	ND	ND	ND	ND	ND	ND	-	-	-

[a] Lowest quantifiable concentration in the fuels.

[b] Values represent levels in original JP-4 fuel samples.

[c] ND means not detected at stated limit.

Analyses were conducted to identify the component which was believed to be a contaminant of the fuel.

GC/MS was the analytical technique of choice for this identification. Figure 69 illustrates a total ion chromatogram of a portion of the fuel and of a hydrocarbon standard. Deuterated (d_{10}) anthracene which has a retention time of about 20.2 minutes, was added to both the fuel and the standard hydrocarbon mixture. The fuel component to be identified had a retention time of 25.5 minutes and eluted just after the C_{21} n-paraffin. The mass spectrum of the unknown component indicated the presence of two atoms of sulfur in the molecule and showed that the molecule could readily cleave to give two identical fragments. The molecular weight was established as 290. A search of all available mass spectral libraries produced no match for the mass spectrum. However, based on information from the mass spectrum, a di-C_8 alkyldisulfide was proposed as the general compound type with the di-n-octyl being the most likely. The presence of sulfur was confirmed by x-ray emission analysis.

Combined gas chromatography/Fourier transform infrared spectroscopy was used to assist in the identification. The component in question was concentrated by evaporation of the more volatile portion of the fuel in a stream of dry nitrogen. The infrared spectrum obtained for the component established with certainty that the compound was non-aromatic and the data supported the proposed structure, though it did not conclusively establish the identity of the compound.

The compound di-n-octyldisulfide was not readily available from regular chemical supply houses such as Aldrich, Sigma, Alfa, etc., but was finally procured through a listing of rare and fine chemicals (K&K Life Science Div. of ICN, Inc.). A mass spectrum of di-n-octyldisulfide was recorded and was found to exactly match the spectrum obtained for the fuel components as shown in

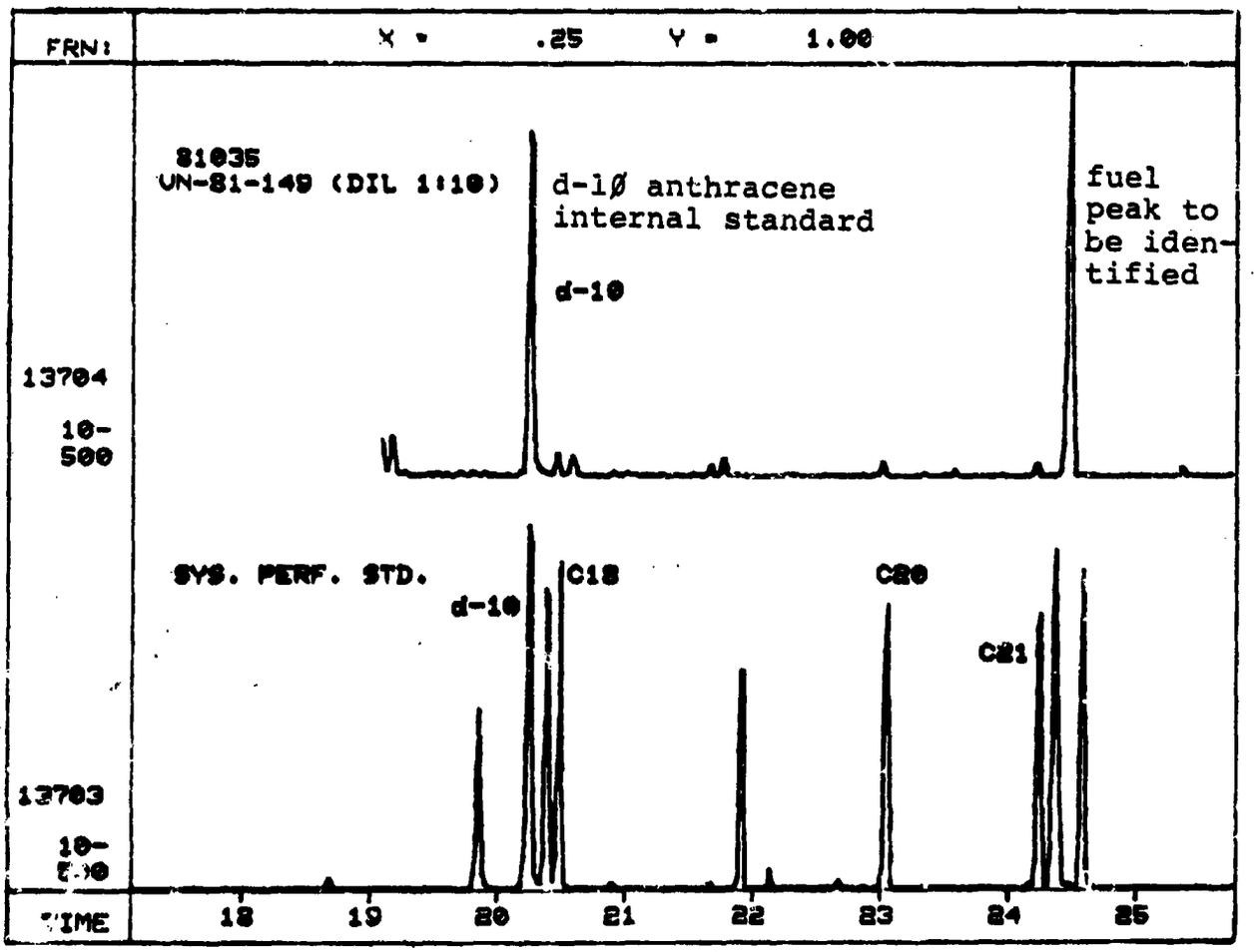

Figure 69. Reconstructed total ion chromatogram from GC/MS analysis. The fuel component is compared to a standard hydrocarbon mixture.

Figure 70. A comparison of the FTIR spectra of the fuel component and reference materials are shown in Figure 71. The fuel component has thus been unequivocally identified as di-n-octyldisulfide.

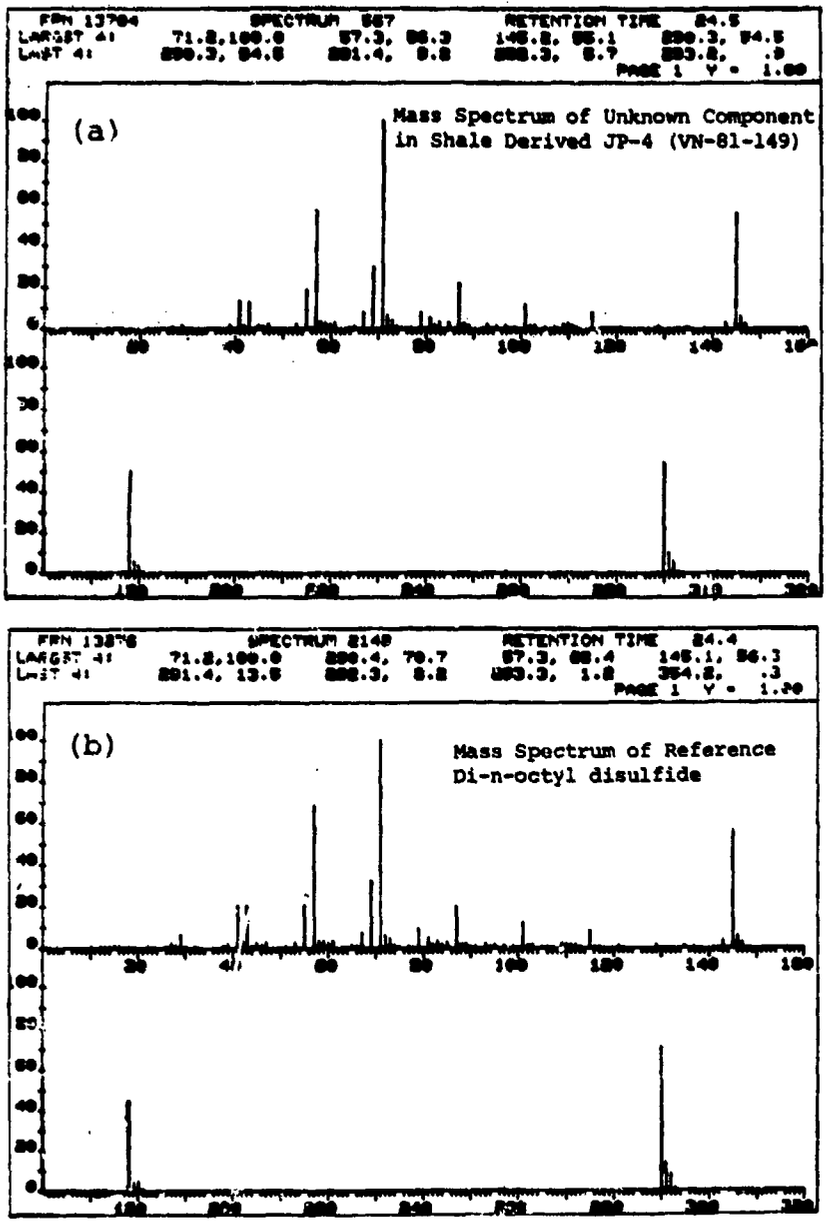

Figure 70. Mass spectra of, (a) unknown compound in shale JP-4 and (b) reference compound di-n-octyldisulfide.

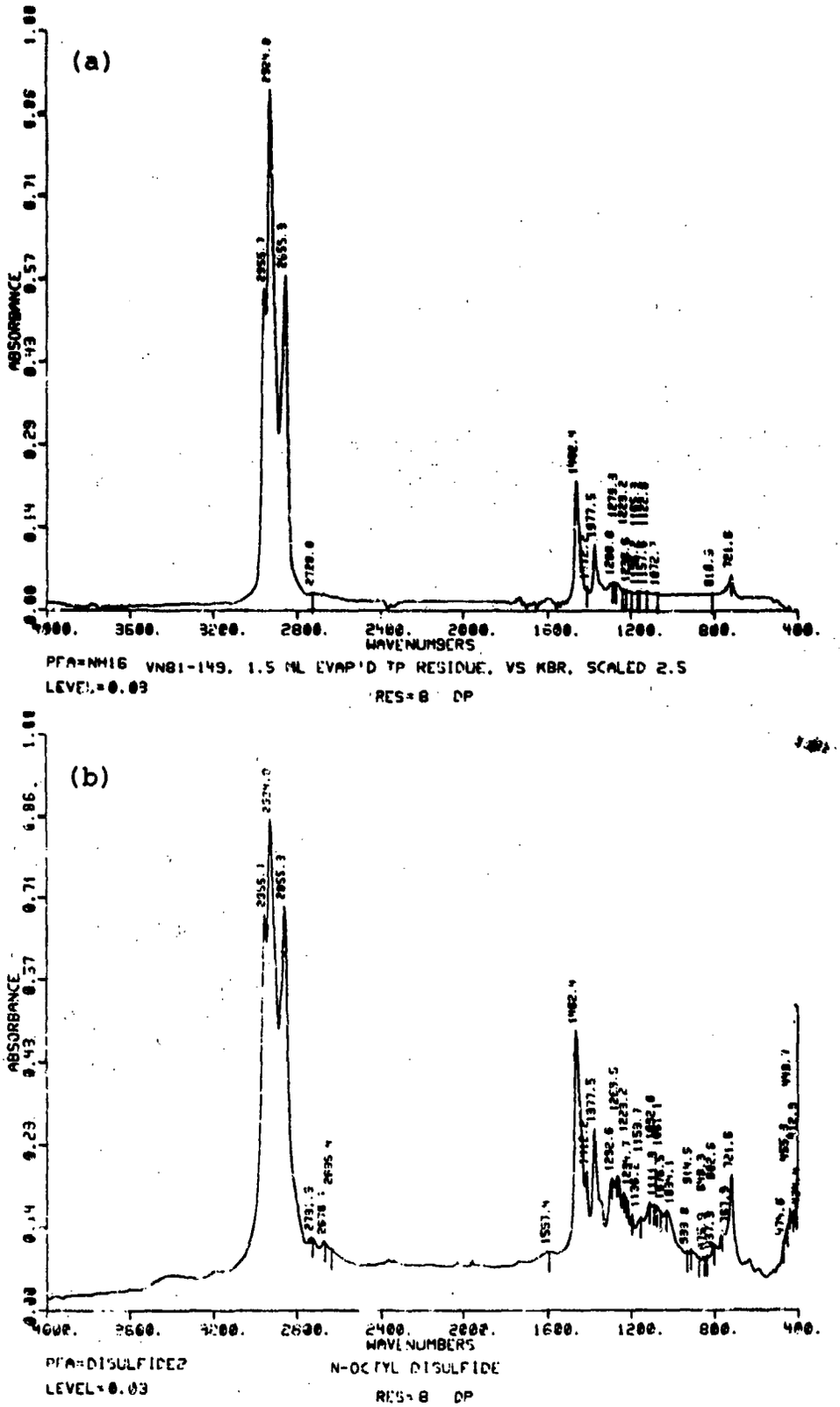

Figure 71. FTIR spectra: (a) contaminant in shale-derived JP-4, (b) reference compound, di-n-octyldisulfide.

25. OPERATION AND EVALUATION OF CARLO ERBA CHN/O ELEMENTAL ANALYZER

The capability for performing accurate and reliable elemental analyses of fuel samples is required in support of current and planned APL fuel development programs. Because of the anticipated large number of samples to test, it was considered advantageous to APL to develop this capability in-house. A Model 1104 Carlo Erba CHN/O elemental analyzer was available within the Aero Propulsion Laboratory facilities for this purpose.

The Model 1104 Carlo Erba analyzer was purchased in 1974 and had been periodically operated by Air Force personnel during subsequent years. The data from these intermittent analyses usually indicated that unreliable results were being obtained. The goals of this program were to determine why reliable data were not being obtained and then to make the analyzer functional for routine analyses of hydrocarbon fuels.

Carlo Erba Operating Procedure

Up to 23 discrete weighed samples loaded in metal containers are placed in the revolving magazine of the automatic sampler. The sampler is placed on top of a reactor where samples are introduced step-by-step and processed. Sample combustion is carried out in one of two independently heated reactors, each one linked to a chromatographic column connected in parallel to the same thermal conductivity detector.

One reactor performs the oxidation-reduction process to determine carbon, hydrogen, and nitrogen. The sample is instantaneously pyrolyzed at about 1,150°C and is then simultaneously oxidized by the combination of introduced oxygen and the action of a chromate catalyst to produce CO_2, H_2O, and nitrogen oxides. The combustion products then pass through the copper reduction reactor at about

700°C where nitrogen oxides are reduced to nitrogen gas and the excess combustion oxygen is irreversibly absorbed. The final products pass through a Porapak Q analytical column which produces a three-peak gas chromatogram of CO_2, H_2O, and N_2.

A second reactor with its own gas chromatographic column is used for the oxygen determination. The only requirements are that another magazine be loaded with up to 23 samples and the automatic sampler be switched to the oxygen side. The sample is pyrolyzed at 1,150°C and any oxygen present is converted to CO which is then separated from nitrogen, if present, by a molecular sieve analytical column.

A CHN analysis requires 10 minutes per sample. The oxygen analysis requires 5 minutes per analysis. The Model 1120 electronic integration is recommended for determining the peak area at an accuracy of ±0.1%. An overall analytical accuracy of at least ±0.3% is claimed for the Carlo Erba Analyzer.

Instrument Set-up

A fresh cylinder of 99.99% pure oxygen gas was procured and the Carlo Erba Model 1104 was set up according to specifications for measuring C, H, and N. The oxygen side of the analyzer was not evaluated. The recommended integrator was not available so the recorder was initially connected in parallel to both a Columbia Scientific Supergrator II and a Minigrator. When it became apparent that both integrators were producing similar results, only the Minigrator was subsequently used for measuring peak areas. Upon initial start up, there was a significant amount of baseline noise in the recorder. This was found to be due to a loose wire. After this was repaired, other problems continued to appear and Mr. E. M. Becker, who is the United States representative for Carlo Erba Company (located in Italy), was contacted for guidance in solving these problems. The instrument was leak-checked after

each problem was investigated, and several times the oxidation and reduction tubes were repacked with fresh catalysts in attempts to remedy persistent problems. After making all instrument modifications and repairs suggested by Mr. Becker, the accuracy and precision of the resulting test data were still not up to specifications. This is illustrated by subsequent data from replicate injections of the acetanilide standard and actual analyses of toluene, JP-7 fuel, and cyclohexanone-2,4-dinitrophenyl-hydrazone against the standard.

Precision for Multiple Injections of the Acetanilide Standard

A series of standards was injected into the Carlo Erba analyzer after each major or minor modification of the instrument. The results of most of these injections are reproduced in Table 67 which contains k-factor values for N_2, CO_2, and H_2O. The k-factor is a normalized peak area per unit sample weight. The results showed that the instrument repeatability varied from day to day and in general was not very consistent.

Analysis of Samples and a Comparison With Data From Other Laboratories

Several other samples also were analyzed during the latter part of the evaluation period for the Carlo Erba instrument. These samples included two reference materials, toluene and cyclohexanone-2,4-dinitrophenylhydrazone, plus JP-7 jet fuel. The test results are shown in Table 68. As can be observed, the accuracy was not near the specified ±0.3% value, for any of the elements.

A sample of JP-7 jet fuel was then taken to an alternate cooperating laboratory for elemental analysis on a Carlo Erba Model 1106 analyzer. This model is a newer instrument than the Model 1104. One obvious difference between the two is that the liquid samples are maintained under pressure in the Model 1106 while awaiting the automatic injections from the sample magazine.

TABLE 67. PRECISION FOR REPLICATE ACETANILIDE INJECTIONS

	Replicate k-factors and calculated precision on the following dates														
	11-19-80	12-4-80	1-8-81	1-13-81	1-14-81	1-21-81	1-22-81	1-28-81	1-29-81	1-30-81	2-2-81	2-4-81	2-9-81	2-24-81	2-25-81
Nitrogen k-factors x 10^4	2.720	2.503	2.257	2.38	2.18	2.13	2.21	2.13	2.49	2.53	2.64	2.36	2.29	2.43	2.43
	2.778	2.580	2.287	2.37	2.23	2.12	2.19	2.12	2.46	2.53	2.49	2.40	2.19	2.70	2.43
	2.354	2.807	2.337	2.39	2.18	2.09	2.27	2.09	2.48	2.52	2.43	2.44	2.27	2.44	2.56
		3.211	2.340	2.16	2.22	2.06	2.26		2.47			2.44	2.29	2.58	2.31
		2.934	2.373	2.29	2.19	2.16	2.32		2.50			2.36	2.28		
			2.369	2.34	2.23		2.12		2.49			2.41	2.28		
				2.29	2.25										
			2.391	2.27	2.25		2.29					2.35	2.28		
				2.22	2.06										
				2.18	2.16		2.29						2.29		
Mean	2.617	2.807	2 336	2.28	2.197	2.112	2.24	2.11	2.482	2.527	2.52	2.39	2.271	2.54	2.43
Percent relative, σ	8.8	10.1	2.1	3.4	2.6	1.8	2.9	1.0	0.6	0.6	4.3	1.6	1.5	5.0	4.2
Carbon k-factors x 10^5	1.935	7.596	7.96	7.95	7.59	7.52	8.08	7.18	8.68	9.13	9.15	8.06	8.00	9.13	9.02
	2.360	8.202	7.94	7.83	7.63	7.66	7.90	7.66	8.53	9.11	8.66	8.34	7.53	9.21	9.00
	3.557	7.856	8.60	7.99	7.60	7.45	8.12	7.45	8.68	9.38	8.41	8.45	7.72	9.05	8.90
		8.477	8.14	7.54	7.59	7.32	8.12		8.67			8.42	8.10	9.06	9.00
		-	8.12	7.98	7.68	7.59	8.37		8.71			8.14	7.92		
			8.17	7.96	7.61		7.90		8.68			8.32	7.92		
			8.28	7.54	7.70		8.16					8.08	7.47		
				7.84	7.69		8.22						7.02		
				7.69	7.47										
				7.79	7.55										
Mean	2.617	8.033	8.174	7.81	7.61	7.508	8.11	7.43	8.658	9.207	8.74	8.26	7.71	9.11	8.98
Percent relative, σ	32.1	4.8	2.7	2.2	0.9	1.7	1.9	3.2	0.7	1.6	4.3	2.0	4.6	0.8	0.6
Hydrogen k-fectors x 10^5	5.172	3.479	3.13	3.78	3.01	2.71	3.17	2.71	3.11	3.48	4.00	3.12	2.97	3.46	3.10
	2.360	3.197	3.21	3.18	3.37	2.91	2.69	2.91	2.99	3.45	3.15	3.67	2.71	3.41	3.12
	3.557	3.218	3.28	3.63	3.02	2.77	2.90	2.77	3.08	3.50	3.81	5.02	3.46	3.17	3.15
		2.705	3.44	3.17	3.14	2.57	2.91		3.13			4.66	3.36	3.22	3.16
		3.058	3.16	3.26	3.04	3.02	3.00		3.30			3.19	3.03		
			3.61	3.70	3.13		2.77		3.16			3.44	2.93		
			3.28	4.19	3.26		2.96					3.07	3.10		
				3.19	3.32		3.17						3.13		
				2.98	2.77										
				3.75	2.50										
Mean	3.700	3.131	3.301	3.46	3.056	2.796	2.95	2.80	3.13	3.48	3.65	3.74	3.09	3.32	3.13
Percent relative, σ	38.1	9.0	5.1	10.7	8.6	6.3	5.8	3.7	3.3	0.7	12.2	21.0	7.7	4.3	0.9

TABLE 68. ANALYTICAL RESULTS FOR SAMPLES

Date	Sample	Percent nitrogen			Percent carbon			Percent hydrogen		
		Theory	Found	Deviation	Theory	Found	Deviation	Theory	Found	Deviation
1-20-81	Toluene	0.0	0.0	0.0	91.25	58.50	-32.75	8.75	5.38	-3.37
			0.0	0.0		52.40	-38.85		4.99	-3.76
1-21-81	Toluene	0.0	0.0	0.0	91.25	90.4	-0.9	8.75	16.4	+7.6
			0.0	0.0		93.4	+2.1		16.6	+7.8
1-21-81	JP-7 fuel	0.0	0.0	0.0	~85.1	79.4	-5.7	~14.9	13.6	-1.3
			0.0	0.0		79.9	-5.2		12.3	-2.6
1-28-81	JP-7	0.0	0.0	0.0	~85.1	99.3	+14.2	~14.9	16.2	+1.3
			0.0	0.0		79.2	-5.9		13.8	-1.1
			0.0	0.0		79.8	-5.3		12.6	-2.3
2-2-81	JP-7	0.0	0.0	0.0	~85.1	92.7	+7.6	~14.9	14.3	-0.6
			0.0	0.0		86.7	+1.6		16.9	+2.0
			0.0	0.0		84.6	-0.5		14.1	-0.8
2-4-81	CDNH[a]	20.14	20.3	+0.2	51.79	51.1	-0.7	5.07	5.1	0.0
			19.7	-0.4		50.1	-1.7		4.0	-1.1
2-5-81	CDNH[a]	20.14	17.5	-2.6	51.79	46.3	-5.5	5.07	3.2	-1.9
			19.5	-0.6		81.5	+29.7		4.2	-0.9
2-5-81	JP-7 fuel	0.0	0.1	0.1	~85.1	91.0	+5.9	~14.9	14.3	-0.6
			0.1	+0.1		81.8	-3.3		15.8	+0.9
			0.1	+0.1		130.9	+44.8		17.3	+2.4
2-23-81	JP-7 fuel	0.0	0.0	0.0	~85.1	88.6	+3.5	~14.9	15.8	+0.9
			0.0	0.0		89.0	+3.9		16.5	+1.6

[a] CDNH = cyclohexanone-2,4-dinitrophenylhydrazone ($C_{12}H_{14}O_4N_4$).

The test results from this instrument over a two-day period are shown in Table 69. Also shown in Table 69 are test results for reference chemicals analyzed at Carlo Erba Company using a Model 1104 instrument.

Conclusions and Recommendations

After making all instrument modifications and adjustments recommended by E. M. Becker and still not improving on the poor accuracy and repeatability of the Carlo Erba analyzer, it was concluded that the problem must be in the instrument electronics. As a minimum solution, it appeared that the instrument needed to be completely reworked by a qualified representative from Carlo Erba Company. If the analyzer could not be repaired on site, high costs probably would have made sending the unit back to Carlo Erba Company in Italy for repair an impractical alternative.

26. DETERMINATION OF AROMATIC CARBON IN TWO FUELS BY ^{13}C FTNMR

Values for carbon aromaticity were determined on two fuel specimens by carbon-13 NMR using a Varian CFT-20 Fourier transform spectrometer. That instrument utilizes a Varian 602L computer for data acquisition, data reduction, and system control. The spectrometer was operated at 20 megahertz and the following instrument conditions were utilized for the analyses:

Sample probe	8 mm
Sweep width	4,000 Hz
Number of transients	1,000
Acquisition time	1.023 s
Pulse width 90°	17 μ/s
Pulse delay	5 s
Data points	8,192

TABLE 69. COMPARATIVE DATA FROM A MODEL 1104 AT CARLO ERBA COMPANY AND A MODEL 1106 AT ALTERNATE LABORATORY

Analyzing organization	Sample	Percent nitrogen			Percent carbon			Percent hydrogen		
		Theory	Found	(Deviation from mean)	Theory	Found	(Deviation from mean)	Theory	Found	(Deviation from mean)
Carlo Erba	Benzoic acid $C_7H_6O_2$	0.0	0.0	0.0	68.85	68.91	+0.10	4.95	4.98	+0.12
			0.0	0.0		68.55	-0.26		4.77	-0.09
			0.0	0.0		68.98	+0.17		4.83	-0.03
		mean	-	-		68.81	0.18[b]		4.86	0.08[b]
Carlo Erba	CDNH[a]	20.14	20.25	+0.13	51.79	51.48	-0.24	5.07	4.95	-0.18
			19.96	-0.16		52.03	+0.31		5.15	+0.02
			20.15	+0.03		51.65	-0.07		5.30	+0.17
		mean	20.12	0.11[b]		51.72	0.21[b]		5.13	0.12[b]
Alternate Laboratory	JP-7 fuel		0.19	+0.03		86.14	+0.14		15.10	0.00
			0.14	-0.02		86.07	+0.07		15.10	0.00
			0.13	-0.03		86.15	+0.15		15.09	-0.01
			0.16	0.00		85.93	-0.07		15.05	-0.05
			0.11	-0.05		85.70	0.30		15.23	+0.13
			0.25	+0.09		86.08	+0.08		15.05	+0.05
			0.17	+0.01		85.90	-0.10		15.11	+0.01
			0.15	-0.01		86.72	+0.12		15.10	0.00
		mean	0.16	0.03[b]		86.08	0.13[b]		15.10	0.03[b]

[a] CDNH = cyclohexanone-2,4-dinitrophenylhydrazone ($C_{12}H_{14}O_4N_4$).

[b] Computed without regard to sign.

Decoupler mode		3[a]
Chemical shift region or integral data	- aromatics	~150-110 ppm
	- aliphatics	~70-4 ppm

The samples were prepared by mixing the following components:

Jet fuel sample - 2 ml

NMR lock solvent - 1 ml deuterated chloroform

Chemical shift reference - 50 µl hexamethyldisiloxane

Relaxation agent - 50 mg 2.4 pentadione chromium III derivative

Results

Sample Number	Carbon aromaticity, C_{ar}/C_{tot}
POSF-D-81-65	0.103
POSF-D-81-69	0.128

[a]The gated proton decoupler was on during acquisition and off during delay.

SECTION III

CONVENTIONAL FUELS

Jet turbine fuels are essentially hydrocarbon mixtures having inexact compositions that vary depending upon the kind and source of the crude oil used for their production. Despite these inherent compositional variations, different types of fuel can be consistently produced to meet a variety of exacting fuel specifications. Conventional jet fuels include grades JP-4, JP-5, Jet-A, JP-7 and JP-8, with JP-4 currently being the most widely used fuel by the Air Force. The investigations described in this section were conducted to define the composition and properties of specific samples of these fuels for engineering applications, to support on-going studies or to aid in solving operational problems related to the use of these fuels.

1. TRACE METAL TRANSFER FROM SUMP WATER TO FUELS

Sample Descriptions

Analyses were conducted in support of an Air Force program to determine the amount of dissolved metals transferred to jet fuels from tank water bottoms.

Nine fuel samples were analyzed for metals by atomic absorption (AA) and emission spectroscopy. Additionally, one of the fuels was dispersed with a synthetic sump (metal chloride) solution, and then was reanalyzed by AA after a period of 4 hours. The nine fuels and one fuel dispersion are described in Table 70.

Fuel numbers 1 through 6 and number 10 were semiquantitatively analyzed by the emission spectrographic technique for all metals present, then were quantitatively analyzed by AA for copper, lead, and cadmium. Samples 7. 8, and 9 were analyzed only for copper and cadmium, by AA.

TABLE 70. DESCRIPTION OF SAMPLES FOR TRACE METAL ANALYSES

MRC Fuel No.	Container Type	WPAFB Sample Identification
1	Can	78-3346 Truck 73L-1180
2	Can	78-3348 Truck 73L-1147
3	Can	78-3348 Truck 72L-997
4	Can	78-3348 Truck 72L-1010
5	Can	F-16A-7 SN-780001
6	Can	F-16 SN, JP-4, fuel spec. 0748
7	Bottle	Standard JRF plain (no metals added)
8	Bottle	JRF spiked with 1.5 ppm copper and cadmium
9	Bottle	JP-4 spiked with 1.5 ppm copper and cadmium
10	Can/flask	258 g of Truck 73L-1180 Fuel #1 after dispersion with 87 g of a metal chloride solution

Sample Processing in Preparation for Analyses

Dispersion Technique for Fuel No. 10

A metal ion synthetic sump solution having the composition shown in Table 71 was dispersed with fuel number 10. The procedure for dispersal was simply a 15-second wrist oscillation of a pint bottle containing the fuel/solution mixture. The metal chloride solution and fuel phases were then allowed to separate overnight, after which the metal chloride solution was drained and discarded. The separated fuel was then acid extracted in preparation for the AA analyses.

Acid Extraction for AA Analyses

The fuels were extracted with high purity acid to sufficiently concentrate the metals in a nonvolatile form that could be quantified by AA. Two-milliliter quantities of metal-free concentrated

TABLE 71. CONCENTRATION OF SALTS AND METAL IONS IN SYNTHETIC SUMP SOLUTION

Salt Formula	Salt, ppm	Metal Ion, ppm
$CaCl_2$	50	18
$CdCl_2$	1000	490
$MgCl_2 \cdot H_2O$	50	6
NaCl	100	20
$ZnCl_2$	10	4.7
$CrCl_3 \cdot 6H_2O$	1	0.2
$CuCl_2 \cdot 2H_2O$	1	0.8
$FeCl_3$	5	1.7
$MnCl_2 \cdot 4H_2O$	5	1.4
$NiCl_2 \cdot 6H_2O$	1	0.2
$PbCl_2$	1	0.7

HCl[a] were added to 250-g quantities of fuel number 10. The fuel/acid dispersions were shaken on a platform shaker for 10 min, after which 18-ml quantities of deionized and distilled water were added. The mixtures were shaken for an additional 20-min period and then the water and fuel phases were allowed to separate. The acidic water layers were analyzed for lead and/or copper and cadmium by AA.

Metals Concentration for Emission Spectrographic Analyses

Two-gram quantities of fuel were deposited into the carbon electrodes by the dropwise addition/fuel evaporation technique. This was followed by the addition of 10 mg lithium carbonate to simulate the matrix of the metal standards. The fuels were then analyzed against 10-mg quantities of lithium carbonate containing 10-, 100-, and 1,000-ppm quantities of about 50 different metals.

[a]UltraR® hydrochloric acid; available from Hopkins and Williams; Essex, England.

The analyses of the 2-g quantities of fuel provided an effective concentration factor of 200. The estimated detection levels with this concentration factor were 0.05 ppm for copper, 1.0 ppm for cadmium, and 0.5 ppm for lead.

Results

The results of the emission and AA analyses for all the fuels are shown in Table 72. The emission analysis is estimated to have a precision of ±50%. A dash under a heading in the table indicates that none of the metal was detected. No copper, lead, or cadmium was detected in any of the samples by emission spectroscopy.

TABLE 72. EMISSION AND AA ANALYSIS RESULTS FOR FUELS

MRC Fuel No.	Brief Description	Emission Analysis Results for Fuels, ppm								AA Results for Acid Extracts of Fuels, ppm		
		Mg	Si	Fe	Al	Ca	Na	Ti	Ni	Cu	Pb	Cd
1	73L-1180	0.04	0.2	0.1	-	-	-	-	0.1	<0.016	0.071	0.014
2	73L-1147	0.4	1	0.1	0.2	3	0.1	-	-	<0.016	0.070	<0.006
3	72L-997	1	20	0.1	0.4	2	2	0.1	-	<0.016	0.071	<0.006
4	72L-1010	0.05	0.2	0.1	0.1	-	-	-	-	<0.016	0.045	<0.006
5	SN 780001	0.03	0.1	0.05	0.005	-	-	-	-	<0.016	0.053	0.018
6	SN, spec. 0748	0.04	1	0.2	0.2	-	-	-	-	<0.016	0.091	0.010
7	Plain JRF									<0.040		<0.015
8	Spiked JRF									1.93		0.74
9	Spiked JP-4									0.26		0.21
10	Conditioned No. 1	0.5	4	0.1	0.2	-	1	-	-	0.018	<0.04	1.06

The AA analysis is estimated to have a precision of ±2%. Values preceded by a "less than" (<) symbol indicate that none of this metal was detected at that level. The AA results showed that fuel number 8 contained copper and cadmium levels reasonably close to the expected 1.5-ppm levels, whereas fuel number 9 contained levels much lower. Fuel number 10 showed copper and cadmium levels that were increased over those in fuel number 1 in amounts proportional to the amounts in the metal chloride solution. Surprisingly, the amount of lead in fuel number 10 decreased to a nondetectable level.

2. TRACE METALS ANALYSIS OF JP-4 FUELS

Five fuel specimens were analyzed for trace metals content, with particular attention being given to copper, lead, and cadmium. An initial emission spectrographic analysis was conducted to semi-quantitatively survey the metals content of each fuel. In order to accomplish this analysis, a 2-g portion of each fuel was deposited dropwise into the cup of a graphite electrode which was maintained at a temperature sufficient to vaporize the volatile hydrocarbons. Care was taken to insure that the electrode did not become hot enough to cause loss of volatile metals. The electrode was then used for analysis by the arc emission procedure using a Bausch and Lomb two-meter dual grating spectrograph.

Atomic absorption analyses were conducted on four fuels for copper and lead and one fuel for cadmium and lead, using an analytical method previously developed for that purpose (ref. 11). The procedure consists of extracting 150 to 200 grams of fuel with high purity hydrochloric acid (UltraR) followed by analysis of the combined acid and water rinses of the fuel. Aqueous standard solutions of metals were used for calibration. A reagent blank was analyzed along with each fuel. A Perkin-Elmer Model 303 atomic absorption spectrophotometer was used for the analysis.

Results of the emission spectrographic and atomic absorption analyses are presented in Tables 73 and 74.

3. PHYSICAL AND CHEMICAL PROPERTIES OF JP-5 FUEL

A JP-5 fuel was analyzed for certain physical and chemical properties by analytical techniques described in the appendix. The data were required for a NASA-generated computer program that predicts combustion parameters.

TABLE 73. SEMIQUANTITATIVE ANALYSIS OF FUELS FOR TRACE METALS BY EMISSION SPECTROSCOPY

Fuel	Concentration, ppm							
	Mg	Si	Fe	Pb	Cd	Cu	Mn	Na
JP-4, A-4	0.005	0.05	0.005	<0.05	<0.1	<0.005	<0.01	<0.05
JP-4, A-7	0.03	0.05	0.01	<0.05	<0.1	<0.005	<0.01	<0.05
JP-4, Edwards Storage Tank 28	0.02	0.05	0.01	<0.05	<0.1	0.01	<0.01	<0.05
JP-4, Hercules 88 + 88n (Edwards)	0.02	0.05	0.02	<0.05	<0.2	0.01	<0.01	<0.05
JP-4, 1197	<0.05	<0.05	0.03	<0.05	<0.1	0.30	0.02	0.20

TABLE 74. ATOMIC ABSORPTION SPECTROPHOTOMETRIC METALS ANALYSIS

Fuel	Concentration, ppm		
	Copper	Cadmium	Lead
JP-4, A-4	0.01	-	None detected
JP-4, A-7	0.007	-	0.030
JP-4, Edwards Storage Tank 28	0.005	-	0.026
JP-4, Hercules 88 + 88n (Edwards)	0.007	-	0.030
JP-4, 1197	-	<0.004	0.02

Note: Dash indicates analysis not conducted.

Vapor pressure and heat of combustion data are presented in Table 75. Gas chromatographic simulated distillation results are shown in Table 76, hydrocarbon type distribution values are in Table 77, and elemental analysis results from a commercial micro-analytical laboratory (Galbraith Laboratories, Inc.) are presented in Table 78.

4. EVALUATION OF JP-8 FROM SHALE OIL

Chemical property data were provided for the first batch of JP-8 fuel produced from shale oil crude at the Sohio Toledo refinery. The properties requested included elemental analysis, hydrocarbon-type distribution, simulated distillation by gas chromatography, and net heat of combustion.

TABLE 75. VAPOR PRESSURE AND HEAT OF COMBUSTION OF JP-5

Property	Determined value
Vapor pressure, mm Hg @ 100°F	31.0
Heat of combustion, Btu/lb	
Gross value, duplicate tests	19,752 19,784
Average	19,768
Net value	18,533

TABLE 76. GAS CHROMATOGRAPHIC SIMULATED DISTILLATION OF JP-5

Percent recovered	Boiling point °C	Boiling point °F
0.5, IBP	44	111
1	106	223
5	161	322
10	174	345
20	190	374
30	201	394
40	211	412
50	220	428
60	230	446
70	239	462
80	250	482
90	263	505
95	271	520
99	289	552
99.5, FBP	295	563

TABLE 77. HYDROCARBON-TYPE ANALYSIS OF JP-5 (MOD. ASTM D 2789)

Compound type	Volume, %
Paraffins	45.3
Monocycloparaffins	37.0
Dicycloparaffins	3.1
Alkylbenzenes	8.7
Indans and Tetralins	3.2
Naphthalenes	2.7

TABLE 78. ELEMENTAL ANALYSIS OF JP-5

	Weight percent	
	Carbon	Hydrogen
	82.80	12.92
	83.06	13.08
Mean	82.93	13.00

Elemental Analysis

The elemental analysis was conducted by a commercial microanalytical laboratory (Galbraith Laboratories, Knoxville). The results of duplicate analyses are shown below in weight percents in Table 79.

TABLE 79. ELEMENTAL ANALYSIS OF SHALE JP-8

Element	Duplicate results, %		Average %
Carbon	86.22,	86.14	86.18
Hydrogen	13.76,	13.82	13.79
Oxygen	0.10,	0.14	0.12
Sulfur	0.086,	0.090	0.088
Nitrogen	0.0042,	0.0044	0.0043 (43 ppm)
Total			100.22

Hydrocarbon Type Distribution

The hydrocarbon type distribution was determined by mass spectroscopy, using a procedure (ASTM D 2789-Modified) whereby characteristic mass fragments were summed to determine the various concentrations. The analysis was conducted on a CEC-21-103C mass spectrometer having a heated batch inlet. The distribution is shown in Table 80.

The total aromatic content of 20.5% is well within the specific maximum limit of 25% for JP-8. The indan/tetralin content for this fuel is somewhat higher than that found in most JP-8 fuels.

TABLE 80. HYDROCARBON TYPE ANALYSIS OF SHALE JP-8 (ASTM D 2789-Modified)

Hydrocarbon type	Volume %
Paraffin	46.7
Cycloparaffins	32.8
Dicycloparaffins	0.0
Alkylbenzenes	10.5
Indans/tetralins	9.2
Naphthalenes	0.8
Total	100.0

Simulated Distillation by Gas Chromatography

The boiling point distribution was determined by gas chromatography as described in ASTM D 2887. A gas chromatograph equipped with a flame ionization detector and a 6-foot by 1/8-inch OV-1 column was used for this work. The column was initially held 4 min at 50°C and then programmed up to 200°C at a rate of 8°C/min. A mixed hydrocarbon standard from C_4 to C_{18} was used to correlate boiling point with retention time. Percent recovered values were determined from an integrating computer program which provided elapsed time, slice area, corrected area, accumulated area of the chromatogram, and percent recovered. The results are shown in Table 81.

Net Heat of Combustion

Net heat of combustion was determined by ASTM Method D 240, employing the oxygen bomb calorimeter. The 13.89% hydrogen value from the NMR analysis was used in the calculation rather than the very similar 13.79% value from the elemental analysis. The results are shown in Table 82.

TABLE 81. SIMULATED DISTILLATION OF SHALE JP-8 BY GC

Percent recovered	Retention time, min	Boiling point °C	Boiling point °F
0.5	4.28	148	298
1	4.83	153.5	309
5	6.06	162.5	324.5
10	6.77	171	340
20	7.62	179	354
30	8.37	185.5	366
40	9.73	198	388
50	10.32	203.5	398
60	11.32	213	415
70	11.99	219.5	427
80	13.04	230	446
90	14.04	240	464
95	15.28	252	486
99	17.50	277	531
99.5	19.17	295.5	564

TABLE 82. HEAT OF COMBUSTION OF JP-5

Btu/lb		
Gross	Average	Net
19,811		
19,805		
	19,808	18,541

5. TRACE METALS ANALYSIS OF SHALE DERIVED JP-8

A series of five samples, which consisted of shale derived JP-8 stored in different containers under various conditions, were analyzed for trace metals content. The fuels were treated with high purity acid (metal-free) to extract trace metals according to methodology developed earlier for analysis of metals in fuels (ref. 11). An aliquot of the acidic extract was concentrated by dropwise addition and evaporation into the carbon electrodes used for emission spectrographic analysis.

Lower detection limits for metals of interest are as follows: Zn - 200 ppb; Pb - 20 ppb; Al - 4 ppb; Cu - 2 ppb; Sn - 10 ppb; Fe - 6 ppb. Analytical results are shown in Table 83 below.

TABLE 83. EMISSION SPECTROGRAPHIC ANALYSIS OF FUELS

Fuel sample	Parts-per-billion Copper	Tin
JP-8, fuel rinsed, lined can	-	-
JP-8, fuel rinsed, unlined can	2	14
JP-8, solvent rinsed, lined can	4	-
JP-8, solvent rinsed, unlined can	6	-
JP-8, control	-	-

[a]Dash (-) indicates none detected.
No Zn, Pb, Al or Fe was detected.

6. CHEMICAL AND PHYSICAL PROPERTIES OF AMRL JP-8 FUEL

Chemical and physical property determinations were performed on a JP-8 fuel sample to provide data required by the Air Force Civil and Environmental Engineering Office at Tyndall Air Force Base, Florida.

Kinematic viscosity, density, vapor pressure and surface tension were determined as a function of temperature. Net heat of combustion was measured by oxygen bomb calorimetry. Simulated distillation was conducted by gas chromatography, and mass spectrometry by ASTM Method D 2425 was used for hydrocarbon type distribution. All test methods are described in the Appendix. The JP-8 fuel was fractionated before the hydrocarbon type analysis, and this is described below.

Table 84 lists data for density, kinematic viscosity, surface tension, and vapor pressure; Table 85 presents heat of combustion values; and Table 86 provides simulated distillation data. Figure 72 shows the viscosity/temperature relationship.

TABLE 84. PHYSICAL PROPERTIES OF AMRL JP-8

Property	Temperature, °F	
Density, g/cc	32	0.8172
	70	0.8018
	100	0.7894
Kinematic viscosity, centistokes	0	4.553
	77	1.737
	100	1.417
Surface tension, dynes/cm	32	28.15
	70	26.18
	100	24.58
Vapor pressure, mm Hg	32	3.3
	70	11.0
	100	25.7

TABLE 85. HEAT OF COMBUSTION OF AMRL JP-8

Gross, Btu/lb		Net, Btu/lb
Duplicate	Average	Average
19,657		
19,710		
	19,684	18,407

TABLE 86. GAS CHROMATOGRAPHIC SIMULATED DISTILLATION OF AMRL JP-8

Percent Recovered	Temperature °C	Temperature °F
0.5 (IBP)	102	216
1	115	239
5	144	291
10	165	329
20	182	360
30	194	381
40	202	396
50	210	410
60	218	424
70	227	441
80	238	460
90	256	493
95	270	518
99	294	561
99.5 (FBP)	303	577

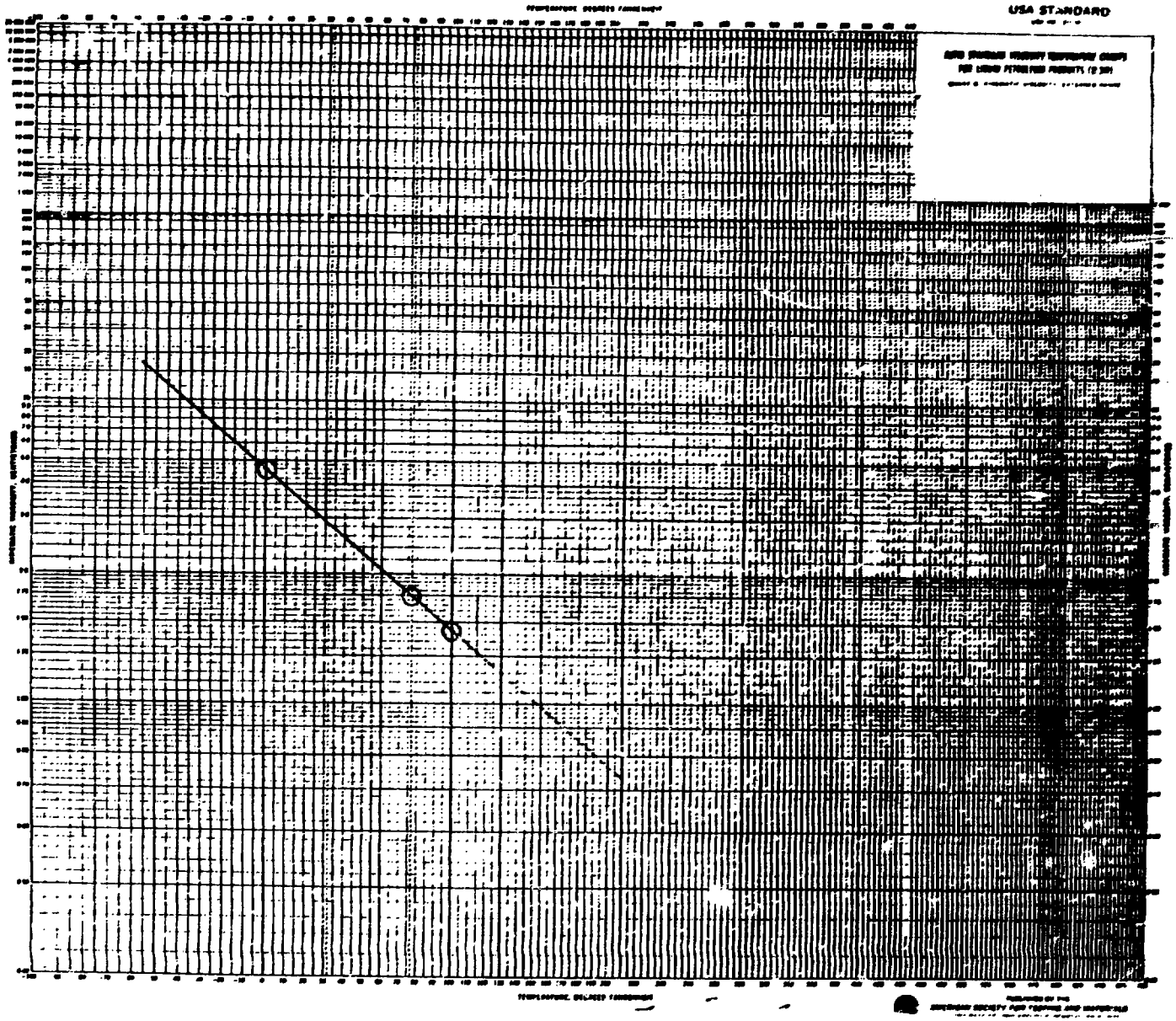

Figure 72. Viscosity/temperature plot for AMRL JP-8.

A hydrocarbon type analysis was conducted on the fuel using the approach of isolating aromatic and paraffinic fractions by elution chromatography (ASTM D 2549) and then analyzing each fraction by a mass spectrometric procedure (ASTM D 2425). The preliminary separation was conducted on a 50-cm column of activated bauxite and silica gel by sequential elution with pentane, ethyl ether, chloroform, and ethyl alcohol.

The mass spectrometric analysis provided quantitative information on 11 hydrocarbon types. The analysis was based on the summation of characteristic fragment mass intensities to determine the concentration of various hydrocarbon types.

By summation of various combinations of more than 110 mass spectral peaks, matrices consisting of sets of 5 linear simultaneous equations for the saturate fraction and 10 for the aromatic fraction were constructed. Alkylbenzenes, which were calculated in the saturate fraction and paraffins calculated in the aromatic fraction, demonstrated the completeness of the chromatographic separation. Computer solution of each matrix yielded weight percent of each compound type. Hydrocarbon type data are presented in Table 87.

TABLE 87. HYDROCARBON-TYPE DISTRIBUTION OF AMRL JP-8 BY ASTM D 2425

Compound type	Weight percent
Paraffins	42.29
Cycloparaffins	35.28
Dicycloparaffins	9.10
Tricycloparaffins	1.64
Alkylbenzenes	8.57
Indans and tetralins	1.83
Indenes	0.04
Naphthalene	0.34
Naphthalenes	0.90
Acenaphthenes	-[a]
Acenaphthylenes	-
Tricyclic aromatics	0.01

[a]Dash indicates none was detected.

7. DIELECTRIC CONSTANT OF JP-8 FUEL WITH ANTISTATIC ADDITIVES

The dielectric constant as a function of temperature was determined for JP-8 with and without antistatic additives. The purpose of the work was to determine whether the presence of these additives in the fuel has a significant effect on its dielectric constant.

A General Radio 1615A capacitance bridge and guard circuit were used for the measurements. The bridge signal generator was a General Radio 1311A audio oscillator and the bridge detector was a Type 1232A tuned amplifier and null detector.

Capacitance measurements were made in a three-terminal guarded cell relative to air at the same temperature.

Dielectric constant values are given in Table 88 below.

TABLE 88. DIELECTRIC CONSTANT OF JP-8 WITH/ WITHOUT ANTISTATIC ADDITIVES

	Temperature, °F		
	0	74	100
JP-8, Tank F-3	2.192	2.144	2.127
JP-8 + 2PPM ASA-3	2.186	2.137	2.120
JP-8 + 2PPM S-450	2.181	2.132	2.115

8. CHEMICAL PROPERTIES OF ENGLISH JP-8 FUEL

Hydrocarbon type and distillation temperature range data were provided for a sample of JP-8 from Bendix fuel control division. The effect of this fuel on elastomeric seals was evaluated as part of another Air Force program.

Simulated distillation was conducted according to ASTM procedure D 2887 to determine boiling point range. A gas chromatograph equipped with a 3% OV-1 column and a hydrogen flame ionization detector was used for this work. Hydrocarbon type analysis by mass spectrometry was conducted according to ASTM Method D 2789-71.

Data are presented in Tables 89 and 90.

TABLE 89. SIMULATED DISTILLATION OF ENGLISH JP-8 BY GAS CHROMATOGRAPHY

Percent recovered	English JP-8 BP, °C	English JP-8 BP, °F
0.5, IBP	92	198
1	104	219
5	141	206
10	156	313
20	170	338
30	180	356
40	190	374
50	198	388
60	209	408
70	218	424
80	231	448
90	245	473
95	254	489
99	270	518
99.5, FBP	276	529

TABLE 90. HYDROCARBON TYPE DISTRIBUTION OF ENGLISH JP-8 BY MASS SPECTROMETRY

Compound type	Volume, %
Paraffins	55.4
Monocycloparaffins	30.1
Dicycloparaffins	-
Alkylbenzenes	11.7
Indans and tetralins	2.0
Naphthalenes	0.8

9. ANALYSIS OF TWO BROAD SPECTRUM ERBS FUELS

Two samples of experimental reference broad spectrum fuels were analyzed in support of Alternate Source Development.

Simulated distillation was conducted by gas chromatography as described in ASTM D 2887. A gas chromatograph, equipped with a flame ionization detector and a column of SP-2100, was used for this work. Data are presented in Table 91.

TABLE 91. SIMULATED DISTILLATION OF BROAD SPECTRUM FUELS

	ERBS #1 Boiling Point		ERBS #2 Boiling Point	
Percent Recovered	°C	°F	°C	°F
0.5, IBP	132	270	129	264
1	141	286	140	284
5	163	325	162	324
10	173	343	173	343
20	188	370	188	370
30	197	387	197	387
40	208	406	208	406
50	218	424	218	424
60	230	446	231	448
70	240	464	244	471
80	258	496	261	502
90	287	549	290	554
95	313	595	315	601
99	355	671	366	691
99.5, FBP	365	689	377	711

Hydrocarbon type analyses were conducted using ASTM procedure D 2789-71. Data are presented in Table 92.

Nitrogen analyses were obtained from Galbraith Laboratories, Inc. (Knoxville, TN). Data are presented in Table 93.

TABLE 92. HYDROCARBON TYPE DISTRIBUTION OF BROAD SPECTRUM FUELS BY MASS SPECTROMETRY

Compound type	Volume percent ERBS #1	ERBS #2
Paraffins	46.6	46.8
Monocycloparaffins	32.6	32.4
Dicycloparaffins	-	-
Alkylbenzenes	9.5	9.5
Indans and Tetralins	5.3	5.3
Naphthalenes	6.0	6.0

TABLE 93. ELEMENTAL ANALYSIS OF BROAD SPECTRUM FUELS

	Nitrogen, ppm ERBS #1	ERBS #2
	84	85
	82	78
Mean	83	82

10. HYDROCARBON-TYPE DISTRIBUTION IN NASA JET "A" AND DIESEL FUELS

Chemical property data were required for two fuel specimens being studied independently at AFAPL and NASA Lewis Research Center. A hydrocarbon-type distribution analysis was requested along with an independent check for total naphthalenes content by conventional ASTM procedure D 1840.

Analytical Procedures

Modified ASTM Method D 2789 was used to determine the concentration of six different hydrocarbon types present in two fuels. Mass spectra of the fuels were recorded, and summations of characteristic mass fragments for the hydrocarbon types were related to concentrations by means of calibration mixtures.

ASTM Method D 1840 was used to determine the total concentration of naphthalene, acenaphthene, and alkylated derivatives of both of these compounds. Ultraviolet spectrophotometry is employed in this method, with absorbance at 285 nm being measured for known concentrations of fuel in cyclohexane. Phenanthrenes, dibenzothiophenes, biphenyls, benzathiophenes, and anthracenes interfere with the method if present and add to the apparent naphthalene content.

Results

The analytical results from both procedures are shown in Table 94.

TABLE 94. RESULTS OF HYDROCARBON TYPE AND NAPHTHALENES ANALYSES FOR TWO FUELS

		Concentrations of compound types			
		NASA Jet "A"		NASA diesel fuel	
Compound types	Method	(Vol %)	(Wt %)	(Vol %)	(Wt %)
Paraffins	MS[a]	45.8		38.4	
Monocyclo-paraffin	MS	37.4		27.0	
Dicyclo-paraffin	MS	1.0		0.8	
Alkylbenzenes	MS	9.0		8.4	
Indans and Tetralins	MS	4.4		10.5	
Naphthalenes	MS	2.4	3.1	14.9	19.2
Naphthalenes	UV Absorption		2.4, 2.4[b]		25.6, 25.8[b]

[a]Mass Spectrometric.

[b]Duplicate analyses.

The mass spectral hydrocarbon type analysis yields results in liquid volume percent, while the naphthalene determination (ASTM D 1840) is computed in weight percent. In order to compare data, the volumetric naphthalene value was converted to weight percent. The higher naphthalene content for the diesel fuel by ASTM D 1840 indicates the probable presence of interfering compounds.

11. METALS ANALYSIS OF SHALE-DERIVED JET FUEL

Shale-derived jet fuel, which was shipped in an unlined metal can, was found during evaluation at AFAPL to fail the thermal stability tests. A metals analysis was requested to determine if contamination from the sample container was responsible for the fuel instability.

An emission spectrographic analysis of the fuel sample, labeled 9105-1, showed the presence of 200 ppb tin and 8 ppb nickel. No other metals were detected. The tin source may be the solder seam in the fuel can, and its presence is the likely cause of the poor thermal stability.

12. VAPOR PRESSURE OF JP-4 FROM BOTH PETROLEUM AND SHALE OILS

Vapor pressure was determined for petroleum- and shale-derived JP-4 samples by use of the microvapor pressure apparatus and procedure described in ASTM Method D 2251 and reference 9. Results are presented below.

	Vapor pressure, mm Hg	
Sample number	135°F	150°F
145-400-792033	229	297
HRI-LO-2054	150	191

13. GC, MS, AND NMR ANALYSES OF EIGHT SHALE-DERIVED JET FUELS

Samples of eight shale-derived jet fuels were analyzed for boiling range distribution by GC-simulated distillations, hydrocarbon-type distribution by mass spectrometry, and aromaticity by carbon-13 and proton high-resolution NMR spectroscopy. The eight shale-derived jet fuel samples were identified as follows.

1. HRI-LO-2054 (80-PHJ-084A)
2. HRI-LO-2057 (80-PHJ-084B)
3. UOC-A-1655 Rehydrotreated
4. UOC-B-1656 Single Pass
5. UOC-9H15-6
6. UOC-9I05-1
7. UOC-9H15-7
8. UOC-9I05-2

The simulated distillations were conducted by gas chromatography as described in ASTM Method D 2887. A gas chromatograph equipped with a flame ionization detector and a column of 3% OV-1 on Chromosorb W was used for this work. Data are presented in Table 95.

The hydrocarbon-type analyses were conducted using the modified ASTM procedure D 2789 for all samples. Additionally, Monsanto Method 21-PQ-38-63 was used for two samples. Data are presented in Table 96.

The carbon-13 NMR analyses were conducted to determine carbon aromaticity, which is a ratio of the aromatic carbon to the total carbon in the fuel. Likewise, the proton NMR analyses were conducted to determine hydrogen aromaticity, which is a ratio of the aromatic hydrogen in the fuel to the total hydrogen. Using these aromaticity values and the ratio of total hydrogen to total carbon in the fuels (obtained from elemental hydrogen analyses conducted at AFAPL), the ratio of aromatic hydrogen to aromatic carbon was then calculated for the eight fuels. This ratio was to be used to correlate the composition of the fuel with its combustion behavior. The total area under the peaks in specified spectral regions of the proton NMR curves was also provided for use in a computer program.

NMR Analytical Parameters

The NMR analyses were conducted on a Varian CFT-20 Fourier transform spectrometer containing a Varian 602L computer for data acquisition, data reduction, and system control. The spectrometer

TABLE 95. SIMULATED DISTILLATION BY GAS CHROMATOGRAPHY

Percent Recovered	HRI-LO-2054 (80-PHJ-084A)		HRI-LO-2057 (80-PHJ-084B)		UOC-A-1655		UOC-B-1656		UOC-9H15-6		UOC-9I05-1		UOC-9H15-7		UOC-9I05-2	
	°C	°F	°C	°F	°C	°F	°C	°F	°C	°F	°C	°F	°C	°F	°C	°F
0.5 (IBP)	25	77	28	82	55	131	57	135	82	180	51	124	143	289	145	293
1	34	93	36	97	65	149	66	151	89	192	58	136	151	304	153	307
5	88	190	95	203	100	212	98	208	116	241	96	205	175	347	174	345
10	107	225	112	234	121	250	117	243	128	262	116	241	196	385	195	383
20	136	277	128	262	144	291	135	275	145	293	139	282	228	442	218	424
30	154	309	149	300	161	322	151	304	159	318	153	307	249	480	238	460
40	171	340	166	331	174	345	166	331	168	334	167	333	266	511	258	496
50	184	363	180	356	186	367	177	351	175	347	175	347	284	543	277	531
60	197	387	195	383	196	38'	190	374	183	361	185	365	300	572	298	568
70	206	403	207	405	208	406	201	394	194	381	196	395	313	595	312	594
80	219	426	222	432	217	423	216	421	200	392	203	397	327	621	330	626
90	236	457	240	464	228	442	228	442	212	414	215	419	343	649	350	662
95	255	491	258	496	235	455	236	457	217	423	220	428	354	669	367	693
99	303	577	293	559	251	484	252	486	230	446	236	457	381	718	397	747
99.5(FBP)	307	585	304	579	257	495	261	502	240	464	244	471	388	730	408	766

TABLE 96. HYDROCARBON-TYPE ANALYSIS

	Volume Percent									
	HRI-LO-2054[a] (80-PHJ-084A)	HRI-LO-2057[a] (80-PHJ-084B)	UOC-A-1655[a]	UOC-B-1656[a]	UOC-9H15-6[a]	UOC-9I05-1[a]	UOC-9H15-7 Method 1[a]	UOC-9H15-7 Method 2[b]	UOC-9I05-2 Method 1	UOC-9I05-2 Method 2
Paraffins	46.5	44.8	46.0	50.7	46.7	49.5	46.0	46.2	45.4	45.5
Monocycloparaffins	42.5	42.9	50.2	46.8	42.6	39.5	37.2	38.3[c]	37.4	38.1[c]
Dicycloparaffins	1.9	1.2	0	0	0	0.4	2.1		1.4	
Alkylbenzene	6.2	9.1	3.0	2.0	9.0	8.4	6.0	6.8	6.5	7.6
Indans/Tetralin	2.9	2.1	0.8	0.5	1.7	2.2	7.4	7.8	8.0	7.7
Naphthalenes	Trace	Trace	0	0	0	0	1.3	0.9	1.3	1.1

[a] Method 1. Modified ASTM D2789-71

[b] Method 2. Monsanto 21-PQ-38-63.

[c] This method combines mono- and dicycloparaffins into a single value.

was operated at 20 megahertz for the ^{13}C analyses and 79.54 megahertz for the proton NMR analyses. The following instrument conditions were utilized for the two analyses:

Type NMR Analysis		Carbon-13	Proton (^{1}H)
Sample Probe		10 mm	5 mm
Sweep Width		4,000 Hz	1,000 Hz
Number of Transients		1,000	50
Acquisition Time		1.023 s	4.095 s
Pulse Width 90°		17 µs	24 µs
Pulse Delay		5 s	8 s
Homo-Spoil Time[a]		Not on	8 ms
Data Points		8,192	8,192
Decoupler Mode		3[b]	--
Chemical Shift Regions for Integral Data	Aromatics	~150-110 ppm	8.3-6.5 ppm
	Aliphatics	~70-4 ppm	4.0-0.2 ppm

[a]Homospoil was on during pulse delay.

[b]The gated proton decoupler was on during acquisition and off during delay.

The analytical samples were prepared for carbon-13 analysis by mixing the following components:

Jet Fuel Sample - 1 ml
NMR lock solvent - 0.5 ml deuterated chloroform ("100%" $CDCl_3$)
Chemical shift reference - 50 µl hexamethyl disiloxane
Relaxation agent - ~25 mg 2,4-pentanedione chromium III derivative

For the proton NMR analysis, a 20 µl quantity of the above mixture was added to 0.5 ml additional $CDCl_3$.

Calculations and Results

The carbon aromaticity values were obtained by integrating the peak areas in the aromatic region of the ^{13}C spectra relative to the total peak area in the spectra. The hydrogen aromaticities were obtained in the same manner from peak areas in the proton NMR spectra. The ratio of aromatic hydrogen to aromatic carbon was obtained from the following equation:

$$\frac{H_{ar}}{C_{ar}} = \underset{I}{\frac{C_T}{C_{ar}}} \times \underset{II}{\frac{H_{ar}}{H_T}} \times \underset{III}{\frac{H_T}{C_T}}$$

where I = the inverse of carbon aromaticity determined by ^{13}C NMR

II = the hydrogen aromaticity determined by proton NMR

III = total hydrogen/carbon ratio determined from percent hydrogen data provided by AFAPL

The aromaticity values for the eight fuels and their aromatic and total hydrogen/carbon ratios are presented in Table 97. The integrated areas for the specified spectral regions of the proton NMR spectra are listed in Table 98.

In general, no specific compounds were identified by the ^{13}C and proton NMR analyses. However, the one exception was fuel HRI-LO-2057 which was observed to contain a significant quantity of toluene.

Comparison of Carbon Aromaticities With Values From Mass Spectrometric Analyses

Carbon aromaticity was calculated from the hydrocarbon-type analysis data. The volume percents were recomputed to weight percents and an average compound structure was formulated for each fuel constituent using an average carbon number determined from the GC

TABLE 97. AROMATICITY VALUES AND HYDROGEN/CARBON RATIOS

Sample designation	Carbon aromaticity, C_{ar}/C_T [a]	Hydrogen aromaticity, H_{ar}/H_T	Percent H_T [b]	Mole ratio [c] H_T/C_T	Mole ratio H_{ar}/C_{ar}
HRI-LO-2054	0.062	0.022	14.43	2.01	0.714
HRI-LO-2057	0.099	0.039	14.22	1.98	0.774
UOC-A-1655	0.045	0.018	14.68	2.05	0.821
UOC-B-1656	0.033	0.009	14.82	2.07	0.560
UOC-9H15-6	0.086	0.029	14.34	1.99	0.667
UOC-9I05-1	0.086	0.031	14.36	2.00	0.726
UOC-9H15-7	0.086	0.033	13.77	1.90	0.726
UOC-9I05-2	0.089	0.040	13.70	1.89	0.845

[a] These values may not be as accurate as the hydrogen aromaticity values because of a low signal/noise ratio in the aromatic region of the ^{13}C spectrum.

[b] Data from AFAPL by ASTM D 3701.

[c] Total carbon data were obtained by subtracting the % H_T from 100.

TABLE 98. INTEGRATED AREAS[a] OF SPECIFIED PROTON NMR SPECTRAL REGIONS

	Spectral Regions							
Sample	HMONO 6.6-7.3, ppm	HDI 7.3-7.8, ppm	HTRI 7.8-8.3, ppm	HALP 1 2.3-4.0, ppm	HALP 2 1.9-2.3, ppm	H BETA 1.9-1.0, ppm	H GAMA 1.0-0.5, ppm	H BETH 1.90-1.65, ppm
HRI-LO-2054	6	ND[b]	ND	2	7	139	111	9
HRI-LO-2057	8	ND	ND	1	7	105	84	6
UOC-A-1655	3	1	ND	ND	4	121	98	7
UOC-B-1656	2	ND	ND	1	2	125	96	6
UOC-9H15-6	6	ND	ND	1	8	108	82	5
UOC-9I05-1	6	ND	ND	ND	6	99	83	5
UOC-9H15-7	6	1	ND	3	6	117	74	6
UOC-9I05-2	7	1	1	7	8	128	74	8

[a] The listed integral areas are accurate to ±0.5. Fractional values are rounded to the nearest whole number by the data system.

[b] ND shows a total area less than 0.5.

simulated distillation analysis. The percents of aromatic and aliphatic carbon in each fuel constituent were calculated from the weight percentages and compound structures. The carbon aromaticity of the entire fuel was then calculated from the ratio of total aromatic carbon to total carbon in the fuel. These calculated carbon aromaticity values and all data used in the calculations are shown in Table 99. The calculated carbon aromaticity values and those obtained from ^{13}C NMR are compared in Table 100.

Conclusions

In general, the aromaticity values calculated from the hydrocarbon type analyses were slightly lower than the corresponding values calculated from the ^{13}C NMR analyses. However, the overall agreement of data was good considering the diversity of the two methods and the experimental error inherent in the component parts of each analysis. The relative differences in the fuels were highlighted by the aromaticity values obtained by both analytical approaches.

It is interesting to note the generally good correlation of the total hydrogen values with aromaticity values. As expected, the hydrogen content increased as aromaticity decreased. The only notable exception occurs for fuel number HRI-LO-2057. This fuel showed the highest aromaticity of all the fuels by all three analytical techniques, yet it did not have the lowest hydrogen content. Coincidentally, this was also the only fuel that was shown earlier to contain toluene.

The H_{ar}/C_{ar} value, given in the last column of Table 97, is useful in evaluating the nature of a fuel's aromatic fraction. However, both C_{ar}/C_T and H_{ar}/C_{ar} values should be used for correlation with the fuels combustion characteristics.

TABLE 99. CARBON AROMATICITY FROM HYDROCARBON TYPE ANALYSES

Fuel constituents	Volume percent[a]	Weight percent[b]	Average compound[c]	Mole percent aromatic carbon[d]	Mole percent aliphatic carbon[d]	Carbon aromaticity[e]
		Fuel HRI-LO-2054				
Paraffins	46.5	44.2	$C_{10}H_{22}$	0	43.6	
Monocycloparaffins	42.5	43.6	$C_{10}H_{20}$	0	43.6	
Dicycloparaffins	1.9	1.9	$C_{10}H_{18}$	0	2.0	
Alkylbenzenes	6.2	6.9	C_9H_{12}	4.8	2.4	
Indans/Tetralin	2.9	3.4	C_9H_{10}	2.4	1.2	
Total				7.2	92.8	0.072
		Fuel HRI-LO-2057				
Paraffins	44.8	42.5	$C_{10}H_{22}$	0	41.9	
Monocycloparaffins	42.9	43.8	$C_{10}H_{20}$	0	43.7	
Dicycloparaffins	1.1	1.2	$C_{10}H_{18}$	0	1.2	
Alkylbenzenes	9.1	10.1	C_9H_{12}	7.1	3.5	
Indans/Tetralin	2.1	2.4	C_9H_{10}	1.8	0.8	
Total				8.9	91.1	0.089
		Fuel UOC-A-1655				
Paraffins	46.0	44.1	$C_{10}H_{22}$	0	43.6	
Monocycloparaffins	50.2	51.7	$C_{10}H_{20}$	0	51.8	
Dicycloparaffins	0.0	0.0	$C_{10}H_{18}$	0	0.0	
Alkylbenzenes	3.0	3.3	C_9H_{12}	2.4	1.2	
Indans/Tetralin	0.8	0.9	C_9H_{10}	0.7	0.3	
Total				3.1	96.9	0.031

(continued)

TABLE 99 (continued)

Fuel constituents	Volume percent[a]	Weight percent[b]	Average compound[c]	Mole percent aromatic carbon[d]	Mole percent aliphatic carbon[d]	Carbon aromaticity[e]
	Fuel UOC-B-1656					
Paraffins	50.7	48.8	$C_{10}H_{22}$	0	48.3	
Monocycloparaffins	46.8	48.4	$C_{10}H_{20}$	0	48.6	
Dicycloparaffins	0.0	0.0	$C_{10}H_{18}$	0	0.0	
Alkylbenzenes	2.0	2.3	C_9H_{12}	1.6	0.2	
Indans/Tetralin	0.5	0.6	C_9H_{10}	0.5	0.2	
Total				2.1	97.9	0.021
	Fuel UOC-9H15-6					
Paraffins	46.7	44.4	$C_{10}H_{22}$	0	43.7	
Monccycloparaffins	42.6	43.7	$C_{10}H_{20}$	0	43.7	
Dicycloparaffins	0.0	0.0	$C_{10}H_{18}$	0	0.0	
Alkylbenzenes	9.0	10.0	C_9H_{12}	7.0	3.5	
Indans/Tetralin	1.7	2.0	C_9H_{10}	1.4	0.7	
Total				8.4	91.6	0.084
	Fuel UOC-9I05-1					
Paraffins	49.5	47.0	$C_{10}H_{22}$	0	46.4	
Monocycloparaffins	39.5	40.5	$C_{10}H_{20}$	0	40.5	
Dicycloparaffins	0.4	0.5	$C_{10}H_{18}$	0	0.5	
Alkylbenzenes	8.4	9.4	C_9H_{12}	6.5	3.3	
Indans/Tetralin	2.2	2.6	C_9H_{10}	1.9	0.9	
Total				8.4	91.6	0.084

(continued)

TABLE 99 (continued)

Fuel Constituents	Volume percent[a]	Weight percent[b]	Average compound[c]	Mole percent aromatic carbon[d]	Mole percent aliphatic carbon[d]	Carbon aromaticity[e]
	Fuel UOC-9H15-7					
Paraffins	46.0	43.3	$C_{15}H_{32}$	0	42.8	
Monocycloparaffins	37.2	37.7	$C_{15}H_{30}$	0	37.6	
Dicycloparaffins	2.1	2.1	$C_{15}H_{28}$	0	2.1	
Alkylbenzenes	6.0	6.6	$C_{14}H_{22}$	2.9	3.8	
Indans/Tetralin	7.4	8.6	$C_{14}H_{20}$	3.9	5.1	
Naphthalenes	1.3	1.7	$C_{14}H_{16}$	0.8	1.0	
Total				7.6	92.4	0.076
	Fuel UOC-9I05-2					
Paraffins	45.4	42.5	$C_{15}H_{32}$	0	42.0	
Monocycloparaffins	37.4	37.8	$C_{15}H_{30}$	0	37.6	
Dicycloparaffins	1.4	1.4	$C_{15}H_{28}$	0	1.4	
Alkylbenzenes	6.5	7.2	$C_{14}H_{22}$	3.2	4.2	
Indans/Tetralin	8.0	9.4	$C_{14}H_{20}$	4.2	5.6	
Naphthalenes	1.3	1.7	$C_{14}H_{16}$	0.8	1.0	
Total				8.2	91.8	0.082

[a] Results from mass spectrometric hydrocarbon type analyses.

[b] Calculated using density values.

[c] Determined using an average carbon number obtained from simulated distillation analyses.

[d] Calculated from structure of average compound.

[e] Calculated by dividing the percent aromatic carbon by the percent total carbon in the fuel.

TABLE 100. COMPARISON OF CARBON AROMATICITY VALUES

Fuel	Values from ^{13}C NMR	Values from mass spectrometry[a]
HRI-LO-2054	0.062	0.072
HRI-LO-2057	0.099	0.089
UOC-A-1655	0.045	0.031
UOC-B-1656	0.033	0.021
UOC-9H15-6	0.086	0.084
UOC-9I05-1	0.086	0.084
UOC-9H15-7	0.086	0.076
UOC-9I05-2	0.089	0.082

[a]Using average carbon numbers from simulated distillations by GC.

14. VAPOR COMPOSITION OF JP-4 AND JP-8 FUELS IN EQUILIBRIUM WITH THEIR BULK LIQUIDS

Fuel flammability studies conducted within the Fire Protection Branch of the Aero Propulsion Laboratory generated a need for information concerning the precise composition of vapors in equilibrium with bulk aircraft fuels. Therefore, a study was conducted to determine equilibrium vapor compositions of two fuels, a JP-4 (Tank 15) and a JP-8 (Tank F-3), at various temperatures. The procedures and results of this work are documented below.

Procedure

A vapor equilibration system was constructed which consisted essentially of a 400-ml glass vessel immersed into a constant temperature bath. A quantity of 200 ml of fuel was placed into

the vessel, giving a 1:1 ratio in the volumes of fuel and vapor. A 1-ml sampling loop was attached to the system for withdrawing vapor samples. The loop could be evacuated by means of a vacuum pump prior to sampling the vapor. The head space and vapor sample volumes were selected in order to minimize disruption of the equilibrium by removal of vapor phase.

Vapor analyses were conducted using a Hewlett-Packard GC/MS unit with attached data system, and a Perkin Elmer 3920 gas chromatograph having a 50-meter glass capillary column coated with SF-96 liquid phase. The mass spectral data were recorded in the continuous scanning mode and were used primarily for compound identification. The high-resolution GC system was used for quantitation by means of a hydrogen flame ionization detector (FID). In some cases, a precise structural configuration could not be unambiguously determined from the mass spectrum alone. Reference hydrocarbons were used to establish a boiling point/retention time relationship which was then used to aid in selecting the correct compound from the several possible configurations.

Results

Vapor compositions are presented in Tables 101 and 102 at four different temperatures. Linear and cyclic paraffins, which comprised the bulk of the vapor phase, responded uniformly by FID on essentially a carbon number basis making the response proportional to weight composition. These compounds were consequently assigned a weight response factor of unity. Several aromatic constituents were found in the vapor phase and individual response factors for these compounds were applied in calculating compositions.

All components present at concentrations of 1% or greater in the vapors were reported. These components accounted for a major part of the vapor. The remaining portion consisted of low levels of a myriad of compounds. Each component of the fuel, even though it

TABLE 101. VAPOR COMPOSITIONS OF JP-4, TANK 15

Component	Weight Percent			
	0°F	35°F	70°F	105°F
Cyclopropane	5.1	4.4	3.3	
2-Methylpropane	8.0	6.4	5.7	1.5
Butane	15.6	11.9	12.0	3.5
2-Methylbutane	16.6	13.3	15.4	4.3
Pentane	14.6	10.8	13.4	4.2
2,3-Dimethylbutane	4.8	5.0	5.8	1.3
3-Methylpentane	3.0	3.3	4.1	1.5
Hexane	7.5	5.9	7.4	3.9
2,2-Dimethylpentane	2.3	2.2	2.4	1.4
Cyclohexane	2.3	2.3	2.6	1.5
3,3-Dimethylpentane	2.3	2.4	2.6	2.8
2,3-Dimethylpentane	2.7	2.7	3.0	2.8
Heptane	2.8	4.1	3.2	4.4
Methylcyclohexane	2.1	2.8	2.4	2.9
2,2,3,3-Tetramethylbutane				1.4
Toluene				1.2
2,3-Dimethylhexane	1.5	2.9	1.8	6.1
3-Ethylhexane		1.9	1.3	4.0
Octane	0.9	1.9	1.1	5.2
2,4,4-Trimethylhexane				1.1
Dimethylheptanes, 4,4/2,6				1.4
1,4-Dimethylbenzene				2.4
4-Methyloctane				2.6
3-Methyloctane				1.1
1,2-Dimethylbenzene				1.6
Nonane		0.8	0.3	4.0
Dimethyloctanes, 2,7/3,5/3,6				1.0
3,3-Diethylhexane & Ethyloctane, 3/4				1.1
Decane		0.3		1.9
Total	92.1	85.3	87.8	72.1

TABLE 102. VAPOR COMPOSITIONS OF JP-8, TANK F-3

Component	Weight Percent 32°F	100°F	135°F	170°F
Butane	46.0	3.9	2.1	2.3
2-Methylbutane	18.3	1.1	-	-
1,1,2-Trimethylcyclopropane	1.3	-	-	1.7
Heptane	1.3	-	-	-
3-Ethylhexane	1.1	-	-	-
Octane	1.1	0.4	0.2	0.4
2,4-Dimethylheptane	1.4	-	-	-
Nonane	2.3	1.0	1.1	1.4
2,3,4-Trimethylheptane	1.0	-	1.2	1.2
Trimethyloctanes, (2,2,6/2,2,7/2,4,4)	-	-	1.0	1.1
Decane	3.1	3.4	4.1	3.6
5-Ethylnonane	1.4	1.8	2.0	2.0
Dimethylnonanes, (3,5/3,6)	-	-	1.1	1.0
3,3-Dimethylnonane	1.3	1.3	1.4	1.4
Trimethyloctanes, (4,4,5/3,4,4/2,3,4)	1.0	1.5	1.6	1.6
5-Methyldecane	-	1.1	1.2	1.2
3-Ethylnonane	-	1.0	1.1	1.1
2-Methyldecane	-	1.9	1.8	1.8
2,5,8-Trimethylnonane & Dimethylethylbenzenes *	-	1.8	1.9	2.0
4,5-Diethyloctane	-	1.4	2.3	3.4
Hendecane & Methyl Isobutylbenzenes **	4.4	11.1	10.6	8.2
2,6-Dimethyldecane	-	3.0	2.9	3.1
3,6-Diethyloctane	-	2.6	2.6	2.7
Hexylcyclopentane	-	2.9	2.5	2.5
5-Methylhendecane	-	1.4	1.4	1.3
4-Cyclopentylheptane	-	1.4	1.3	1.2
3-Methylhendecane	-	2.3	2.3	2.2
1,6-Dimethylindan	-	1.8	1.8	1.8
1,4-Diisopropylhexane	-	1.7	1.5	1.3
Hexamethylcyclohexane	-	-	1.3	1.2
3,5-Dimethyl-5-Ethylnonane	-	1.1	1.1	1.0
4-Propyldecane	-	1.5	1.4	1.3
Dodecane	1.7	6.5	6.6	5.7
Butylcyclooctane	-	2.2	2.0	1.7
Tridecane	-	1.8	1.6	1.6
Total	86.7	64.5	66.7	64.0

* Weight ratio of 3:1
**Weight ratio of 10:1

may have had a low vapor pressure, made some contribution to the composition of the vapor. A total vapor analysis would consequently have included most of the compounds present in the fuel, particularly at temperatures above ambient. The portion of the vapor that is accounted for by the reported compounds is given as a summation at the bottom of each column in the tables.

It should be noted that values presented in the tables are relative vapor compositions. The concentration of any given component in the air head space could be estimated using these data along with appropriate vapor pressure values.

Discussion

As shown in Table 102, JP-8 vapors at 32°F consisted largely of the very volatile constituents, mainly butane (46%) and 2-methylbutane (18%). These components were present only as trace constituents of the fuel liquid phase, being scarcely perceptible in a chromatogram of the fuel. Replicate vapor analyses at 32°F, however, showed their preponderance in the vapor phase. As temperature was increased, the other JP-8 components contributed increasingly to the vapor composition. At 170°F, butane and 2-methylbutane constituted only a small part of the vapor. This observation emphasizes the need to consider the total amount of vapor (vapor pressure) as well as its composition in applying these data to specific problems.

In several cases, where components were chromatographically unresolved, approximate weight ratios were determined by mass spectrometry and these are reported in Table 102.

15. PARTIAL CHARACTERIZATION OF SHALE-DERIVED FUELS

Five samples of shale-derived fuel were characterized by simulated distillations, elemental analyses, and hydrocarbon-type analyses.

Simulated distillations were conducted by gas chromatography as described in ASTM Method D 2887. A gas chromatograph, equipped with a flame ionization detector and a column of 3% OV-1 on Chromosorb W, was used for this work. Data are presented in Table 103.

TABLE 103. SIMULATED DISTILLATION BY GAS CHROMATOGRAPHY

Percent Recovery	X090-176 °C	X090-176 °F	X090-177 °C	X090-177 °F	X090-178 °C	X090-178 °F	X090-179 °C	X090-179 °F	X090-180 °C	X090-180 °F
0.5 (IBP)	51	124	116	241	28	83	27	81	88	190
1	59	138	120	248	34	93	29	84	92	198
5	77	171	140	284	64	147	60	140	120	248
10	92	198	156	312	83	181	79	174	137	279
20	116	241	174	345	98	208	110	230	161	322
30	131	268	188	370	115	239	142	288	181	358
40	144	291	198	388	123	253	170	338	199	390
50	165	329	210	410	135	275	206	403	216	421
60	185	365	218	424	146	295	222	432	231	448
70	206	403	225	437	164	327	235	455	249	480
80	226	439	236	457	183	361	252	486	266	511
90	244	471	253	487	212	414	280	536	281	538
95	257	495	269	516	230	446	301	574	290	554
99	299	570	288	550	249	480	324	615	309	588
99.5 (FBP)	308	586	291	556	254	489	328	622	312	594

Elemental analysis was obtained from a commercial microanalytical laboratory, Galbraith Laboratories, Inc., Knoxville, Tennessee. Data are presented in Table 104.

Hydrocarbon-type analyses were conducted by mass spectrometry using a modification of ASTM D 2789. Data are presented in Table 105.

TABLE 104. ELEMENTAL ANALYSIS OF SHALE-DERIVED FUELS

Sample	Weight % Carbon	Hydrogen	Nitrogen
X090-176	86.24	13.55	0.004
	86.53	13.50	0.004
Mean	86.36	13.53	0.004
X090-177	85.99	13.79	0.006
	86.19	13.68	0.006
Mean	86.09	13.74	0.006
X090-178	85.14	14.66	0.002
	84.96	14.43	0.002
Mean	85.05	14.55	0.002
X090-179	86.21	13.34	0.005
	86.32	13.67	0.005
Mean	86.27	13.51	0.005
X090-180	86.55	13.38	0.004
	86.73	13.12	0.004
Mean	86.64	13.25	0.004

TABLE 105. HYDROCARBON-TYPE ANALYSIS BY MASS SPECTROMETRY

Components	Volume % X090-176	X090-177	X090-178	X090-179	X090-180
Paraffins	46.7	46.4	55.2	46.0	34.0
Monocycloparaffins	39.6	40.3	35.8	40.7	46.0
Dicycloparaffins	-	-	2.1	-	3.2
Alkylbenzenes	9.5	6.8	5.5	7.3	9.2
Indans & Tetralins	4.2	6.0	0.9	5.7	6.9
Naphthalenes	Trace	0.5	0.5	0.3	0.7

- Dash indicates none found.

16. DIELECTRIC CONSTANT OF A JP-4 SAMPLE LABELED KI SAWYER

Dielectric constant was measured at three temperatures for KI Sawyer JP-4 sample #80-37, Tank 5, drawn 14 November 1980. The measurements were made relative to air at 400 hertz using a three-terminal guarded cell and a General Radio 1615A capacitance bridge and guarded circuit. The bridge signal generator was a General Radio 1311A audio oscillator, and the bridge detector was a Type 1232A tuned amplifier and null detector. The test results are listed below.

Test temperature, °F	Dielectric constant
32	2.102
77	2.052
100	2.028

17. COMPARATIVE CARBON-HYDROGEN ANALYSES OF EIGHT FUEL SAMPLES BY TWO COMMERCIAL LABORATORIES

Six samples comprising a mixture of actual jet fuels and synthetic fuel blends were submitted to two commercial analytical laboratories for duplicate carbon and hydrogen analyses. The two commercial companies were Galbraith Laboratories, Inc., and Schwartzkopf Microanalytical Laboratory, both of which use the classical combustion technique for their analytical approach. The analyses were required as part of a program to evaluate different methods for measuring hydrogen content. Two of the six samples were resubmitted six weeks later to the same two laboratories as blind duplicates for a measure of method reproducibility. All data are presented in Table 106.

TABLE 106. DUPLICATE CARBON AND HYDROGEN ANALYSIS RESULTS FROM TWO COMMERCIAL LABORATORIES FOR JET FUELS

Sample Number	Replicate Number		Percent Carbon Data From Galbraith	Percent Carbon Data From Schwarzkopf	Percent Hydrogen Data From Galbraith	Percent Hydrogen Data From Schwarzkopf
80-304-1	1		87.69	87.50	12.35	12.68
	2		87.50	87.48	12.47	12.59
		Avg.	87.60	87.49	12.41	12.64
80-304-2	1		88.26	87.90	11.72	11.95
	2		88.25	88.10	11.80	11.87
		Avg.	88.26	88.00	11.76	11.91
80-304-3	1		87.63	87.55	12.38	12.45
	2		87.68	87.54	12.37	12.70
		Avg.	87.66	87.55	12.38	12.58
80-304-4	1		88.00	87.97	12.07	11.79
	2		88.03	88.00	11.94	11.67
		Avg.	88.02	87.99	12.01	11.73
80-304-5	1		86.30	85.58	13.68	14.57
	2		86.34	85.36	13.88	14.48
		Avg.	86.32	85.47	13.78	14.53
80-304-5 Blind Repeat 6 wks. later	1		85.54	85.75	14.35	14.31
	2		85.70	85.52	14.23	14.52
		Avg.	85.62	85.64	14.29	14.42
80-304-6 (DF-2)	1		86.54	86.81	12.89	13.05
	2		86.59	86.92	12.68	13.04
		Avg.	86.57	86.87	12.79	13.05
80-304-6 Blind Repeat 6 wks. later	1		87.20	86.96	12.79	12.96
	2		87.24	86.90	12.70	13.17
		Avg.	87.22	86.93	12.75	13.07

Conclusions

1. With the exception of Sample 80-304-4, Galbraith Laboratories consistently obtained lower hydrogen values than Schwartzkopf.

2. The Schwartzkopf percent hydrogen data appeared to be in good agreement with data obtained on similar samples analyzed at APL by an NMR technique.

3. Good reproducibility was obtained by Schwartzkopf Laboratories for the blind repeat analyses of both diesel fuel and JP-4. Good reproducibility was also obtained by Galbraith Laboratories for the diesel fuel analyses, but the dissimilar results for the JP-4 fuel analyses indicates that Galbraith may have problems in handling volatile samples.

It should be noted that both of the laboratories quote an absolute accuracy of ±0.3% for carbon and hydrogen determinations. Analysis from the two laboratories do not differ by more than this amount for any sample except sample 80-304-5.

18. EFFECT OF ANTISTATIC ADDITIVES ON THE DIELECTRIC CONSTANT OF JP-4 FUEL

Dielectric constant values were determined for a specimen of JP-4 fuel coded 81-3-CRM and separated portions of that fuel containing either 2 ppm ASA-3 additive or 2 ppm Stadis 450 additive. The purpose of the analyses was to determine if the presence of antistatic additives had a significant impact on the dielectric constant of the fuel, thereby affecting the accuracy of aircraft fuel gauges. This same fuel and additives were also evaluated for electrical conductivity and charging tendency as documented in subsection II-2. The dielectric constant values are listed below.

Test sample	Dielectric constant at 77°F
81-3-CRM JP-4 Fuel	2.046
JP-4 + 2.0 ppm ASA-3	2.031
JP-4 + 2.0 ppm Stadis 450	2.021

The above variations in dielectric constant are not any greater than would be expected for different lots of JP-4 without additives.

19. HYDROCARBON-TYPE ANALYSES OF JP-5 AND JP-8

Nine samples of JP-5, JP-8, and shale-derived broad range fuels were analyzed by mass spectrometry to determine their hydrocarbon-type distributions. The modified ASTM D 2789 method and Monsanto Method 21-PQ-38-63 were used for these determinations. Average density values were used to convert ASTM D 2789 volume percent data (Table 107) to weight percent. The converted values are compared with those obtained by the Monsanto Method in Table 108.

TABLE 107. HYDROCARBON-TYPE ANALYSIS BY MODIFIED ASTM D 2789

	Volume Percent								
Compound Type	VN-81 -132	VN-81 -133	VN-81 -134	VN-81 -135	VN-81 -136	VN-81 -137	VN-81 -138	VN-81 -139	VN-81 -140
Paraffins	49.6	50.1	49.8	39.5	35.5	40.9	42.1	50.2	48.6
Cycloparaffins	38.7	33.0	34.5	40.1	51.0	42.8	32.5	20.7	28.3
Dicyclo-paraffins	0.0	0.0	0.0	12.9	3.4	9.2	4.3	0.0	0.9
Alkylbenzenes	5.5	8.1	7.7	4.0	6.6	3.7	10.3	17.6	13.9
Indans & Tetralins	5.6	7.2	6.6	3.1	3.1	3.0	9.8	10.7	7.7
Naphthalenes	0.6	1.6	1.4	0.4	0.4	0.4	1.0	0.8	0.6

TABLE 108. COMPARISON OF HYDROCARBON-TYPE ANALYSES

	Weight Percent																	
	81-132		81-133		81-134		81-135		C1-136		81-137		81-138		81-139		81-140	
	D2789[a]	MONS[b]	D2789	MONS	D2789	MONS	D2789	MONS	D2789	MONS	D2789	MONS	D2789	MONS	D2789	MONS	D2789	MONS
Paraffins	47.0	49.0	47.3	49.5	47.0	49.1	37.3	36.7	33.4	33.0	38.7	38.3	39.3	39.9	46.8	45.5	45.6	44.3
Cycloparaffins	39.6	36.9[c]	33.5	29.7	35.1	31.6	41.0	54.8	51.8	54.8	43.8	53.6	32.7	35.3	20.8	18.0	28.6	27.6
Dicycloparaffins	-		-		-		13.1		3.5		9.5		4.3		-		0.9	
Alkylbenzenes	6.0	7.5	8.8	11.5	8.4	10.7	4.4	4.9	7.2	8.5	4.0	4.4	11.2	13.9	19.0	24.7	15.1	19.3
Indans & Tetralins	6.6	5.7	8.4	6.8	7.7	6.3	3.7	3.0	3.6	3.3	3.5	3.1	11.3	9.5	12.4	10.9	9.0	7.9
Indenes & DHN	[d]	[e]		0.1		0.1		-		-		-		-		-		-
Naphthalenes	0.8	0.9	2.0	2.4	1.8	2.2	0.5	0.6	0.5	0.4	0.5	0.6	1.2	1.4	1.0	0.9	0.8	0.9

[a] Value from modified ASTM D 2789 was converted from volume percent using average density values.

[b] Monsanto method 21-PQ-38-63.

[c] Total cycloparaffins.

[d] Method does not provide this information.

[e] Dash indicates none was detected.

20. HYDROCARBON-TYPE ANALYSES OF SHALE-DERIVED GASOLINE, JP-4, JP-8, AND DF-2 BY TWO MASS SPECTRAL METHODS

Six shale-derived fuel samples consisting of two diesel fuels, two JP-8s, a JP-4, and a gasoline were analyzed by mass spectrometry to determine hydrocarbon-type distributions. The modified ASTM D 2789 method and Monsanto Method 21-PQ 38-63 were used for these determinations. The Monsanto method was used for all fuels because it was specifically requested although that procedure is not very appropriate for two of the samples. Samples VN 81-141 and VN 81-142 are shale-derived JP-4 and gasoline, respectively. Their average carbon numbers of 8.4 and 8.6, respectively, place them outside the range intended for this method. The ASTM D 2789 data are considered to be the more reliable for these two samples.

Average density values were used to convert ASTM D 2789 volume percent data (Table 109) to weight percents. The converted values are compared with those obtained by the Monsanto method in Table 110.

TABLE 109. HYDROCARBON-TYPE ANALYSES BY MODIFIED ASTM D 2789

	Volume Percent					
Compound Type	81-141	81-142	81-143	81-144	81-145	81-146
Paraffins	43.4	43.2	50.7	48.6	39.8	40.4
Cycloparaffins	35.5	6.0	28.6	29.3	37.3	27.8
Dicyloparaffins	9.0	0.3	2.7	1.0	5.6	1.8
Alkylbenzenes	9.6	42.5	4.4	5.2	9.6	14.7
Indans & Tetralenes	2.0	6.9	11.7	13.8	6.9	14.0
Naphthalenes	0.5	1.1	1.9	2.1	0.8	1.3

TABLE 110. COMPARISON OF HYDROCARBON-TYPE ANALYSES

Hydrocarbon type	Weight percent											
	81-141		81-142		81-143		81-144		81-145		81-146	
	D2789[a]	MON[b]	D2789	MON	D2789	MON	D2789	MON	D2789	MON	D2789	MON
Paraffins	41.0	32.1	39.5	29.6	47.5	49.2	45.4	46.9	37.3	36.5	37.2	36.9
Cycloparaffins	36.2	50.2[c]	6.0	3.3	29.0	30.2	29.5	28.7	37.6	42.8	27.7	28.0
Dicycloparaffins	9.2		0.2		2.8		1.0		5.6		1.8	-
Alkylbenzenes	10.6	14.9	45.1	59.8	4.8	6.0	5.6	7.1	10.5	12.5	15.7	20.1
Indans and tetralins	2.4	2.8	7.8	6.5	13.5	10.3	15.9	13.4	8.0	7.2	16.0	13.5
Indenes and DHN[d]	-[e]	-[f]		-		1.7		1.6		0.1		0.5
Naphthalenes	0.6	-	1.4	0.8	2.4	2.6	2.6	2.3	1.0	0.8	1.6	1.1

[a]Values from modified ASTM D 2789 were converted from volume percent using average density values.

[b]Monsanto method.

[c]Total cycloparaffins.

[d]DHN = dihydronaphthalenes.

[e]Method does not provide this information.

[f]Dash indicates none detected.

21. HYDROCARBON-TYPE ANALYSES OF SHALE-DERIVED JP-4, JP-5, JP-8, DF-2, AND DFM BY TWO MASS SPECTRAL METHODS

Nine shale-derived fuels including marine diesel fuel, DF-2, JP-4, JP-5, and JP-8; and two blend stock samples were analyzed for hydrocarbon types by two mass spectral methods. Analysis results from ASTM Method D 2789 (modified), in volume percents, are presented in Table 111. The same analysis results converted to weight percents and weight percent data from Monsanto Method 21-PQ-38-63 are presented in Table 112 for direct comparison.

The three JP-4 fuels in this set of samples had average carbon numbers, as determined by mass spectrometry, of 9.6 for 81-149; 7.9 for 81-150 and 8.5 for 81-155. The average carbon number for the latter two fuels placed them outside the intended range of the Monsanto method, thus the ASTM Method D 2789 (modified) data were considered more reliable. However, both sets of values were reported as specifically requested.

22. HYDROCARBON-TYPE ANALYSES BY TWO MASS SPECTRAL METHODS FOR TEN SHALE-DERIVED JP-4 AND JP-8 FUELS; SIMULATED DISTILLATIONS FOR TWO FUELS

Ten shale-derived JP-4 and JP-8 fuel samples were analyzed for hydrocarbon types by two mass spectral methods, ASTM D 2789 and Monsanto Method 21-PQ-38-63. Analytical data from ASTM D 2789, in volume percents are presented in Table 113. Weight percent data from both the ASTM and Monsanto methods are presented in Table 114 for direct comparison.

Two of the JP-4 samples, WEH-81-37 and VN-81-158, were also analyzed for boiling range distributions via simulated distillations by gas chromatography (ASTM D 2887). These results are provided in Table 115.

TABLE 111. HYDROCARBON-TYPE ANALYSES BY ASTM D 2789 - VOLUME PERCENTS

Sample Number	Fuel Type	Source	Paraffins	Monocyclo-Paraffins	Dicyclo-Paraffins	Alkyl Benzenes	Indans & Tetralins	Naphthalenes
[illegible]	JP-4	Shale	51.0	41.0	0.0	4.7	3.1	0.2
[illegible]	JP-4	Shale	50.8	36.4	3.6	6.2	2.4	0.6
[illegible]	JP-5	Shale	37.7	37.0	1.9	11.7	10.7	1.0
[illegible]	JP-8	Shale	37.2	39.5	0.0	13.3	9.1	0.9
[illegible]	DF-2	Shale	46.8	36.1	1.3	7.9	6.7	1.2
VR-81-154	Marine-DF	Shale	53.9	34.6	0.4	4.3	5.3	1.5
[illegible]	JP-4	Shale	53.5	37.3	3.7	4.2	1.1	0.2
[illegible]	JP-8	Shale	44.2	44.9	0.0	6.1	4.4	0.4
[illegible]	JP-5	Shale	43.5	41.9	0.0	6.7	7.2	0.7
WEH-81-39	Blend	Stock	18.1	6.9	0.9	54.9	4.8	14.4
WEH-81-40	Blend	Stock	46.0	28.1	2.4	7.5	8.5	7.5

TABLE 112. HYDROCARBON-TYPE DATA FROM TWO MASS SPECTRAL METHODS - WEIGHT PERCENTS

Components	VN-81-149 Shale JP-4		VN-81-150 Shale JP-4		VN-81-151 Shale JP-5		VN-81-152 Shale JP-8		VN-81-153 Shale DF-2		VN-81-154 Shale Marine DF-2	
	D2789[a]	MONS[b]	D2789	MONS	D2789	MONS	D2789	MONS	D2789	MONS	D2789	MONS
Paraffins	48.6	51.9	48.4	41.0	34.4	35.1	34.5	34.2	44.1	44.8	51.3	52.6
Cycloparaffins	42.2	37.4	41.2	45.2	38.2	38.2	39.6	38.2	38.0	36.7	35.9	33.6
Alkylbenzenes	5.2	6.8	6.8	10.3	14.1	16.0	14.3	18.2	8.6	10.3	4.7	5.3
Indans/Tetralins	3.7	3.4	2.8	3.5	12.1	9.4	10.5	8.2	7.8	6.1	6.2	5.0
Indenes[c]	-	0.0	-	0.0	-	0.0	-	0.0	-	0.4	-	1.0
Naphthalenes	0.3	0.5	0.8	0.0	1.2	1.3	1.1	1.2	1.5	1.7	1.9	2.5

Components	VN-81-155 Shale JP-4		VN-81-156 Shale JP-8		VN-81-157 Shale JP-5		WEH-81-39 Blended Stock		WEH-81-40 Blended Stock	
	D2789	MONS	D2789	MONS	D2789	MONS	D2789	MONS	D2789	MONS
Paraffins	51.3	45.8	41.8	42.0	40.9	41.2	15.7	12.8	42.6	41.0
Cycloparaffins	42.4	45.2	45.8	45.0	42.5	41.8	7.3	6.3	30.5	29.2
Alkylbenzenes	4.7	7.4	6.7	8.2	7.3	9.1	55.2	56.1	8.0	10.0
Indans/Tetralins	1.3	1.6	5.2	4.3	8.4	6.9	5.2	5.1	9.7	7.8
Indenes[c]	-	0.0	-	0.0	-	0.0	-	0.0	-	0.0
Naphthalenes	0.3	0.0	0.5	0.5	0.9	1.0	16.6	19.7	9.2	12.0

[a] ASTM Method D2789 provides data in volume percents (see Table 1). The weight percent data were calculated from average density values for the compound classes.

[b] Monsanto mass spectral method 21-PQ-38-63 was developed for hydrocarbon fuel stocks.

[c] Also includes dihydronaphthalenes in the analysis. This compound class is not detected by ASTM D2789.

TABLE 113. HYDROCARBON-TYPE ANALYSES BY ASTM D 2789 (MODIFIED) - VOLUME PERCENTS

Sample Number	Fuel Type	Source	Paraffins	Monocyclo-Paraffins	Dicyclo-Paraffins	Alkyl Benzenes	Indans & Tetralins	Naphtha-lenes
VN-81-120	JP-4	Shale	44.8	43.3	6.1	4.5	0.8	0.5
VN-81-121	JP-4	Shale	39.5	53.5	0.2	3.4	3.0	0.4
VN-81-122	JP-4	Shale	47.4	46.9	3.8	1.3	0.2	0.4
VN-81-123	JP-4	Shale	51.6	41.2	0.0	3.5	3.4	0.3
VN-81-124	JP-4	Shale	61.9	26.9	3.9	4.4	2.3	0.6
VN-81-125	JP-8	Shale	48.3	42.4	0.0	4.6	4.1	0.6
VN-81-126	JP-4	Shale	58.7	28.8	6.0	4.2	2.0	0.3
VN-81-158	JP-4	Shale	47.6	35.3	0.0	11.5	5.2	0.4
VN-81-159	JP-8	Shale	47.5	33.7	0.0	10.4	7.7	0.7
WEH-81-37	JP-4	Shale	50.2	29.3	4.8	10.7	4.5	0.5

TABLE 114. HYDROCARBON-TYPE DATA FROM TWO MASS SPECTRAL METHODS - WEIGHT PERCENT

Components	VN-81-120 Shale JP-4		VN-81-121 Shale JP-4		VN-81-122 Shale JP-4		VN-81-123 Shale JP-4		VN-81-124 Shale JP-4	
	D2789[a]	MONS[b]	D2789	MONS	D2789	MONS	D2789	MONS	D2789	MONS
Paraffins	42.7	34.5	37.4	38.2	45.4	37.3	49.2	52.3	59.5	56.2
Cycloparaffins	50.6	57.5	54.9	53.7	52.5	60.2	42.5	38.4	32.1	33.2
Alkylbenzenes	5.0	7.1	3.7	4.0	1.4	2.2	3.9	4.9	4.9	7.4
Indans/Tetralins	0.9	0.9	3.5	3.4	0.2	0.3	4.0	3.8	2.7	3.2
Indenes[c]	-	0.0	-	0.0	-	0.0	-	0.0	-	0.0
Naphthalenes	0.6	0.0	0.5	0.7	0.5	0.0	0.4	0.6	0.8	0.0
Average Carbon No.	8.3		10.3		8.0		9.8		8.6	

Components	VN-81-125 Shale JP-8		VN-81-126 Shale JP-4		VN-81-158 Shale JP-4		VN-81-159 Shale JP-8		WEH-81-37 Shale JP-4	
	D2789	MONS	D2789	MONS	D2789	MONS	D2789	MONS	D2789	MONS
Paraffins	45.8	47.8	56.4	53.3	44.9	42.0	44.6	46.3	47.6	42.7
Cycloparaffins	43.5	41.0	36.1	36.5	35.9	34.2	34.2	31.0	34.8	33.9
Alkylbenzenes	5.1	6.0	4.7	7.0	12.6	17.4	11.3	14.4	11.7	17.0
Indans/Tetralins	4.8	4.2	2.4	2.9	6.1	5.9	9.0	7.0	5.3	5.8
Indenes[c]	-	0.0	-	0.0	-	0.0	-	0.0	-	0.0
Naphthalenes	0.8	1.0	0.4	0.3	0.5	0.5	0.9	1.3	0.6	0.6
Average Carbon No.	-		9.1		9.5		-		9.3	

[a] ASTM Method D2789 provides data in volume percents (see Table 113). The weight percent data were calculated from average density values for the compound classes.

[b] Monsanto mass spectral Method 21-PQ-38-63 was developed for hydrocarbon feed stocks.

[c] Also includes dihydronaphthalenes in the analysis. This compound class is not detected by ASTM D 2789.

TABLE 115. SIMULATED DISTILLATION BY GC (ASTM D 2887)

Percent Recovered	WEH-81-37 Shale JP-4 °C	WEH-81-37 Shale JP-4 °F	VN-81-158 Shale JP-4 °C	VN-81-158 Shale JP-4 °F
0.5 (IBP)	26	79	34	93
1	34	93	56	133
5	69	156	75	167
10	91	196	97	207
20	118	244	121	250
30	140	284	142	288
40	161	322	164	327
50	181	358	183	361
60	202	396	202	396
70	220	428	221	430
80	236	457	236	457
90	257	495	257	495
95	269	516	269	516
99	293	559	292	558
99.5 (FBP)	300	572	299	570

The average carbon numbers for all JP-4 fuels were calculated and are presented in Table 114. Samples 81-120, 81-122, and 81-124 had carbon numbers outside the intended range of the Monsanto method, thus the ASTM D 2789 data were more reliable for these samples. However, both sets of data were reported as requested.

23. HYDROCARBON-TYPE ANALYSES OF FIVE SHALE-DERIVED JP-8, DF-2, AND DFM SAMPLES BY TWO MASS SPECTRAL METHODS

Five shale-derived fuel samples were analyzed for hydrocarbon-type distribution by two mass spectral methods, modified ASTM Method D 2789 and Monsanto Method 21-PQ-38-63. The data from ASTM Method D 2789 are provided in Table 116 in volume percents. The same data were converted to weight percent values by the use of average densities for the compound classes, and these values are presented in Table 117 along with the weight percent values from Monsanto Method 21-PQ-38-63.

TABLE 116. HYDROCARBON-TYPE ANALYSES BY MODIFIED ASTM D 2789 - VOLUME PERCENTS

Compound Type	Shale Marine Diesel Fuel VN-81-160	Shale DF-2 VN-81-161	Shale Broad Range JP-8 VN-81-162	Shale Broad Range JP-8 VN-81-163	Shale JP-8 VN-81-164
Paraffins	48.1	48.0	46.1	46.9	50.5
Cycloparaffins	38.3	38.6	39.9	40.2	41.4
Dicycloparaffins	0.9	0.7	0.2	0.0	0.0
Alkylbenzenes	5.3	5.3	5.8	5.6	4.0
Indans/Tetralins	6.0	6.1	6.7	6.1	3.5
Naphthalenes	1.4	1.3	1.3	1.2	0.6

24. DENSITY OF 14 MULTI-TYPE SHALE-DERIVED FUELS AT 15°C

Density was determined by the dilatometer method for 14 shale-derived fuels at 15°C. Results are shown in Table 118.

TABLE 117. HYDROCARBON-TYPE DATA FROM TWO MASS SPECTRAL METHODS - WEIGHT PERCENTS

Components	Shale Marine Diesel Fuel VN-81-160		Shale DF-2 VN-81-161		Shale Broad Range JP-8 VN-81-162		Shale Broad Range JP-8 VN-81-163		Shale JP-8 VN-81-164	
	D2789[a]	MONS[b]	D2789	MONS	D2789	MONS	D2789	MONS	D2789	MONS
Paraffins	45.4	46.3	45.3	46.1	43.4	44.5	44.3	45.2	48.1	50.6
Cycloparaffins	39.9	38.4	40.1	38.5	40.8	39.0	41.0	39.0	42.6	39.6
Alkylbenzenes	5.8	6.7	5.8	5.8	6.4	7.5	6.1	7.3	4.4	5.2
Indans/Tetralins	7.1	5.6	7.1	5.7	7.8	6.3	7.1	5.8	4.1	3.6
Indenes[c]	-	0.9	-	0.9	-	1.0	-	0.9	-	0.0
Naphthalenes	1.8	2.1	1.7	2.0	1.6	1.7	1.5	1.8	0.8	1.0

[a] ASTM Method D 2789 (Modified) provides data in volume percents (see Table 116). These weight percent data were calculated from average density values for the compound classes.

[b] Monsanto mass spectral Method 21-PQ-38-63.

[c] Also includes dihydronaphthalenes in the analysis. This compound class is not detected by ASTM D 2789.

TABLE 118. DENSITY OF SHALE FUELS AT 15°C

Sample number	Type fuel	Density, g/cc
VN-81-141	Shale JP-4	0.7825
VN-81-142	Shale gasoline	0.8034
VN-81-143	Shale DF-2	0.8345
VN-81-144	Shale DF-2	0.8359
VN-81-145	Shale JP-8	0.8178
VN-81-146	Shale broad range JP-8	0.8269
VN-81-149	Shale JP-4	0.7801
VN-81-158	Shale JP-4	0.7871
VN-81-159	Shale JP-8	0.8094
VN-81-160	Shale DFM	0.8308
VN-81-161	Shale DF-2	0.8307
VN-81-162	Shale JP-8 blend	0.8205
VN-81-163	Shale JP-4 blend	0.8217
VN-81-164	Shale JP-8	0.7969

25. DENSITY AND BOILING RANGE DISTRIBUTION FOR EIGHT BP-IF CODED FUELS

Eight coded fuel samples were evaluated for density at 15°C and boiling range distribution. Density was determined by the dilatometer method and results are presented in Table 119. Simulated distillations were conducted by gas chromatography according to ASTM Method D 2887, and these results are provided in Table 120.

TABLE 119. DENSITY OF FUEL SAMPLES

Sample code	Grams/cc
BP-IP-1	0.7989
BP-IP-2	0.7888
BP-IP-3	0.7948
BP-IP-4	0.8002
BP-IP-5	0.7990
BP-IP-6	0.8293
BP-IP-7	0.8180
BP-IP-9	0.8309

TABLE 120. SIMULATED DISTILLATIONS

Percent Recovered	BP-IP-1 °C	BP-IP-1 °F	BP-IP-2 °C	BP-IP-2 °F	BP-IP-3 °C	BP-IP-3 °F	BP-IP-4 °C	BP-IP-4 °F
0.5 (IBP)	124	255	117	243	100	212	123	253
1	138	280	128	262	115	239	138	280
5	169	336	148	298	139	282	171	340
10	180	356	154	309	149	300	184	363
20	194	381	164	327	162	324	194	381
30	202	396	172	342	174	345	202	396
40	211	412	179	354	185	365	210	410
50	217	423	187	369	196	385	216	421
60	225	437	196	385	209	408	225	437
70	233	451	204	399	220	428	233	451
80	240	464	215	419	233	451	242	468
90	252	486	231	448	249	480	251	484
95	258	496	244	471	258	496	256	493
99	271	520	269	516	279	534	267	513
99.5 (FBP)	281	538	283	541	290	554	269	516

	BP-IP-5 °C	BP-IP-5 °F	BP-IP-6 °C	BP-IP-6 °F	BP-IP-7 °C	BP-IP-7 °F	BP-IP-9 °C	BP-IP-9 °F
0.5 (IBP)	114	237	102	216	101	214	103	217
1	119	246	117	243	110	230	116	241
5	137	279	153	307	147	297	154	309
10	146	295	170	338	164	327	170	338
20	155	311	185	365	177	351	185	365
30	163	325	197	387	189	372	196	385
40	171	340	206	403	197	387	204	399
50	178	352	215	419	207	405	213	415
60	191	376	223	433	217	423	222	432
70	204	399	231	448	227	441	232	450
80	221	430	240	464	236	457	239	462
90	239	462	252	486	250	482	253	487
95	252	486	259	498	257	495	258	496
99	266	511	271	520	273	523	273	523
99.5 (FBP)	271	520	274	525	281	538	278	532

26. ICP TRACE METALS ANALYSES FOR TEN SHALE- AND PETROLEUM-DERIVED JP-4 AND JP-8 FUELS

Two samples of JP-4 and JP-8 fuels derived from both shale and petroleum sources were analyzed for trace metals content using an ISA Model JY48P inductively coupled plasma (ICP) spectrometer. The ICP analyses were conducted on aqueous acid (ultrapure HCl) extracts of the fuels which provided a concentration factor of 21.25 for the metals. The test results for an acid extraction blank, the fuel samples (one in duplicate), and a reference standard are shown in Table 121.

27. ICP TRACE METALS ANALYSES FOR THREE JP-4 FUELS

Three fuel samples were analyzed for trace metals content by inductively coupled argon plasma (ICP) spectroscopy. The instrument used was an ISA Model JY48P ICP spectrometer. The analyses were conducted on aqueous acid extracts of the fuels which were obtained using ultrapure hydrochloric acid. The concentration factor for metals in the acid extract was 21.25. The analytical results for an acid extraction blank, the three fuel samples and a reference standard are presented in Table 122.

Though sodium is not always included in ICP analyses, the instrument was configured to include sodium for these analyses. Because of the ubiquitous nature of sodium and the fuel's history of contact to soft glass, the analysis for sodium is not considered to have the same significance as the analyses for other metals, and it was thus excluded from the table. As these values could have served to monitor gross sodium contamination, they were provided in a separate listing as follows.

TABLE 121. TRACE METALS ANALYSES BY ICP SPECTROMETRY

Elements of Detection:	Ag	Be	Co	Mn	Sn	Al	Cd	Fe	Ni	Ti	B	Cr	Mg	Pb	Zn	Ba	Cu	Mo	Sb
Instrument detection limits, ppb	110	2	24	3	250	150	4	10	86	8	35	22	120	175	8	10	22	125	270
MDL after concentration[a], ppb	5	0.1	1.1	0.2	12	7	0.2	0.5	4	0.4	1.6	1	5.7	8.2	0.4	0.5	1	6	13
Acid Extraction Blank[b]	x	x	x	x	x	x	x	x	x	x	x	x	x	x	x	x	x	x	x
Elements Concentration in Fuel Samples,[c] ppb																			
UOP-3794-157C	x	x	x	2.4	x	x	x	20	x	x	3.0	x	x	x	0.7	1.7	x	x	x
FOSF-D-81-124	x	x	x	x	x	x	x	3.9	x	x	x	x	x	x	x	1.5	x	x	x
-117	x	x	x	x	x	x	x	3.6	x	x	x	x	x	x	1.4	1.7	x	x	x
- 66	x	x	x	x	x	x	x	2.9	x	x	x	x	x	x	1.6	1.7	x	x	x
- 67	x	x	x	0.3	x	x	x	6.3	x	x	2.3	x	x	x	x	1.7	x	x	x
- 63	x	x	x	x	x	x	x	2.0	x	x	x	x	x	x	x	1.5	x	x	x
-114	x	x	x	0.2	x	x	x	8.0	x	x	2.0	x	x	x	1.6	1.8	x	x	x
- 43	x	x	x	0.2	x	x	x	8.0	x	x	x	x	x	x	1.1	1.6	x	x	x
- 44	x	x	x	x	21	x	x	1.8	x	x	x	x	x	x	3.6	1.8	x	x	x
Repeat - 44	x	x	x	x	19	x	x	2.1	x	x	x	x	x	x	3.6	1.9	x	x	x
JP-4-P-05288-1	x	x	x	0.2	x	x	x	3.6	x	x	1.7	x	x	43	x	1.5	x	x	x
Analysis of Reference Standard, ppb																			
True Value	-	1000	1000	1000	-	1000	1000	1000	1000	1000	1000	1000	1000	1000	1000	1000	1000	1000	1000
Observed Value	x	1010	1070	1040	x	955	1020	1040	986	1020	1110	1020	1100	1000	1030	1030	1000	994	1040
% Recovery		101	107	104		96	102	104	99	102	111	102	110	100	103	103	100	99	104

[a] The fuel samples were effectively concentrated by a factor of 21.25 when they were extracted with a much smaller volume of aqueous acid for the analysis.

[b] The aqueous ultrapure acid used to extract the fuel samples for analysis. An "x" shows that the element was not detected at the instrument detection limit

[c] An "x" shows that the element was not detected at the MDL after concentration. The numerical values were obtained by dividing the observed value by 21.25 to take into account the concentration effect, and these values represent the element concentration in the original fuels.

TABLE 122. TRACE METALS ANALYSES BY ICP SPECTROMETRY

Elements of Detection:	Ag	Be	Co	Mn	Sn	Al	Cd	Fe	Ni	Ti	B	Cr	Mg	Pb	Zn	Ba	Cu	Mo	Sb	Ca	Sr	V
Instrument detection limits, ppb	110	2	24	3	250	150	4	10	86	8	35	22	120	175	8	10	22	125	270	140	5	60
MDL after concentration[a], ppb	5	0.1	1.1	0.2	12	7	0.2	0.5	4	0.4	1.6	1	5.7	8.2	0.4	0.5	1	6	13	6.6	0.2	2.8
Acid Extraction Blank[b]	x	x	x	x	x	x	x	x	x	x	x	x	x	x	x	x	x	x	x	x	x	
Elements Concentration in Fuel Samples,[c] ppb																						
JP-4-103081-3	x	x	x	x	x	7.1	x	x	x	x	x	x	x	x	x	0.8	4.7	x	x	x	x	x
JP-4-103081-4	x	x	x	x	x	x	x	x	x	x	x	x	x	x	x	0.7	7.3	x	x	x	x	x
VN-81-119	x	x	x	x	x	7.6	x	x	x	x	x	x	x	x	0.6	0.8	1.6	x	x	x	x	x
Analysis of Reference Standard, ppb																						
True Value	1000	1000	1000	1000	1000	1000	1000	1000	1000	1000	1000	1000	1000	1000	1000	1000	1000	1000	1000	1000	1000	1000
Observed Value	991	1030	1090	1050	1060	965	1040	1020	990	1010	1090	978	1030	1070	1050	100	984	1040	972	1020	1020	1010
% Recovery	99	103	109	105	106	97	104	102	99	101	109	98	103	107	105	100	98	104	97	102	102	101

[a] The fuel samples were effectively concentrated by a factor of 21.25 when they were extracted with a much smaller volume of aqueous acid for the analysis.

[b] The aqueous ultrapure acid used to extract the fuel samples for analysis. An "x" shows that the element was not detected at the instrument detection limit

[c] An "x" shows that the element was not detected at the MDL after concentration. The numerical values were obtained by dividing the observed value by 21.25 to take into account the concentration effect, and these values represent the element concentration in the original fuels.

Sample	Sodium concentration, ppb
Blanks[a]	140
JP-4 103081-3	640
JP-4 103081-4	730
VN 81-119	520

[a]Blank value has been subtracted from those of fuels.

SECTION IV

COMBUSTION SUPPORT

Certain Air Force programs require the determination of data describing the detailed chemistry of fuels being used in combustion studies. As a class, aromatic compounds are of greatest interest because they tend to have the poorest combustion characteristics. High concentrations of aromatics have been known to produce excessive exhaust emissions in the form of unburned hydrocarbons and smoke. Paraffins and cyclic paraffins, on the other hand, are clean burning and have a high gravimetric heat of combustion. Accurate compositional data are therefore often required as an integral part of fuel combustion studies.

The test programs described in this section have involved a wide range of fuel physical property and analytical determinations to complement the information being generated by the Air Force in separate fuel combustion studies.

1. CHEMICAL AND PHYSICAL PROPERTIES OF SIX CONVENTIONAL AND SYNTHETIC FUELS

Six fuels of widely varying types, including those of conventional and synthetic origin, were subjected to several physical and chemical property tests using procedures detailed in the Appendix. Results for density and vapor pressure as a function of temperature are presented in Tables 123 and 124; net heat of combustion values by oxygen bomb calorimetry are shown in Table 125; results for simulated distillation by gas chromatography are presented in Table 126; and data for hydrocarbon type analysis by mass spectrometry are tabulated in Table 127.

TABLE 123. DENSITY OF TEST FUELS AS A FUNCTION OF TEMPERATURE

Sample	Density, g/cc		
	32°F	70°F	100°F
Conventional JP-4	0.7649	0.7484	0.7353
Shale JP-4	0.7633	0.7466	0.7332
Conventional JP-5	0.8226	0.8076	0.7955
Shale JP-5	0.8176	0.8024	0.7903
JP-9 (6-22-78)	0.9588	0.9421	0.9289
JP-10 (6-22-78)	0.9516	0.9355	0.9230

TABLE 124. VAPOR PRESSURE OF TEST FUELS AS A FUNCTION OF TEMPERATURE

Sample	Vapor Pressure, mm Hg		
	32°F	70°F	100°F
Conventional JP-4	28.5	67.0	122.0
Shale JP-4	24.0	55.5	99.5
Conventional JP-5	10.8	15.7	20.3
Shale JP-5	6.6	11.0	15.7
JP-9 (6-22-78)	7.5	17.5	29.0
JP-10 (6-22-78)	4.6	8.6	13.5

TABLE 125. HEAT OF COMBUSTION OF TEST FUELS (ASTM D 240-64)

Sample	Gross, Btu/lb		Net, Btu/lb
	Duplicate	Average	Average
Conventional JP-4	20,099 20,098	20,099	18,768
Shale JP-4	20,091 20,102	20,097	18,772
Conventional JP-5	19 92 19,777	19,785	18,511
Shale JP-5	19,749 19,748	19,749	18,497
JP-9 (6-22-78)	19,098 19,071	19,085	18,020
JP-10 (6-22-78)	19,146 19,163	19,155	18,074

TABLE 126. GAS CHROMATOGRAPHIC SIMULATED DISTILLATION OF TEST FUELS

Percent Recovered	°C	°F	°C	°F
	Conventional JP-4		Shale JP-4	
0.5 (IBP)	4	39	2	36
1	22	72	22	72
5	58	136	70	158
10	79	174	90	194
20	96	205	107	225
30	115	239	122	252
40	135	275	136	277
50	158	316	148	298
60	181	358	161	322
70	202	396	174	345
80	217	423	187	369
90	236	457	202	396
95	251	484	214	417
99	269	516	241	466
99.5 (FBP)	277	531	260	500
	Conventional JP-5		Shale JP-5	
0.5 (IBP)	112	234	141	286
1	126	259	147	297
5	162	324	164	327
10	174	345	173	343
20	190	374	190	374
30	201	394	202	396
40	211	412	215	419
50	222	432	225	437
60	231	448	235	455
70	242	468	248	478
80	252	486	258	496
90	265	509	273	523
95	273	523	285	545
99	291	556	311	592
99.5 (FBP)	299	570	323	613

TABLE 127. HYDROCARBON-TYPE ANALYSIS OF TEST FUELS

Compound Type	Volume Percent			
	Conventional JP-4	Shale JP-4	Conventional JP-5	Shale JP-5
Paraffins	67.6	67.9	47.2	62.0
Cycloparaffins	19.8	19.5	37.7	16.9
Dicycloparaffins	3.2	1.7	2.2	0.6
Alkylbenzenes	7.6	9.6	7.6	8.9
Indans and tetralins	1.8	1.3	2.9	9.0
Naphthalenes	<0.1	-	2.3	2.6

2. SIMULATED DISTILLATION OF DF-2 FUEL

A simulated distillation was conducted on a fuel coded 78-8-TJ DF-2. The gas chromatographic method described in ASTM D 2887 was used. Data are presented in Table 128 and a gas chromatogram of the fuel is shown in Figure 73.

TABLE 128. SIMULATED DISTILLATION OF DF-2 FUEL 78-8-TJ DF-2

Percent Recovered	Temperature	
	°C	°F
0.5 (IBP)	95	203
5.0	175	347
10.0	194	381
20.0	216	421
30.0	232	450
40.0	248	478
50.0	260	500
60.0	274	525
70.0	290	554
80.0	308	586
90.0	332	629
95.0	349	659
99.5 (FBP)	390	734

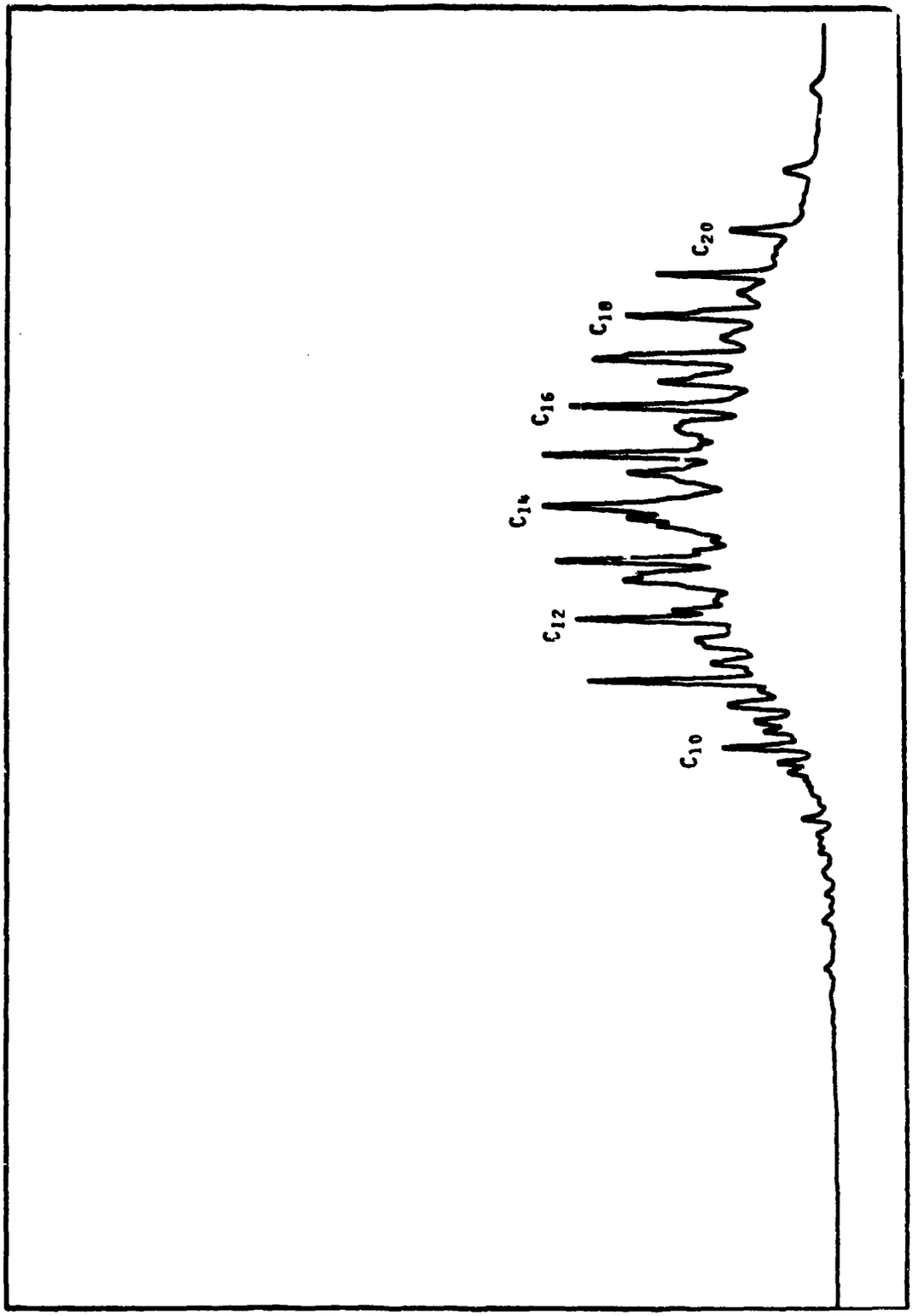

Figure 73. Gas chromatogram of 78-8-TJ DF-2.

3. DENSITY OF DIESEL FUELS

Density as a function of temperature was determined for four diesel fuel specimens by the dilatometer method. The results are shown in Table 129.

TABLE 129. DENSITY OF DIESEL FUELS

Sample	Density, g/cc 32°F	70°F	100°F
78-17-TJ DF-2	0.8481	0.8337	0.8221
78-18-TJ DF-2	0.8490	0.8339	0.8220
78-19-TJ DF-2	0.8485	0.8335	0.8215
78-20-TJ DF-2	0.8489	0.8338	0.8215

4. PROPERTIES AND ANALYSIS OF AROMATIC STOCK (XYLENE BOTTOMS)

An aromatic stock (xylene bottoms) used in Air Force studies for modifying the aromatic content of experimental fuels was characterized by a series of test procedures described in the Appendix. The material was originally thought to consist essentially of xylene isomers, but subsequent analyses showed it to consist mainly of C_3 substituted benzenes.

Kinematic viscosity, density, vapor pressure, and surface tension values as a function of temperature are presented in Table 130. Heat of combustion values are presented in Table 131 and compositional analyses in Table 132. The viscosity/temperature relationship is graphed in Figure 74. The GC analytical trace for the compositional analysis, presented in Figure 75, shows that the sample contained only a small amount of the reported xylene isomers. Further analyses by gas chromatography-mass spectrometry showed that C_3 substituted benzenes made up the bulk of the stock.

TABLE 130. PHYSICAL PROPERTIES OF XYLENE BOTTOMS

	Temperature, °F	
Kinematic viscosity, centistokes	0	1.730
	77	0.8784
	100	0.7565
Density, g/cc	32	0.8830
	70	0.8660
	100	0.8524
Vapor pressure, mm Hg	32	3.7
	70	9.6
	100	18.7
Surface tension, dynes/cm	32	30.56
	70	28.42
	100	26.76

TABLE 131. HEAT OF COMBUSTION OF XYLENE BOTTOMS

Gross, Btu/lb		Net, Btu/lb
Duplicate	Average	Average
18,594		
18,560		
	18,577	17,710

TABLE 132. GAS CHROMATOGRAPHIC-MASS SPECTROMETRIC ANALYSIS OF XYLENE BOTTOMS

Retention Time, minutes	Volume Percent		Retention Time, minutes	Volume Percent	
6.44	0.60		8.01	10.37	
6.65	3.79		8.76	8.74	
7.16	3.79		9.01	25.24	
Total xylenes		8.18	9.05	7.87	
			9.19	8.20	
			9.40	7.17	
			9.82	19.33	
			10.19	0.36	
			10.25	0.42	
			10.45	1.92	
			Total C_3 alkylbenzenes		89.62
			10.55	0.43	
			10.69	0.53	
			11.30	0.57	
			11.40	0.36	
			11.48	0.31	
			Total C_4 alkylbenzenes		2.20

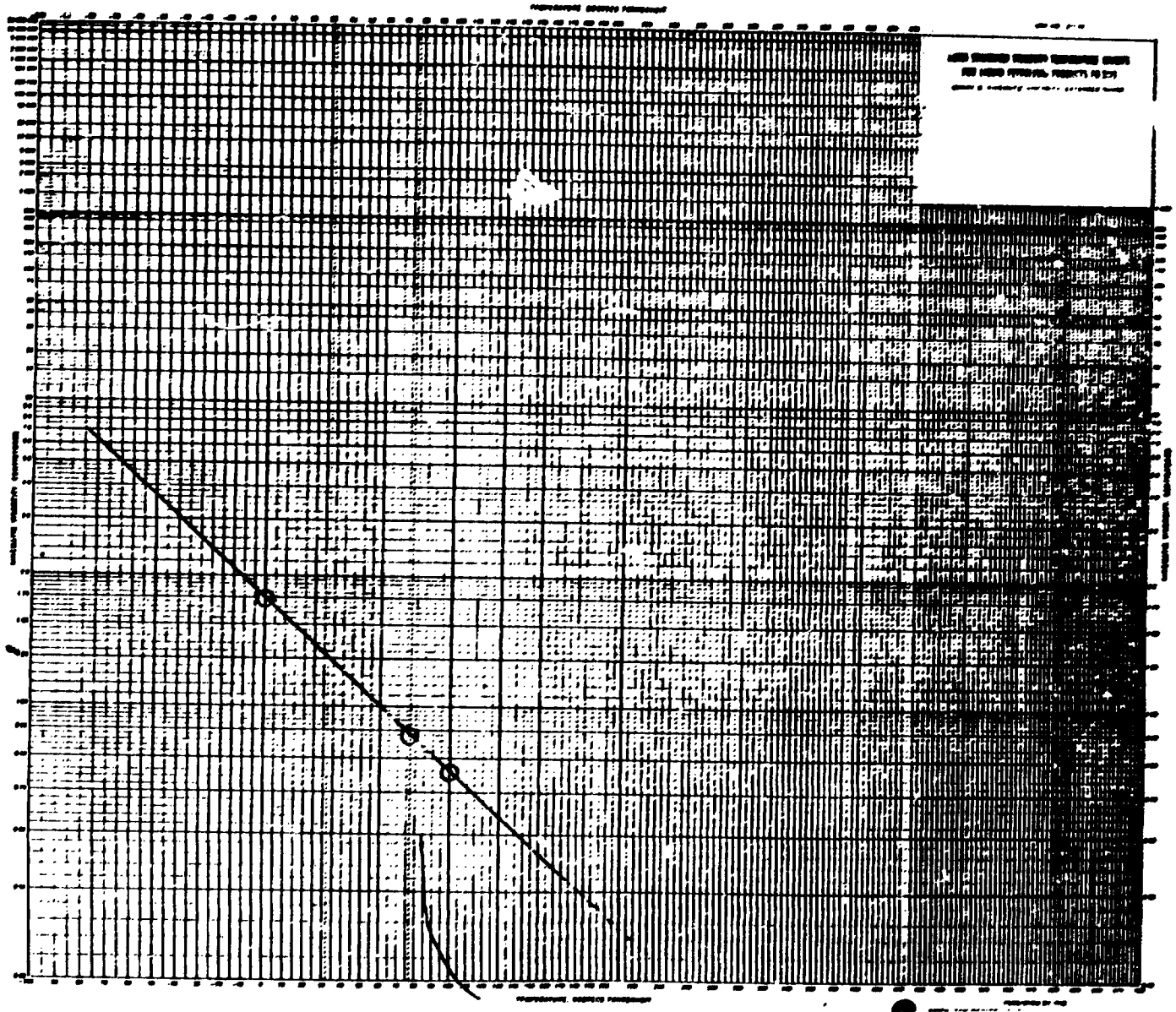

Figure 74. Viscosity/temperature plot for xylene bottoms.

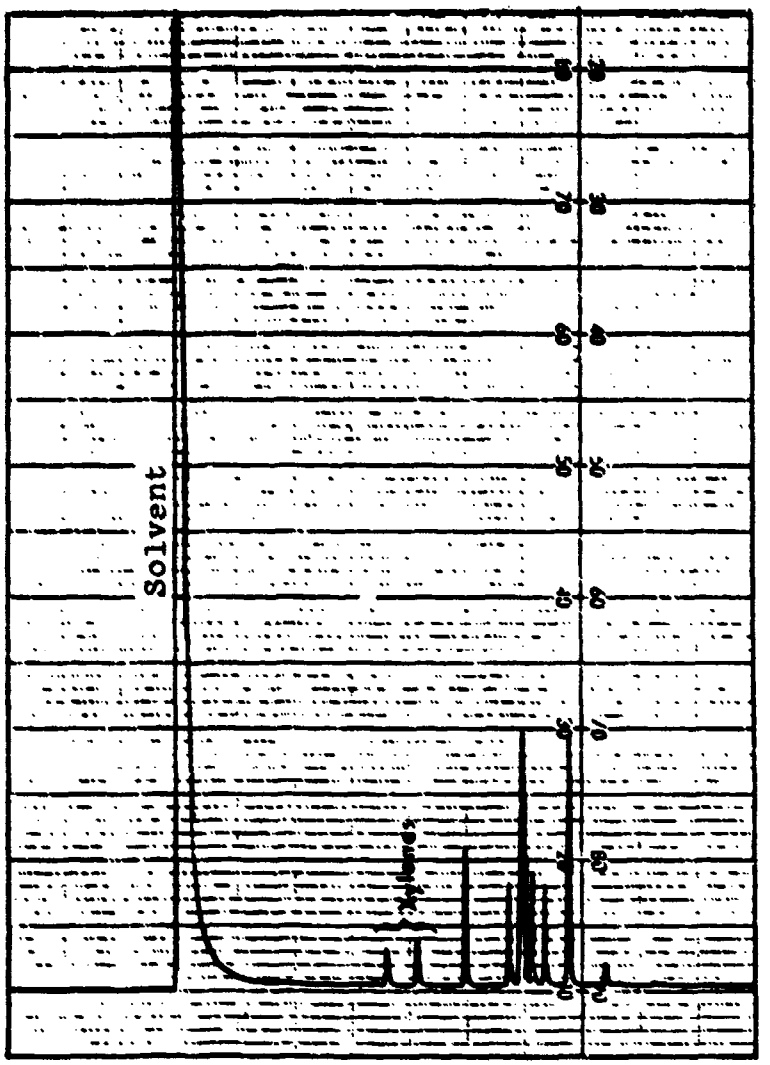

Figure 75. Chromatogram of xylene bottoms.

5. PROPERTIES AND ANALYSIS OF JP-8, TANK F-3

A multitude of tests were performed on a reference sample of JP-8 fuel in support of an Air Force-sponsored program in combustion technology. The test procedures used are described in the Appendix.

Test results for density, kinematic viscosity, surface tension, and vapor pressure as a function of temperature are shown in Table 133. Heat of combustion values are shown in Table 134, and hydrocarbon type analysis results are presented in Table 135. The temperature/viscosity relationship is illustrated in Figure 76.

TABLE 133. PHYSICAL PROPERTIES OF JP-8, TANK F-3

	Temperature, °F	
Density, g/cc	32	0.8255
	70	0.8102
	100	0.7980
Kinematic viscosity, centistokes	0	6.082
	77	2.080
	100	1.672
Surface tension, dynes/cm	32	28.81
	70	26.77
	100	25.14
Vapor pressure, mm Hg	32	8.4
	70	12.7
	100	16.7

TABLE 134. HEAT OF COMBUSTION OF JP-8, TANK F-3

Gross, Btu/lb		Net, Btu/lb
Duplicate	Average	Average
19,786 19,806	19,796	18,519

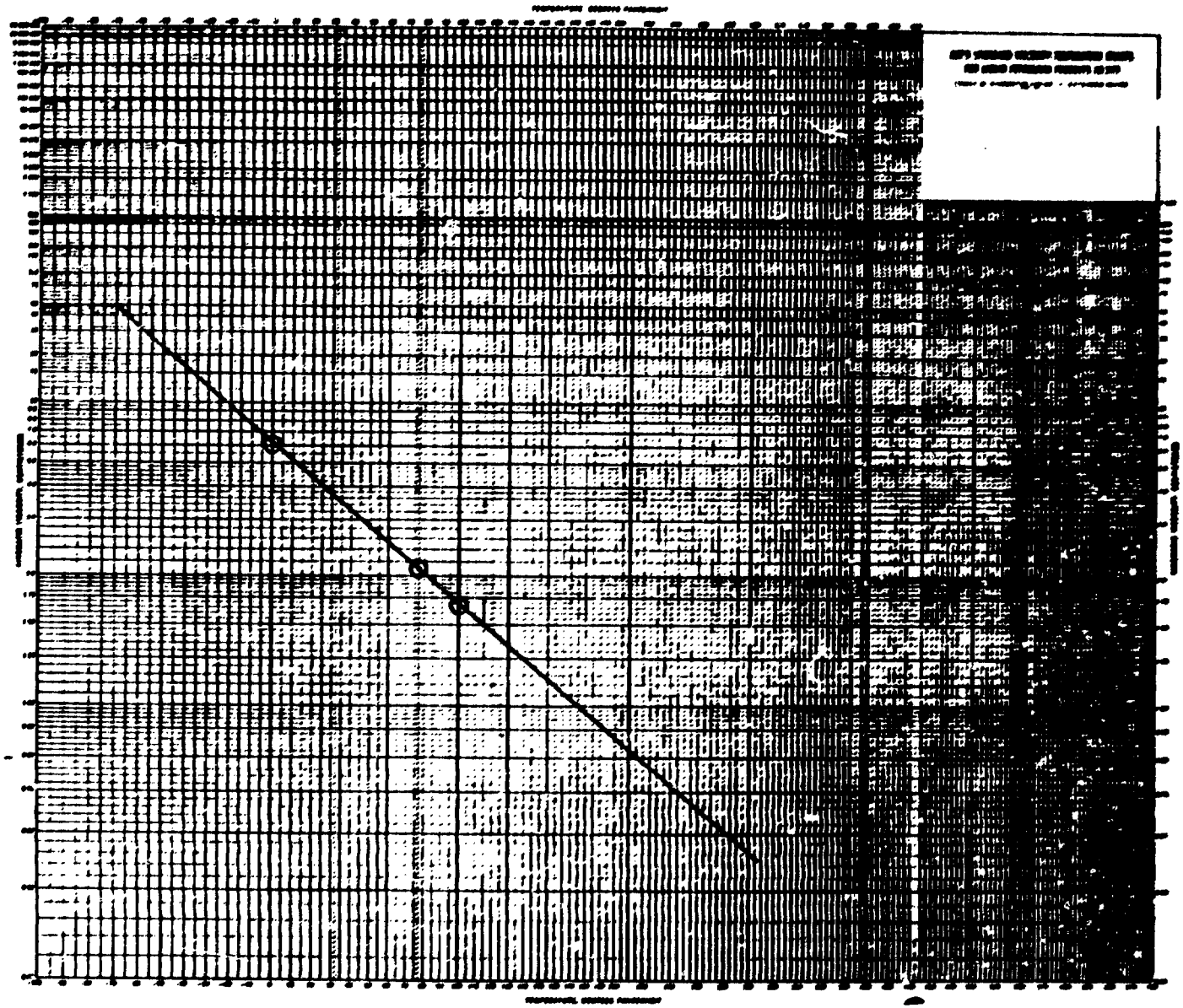

Figure 76. Viscosity/temperature plot for JP-8, tank F-3.

TABLE 135. HYDROCARBON TYPE ANALYSIS OF JP-8, TANK F-3, BY ASTM D 2789 (MODIFIED)

Compound type	Volume percent
Paraffins	43.4
Cycloparaffins	39.8
Dicycloparaffins	3.3
Alkylbenzenes	7.4
Indans and tetralins	4.1
Naphthalenes	2.0

6. HEAT OF COMBUSTION OF GULF MINERAL SEAL OIL

Gulf Mineral Seal Oil, used for blending special fuels to be used in full-scale combustion tests, was evaluated for net heat of combustion using the oxygen bomb calorimeter according to ASTM procedure D 240-64. The results are given below in Table 136.

TABLE 136. HEAT OF COMBUSTION OF MINERAL SEAL OIL

Gross, Btu/lb		Net, Btu/lb
Duplicate	Average	Average
19,937		
19,902		
	19,920	18,627

7. HEAT OF COMBUSTION OF JP-4

JP-4 fuel samples were routinely given in-house full-scale engine tests by the AFAPL Turbine Engine Division. Heat of combustion data were required for these fuels to evaluate their performance in the tests. These data are shown in Table 137.

8. CHEMICAL AND PHYSICAL PROPERTIES OF MODIFIED JP-4 AND JP-8 FUELS

A large number of modified JP-4 and JP-8 fuels were subjected to multiple physical and chemical tests, as described in the Appendix. The number and letter designations after the second

TABLE 137. HEAT OF COMBUSTION OF JP-4 TEST FUELS

JP-4 sample	Report date	Heat of combustion, Gross, Btu/lb Duplicate	Gross, Btu/lb Average	Net, Btu/lb Average
Scrap tank, 'D' bay	2-7-79	20,137 20,134	20,136	18,811
B-3 tank	2-7-79	20,140 20,097	20,119	18,794
'D' bay engine cell	2-7-79	20,094 20,147	20,121	18,796
B-2 tank	2-7-79	20,076 20,107	20,092	18,767
Test fuel from AFAPL Turbine Engine Division	8-31-78	19,934 20,008	19,996	18,686
Test fuel from TF-41 engine test facility	10-9-78	20,152 20,111	20,132	18,818
Test fuel from AFAPL full-scale engine	12-15-78	20,137 20,171	20,154	18,831
Test facility AFAPL turbine engine test fuel	3-26-79	20,117 20,100	20,109	18,786

hyphen in the sample number indicate the type of fuel (JP-4 or JP-8) and the blending stock used to modify the fuel. The letters AR (2040 aromatic solvent), XY (xylene bottoms), DF-2 (diesel fuel), XG (xylene bottoms and Gulf Mineral Seal Oil) are used. The number following the third hyphen indicates the nominal hydrogen content resulting from the modification (12.0%, 13.0%, or 14.0%).

The data are presented in Tables 138 through 144 and Figures 77 through 108 as follows:

TABLE 138. DENSITY OF MODIFIED FUELS AS A FUNCTION OF TEMPERATURE

Sample number	Density, g/cc 32°F	70°F	100°F
GE/TJ-78-4AR-12.0	0.8506	0.8343	0.8210
GE/TJ-78-4AR-12.0-02	0.8543	0.8375	0.8243
GE/TJ-78-4AR-12.0-03	0.8525	0.8357	0.8225
GE/TJ-78-4AR-12.0-05	0.8489	0.8323	0.8193
GE/TJ-78-4AR-13.0	0.8171	0.8007	0.7878
GE/TJ-78-4AR-13.0-02	0.8168	0.8003	0.7872
GE/TJ-78-4AR-13.0-03	0.8178	0.8010	0.7878
GE/TJ-78-4AR-13.0-05	0.8184	0.8023	0.7895
GE/TJ-78-4XY-12.0 (5/23/78)	0.8305	0.8135	0.8000
GE/TJ-78-4XY-12.0 (5/30/78)	0.8307	0.8134	0.8002
GE/TJ-78-4XY-12.0 (Batch 2)	0.8298	0.8126	0.7990
GE/TJ-78-4XY-12.0-02	0.8306	0.8135	0.7999
GE/TJ-78-4XY-13.0 (5/13/78)	0.8064	0.7899	0.7740
GE/TJ-78-4XY-13.0 (5/30/78)	0.8079	0.7909	0.7771
GE/TJ-78-4XY-13.0 (Batch 2)	0.8081	0.7912	0.7776
GE/TJ-78-4XY-13.0-02	0.8091	0.7922	0.7787
GE/TJ-78-4XG-14.0 (5/23/78)	0.7904	0.7740	0.7608
GE/TJ-78-4XG-14.0 (5/30/78)	0.7906	0.7740	0.7611
GE/TJ-78-4XG-14.0-02	0.7915	0.7749	0.7617
DF-2 (5/25/78)	0.8561	0.8413	0.8295
GE/TJ-78-DF2-13.0-02	0.8491	0.8338	0.8218
GE/TJ-78-8AR-13.0	0.8452	0.8295	0.8171
GE/TJ-78-8AR-13.0-02	0.8454	0.8298	0.8174
GE/TJ-78-8AR-13.0-03	0.8457	0.8300	0.8175
GE/TJ-78-8AR-13.0-05	0.8454	0.8298	0.8177
GE/TJ-78-8AR-12.0-08	0.8728	0.8568	0.8444
GE/TJ-78-8AR-12.0-09	0.8726	0.8568	0.8444
GE/TJ-78-8XY-12.0-05	0.8490	0.8326	0.8195
GE/TJ-78-8XY-12.0-08	0.8489	0.8323	0.8191
GE/TJ-78-8XY-12.0-09	0.8486	0.8320	0.8190
GE/TJ-78-8XY-13.0-08	0.8339	0.8180	0.8055
GE/TJ-78-8XY-13.0-09	0.8343	0.8182	0.8053

TABLE 139. KINEMATIC VISCOSITY OF MODIFIED FUELS AS A FUNCTION OF TEMPERATURE

Sample Number	Viscosity, centistokes 0°F	77°F	100°F
GE/TJ-78-4AR-12.0	2.605	1.175	0.989
GE/TJ-78-4AR-12.0-02	2.598	1.173	0.990
GE/TJ-78-4AR-12.0-03	2.632	1.173	0.994
GE/TJ-78-4AR-12.0-05	2.598	1.173	0.988
GE/TJ-78-4AR-13.0	2.204	1.053	0.903
GE/TJ-78-4AR-13.0-02	2.199	1.059	0.903
GE/TJ-78-4AR-13.0-03	2.227	1.063	0.908
GE/TJ-78-4AR-12.0-05	2.288	1.081	0.920
GE/TJ-78-4XY-12.0 (5/23/78)	1.623	0.851	0.739
GE/TJ-78-4XY-12.0 (5/30/78)	1.618	0.851	0.738
GE/TJ-78-4XY-12.0 (Batch 2)	1.616	0.852	0.738
GE/TJ-78-4XY-12.0-02	1.662	0.836	0.726
GE/TJ-78-4XY-13.0 (5/23/78)	1.685	0.864	0.748
GE/TJ-78-4XY-13.0 (5/30/78)	1.676	0.859	0.745
GE/TJ-78-4XY-13.0 (Batch 2)	1.662	0.855	0.742
GE/TJ-78-4XY-13.0-02	1.688	0.864	0.747
GE/TJ-78-4XG-14.0 (5/23/78)	2.231	1.089	0.927
GE/TJ-78-4XG-14.0 (5/23/78)	2.236	1.085	0.927
GE/TJ-78-4XG-14.0-02	2.261	1.093	0.932
DF-2 (5/25/78)	14.99*	3.356	2.561
GE/TJ-78-DF2-13.0-02	11.19	3.006	2.318
GE/TJ-78-8AR-13.0	5.209	1.864	1.508
GE/TJ-78-8AR-13.0-02	5.212	1.871	1.513
GE/TJ-78-8AR-13.0-03	5.193	1.861	1.505
GE/TJ-78-8AR-13.0-05	5.183	1.858	1.511
GE/TJ-78-8AR-12.0-08	5.409	1.876	1.514
GE/TJ-78-8AR-12.0-09	5.386	1.870	1.509
GE/TJ-78-8XY-12.0-05	2.635	1.195	1.007
GE/TJ-78-8XY-12.0-08	2.633	1.192	1.008
GE/TJ-78-8XY-12.0-09	2.618	1.196	1.006
GE/TJ-78-8XY-13.0-08	3.520	1.471	1.223
GE/TJ-78-8XY-13.0-09	3.569	1.470	1.220

*Forms gel at this temperature.

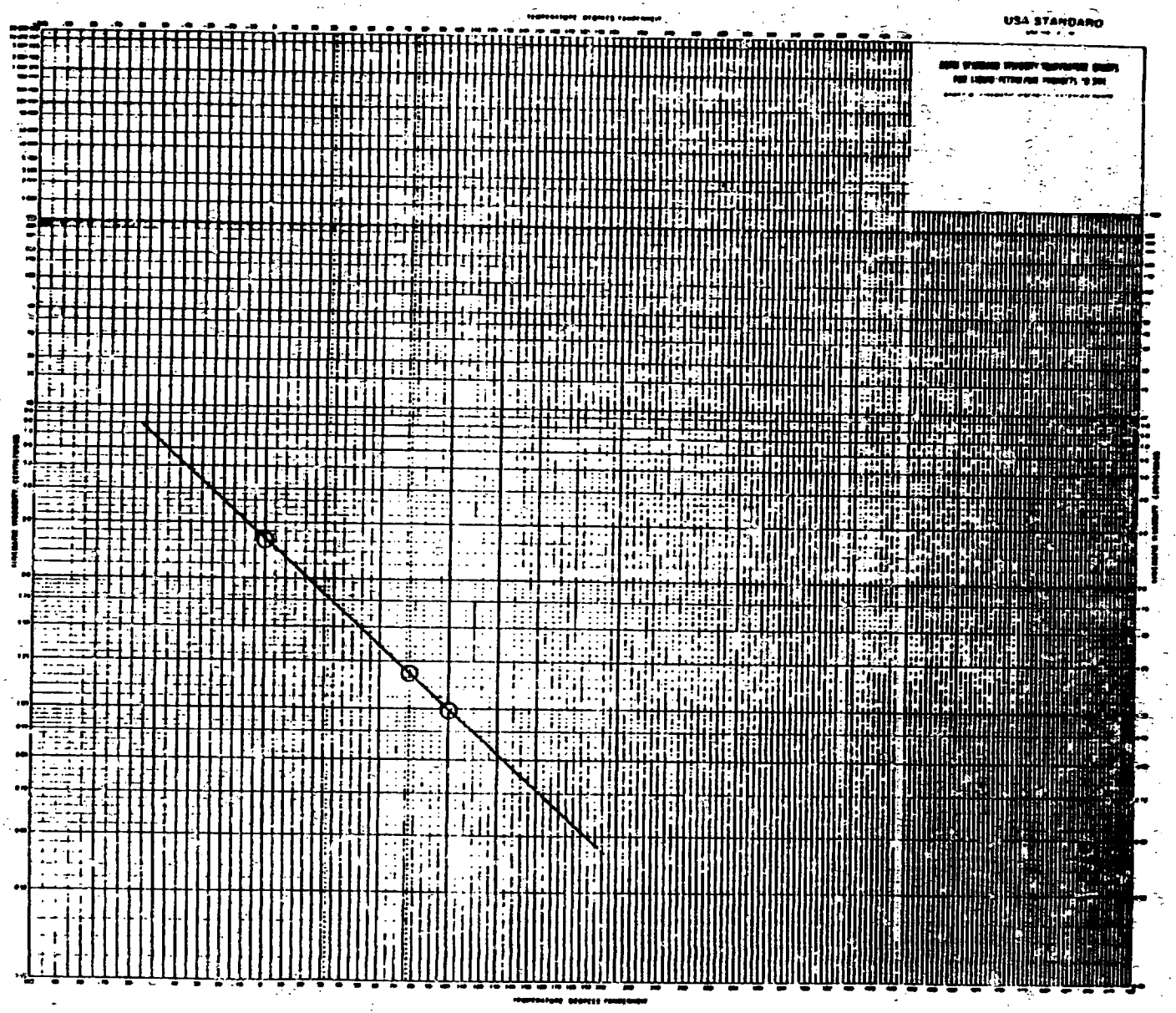

Figure 77. Viscosity/temperature plot for GE/TJ-78-4AR-12.0.

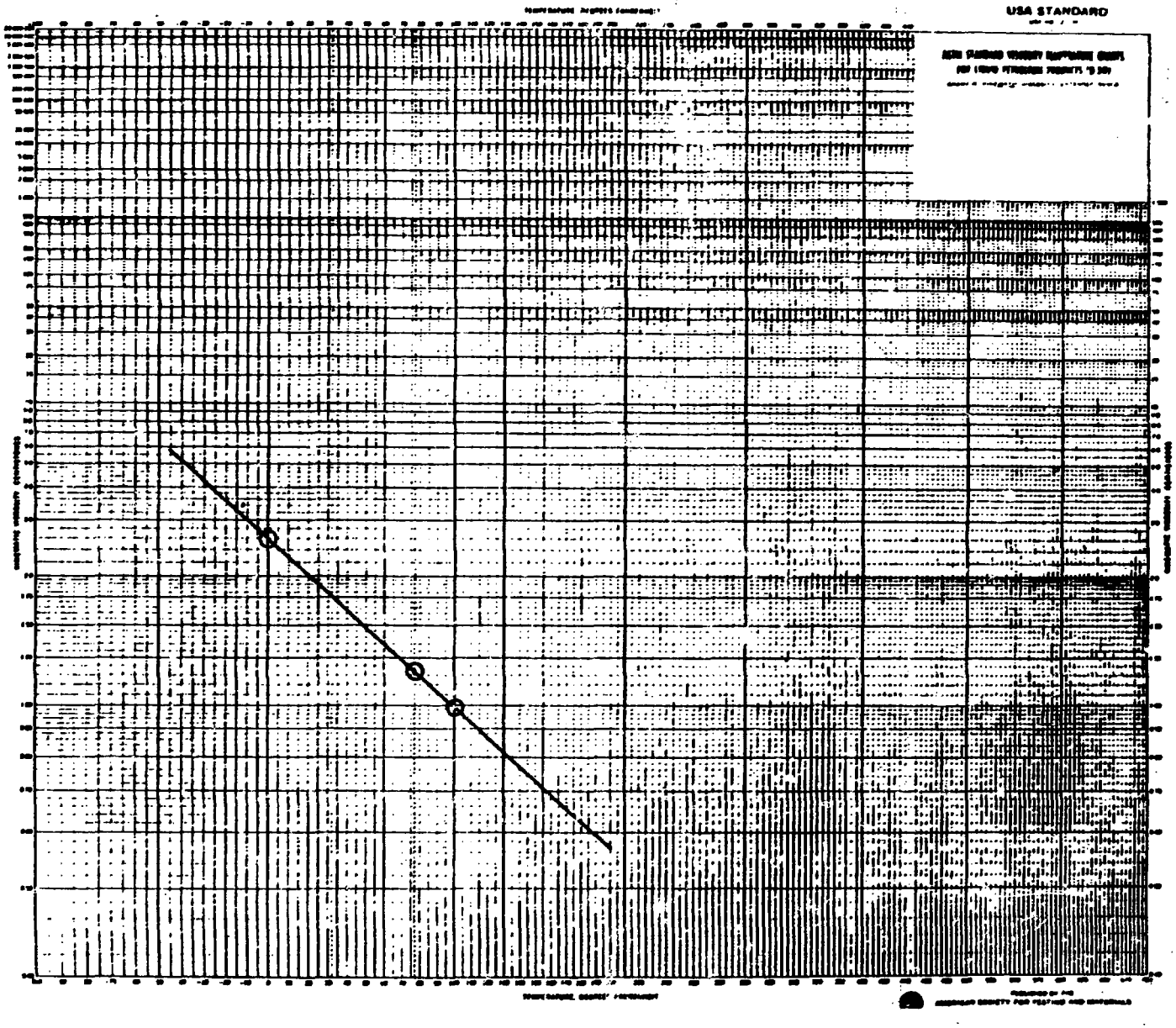

Figure 78. Viscosity/temperature plot for GE/TJ-78-4AR-12.0-02.

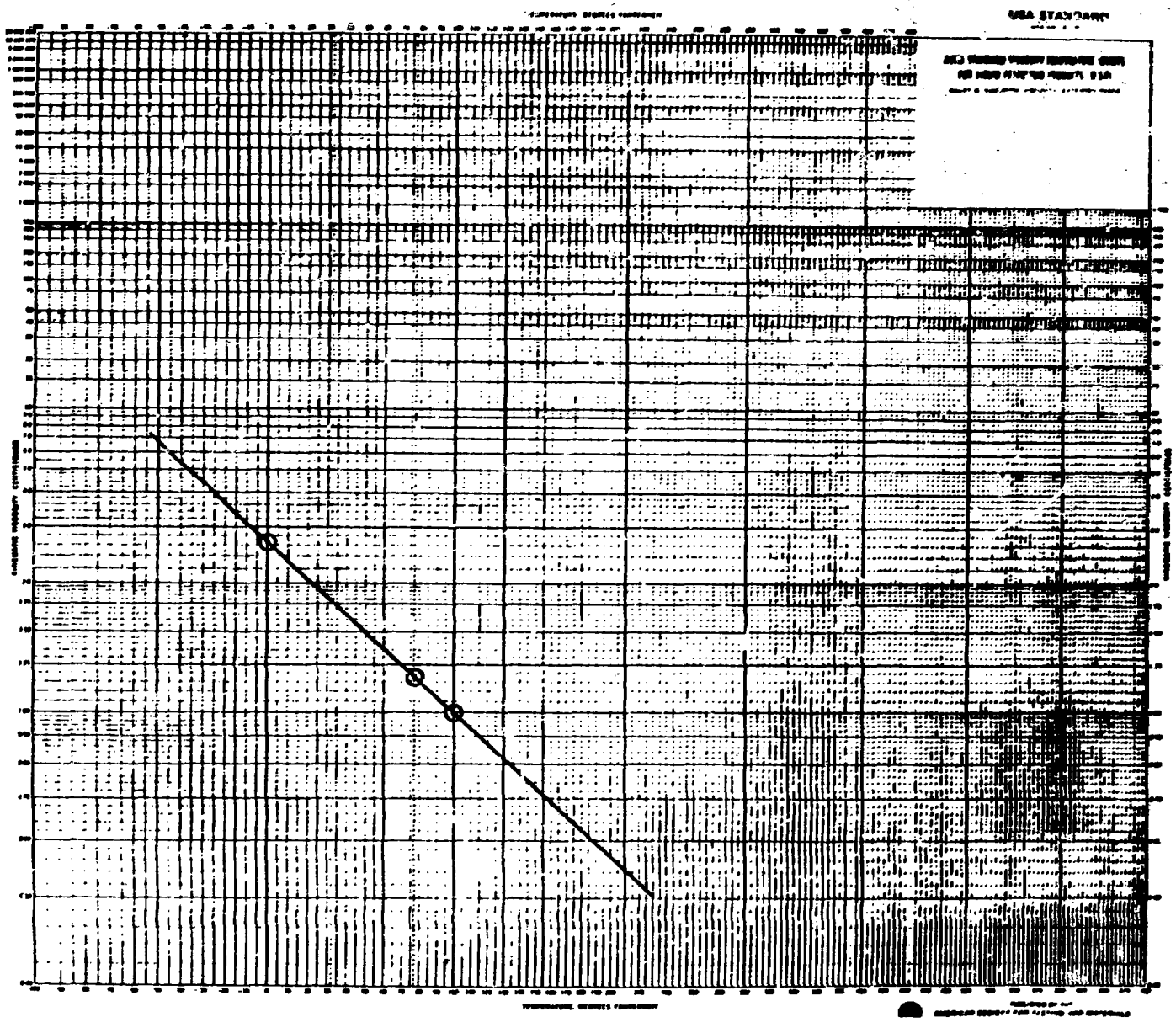

Figure 79. Viscosity/temperature plot for GE/TJ-78-4AR-12.0-03.

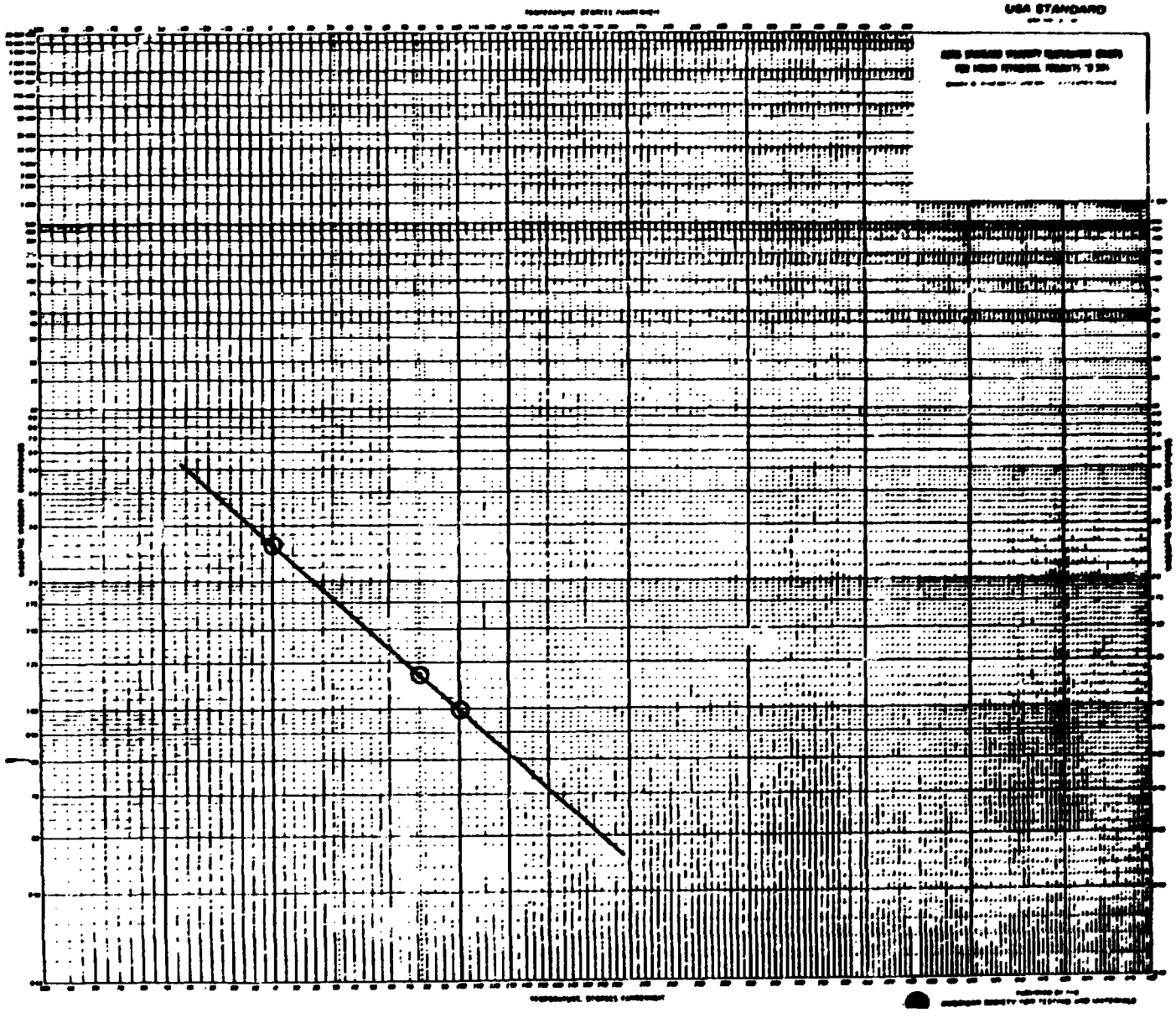

Figure 80. Viscosity/temperature plot for GE/TJ-78-4AR-12.0-05.

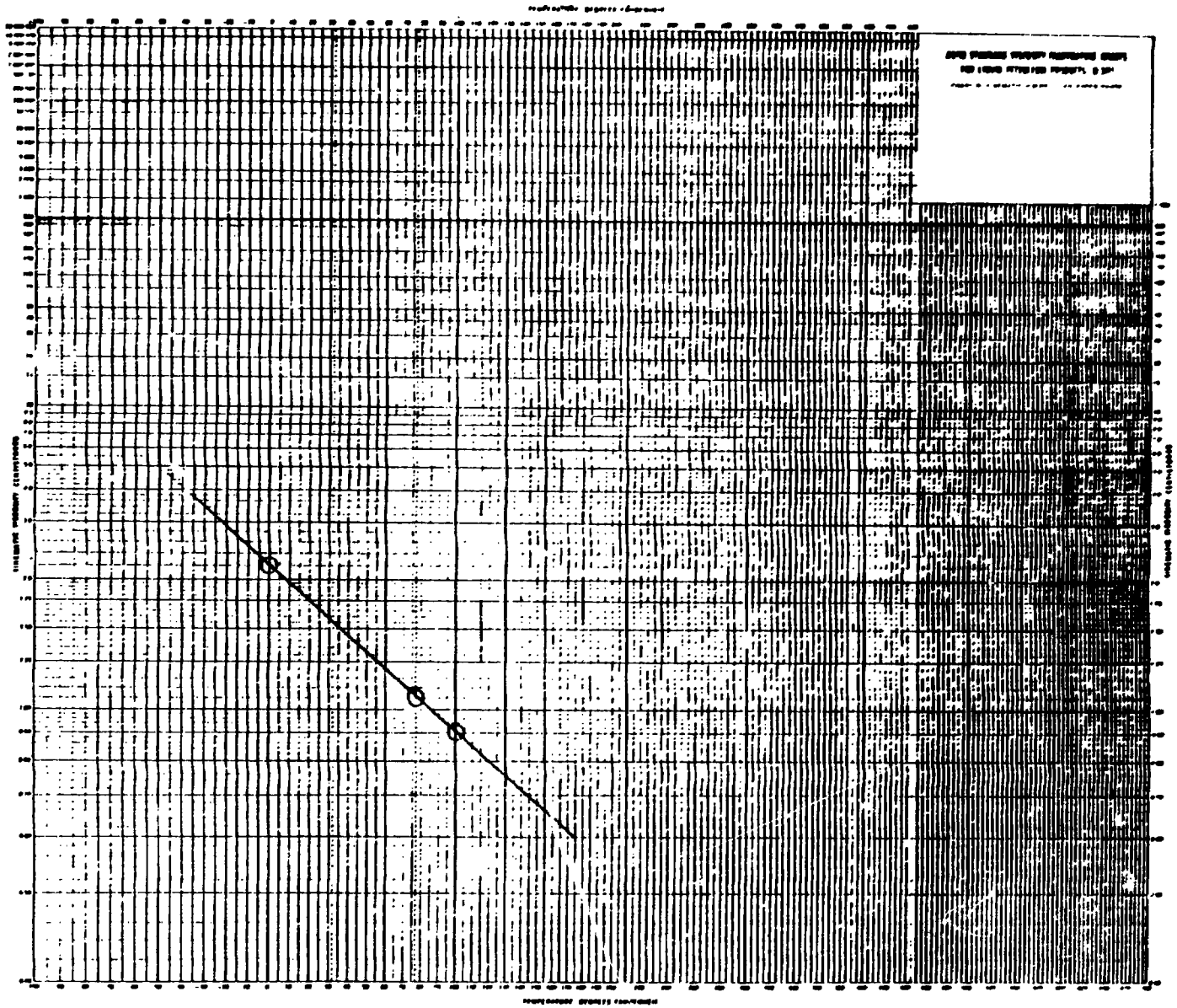

Figure 81. Viscosity/temperature plot for GE/TJ-78-4AR-13.0.

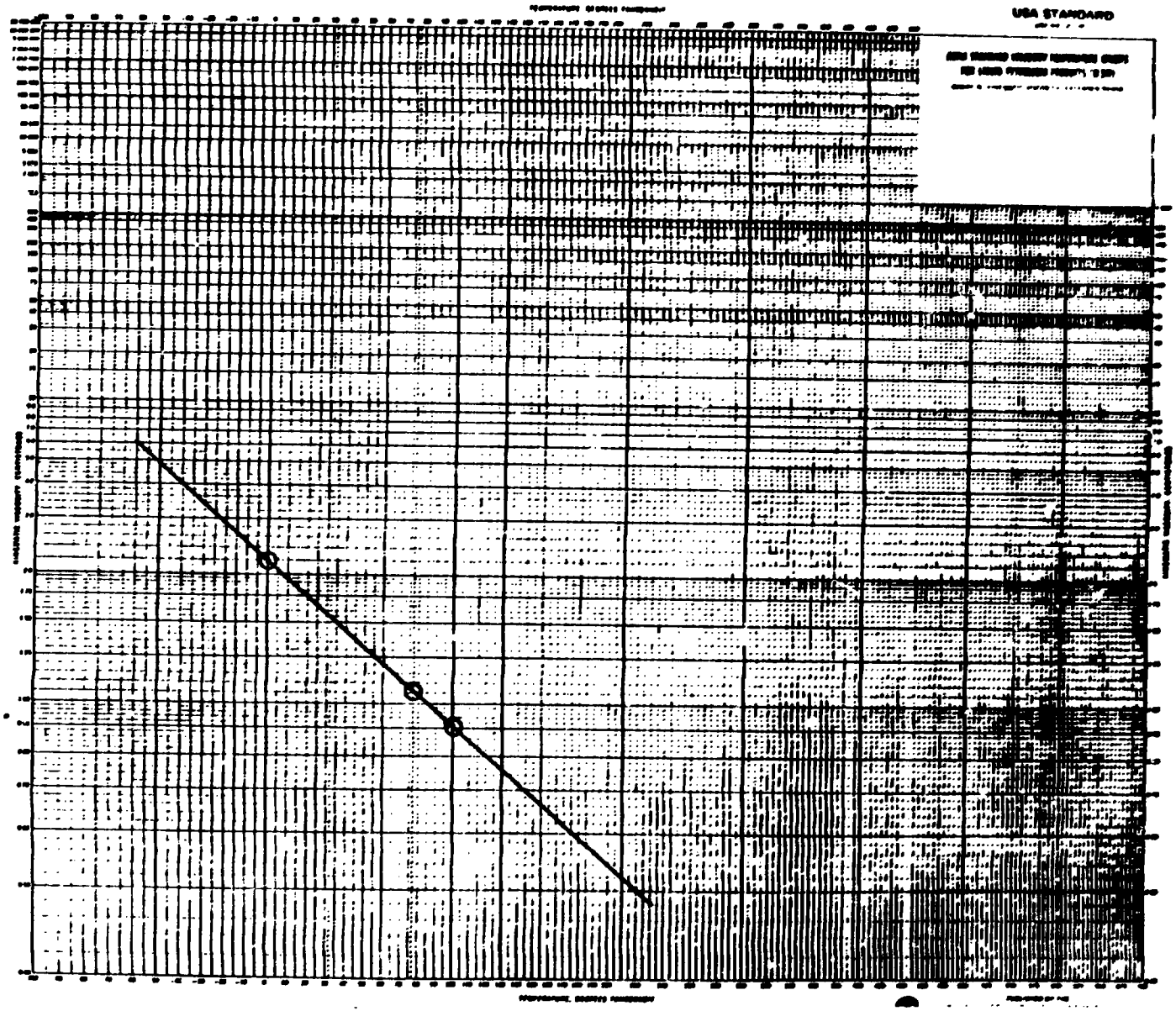

Figure 82. Viscosity/temperature plot for GE/TJ-78-4AR-13.0-02.

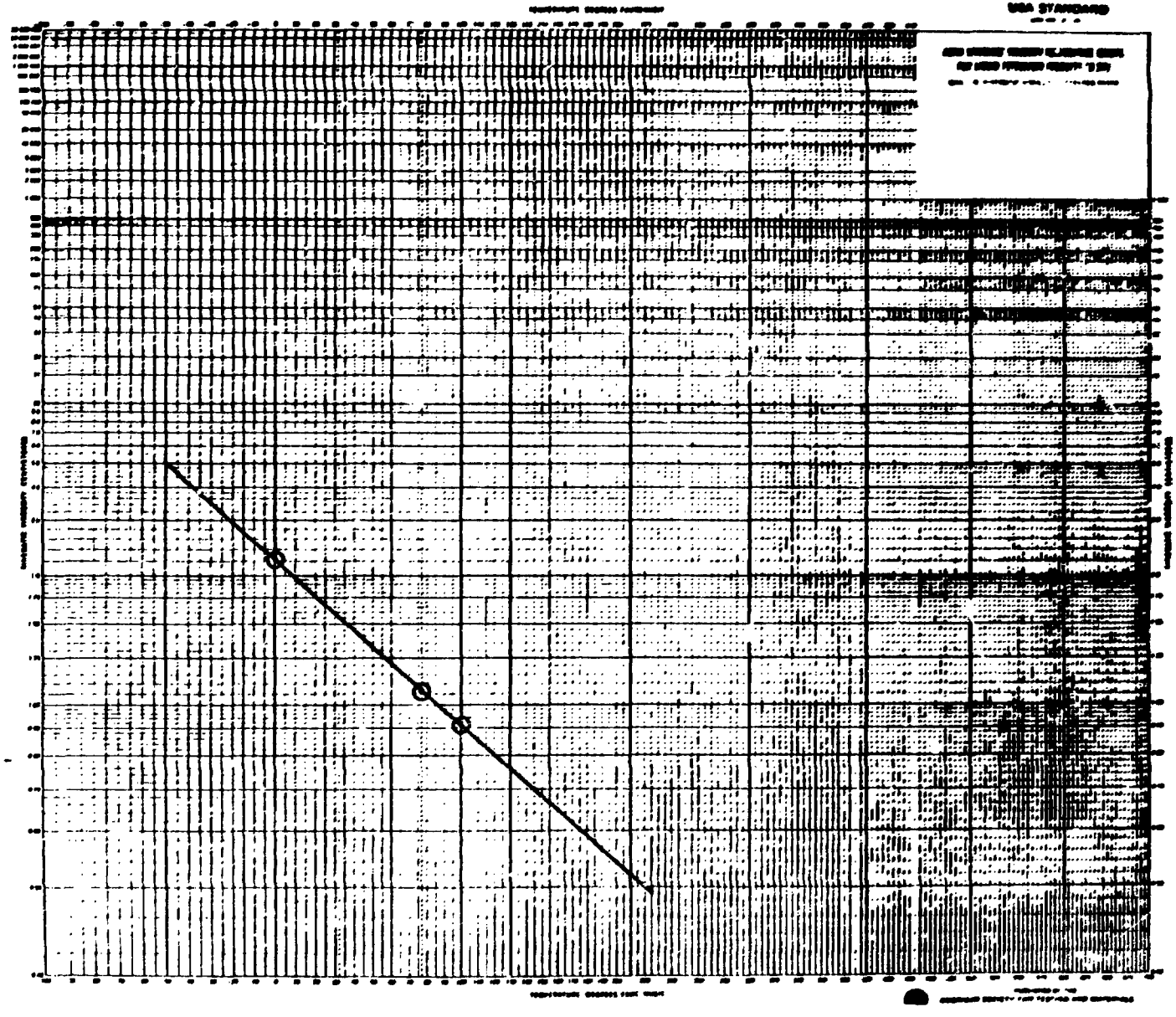

Figure 83. Viscosity/temperature plot for GE/TJ-78-4AR-13.0-03.

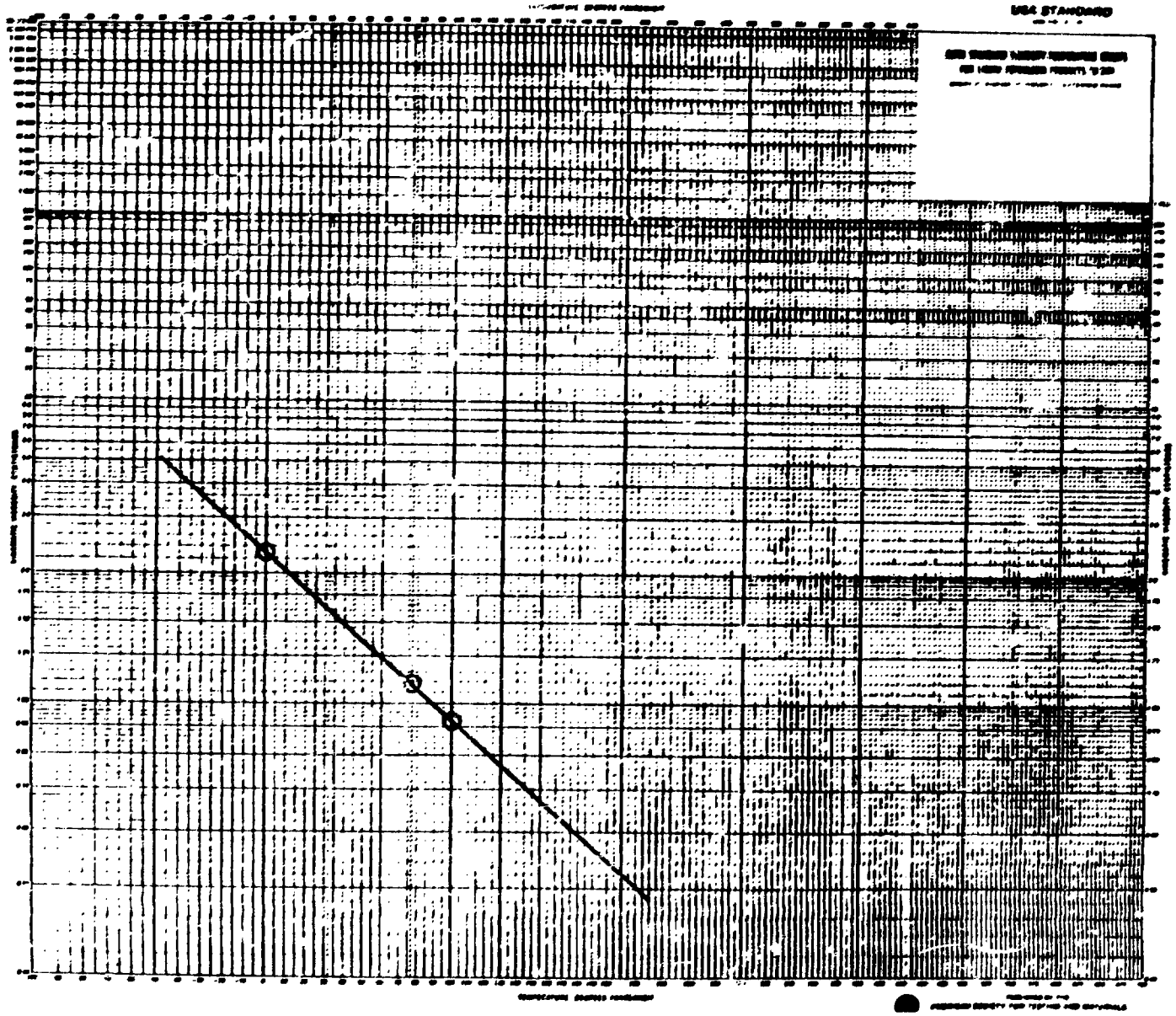

Figure 84. Viscosity/temperature plot for GE/TJ-78-4AR-13.0-05.

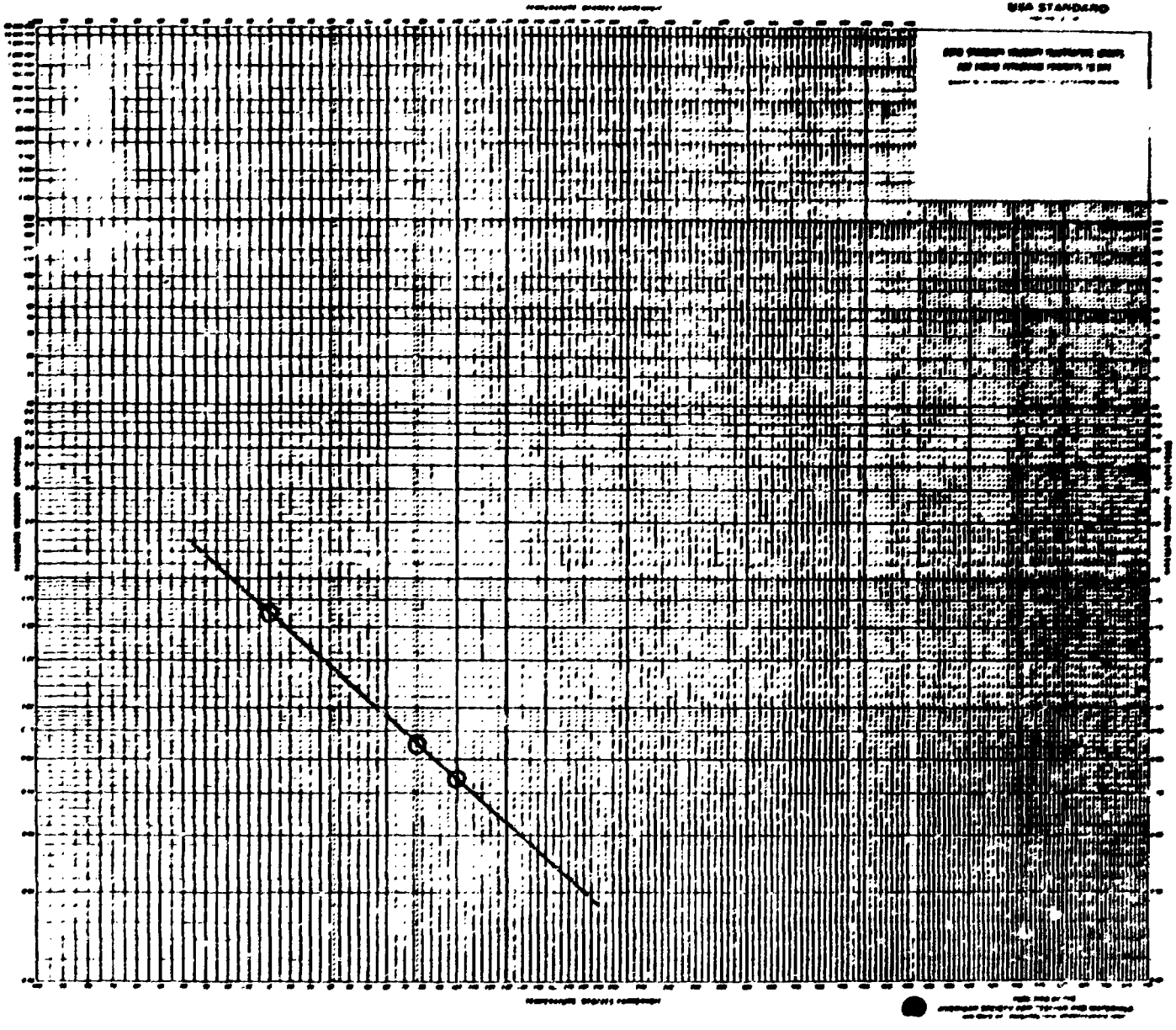

Figure 85. Viscosity/temperature plot for GE/TJ-78-4XY-12.0 (5-23-78).

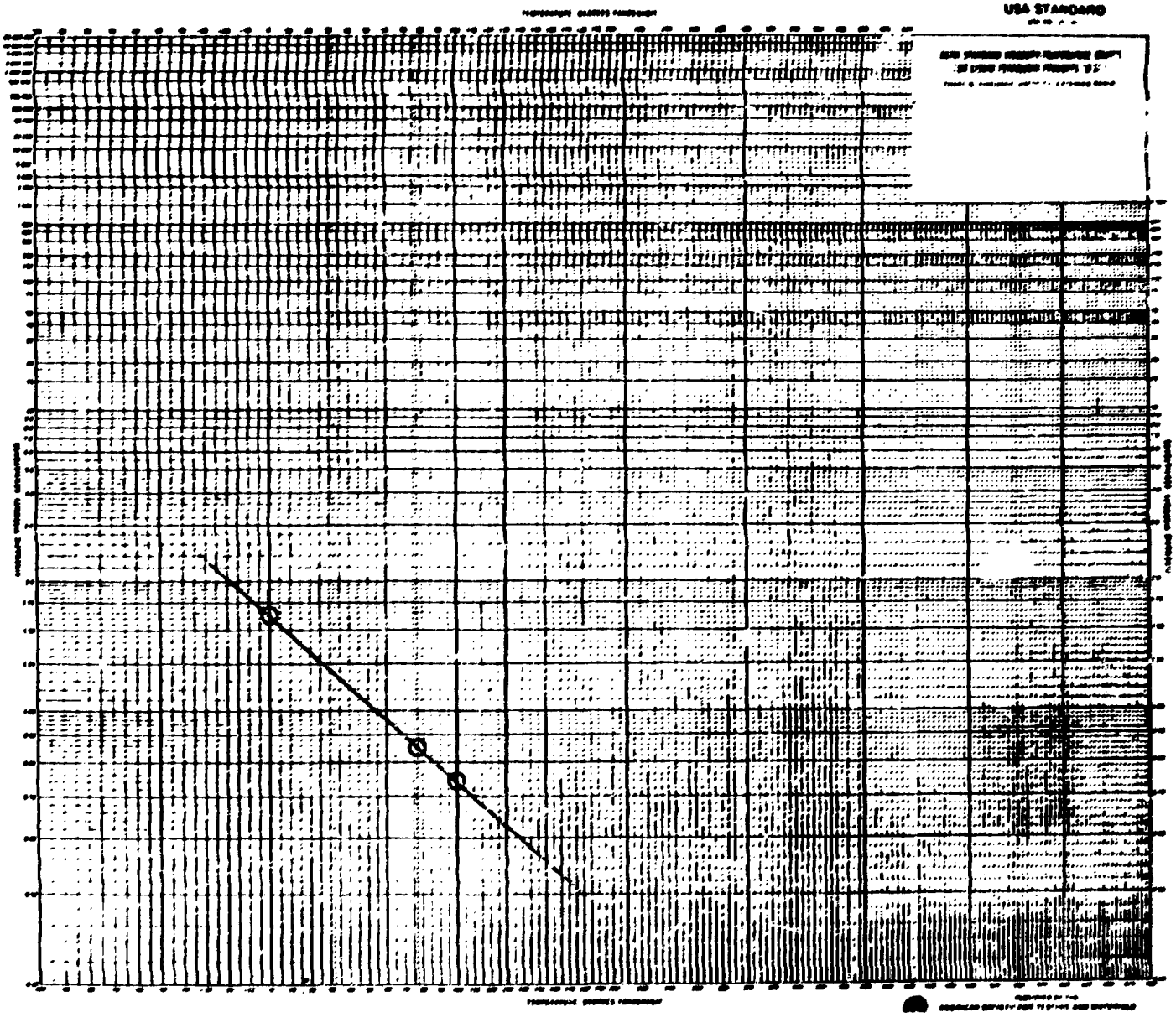

Figure 86. Viscosity/temperature plot for GE/TJ-78-4XY-12.0 (5-30-78).

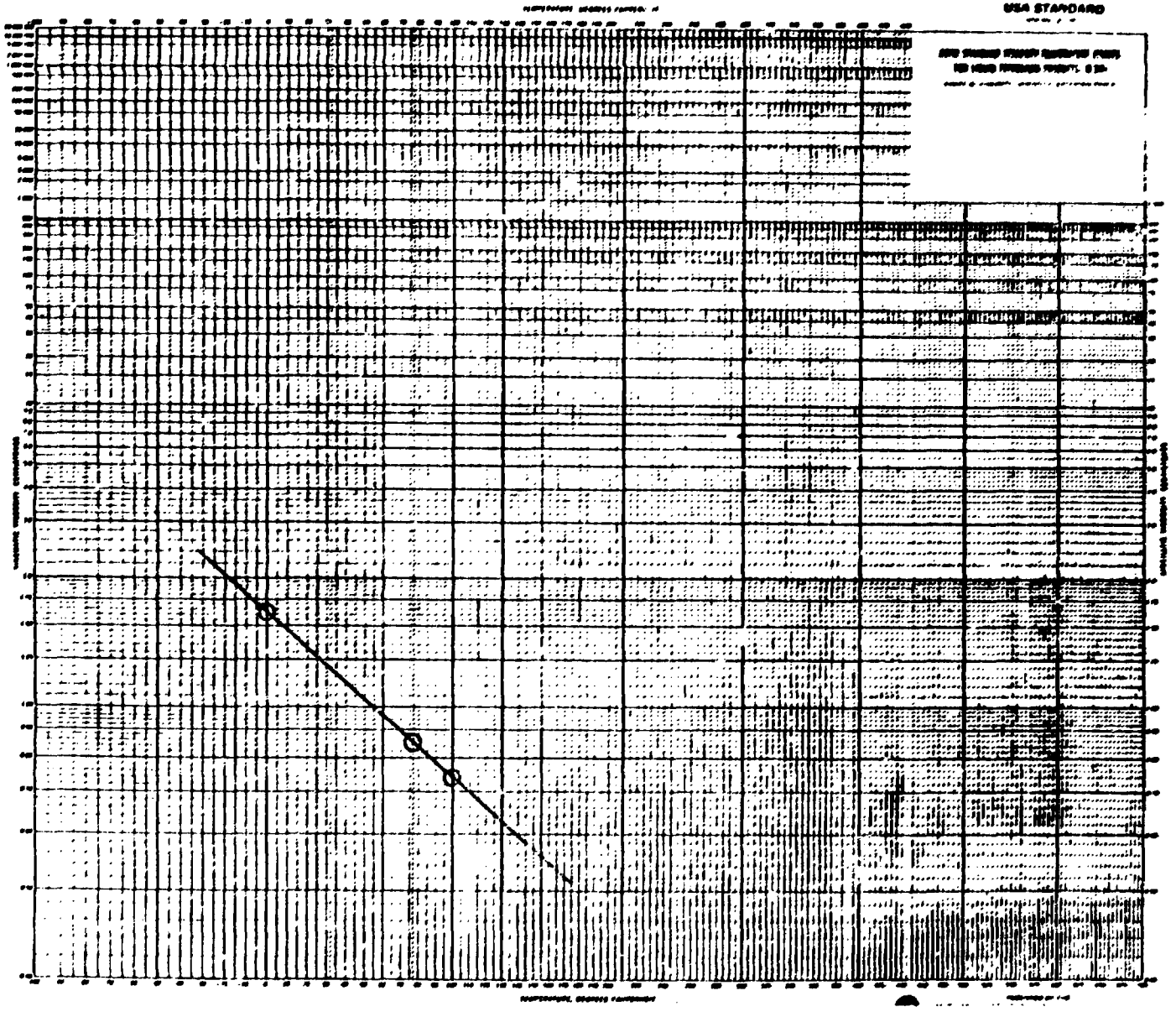

Figure 87. Viscosity/temperature plot for GE/TJ-78-4XY-12.0 (Batch 2).

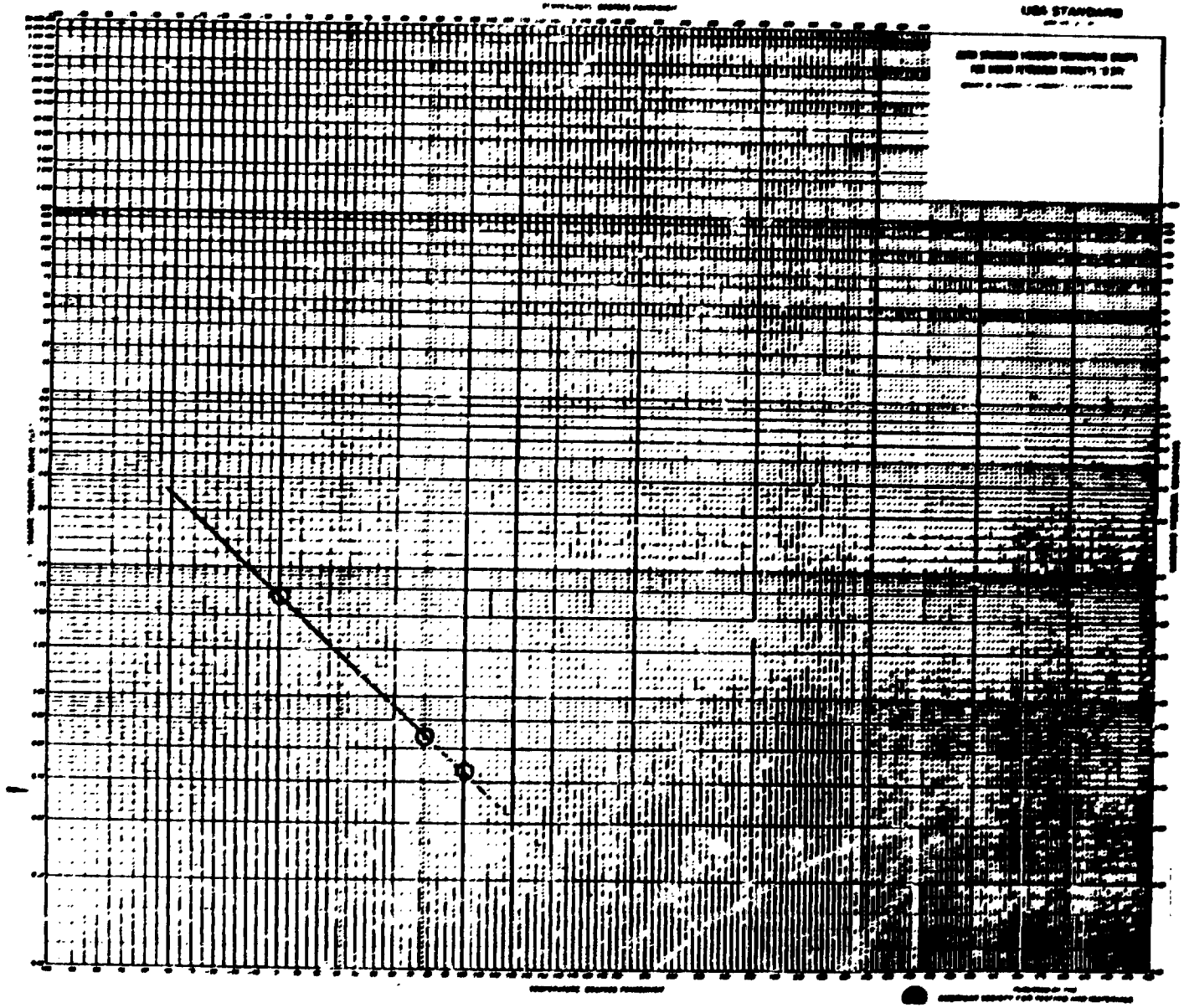

Figure 88. Viscosity/temperature plot for GE/TJ-78-4XY-12.0-02.

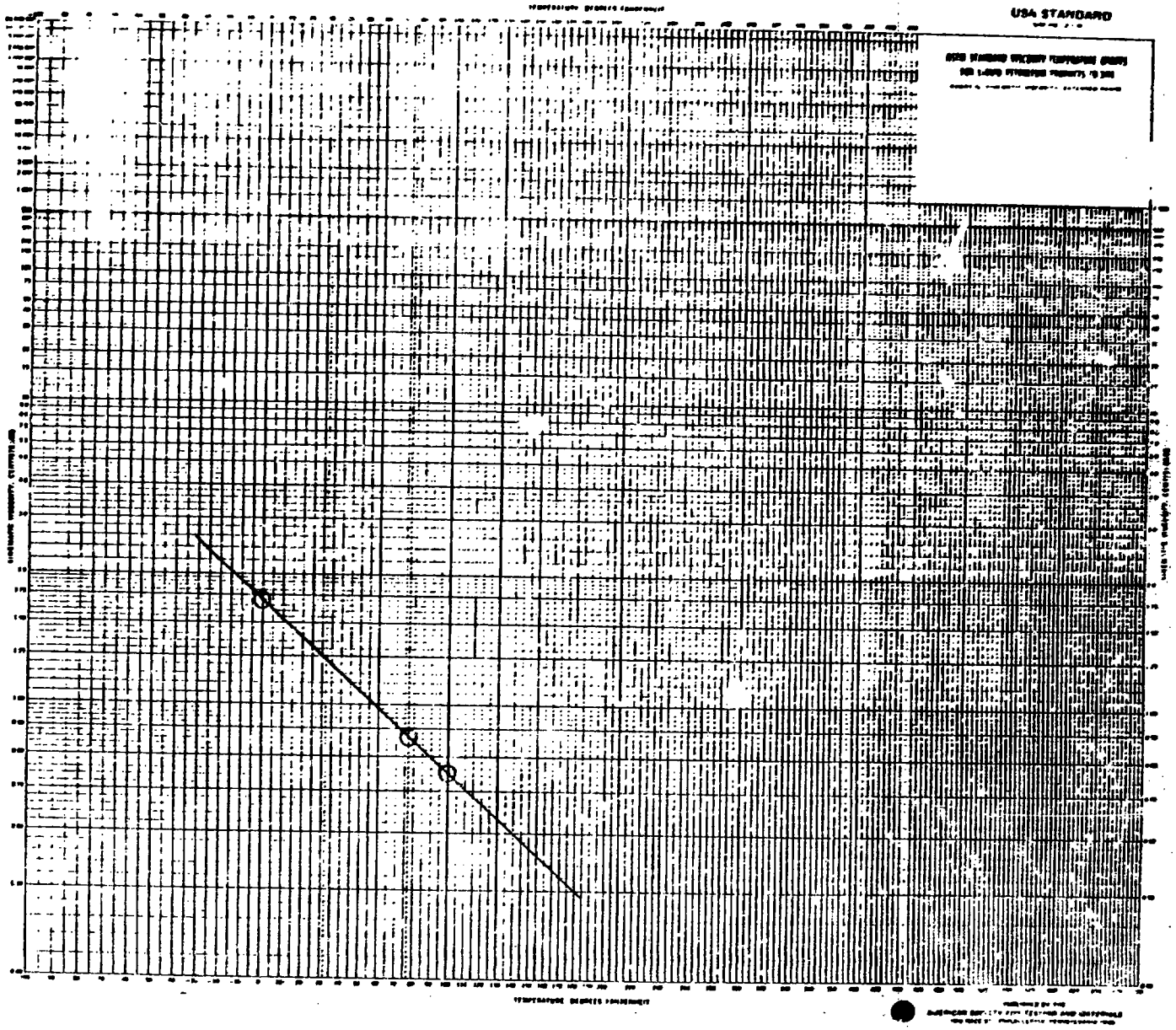

Figure 89. Viscosity/temperature plot for GE/TJ-78-4XY-13.0 (5-23-78).

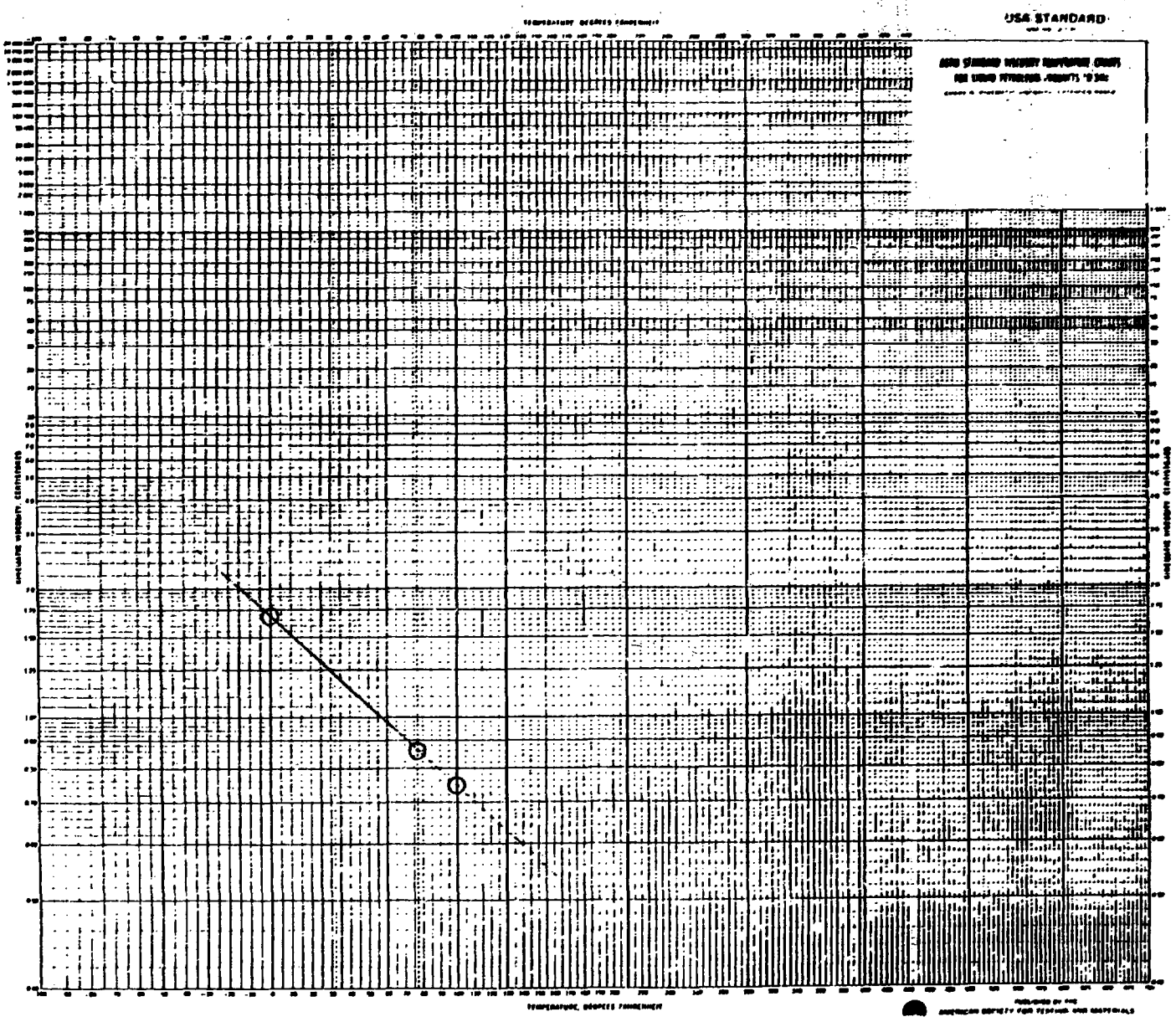

Figure 90. Viscosity/temperature plot for GE/TJ-78-4XY-13.0 (5-30-78).

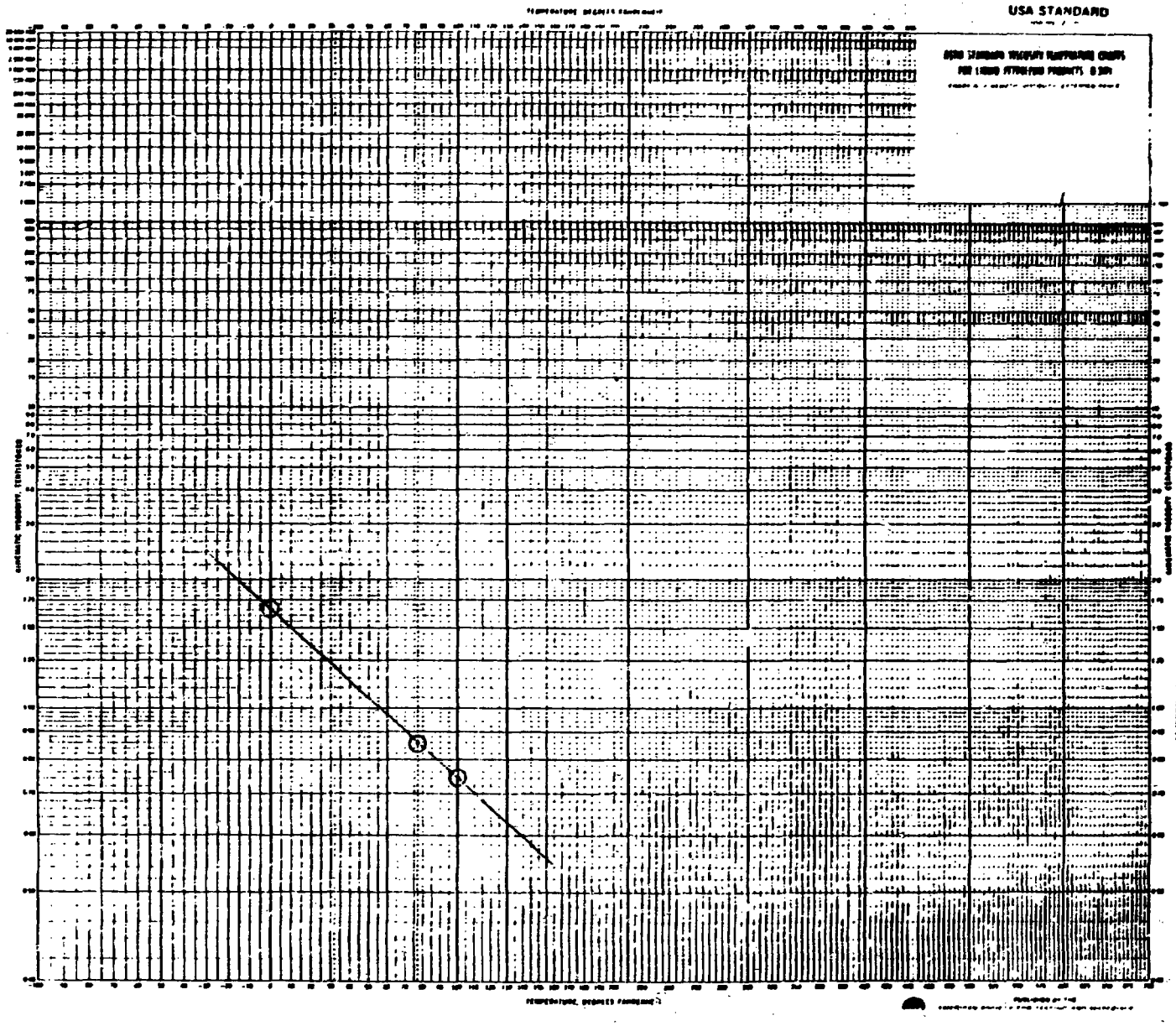

Figure 91. Viscosity/temperature plot for GE/TJ-78-4XY-13.0 (Batch 2).

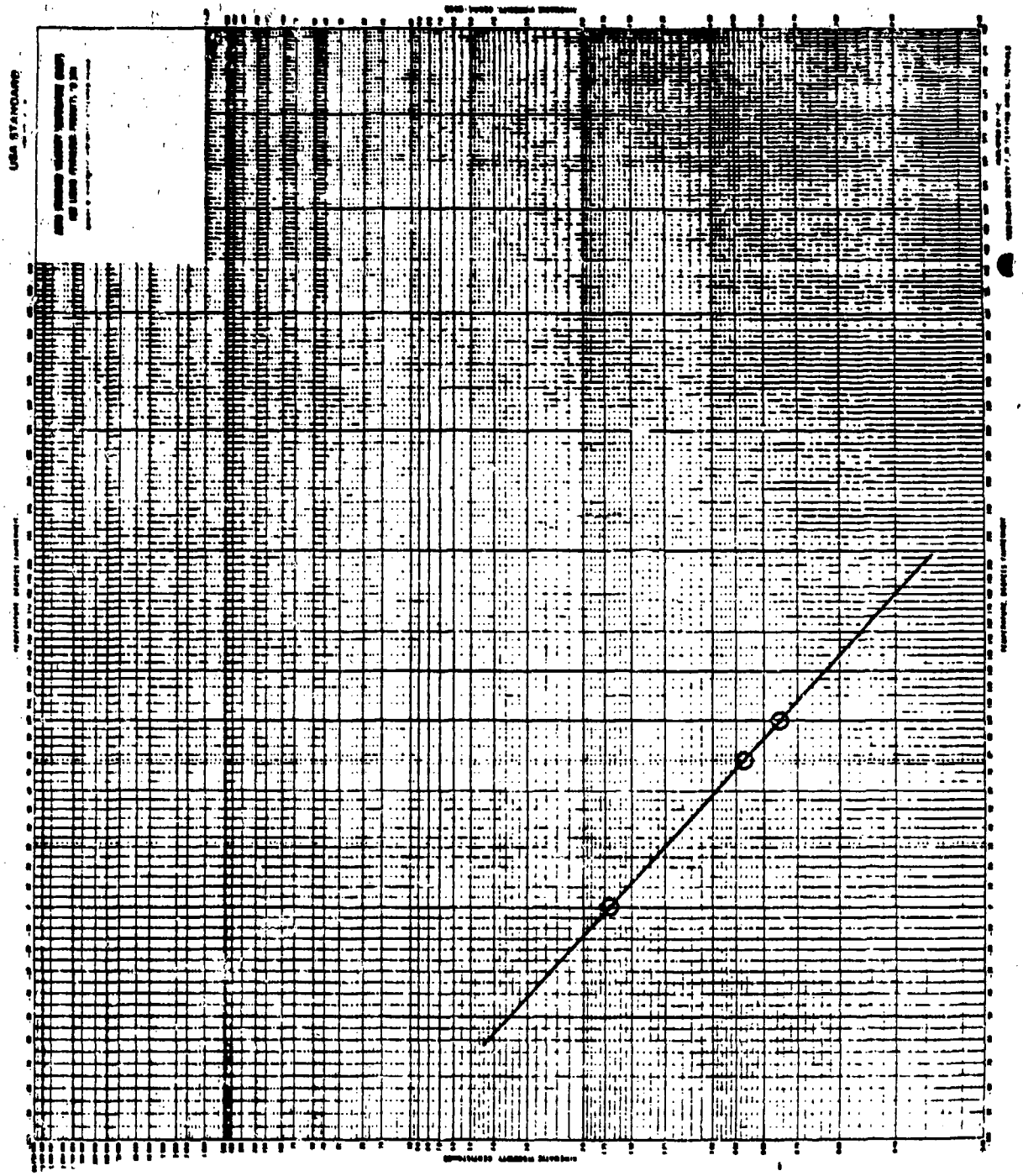

Figure 92. Viscosity/temperature plot for GE/TJ-78-4XY-13.0-02.

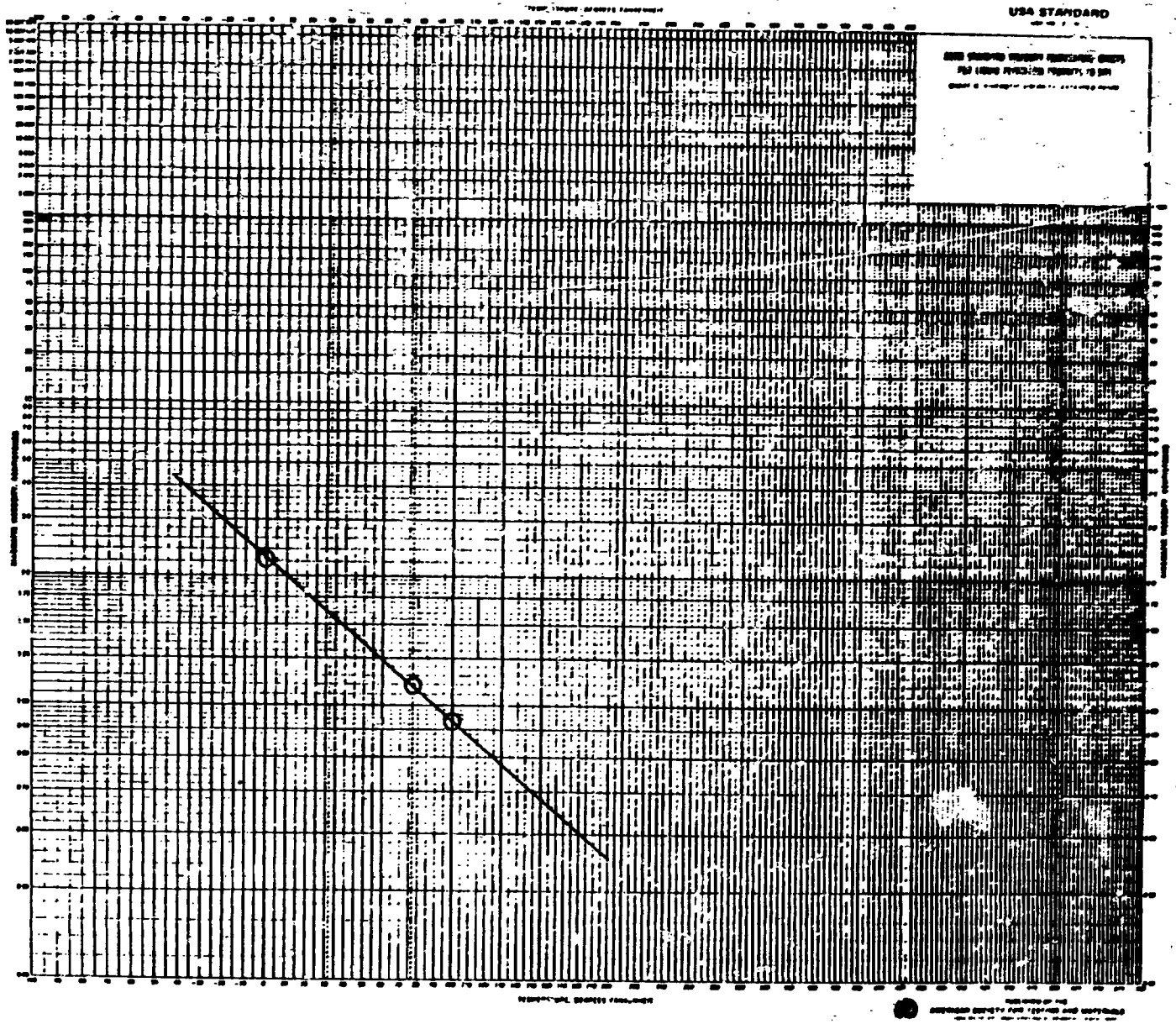

Figure 93. Viscosity/temperature plot for GE/TJ-78-4XG-14.0 (5-23-78).

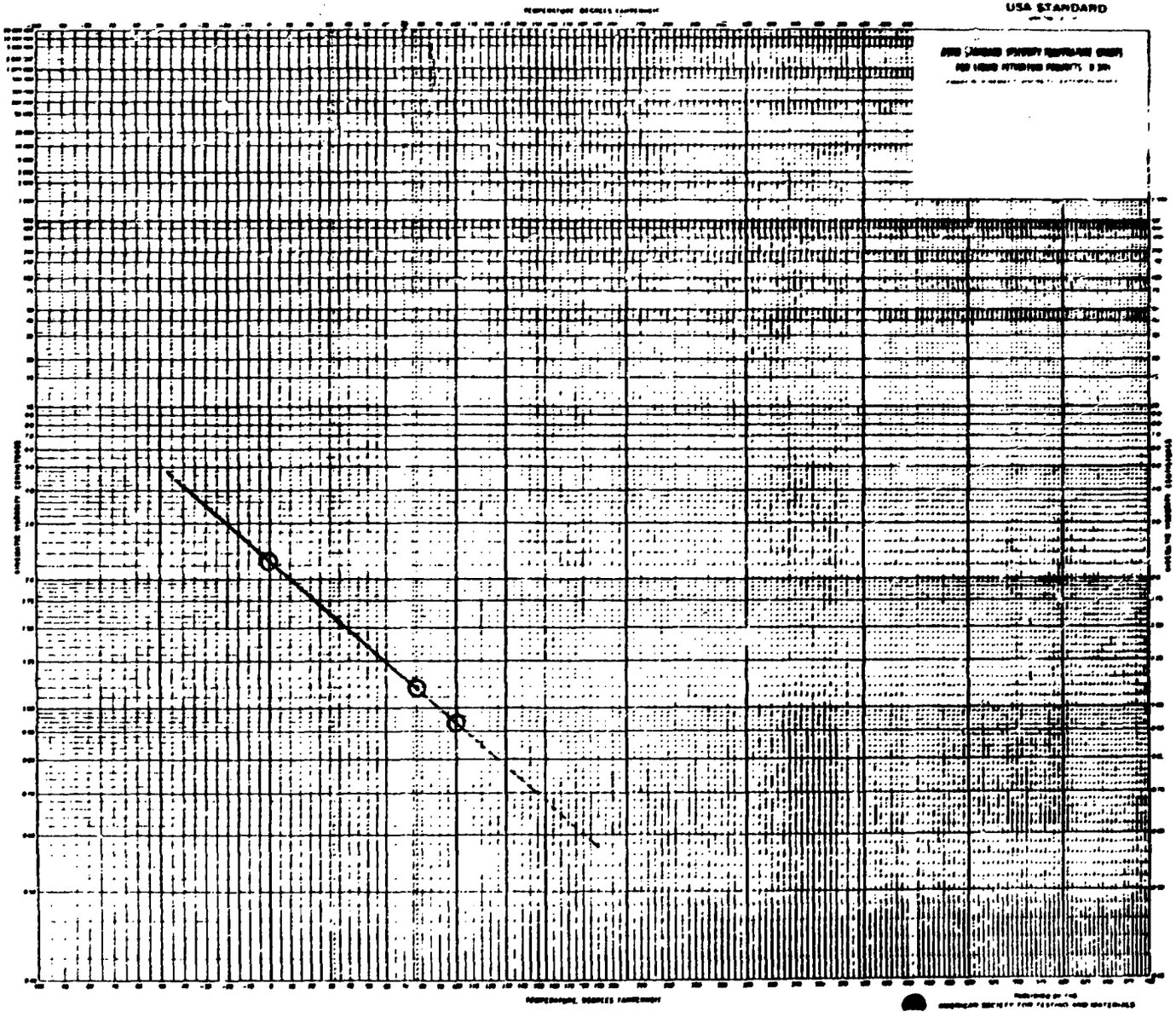

Figure 94. Viscosity/temperature plot for GE/TJ-78-4XG-14.0 (5-30-78).

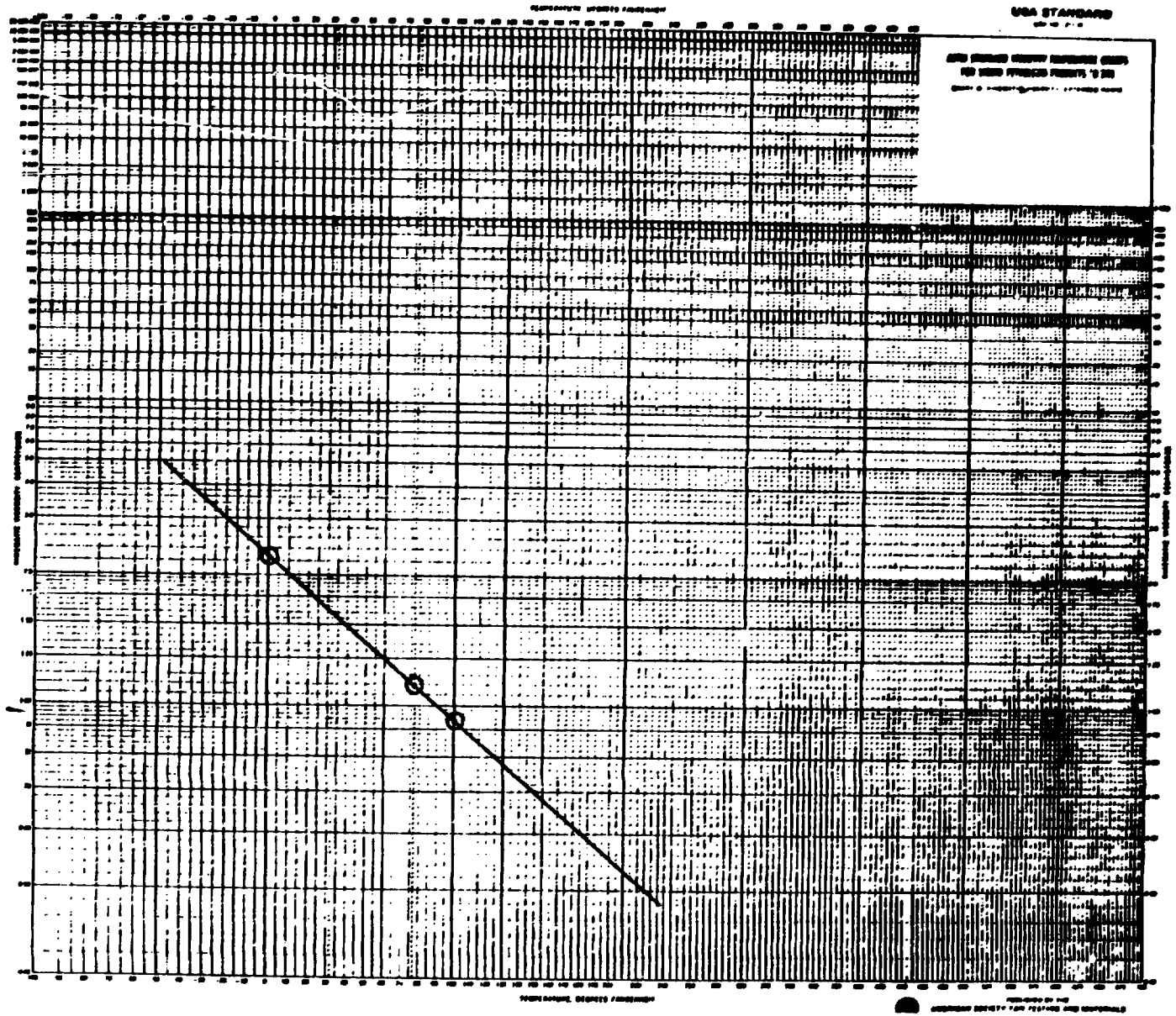

Figure 95. Viscosity/temperature plot for GE/TJ-78-4XG-14.0-02.

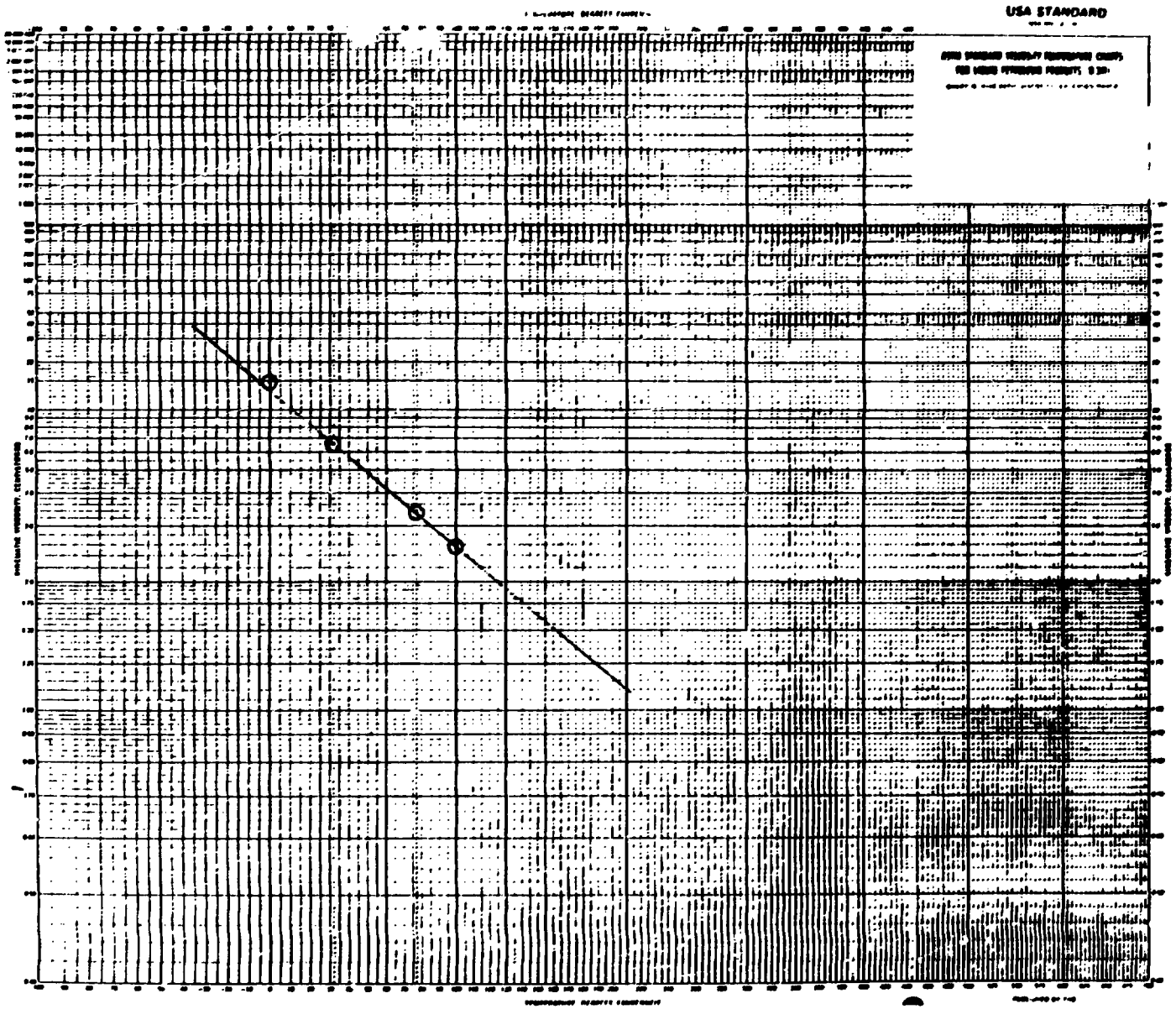

Figure 96. Viscosity/temperature plot for DF-2 (5-25-78).

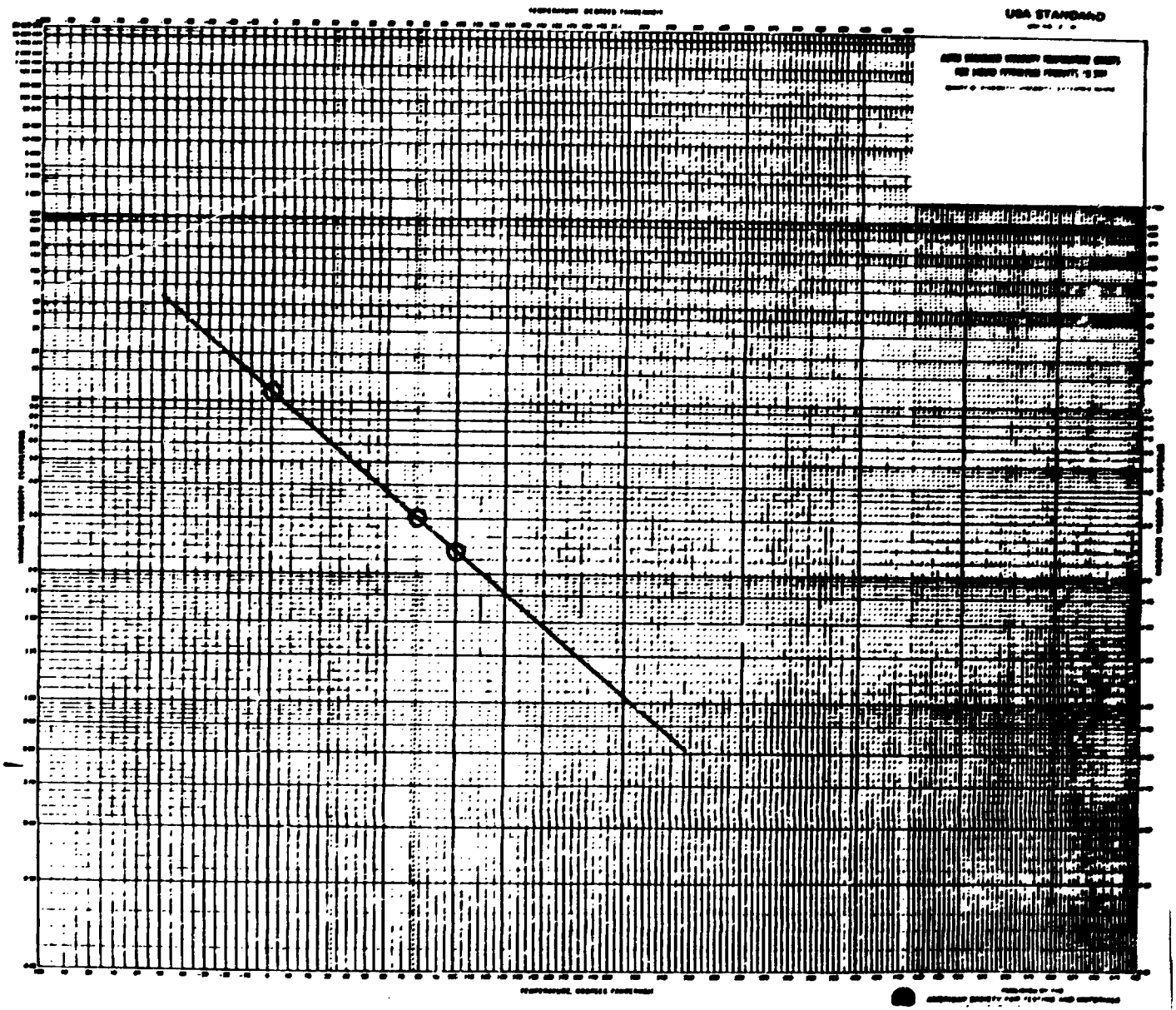

Figure 97. Viscosity/temperature plot for GE/TJ-78-DF2-13.0-02.

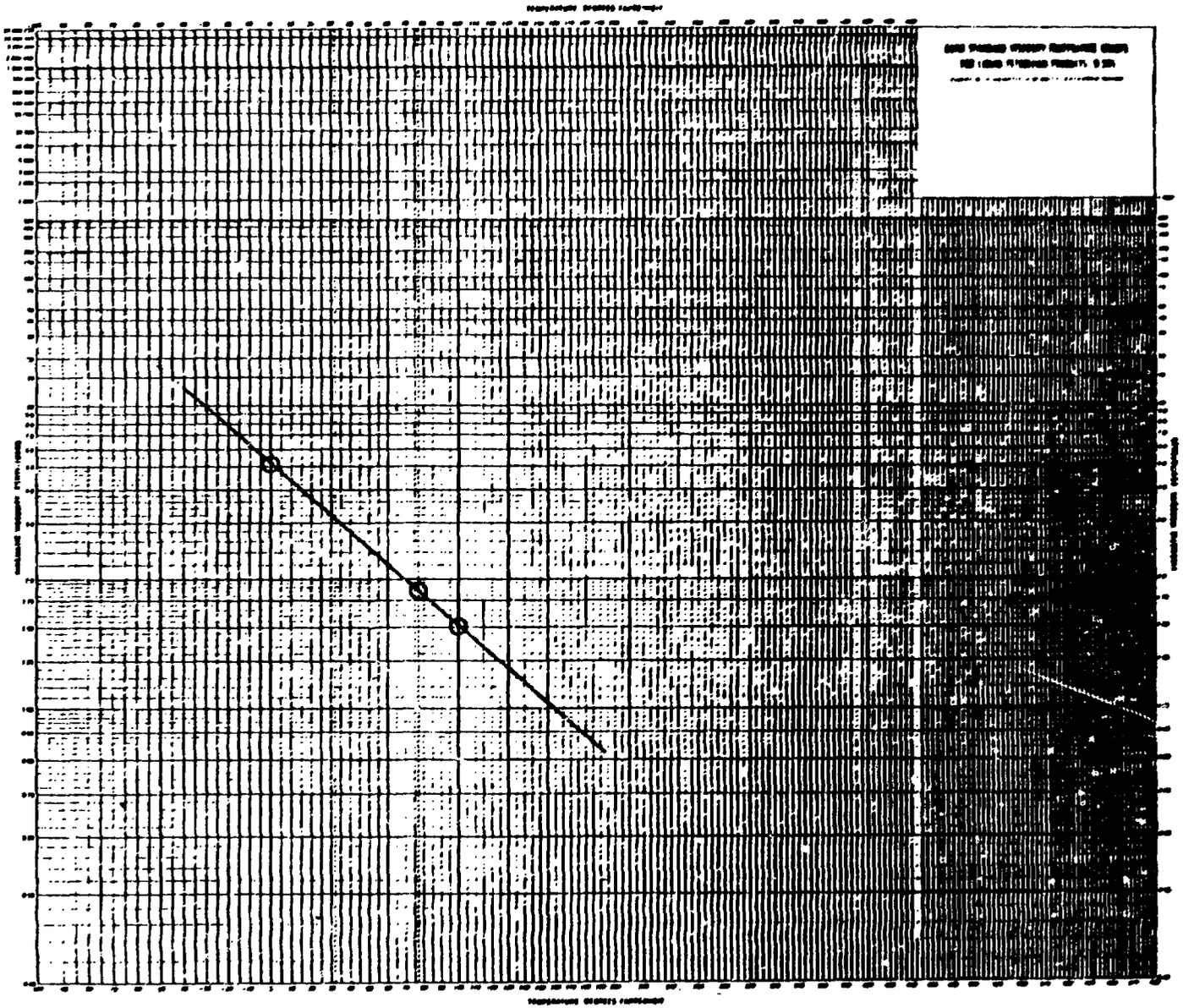

Figure 98. Viscosity/temperature plot for GE/TJ-78-8AR-13.0

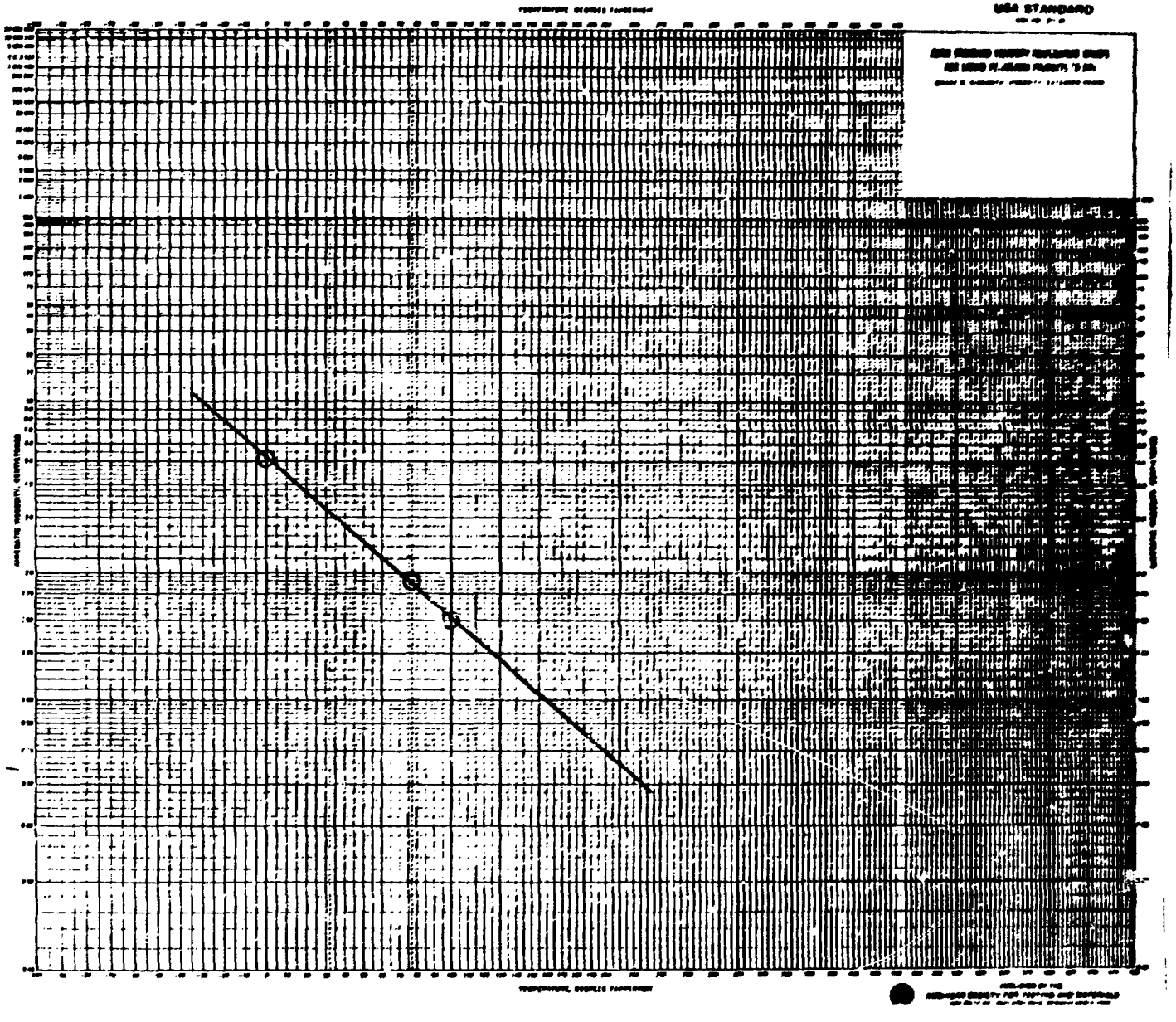

Figure 99. Viscosity/temperature plot for GE/TJ-78-8AR-13.0-02.

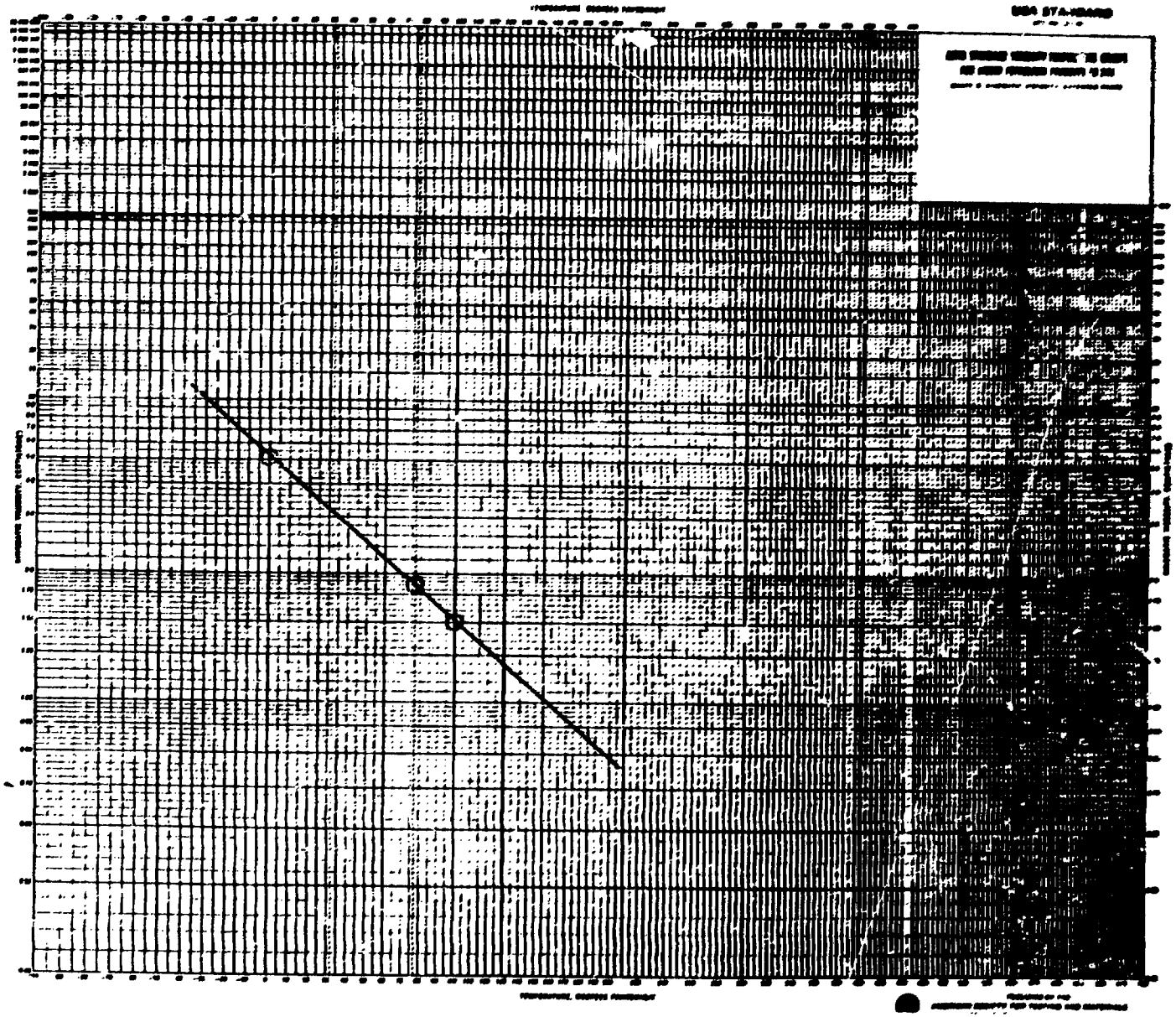

Figure 100. Viscosity/temperature plot for GE/TJ-78-8AR-13.0-03.

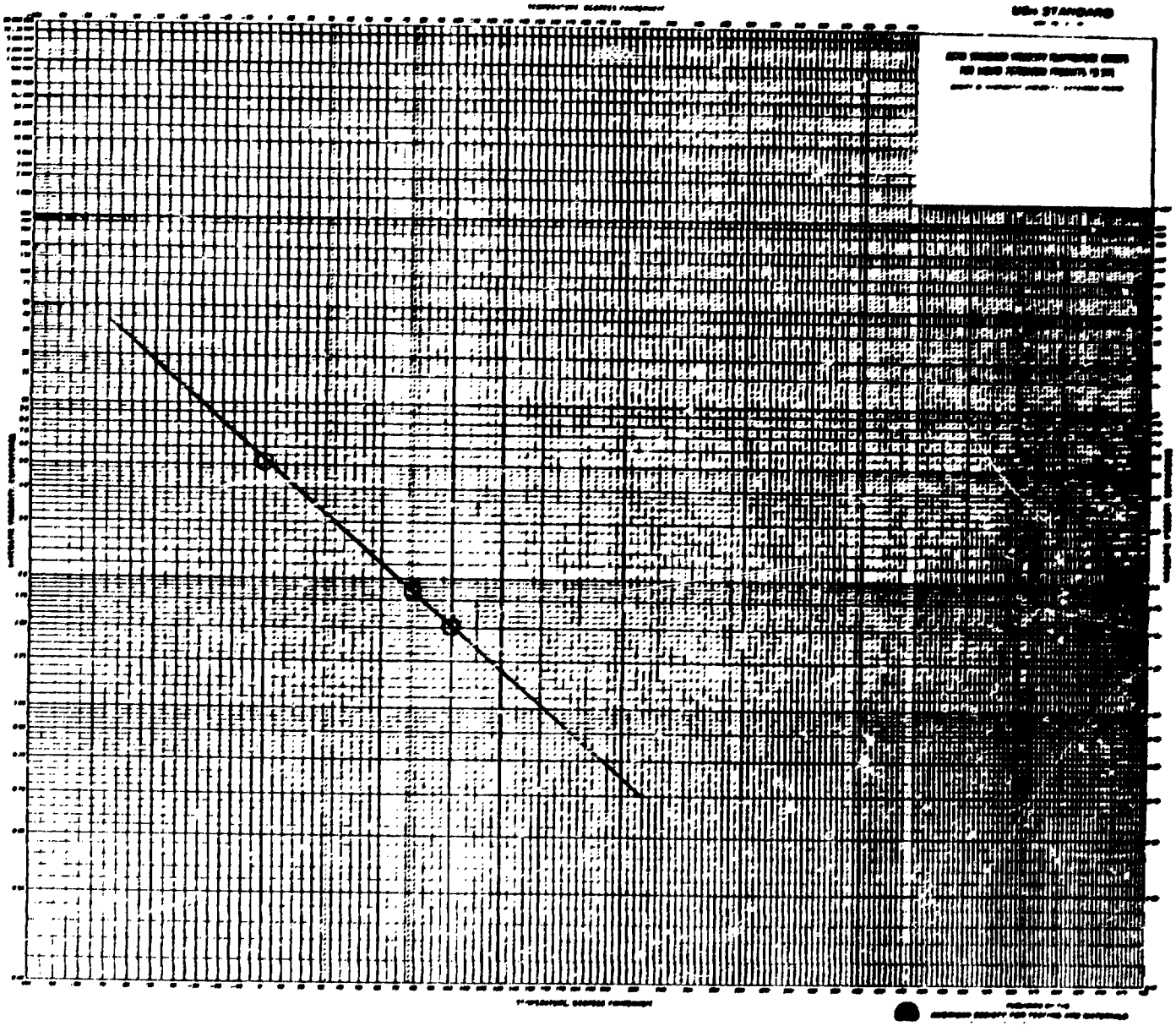

Figure 101. Viscosity/temperature plot for GE/TJ-78-8AR-13.0-05.

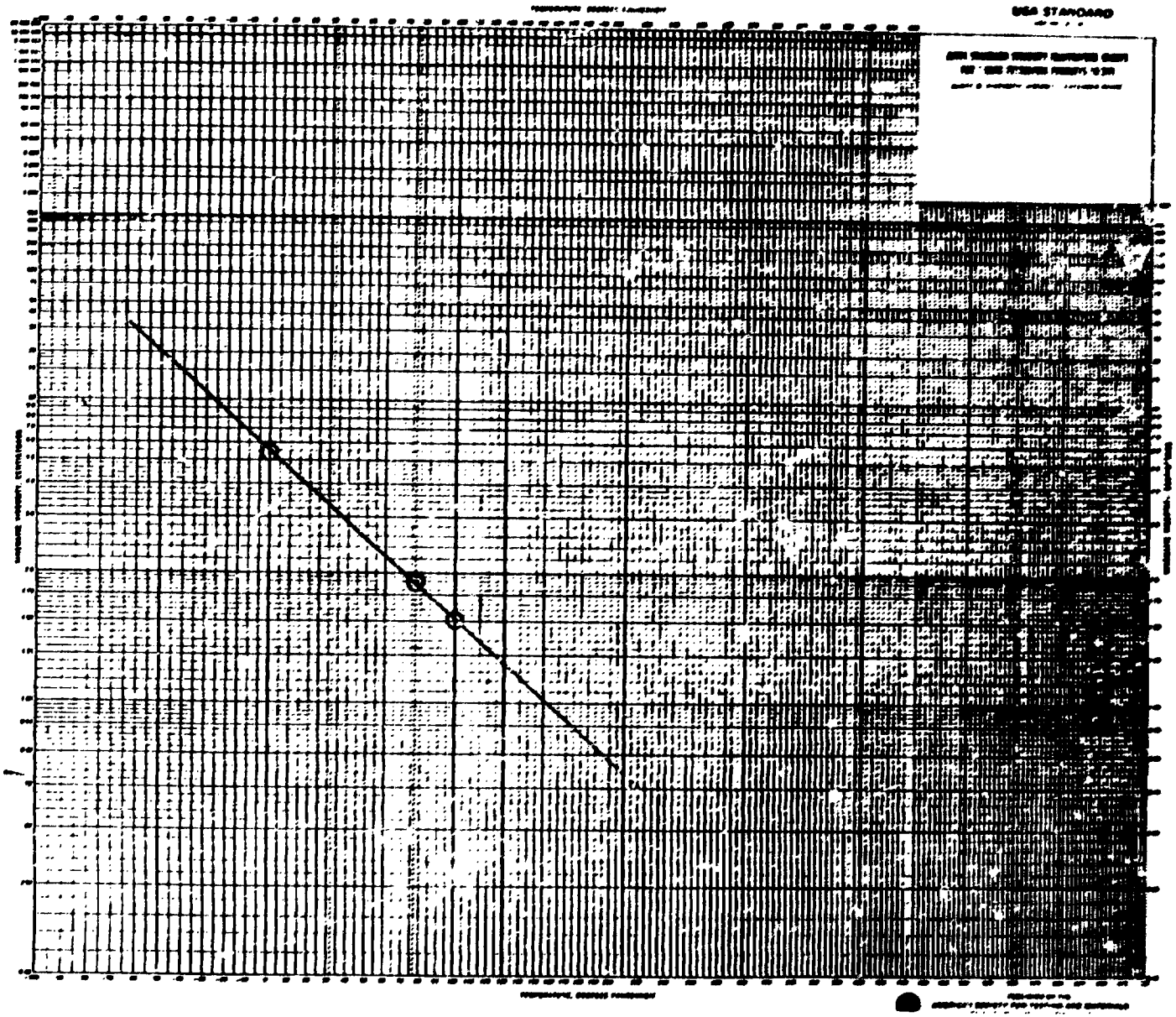

Figure 102. Viscosity/temperature plot for GE/TJ-78-8AR-12.0-08.

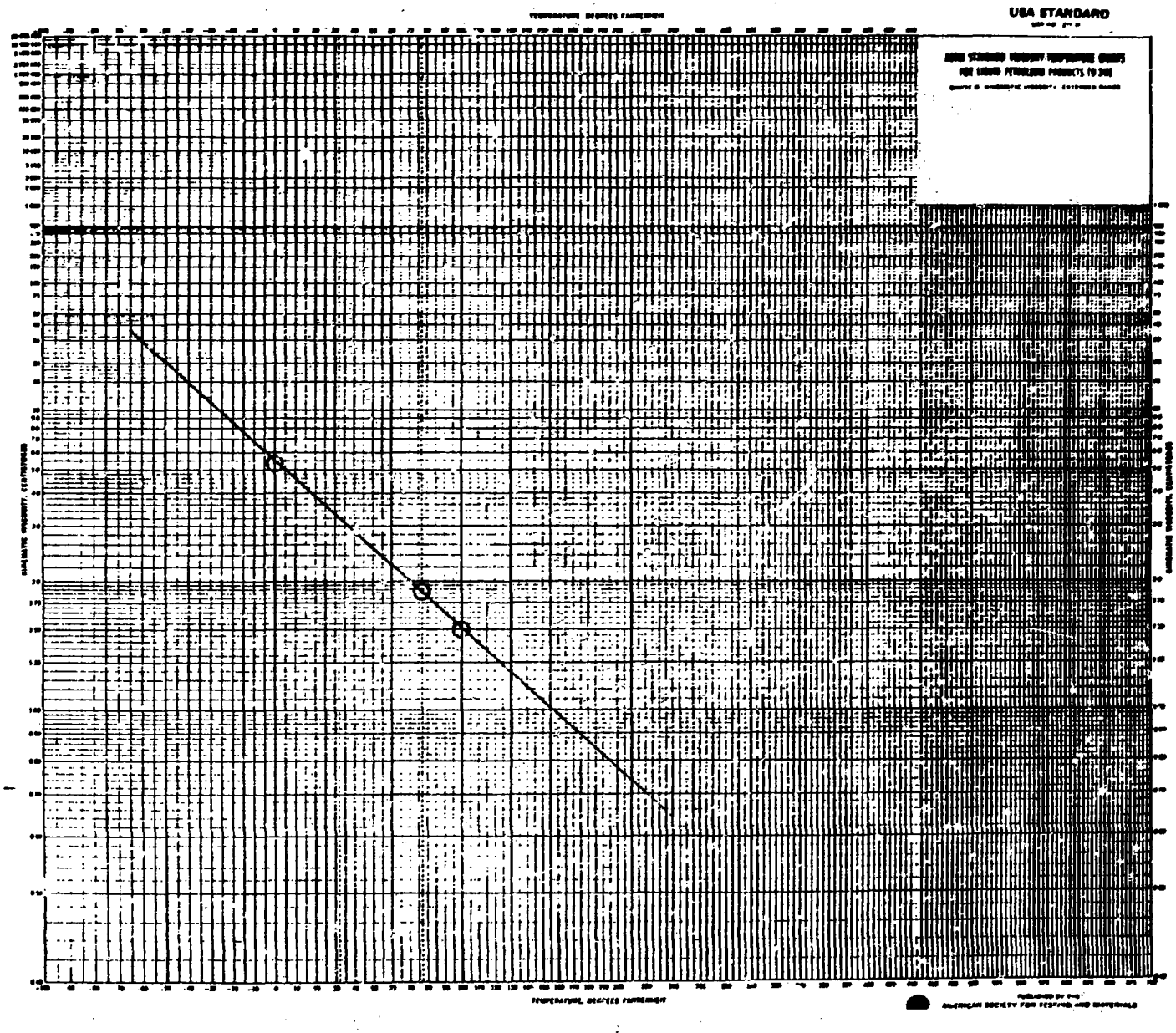

Figure 103. Viscosity/temperature plot for GE/TJ-78-8AR-12.0-09.

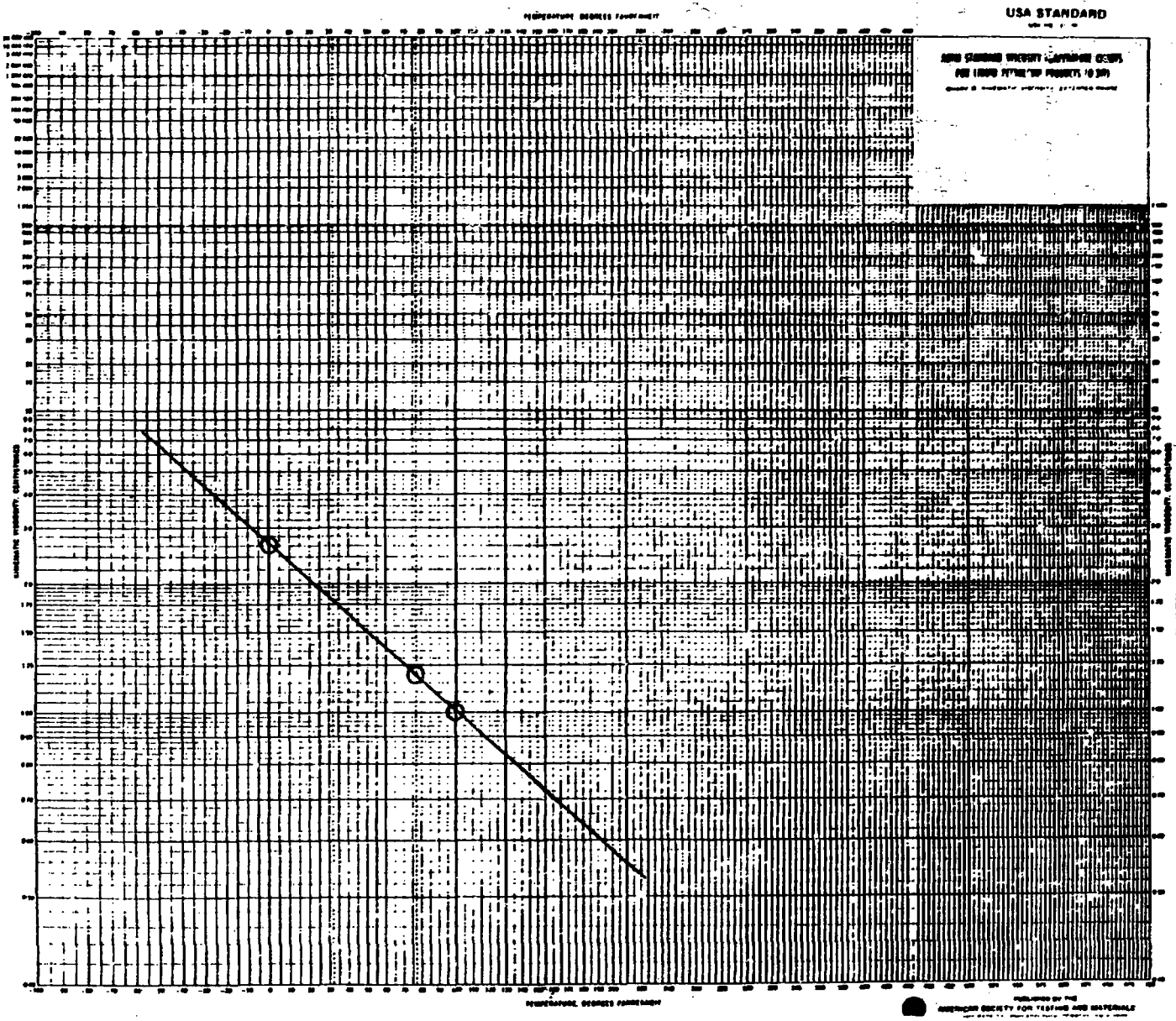

Figure 104. Viscosity/temperature plot for GE/TJ-78-8XY-12.0-05.

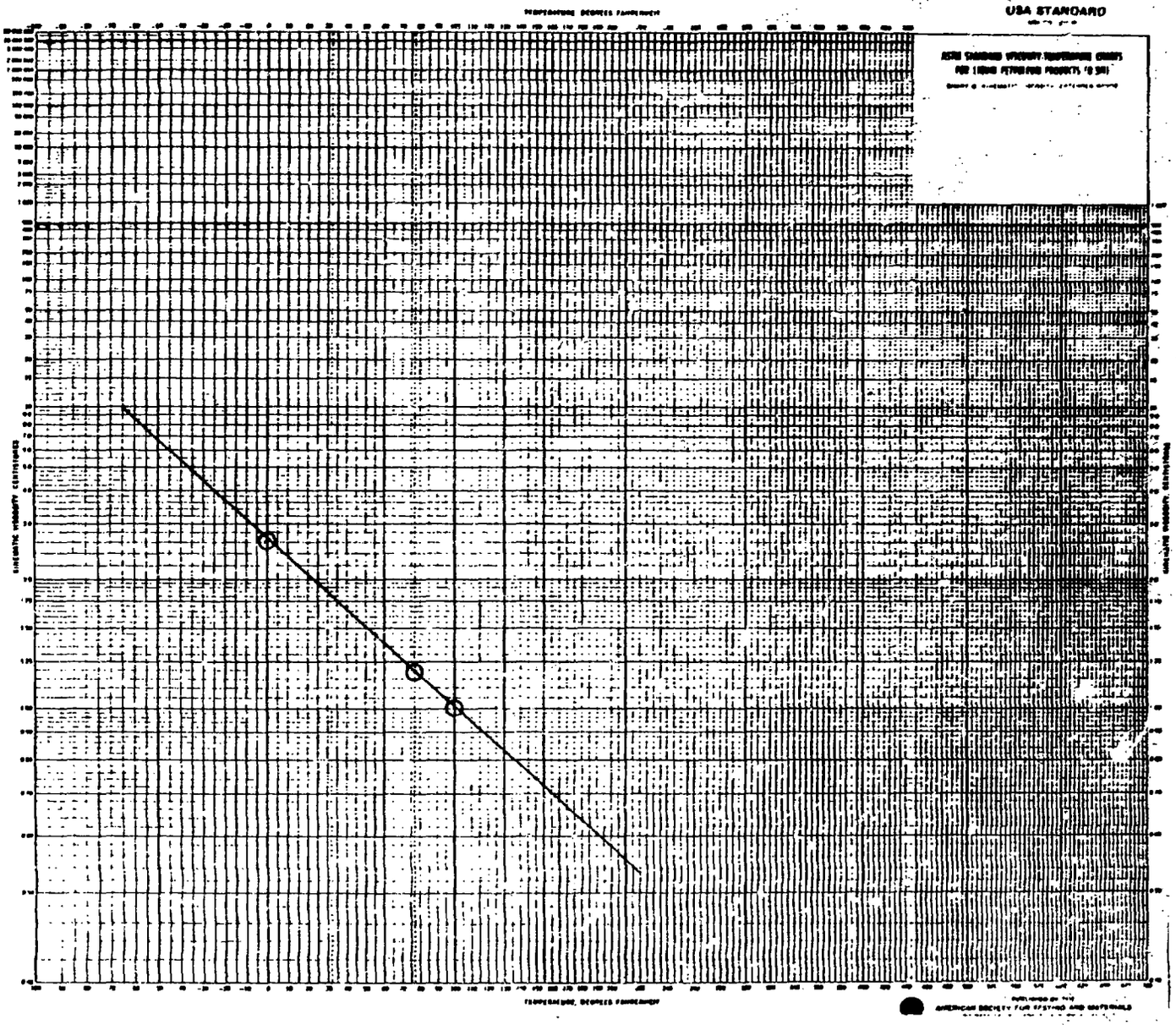

Figure 105. Viscosity/temperature plot for GE/TJ-78-8XY-12.0-08.

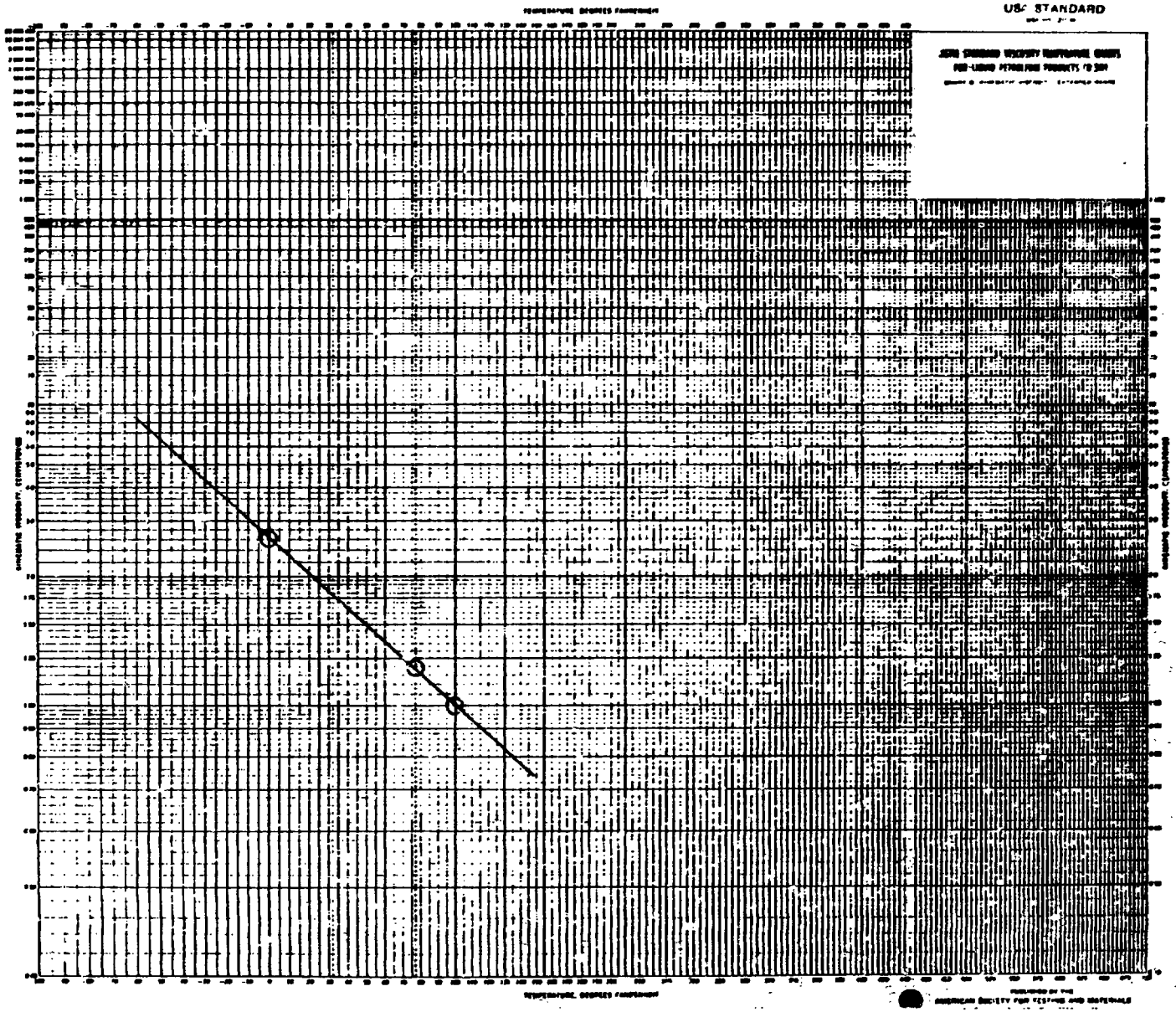

Figure 106. Viscosity/temperature plot for GE/TJ-78-8XY-12.0-09.

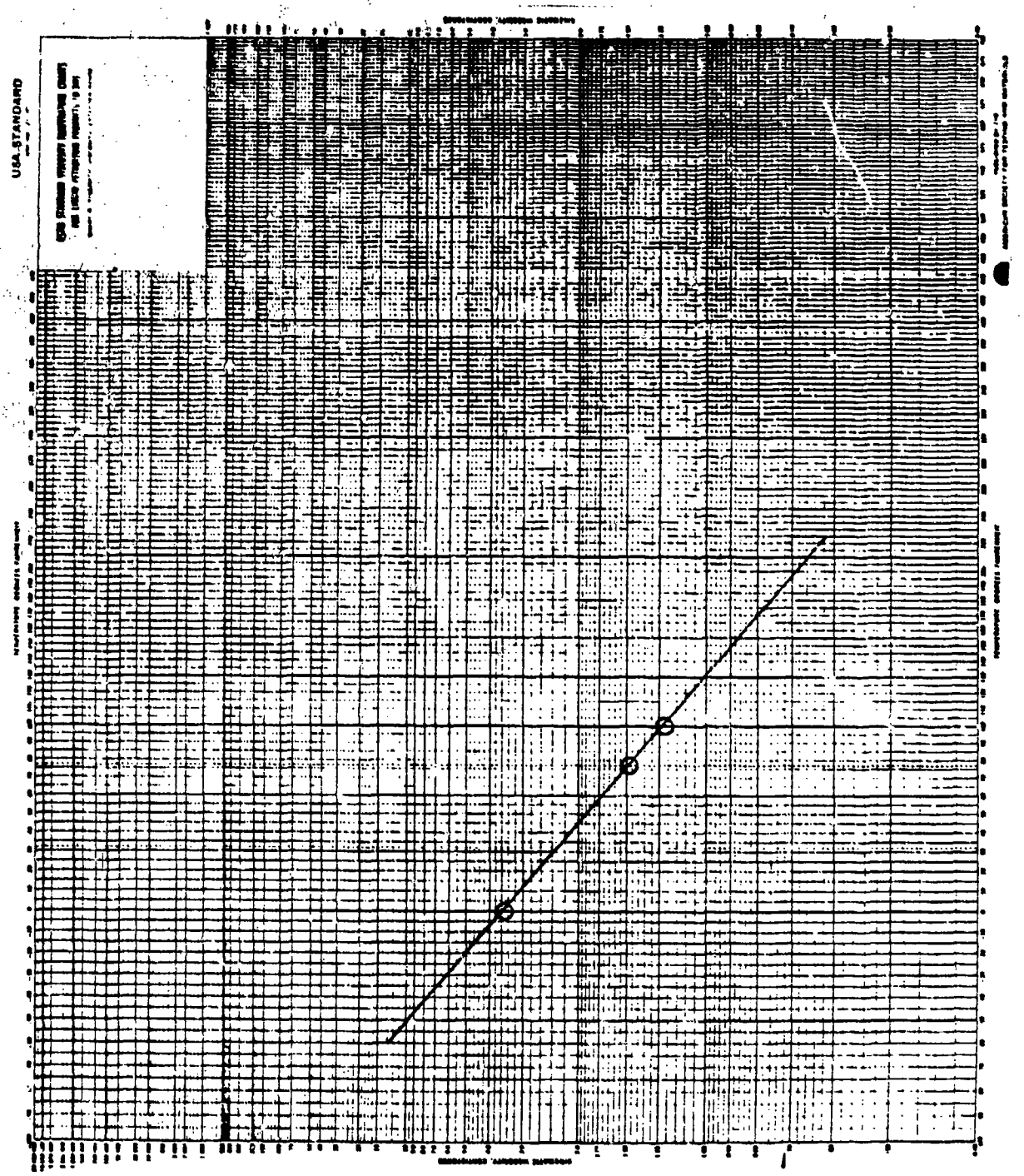

Figure 107. Viscosity/temperature plot for GE/TJ-78-8XY-13.0-08.

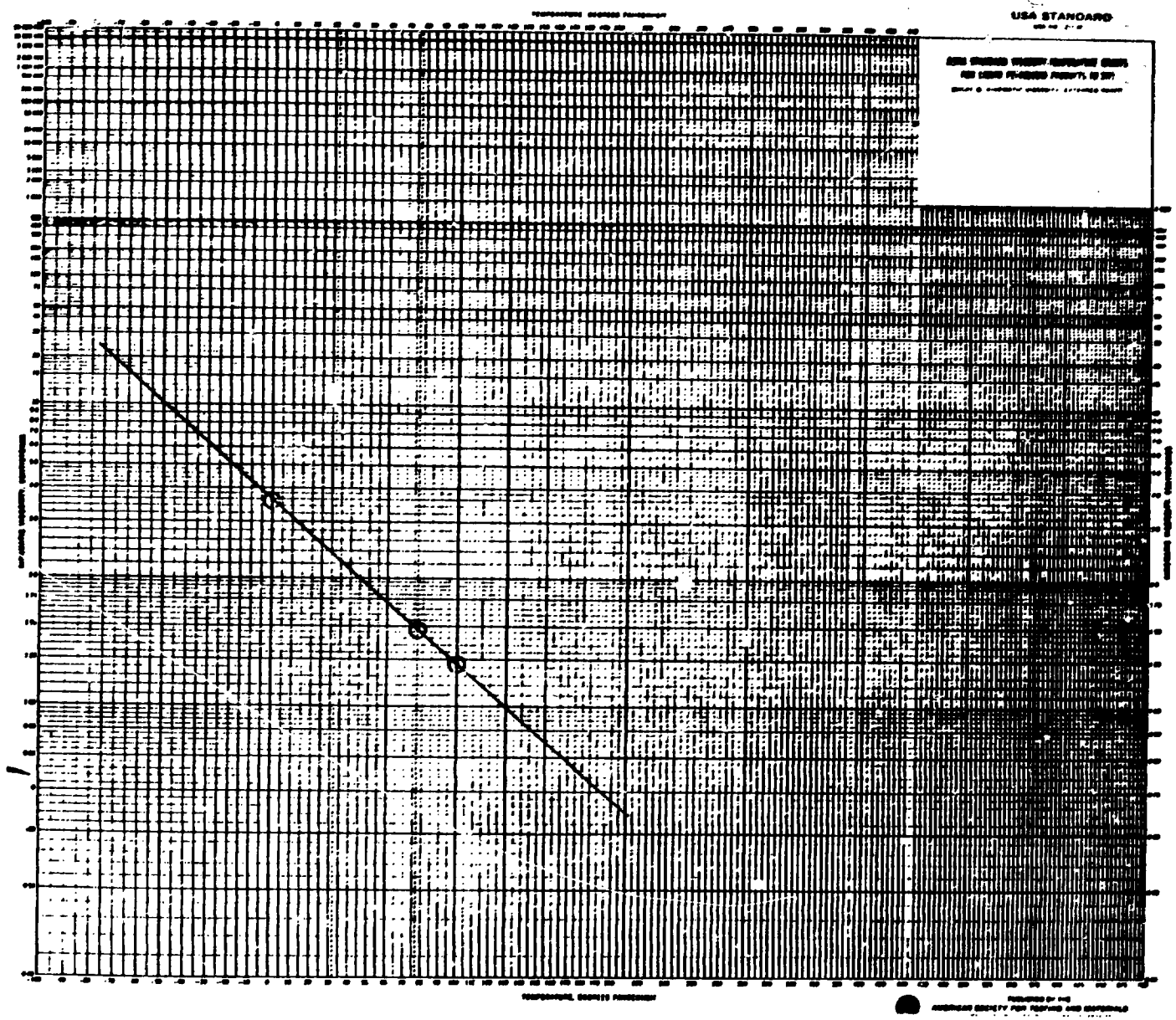

Figure 108. Viscosity/temperature plot for GE/TJ-78-8XY-13.0-09.

TABLE 140. SURFACE TENSION OF MODIFIED FUELS AS A FUNCTION OF TEMPERATURE

Sample Number	Surface Tension, dynes/cm 32°F	70°F	100°F
GE/TJ-78-4AR-12.0	27.18	25.63	24.42
GE/TJ-78-4AR-12.0-02	27.74	25.83	24.50
GE/TJ-78-4AR-12.0-03	27.56	25.82	24.51
GE/TJ-78-4AR-12.0-05	27.19	25.54	24.41
GE/TJ-78-4AR-13.0	25.62	24.14	23.00
GE/TJ-78-4AR-13.0-02	26.46	24.80	23.45
GE/TJ-78-4AR-13.0-03	26.13	24.58	23.47
GE/TJ-78-4AR-13.0-05	25.91	24.64	23.34
GE/TJ-78-4XY-12.0 (5/23/78)	26.48	25.54	24.31
GE/TJ-78-4XY-12.0 (5/30/78)	27.23	25.60	24.30
GE/TJ-78-4XY-12.0 (Batch 2)	27.34	25.67	24.33
GE/TJ-78-4XY-12.0-02	27.78	25.87	24.36
GE/TJ-78-4XY-13.0 (5/23/78)	25.83	24.36	23.37
GE/TJ-78-4XY-13.0 (5/30/78)	25.67	24.50	23.57
GE/TJ-78-4XY-13.0 (Batch 2)	25.65	24.52	23.61
GE/TJ-78-4XY-13.0-02	25.97	24.48	23.20
GE/TJ-78-4XG-14.0 (5/23/78)	25.45	23.87	22.63
GE/TJ-78-4XG-14.0 (5/30/78	25.38	23.87	22.66
GE/TJ-78-4XG-14.0-02	25.70	24.12	22.97
DF-2 (5/25/78)	29.07	27.73	26.67
GE/TJ-78-DF2-13.0-02	28.53	27.33	26.44
GE/TJ-78-8AR-13.0	28.08	26.77	25.74
GE/TJ-78-8AR-13.0-02	29.78	27.69	26.19
GE/TJ-78-8AR-13.0-03	30.11	27.82	26.36
GE/TJ-78-8AR-13.0-05	29.63	27.53	26.02
GE/TJ-78-8AR-12.0-08	30.42	28.66	27.23
GE/TJ-78-8AR-12.0-09	30.48	28.19	26.36
GE/TJ-78-8XY-12.0-05	29.72	27.47	25.63
GE/TJ-78-8XY-12.0-08	29.40	27.40	25.80
GE/TJ-78-8XY-12.0-09	29.86	27.75	26.05
GE/TJ-78-8XY-13.0-08	29.01	27.17	25.86
GE/TJ-78-8XY-13.0-09	29.02	26.87	25.49

TABLE 141. VAPOR PRESSURE OF MODIFIED FUELS AS A FUNCTION OF TEMPERATURE

Sample Number	Vapor Pressure, mm Hg 32°F	70°F	100°F
GE/TJ-78-4AR-12.0	18.5	45.0	83.0
GE/TJ-78-4AR-12.0-02	22.5	51.5	93.0
GE/TJ-78-4AR-12.0-03	27.5	60.5	104.0
GE/TJ-78-4AR-12.0-05	23.5	53.5	95.5
GE/TJ-78-4AR-13.0	22.0	53.0	96.0
GE/TJ-78-4AR-13.0-02	28.0	63.0	110.0
GE/TJ-78-4AR-13.0-03	22.5	51.5	94.5
GE/TJ-78-4AR-13.0-05	26.5	60.0	106.0
GE/TJ-78-4XY-12.0 (5/23/78)	19.0	42.0	73.5
GE/TJ-78-4XY-12.0 (5/30/78)	16.5	39.0	72.0
GE/TJ-78-4XY-12.0 (Batch 2)	16.0	37.5	69.0
GE/TJ-78-4XY-12.0-02	19.0	43.0	75.5
GE/TJ-78-4XY-13.0 (5/23/78)	23.5	53.0	93.0
GE/TJ-78-4XY-13.0 (5/30/78)	27.0	59.5	103.0
GE/TJ-78-4XY-13.0 (Batch 2)	25.5	55.5	99.0
GE/TJ-78-4XY-13.0-02	25.5	56.5	99.0
GE/TJ-78-4XG-14.0 (5/23/78)	22.5	50.5	89.5
GE/TJ-78-4XG-14.0 (5/30/78)	28.5	63.0	112.0
GE/TJ-78-4XG-14.0-02	25.5	56.5	98.0
DF-2 (5/25/78)	6.5	10.5	15.0
GE/TJ-78-DF2-13.0-02	5.0	9.0	14.0
GE/TJ-78-8AR-13.0	5.0	9.0	13.5
GE/TJ-78-8AR-13.0-02	5.0	9.0	13.5
GE/TJ-78-8AR-13.0-03	5.5	10.0	15.0
GE/TJ-78-8AR-13.0-05	6.0	11.5	17.0
GE/TJ-78-8AR-12.0-08	9.0	14.0	19.5
GE/TJ-78-8AR-12.0-09	6.0	10.0	14.0
GE/TJ-78-8XY-12.0-05	3.5	8.0	15.5
GE/TJ-78-8XY-12.0-08	3.5	9.0	17.0
GE/TJ-78-8XY-12.0-09	4.0	9.5	18.0
GE/TJ-78-8XY-13.0-08	6.0	12.5	21.0
GE/TJ-78-8XY-13.0-09	6.0	12.5	21.0
GE/TJ-78-8AR-12.0-01	4.2	7.5	11.5
GE/TJ-78-8XY-12.0-01	3.6	8.2	14.5
GE/TJ-78-8XY-13.0-0	4.0	9.1	16.3

TABLE 142. HEAT OF COMBUSTION OF MODIFIED FUELS

Sample Number	Gross, Btu/lb Duplicates		Gross, Btu/lb Avg	Net, Btu/lb Avg
GE/TJ-78-4AR-12.0	19,243	19,217	19,230	18,144
GE/TJ-78-4AR-12.0-02	19,204	19,194	19,199	18,111
GE/TJ-78-4AR-12.0-03	19,127	19,148	19,138	18,054
GE/TJ-78-4AR-12.0-05	19,141	19,140	19,141	18,042
GE/TJ-78-4AR-13.0	19,490	19,531	19,511	18,327
GE/TJ-78-4AR-13.0-02	19,486	19,477	19,482	18,291
GE/TJ-78-4AR-13.0-03	19,490	19,483	19,487	18,313
GE/TJ-78-4AR-13.0-05	19,437	19,467	19,452	18,213
GE/TJ-78-4XY-12.0 (5/23/78)	19,207	19,256	19,232	18,141
GE/TJ-78-4XY-12.0 (5/30/78)	19,263	19,268	19,266	18,178
GE/TJ-78-4XY-12.0 (Batch 2)	19,364	19,340	19,352	18,256
GE/TJ-78-4XY-12.0-02	19,223	19,192	19,208	18,117
GE/TJ-78-4XY-13.0 (5/23/78	19,530	19,532	19,531	18,350
GE/TJ-78-4XY-13.0 (5/30/78)	19,533	19,563	19,548	18,369
GE/TJ-78-4XY-13.0 (Batch 2)	19,459	19,408	19,434	18,253
GE/TJ-78-4XY-13.0-02	19,552	19,515	19,534	18,350
GE/TJ-78-4XG-14.0 (5/23/78)	19,936	19,966	19,951	18,674
GE/TJ-78-4XG-14.0 (5/30/78)	19,843	19,787	19,815	18,538
GE/TJ-78-4XG-14.0-02	19,865	19,828	19,847	18,573
DF-2 (5/25/78)	19,567	19,543	19,555	18,354
GE/TJ-73-DF2-13.0-02	19,613	19,596	19,605	18,393
GE/TJ-78-8AR-13.0	19,453	19,507	19,480	18,296
GE/TJ-78-8AR-13.0-02	19,501	19,462	19,482	18,305
GE/TJ-78-8AR-13.0-03	19,488	19,482	19,485	18,305
GE/TJ-78-8AR-13.0-05	19,455	19,492	19,474	18,291
GE/TJ-78-8AR-12.0-08	19,161	19,150	19,156	18,063
GE/TJ-78-8AR-12.0-09	19,144	19,162	19,153	18,059
GE/TJ-78-8XY-12.0-05	19,216	19,200	19,208	18,111
GE/TJ-78-8XY-12.0-08	19,204	19,205	19,205	18,112
GE/TJ-78-8XY-12.0-09	19,171	19,200	19,186	18,085
GE/TJ-78-8XY-13.0-08	19,458	19,512	19,485	18,301
GE/TJ-78-8XY-13.0-09	19,518	19,500	19,509	18,327

TABLE 143. GAS CHROMATOGRAPHIC SIMULATED DISTILLATION OF MODIFIED FUELS

Percent Recovered	GE/TJ-78-4AR-12.0		GE/TJ-78-4AR-12.0-02		GE/TJ-78-4AR-12.0-03		GE/TJ-78-4AR-12.0-05		GE/TJ-78-4AR-13.0	
	°C	°F	°C	°F	°C	°F	°C	°F	°C	°F
0.5, IBP	24	75	18	64	18	64	19	66	20	68
1	33	91	24	75	23	73	28	82	30	86
5	80	176	65	149	63	145	70	158	68	154
10	95	203	85	184	85	185	88	190	87	187
20	119	246	112	234	112	234	113	235	114	237
30	149	300	137	279	138	280	140	284	133	271
40	179	354	166	331	167	333	170	338	161	322
50	198	388	188	370	190	374	192	378	193	361
60	214	417	207	405	207	405	208	406	203	397
70	230	446	225	437	226	439	226	439	219	426
80	242	468	239	462	240	464	238	460	233	451
90	257	495	257	495	260	500	255	491	253	487
95	272	522	272	522	274	525	272	522	268	514
99	296	565	297	567	298	568	299	570	297	567
99.5, FBP	301	574	305	581	307	585	309	588	305	581

(continued)

TABLE 143 (continued)

Percent Recovered	GE/TJ-78-4AR-13.0-02 °C	GE/TJ-78-4AR-13.0-02 °F	GE/TJ-78-4AR-13.0-03 °C	GE/TJ-78-4AR-13.0-03 °F	GE/TJ-78-4AR-13.0-05 °C	GE/TJ-78-4AR-13.0-05 °F	GE/TJ-78-4XY-12.0 (5/23/78) °C	GE/TJ-78-4XY-12.0 (5/23/78) °F	GE/TJ-78-4XY-12.0 (5/30/78) °C	GE/TJ-78-4XY-12.0 (5/30/78) °F	GE/TJ-78-4XY-12.0 (Batch 2) °C	GE/TJ-78-4XY-12.0 (Batch 2) °F	GE/TJ-78-4XY-12.0-02 °C	GE/TJ-78-4XY-12.0-02 °F	GE/TJ-78-4XY-13.0 (5/23/78) °C	GE/TJ-78-4XY-13.0 (5/23/78) °F	GE/TJ-78-4XY-13.0 (5/30/78) °C	GE/TJ-78-4XY-13.0 (5/30/78) °F	GE/TJ-78-4XY-13.0 (Batch 2) °C	GE/TJ-78-4XY-13.0 (Batch 2) °F
0.5, IBP	16	61	16	61	17	63	16	61	18	64	19	66	18	64	18	64	16	61	12	54
1	19	66	23	73	23	73	24	75	25	77	27	81	26	79	22	72	19	66	19	66
5	62	143	61	142	63	145	63	145	66	151	62	144	67	153	62	144	59	138	59	138
10	84	183	82	180	84	183	84	183	85	185	83	181	86	187	84	183	81	178	80	176
20	109	228	107	225	109	229	111	232	111	232	111	232	113	235	110	230	106	223	104	219
30	129	264	128	262	130	266	133	271	133	271	133	271	135	275	130	266	127	261	126	259
40	155	311	153	307	158	316	144	291	142	288	142	288	146	295	144	291	140	284	141	286
50	179	354	176	349	181	358	158	316	157	315	157	315	159	318	160	320	158	316	158	316
60	199	390	196	385	201	394	168	334	167	333	165	329	169	337	174	345	171	340	172	342
70	216	421	214	417	218	424	186	367	181	358	179	354	186	367	194	381	191	376	192	378
80	232	450	232	450	233	451	209	408	206	403	202	396	211	412	216	421	213	415	214	417
90	252	486	252	486	252	486	232	450	231	448	229	444	234	453	238	460	235	455	236	457
95	267	513	266	511	268	514	248	478	246	475	246	475	251	484	252	486	250	482	250	482
99	291	556	286	547	300	572	271	520	269	516	272	522	278	532	274	525	277	531	275	527
99.5, FBP	301	574	295	563	314	597	284	543	281	538	286	547	297	567	283	541	290	554	287	549

(continued)

TABLE 143 (continued)

Percent Recovered	GE/TJ-78-4XY-13.0-02		GE/TJ-78-4XG-14.0-(5/23/78)		GE/TJ-78-4XG-14.0-(5/30/78)		GE/TJ-78-4XG-14.0-02		DF-2 (5/25/78)		GE/TJ-78-DF2-13.0-02		GE/TJ-78-8AR-13.0		GE/TJ-78-8AR-13.0-02		GE/TJ-78-8AR-13.0-03	
	°C	°F	°C	°F	°C	°F	°C	°F	°C	°F	°C	°F	°C	°F	°C	°F	°C	°F
0.5, IBP	18	64	16	61	12	54	18	64	98	208	106	223	118	244	116	241	97	207
1	19	66	20	68	19	66	22	72	120	248	126	259	130	266	127	261	119	246
5	61	142	59	138	59	138	62	144	168	334	165	329	157	315	159	318	157	315
10	83	181	82	180	81	178	84	183	187	369	181	358	169	336	171	340	170	338
20	109	228	109	228	108	226	111	232	209	408	202	396	185	365	186	367	186	367
30	130	266	132	270	131	268	135	275	227	441	218	424	197	387	200	392	200	392
40	144	291	153	307	152	306	151	304	243	469	233	451	208	406	212	414	211	412
50	159	318	173	343	174	345	171	340	258	496	249	480	220	428	224	435	224	435
60	174	345	197	387	198	388	194	381	273	523	264	507	231	448	235	455	235	455
70	194	380	221	430	222	432	219	426	290	554	281	538	242	468	249	480	248	478
80	216	421	246	475	248	478	244	471	307	585	301	574	253	487	262	504	261	502
90	238	460	290	554	292	558	287	549	328	622	323	613	266	511	278	532	278	532
95	251	484	309	588	310	590	309	588	350	662	345	653	283	541	291	556	290	554
99	271	520	332	630	338	640	332	630	385	725	384	723	306	583	308	586	308	586
99.5, FBP	283	541	344	651	350	662	341	646	406	762	396	745	319	606	318	604	318	604

(continued)

TABLE 143 (continued)

Percent Recovered	GE/TJ-78-8AR-13.0-05		GE/TJ-78-8AR-12.0-08		GE/TJ-78-8AR-12.0-09		GE/TJ-78-8XY-12.0-05		GE/TJ-78-8XY-12.0-08		GE/TJ-78-8XY-12.0-09		GE/TJ-78-8XY-13.0-08		GE/TJ-78-8XY-13.0-09	
	°C	°F	°C	°F	°C	°F	°C	°F	°C	°F	°C	°F	°C	°F	°C	°F
0.5, IBP	110	230	108	226	121	250	109	228	121	250	120	248	107	225	120	248
1	124	255	125	257	135	275	127	261	132	270	131	268	121	250	129	264
5	157	315	162	324	163	325	142	288	142	288	143	289	143	289	143	289
10	170	338	172	342	173	343	148	298	147	297	148	298	151	304	152	306
20	186	367	189	372	190	374	164	327	163	325	161	322	168	334	168	334
30	200	392	203	397	203	397	173	343	172	342	172	342	182	360	181	358
40	211	412	215	419	215	419	186	367	186	367	186	367	197	387	196	385
50	224	435	227	441	227	441	202	396	202	396	201	394	212	414	210	410
60	236	457	237	459	238	460	218	424	219	426	218	424	226	439	224	435
70	249	480	251	484	251	484	233	451	234	453	233	451	240	464	238	460
80	261	502	264	507	263	505	250	482	250	482	250	482	257	495	255	491
90	278	532	280	536	280	536	270	518	271	520	270	518	275	527	274	525
95	291	556	292	558	292	558	285	545	286	547	285	545	290	554	288	550
99	307	585	308	586	308	586	303	581	306	583	306	583	307	585	306	583
99.5, FBP	312	594	316	601	314	597	312	594	314	597	314	597	312	594	310	590

TABLE 144. HYDROCARBON-TYPE DISTRIBUTION OF MODIFIED FUELS

Compound Type	Volume Percent							
	GE/TJ-78-4AR-12.0	GE/TJ-78-4AR-12.0-02	GE/TJ-78-4AR-12.0-03	GE/TJ-78-4AR-12.0-05	GE/TJ-78-4AR-13.0	GE/TJ-78-4AR-13.0-02	GE/TJ-78-4AR-13.0-03	GE/TJ-78-4AR-13.0-05
Paraffins	38.4	37.6	37.6	38.0	47.2	46.2	45.9	46.0
Monocycloparaffins	20.4	21.2	20.7	21.1	25.4	25.4	25.3	25.4
Dicycloparaffins	-	-	-	-	-	-	-	-
Alkylbenzenes	12.4	12.7	12.7	12.6	10.7	11.0	11.2	11.0
Indans and tetralins	4.4	4.5	4.5	4.4	3.0	3.1	3.2	3.2
Naphthalenes	24.4	24.0	24.5	23.9	13.7	14.3	14.4	14.4

	GE/TJ-78-4XY-12.0 (5/23/78)	GE/TJ-78-4XY-12.0 (5/30/78)	GE/TJ-78-4XY-12.0 (Batch 2)	GE/TJ-78-4XY-12.0-02	GE/TJ-78-4XY-13.0 (5/23/78)	GE/TJ-78-4XY-13.0 (5/30/78)	GE/TJ-78-4XY-13.0 (Batch 2)	GE/TJ-78-4XY-13.0-02
Paraffins	33.3	33.0	33.0	33.1	45.8	45.8	45.2	46.0
Monocycloparaffins	11.0	11.2	11.3	11.7	15.1	15.1	15.1	15.9
Dicycloparaffins	2.4	2.4	2.5	2.7	3.4	3.4	3.3	3.7
Alkylbenzene	53.0	53.1	52.9	51.9	34.7	34.7	35.5	33.4
Indans and tetralins	<0.1	Trace	Trace	0.2	0.6	0.6	0.5	0.6
Naphthalenes	0.3	0.3	0.3	0.4	0.4	0.4	0.4	0.4

TABLE 144 (continued)

	Volume Percent							
	GE/TJ-78-4XG-14.0 (5/23/78)	GE/TJ-78-4XG-14.0 (5/30/78)	GE/TJ-78-4XG-14.0-02	DF-2 (5/25/78)	GE/TJ-78-DF2-13.0-02	GE/TJ-78-8AR-13.0	GE/TJ-78-8AR-13.0-02	GE/TJ-78-8AR-13.0-03
Paraffins	58.4	58.4	57.7	44.9	44.9	39.1	38.3	38.2
Monocycloparaffins	20.1	20.1	20.9	32.7	32.7	34.1	33.9	34.0
Dicycloparaffins	5.0	5.0	5.3	2.5	2.5	1.5	1.7	1.6
Alkylbenzenes	14.8	14.8	14.1	8.6	8.6	9.5	9.6	9.6
Indans and tetralins	1.1	1.1	1.3	6.1	6.1	3.8	4.2	4.2
Naphthalenes	0.6	0.6	0.7	5.2	5.2	12.0	12.3	12.4

	GE/TJ-78-8AR-13.0-05	GE/TJ-78-8AR-12.0-08	GE/TJ-78-8AR-12.0-09	GE/TJ-78-8XY-12.0-05	GE/TJ-78-8XY-12.0-08	GE/TJ-78-8XY-12.0-09	GE/TJ-78-8XY-13.0-08	GE/TJ-78-8XY-13.0-09
Paraffins	38.3	31.2	31.2	26.4	26.4	26.4	36.2	36.3
Monocycloparaffins	33.9	27.9	27.6	22.3	22.3	22.1	31.8	31.5
Dicycloparaffins	1.7	1.3	1.5	1.6	1.5	1.6	1.8	1.9
Alkylbenzenes	9.5	11.5	11.5	48.8	48.9	49.0	27.9	28.1
Indans and tetralins	4.2	5.4	5.4	-	-	-	0.9	0.9
Naphthalenes	12.4	22.7	22.8	0.9	0.9	0.9	1.4	1.3

Density by the dilatometer method - Table 138,
Kinematic viscosity by ASTM D 445 - Table 139 and Figures 77-108,
Surface tension by the capillary rise method - Table 140,
Vapor pressure by the micro-method - Table 141,
Heat of combustion by ASTM D 240 - Table 142,
GC simulated distillation by ASTM D 2887 - Table 143, and
Hydrocarbon type analyses by ASTM D 2789 - Table 144.

9. CHEMICAL AND PHYSICAL PROPERTIES OF FUELS TESTED IN TF41 COMBUSTOR AND IN J79 LOW-SMOKE COMBUSTOR

Chemical and physical properties were determined for a large number of experimental fuels and blending components scheduled for testing combustors. The analytical data, which were required for correlation with the combustion performances of the fuels, are presented in Tables 145 through 152 and Figures 109 through 133 as follows:

Density by the dilatometer method - Table 145,
Kinematic viscosity by ASTM D 445 - Table 146 and Figures 109-133,
Surface tension by the capillary rise method - Table 147,
Vapor pressure by the micro-method - Table 148,
Specific gravity and API gravity from density - Table 149,
Heat of combustion by ASTM D 240 - Table 150,
GC simulated distillation by ASTM D 2887 - Table 151,
Hydrocarbon type analysis by ASTM D 2789-71 - Table 152.

Specific gravity and API gravity were calculated from density data determined by the dilatomer method. All other analytical methods are described in the Appendix.

The sample number coding system for the fuels presented in this subsection differs slightly from the code used for the samples shown in the previous subsection. The fuels with codes terminating in "(2006).78-C" were tested in the TF41 combustor. The

TABLE 145. DENSITY OF TESTED FUELS AS A FUNCTION OF TEMPERATURE

Sample Designation	Density, g/cc -20°F	32°F	70°F	100°F
JP-8 (2006), 78-C		0.8252	0.8099	0.7977
8A2 " "		0.8755	0.8600	0.8480
8A3 " "		0.8495	0.8343	0.8225
JP-4 (2006), 78-C		0.7739	0.8574	0.8445
4A2 " "		0.8483	0.8322	0.8193
4A3 " "		0.8183	0.8017	0.7887
8X2 " "		0.8515	0.8352	0.8222
8X3 " "		0.8389	0.8230	0.8106
8GM " "		0.8264	0.8113	0.7994
4X2 " "		0.8324	0.8153	0.8021
4X3 " "		0.8083	0.7913	0.7780
4XG " "		0.7928	0.7763	0.7636
GEC-120-8X0-792033	0.8702	0.8480	0.8314	0.8188
GEC-130-4X0-792033	0.8282	0.8049	0.7878	0.8848
GEC-130-DF2-792033	-	0.8589	0.8434	0.8319
GEC-145-400-792033	0.7957	0.7723	0.7557	0.7423
GEC-140-800-792033	0.8460	0.8252	0.8096	0.7977
GEC-130-8X0-792033	0.8598	0.8380	0.8219	0.8097
GEC-140-4GX-792033	0.8100	0.7876	0.7712	0.7580
GEC-120-8AO-792033	0.8967	0.8746	0.8589	0.8469
GEC-130-8AO-792033	0.8706	0.8488	0.8333	0.8213
GEC-120-4AO-792033	0.8709	0.8475	0.8309	0.8182
GEC-130-4AO-792033	0.8393	0.8156	0.7990	0.7858
GEC-120-X40-792033 Feb	0.8519	0.8281	0.8110	0.7980
GEC-140-8GO-792033 Feb	0.8466	0.8255	0.8104	0.7986

TABLE 146. KINEMATIC VISCOSITY OF TESTED FUELS AS A FUNCTION OF TEMPERATURE

Sample Designation	Centistokes -20°F	0°F	32°F	70°F	77°F	100°F
JP-8 (2006), 78-C		6.068			2.081	1.670
8A2 " "		5.816			1.964	1.576
8A3 " "		5.841			2.004	1.610
JP-4 (2006), 78-C		1.854			0.948	0.819
4A2 " "		2.582			1.143	0.966
4A3 " "		2.208			1.063	0.907
8X2 " "		2.786			1.244	1.047
8X3 " "		3.900			1.562	1.289
8GM " "		7.075			2.316	1.841
4X2 " "		1.705			0.884	0.764
4X3 " "		1.742			0.910	0.785
4XG " "		2.342			1.126	0.957
GEC-120-8X0-792033	3.418		1.844	1.240		0.988
GEC-130-4X0-792033	2.084		1.219	0.910		0.752
GEC-130-DF2-792033	-		5.774	3.267	3.004	2.306
GEC-145-400-792033	2.206		1.288	0.955	0.911	0.786
GEC-140-800-792033	9.101		3.526	2.233	2.075	1.665
GEC-130-8X0-792033	5.655		2.516	1.688	1.583	1.304
GEC-120-X40-792033				1.172		0.948
GEC-140-4GX-792033	2.753		1.521	1.113		0.903
GEC-140-8GO-792033				1.862		1.423
GEC-120-8AO-792033	9.053		3.391	2.134		1.591
GEC-130-8AO-792033	9.020		3.431	2.169		1.620
GEC-120-4AO-792033	3.304		1.688	1.206		0.963
GEC-130-4AO-792033	2.671		1.461	1.072		0.871
GEC-120-X40-792033 Feb	2.077		1.202	0.900		0.744
GEC-140-8GO-792033 Feb	10.70		3.938	2.451		1.807

TABLE 147. SURFACE TENSION OF TESTED FUELS AS A FUNCTION OF TEMPERATURE

Sample designation	Dynes per centimeter			
	-20°F[a]	32°F	70°F	100°F
JP-8 (2006), 78-C		27.56	23.81	24.44
8A2 " "		29.33	27.47	25.99
8A3 " "		28.59	26.83	25.43
JP-4 (2006), 78-C		24.67	22.65	21.05
4A2 " "		26.50	24.78	23.45
4A3 " "		25.85	23.94	22.50
8X2 " "		30.00	27.95	26.33
8X3 " "		29.59	27.45	25.79
8GM " "		29.10	27.13	25.58
4X2 " "		27.90	25.95	24.43
4X3 " "		26.62	24.49	22.84
4XG " "		26.10	24.18	22.72
GEC-120-8X0-792033	32.80[a]	29.85	27.82	26.20
GEC-130-4X0-792033	28.60	26.35	24.73	23.43
GEC-130-DF2-792033	32.10	30.07	28.60	26.68
GEC-145-400-792033	27.52	25.05	23.28	21.73
GEC-140-800-792033	31.17	28.78	27.08	25.69
GEC-130-8X0-792033	31.80	29.47	27.80	26.46
GEC-140-4GX-792033	28.21	25.90	24.20	22.86
GEC-120-8AO-792033	33.00	29.98	27.77	26.05
GEC-130-8AO-792033	31.83	29.03	27.00	25.30
GEC-120-4AO-792033	29.24	26.55	24.59	23.03
GEC-130-4AO-792033	28.08	25.50	23.62	22.10
GEC-120-X40-792033 Feb	29.28	26.70	24.81	23.30
GEC-140-8GO-792033 Feb	31.08	28.47	26.56	25.05

[a]Results at this temperature were extrapolated from higher temperature data.

TABLE 148. VAPOR PRESSURE OF TESTED FUELS AS A FUNCTION OF TEMPERATURE

Sample designation	Millimeters, mercury 32°F	70°F	100°F
JP-8 (2006), 78-C	5.0	8.0	11.0
8A2 " "	8.5	13.0	17.0
8A3 " "	8.0	12.5	16.5
JP-4 (2006), 78-C	46.5	95.0	160.0
4A2 " "	24.0	52.5	91.5
4A3 " "	23.0	53.5	98.0
8X2 " "	7.0	13.5	21.5
8X3 " "	10.5	18.0	25.5
8GM " "	8.5	12.5	16.5
4X2 " "	14.5	33.5	60.5
4X3 " "	19.5	47.0	88.0
4XG " "	16.5	41.0	77.0
GEC-120-8X0-792033	8.0	17.0	29.5
GEC-130-4X0-792033	27.5	61.0	105.0
GEC-130-DF2-792033	11.5	16.5	21.0
GEC-145-400-792033	40.0	82.5	146.0
GEC-140-800-792033	10.5	15.5	20.5
GEC-130-8X0-792033	8.0	14.0	20.5
GEC-140-4GX-792033	27.5	64.0	116.0
GEC-120-8AO-792033	8.5	13.5	17.0
GEC-130-8AO-792033	14.5	20.0	25.0
GEC-120-4AO-792033	30.5	64.0	110.0
GEC-130-4AO-792033	34.0	73.0	127.0
GEC-120-X40-792033 Feb	25.5	54.0	90.0
GEC-140-8GO-792033 Feb	17.0	24.5	31.0

TABLE 149. CALCULATED SPECIFIC GRAVITY AND API GRAVITY FOR TESTED FUELS

Sample designation	Specific gravity, 60/60°F	API gravity, °
GEC-131-DF2	0.8486	35.25
GEC-145-400	0.7607	54.51
GEC-140-800	0.8155	42.01
GEC-130-8XO	0.8268	39.64
GMSO F Farm Annex	0.8820	28.90
2040 Solvent B-19	0.9760	13.48
Xylene bottoms, Bldg. 42D	0.8718	30.81

TABLE 150. HEAT OF COMBUSTION OF TESTED FUELS

Sample designation	Gross, Btu/lb Duplicates		Gross, Btu/lb Average	Net, Btu/lb Average
JP-8 (2006), 78-C	19,785	19,782	19,784	18,514
8A2 " "	19,124	19,144	19,134	18,045
8A3 " "	19,512	19,469	19,491	18,311
JP-4 (2006), 78-C	20,023	20,031	20,027	18,719
4A2 " "	19,207	19,209	19,208	18,114
4A3 " "	19,554	19,518	19,536	18,356
8X2 " "	19,187	19,196	19,192	18,119
8X3 " "	19,438	19,475	19,457	18,309
8GM " "	19,809	19,791	19,800	18,556
4X2 " "	19,242	19,226	19,234	18,149
4X3 " "	19,548	19,538	19,543	18,371
4XG " "	19,899	19,877	19,888	18,619
GEC-120-8X0-792033	19,203	19,169	19,186	18,088
GEC-130-4X0-792033	19,648	19,626	19,637	18,455
GEC-130-DF2-792033	19,465	19,501	19,485	18,307
GEC-145-400-792033	20,089	20,086	20,088	18,767
GEC-140-800-792033	19,845	19,851	19,848	18,576
GEC-130-8X0-792033	19,516	19,530	19,523	18,335
AR79029, GMSO F Farm Annex	19,953	19,950	19,952	18,662
Xylene Bottoms, Bldg. #42D	18,641	18,631	18,636	17,714
2040 Solvent B-19	17,945	17,935	17,940	17,186
GEC-140-4GX-792033	19,939	19,983	19,961	18,685
GEC-120-8AO-792033	19,201	19,244	19,223	18,137
GEC-130-8AO-792033	19,531	19,545	19,538	18,358
GEC-120-4AO-792033	19,294	19,262	19,278	18,189
GEC-130-4AO-792033	19,565	19,537	19,551	18,390
GEC-120-X40-792033 Feb	19,285	19,336	19,311	18,209
GEC-140-8GO-792033 Feb	19,826	19,811	19,819	18,549

TABLE 151. GAS CHROMATOGRAPHIC SIMULATED DISTILLATIONS OF TESTED FUELS

Percent recovered	JP-8		8A2		8A3		JP-4		4A2		4A3		8X2	
	°C	°F	°C	°F	°C	°F	°C	°F	°C	°F	°C	°F	°C	°F
0.5, IBP	129	282	108	226	101	214	21	70	35	95	23	73	120	248
1	152	306	128	262	124	255	22	72	44	111	27	81	139	282
5	178	352	164	327	163	325	61	142	86	187	66	151	147	297
10	191	376	179	354	177	351	80	176	104	219	89	192	155	311
20	206	403	192	378	191	376	95	203	130	266	111	232	165	329
30	215	419	203	397	202	396	111	232	153	307	126	259	167	333
40	224	435	212	414	211	412	126	259	183	361	150	302	173	343
50	231	448	223	433	219	426	143	289	209	408	178	352	189	372
60	240	464	227	441	227	441	168	334	223	433	200	392	208	406
70	247	477	234	453	234	453	190	374	243	469	217	423	222	432
80	260	500	248	478	246	475	210	410	248	478	232	450	237	459
90	272	522	260	500	258	496	230	446	267	513	250	482	256	493
95	281	538	269	516	268	514	245	473	281	538	258	496	270	518
99	297	567	290	554	287	549	263	505	304	579	284	543	295	563
99.5, FBP	303	577	296	565	296	565	268	514	314	597	294	561	306	583

Percent recovered	8X3		8GM		4X2		4X3		4XG		GEC-120-X40-792033 Feb		GEC-140-8GO-792033 Feb	
	°C	°F	°C	°F	°C	°F	°C	°F	°C	°F	°C	°F	°C	°F
0.5, IBP	128	262	129	264	25	77	35	95	26	79	31	88	128	262
1	138	280	143	289	35	95	45	113	35	95	44	111	145	392
5	152	306	169	336	82	180	85	185	70	158	91	196	177	351
10	160	320	183	361	91	196	102	216	91	196	106	223	189	372
20	166	331	197	387	124	255	129	264	117	243	140	284	203	397
30	181	358	208	406	143	289	146	295	128	262	157	315	213	415
40	198	388	217	423	155	311	164	327	152	306	166	331	222	432
50	210	410	227	441	163	325	175	347	168	334	168	334	232	450
60	220	428	235	455	167	333	180	356	187	369	170	338	240	464
70	231	448	247	477	172	342	191	376	212	414	174	345	253	487
80	243	469	259	498	190	374	216	421	236	457	181	358	266	511
90	258	496	281	538	225	437	243	469	273	523	221	430	289	552
95	270	518	302	576	244	471	257	495	305	581	246	475	310	590
99	287	549	325	617	275	527	278	532	331	628	292	558	343	649
99.5, FBP	295	563	331	628	286	547	284	543	339	642	305	581	355	671

(continued)

TABLE 151 (continued)

Percent recovered	GEC-120-8X0-792033 °C	°F	GEC-130-4X0-792033 °C	°F	GEC-130-DF2-792033 °C	°F	GEC-145-400-792033 °C	°F	GEC-140-800-792033 °C	°F	GEC-130-8X0-792033 °C	°F
0.5 IBP	80	176	32	59	132	270	25	77	128	262	136	277
1	97	207	40	104	147	297	34	93	144	291	143	289
5	144	291	82	180	180	356	72	162	176	349	157	315
10	156	313	101	214	197	387	93	199	190	374	165	329
20	165	329	123	253	216	421	108	226	203	397	171	340
30	167	333	145	293	231	448	123	253	214	417	187	369
40	171	340	161	322	245	473	141	286	222	432	202	396
50	177	351	166	331	256	493	160	320	231	448	215	419
60	197	387	170	338	271	520	180	356	239	462	223	433
70	216	421	178	352	284	543	199	390	249	480	235	455
80	232	450	203	397	300	572	218	424	259	498	248	478
90	254	489	232	450	318	604	237	459	272	522	263	505
95	291	556	278	552	333	631	254	489	282	540	274	525
99	301	574	289	552	343	649	273	523	300	572	295	563
99.5 FBP					373	703	281	538	306	583	302	576

Percent recovered	GEC-140-4GX-792033 °C	°F	GEC-120-8AO-792033 °C	°F	GEC-130-8AO-792033 °C	°F	GEC-120-4AO-792033 °C	°F	GEC-130-4AO-792033 °C	°F
0.5 IBP	28	82	133	271	136	277	34	93	30	86
1	36	97	149	300	149	300	47	117	37	99
5	78	172	177	351	176	349	88	190	79	174
10	98	208	190	374	189	372	103	217	96	205
20	121	250	203	397	201	394	129	264	121	250
30	143	289	212	414	211	412	160	320	138	280
40	164	327	221	430	219	426	186	367	164	327
50	178	352	230	446	228	442	208	406	187	369
60	204	399	234	453	234	453	221	430	206	403
70	230	446	243	469	242	468	231	448	223	433
80	264	507	254	489	253	487	237	459	232	450
90	301	574	267	513	266	511	255	491	253	487
95	318	604	277	531	275	527	271	520	264	507
99	342	648	298	568	296	565	296	565	291	556
99.5 FBP	346	655	304	579	303	577	302	576	300	572

TABLE 152. HYDROCARBON-TYPE DISTRIBUTION OF TESTED FUELS (ASTM D 2789)

Compound type	Liquid volume percent												
	JP-8	8A2	8A3	JP-4	4A2	4A3	8X2	8X3	8GM	4X2	4X3	4XG	GEC-120-8XO-792033
Paraffins	42.3	29.1	35.9	62.2	37.6	45.6	23.8	33.0	43.9	30.6	44.4	55.3	27.0
Monocycloparaffins	41.0	28.0	34.4	24.1	20.5	25.0	20.5	30.2	39.1	10.4	15.1	25.4	22.6
Dicycloparaffins	3 1	1.9	2.6	3.4	0.0	0.0	2.3	3.1	3.3	2.4	3.7	1.1	1.0
Alkylbenzenes	7.5	11.3	9.4	8.4	12.6	11.0	52.4	30.3	7.6	55.6	35.3	16.2	48.9
Indans and tetralins	4.1	6.1	5.2	1.3	4.5	3.3	0.0	1.8	4.1	0.6	1.0	1.4	0.0
Naphthalenes	2.0	23.7	12.5	0.6	24.8	15.1	1.0	1.6	2.0	0.4	0.5	0.6	0.5

Compound type	Liquid volume percent						
	GEC-130-4XO-792033	GEC-130-8XO-792033	GEC-140-800-792033	GEC-145-400-792033	GEC-130-DF2-792033[a]	GEC-120-4XO-79203	GEC-140-4GX-792033
Paraffins	45.5	36.2	44.4	61.2	49.1	62.8	59.1
Monocycloparaffins	18.3	33.4	41.4	24.2	26.7	25.1	24.0
Dicycloparaffins	3.3	2.3	2.6	4.9	-[b]	4.6	4.4
Alkylbenzenes	32.2	25.4	6.7	8.2	10.6	6.6	11.8
Indans and tetralins	0.0	1.5	3.4	1.1	4.6	0.9	0.7
Indenes and Dihydronaphthalenes	-	-	-	-	0.8	-	-
Naphthalenes	0 2	1.2	1.5	0.4	8.2	<0.1	<0.1

Compound type	Liquid volume percent						
	GEC-140-8GO-792033	GEC-120-8AO-792033	GEC-130-8AO-792033	GEC-120-4AO-792033	GEC-130-4AO-792033	GEC-120-X40-792033 Feb	GEC-140-8GO-792033 Feb
Paraffins	41.4	35.7	41.2	42.4	48.5	36.2	47.2
Monocycloparaffins	38.2	34.8	40.0	28.1	32.0	15.0	42.7
Dicycloparaffins	1.6	0.3	0.4	0.0	0.0	2.6	1.0
Alkylbenzenes	15.9	9.9	7.7	11.2	9.3	45.9	6.0
Indans and tetralins	2.0	4.4	3.4	3.0	1.6	0.3	2.4
Naphthalenes	0.9	14.9	7.3	15.3	8.6	0.0	0.7

[a] Monsanto Method 21-PQ-38-53 used for this analyses.

[b] Dash indicates that the compound type is not included in the analysis.

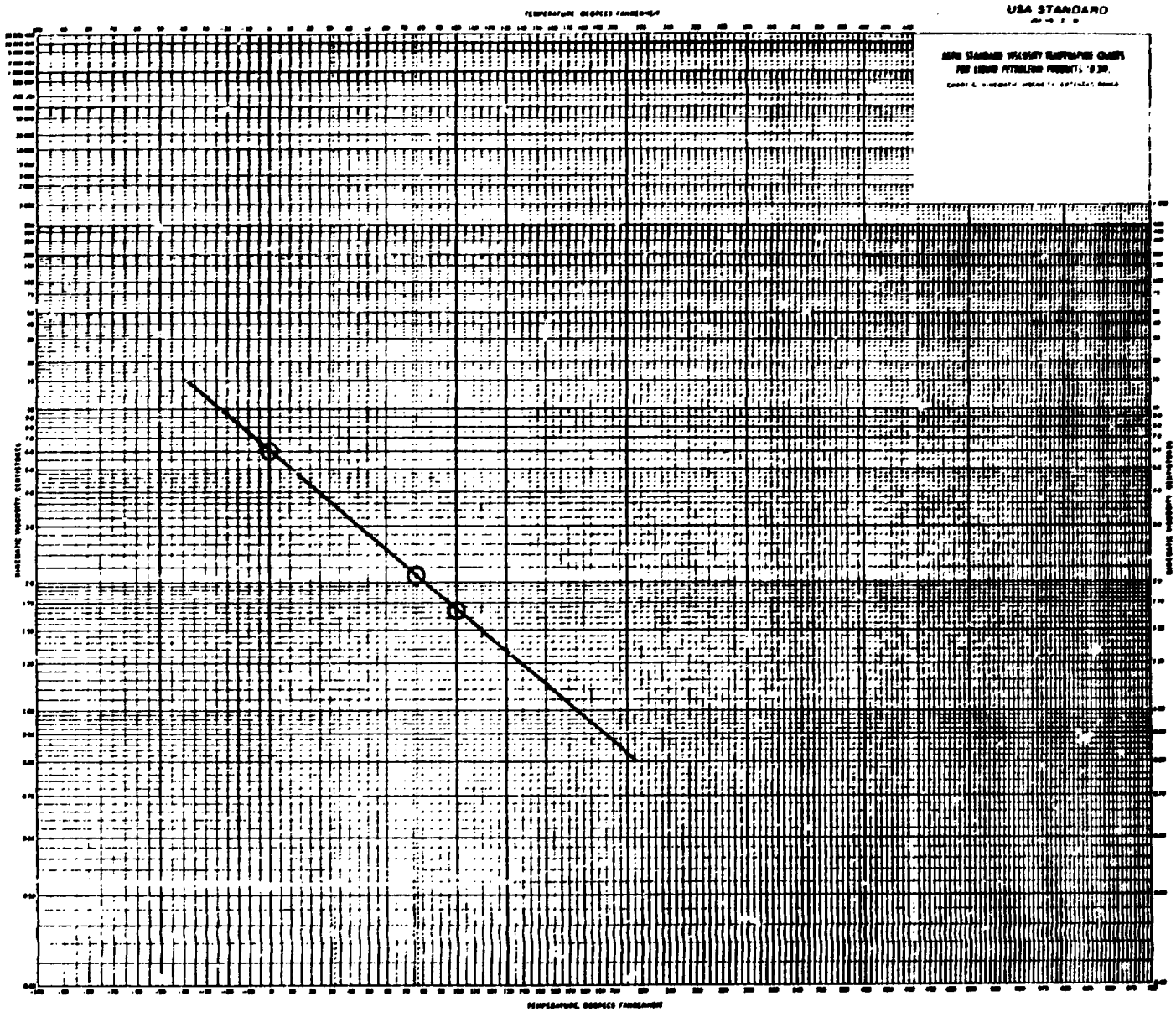

Figure 109. Viscosity/temperature plot for JP-8 fuel, (2006),78C.

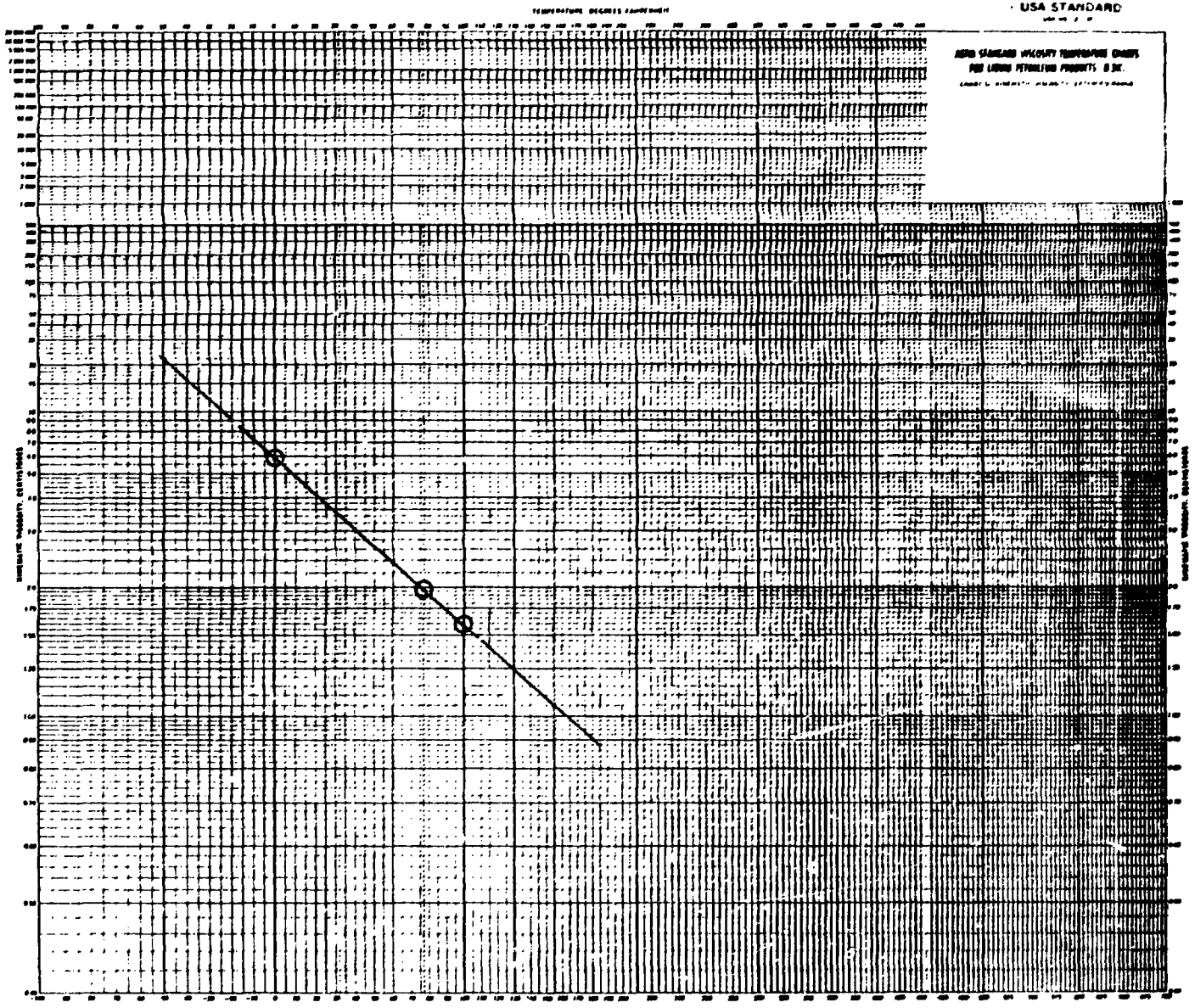

Figure 110. Viscosity/temperature plot for fuel sample 8A2.

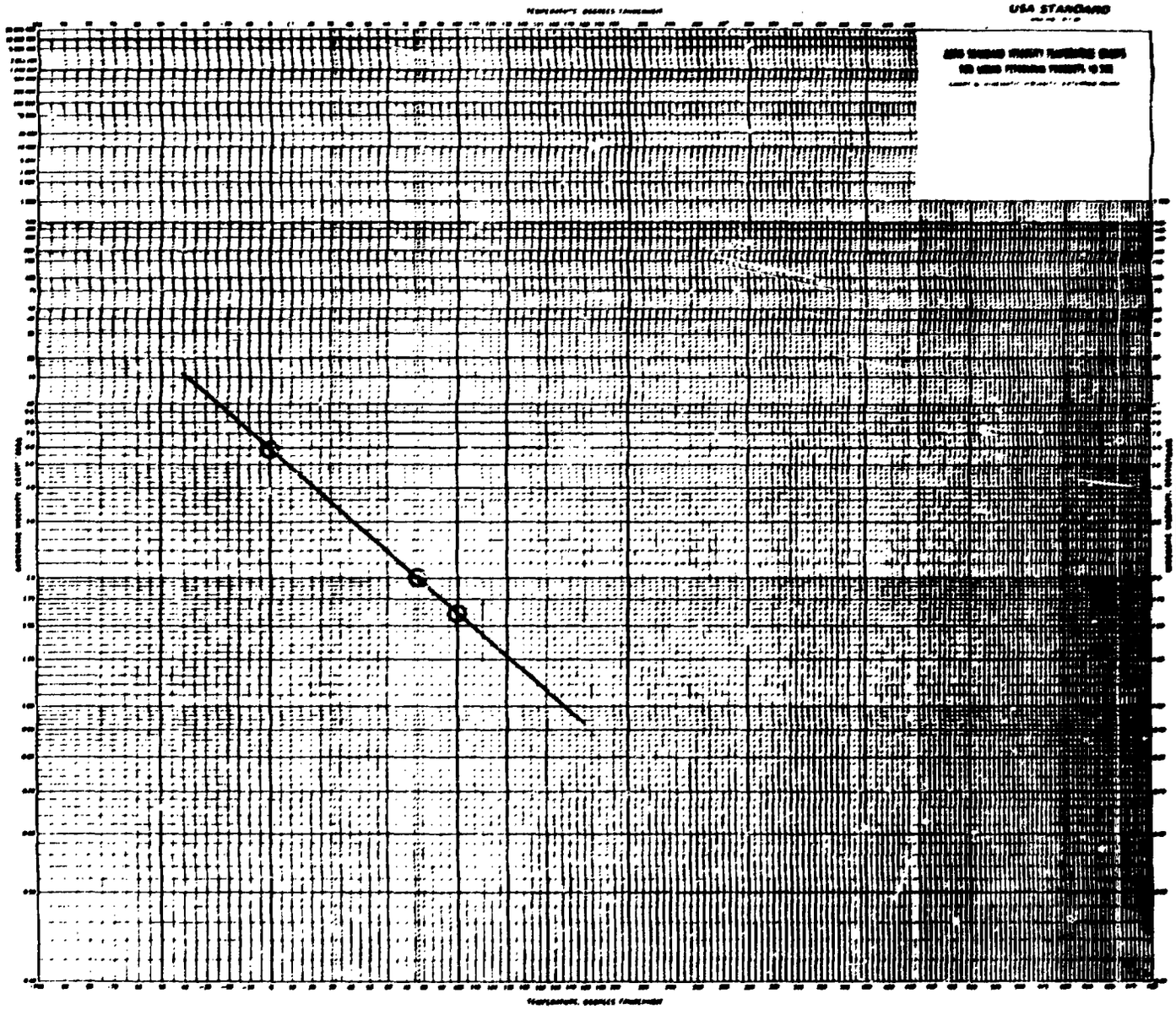

Figure 111. Viscosity/temperature plot for fuel sample 8A3.

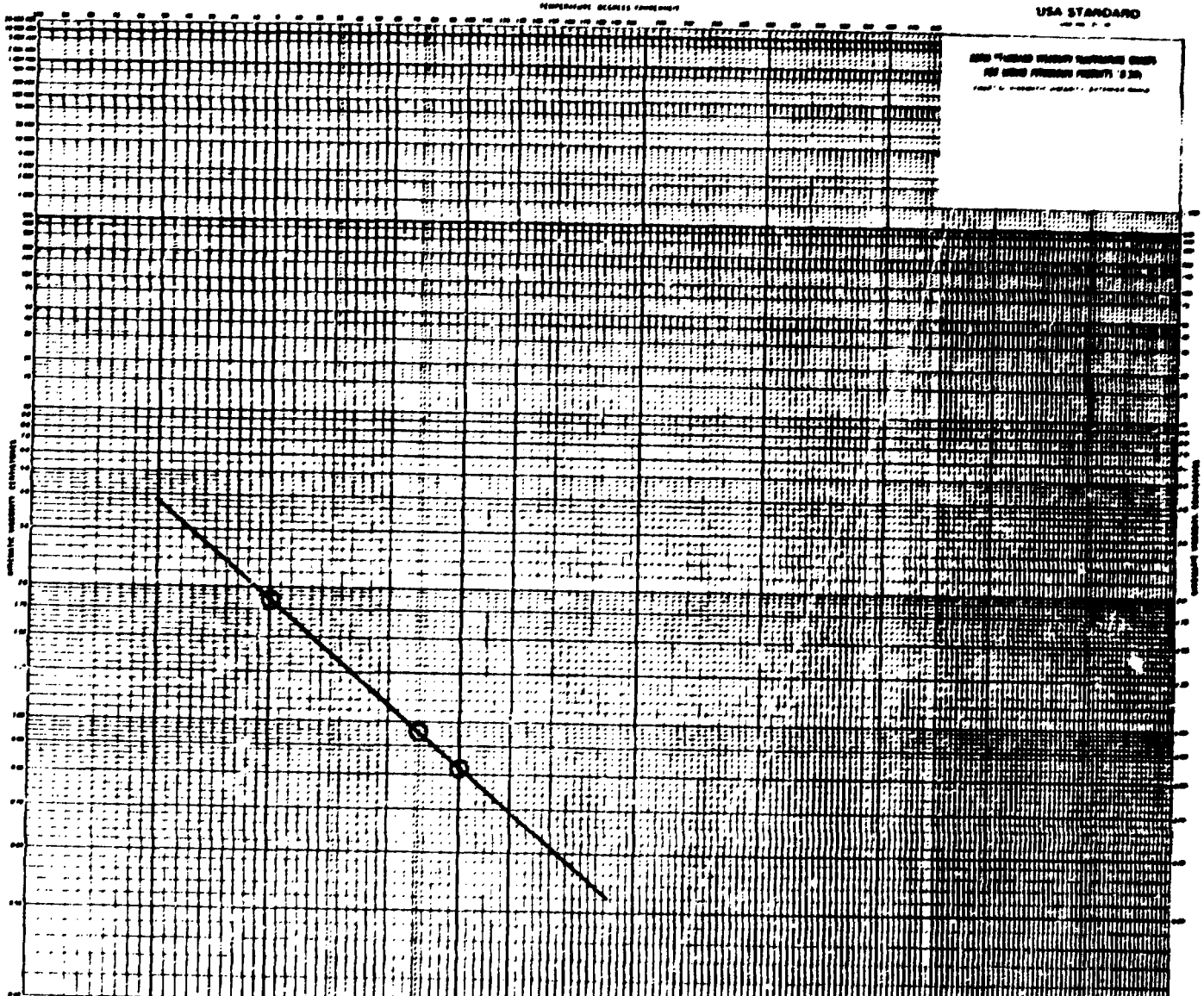

Figure 112. Viscosity/temperature plot for JP-4 fuel, (2006),78C.

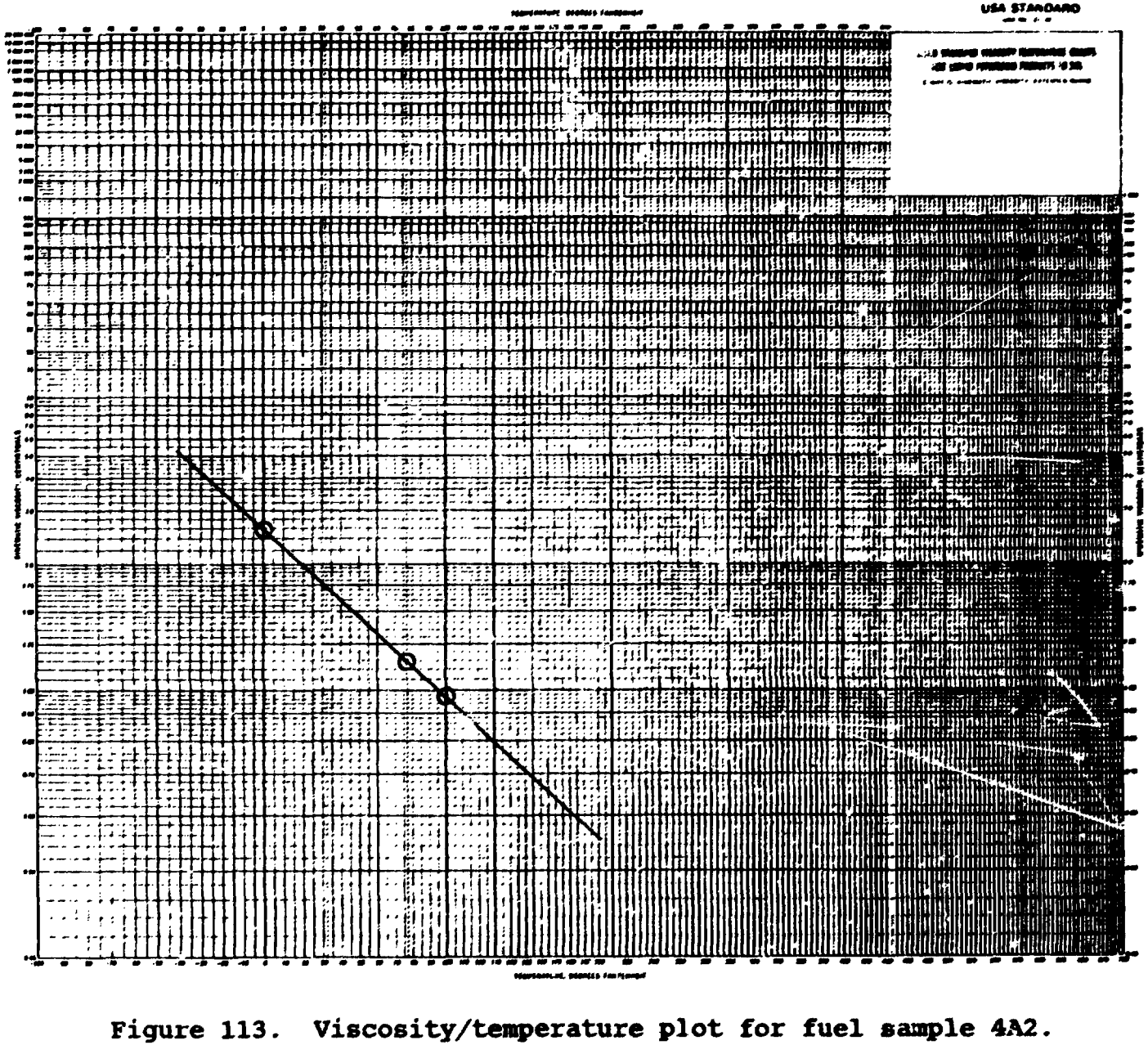

Figure 113. Viscosity/temperature plot for fuel sample 4A2.

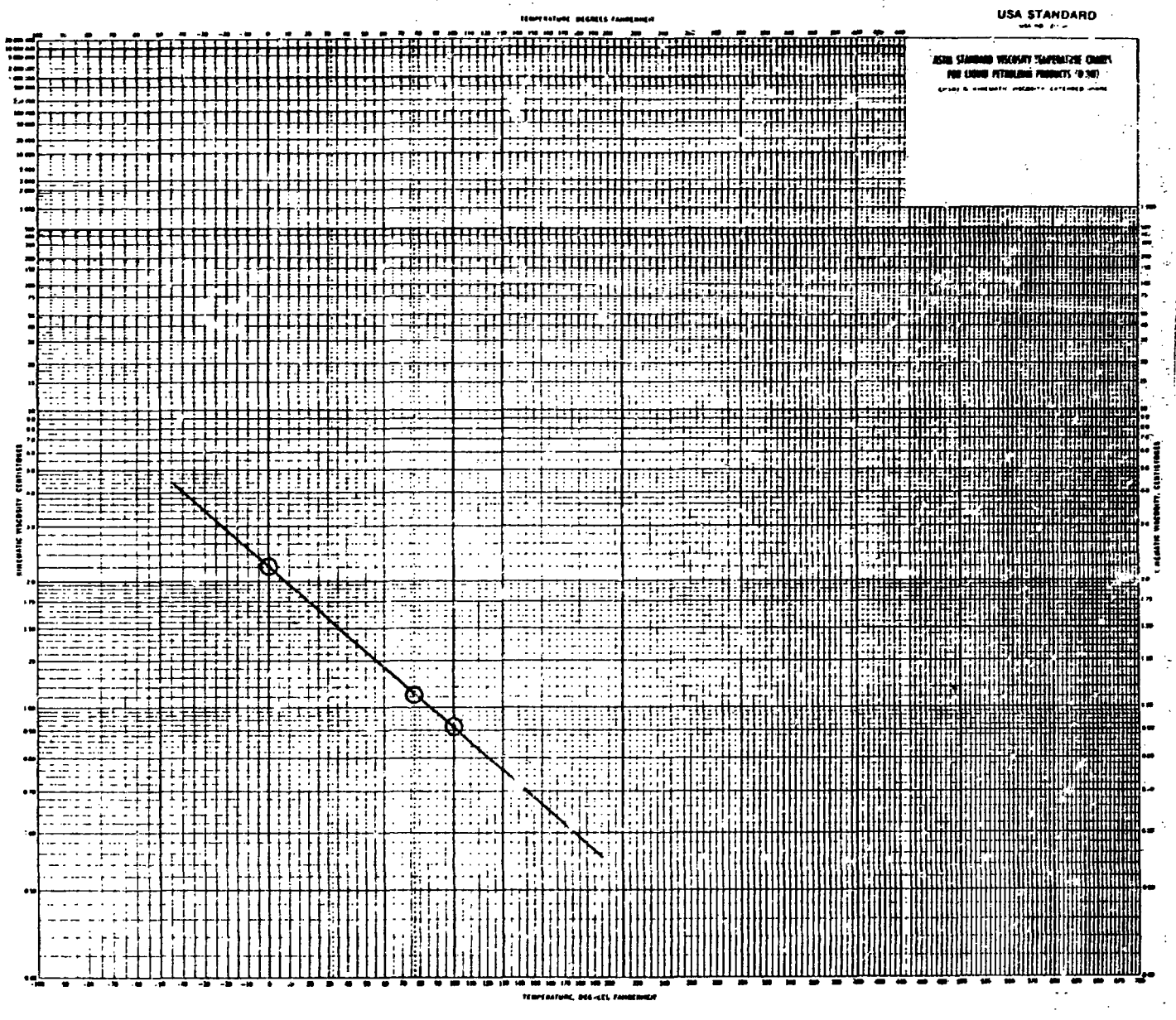

Figure 114. Viscosity/temperature plot for fuel sample 4A3.

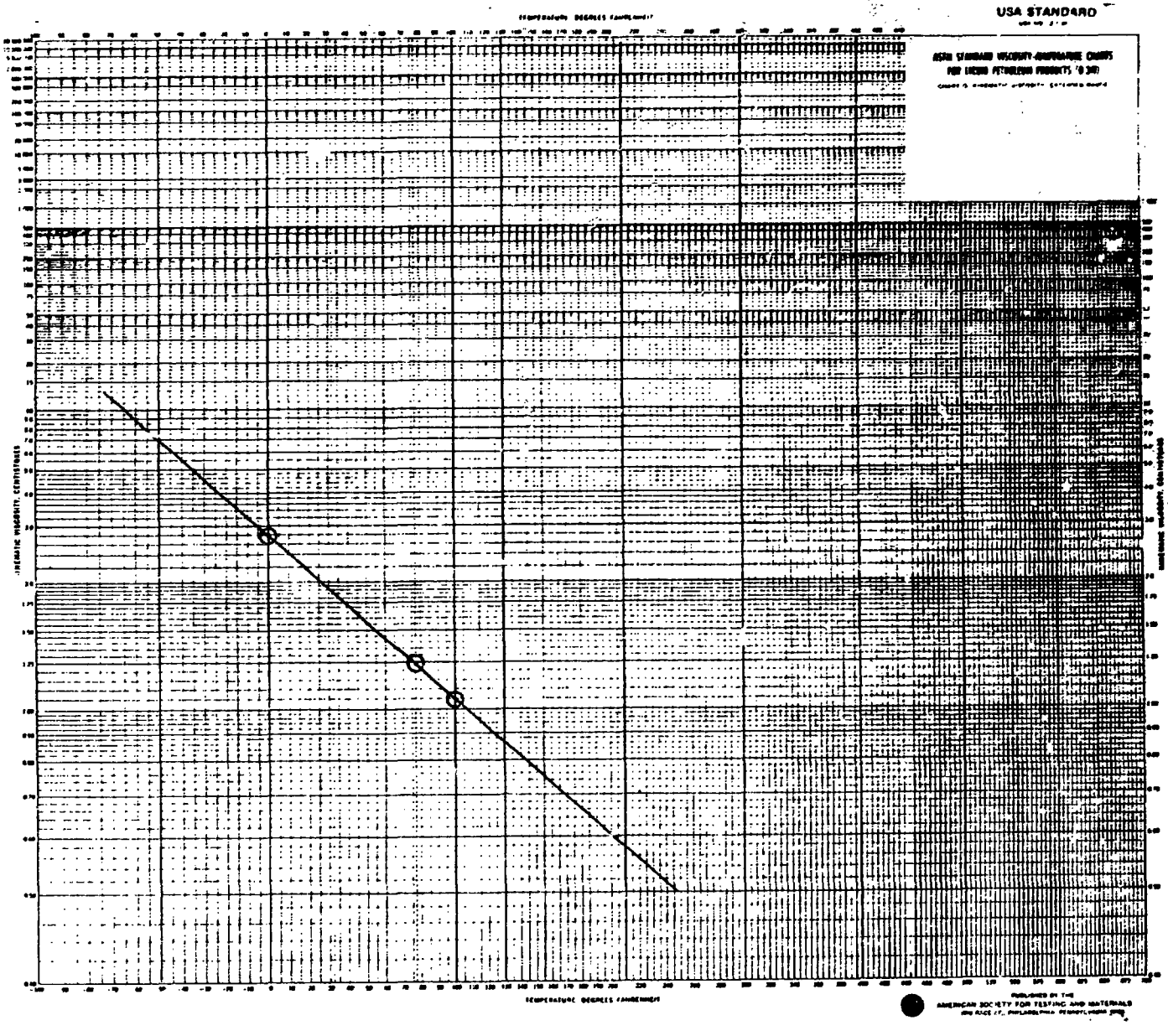

Figure 115. Viscosity/temperature plot for fuel sample 8X2.

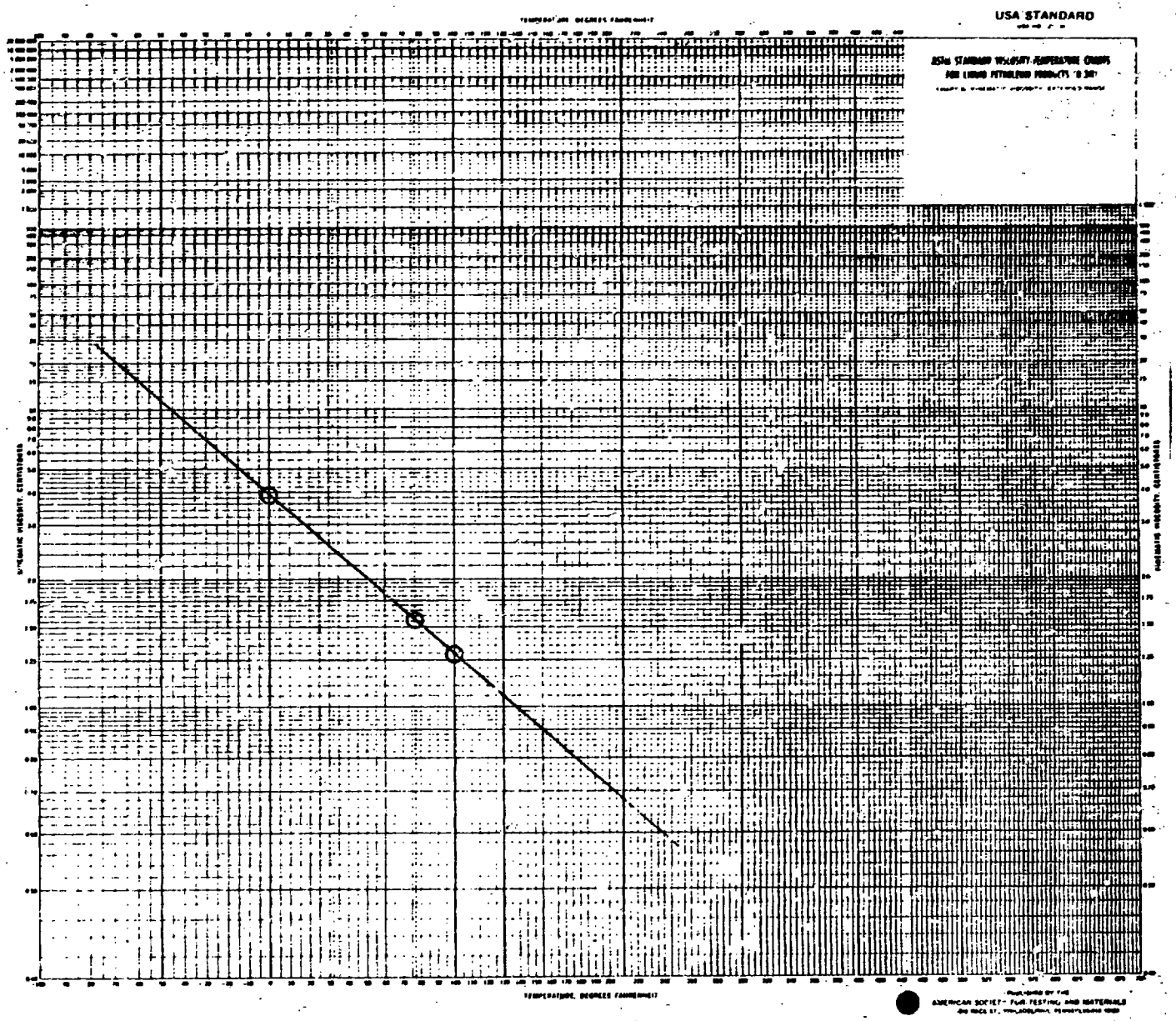

Figure 116. Viscosity/temperature plot for fuel sample 8X3.

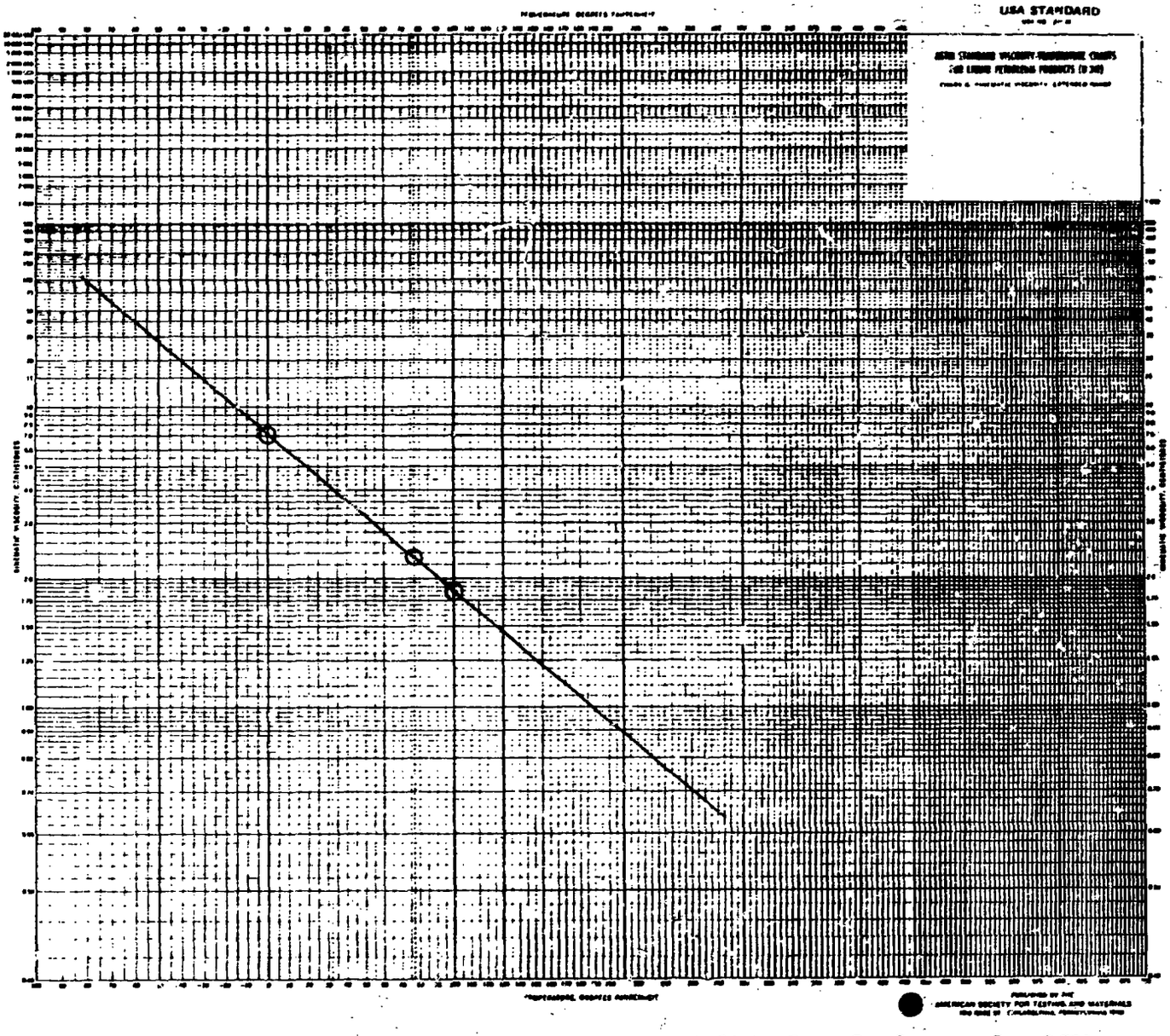

Figure 117. Viscosity/temperature plot for fuel sample 8GM.

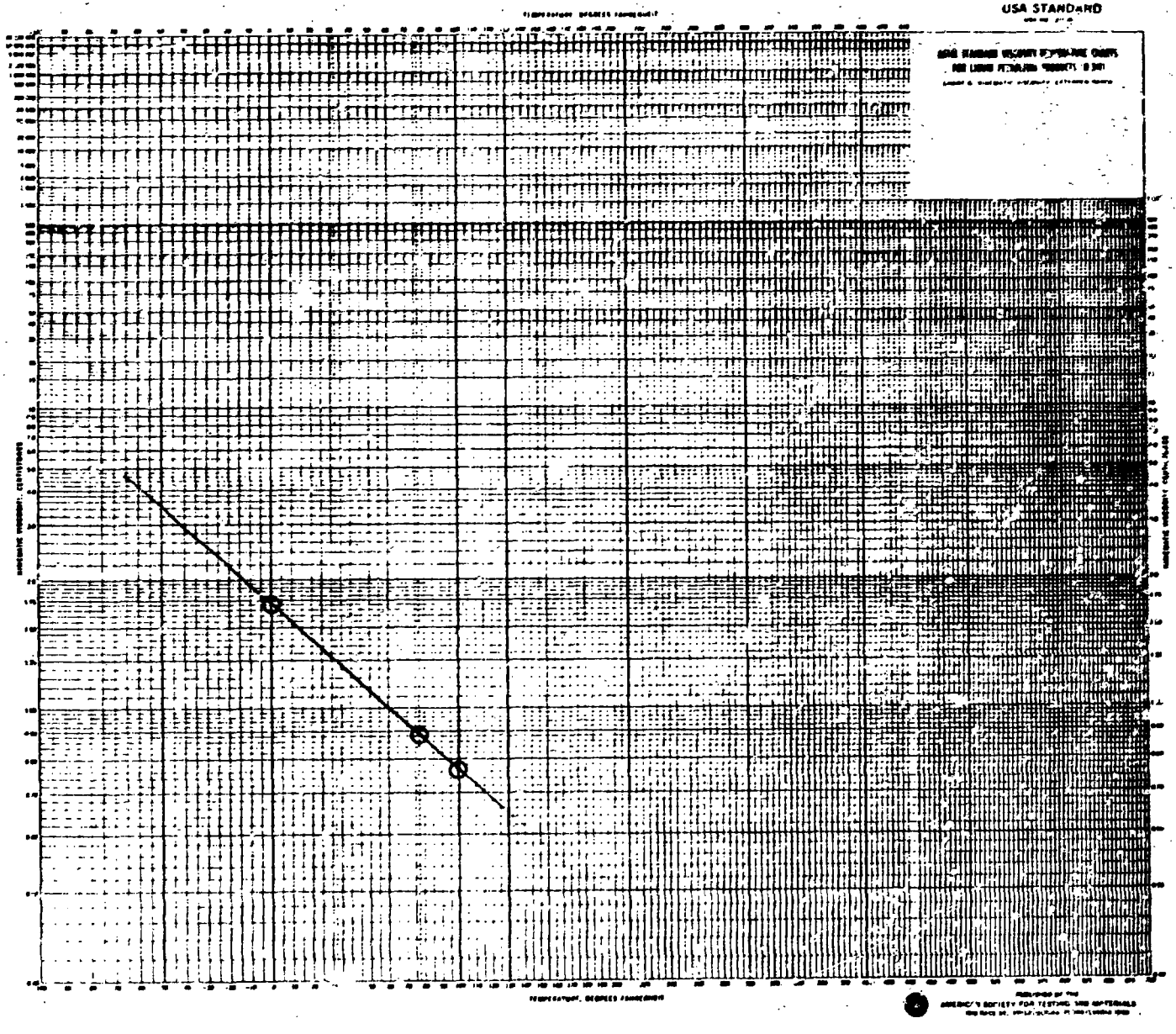

Figure 118. Viscosity/temperature plot for fuel sample 4X2.

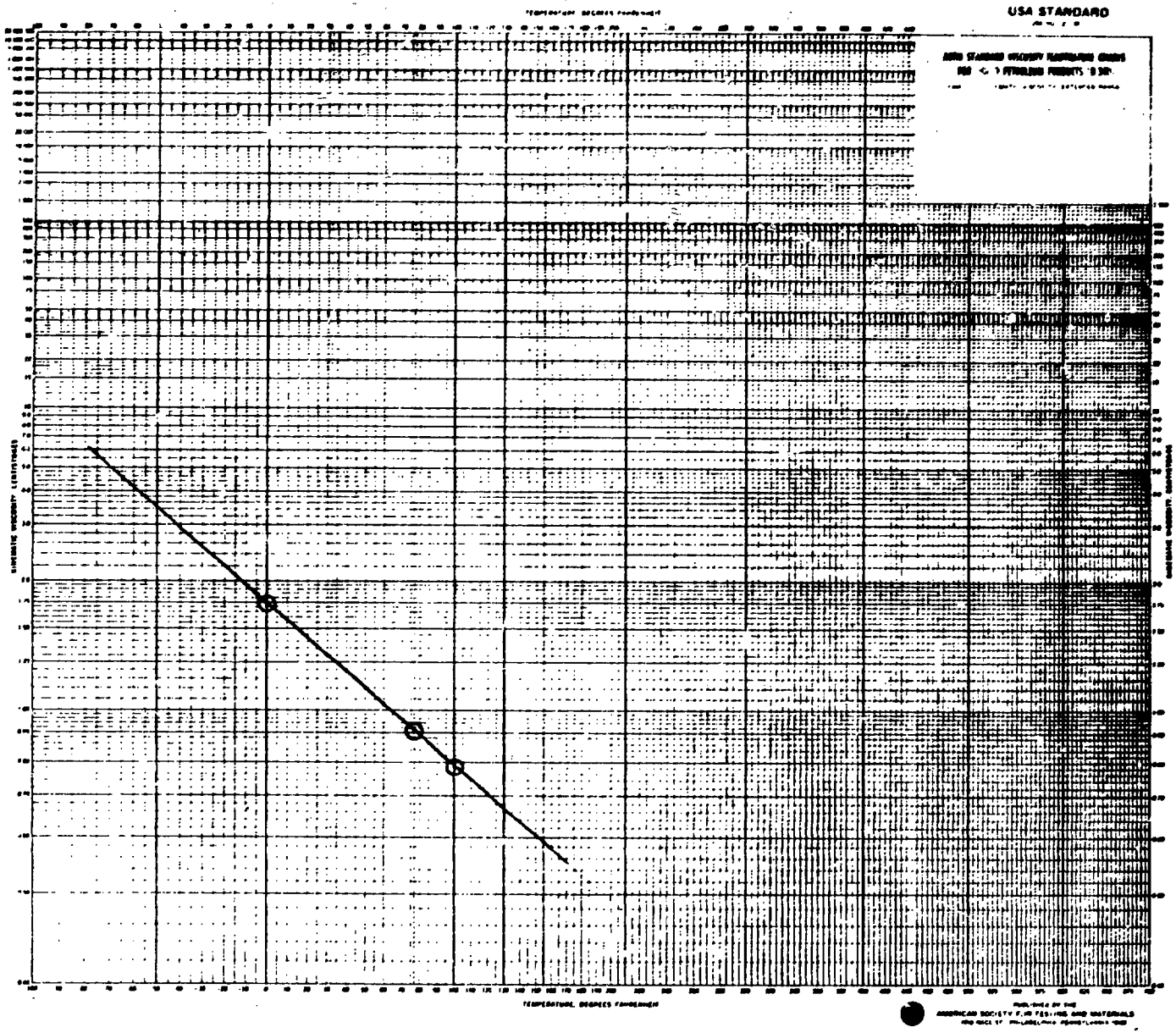

Figure 119. Viscosity/temperature plot for fuel sample 4X3.

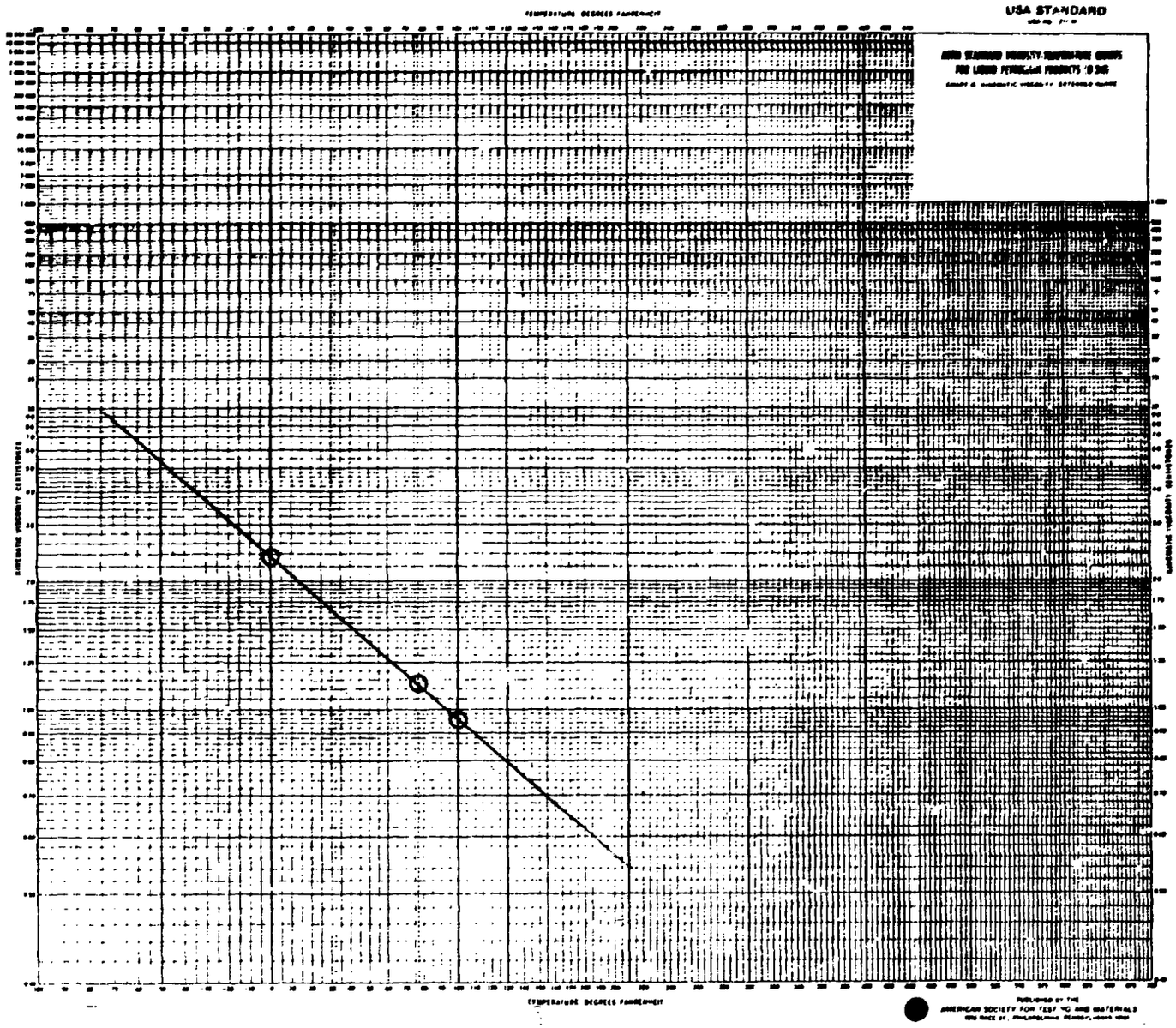

Figure 120. Viscosity/temperature plot for fuel sample 4XG.

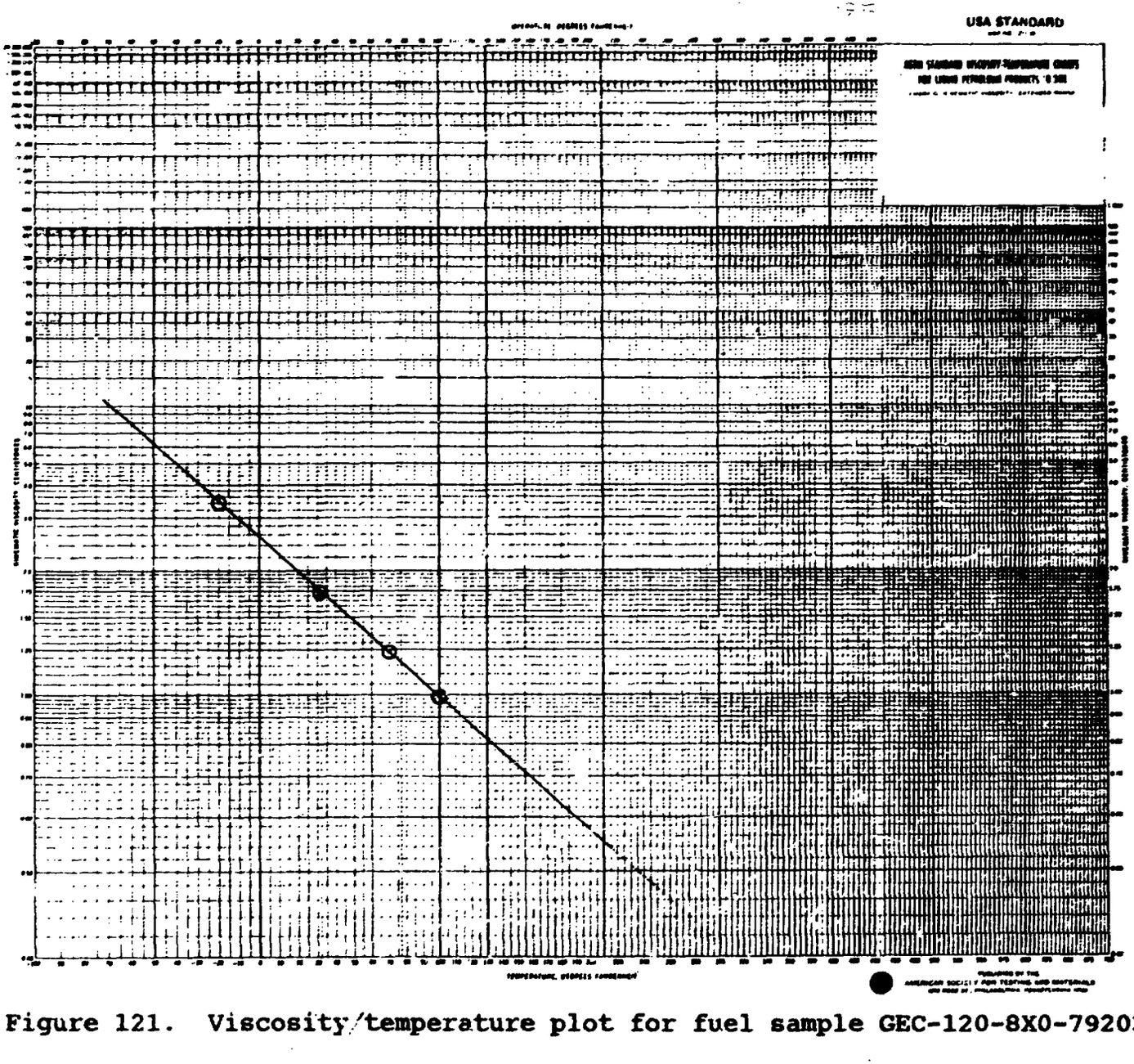

Figure 121. Viscosity/temperature plot for fuel sample GEC-120-8X0-792033.

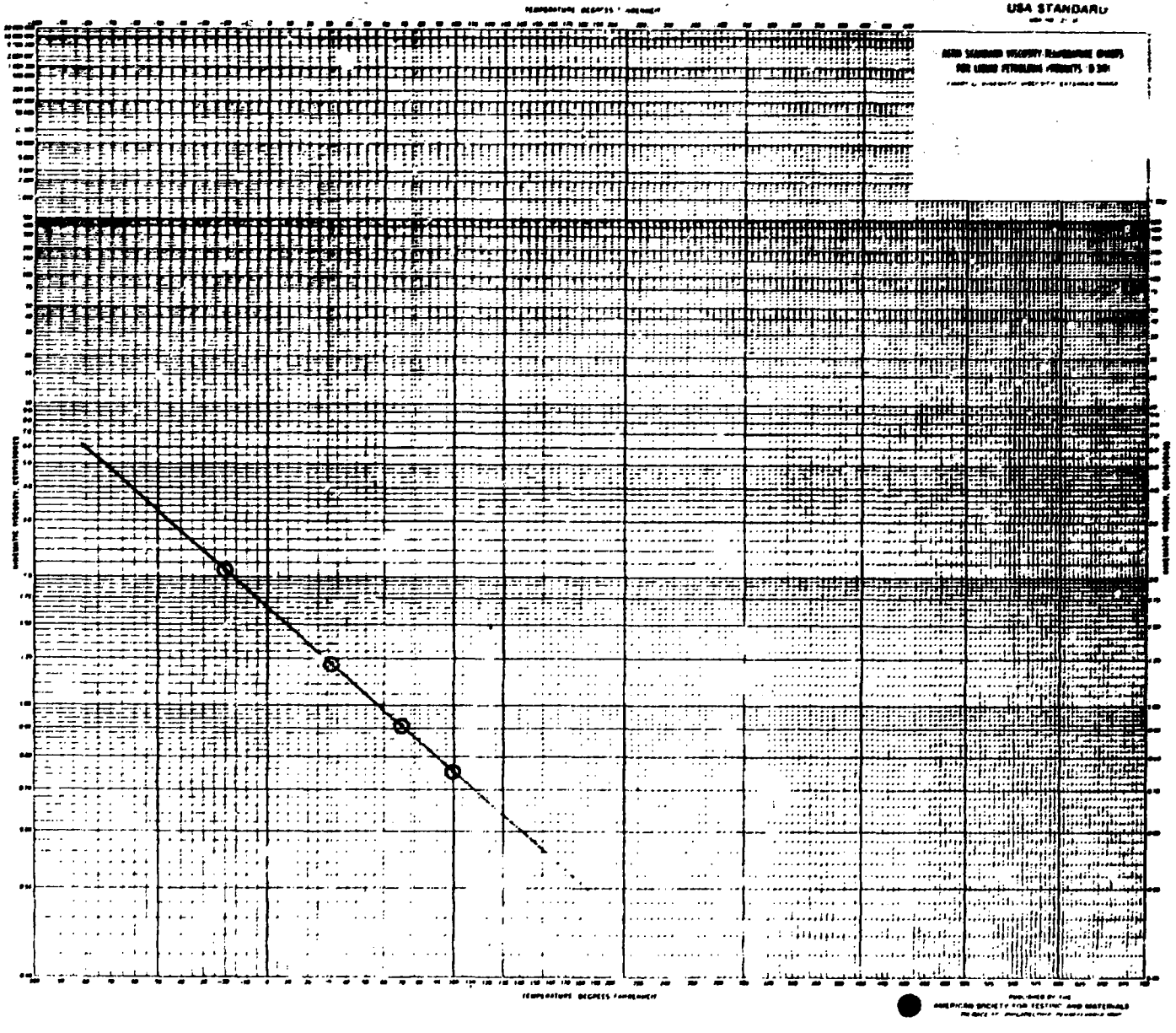

Figure 122. Viscosity/temperature plot for fuel sample GEC-130-4X0-792033.

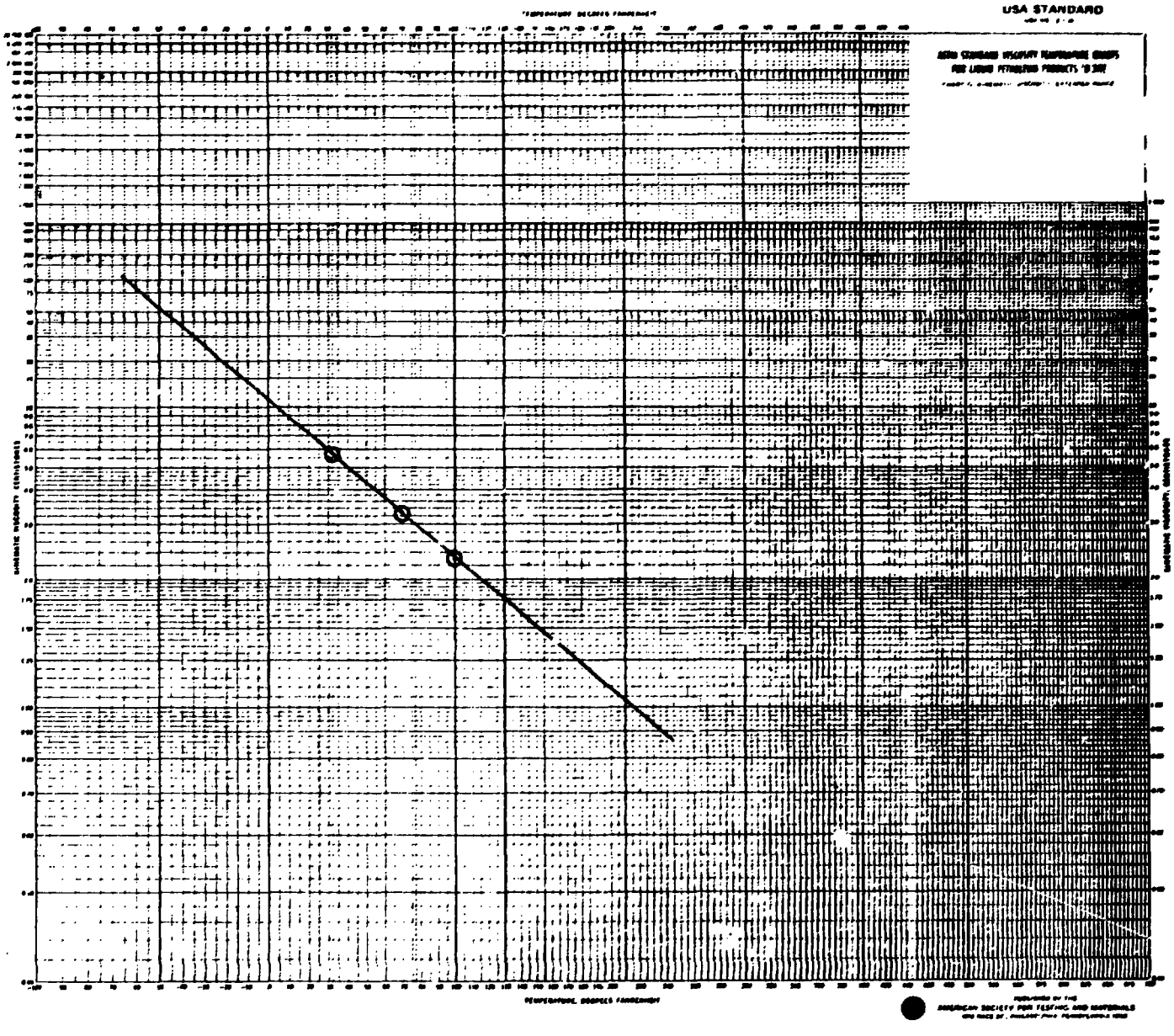

Figure 123. Viscosity/temperature plot for fuel sample GEC-130-DF2-792033.

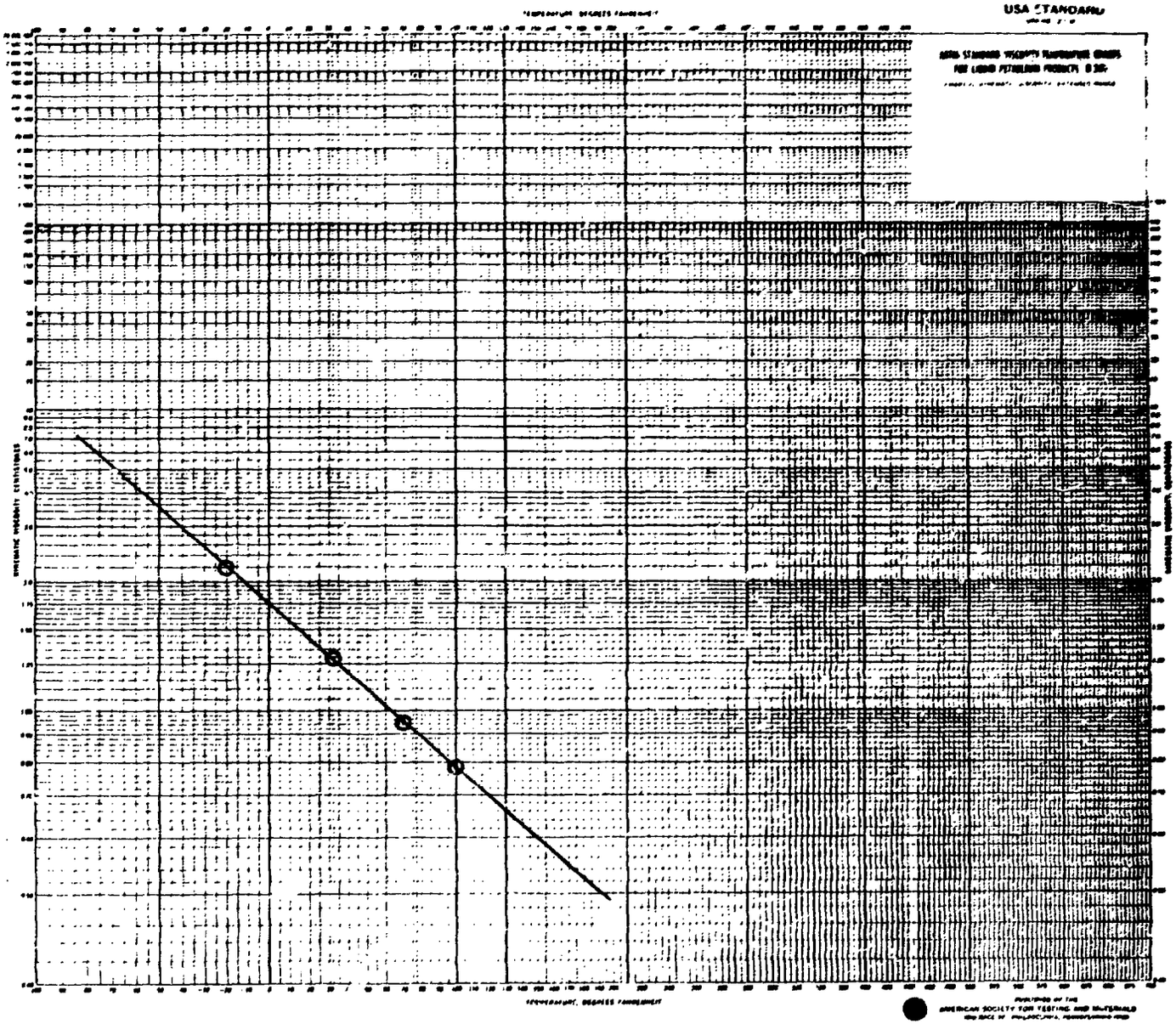

Figure 124. Viscosity/temperature plot for fuel sample GEC-145-400-792033.

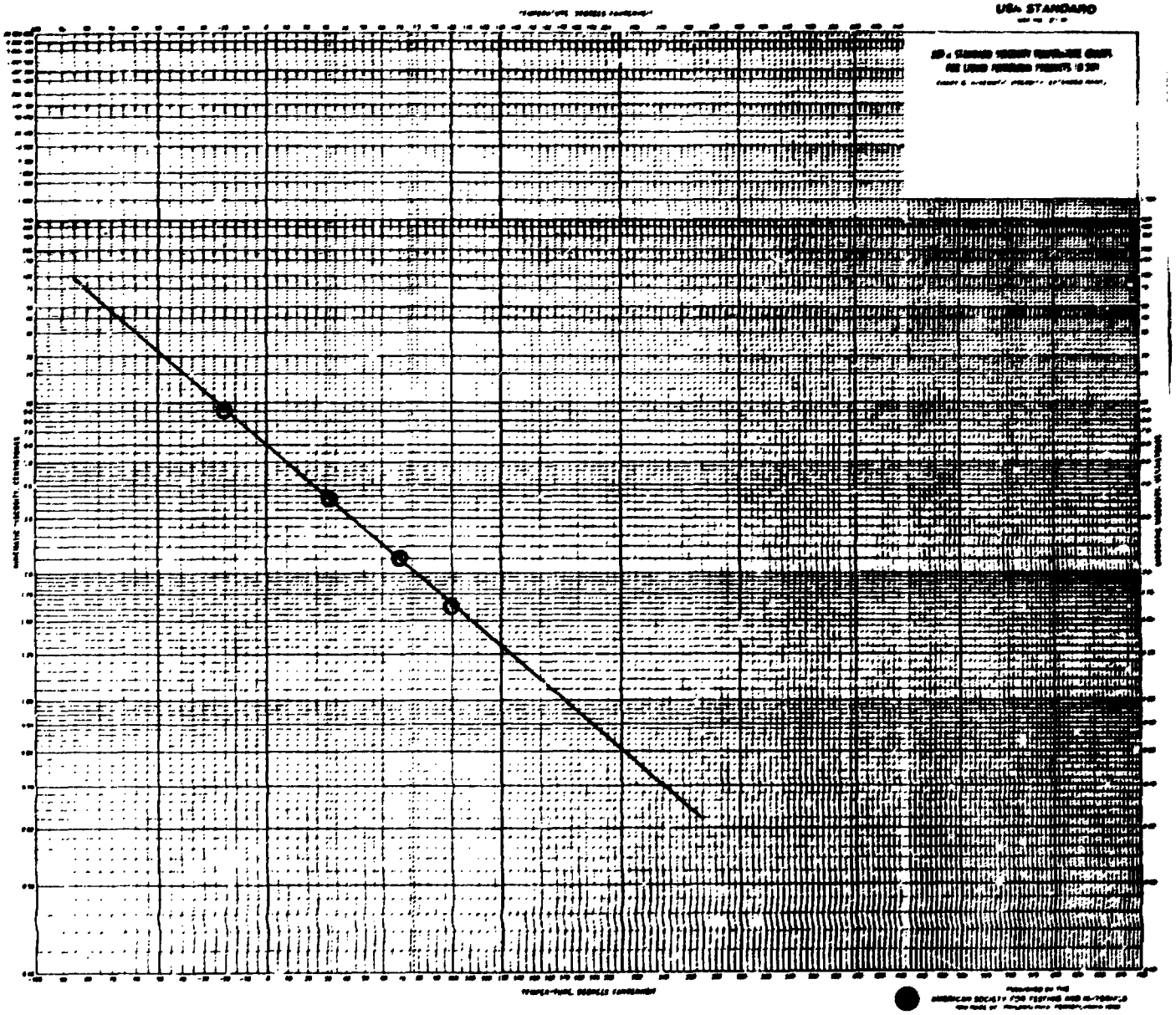

Figure 125. Viscosity/temperature plot for fuel sample GEC-140-800-792033.

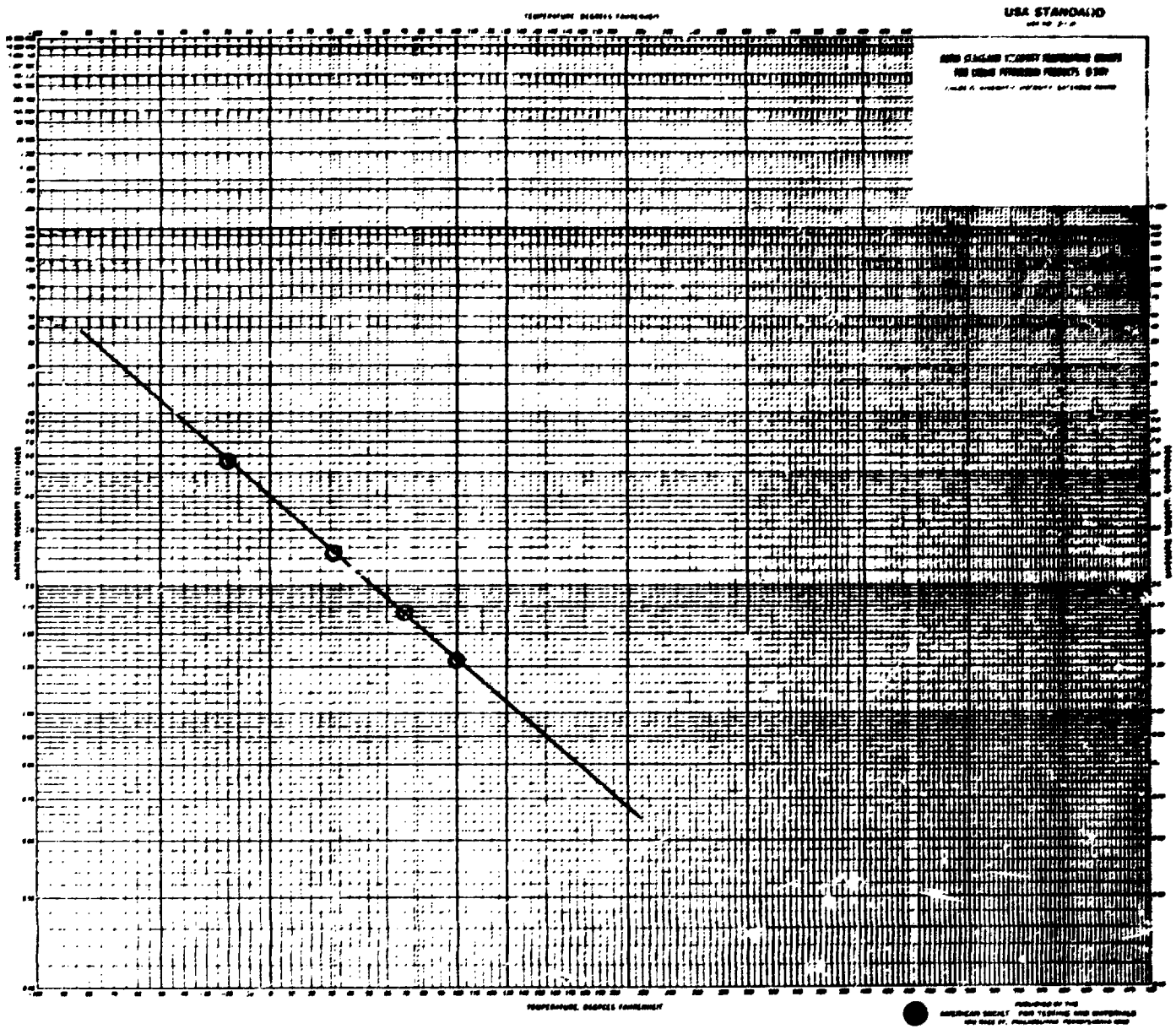

Figure 126. Viscosity/temperature plot for fuel sample GEC-130-8X0-792033.

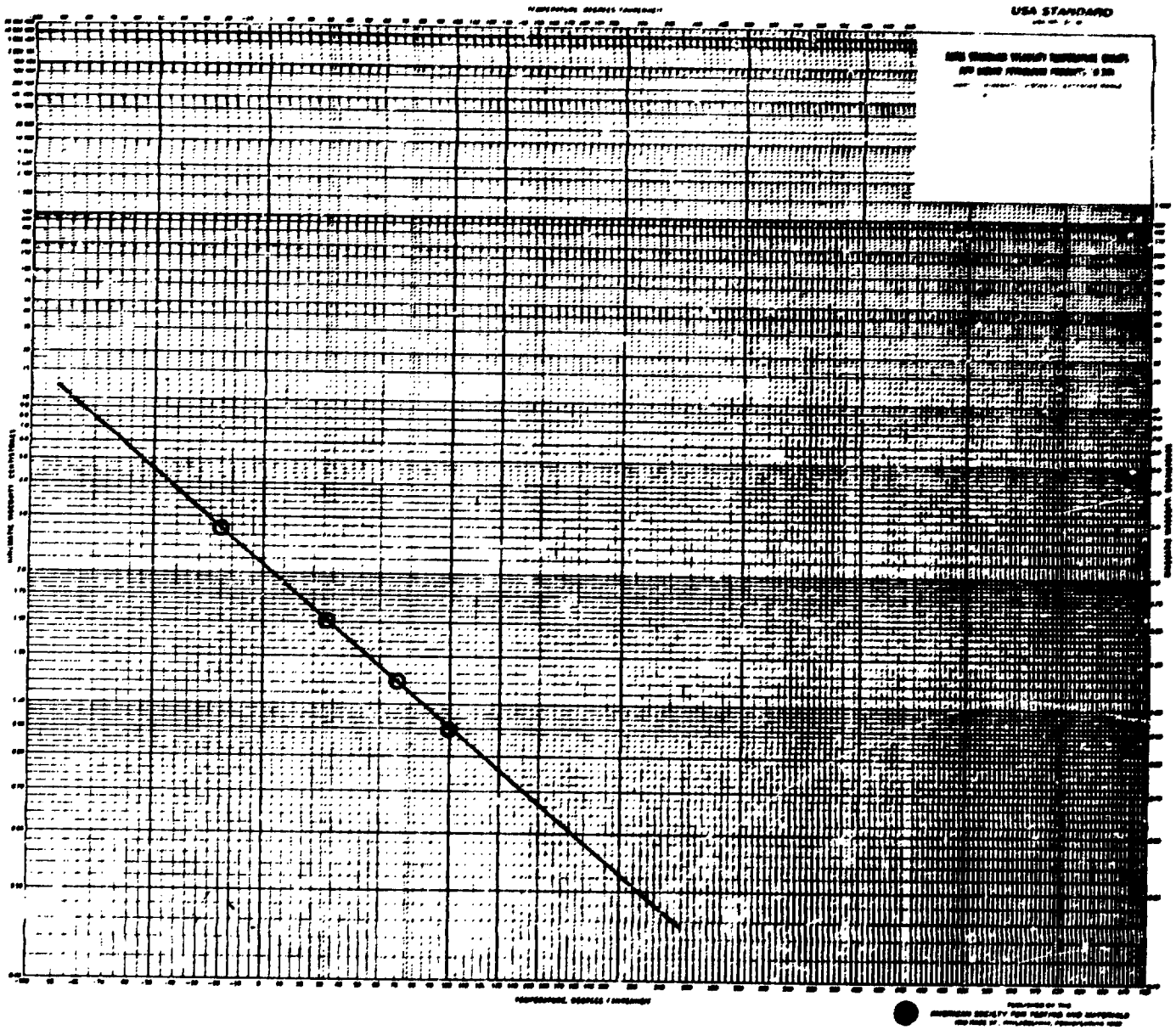

Figure 127. Viscosity/temperature plot for fuel sample GEC-140-4GX-792033.

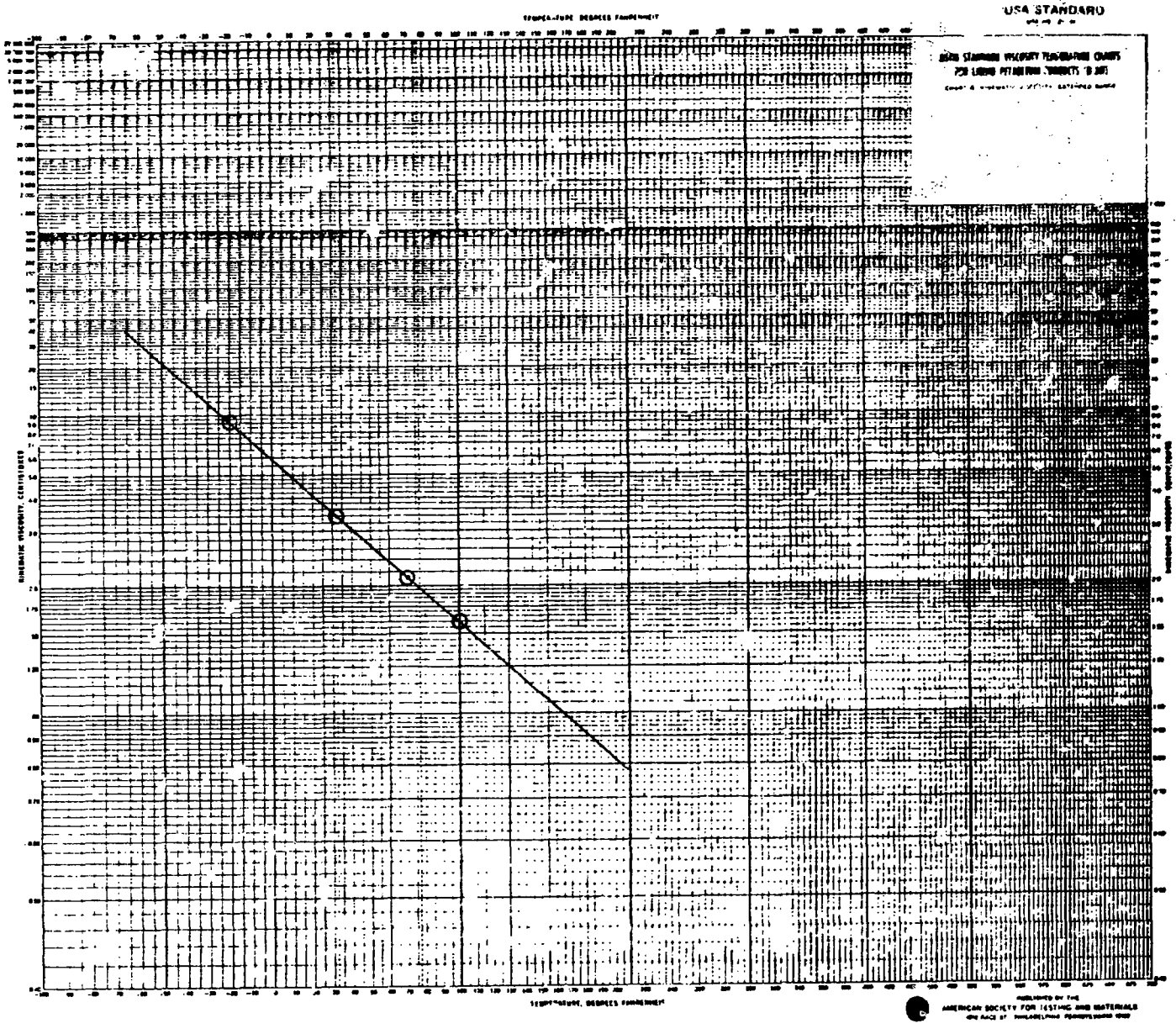

Figure 128. Viscosity/temperature plot for fuel sample GEC-120-8AO-792033.

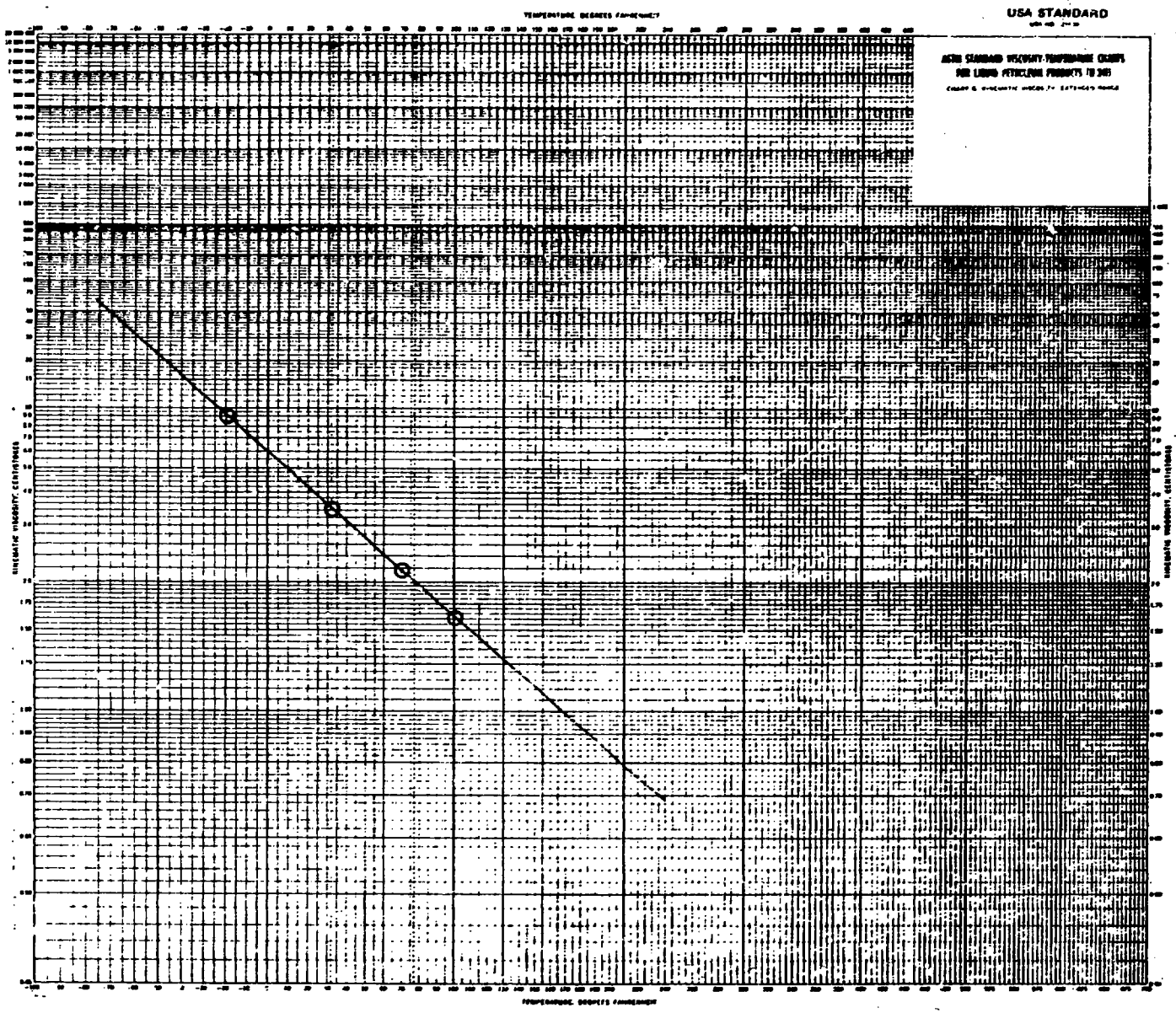

Figure 129. Viscosity/temperature plot for fuel sample GEC-130-8AO-792033.

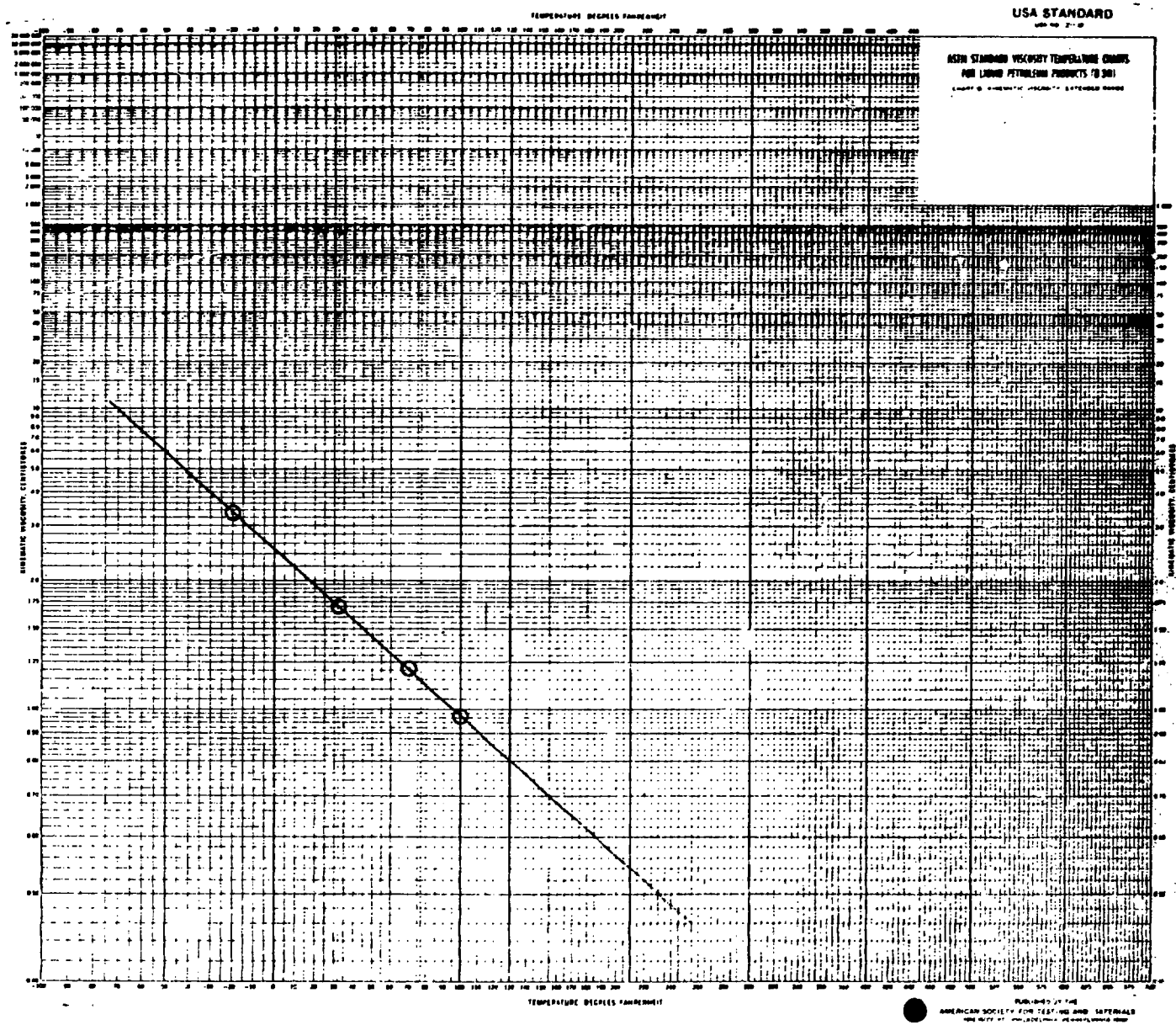

Figure 130. Viscosity/temperature plot for fuel sample GEC-120-4AO-792033.

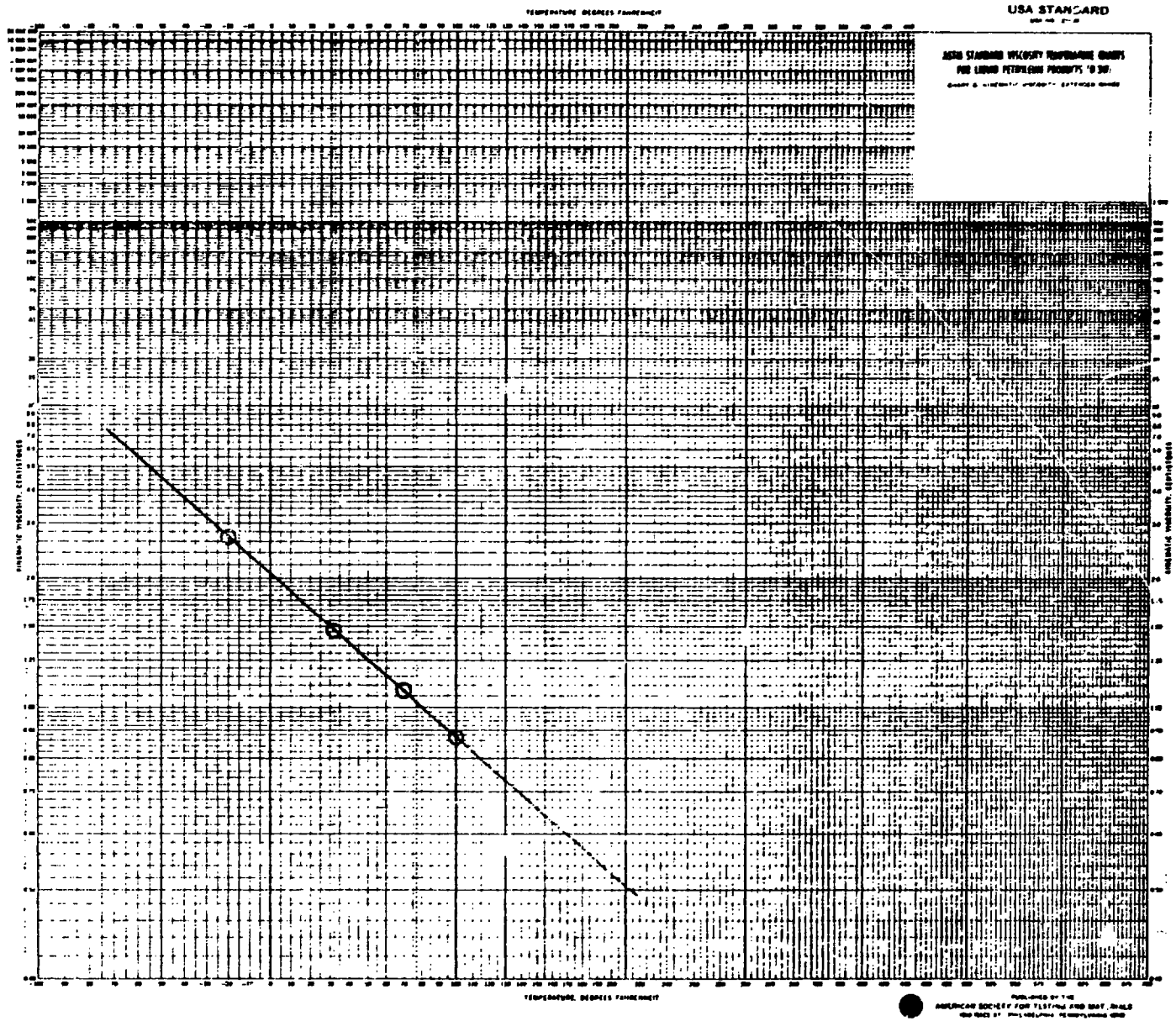

Figure 131. Viscosity/temperature plot for fuel sample GEC-130-4AO-792033.

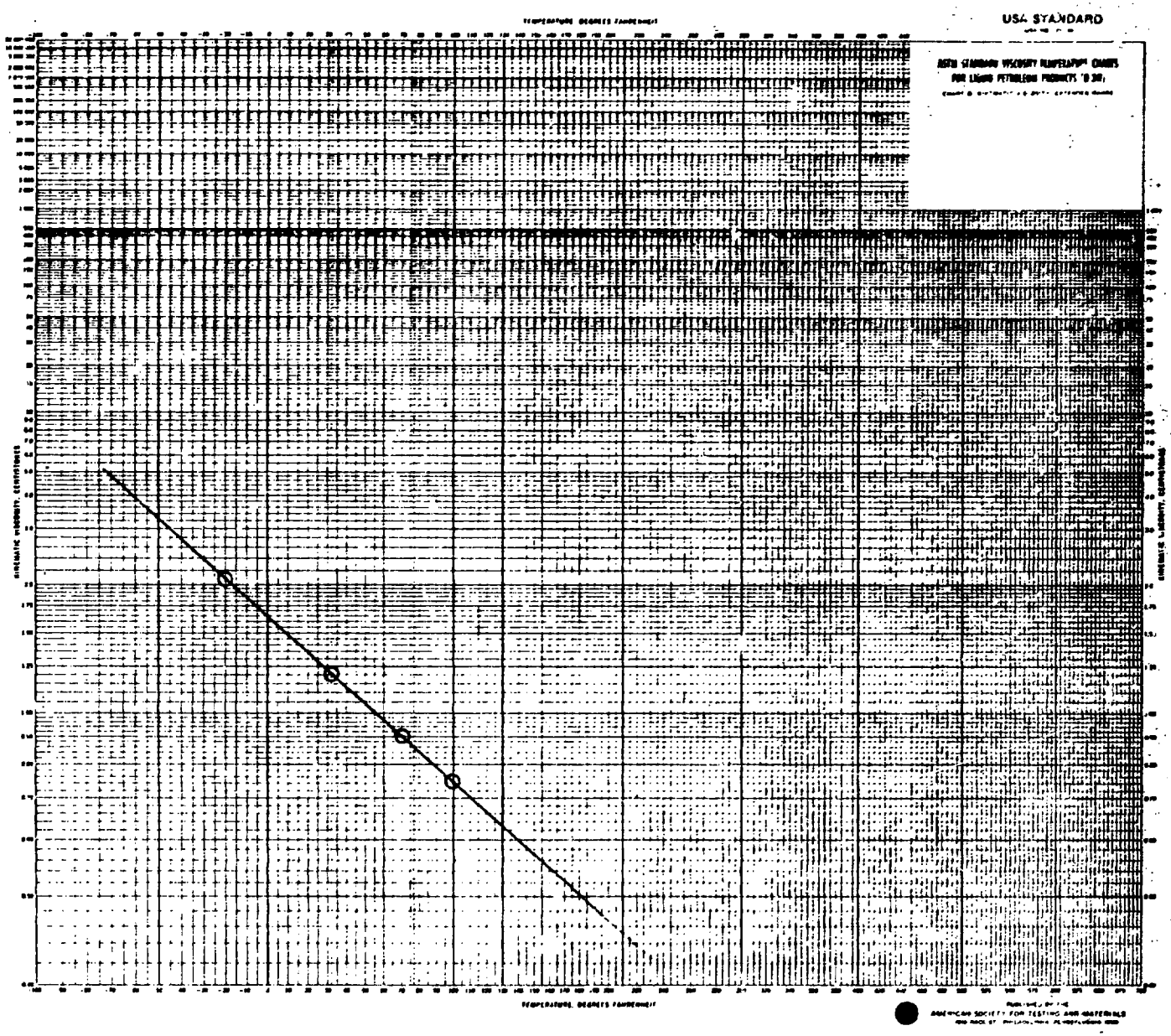

Figure 132. Viscosity/temperature plot for fuel sample GEC-120-X40-792033 Feb.

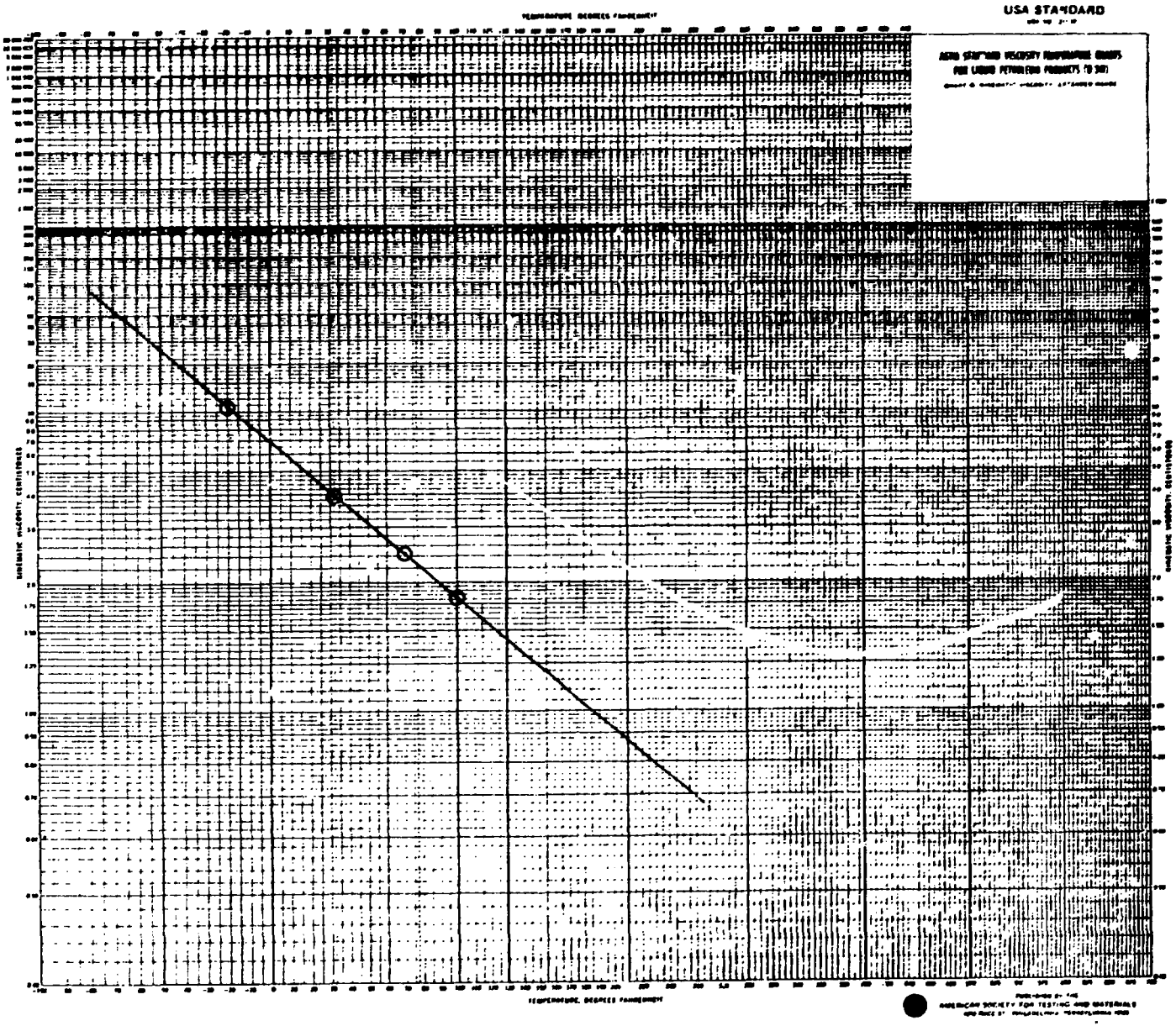

Figure 133. Viscosity/temperature plot for fuel sample GEC-140-8GO-792033 Feb.

first number in the codes for these fuels indicates whether the base fuel was JP-4 (4) or JP-8 (8). The letter(s) following the first number indicate whether the blending stock was 2040 Solvent (A), xylene bottoms (X), or Gulf Mineral Seal Oil (GM). The last number in the initial three characters of the fuel code indicates the nominal hydrogen content 12% (2) or 13% (3). The fuel codes terminating with "792033" were tested in the J79 Low-Smoke Combustor; sample codes for these fuels are as follows. The number following the first hyphen now designates the nominal blended hydrogen content (12.0%, 13.0%, or 14.0%). The number and letters indicate the fuel type (JP-4 or JP-8) and the blending stock. Aromatic 2040 stock only (AO), xylene bottoms only (XO), Gulf Mineral Seal Oil only (GO), and Gulf Mineral Seal Oil and xylene bottoms (GX) are the blending materials used. All fuels were provided to MRC after blending.

10. PHYSICAL PROPERTIES OF EXPERIMENTAL FUEL BLENDS

Before-and-after testing property data were required for a number of experimental fuel blends which had been subjected to full-scale testing by an engine manufacturer. The engine manufacturer's tests included idle point, ignition, and fouling. The physical property measurements were conducted by the procedures described in the Appendix, and the analytical data are shown in the following tables:

Kinematic viscosity by ASTM D 445 - Table 153 and Figures 134-165,
Vapor pressure by the micro-method - Table 154,
Density by the dilatometer method - Table 155,
Specific gravity and API gravity from density data - Table 156,
Surface tension by the capillary rise method - Table 157,
Hydrocarbon type by ASTM D 2789 - Table 158,
Simulated distillation by gas chromatography, ASTM D 2887 - Table 159,

Specific gravity and API gravity were calculated from the density data shown in Table 155.

TABLE 153. KINEMATIC VISCOSITY OF EXPERIMENTAL FUEL BLENDS

Sample	Centistokes 0°F	77°F	100°F
Fouling test			
#1	1.866	0.9315	0.8035
#2	2.601	1.146	0.9665
#4	1.703	0.8860	0.7654
#5	1.765	0.9146	0.7890
#6	2.370	1.133	0.9627
#7	5.974	2.062	1.657
#8	5.793	1.956	1.572
#9	5.834	1.999	1.609
#10	2.750	1.231	1.034
#12	7.105	2.307	1.833
Ignition			
#1, JP-4	1.934	0.9796	0.8407
#2	2.825	1.243	1.044
#3	2.430	1.128	0.9562
#5	2.753	1.240	1.043
#6	2.480	1.161	0.9851
#7, JP-8	5.441	1.942	1.571
#8	5.711	1.938	1.560
#9	5.223	1.864	1.510
#10	2.662	1.209	1.018
#11	3.504	1.450	1.203
#12	3.918	1.580	1.303
Fuel idle point			
#1	1.857	0.9494	0.8185
#2	2.609	1.171	0.9880
#3	2.218	1.062	0.9053
#4	1.716	0.8908	0.7685
#5	1.768	0.9135	0.7879
#7	6.053	2.075	1.667
#8	5.819	1.956	1.572
#9	5.873	2.003	1.611
#10	2.715	1.228	1.034
#11	3.740	1.516	1.253
#12	7.090	2.303	1.829

TABLE 154. VAPOR PRESSURE OF EXPERIMENTAL FUEL BLENDS

Sample		mm HG 32°F	70°F	100°F
Fouling Test	#1	41.0	86.0	146.0
	#2	20.5	47.5	86.0
	#4	21.5	45.5	77.0
	#5	20.5	47.5	86.0
	#6	30.5	66.0	114.0
	#7	9.5	15.0	20.5
	#8	11.0	17.0	27.5
	#9	10.0	16.5	27.5
	#10	7.0	13.5	21.5
	#12	11.5	16.0	21.0
Ignition	#1, JP-4	29.5	65.0	113.0
	#2	19.5	44.0	76.5
	#3	22.0	48.0	83.0
	#5	17.0	39.5	69.0
	#6	22.0	51.0	91.0
	#7, JP-8	11.0	20.5	31.0
	#8	9.5	16.0	22.5
	#9	10.0	19.0	29.5
	#10	12.0	26.0	45.0
	#11	9.5	20.5	34.0
	#12	13.0	26.0	42.0
Fuel [redacted]	#1,	41.5	86.0	143.0
	#2	21.0	48.5	86.0
	#3	28.5	63.5	111.0
	#4	17.5	39.0	67.5
	#5	24.0	53.5	93.5
	#7,	10.0	14.5	18.5
	#8	10.5	16.0	22.0
	#9	7.0	11.5	16.5
	#10	5.0	10.5	19.0
	#11	5.5	11.0	17.5
	#12	10.0	14.5	19.5

TABLE 155. DENSITY OF EXPERIMENTAL FUEL BLENDS

Sample	Grams per cubic centimeter 32°F	70°F	100°F
Ignition #1	0.7769	0.7603	0.7474
Ignition #2	0.8449	0.8285	0.8154
Ignition #3	0.8296	0.8130	0.8001
Ignition #5	0.8230	0.8068	0.7941
Ignition #6	0.7952	0.7795	0.7669
Ignition #7	0.8214	0.8066	0.7946
Ignition #8	0.8709	0.8552	0.8430
Ignition #9	0.8443	0.8288	0.8166
Ignition #10	0.8424	0.8261	0.8132
Ignition #11	0.8395	0.8239	0.8112
Ignition #12	0.8286	0.8128	0.8004

TABLE 156. GRAVITY VALUES FOR EXPERIMENTAL FUEL BLENDS

Sample	Specific Gravity 60/60°F	API Gravity, °
Ignition #1	0.765	53.47
Ignition #2	0.834	38.16
Ignition #3	0.818	41.48
Ignition #5	0.812	42.76
Ignition #6	0.784	48.98
Ignition #7	0.811	42.98
Ignition #8	0.860	33.03
Ignition #9	0.834	38.16
Ignition #10	0.831	38.78
Ignition #11	0.829	39.19
Ignition #12	0.818	41.48

TABLE 157. SURFACE TENSION OF EXPERIMENTAL FUEL BLENDS

Sample	Dynes/cm 32°F	70°F	100°F
Ignition #1	25.81	23.67	22.01
Ignition #2	28.09	26.28	24.86
Ignition #3	27.38	25.93	24.08
Ignition #5	27.98	25.52	24.35
Ignition #6	25.61	24.67	23.17
Ignition #7	28.91	26.89	25.31
Ignition #8	30.47	28.53	27.02
Ignition #9	29.50	27.33	25.63
Ignition #10	28.70	26.80	25.35
Ignition #11	29.09	27.00	25.38
Ignition #12	28.78	26.75	25.18

TABLE 158. HYDROCARBON-TYPE ANALYSIS OF EXPERIMENTAL FUEL BLENDS FROM IGNITION TESTS

Compound Types	Liquid Volume Percent #1	#2	#3	#5	#6	#7	#8	#9	#10	#11	#12
Paraffins	63.8	40.1	42.0	43.5	58.1	45.1	33.4	39.8	32.9	37.8	41.5
Monocycloparaffins	22.0	25.2	25.4	29.6	21.3	41.4	30.8	35.4	24.8	30.8	33.4
Dicycloparaffins	4.8	-	-	-	5.5	1.8	1.6	1.5	0.3	0.8	0.8
Alkylbenzenes	7.7	16.6	22.1	21.0	13.2	7.0	10.7	9.5	37.3	24.7	20.9
Indans & Tetralins	1.3	3.1	1.7	1.5	1.4	3.3	5.2	4.1	0.3	1.8	1.7
Naphthalenes	0.4	15.0	8.8	4.4	0.5	1.4	18.3	9.7	4.4	5.1	1.7

TABLE 159. SIMULATED DISTILLATION BY GAS CHROMATOGRAPHY

Percent Recovered	Fouling Test #1		Fouling Test #2		Fouling Test #4	
	BP, °C	BP, °F	BP, °C	BP, °F	BP, °C	BP, °F
0.5, IBP	-2	28	22	72	11	52
1	-1	30	31	88	18	64
5	28	82	75	167	59	138
10	46	115	89	192	79	174
20	59	138	112	234	102	216
30	75	167	136	277	123	253
40	89	192	168	334	135	275
50	106	223	191	376	144	291
60	130	266	206	403	147	297
70	152	306	224	435	153	307
80	172	342	229	444	171	340
90	193	379	248	478	206	403
95	208	406	262	504	227	441
99	229	444	286	547	256	493
99.5, FBP	251	484	295	563	268	514

Percent Recovered	Fouling Test #5		Fouling Test #6		Fouling Test #7	
	BP, °C	BP, °F	BP, °C	BP, °F	BP, °C	BP, °F
0.5, IBP	23	73	27	81	113	235
1	33	91	35	95	132	270
5	79	174	75	167	170	338
10	106	223	92	198	184	363
20	120	248	116	244	199	390
30	141	286	134	273	208	406
40	155	311	155	311	218	424
50	164	327	170	338	225	437
60	172	342	191	376	234	453
70	190	374	215	419	241	466
80	213	415	237	459	253	487
90	235	455	277	531	265	509
95	251	484	306	583	274	525
99	278	532	335	635	293	559
99.5, FBP	291	556	343	649	301	574

Percent Recovered	Fouling Test #8		Fouling Test #9		Fouling Test #10	
	BP, °C	BP, °F	BP, °C	BP, °F	BP, °C	BP, °F
0.5, IBP	125	257	122	252	102	216
1	142	288	139	282	123	253
5	176	349	173	343	134	273
10	190	374	186	367	143	289
20	204	399	200	392	153	307
30	214	417	210	410	158	316
40	222	432	220	428	165	329
50	233	451	228	442	185	365
60	239	462	235	455	202	396
70	248	478	242	468	216	421
80	257	495	255	491	229	444
90	270	518	267	513	247	477
95	280	536	276	529	261	502
99	302	576	298	568	282	538
99.5, FBP	313	595	306	583	290	554

TABLE 159 (continued)

Percent Recovered	Fouling Test #12 BP, °C	Fouling Test #12 BP, °F	Ignition #1, JP-4 BP, °C	Ignition #1, JP-4 BP, °F	Ignition #2 BP, °C	Ignition #2 BP, °F
0.5, IBP	135	275	25	77	37	99
1	148	298	27	81	49	120
5	172	342	65	149	99	210
10	186	367	87	189	115	239
20	200	392	105	221	143	289
30	212	414	124	255	175	347
40	221	430	141	286	191	376
50	231	448	165	329	213	415
60	240	464	185	365	228	442
70	251	484	205	401	244	471
80	265	509	223	433	253	487
90	290	554	242	468	271	520
95	307	585	256	493	285	545
99	336	637	276	529	307	585
99.5, FBP	346	655	290	554	317	603

Percent Recovered	Ignition #3 BP, °C	Ignition #3 BP, °F	Ignition #5 BP, °C	Ignition #5 BP, °F	Ignition #6 BP, °C	Ignition #6 BP, °F
0.5, IBP	29	84	33	91	9	48
1	39	102	53	127	17	63
5	86	187	91	196	53	127
10	102	216	109	228	74	165
20	128	262	142	288	100	212
30	156	313	163	325	118	244
40	169	336	173	343	139	282
50	184	363	193	379	154	309
60	206	403	210	410	178	352
70	222	432	225	437	201	394
80	238	460	237	459	222	432
90	256	493	256	493	255	491
95	268	514	272	522	287	549
99	292	558	305	581	313	595
99.5, FBP	303	577	317	603	319	606

TABLE 159 (continued)

Percent Recovered	Ignition #7, JP-8 BP, °C	Ignition #7, JP-8 BP, °F	Ignition #8 BP, °C	Ignition #8 BP, °F	Ignition #9 BP, °C	Ignition #9 BP, °F
0.5, IBP	75	167	85	185	69	156
1	95	203	107	225	90	194
5	150	302	156	313	141	286
10	178	352	172	342	170	338
20	198	388	188	370	193	379
30	208	406	199	390	205	401
40	219	426	208	406	217	423
50	226	439	219	426	224	435
60	235	455	224	435	233	451
70	243	469	232	450	240	464
80	255	491	244	471	254	489
90	268	514	257	495	267	513
95	278	532	267	513	279	534
99	296	565	290	554	305	581
99.5, FBP	302	576	298	568	317	603

Percent Recovered	Ignition #10 BP, °C	Ignition #10 BP, °F	Ignition #11 BP, °C	Ignition #11 BP, °F	Ignition #12 BP, °C	Ignition #12 BP, °F
0.5, IBP	31	88	50	122	57	135
1	51	124	64	147	69	156
5	90	194	107	225	118	244
10	115	239	134	273	145	293
20	143	289	152	306	165	329
30	154	309	160	320	175	347
40	160	320	183	361	198	388
50	179	354	198	388	211	412
60	198	388	209	408	223	433
70	213	415	222	432	237	459
80	227	441	233	451	252	486
90	245	473	247	477	273	523
95	258	496	261	502	297	567
99	279	534	281	538	328	622
99.5, FBP	287	549	291	556	337	639

Percent Recovered	Fuel #1, Idle Point BP, °C	Fuel #1, Idle Point BP, °F	Fuel #2 IP BP, °C	Fuel #2 IP BP, °F	Fuel #3 IP BP, °C	Fuel #3 IP BP, °F
0.5, IBP	13	55	26	79	24	75
1	24	75	35	95	27	81
5	61	142	75	167	69	156
10	83	181	93	199	91	196
20	102	216	120	248	115	239
30	121	250	145	293	133	271
40	138	280	174	345	155	311
50	157	315	199	390	183	361
60	180	356	212	414	204	399
70	201	394	232	450	220	428
80	221	430	240	464	236	457
90	240	464	259	498	255	491
95	254	489	274	525	263	505
99	271	520	298	568	289	552
99.5, FBP	276	529	306	583	300	572

TABLE 159 (continued)

Percent Recovered	Fuel #4 IP BP, °C	Fuel #4 IP BP, °F	Fuel #5 IP BP, °C	Fuel #5 IP BP, °F	Fuel #7, Idle Point BP, °C	Fuel #7, Idle Point BP, °F
0.5, IBP	27	81	24	75	126	259
1	35	95	33	91	141	286
5	79	174	70	158	171	340
10	97	207	92	198	184	363
20	122	252	118	244	199	390
30	145	293	136	277	208	406
40	157	315	154	309	218	424
50	167	333	166	331	225	437
60	171	340	173	343	233	451
70	178	352	187	369	241	466
80	199	390	211	412	253	487
90	231	448	236	457	265	509
95	250	482	251	484	274	525
99	280	536	274	525	293	559
99.5, FBP	292	558	284	543	298	568

Percent Recovered	Fuel #8 IP BP, °C	Fuel #8 IP BP, °F	Fuel #9 IP BP, °C	Fuel #9 IP BP, °F	Fuel #10 IP BP, °C	Fuel #10 IP BP, °F
0.5, IBP	116	241	92	198	97	207
1	135	275	123	253	129	264
5	175	347	168	334	143	289
10	188	370	183	361	152	306
20	202	396	198	388	162	324
30	212	414	208	406	165	329
40	221	430	217	423	170	338
50	232	450	226	439	187	369
60	237	459	233	451	206	403
70	244	471	241	466	221	430
80	257	495	253	487	236	457
90	269	516	265	509	254	489
95	280	536	276	529	267	513
99	302	576	301	574	287	549
99.5, FBP	308	586	330	626	295	563

Percent Recovered	Fuel #11 IP BP, °C	Fuel #11 IP BP, °F	Fuel #12 IP BP, °C	Fuel #12 IP BP, °F
0.5, IBP	136	277	132	270
1	143	289	144	291
5	157	315	172	342
10	165	329	186	367
20	170	338	200	392
30	179	354	211	412
40	200	392	221	430
50	212	414	230	446
60	223	433	239	462
70	235	455	251	484
80	247	477	264	507
90	262	504	288	550
95	274	525	307	585
99	293	559	335	635
99.5, FBP	300	572	343	649

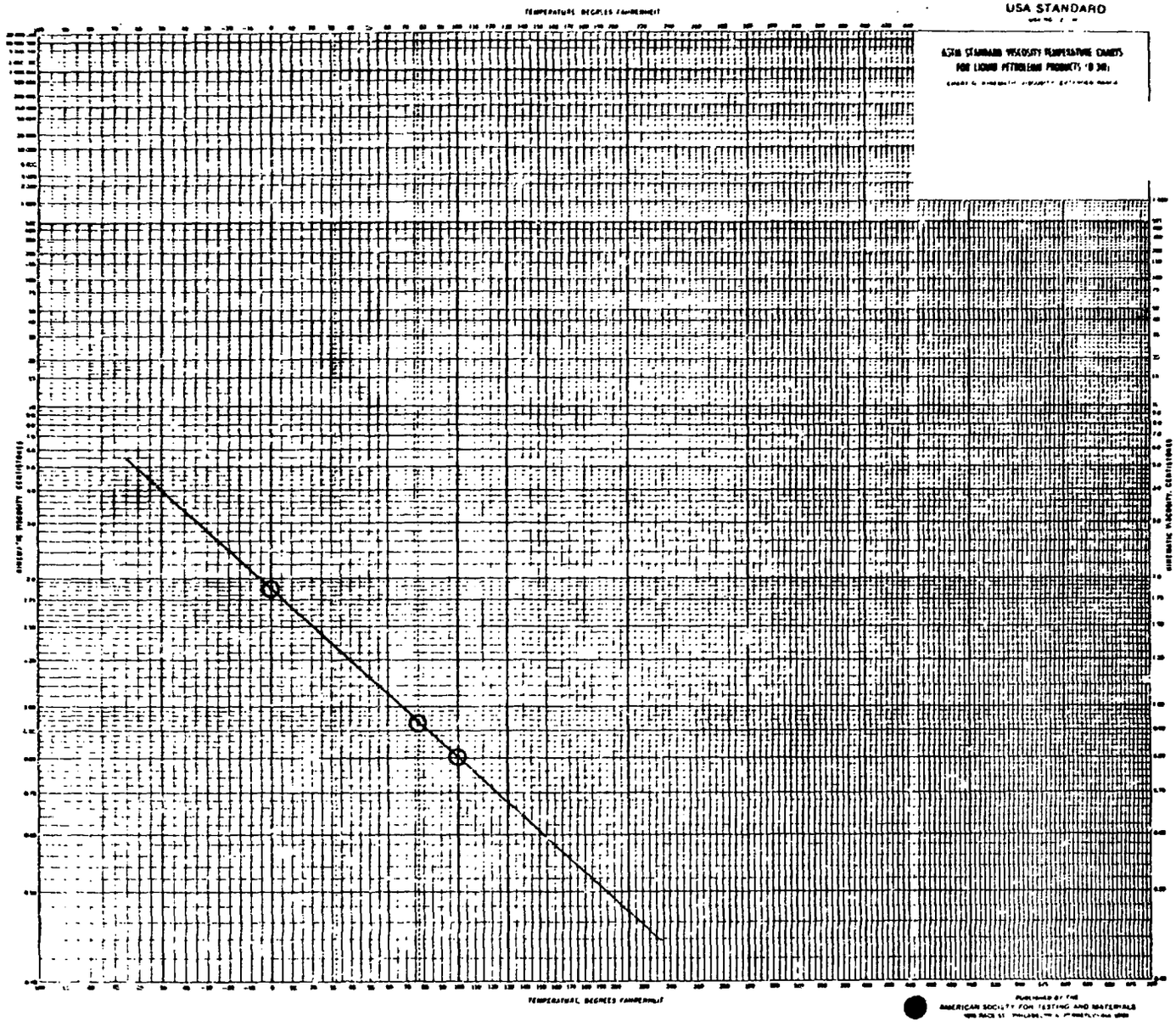

Figure 134. Viscosity/temperature plot for fuel sample from Fouling Test #1.

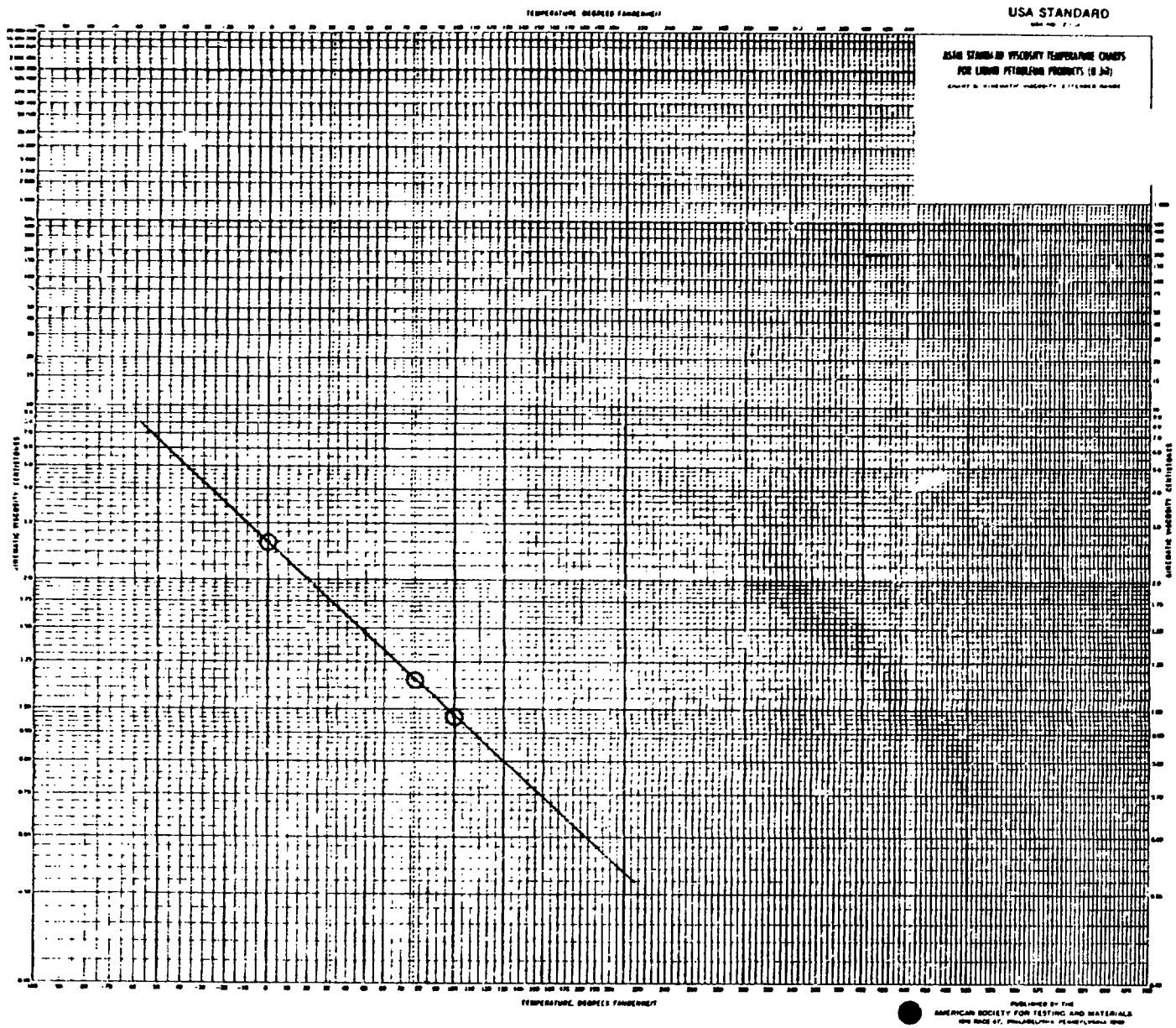

Figure 135. Viscosity/temperature plot for fuel sample from Fouling Test #2.

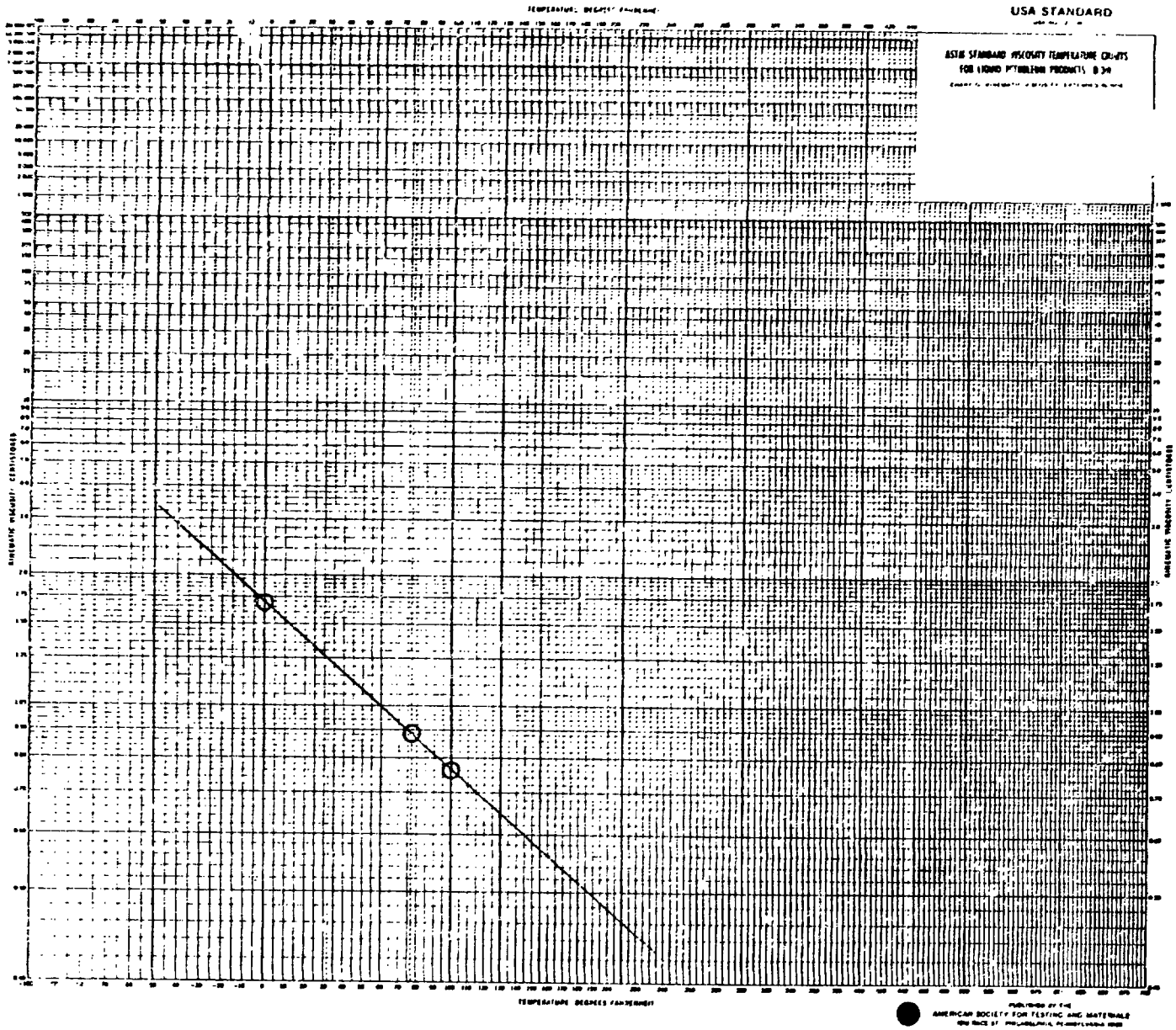

Figure 136. Viscosity/temperature plot for fuel sample from Fouling Test #4.

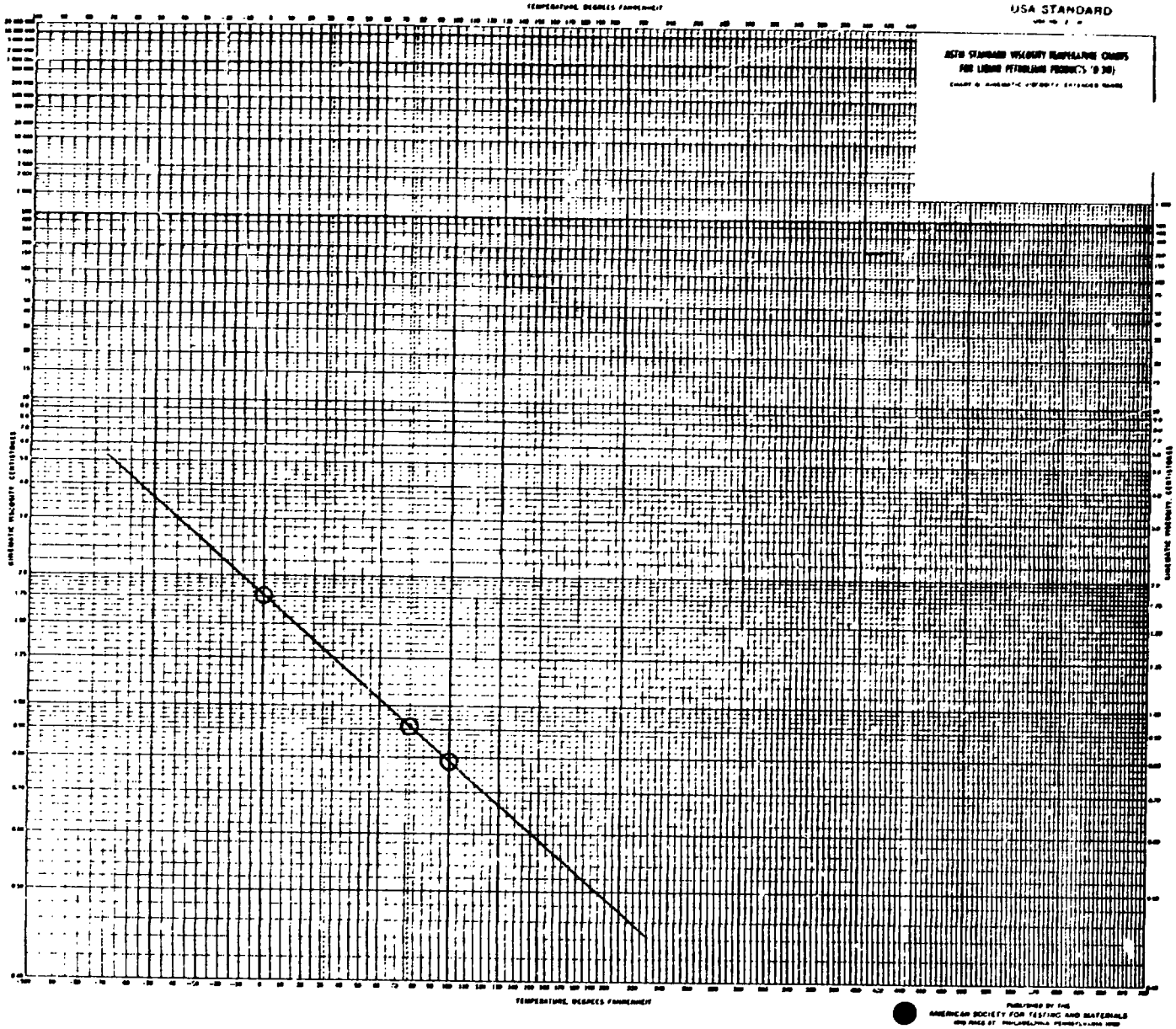

Figure 137. Viscosity/temperature plot for fuel sample from Fouling Test #5.

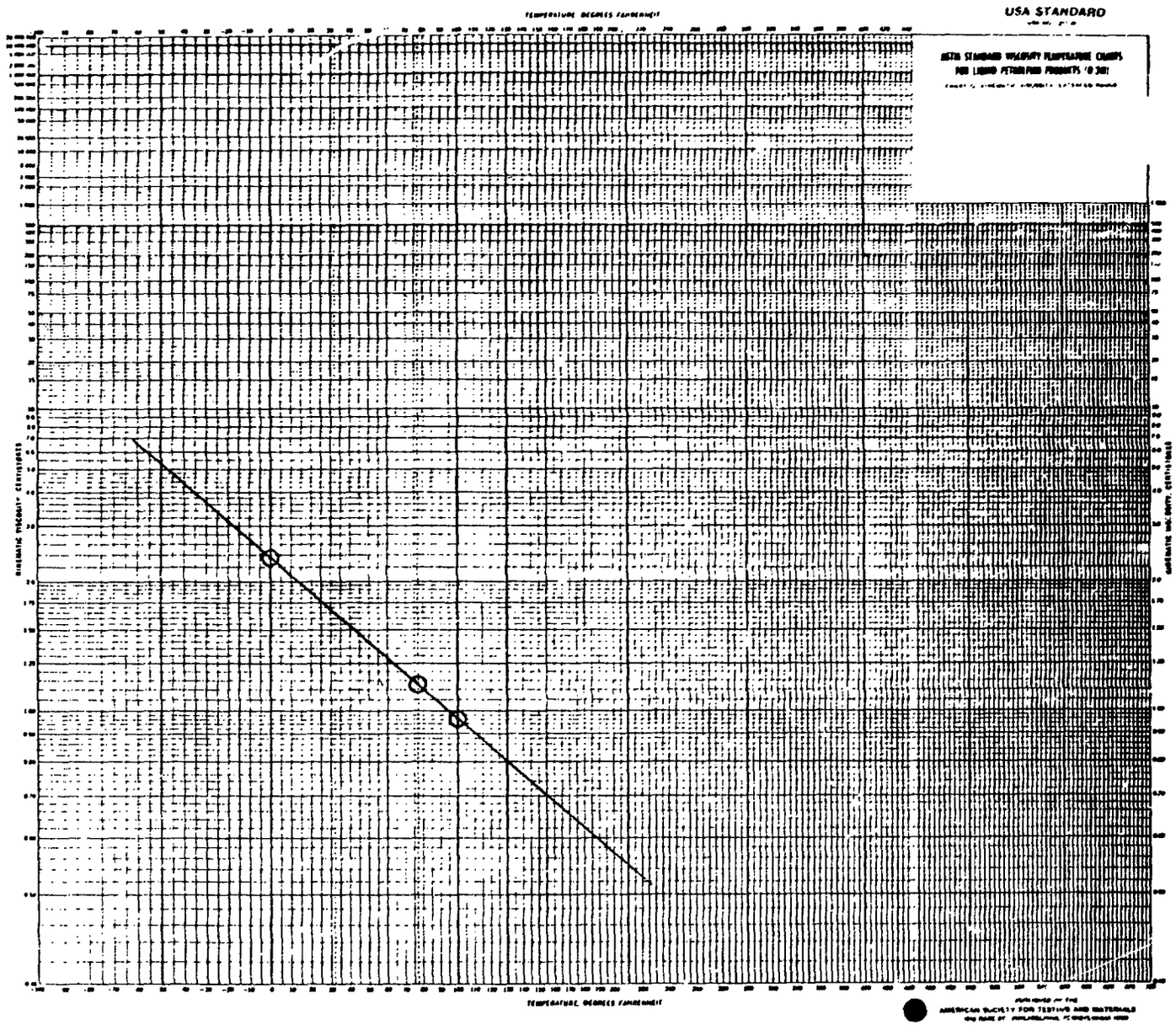

Figure 138. Viscosity/temperature plot for fuel sample from Fouling Test #6.

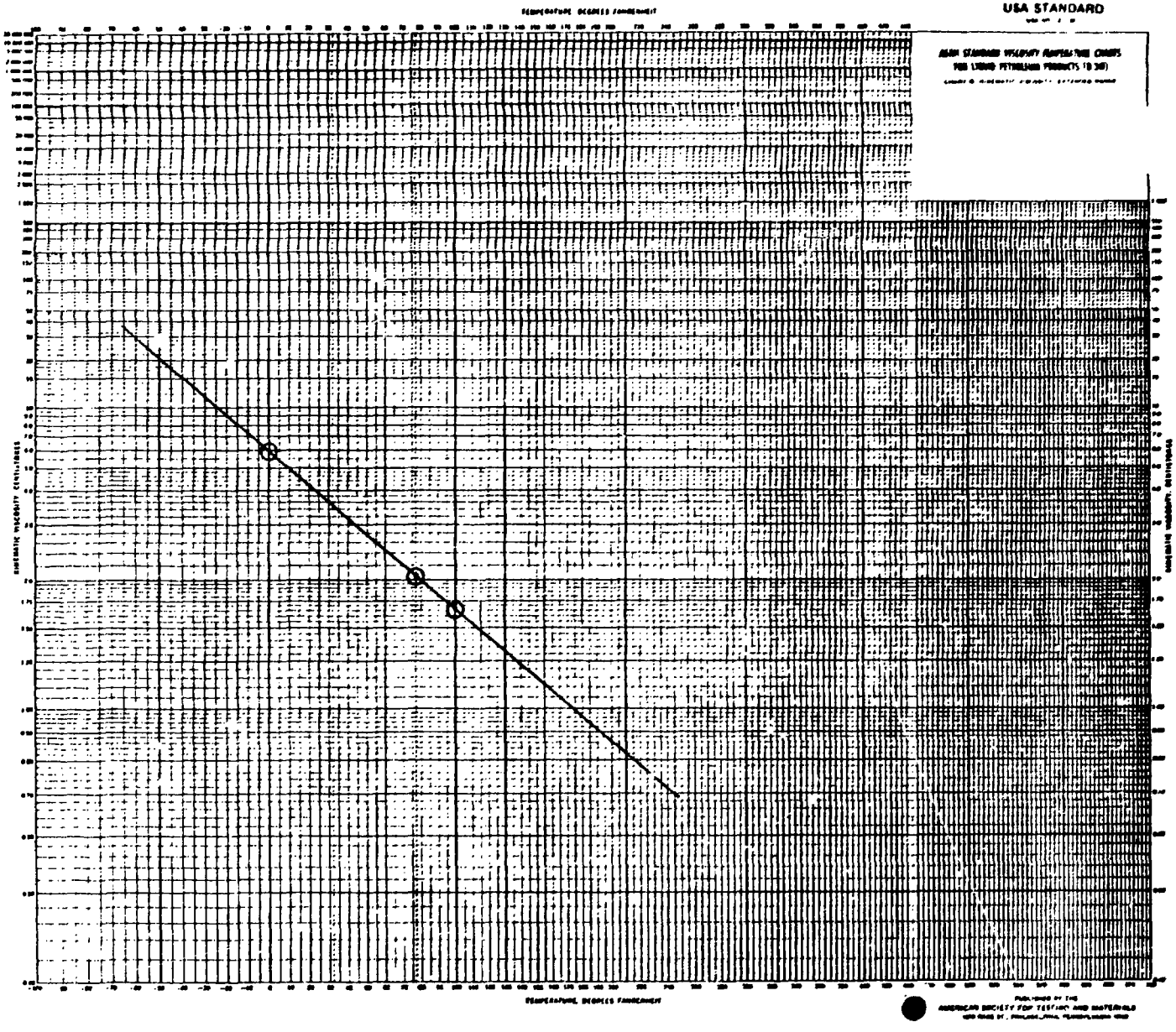

Figure 139. Viscosity/temperature plot for fuel sample from Fouling Test #7.

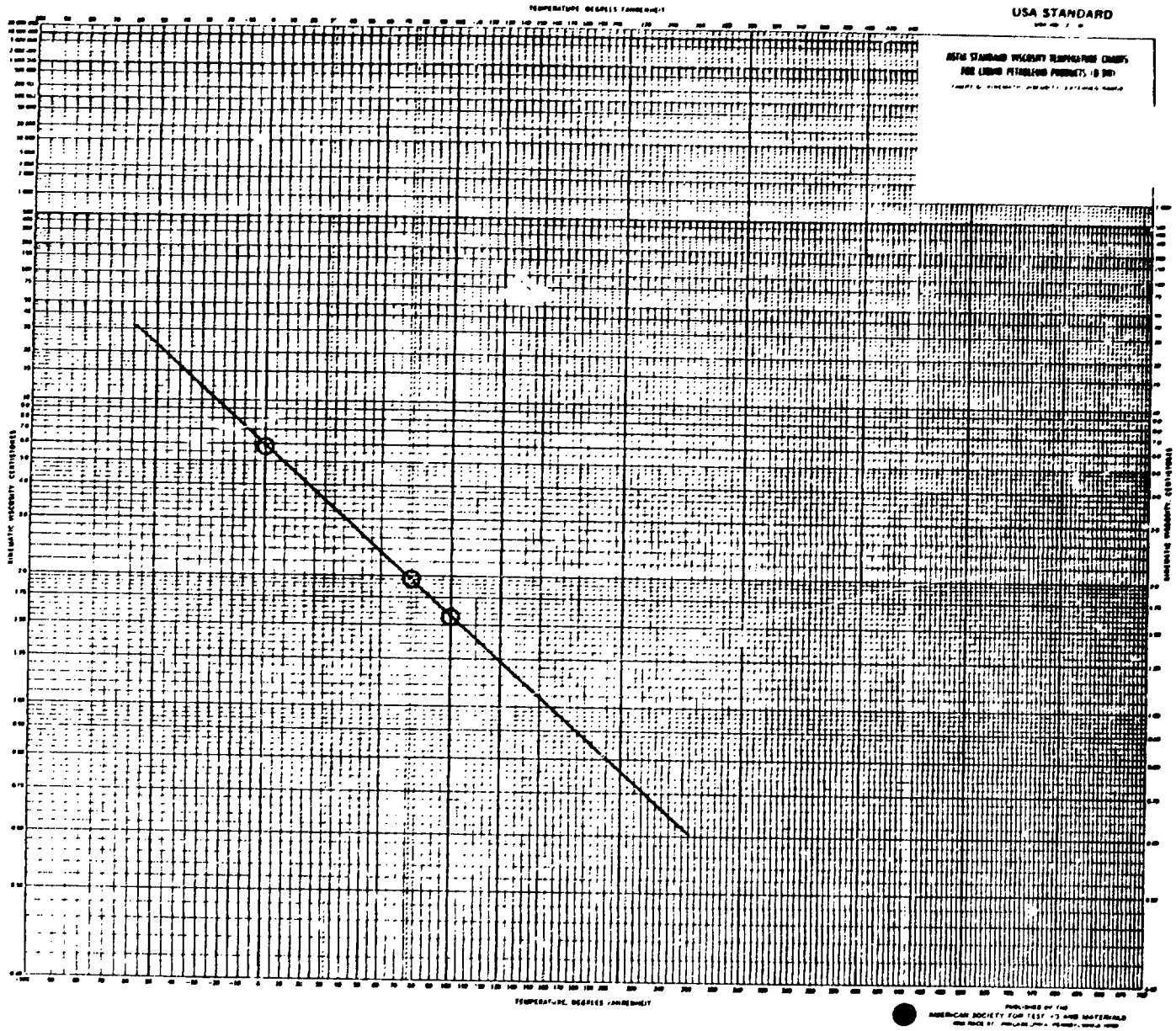

Figure 140. Viscosity/temperature plot for fuel sample from Fouling Test #8.

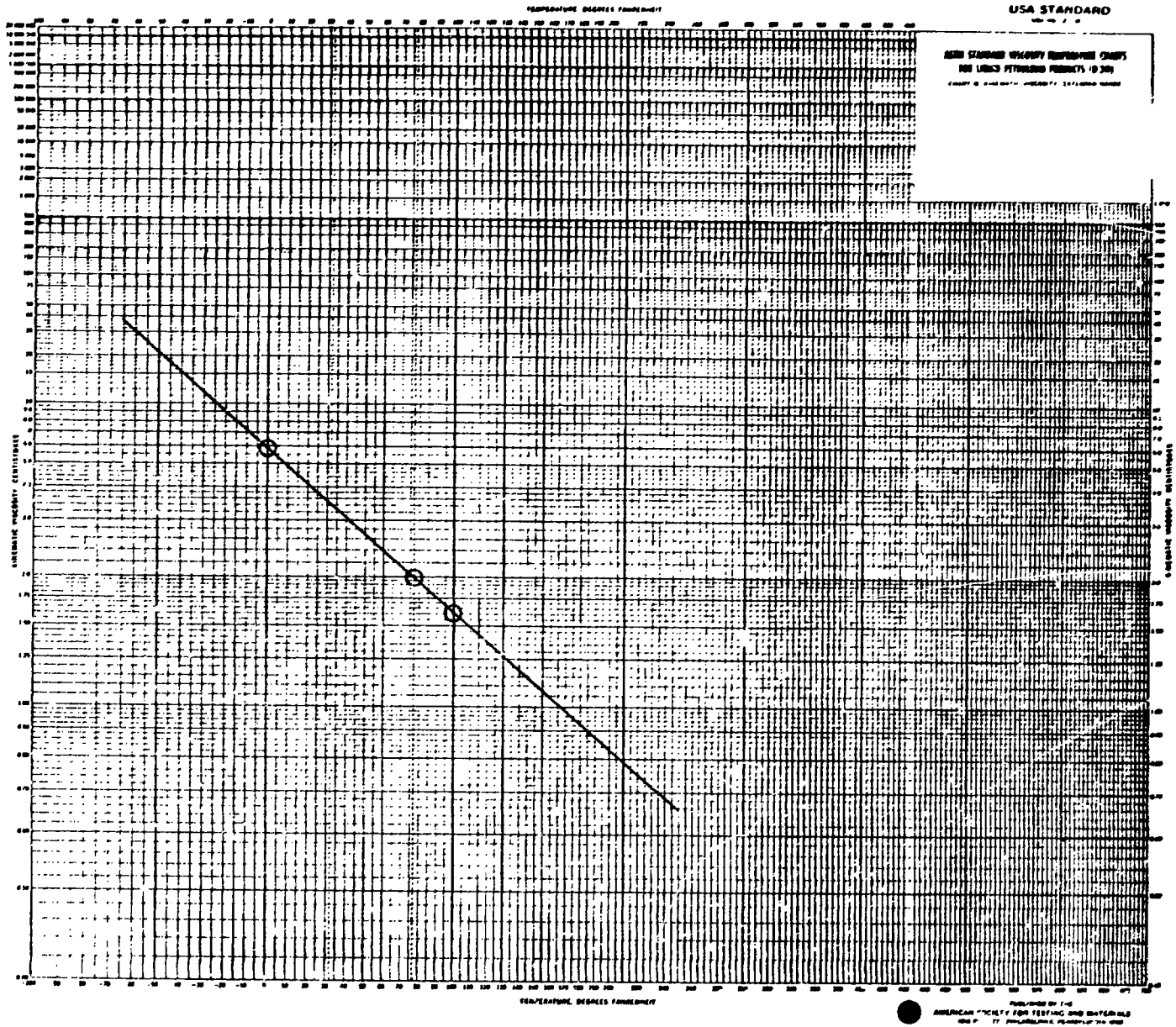

Figure 141. Viscosity/temperature plot for fuel sample from Fouling Test #9.

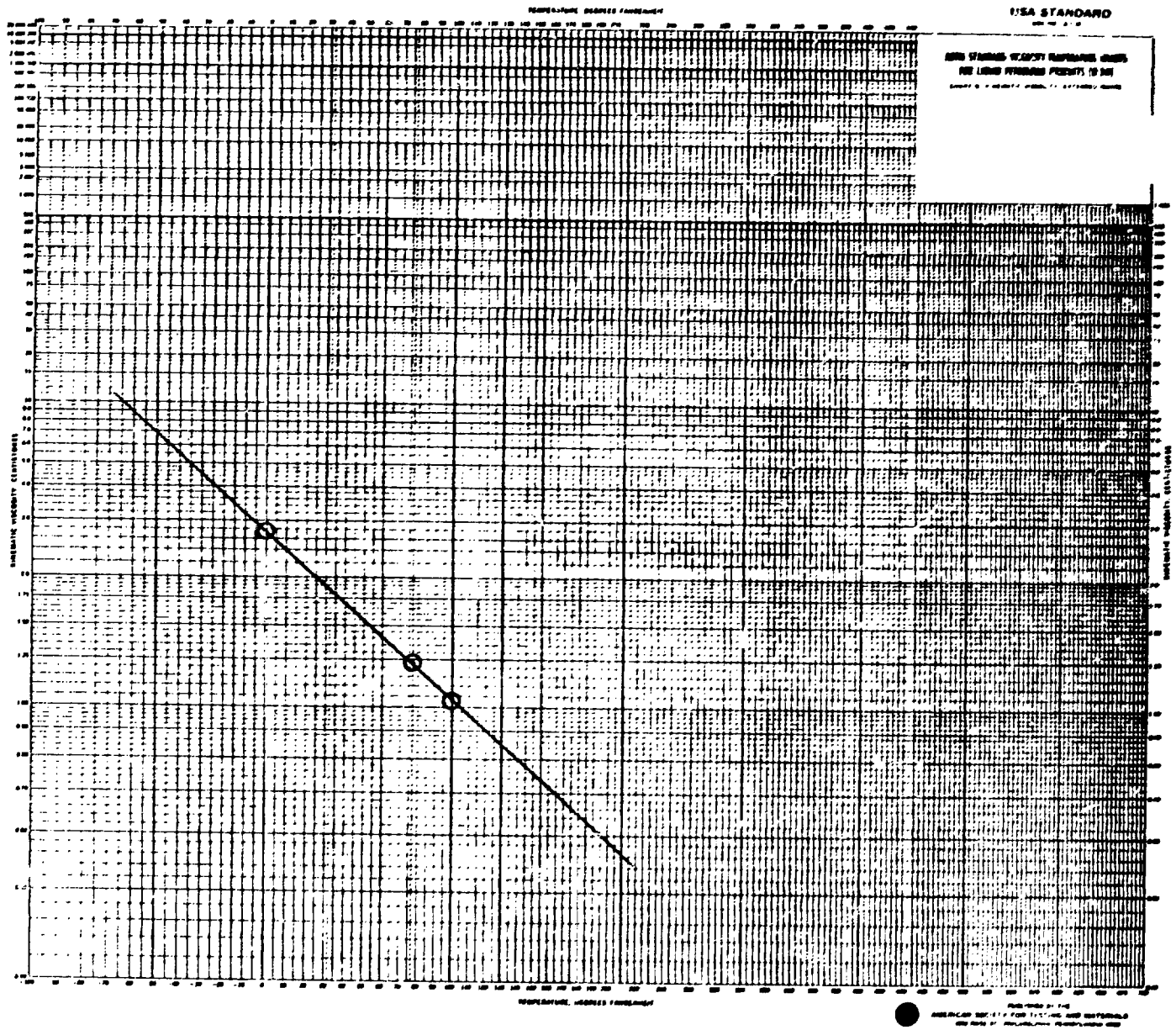

Figure 142. Viscosity/temperature plot for fuel sample from Fouling Test #10

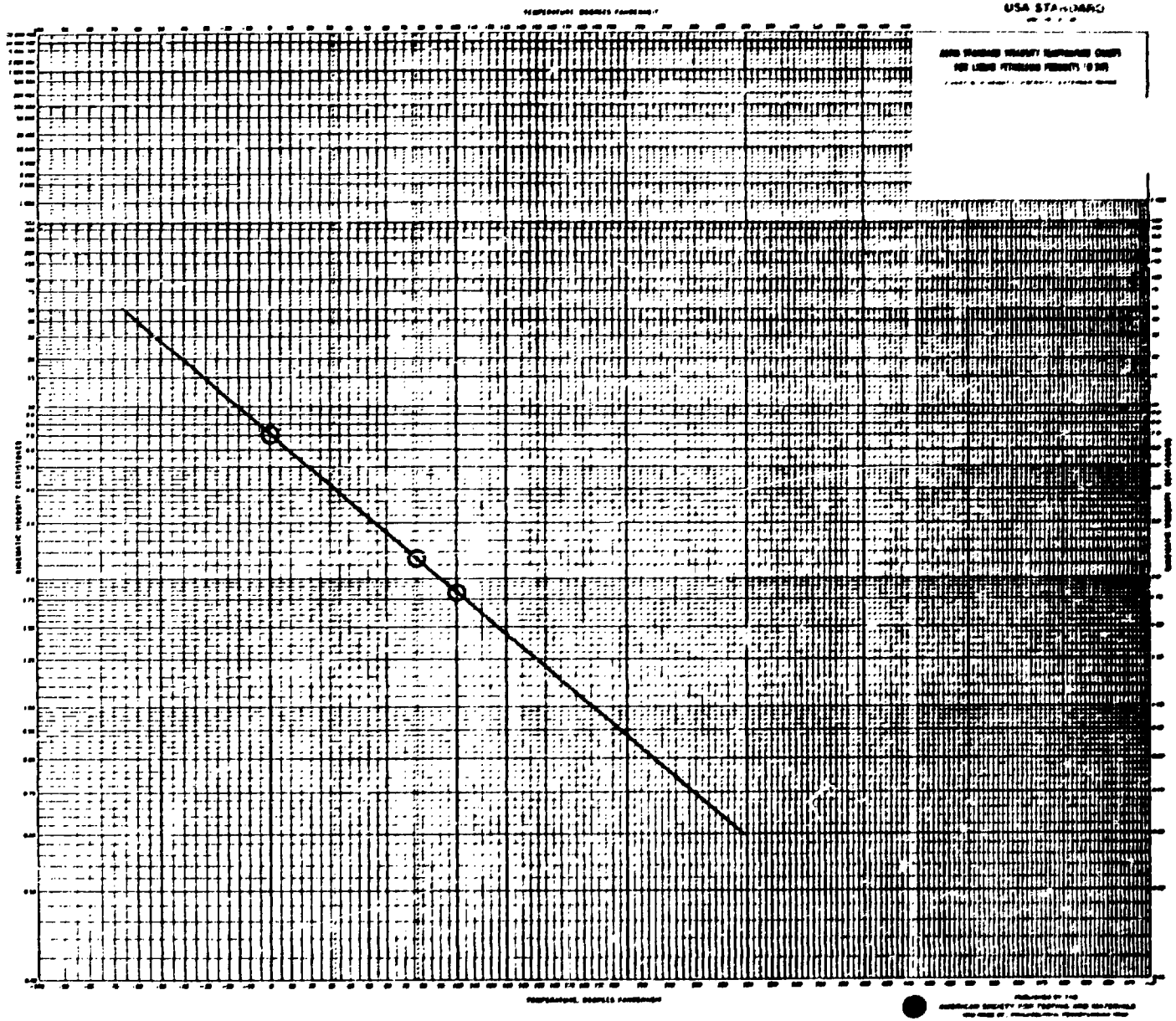

Figure 143. Viscosity/temperature plot for fuel sample from Fouling Test #12.

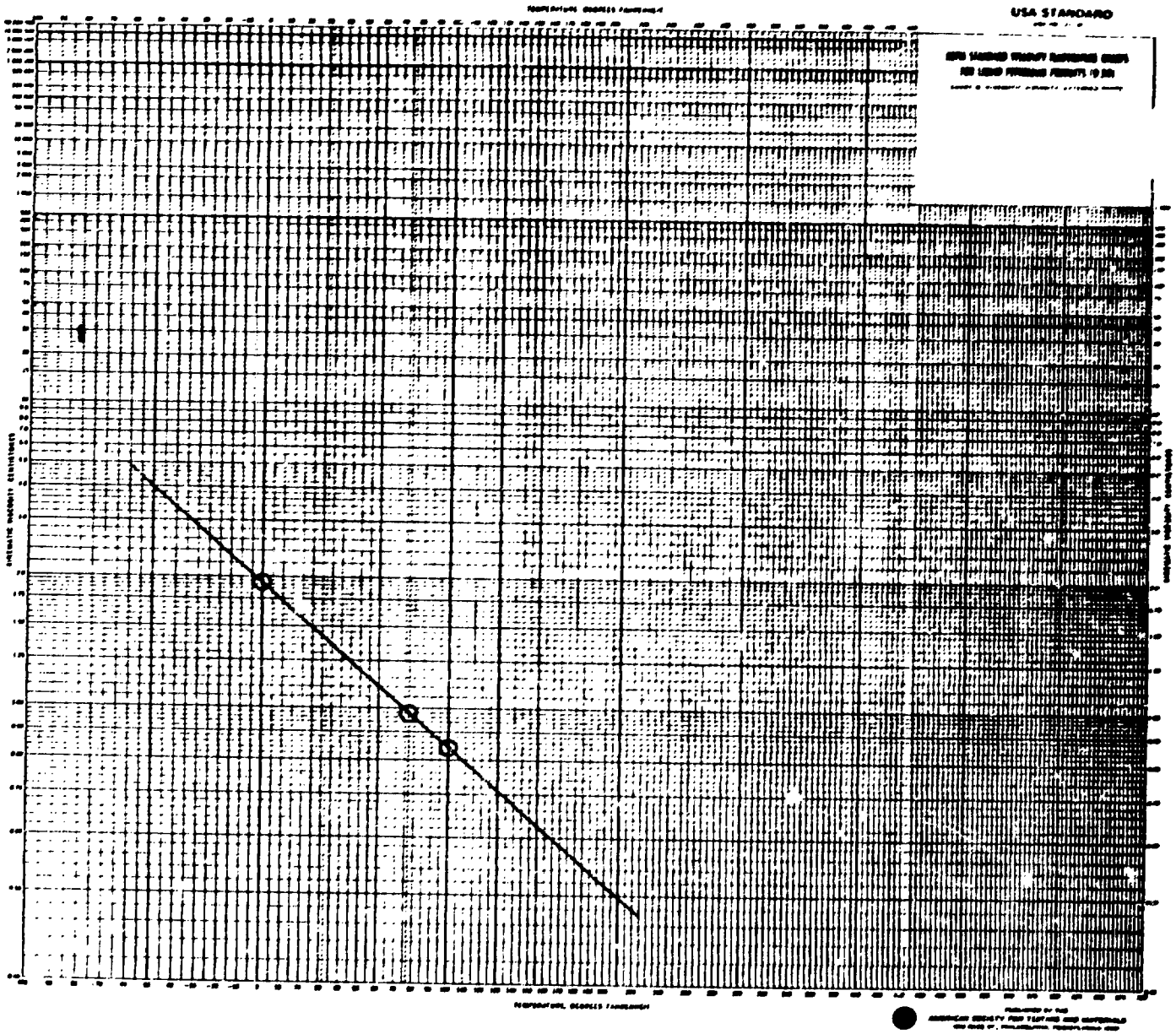

Figure 144. Viscosity/temperature plot for fuel sample from Ignition #1, JP-4.

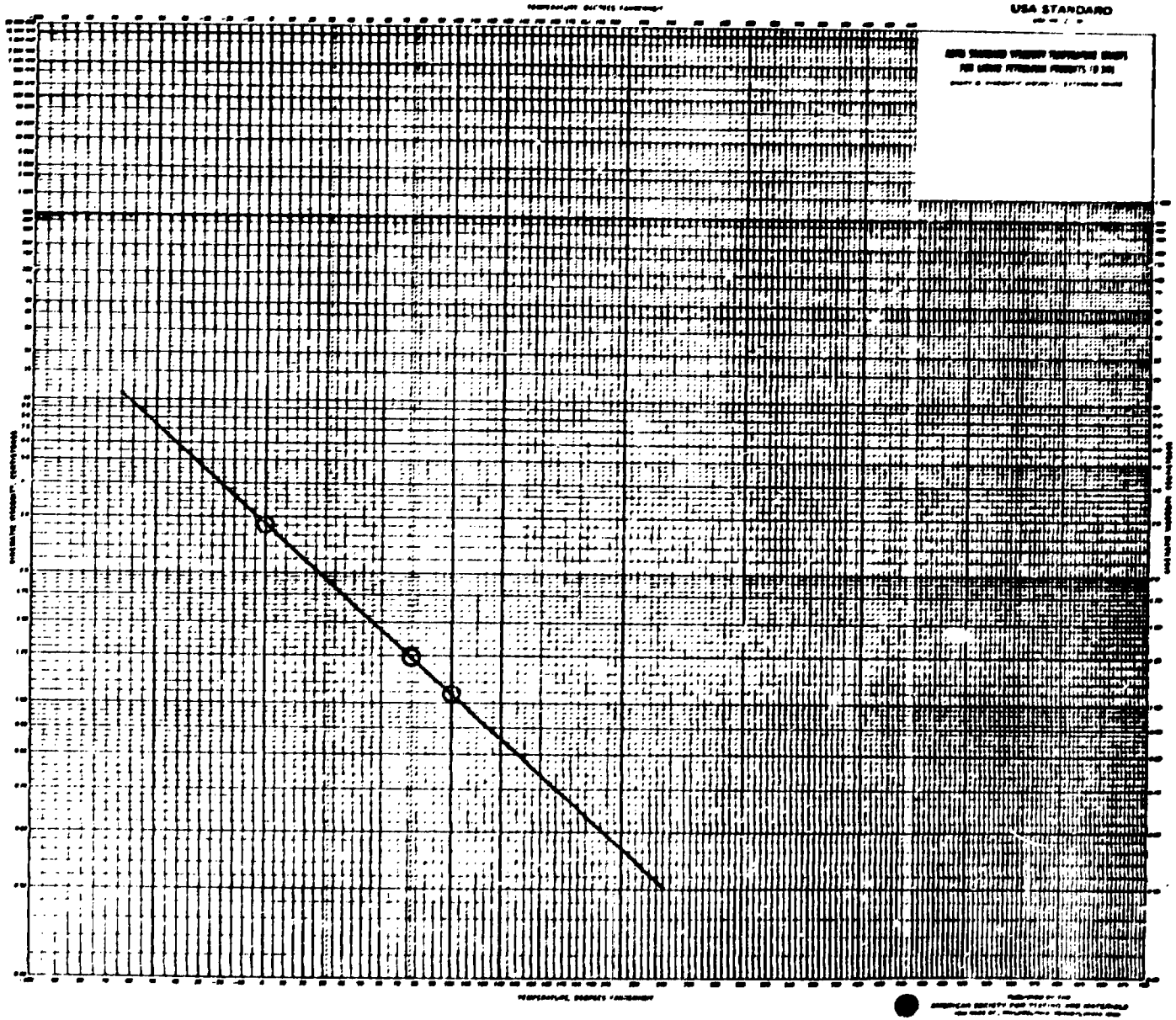

Figure 145. Viscosity/temperature plot for fuel sample fror Ignition #2.

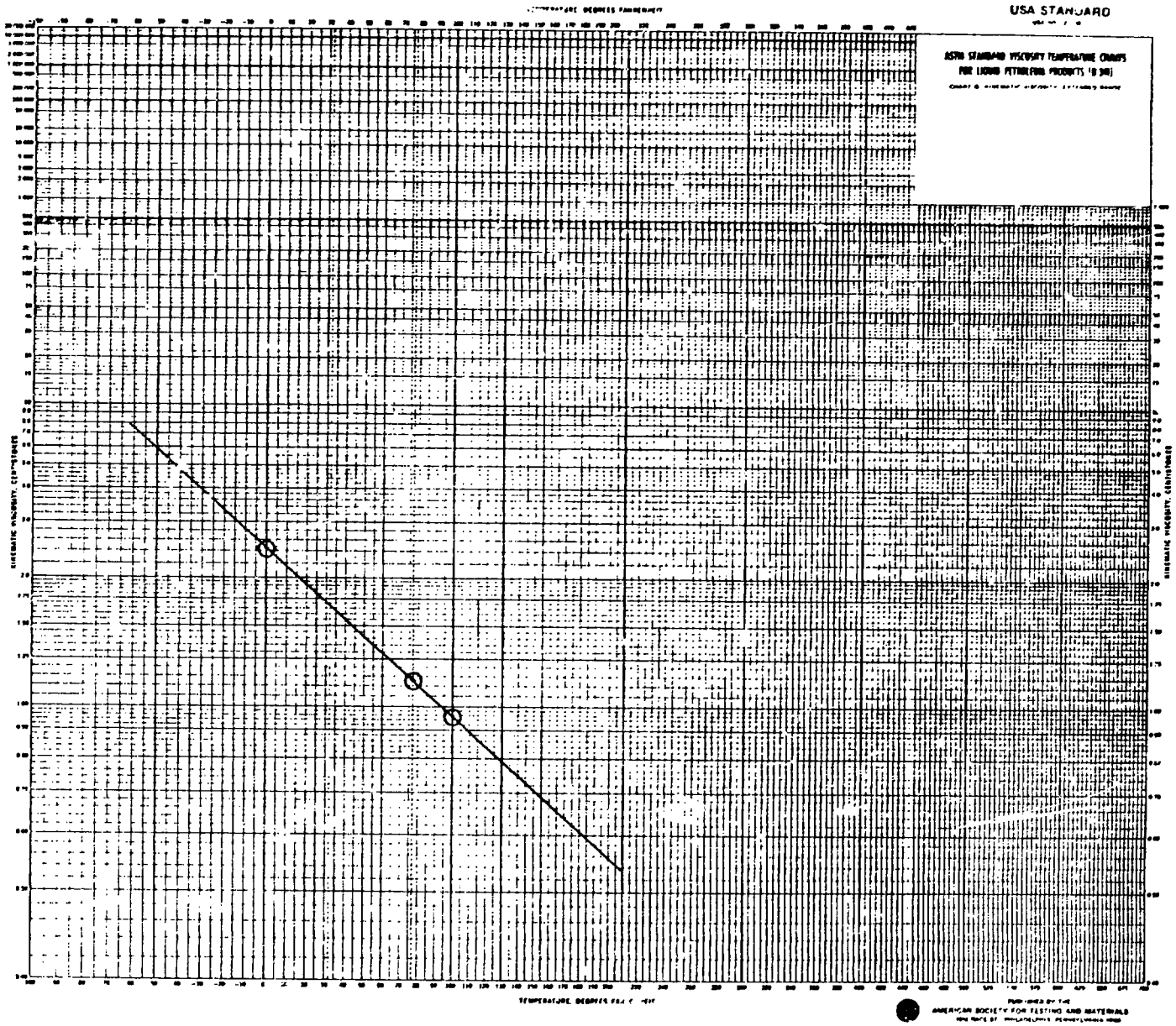

Figure 146. Viscosity/temperature plot for fuel sample from Ignition #3.

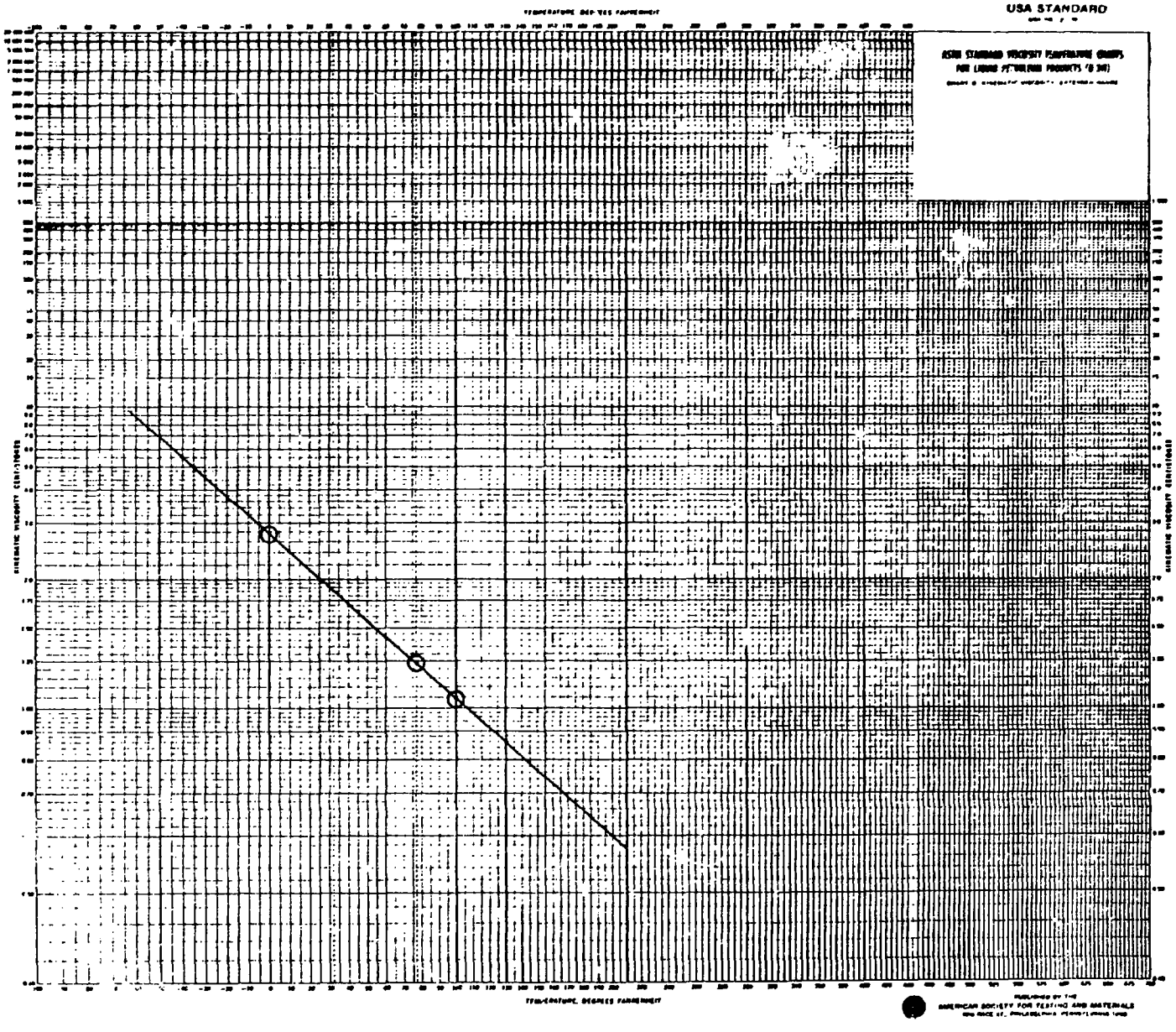

Figure 47. Viscosity/temperature plot for fuel sample from Ignition #5.

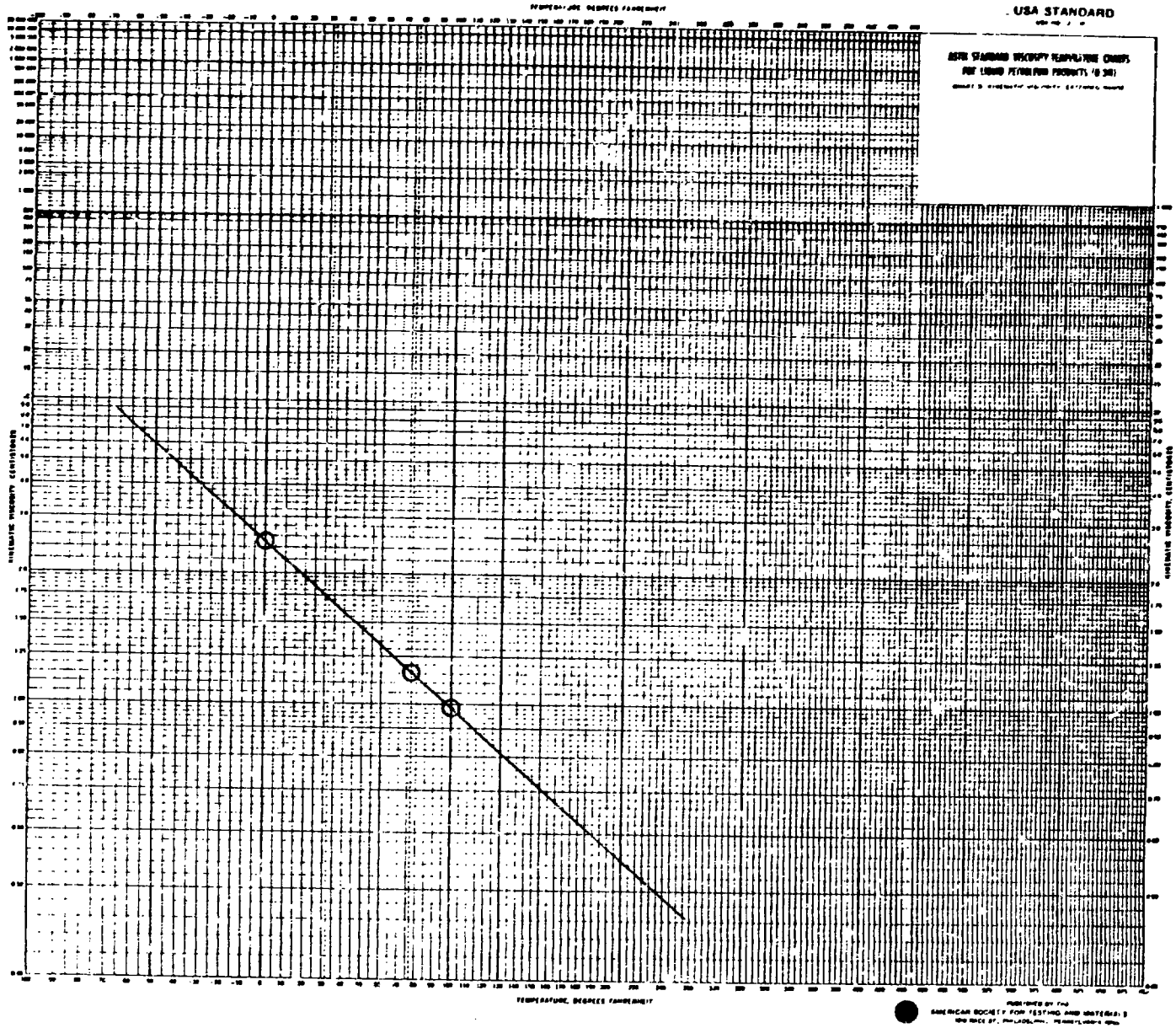

Figure 148. Viscosity/temperature plot for fuel sample from Ignition #6.

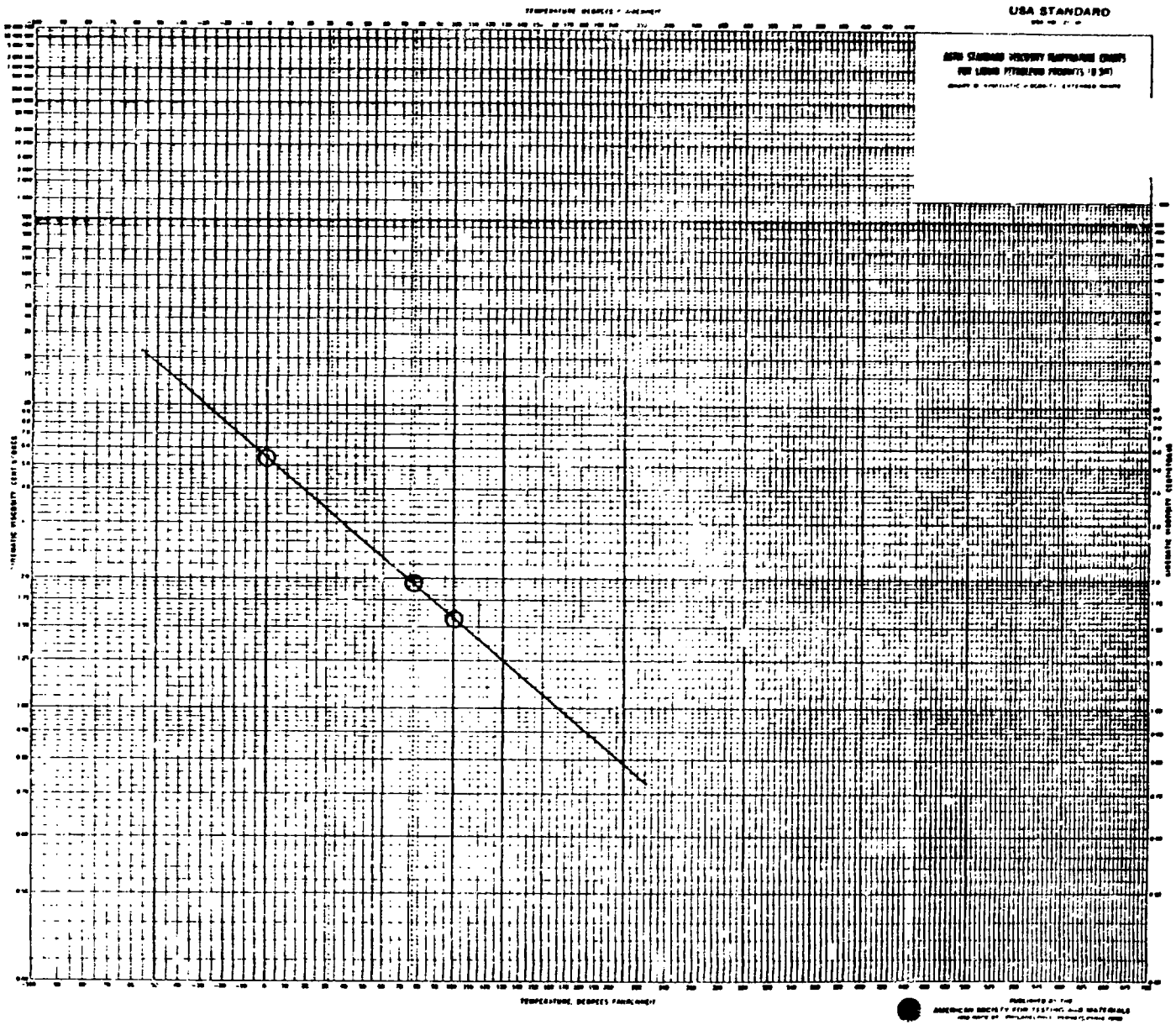

Figure 149. Viscosity/temperature plot for fuel sample from Ignition #7, JP-8.

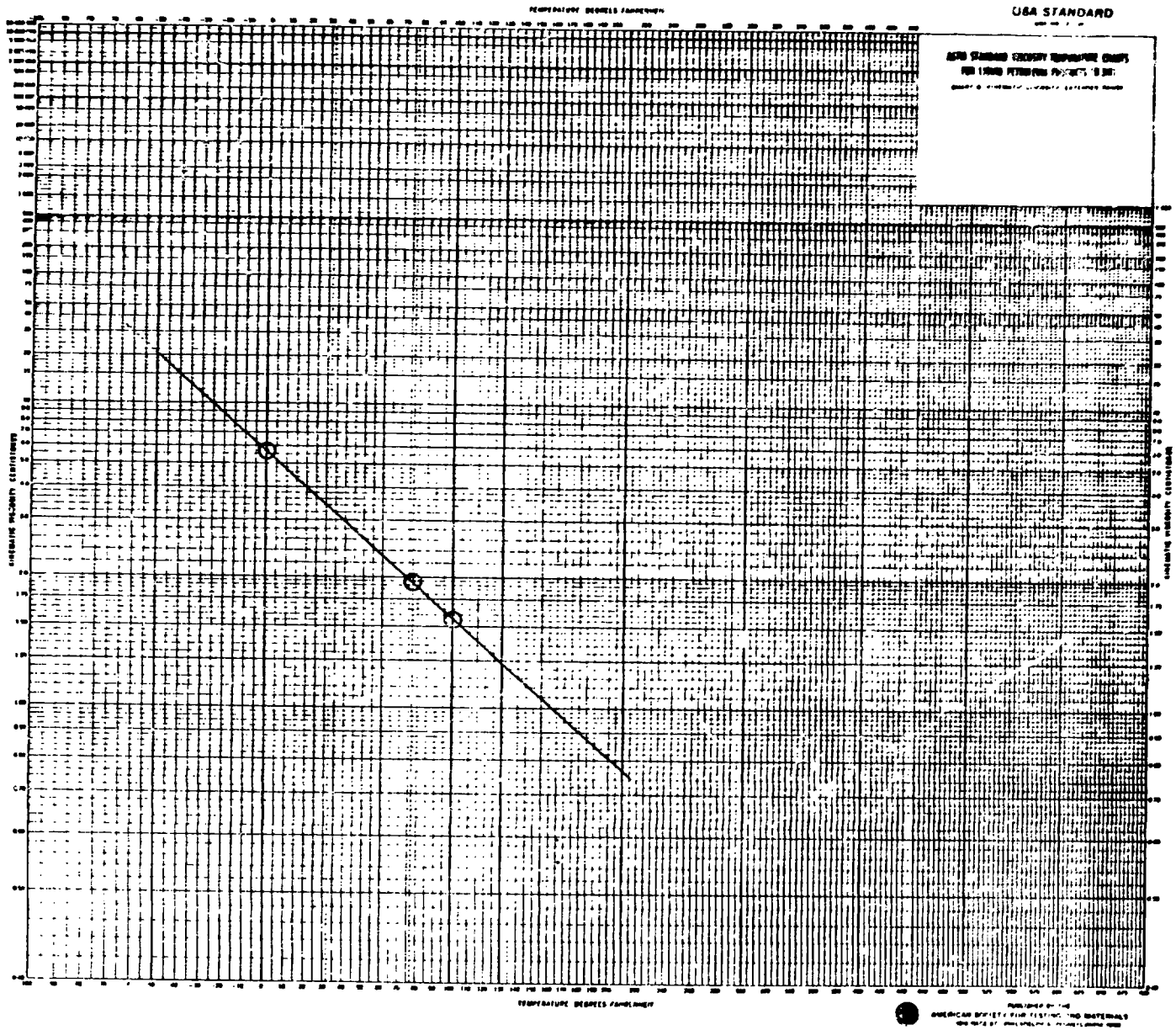

Figure 150. Viscosity/temperature plot for fuel sample from Ignition #8.

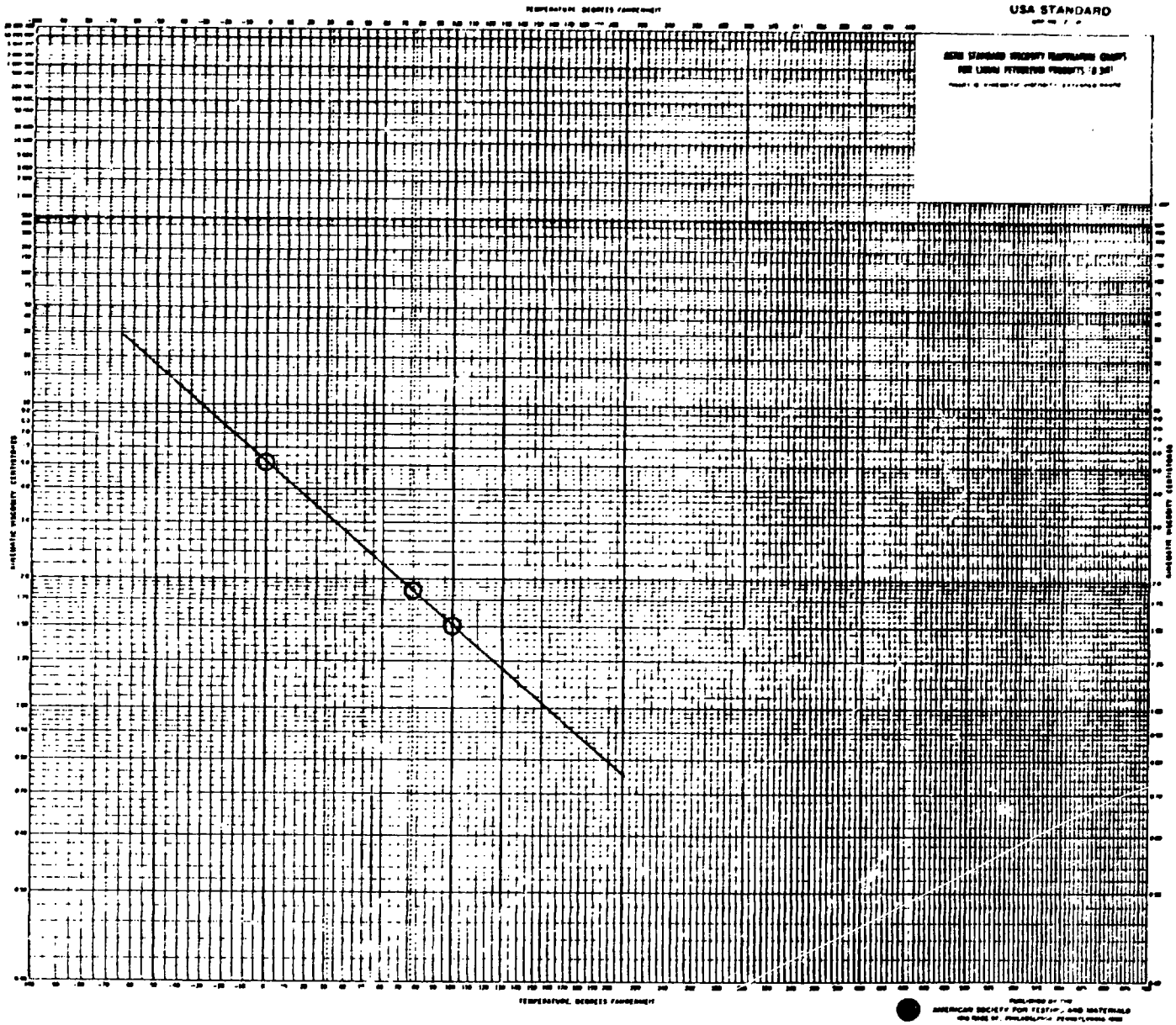

Figure 151. Viscosity/temperature plot for fuel sample from Ignition #9.

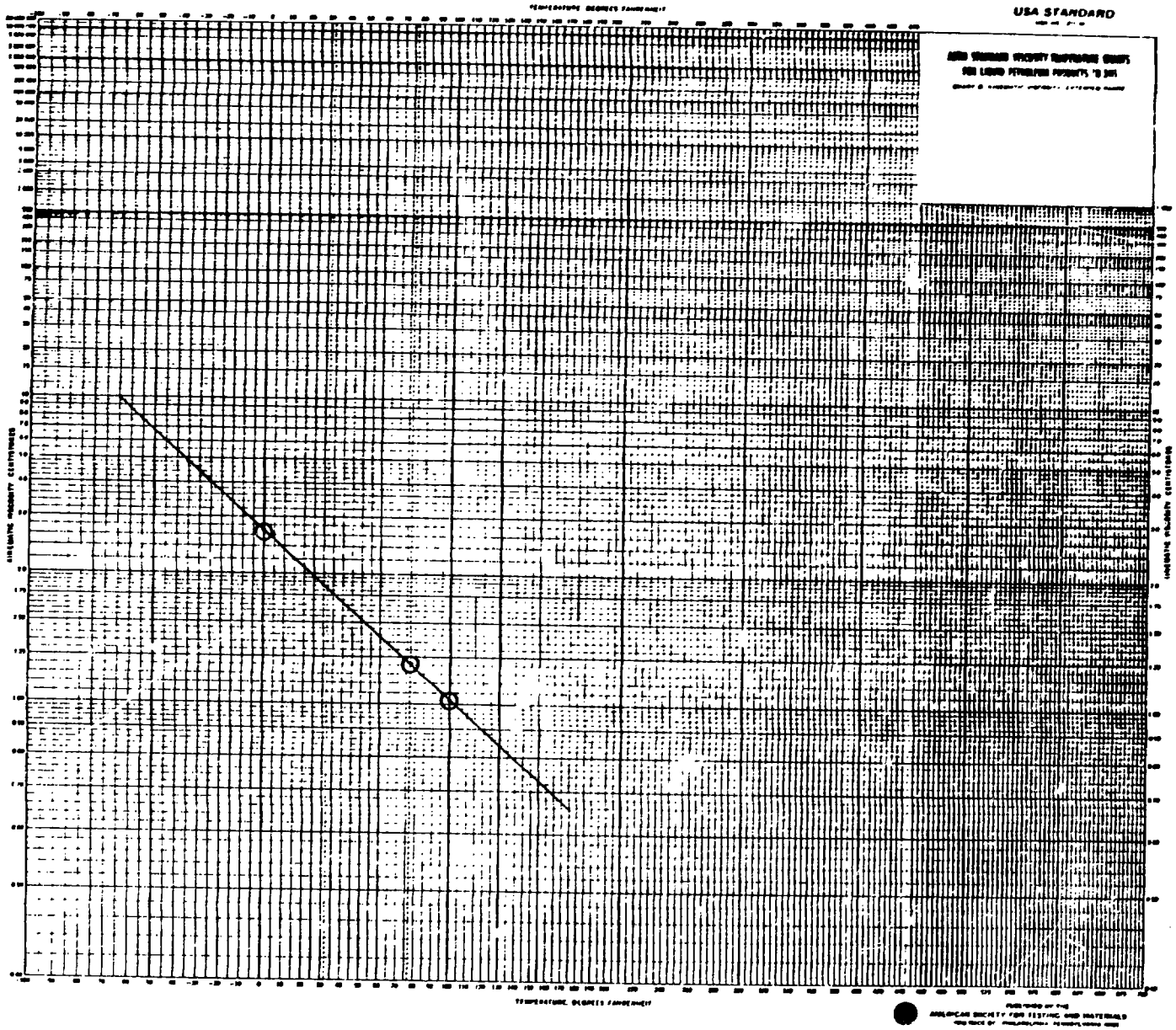

Figure 152. Viscosity/temperature plot for fuel sample from Ignition #10.

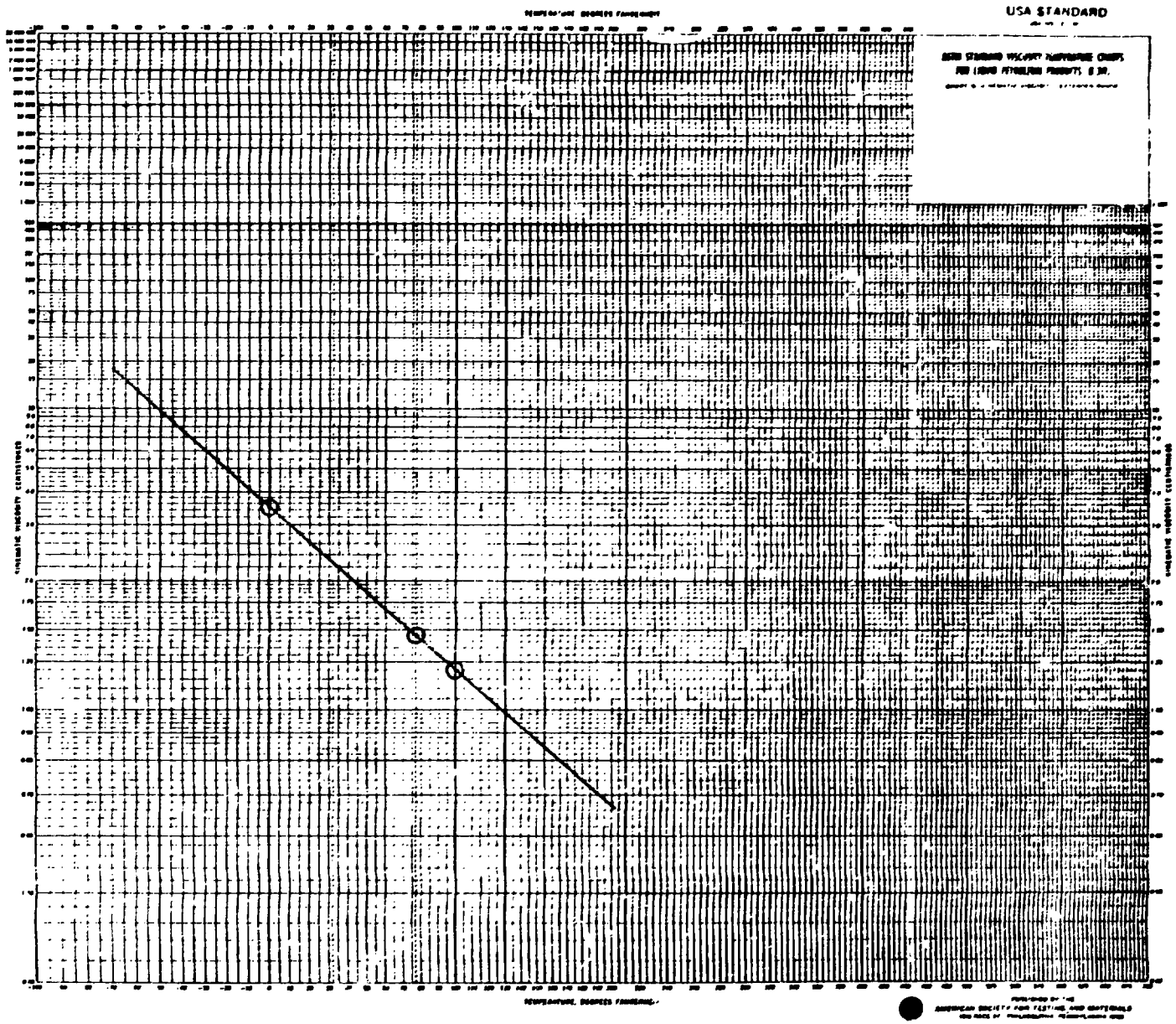

Figure 153. Viscosity/temperature plot for fuel sample from Ignition #11.

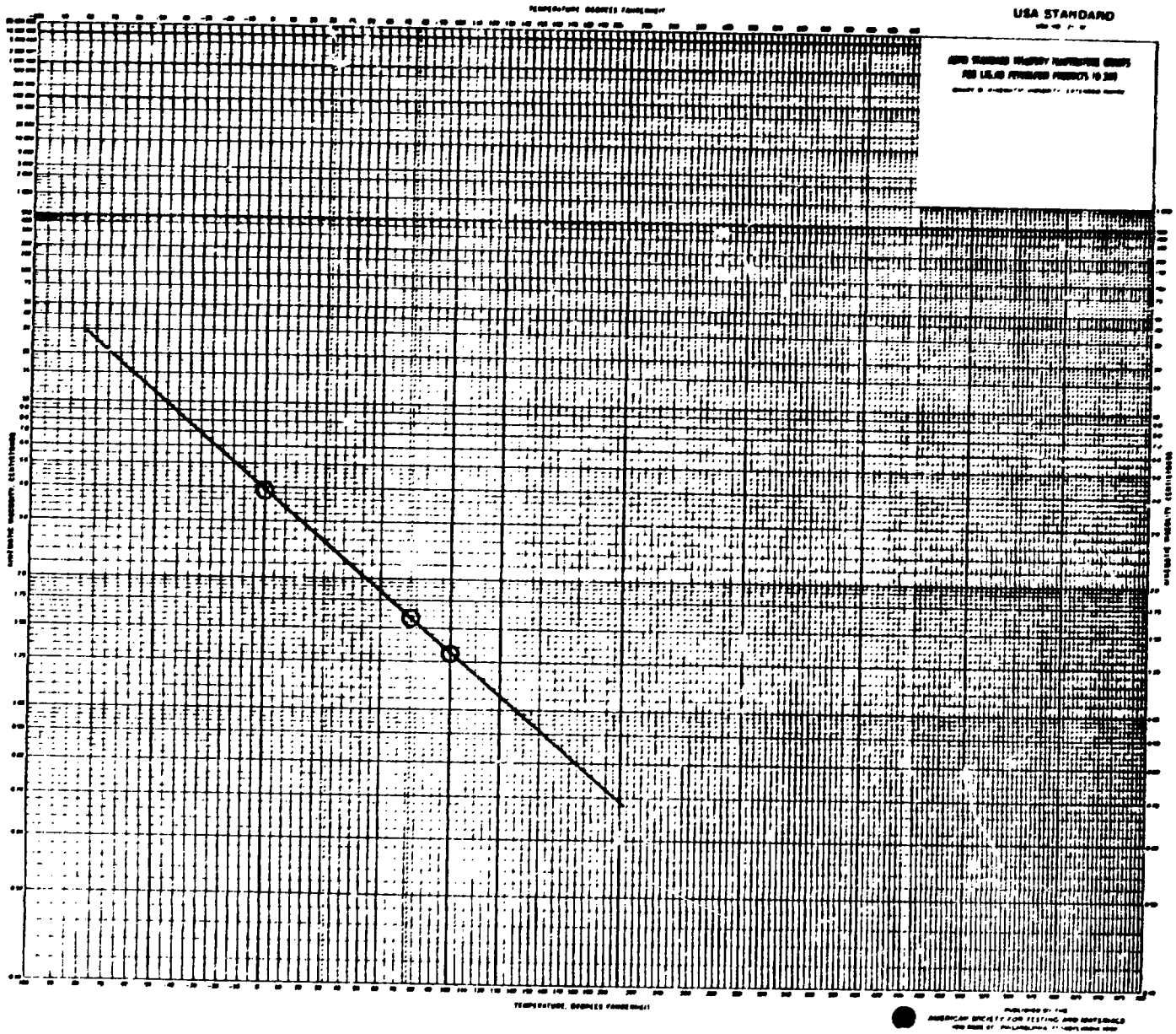

Figure 154. Viscosity/temperature plot for fuel sample from Ignition #12.

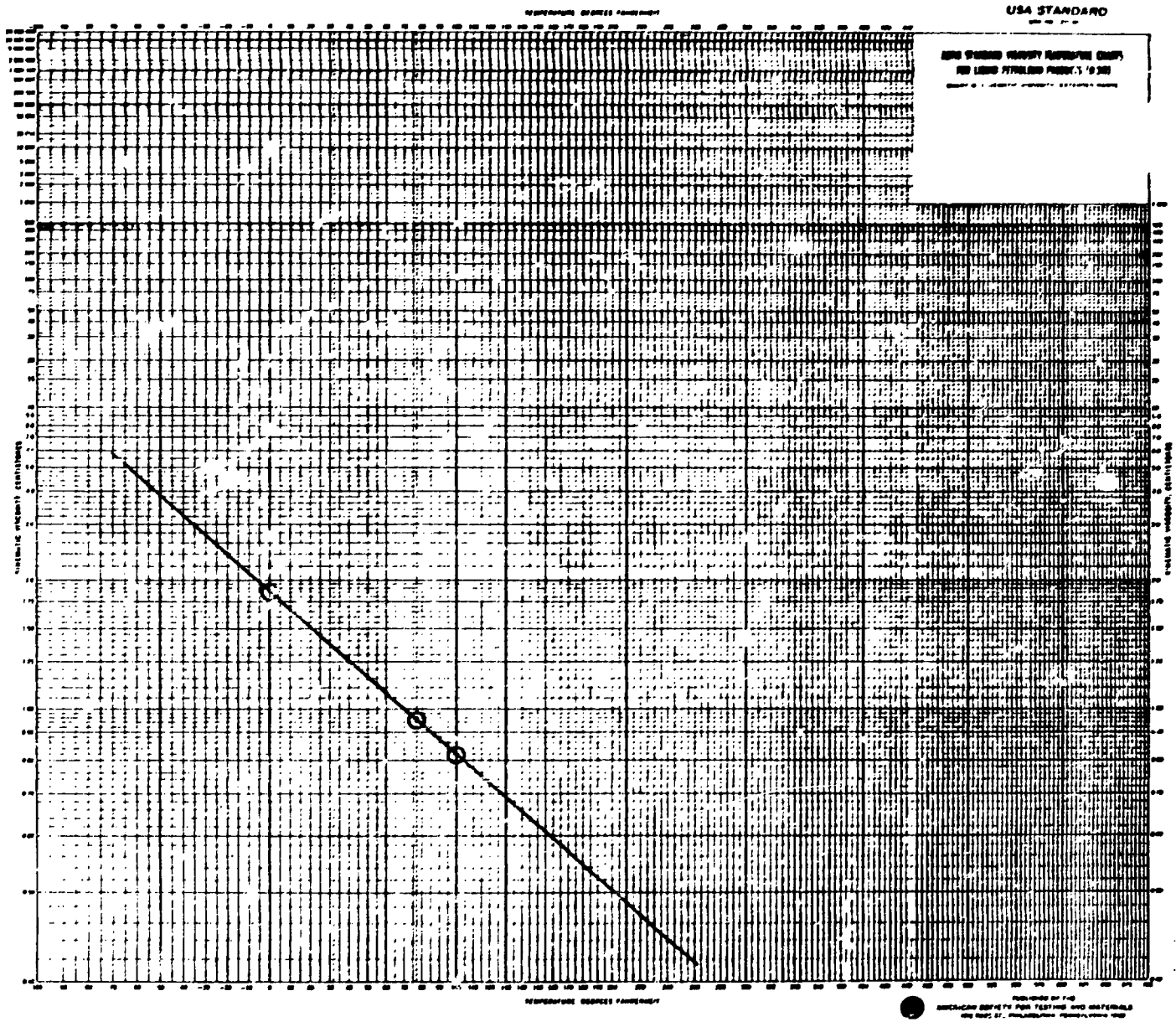

Figure 155. Viscosity/temperature plot for fuel #1, Idle Point.

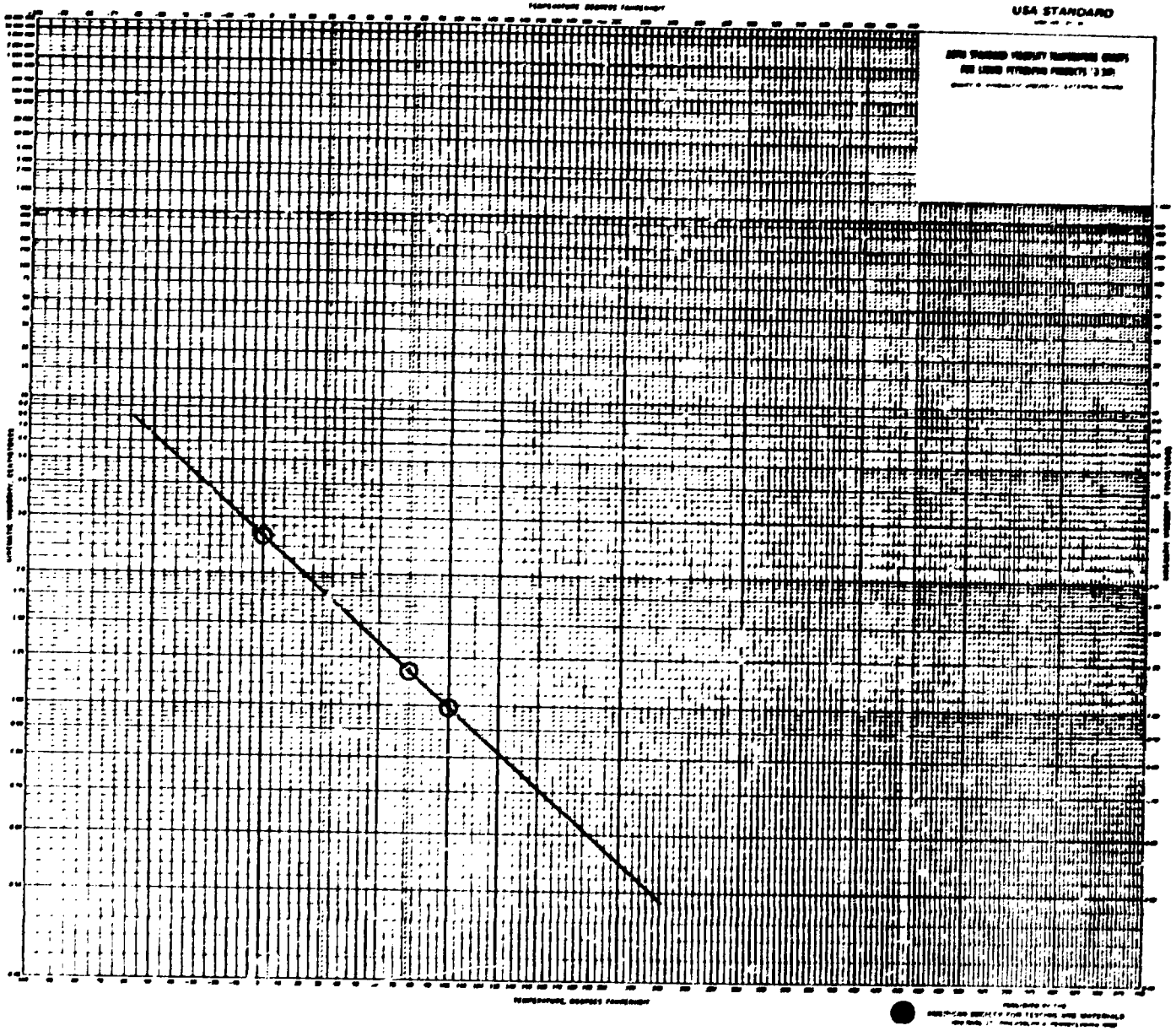

Figure 156. Viscosity/temperature plot for fuel #2.

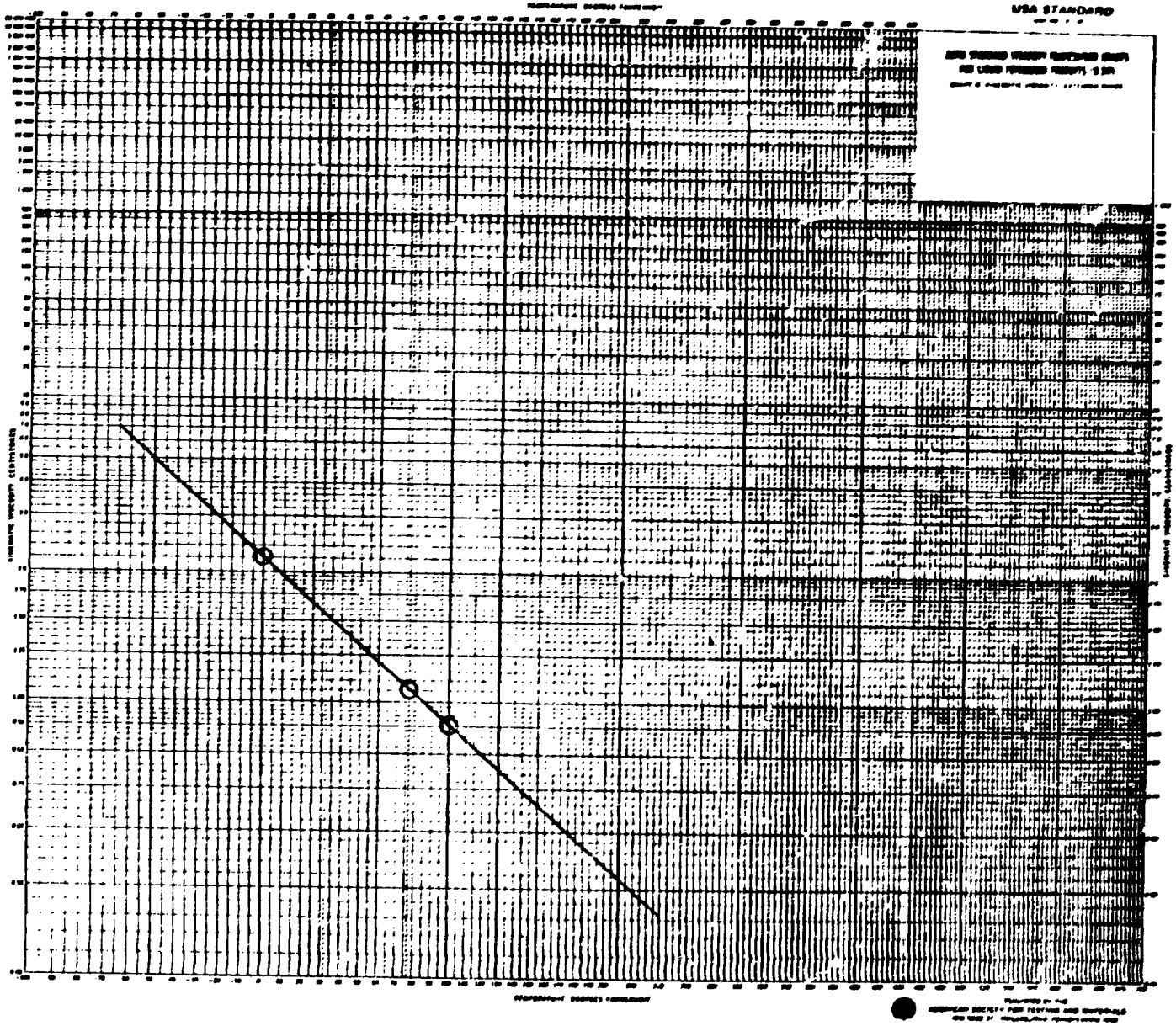

Figure 157. Viscosity/temperature plot for fuel #3.

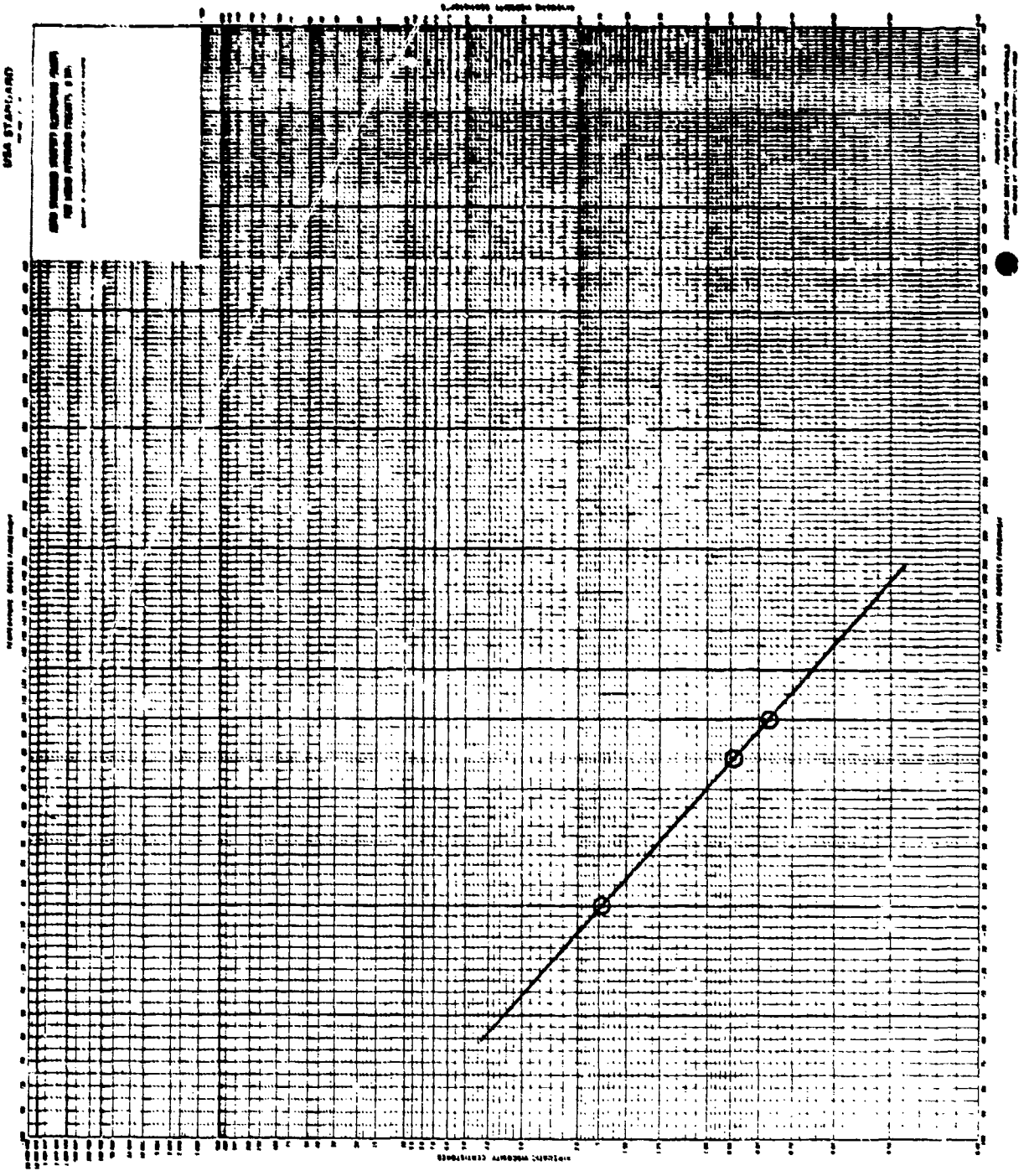

Figure 158. Viscosity/temperature plot for fuel #4.

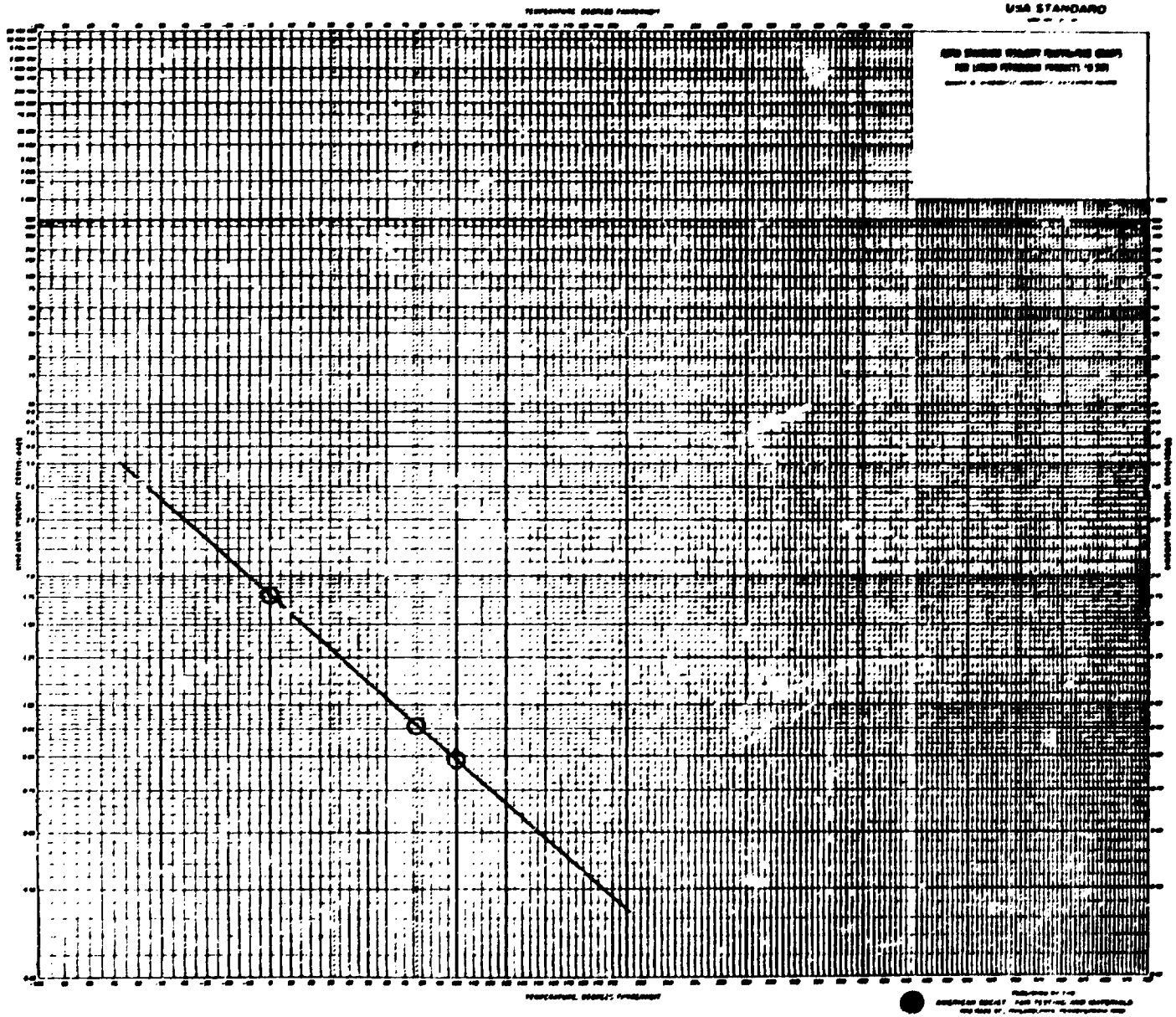

Figure 159. Viscosity/temperature plot for fuel #5.

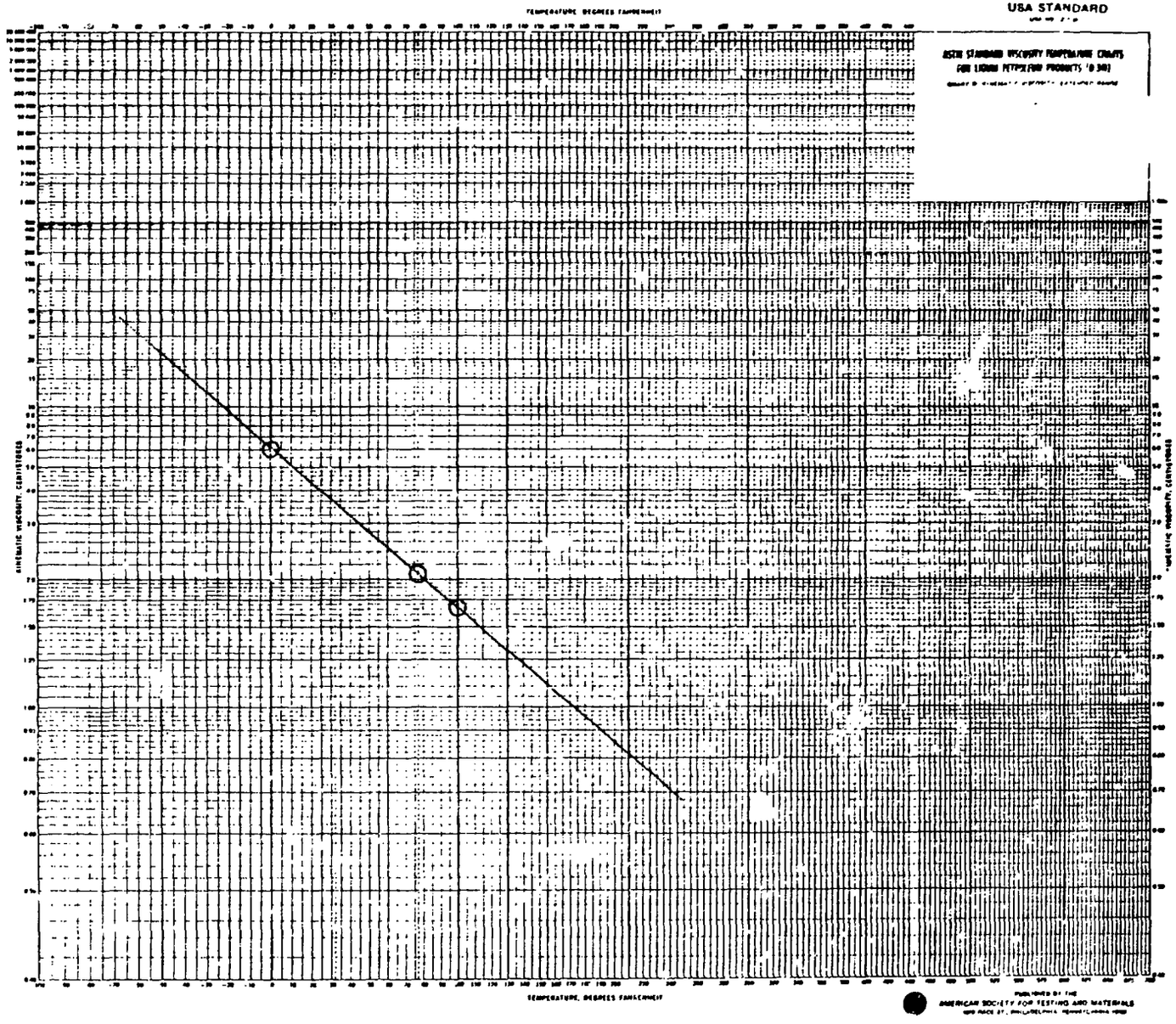

Figure 160. Viscosity/temperature plot for fuel #7, Idle Point.

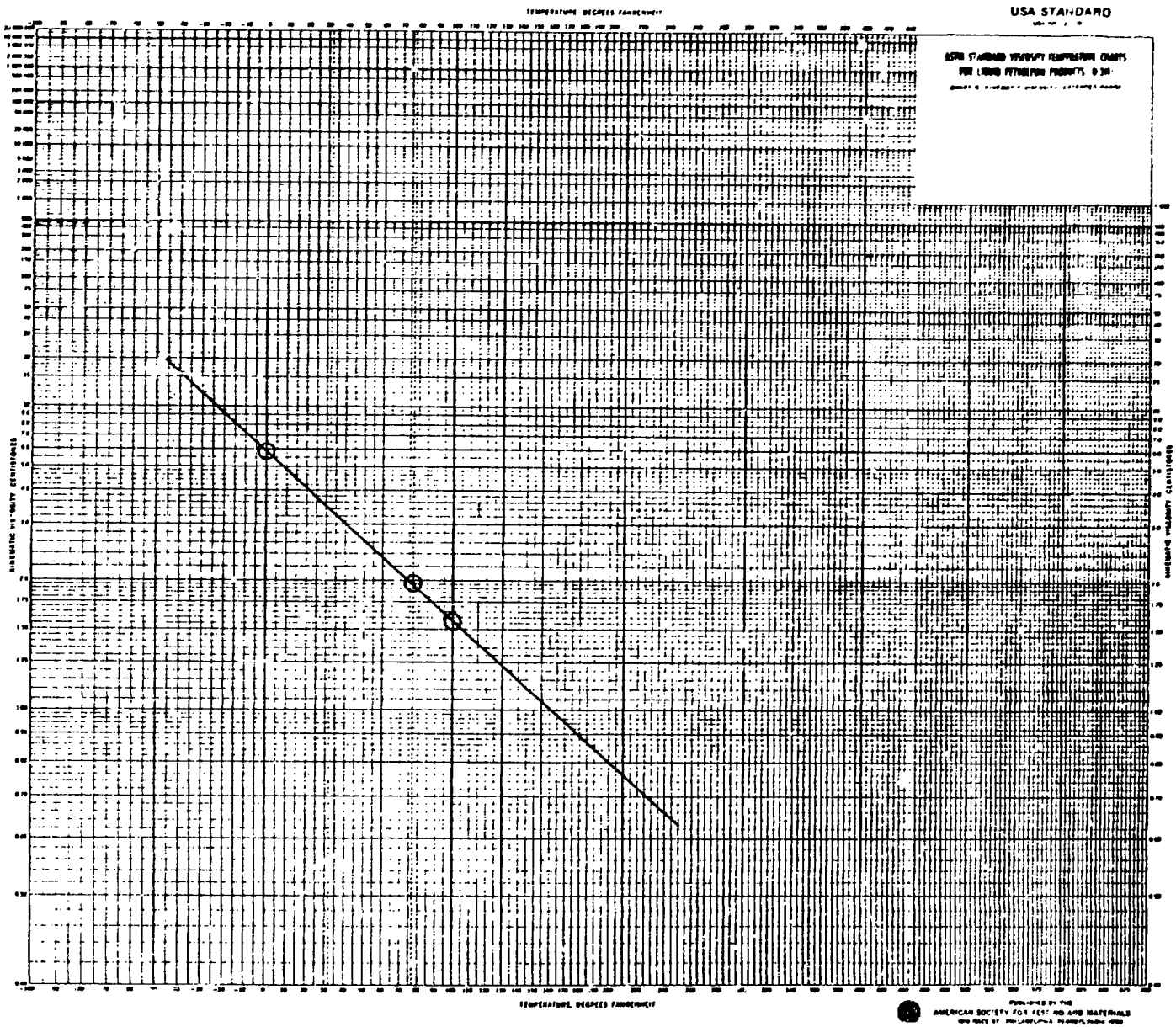

Figure 161. Viscosity/temperature plot for fuel #8.

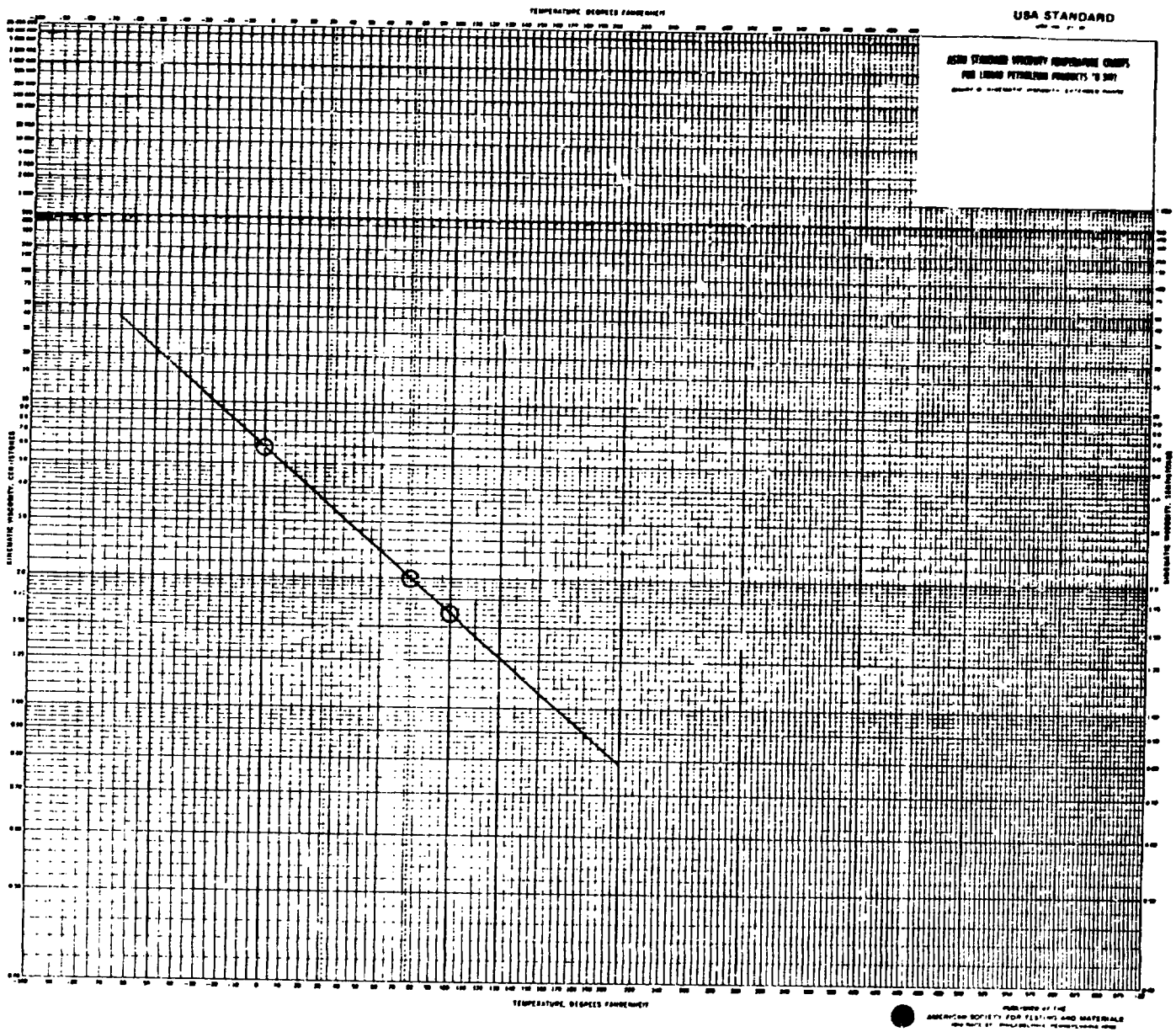

Figure 162. Viscosity/temperature plot for fuel #9.

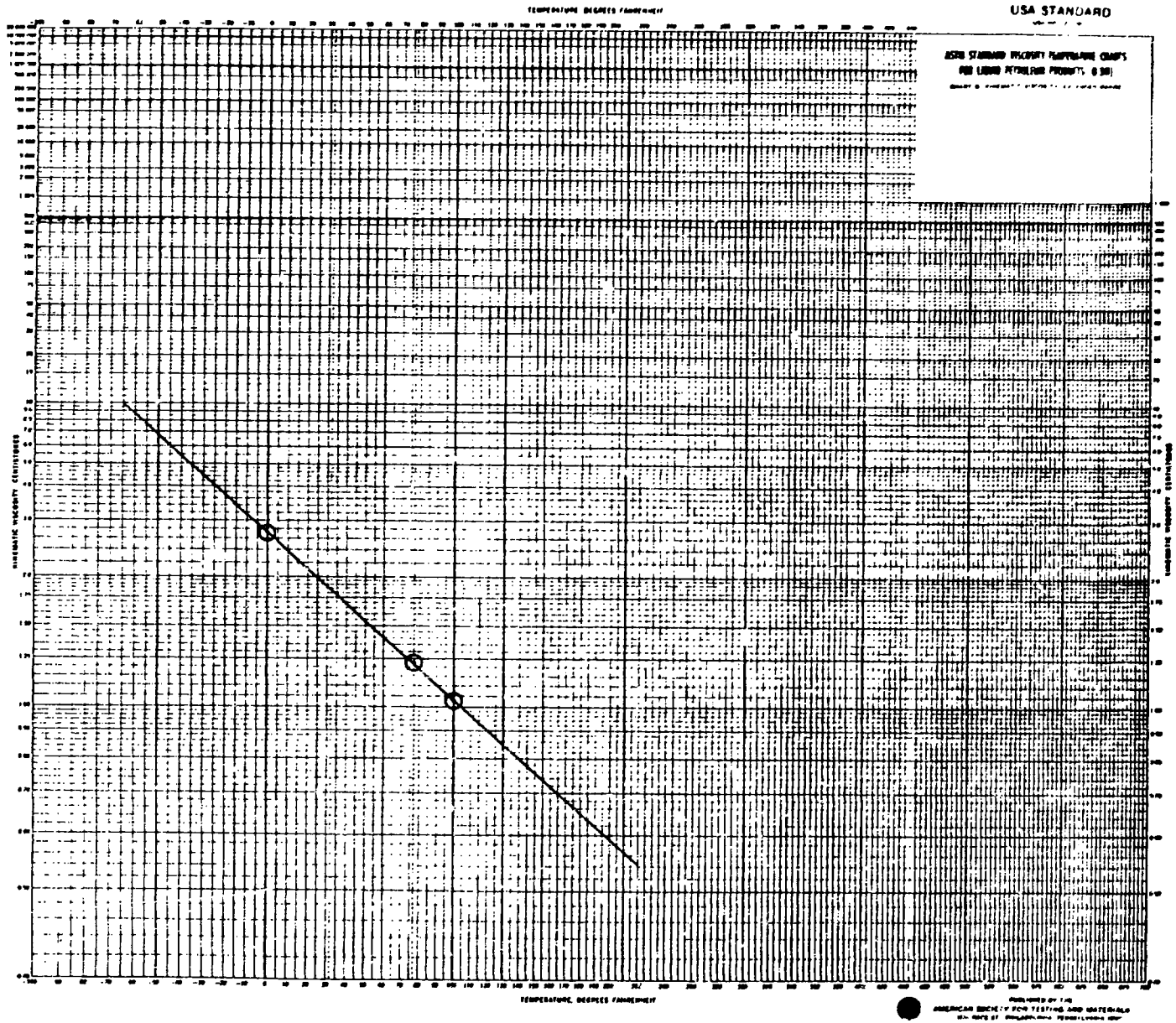

Figure 163. Viscosity/temperature plot for fuel #10.

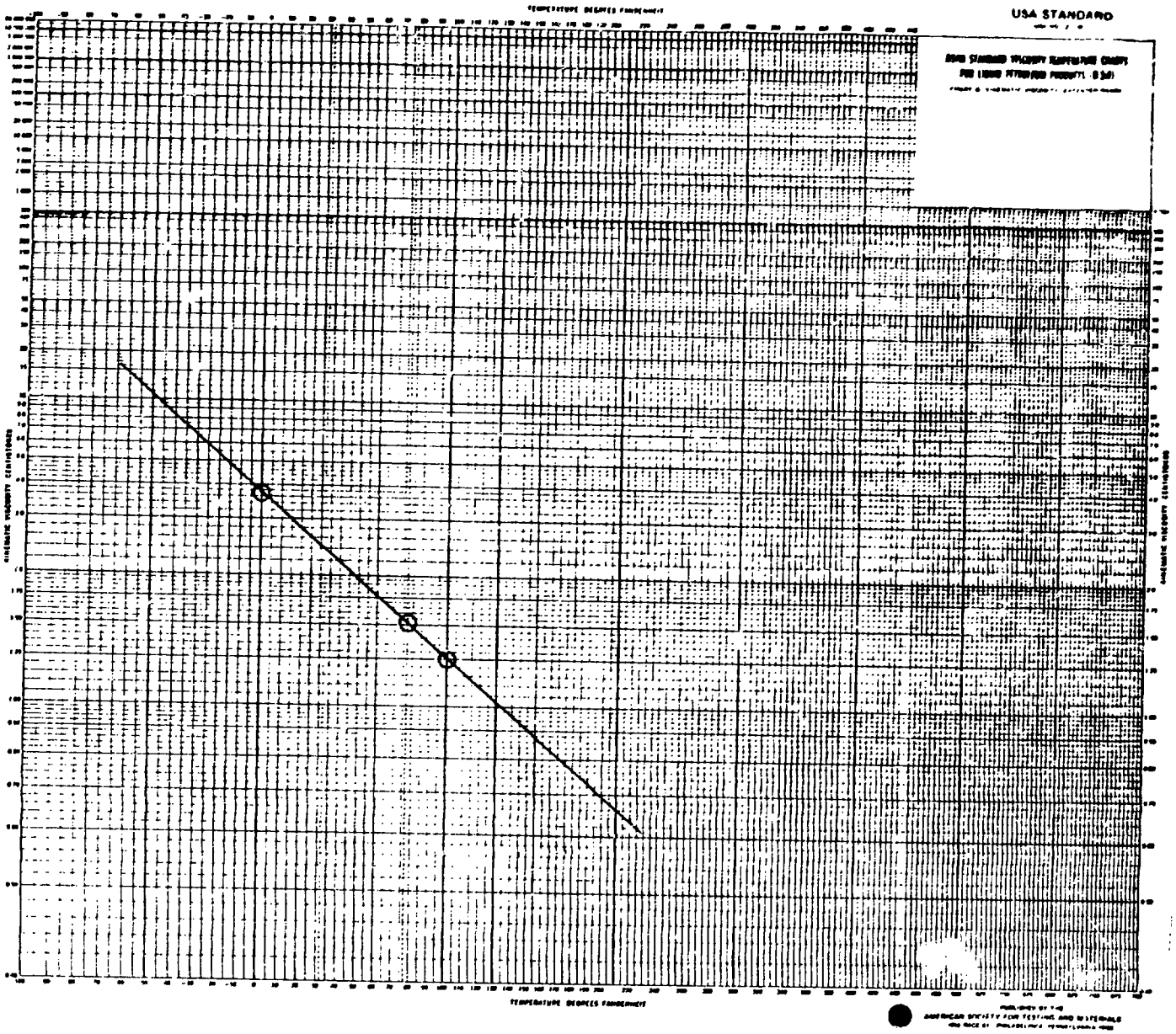

Figure 164. Viscosity/temperature plot for fuel #11.

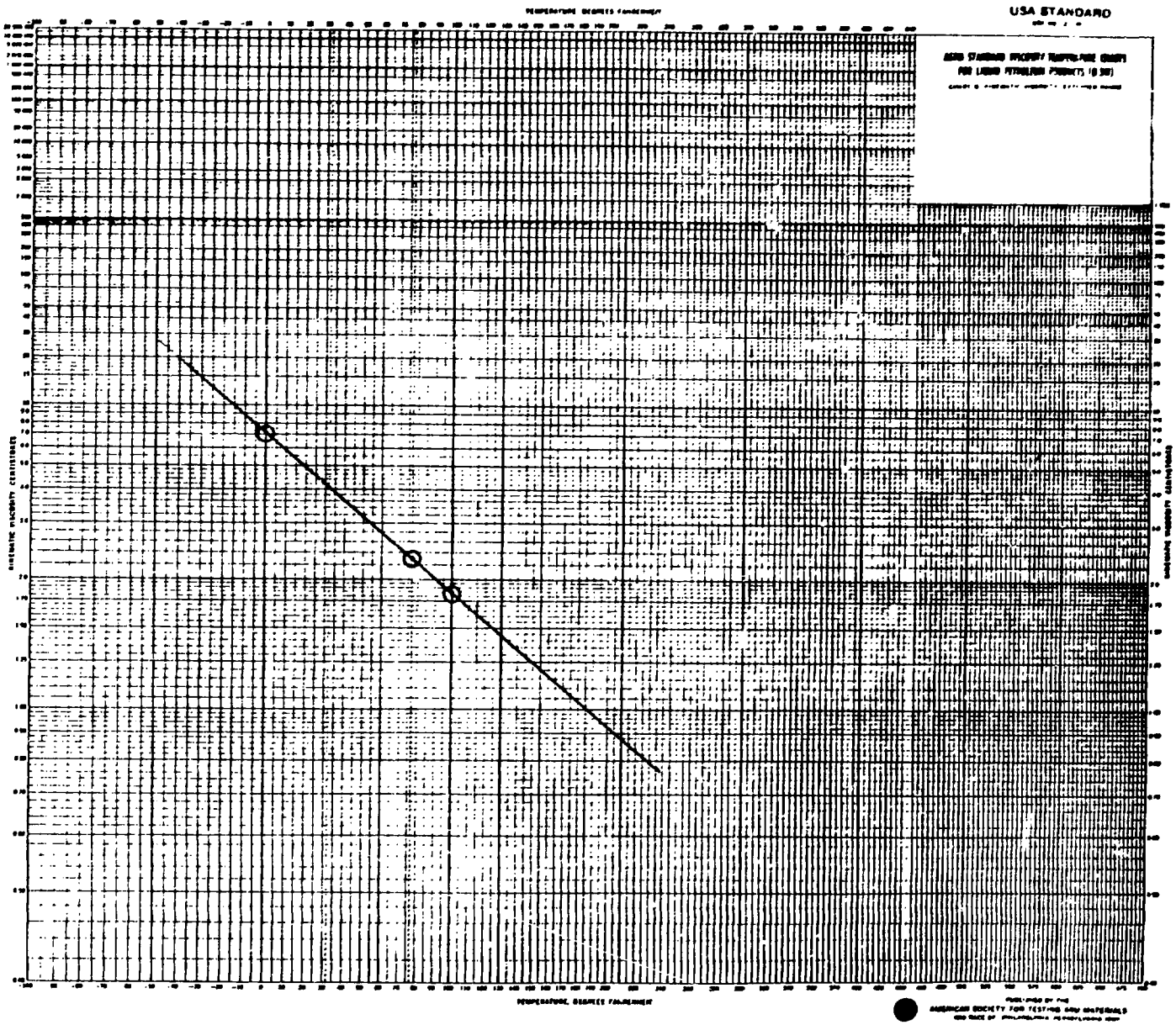

Figure 165. Viscosity/temperature plot for fuel #12.

11. CHARACTERIZATION OF DIESEL FUEL

A diesel fuel, supplied for test programs by an engine manufacturer, was characterized by analyses for hydrocarbon types and boiling range distribution. A simulated distillation by gas chromatography was conducted according to ASTM D 2887. A gas chromatograph equipped with a 3% OV-1 column and a flame ionization detector was employed for this work. Boiling range distribution data are presented in Table 160.

Hydrocarbon type analyses were performed by mass spectrometry using several different methods. The first consisted of a separation into paraffinic and aromatic fractions using the procedure described in ASTM D 2549, followed by mass spectrometric analysis using ASTM Method D 2425. This analysis was performed in duplicate. The second method used was a modification of ASTM D 2789, and was conducted at Monsanto facilities in St. Louis. The third method for hydrocarbon-type analysis was developed within Monsanto for hydrocarbon feed stocks. The boiling range limits of the method match those of the fuel quite well.

The analysis results from all three methods for hydrocarbon type distribution are shown in Table 161. All analyses are in reasonable agreement except for the distribution of the various cycloparaffins which were obtained in greater detail by the ASTM D 2549/ D 2425 analysis.

TABLE 160. SIMULATED DISTILLATION OF DF-2 DIESEL FUEL (ASTM D 2887)

Percent Recovered	Boiling Point °C	Boiling Point °F
0.5 (IBP)	127	261
1	147	297
5	179	354
10	197	387
20	222	432
30	238	460
40	255	491
50	268	514
60	282	540
70	297	567
80	313	595
90	332	630
95	349	660
99	382	720
99.5 (FBP)	391	736

TABLE 161. HYDROCARBON TYPE ANALYSIS OF DF-2 DIESEL FUEL BY THREE METHODS

Compound type	Weight percent: ASTM D 2549/D 2424 duplicate analyses		ASTM D 2789 modified	Monsanto 21-PQ-38-63
Paraffins	39.9	40.0	41.5	40.2
Cycloparaffins	19.7	19.5	34.3	35.1
Dicycloparaffins	8.2	8.0	2.3	-
Tricycloparaffins	2.5	2.5	a	-
Alkylbenzenes	9.0	8.5	8.6	10.0
Indans/Tetralins	4.7	4.6	6.5	5.3
Indens	2.6	2.7	-	1.0
Naphthalene	0.3	0.3	-	-
Naphthalenes	8.0	8.4	6.8	8.4
Acenaphthenes	2.6	2.7	-	-
Acenaphthylenes	1.6	1.8	-	-
Tricyclic Aromatics	0.9	1.0	-	-

[a]Dash indicates that the compound type is not included in the analysis.

12. SODIUM AND WATER ANALYSES OF 2040 SOLVENT SAMPLES

Four samples of 2040 solvent blending stock were analyzed for sodium content by atomic absorption spectroscopy to assure that the salt levels were not high enough to damage fuel handling equipment during combustion testing. Three of the samples were also analyzed for water content by the Karl Fischer method. Each 2040 solvent sample represented a different step in a clean-up procedure conducted by Aero Propulsion Laboratory personnel.

Sample 80036 was collected downstream of the clay filter tower on 12-8-80. It had been treated by a single pass through the filter separator, the NaCl salt tower, and the clay tower.

Sample 80036-a was collected from Compartment 4 of the 8400-gallon trailer after at least three passes through the filter separator, salt tower, and clay tower. No visible free water was detected in the amber liquid, but some black particles up to an inch in length (possibly hose lining or gaskets) and gravel size rust-colored particles were observed in the bottom of the tank.

Sample 80036-b was collected from the bottom-fill line of Compartment 3 of the 8400-gallon trailer. The compartment contained approximately 750 gallons of solvent when it was sampled. Solvent from Compartment 4 was passed through an anhydrous calcium sulfate drying tower, through an 18-element filter separator, and then through a 3-element clay filter before being emptied into Compartment 3, which had been carefully rinsed with methanol, water, methanol, and then clean 2040 solvent prior to filling.

Sample 80036-c was also taken from the bottom fill line of Compartment 3, but after the compartment was completely filled on 12-11-80.

Water analyses were conducted on the foregoing fuel specimens after thorough agitation to insure that both free and dissolved water were included in the determination. The sodium and water analysis results are shown in Table 162.

TABLE 162. ANALYSIS OF FOUR 2040 SOLVENT SAMPLES

Sample	Sodium ppm by wt	Water ppm by wt
80036	0.13	-[a]
80036-a	0.05	175
80036-b	0.10	220
80036-c	0.05	150, 140[b]

[a]Not determined.

[b]Second analysis was conducted 24 hours later.

13. SIMULATED DISTILLATIONS AND VISCOSITY DETERMINATIONS FOR 17 FUEL BLENDS

Samples of blends being considered for use in major engine test programs were analyzed for boiling range distribution and kinematic viscosity, to aid in determining the most suitable blends.

Simulated distillations were conducted by gas chromatography as described in ASTM Method D 2887, and data are presented in Table 163. This table and Table 164 also contain the composition of each of the seventeen fuel blends.

Kinematic viscosity was determined by ASTM Method D 445 at 77°F only. Results are presented in Table 164.

TABLE 163. SIMULATED DISTILLATIONS OF FUEL BLENDS

Sample No.:	M003-1		M003-2		M003-2		M003-4		M003-5		M003-6		M003-7		M003-8		M003-9	
Blend (Vol.%)	30% DF-2 70% JP-6		20% DF-2 80% JP-8		10% DF-2 90% JP-8		50% DF-2 5% Xyl B 45% JP-4		50% DF-2 10% Xyl B 40% JP-4		45% DF-2 5% Xyl B 50% JP-4		40% DF-2 10% Xyl B 50% JP-4		50% DF-2 50% JP-4		JP-8	
Percents	°C	°F	°C	°F	°C	°F	°C	°F	°C	°F	°C	°F	°C	°F	°C	°F	°C	°F
0.5 (IBP)	138	280	137	279	136	277	47	117	48	118	41	106	43	109	46	115	133	271
1.0	148	298	149	300	148	298	60	140	61	142	57	135	59	138	63	145	146	295
5	176	349	174	345	174	345	91	196	93	199	89	192	90	194	97	207	173	343
10	189	372	187	369	187	369	116	241	116	242	107	225	109	228	112	234	185	365
20	201	394	199	390	198	388	148	298	152	306	140	284	141	286	148	298	197	387
30	213	415	211	412	210	410	173	343	168	334	165	329	162	324	185	361	208	406
40	222	432	219	426	218	424	198	388	195	383	192	378	179	354	208	406	216	421
50	232	450	229	444	226	439	218	424	216	421	213	415	204	399	226	439	223	433
60	240	464	236	457	236	457	236	457	234	454	231	448	225	437	243	469	232	450
70	253	487	249	480	245	473	254	489	252	486	249	480	244	471	260	500	240	464
80	265	509	259	498	255	491	274	525	273	523	269	516	265	509	281	538	251	484
90	285	545	278	532	270	518	300	572	301	574	299	570	295	563	308	586	264	507
95	309	588	299	570	285	545	321	610	320	608	317	603	316	601	326	619	272	522
99	353	667	344	651	329	624	344	651	359	678	358	676	356	673	362	684	292	558
99.5 (FBP)	369	696	360	680	347	657	372	702	371	699	371	700	370	698	373	703	301	574

Sample No.:	M003-10		M003-11		M003-12		M003-13		M003-14		M003-15		M003-16		M003-17 Tyndall Shale	
Blend (Vol.%)	90% JP-8 10% Xyl B		85% JP-8 15% [redacted]		80% JP-8 20% Xyl B		95% JP-4 5% Xyl B		90% JP-4 10% Xyl B		85% JP-4 15% Xyl B		JP-4		JP-8	
Percents	°C	°F	°C	°F	°C	°F	°C	°F	°C	°F	°C	°F	°C	°F	°C	°F
0.5 (IBP)	136	277	136	276	138	280	31	88	31	87	34	93	31	88	151	304
1.0	144	291	142	288	143	289	37	98	37	98	40	105	38	101	155	310
5	160	320	159	318	158	316	68	154	68	154	71	160	68	155	164	328
10	166	331	162	324	163	325	89	192	89	191	91	196	87	189	170	338
20	187	369	176	349	170	338	106	222	108	226	115	239	102	215	178	352
30	199	390	195	383	190	374	120	249	125	257	127	261	118	245	184	369
40	211	412	206	404	203	397	141	286	143	289	147	296	135	274	197	386
50	219	426	216	421	215	420	160	320	161	322	162	323	152	306	203	398
60	228	442	226	432	224	435	174	345	169	336	169	336	175	347	213	416
70	236	457	235	455	235	455	196	385	190	375	187	368	196	384	219	427
80	249	480	247	477	247	477	216	421	212	414	210	410	216	421	230	445
90	261	502	260	500	261	501	236	458	234	454	234	453	235	455	240	465
95	271	520	270	518	271	520	252	485	250	482	249	481	250	483	252	486
99	291	556	289	553	290	555	274	525	265	509	273	523	271	520	275	526
99.5 (FBP)	301	574	297	567	298	568	285	545	285	545	284	544	282	539	286	546

TABLE 164. KINEMATIC VISCOSITY OF FUEL BLENDS AT 77°F

Sample number	Fuel compositions in volume percent JP-4	JP-8	DF-2	Xyl B	Viscosity, centistokes
M003-1		70	30		2.298
M003-2		80	20		2.220
M003-3		90	10		2.146
M003-4	45		50	5	1.526
M003-5	40		50	10	1.514
M003-6	50		45	5	1.440
M003-7	50		40	10	1.353
M003-8	50		50		1.544
M003-9		100			2.064
M003-10		90		10	1.821
M003-11		85		15	1.727
M003-12		80		20	1.626
M003-13	95			5	0.9188
M003-14	90			10	0.9118
M003-15	85			15	0.9032
M003-16	100				0.9284
M003-17		100 Tyndall Shale JP-8			1.594

14. SIMULATED DISTILLATIONS, VISCOSITY DETERMINATIONS, AND HYDROCARBON-TYPE ANALYSES (ONE SAMPLE ONLY) FOR 19 AEDC FUEL BLENDS

Simulated distillation analyses and kinematic viscosity determinations at 70°F and 32°F were conducted on the 19 fuel samples. One sample was also analyzed for hydrocarbon type by mass spectrometry. These analyses were conducted to aid in determining the most suitable blends for use in a major engine test program to be conducted at Arnold Engineering and Development Center (AEDC).

The simulated distillation analyses were conducted according to ASTM Method D 2887. The results are presented in Table 165. This table also contains results for selected repeat analyses.

Kinematic viscosity was determined at 32°F and 72°F by ASTM Method D 445. The results are presented in Table 166.

TABLE 165. SIMULATED DISTILLATION OF AEDC FUEL BLENDS

Sample:	M006-1		M006-2A		M006-2B		Repeat M006-2B		M006-2C		Repeat M006-2C		M006-3A		M006-3B		M006-3C		M006-3D		M006-4		M006-5A	
Temp. Scale:	°C	°F	°C	°F	°C	°F	°C	°F	°C	°F	°C	°F	°C	°F	°C	°F	°C	°F	°C	°F	°C	°F	°C	°F
Percents																								
0.5(IBP)	14	57	30	86	36	97	34	93	36	97	34	93	39	103	51	124	51	124	60	139	144	292	136	277
1.0	37	98	37	98	43	109	40	105	44	111	40	104	57	135	63	145	63	145	69	157	160	321	142	288
5.0	67	152	69	155	76	169	76	169	78	172	75	166	91	196	99	210	96	205	104	219	190	375	157	314
10	83	182	90	194	96	204	97	206	97	206	92	198	115	240	125	256	118	245	129	265	203	398	163	326
20	99	210	112	232	118	245	119	246	117	243	117	242	151	304	175	347	162	324	181	358	216	421	170	338
30	117	243	126	258	142	288	143	289	139	282	138	280	188	371	202	395	191	376	210	410	227	440	189	373
40	130	266	145	293	159	319	160	320	153	307	152	305	211	412	222	431	213	416	232	450	236	456	204	399
50	148	298	160	320	163	326	163	326	163	326	162	323	229	444	236	457	230	447	247	477	243	469	217	422
60	169	337	164	328	169	336	169	337	170	337	175	346	245	472	252	485	247	477	260	499	252	486	227	441
70	192	377	175	347	190	375	192	377	194	381	192	378	258	496	265	510	262	503	276	528	260	500	236	457
80	212	413	200	391	215	420	217	422	218	425	216	421	277	530	282	540	278	533	295	564	271	521	249	480
90	233	452	228	442	235	455	237	459	237	459	235	456	301	574	305	580	302	575	318	604	284	543	262	506
95	247	477	245	472	252	486	253	487	252	486	252	485	321	610	325	616	323	614	333	632	293	559	274	525
99	267	512	273	523	289	552	291	555	289	552	287	548	361	682	363	685	364	687	370	699	316	601	302	575
99.5(FBP)	275	526	288	550	307	584	309	588	308	587	304	575	377	711	379	713	379	715	386	728	330	627	318	604

Sample:	M006-5B		Repeat M006-5B		M006-5C		M006-6A		Repeat M006-6A		M006-6B		M006-6C		M006-6D		M006-6E		M006-6F		M006-7	
Temp. Scale:	°C	°F	°C	°F	°C	°F	°C	°F	°C	°F	°C	°F	°C	°F	°C	°F	°C	°F	°C	°F	°C	°F
Percents																						
0.5(IBP)	177	351	143	290	146	296	147	297	156	312	136	277	154	309	140	283	138	281	139	282	151	304
1.0	180	356	145	294	160	321	159	318	168	335	149	300	164	327	151	304	150	301	150	303	165	328
5.0	191	375	157	315	187	368	185	365	194	382	177	350	195	383	178	352	177	351	178	352	205	401
10	197	387	166	330	199	391	198	388	209	408	191	377	212	413	192	378	192	378	192	378	230	445
20	200	391	168	335	212	414	213	421	224	435	207	405	234	454	208	407	209	408	208	407	256	493
30	203	398	174	345	222	432	225	437	237	458	219	427	252	485	220	429	221	430	222	432	272	522
40	209	409	186	366	232	449	237	459	249	481	232	449	263	506	233	451	234	453	234	453	286	547
50	234	454	203	398	242	467	246	475	259	499	242	467	276	528	245	473	246	474	247	476	298	568
60	253	488	218	425	246	475	258	496	273	523	254	489	288	551	255	492	255	490	256	493	311	592
70	267	513	230	447	255	490	269	516	284	544	265	510	301	574	268	514	268	515	269	517	324	615
80	283	541	242	468	265	510	283	541	300	572	280	536	310	591	284	543	284	543	286	547	339	642
90	304	579	259	499	278	532	309	588	326	618	303	578	325	617	308	587	306	583	308	587	357	675
95	319	605	273	524	287	549	331	628	346	655	325	616	339	643	329	624	326	619	327	620	371	700
99	338	640	295	562	307	585	380	716	383	722	367	692	375	706	368	695	367	692	366	690	394	741
99.5(FBP)	345	653	305	580	314	597	404	759	395	742	383	722	393	739	383	722	383	722	382	719	403	758

TABLE 166. KINEMATIC VISCOSITY OF AEDC FUEL BLENDS

Sample number	Centistokes 32°F	70°F
M006-1	1.271	0.9493
M006-2A	1.223	0.9204
M006-2B	1.309	0.9689
M006-2C	1.267	0.9455
M006-3A	2.844	1.870
M006-3B	3.402	2.143
M006-3C	3.039	1.964
M006-3D	3.660	2.291
M006-4	3.524	2.223
M006-5A	2.572	1.710
M006-5B	2.161	1.485
M006-5C	3.407	2.130
M006-6A	4.657	2.765
M006-6B	4.795	2.832
M006-6C	7.610	4.091
M006-6D	4.895	2.888
M006-6E	5.013	2.934
M006-6F	5.209	3.045
M006-7	10.75	5.361, 5.369
Mixture[a]	3.715	2.330

[a]Mixture of 3 parts Sample M006-7 with 2 parts M006-1.

Mass spectrometric hydrocarbon-type analyses were conducted for sample M006-7 using both a modification of ASTM D 2789 and Monsanto Method 21-PQ-38-63. Results are given in Table 167.

TABLE 167. HYDROCARBON-TYPE ANALYSIS OF AEDC FUEL BLEND M006-7

Components	ASTM D 2789 volume %	Monsanto 21-PQ-38-63 weight %
Paraffins	46.0	43.0
Monocycloparaffins	30.9	39.9
Dicycloparaffins	2.0	-
Alkylbenzenes	5.8	7.0
Indans/tetralins	3.5	3.4
Naphthalenes	2.2	5.5
Indenes/dihydronaphthalenes	-	1.2

15. PARTIAL CHARACTERIZATION OF SIX AEDC BLENDING STOCKS

Kinematic viscosity, simulated distillations, and hydrocarbon-type analyses were conducted on six JP-4 and JP-5 fuels blended with two aromatic stocks designated as xylene bottoms and A-400. These fuels were to serve as blending stocks for use in preparing other fuels for test programs at AEDC.

Kinematic viscosity was determined by ASTM Method D 445 at 70°F only. Results are presented in Table 168.

TABLE 168. KINEMATIC VISCOSITY AT 70°F

	Sample description				
Number	Percent JP-4	Percent JP-5	Percent Xy-B	Percent A-400	Centistokes
WEH-81-5	82.7		11.6	5.7	0.9605
WEH-81-6	82.5		12.0	5.5	0.9708
WEH-81-7	82.0		13.0	5.0	0.9588
WEH-81-8		69.5	24.5	6.0	1.659
WEH-81-9		69.0	25.5	5.5	1.643
WEH-81-10		69.0	26.0	5.0	1.637

Simulated distillations were conducted by gas chromatography as described in ASTM Method D 2887. Data are presented in Table 169.

Hydrocarbon-type analyses were conducted by mass spectrometry using modified ASTM Method D 2789. Data are presented in Table 170.

16. PARTIAL CHARACTERIZATION OF 24 COMBUSTION TEST FUELS WITH VN NUMBERS

Samples of fuels from engine test programs were sufficiently characterized to correlate fuel composition and properties with fuel performance.

TABLE 169. SIMULATED DISTILLATION OF FUEL BLENDS

Percent Recovery	WEH-81-5 82.7 JP-4 11.6 Xy-B 5.7 A-400 °C	°F	WEH-81-6 82.5 JP-4 12.0 Xy-B 5.5 A-400 °C	°F	WEH-81-7 82.0 JP-4 13.0 Xy-B 5.0 A-400 °C	°F	WEH-81-8 69.5 JP-5 24.5 Xy-B 6.0 A-400 °C	°F	WEH-81-9 69.0 JP-5 25.5 Xy-B 5.5 A-400 °C	°F	WEH-81-10 69.0 JP-5 26.0 Xy-B 5.0 A-400 °C	°F
0.5(IBP)	35	94	40	103	37	98	141	286	141	286	142	287
1	53	128	57	134	56	132	146	295	145	294	146	295
5	72	162	76	168	73	163	154	309	152	306	152	306
10	88	191	89	191	98	191	158	316	158	316	158	316
20	112	234	113	235	113	236	164	328	163	326	163	326
30	127	261	130	267	130	266	184	363	181	358	180	357
40	150	303	152	306	154	309	197	387	196	385	196	384
50	162	324	162	324	162	323	208	407	207	405	207	405
60	185	365	186	366	184	363	219	425	218	424	218	424
70	205	400	205	401	205	400	230	445	229	444	229	445
80	225	438	225	437	224	435	243	470	243	469	243	469
90	245	474	247	476	246	474	259	498	258	497	258	497
95	260	501	261	502	261	502	272	522	272	521	271	520
99	296	564	299	571	297	566	306	583	303	577	301	574
99.5(FBP)	312	593	315	599	312	593	320	608	312	594	311	591

TABLE 170. HYDROCARBON-TYPE ANALYSES BY ASTM D 2789 (MODIFIED)

Components	WEH-81-5 82.7 JP-4 11.6 Xy-B 5.7 A-400	WEH-81-5 82.5 JP-4 12.0 Xy-B 5.5 A-400	WEH-81-7 82.0 JP-4 13.0 Xy-B 5.0 A-400	WEH-81-8 69.5 JP-5 24.5 Xy-B 6.0 A-400	WEH-81-9 69.0 JP-5 25.5 Xy-B 5.5 A-400	WEH-81-10 69.0 JP-5 26.0 Xy-B 5.0 A-400
Paraffins	54.6	54.5	54.1	32.4	32.0	31.9
Monocyclo-paraffins	16.1	16.1	16.0	24.5	23.9	24.2
Dicyclo-paraffins	2.9	2.9	2.9	2.5	2.6	2.4
Alkyl benzenes	20.7	21.1	21.7	31.2	32.5	32.8
Indans & Tetralins	2.6	2.5	2.5	4.8	4.6	4.5
Naphthalenes	3.1	2.9	2.8	4.6	4.4	4.2

Density was determined at 32°F, 70°F, and 100°F by the dilatometer method. Data are presented in Table 171.

TABLE 171. DENSITY AS A FUNCTION OF TEMPERATURE

Sample	Grams per cubic centimeter 32°F	70°F	100°F
VN-81-84	0.7739	0.7575	0.7441
-85	0.8197	0.8044	0.7915
-86	0.8213	0.8059	0.7937
-87	0.8708	0.8552	0.8427
-88	0.8337	0.8182	0.8053
-89	0.8487	0.8324	0.8195
-90	0.8458	0.8298	0.8172
-91	0.8505	0.8342	0.8212
-92	0.8179	0.8007	0.7879
-93	0.8307	0.8130	0.7999
-94	0.8075	0.7910	0.7774
-95	0.7905	0.7740	0.7610
-96	0.8561	0.8413	0.8294
-97	0.7743	0.7575	0.7448
-98	0.8489	0.8324	0.8192
-99	0.8181	0.8019	0.7884
-100	0.8327	0.8151	0.8018
-101	0.8081	0.7914	0.7780
-102	0.7926	0.7763	0.7631
-103	0.8254	0.8104	0.7978
-104	0.8763	0.8602	0.8482
-105	0.8497	0.8339	0.8217
-106	0.8518	0.8353	0.8225
-107	0.8402	0.8237	0.8113

Naphthalenes content was determined by ASTM D 1840. This method covers the determination by ultraviolet spectrometry of the total concentration of naphthalene, acenaphthene, and alkylated derivatives of these hydrocarbons in straight-run jet fuels containing not more than 5 percent of such components and having end points below 315°C. The method determines the maximum amount of naphthalenes that could be present by measurement of the absorbance at 285 nm of a solution with a known concentration of fuel. The results are presented in Table 172 where they are compared against naphthalenes content determined by the ASTM D 2789 hydrocarbon-type analysis. The results by the UV absorbance method are obviously

TABLE 172. NAPHTHALENES BY ASTM D 1840 METHOD

Sample	D 1840 weight %	Comparative D 2789 analysis, volume %
VN-81-84	6.3	0.7
-85	10.8	1.8
-86	10.3	1.7
-87	106, 110	22.9
-88	8.0	1.4
-89	5.8	0.9
-90	63.7	12.5
-91	124	25.1
-92	78.3	14.7
-93	3.0	0.4
-94	4.3	0.5
-95	5.7	0.6
-96	52.9	6.0
-97	6.2	0.7
-98	116	25.0
-99	81.7	14.8
-100	3.0	0.4
-101	4.2	0.5
-102	5.4	0.6
-103	10.6	2.1
-104	116	23.2
-105	60.6	12.3
-106	2.8	1.0
-107	4.1	1.5

not meaningful as they are three to nine times higher than those from the hydrocarbon-type analysis, and three values are actually greater than 100%.

Simulated distillations were conducted by gas chromatography as described in ASTM Method D 2887. As requested because of the large number of samples, the GC runs were conducted in an automated fashion with some of the customary individual handling of data being eliminated. The percent cumulative area counts are reported directly as recorded by the data system. Results are presented in Table 173.

TABLE 173. SIMULATED DISTILLATIONS BY GAS CHROMATOGRAPHY

Percent Recovered	VN-81-84 °C	VN-81-84 °F	VN-81-85 °C	VN-81-85 °F	VN-81-86 °C	VN-81-86 °F	VN-81-87 °C	VN-81-87 °F	VN-81-88 °C	VN-81-88 °F	VN-81-89 °C	VN-81-89 °F	VN-81-90 °C	VN-81-90 °F	VN-81-91 °C	VN-81-91 °F	VN-81-92 °C	VN-81-92 °F	VN-81-93 °C	VN-81-93 °F	VN-81-94 °C	VN-81-94 °F	VN-81-106 °C	VN-81-106 °F
0.5 (IBP)	26	79	114	237	119	246	117	243	120	248	127	261	144	291	50	122	33	91	36	97	29	84	130	266
1	29	84	125	257	129	264	130	266	132	270	136	277	159	318	61	142	41	106	55	131	38	100	138	280
5	66	151	156	313	158	316	162	324	140	284	139	282	195	383	111	232	84	183	88	190	81	178	150	302
10	86	187	167	333	169	336	174	345	145	293	140	284	207	405	125	257	103	217	112	234	96	205	155	311
20	100	212	180	356	184	363	190	374	162	324	148	298	223	433	151	304	126	262	138	280	120	248	162	324
30	117	243	194	381	198	388	203	397	169	336	162	324	235	455	183	361	144	291	142	288	139	282	164	327
40	127	261	204	399	211	412	214	417	181	358	165	329	247	477	215	419	179	354	146	295	145	293	168	334
50	147	297	217	423	223	433	228	442	197	387	171	340	257	495	235	455	205	401	160	320	155	311	172	342
60	174	345	228	442	237	459	234	453	212	414	183	361	268	514	250	482	223	433	164	327	164	327	195	383
70	197	387	240	464	253	487	241	466	227	441	202	396	276	529	264	507	243	469	169	336	172	342	216	421
80	218	424	255	491	270	518	257	495	243	469	226	439	291	556	270	518	250	482	177	351	196	385	233	451
90	239	462	273	523	295	563	275	527	266	511	255	491	308	586	289	552	268	514	213	415	228	442	255	491
95	254	489	286	547	312	594	288	550	281	538	273	523	321	610	305	581	279	534	238	460	247	477	270	518
99	272	522	309	588	341	646	313	595	306	583	303	577	339	642	333	631	310	590	271	520	276	529	296	565
99.5(FBP)	277	531	314	597	352	666	325	617	313	595	312	594	348	658	343	649	323	613	286	547	286	550	308	586

Percent Recovered	VN-81-95 °C	VN-81-95 °F	VN-81-96 °C	VN-81-96 °F	VN-81-97 °C	VN-81-97 °F	VN-81-98 °C	VN-81-98 °F	VN-81-99 °C	VN-81-99 °F	VN-81-100 °C	VN-81-100 °F	VN-81-101 °C	VN-81-101 °F	VN-81-102 °C	VN-81-102 °F	VN-81-103 °C	VN-81-103 °F	VN-81-104 °C	VN-81-104 °F	VN-81-105 °C	VN-81-105 °F	VN-81-107 °C	VN-81-107 °F
0.5 (IBP)	28	82	124	255	26	79	30	86	28	82	38	100	30	86	30	86	133	271	126	259	130	266	137	279
1	35	95	141	286	30	86	41	106	35	95	57	135	41	106	38	100	145	293	145	293	144	291	140	284
5	71	160	176	349	65	149	82	180	72	162	89	192	81	178	74	165	172	342	175	347	174	345	154	309
10	89	192	194	381	87	189	97	207	89	192	115	239	96	205	90	194	184	363	188	370	184	363	162	324
20	115	239	216	421	100	212	119	246	116	241	141	286	118	244	116	241	198	388	201	394	199	390	165	329
30	126	259	233	451	117	243	150	302	128	262	154	309	143	289	130	266	208	406	211	412	210	410	175	347
40	143	289	249	480	130	266	183	361	156	313	163	325	159	318	152	306	218	424	221	430	220	428	197	387
50	162	324	262	504	150	302	204	399	184	363	165	329	163	325	167	333	224	435	232	450	228	442	210	410
60	182	360	277	531	175	347	220	428	200	403	167	333	167	333	187	369	234	453	235	455	235	455	221	430
70	208	406	294	561	197	387	234	453	223	433	171	340	174	345	212	414	242	468	243	469	243	469	234	453
80	235	455	313	595	219	426	238	460	235	455	178	352	199	390	237	459	255	491	256	493	256	493	246	475
90	276	529	339	642	239	462	258	495	255	491	219	426	231	448	277	531	268	514	270	518	269	516	262	504
95	310	590	358	676	255	491	273	523	264	507	243	469	250	482	311	592	278	532	281	538	279	534	276	529
99	341	646	398	748	277	531	304	579	295	563	283	541	278	532	341	646	301	574	307	585	304	579	298	568
99.5(FBP)	350	662	415	779	288	550	315	599	308	586	298	568	290	554	350	662	312	594	316	601	315	599	310	590

Hydrocarbon-type analyses were conducted by mass spectrometry using a modification of ASTM D 2789. Data are presented in Table 174. Twelve of the samples were also analyzed by the Monsanto mass spectral method for hydrocarbon feed stocks, and these data are presented in Table 175, along with comparative data from the ASTM method.

TABLE 174. HYDROCARBON-TYPE ANALYSES BY ASTM D 2789 (MODIFIED)

	Volume Percents					
Sample	Paraffins	Monocyclo-paraffins	Dicyclo-paraffins	Alkyl-benzenes	Indans & Tetralins	Naphtha-lenes
VN-81-84	63.4	21.3	5.2	8.1	1.3	0.7
85	45.3	40.0	2.0	7.8	3.1	1.8
86	46.5	39.8	1.6	7.4	3.0	1.7
87	31.3	27.5	1.3	11.6	5.4	22.9
88	36.0	31.3	1.8	28.7	0.8	1.4
89	25.9	21.3	1.6	50.3	0.0	0.9
90	38.1	33.7	1.7	9.7	4.3	12.5
91	37.5	20.1	0.0	12.7	4.6	25.1
92	46.2	24.9	0.0	11.0	3.2	14.7
93	32.4	10.7	2.6	53.8	0.1	0.4
94	45.2	14.9	3.6	35.2	0.6	0.5
95	58.0	20.1	5.0	15.2	1.1	0.6
96	43.0	33.9	2.3	8.5	6.3	6.0
97	62.9	21.6	5.3	8.2	1.3	0.7
98	37.6	20.2	0.0	12.6	4.6	25.0
99	46.1	24.8	0.0	11.1	3.2	14.8
100	31.5	10.8	2.5	54.0	0.7	0.4
101	45.3	15.4	3.7	34.1	1.0	0.5
102	57.6	20.2	5.1	15.0	1.5	0.6
103	42.7	40.3	3.3	7.5	4.1	2.1
104	29.5	27.6	2.2	11.4	6.1	23.2
105	36.2	34.2	2.8	9.4	5.1	12.3
106	24.4	21.4	2.0	51.2	0.0	1.0
107	33.7	31.1	2.7	29.2	1.8	1.5

17. CHARACTERIZATION OF 131 VARIOUS FUEL SAMPLES BETWEEN MAY 1980 AND JANUARY 1982

Twenty-nine groups of fuel samples comprising a total of 131 fuels were characterized either in detail or in part from May 1980 to January 1982 to obtain data that would allow correlation of physical and chemical properties with combustion performance. Most

TABLE 175. COMPARATIVE HYDROCARBON-TYPE DATA FROM TWO ANALYTICAL METHODS, IN WEIGHT PERCENTS

	VN-81-85		VN-81-86		VN-81-87		VN-81-88		VN-81-89		VN-81-90	
Components	D 2789[a]	MONS[b]	D 2789	MONS	D 2789	MONS	D 2789	MONS	D 2789	MONS	D 2789	MONS
Paraffins	42.8	41.6	44.0	43.2	27.7	26.3	33.4	30.4	23.5	20.4	34.7	33.6
Cycloparaffins	42.8	42.5	42.2	41.7	27.5	26.7	33.1	31.1	22.4	20.6	34.9	34.2
Alkylbenzenes	8.5	10.1	8.1	9.5	11.9	14.8	30.9	34.6	53.0	56.8	10.3	12.6
Indans/Tetralins	3.6	3.2	3.5	3.1	5.9	4.7	0.9	1.7	0.0	0.3	4.9	4.0
Indenes[c]	-	0.0	-	0.1	-	0.5	-	0.0	-	0.0	-	0.2
Naphthalenes	2.3	2.6	2.2	2.4	27.0	27.0	1.7	2.2	1.1	1.9	15.2	15.4

	VN-81-96		VN-81-103		VN-81-104		VN-81-105		VN-81-106		VN-81-107	
Components	D 2789[a]	MONS[b]	D 2789	MONS	D 2789	MONS	D 2789	MONS	D 2789	MONS	D 2789	MONS
Paraffins	39.9	39.2	40.1	39.6	26.0	24.9	33.0	32.2	22.1	19.1	31.1	28.6
Cycloparaffins	36.2	34.5	44.3	43.9	28.4	27.6	36.4	35.8	22.9	20.8	33.7	31.7
Alkylbenzenes	9.2	10.7	8.2	9.7	11.7	14.5	9.9	12.2	53.8	57.2	31.3	35.0
Indans/Tetralins	7.3	5.9	4.8	4.1	6.6	5.2	5.8	4.6	0.0	1.0	2.1	2.4
Indenes[c]	-	0.8	-	0.0	-	0.6	-	0.2	-	0.0	-	0.0
Naphthalenes	7.4	8.9	2.6	2.7	27.3	27.2	14.9	15.0	1.2	1.9	1.8	2.3

[a] ASTM Method D 2789 provides data in volume percents. The weight percent data were calculated from average density values for the compound classes.

[b] Monsanto mass spectral method developed for hydrocarbon feed stocks.

[c] Also includes dihydronaphthalenes.

of the fuel samples had been combustion-tested at either General Electric Company, Pratt and Whitney Company, or AEDC. Generally, however, the only information submitted with the samples was a sample identification. For the sake of conciseness, data for these twenty-nine groups of samples have been consolidated in this single subsection.

Density was determined as a function of temperature for 67 samples, and these data are presented in Table 176. Kinematic viscosity was determined for 55 samples as a function of temperature, and these data are presented in Table 177. The viscosity/temperature relationships are graphed in Figures 166 through 219. Surface tension versus temperature was also determined for 55 samples as presented in Table 178. Vapor pressure versus temperature was determined for 49 of the samples, and results are provided in Table 179. Heat of combustion was also determined for 49 samples and these data are presented in Table 180. Boiling range distribution was determined for 91 samples by GC simulated distillation, and these results are provided in Tables 181 and 182. Table 181 provides results in degrees Celsius while Table 182 provides the same results in degrees Fahrenheit. Hydrocarbon-type analyses by modified ASTM Method D 2789 were conducted on 102 of the samples, and these data, in volume percent, are provided in Table 183. Thirty-four of these samples were also analyzed for hydrocarbon type by Monsanto Method 21-PQ-38-63, and comparative data from both modified ASTM D 2789 and the Monsanto method in weight percents are presented in Table 184. Six other samples were analyzed for hydrocarbon types by ASTM D 2425 in addition to modified ASTM D 2789 (four of the samples were also analyzed by the Monsanto method), and comparative data from all three methods are presented in Table 185

TABLE 176. DENSITY AS A FUNCTION OF TEMPERATURE FOR FUELS TESTED AFTER 1 MAY 1980

Sample description	Grams per cubic centimeter			
	-20°F	32°F	70°F	100°F
1B-792009, JP-4	0.7875	0.7643	0.7475	0.7346
2B-792009, JP-8	0.8440	0.8227	0.8075	0.7955
13B-792009, DF-2	gel	0.8573	0.8427	0.8313
14B-792009, DF-2 Aromatic Blend	gel	0.8871	0.8722	0.8600
8B-792009	0.8618	0.8385	0.8220	0.8086
9B-792009	0.8300	0.8065	0.7900	0.7771
15B-792009	0.8152	0.7925	0.7765	0.7637
GEC-49B-1	0.7891	0.7655	0.7492	0.7355
1C-792009	0.8014	0.7785	0.7619	0.7486
8C-792009	0.8714	0.8492	0.8330	0.8202
9C-792009	0.8393	0.8170	0.8002	0.7875
13C-792009	--	0.8613	0.8462	0.8340
14C-792009	--	0.8929	0.8777	0.8655
15C-792009	0.8196	0.7980	0.7824	0.7700
JP-5, Tank 13	0.8503	0.8290	0.8134	0.8016
P&W 79-C-2086, Petroleum JP-4	0.7938	0.7708	0.7540	0.7411
P&W 79-C-2086, Shale JP-4	0.8146	0.7925	0.7765	0.7637
P&W 79-C-2086, Blend #1	0.8215	0.7997	0.7839	0.7715
P&W 79-C-2086, Blend #2	0.8304	0.8080	0.7915	0.7785
P&W 79-C-2086, Blend #3	0.8336	0.8125	0.7967	0.7843
P&W 79-C-2086, Blend #4	0.8350	0.8099	0.7920	0.7778
P&W 79-C-2009-62B-1, DF-2	0.7911	0.7681	0.7513	0.7376
P&W 792086, M50001	0.8132	0.7918	0.7753	0.7623
P&W 792086, M60001	0.8483	0.8262	0.8097	0.7968
P&W 792086, M70001	0.9119	0.8907	0.8750	0.8624
P&W 792086, M80001	frozen	0.8974	0.8818	0.8695
GEC 792009, 77B	0.7910	0.7681	0.7508	0.7377
GEC 792009, 78B	slushy	0.8699	0.8541	0.8425
GEC 792009, 13C-2	frozen	0.8615	0.8461	0.8340
P&W M50014A-2	0.8500	0.8282	0.8126	0.8008
P&W MJ0016A	0.7952	0.7733	0.7563	0.7434
P&W MJ0013B	0.7970	0.7746	0.7584	0.7447
POSF-D-81-043, GECF-1D, JP-4	0.7910	0.7689	0.7520	0.7390
AEDC, POSF-C-81-134, A-1, JP-4	0.7992	0.7767	0.7598	0.7468
POSF-D-81-044, GECF-13D, DF-2	frozen	0.8588	0.8440	0.8319
POSF-D-81-042, GECF-14D, DF-2/ARO	frozen	0.8840	0.8687	0.8571

(continued)

TABLE 176 (continued)

Sample description	Grams per cubic centimeter -20°F	32°F	70°F	100°F
POSF-D-81-046, GECF-1E, JP-4	0.8018	0.7797	0.7633	0.7504
POSF-D-81-045, GECF-13E, DF-2	frozen	0.8611	0.8458	0.8344
DDP-81-25 Blending JP-4, Tank B-1, 5-5-81	--	0.7684	0.7519	0.7386
DDP-81-26 DF-2 Base stock, 5-5-81	--	0.8639	0.8483	0.8368
GECS-24-D, Reference JP-4	0.7909	0.7680	0.7509	0.7379
GECS-26-D, Reference JP-4	0.7964	0.7745	0.7577	0.7444
DDP-81-08 Blending JP-5, Tank F-1, 4-23-81	0.8367	0.8241	0.8085	0.7961
GECS-81B-1, DF-2	frozen	0.8552	0.8402	0.8285
GECS-82B, DF-2	frozen	0.8526	0.8368	0.8248
POSF-81-59, Blend of JP-4, DF-2, 2040 Solvent	0.8556	0.8331	0.8174	0.8047
AEDC Blending Stocks				
DDP-81-22, Tank B-11, JP-4	--	0.7684	0.7517	0.7384
DDP-81-23, Tank B-12, JP-4	--	0.7689	0.7517	0.7385
DDP-81-24, Tank B-13, JP-4	--	0.7683	0.7515	0.7386
DDP-82-20, Tank F-6, JP-5	--	0.8263	0.8111	0.7990
DDP-82-21, Tank F-7, JP-5	--	0.8273	0.8120	0.7992
DDP-81-17, Tank F-9, DF-2	--	0.8523	0.8375	0.8264
DDP-81-18, Tank F-10, DF-2	--	0.8520	0.8372	0.8258
DDP-81,19, Tank F-11, DF-2	--	0.8523	0.8374	0.8259
DDP-81-12, Tank F-8, Xy-B	--	0.8856	0.8680	0.8542
DDP-81-14, Tank B-18, A-400	--	0.9772	0.9611	0.9482
DDP-81-28, Tank F-12, AEDC Blend 2 (6 July 81)	--	0.7950	0.7783	0.7649
DDP-81-29, Tank F-11, AEDC Blend 3 (6 July 81)	--	0.8248	0.8093	0.7968
DDP-81-30, Tank F-7, AEDC Blend 5 (6 July 81)	--	0.8497	0.8336	0.8203
DDP-81-31, Tank F-9, AEDC Blend 6 (6 July 81)	--	0.8485	0.8327	0.8209
E314A, JP-8 Blend #3 (P&W)	0.8318	0.8109	0.7948	0.7821
M50003B, JP-4 Blend #5 (P&W)	0.8501	0.8291	0.8139	0.8011
M50008B, JP-4 Blend #5 (P&W)	0.8489	0.8280	0.8124	0.7997
MS0007A, Shale JP-4 (P&W)	0.8184	0.7970	0.7810	0.7682
MS0010A, Shale JP-4 (P&W)	0.8169	0.7950	0.7792	0.7666
MS0011A, Shale JP-4 (P&W)	0.8201	0.7982	0.7820	0.7691
EJ0020B, JP-4 (P&W)	0.7966	0.7748	0.7574	0.7440

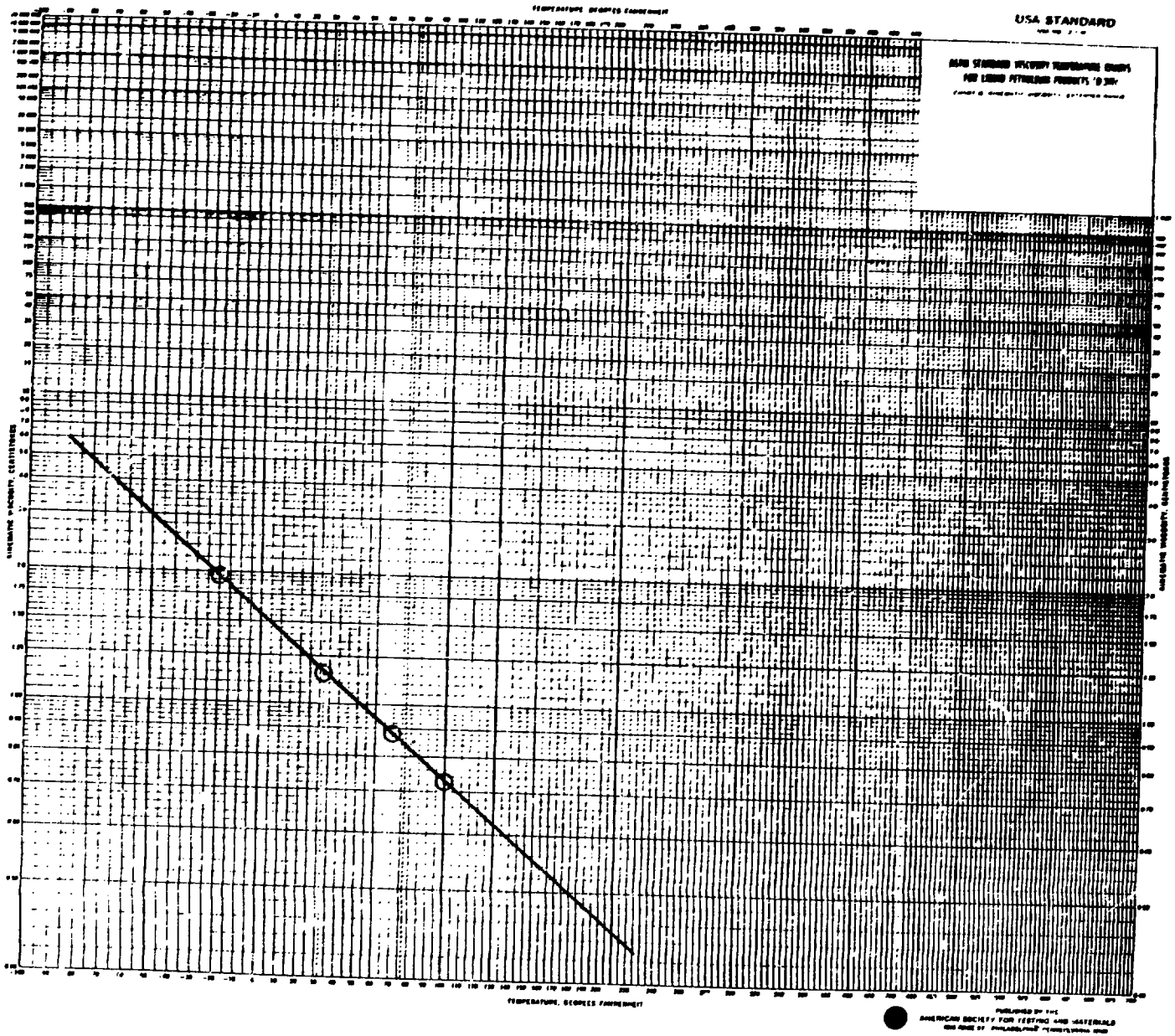

Figure 166. Viscosity/temperature plot for fuel 1B-792009 JP-4.

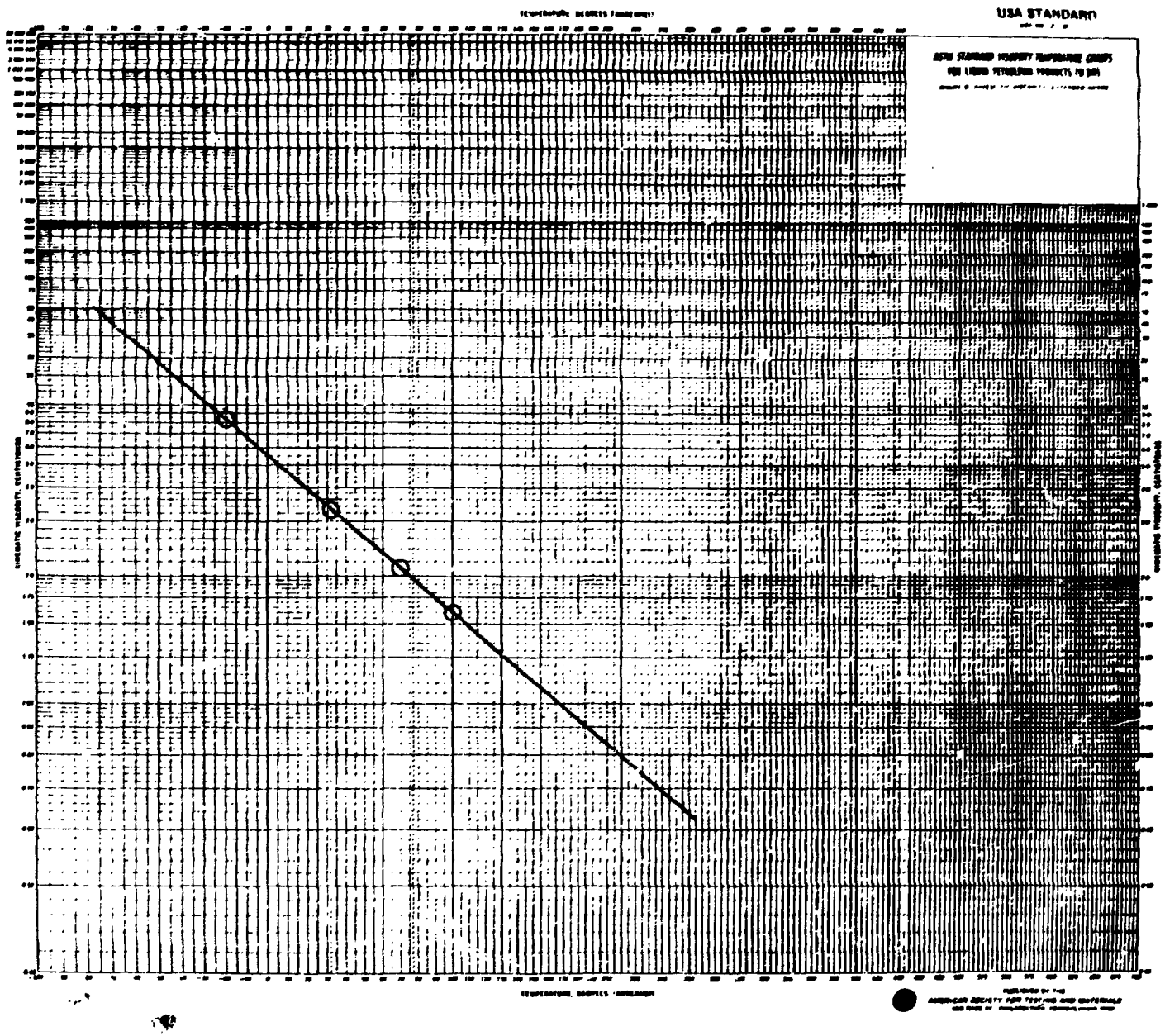

Figure 167. Viscosity/temperature plot for fuel 2B-792009 JP-8.

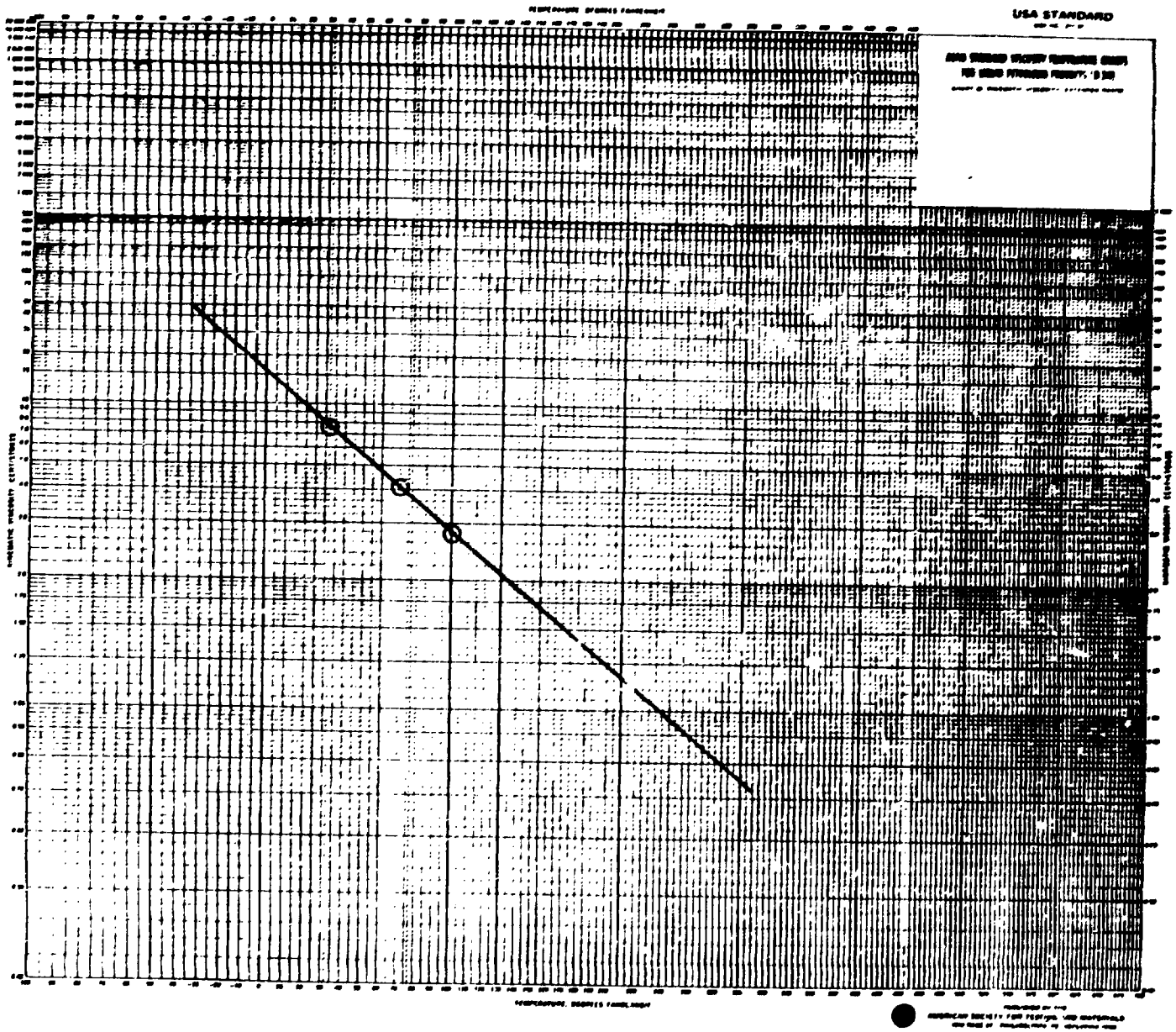

Figure 168. Viscosity/temperature plot for fuel 13B-792009 DF-2.

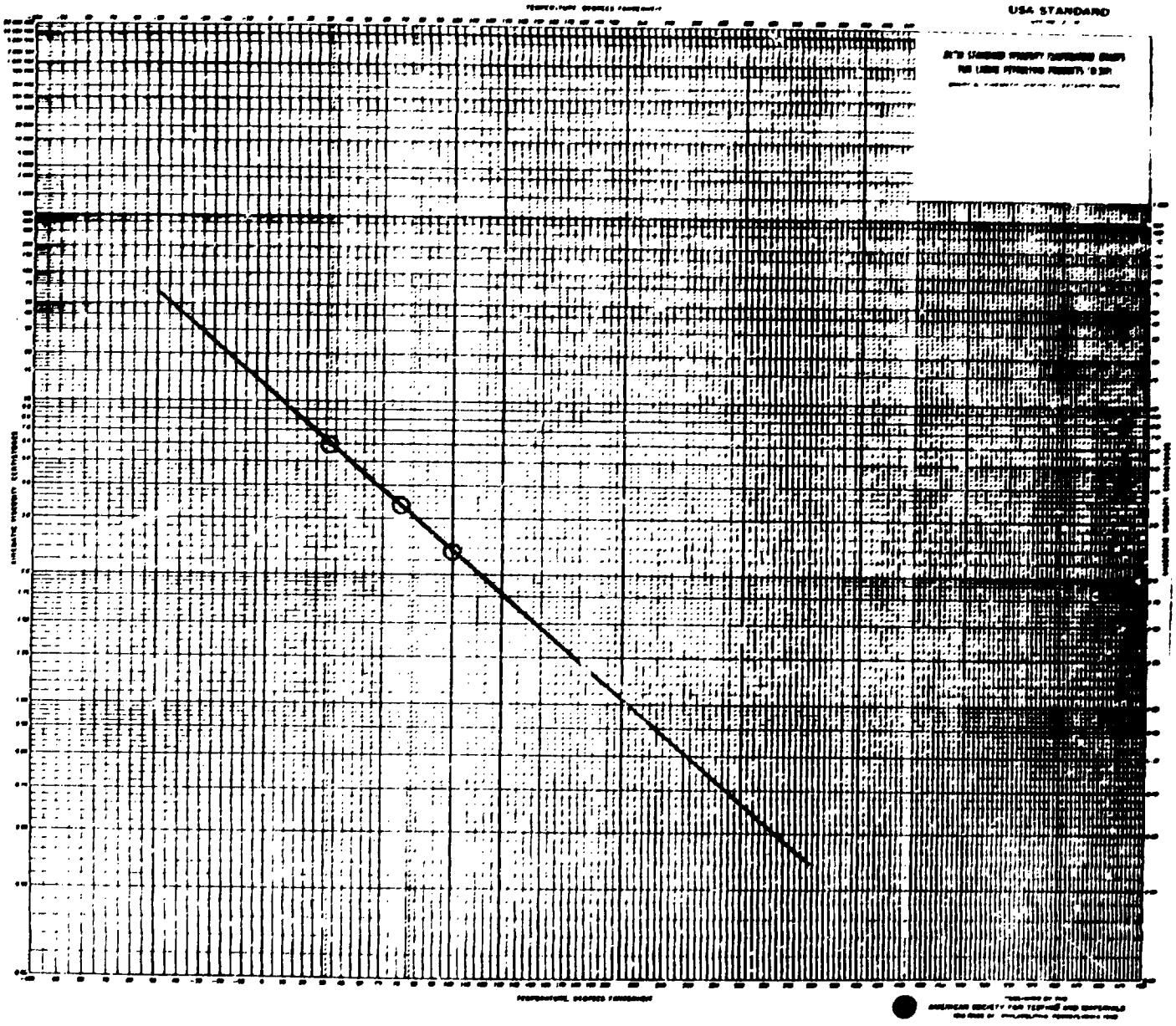

Figure 169. Viscosity/temperature plot for fuel 14B-792009 DF-2 aromatic blend.

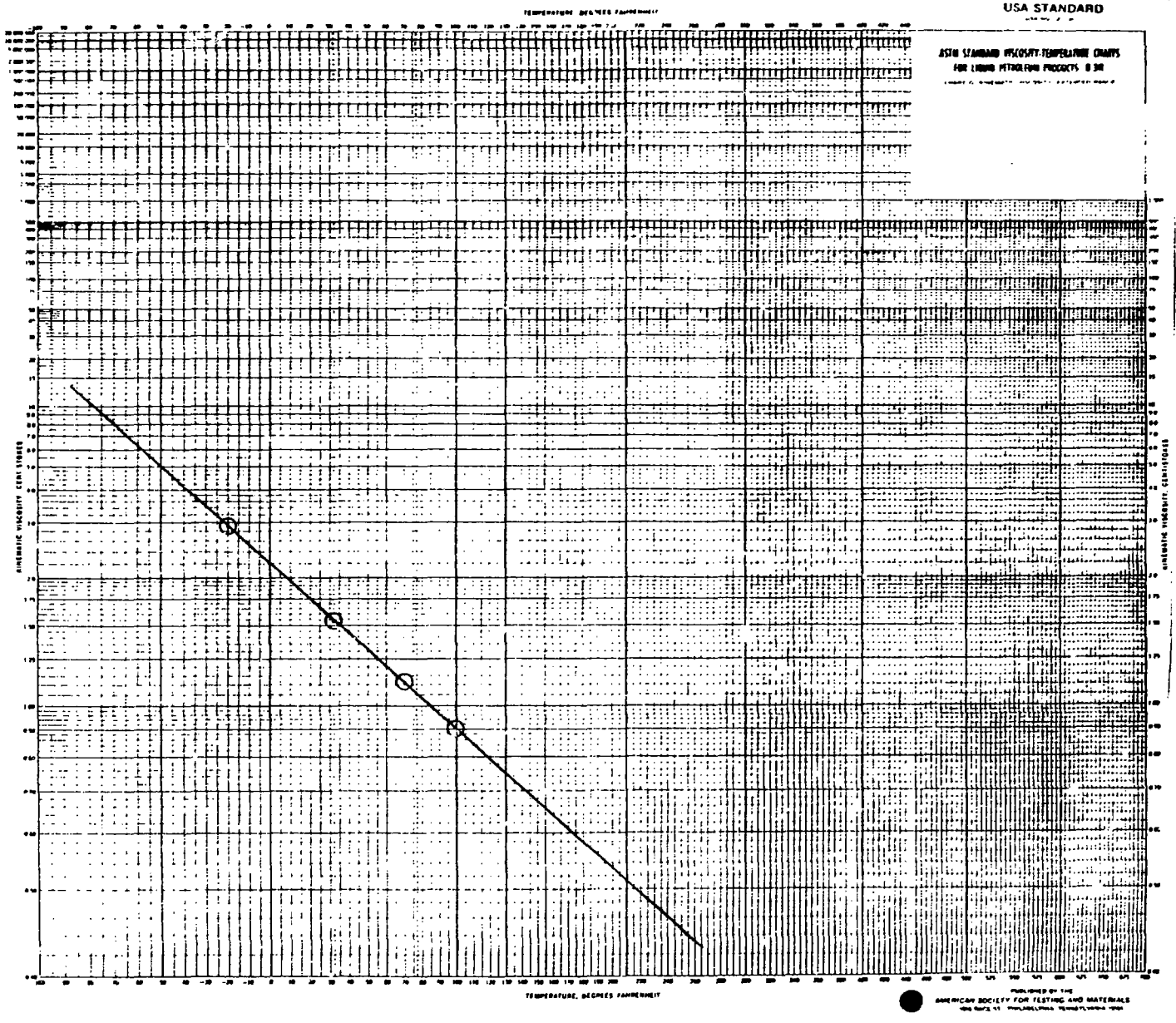

Figure 170. Viscosity/temperature plot for fuel 8B-792009.

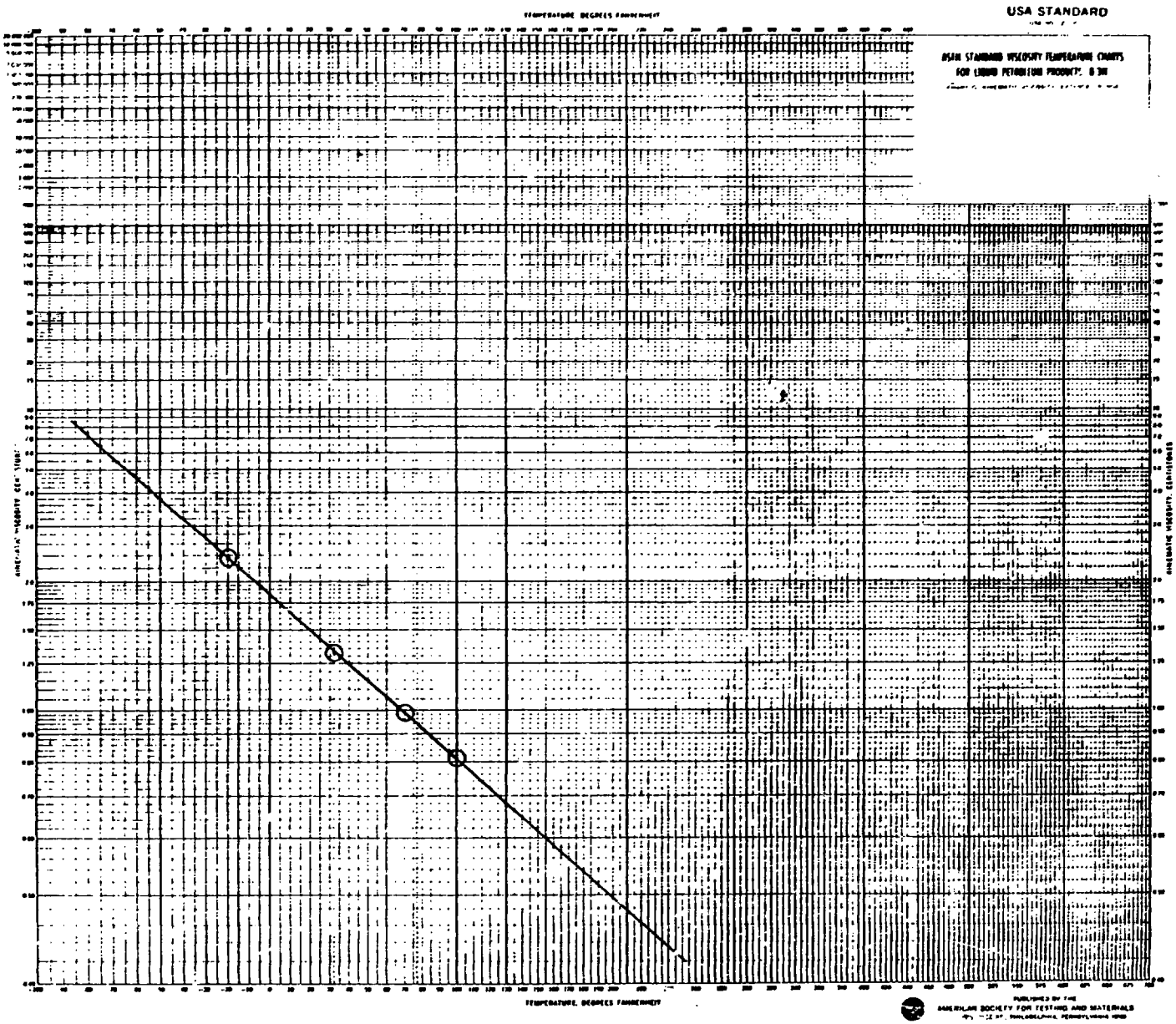

Figure 171. Viscosity/temperature plot for fuel 9B-792009.

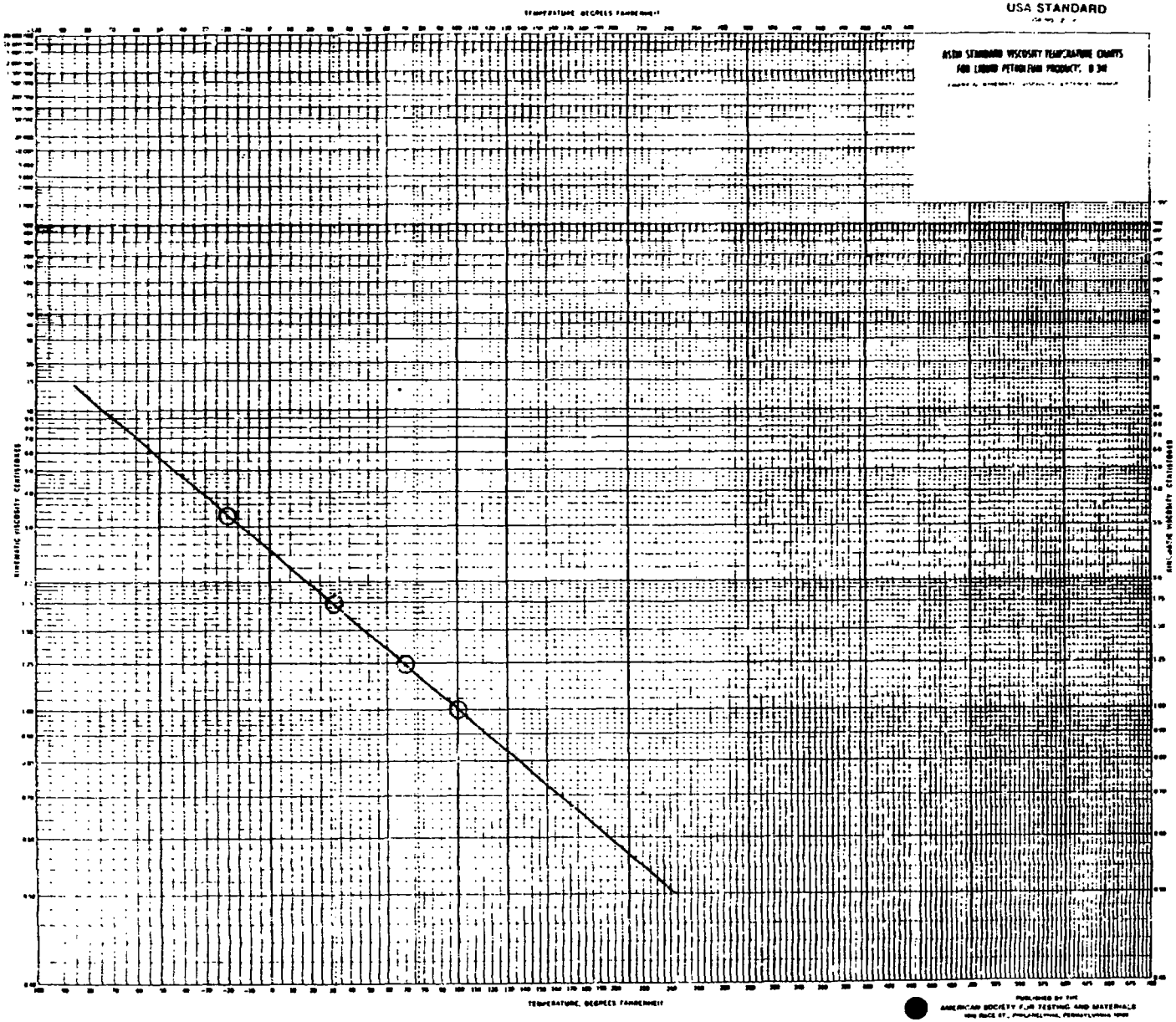

Figure 172. Viscosity/temperature plot for fuel 15B-792009.

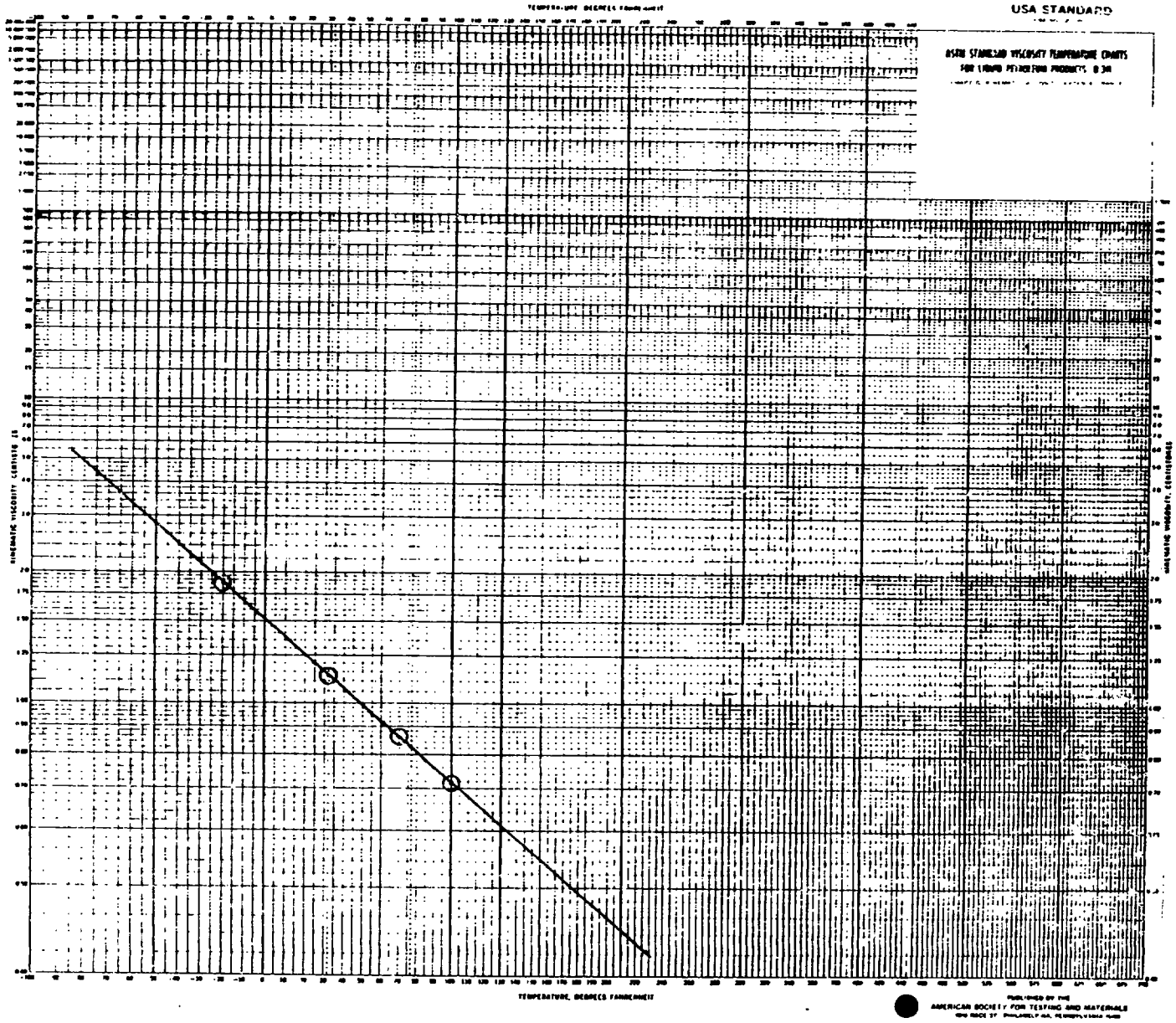

Figure 173. Viscosity/temperature plot for fuel GEC-49B-1.

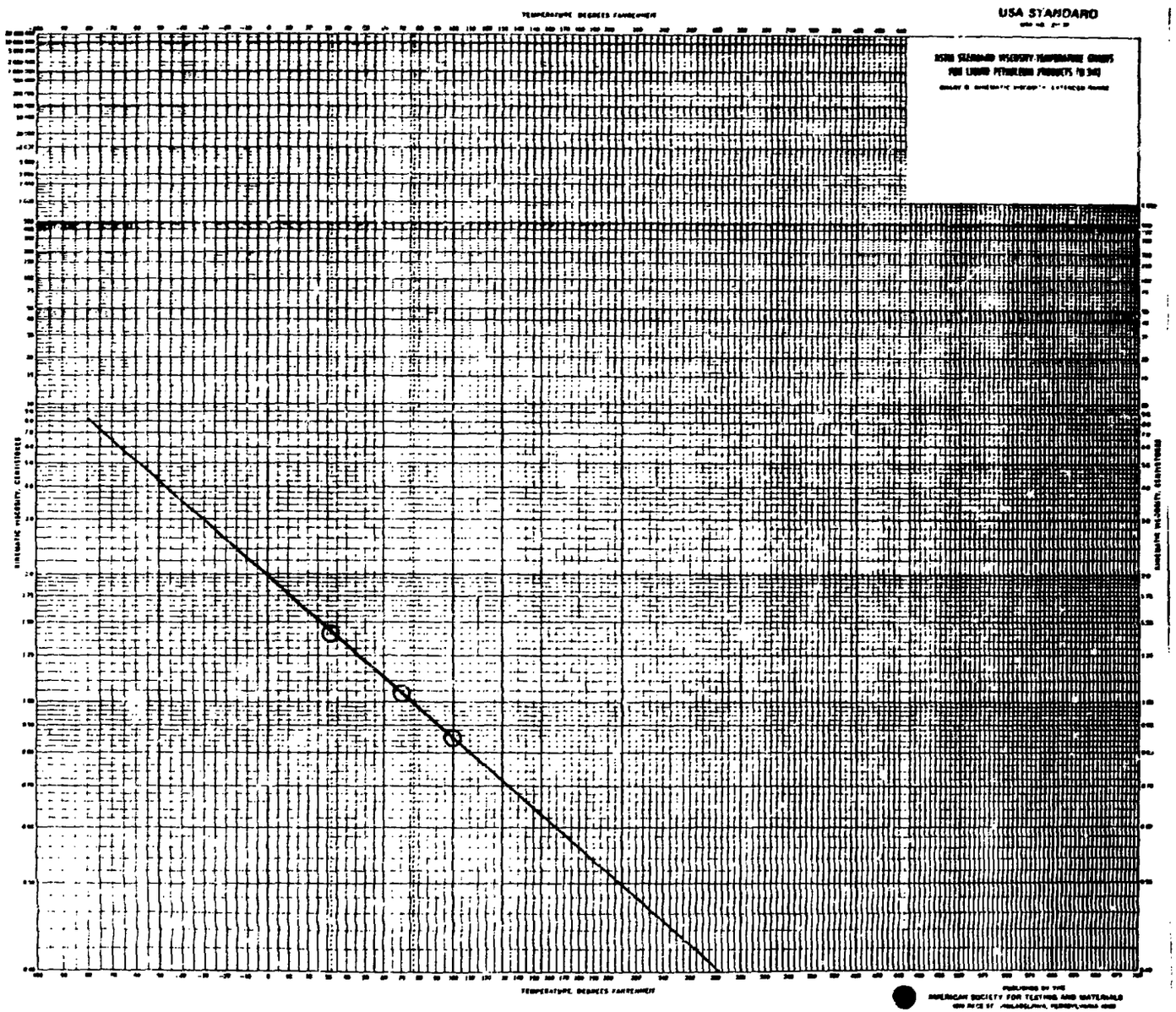

Figure 174. Viscosity/temperature plot for fuel 1C-792009.

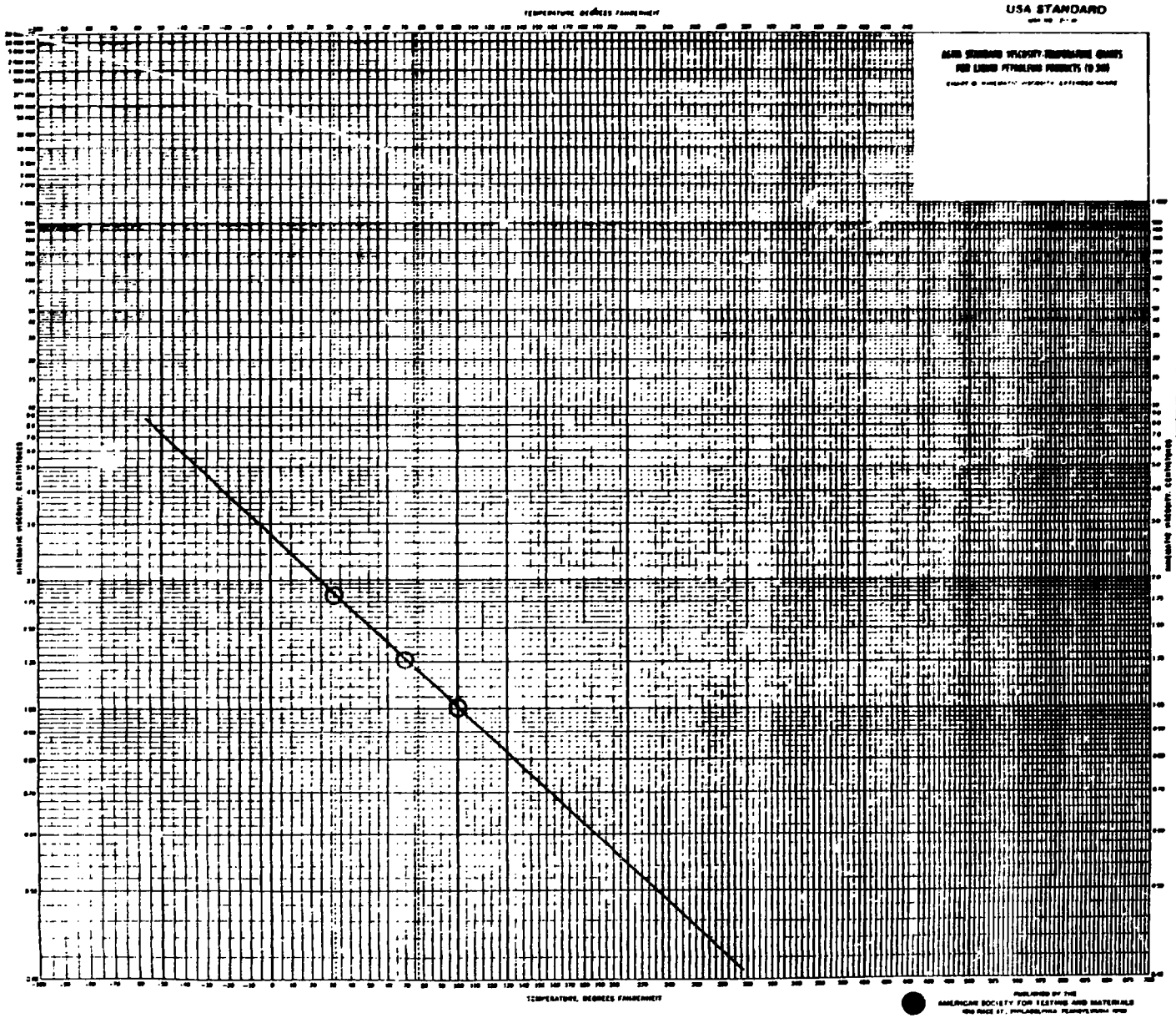

Figure 175. Viscosity/temperature plot for fuel 8C-792009.

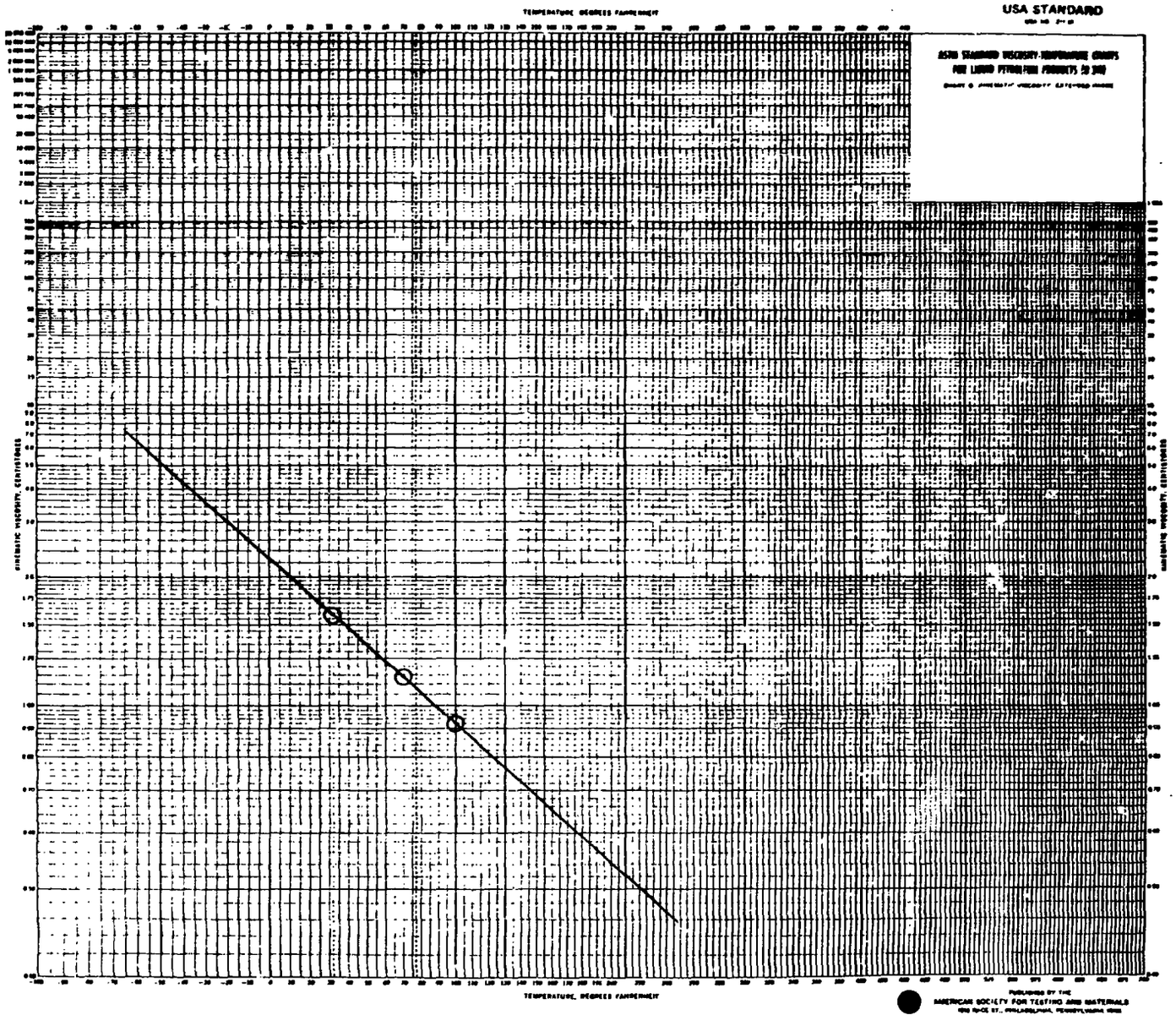

Figure 176. Viscosity/temperature plot for fuel 9C-792009.

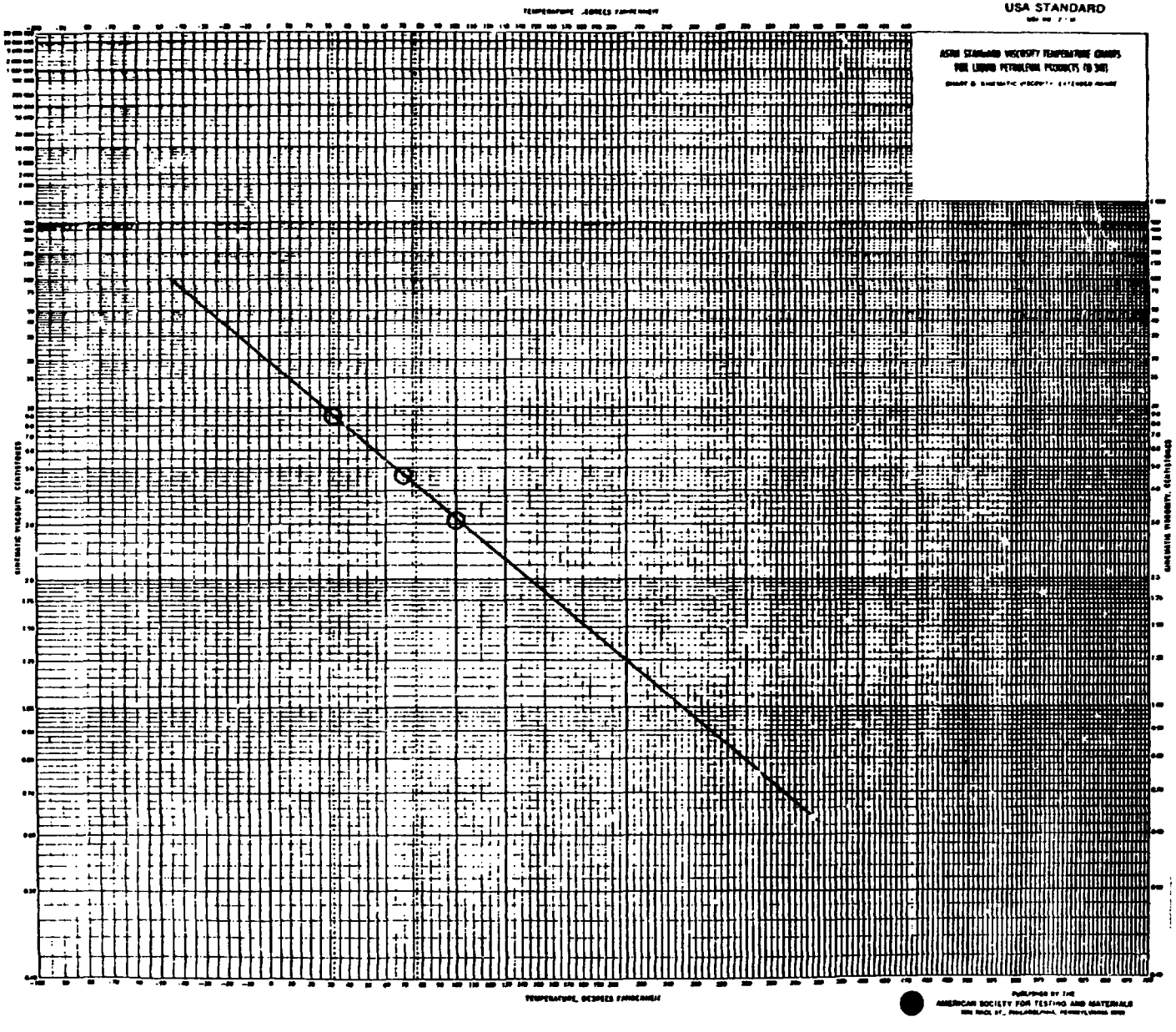

Figure 177. Viscosity/temperature plot for fuel 13C-792009.

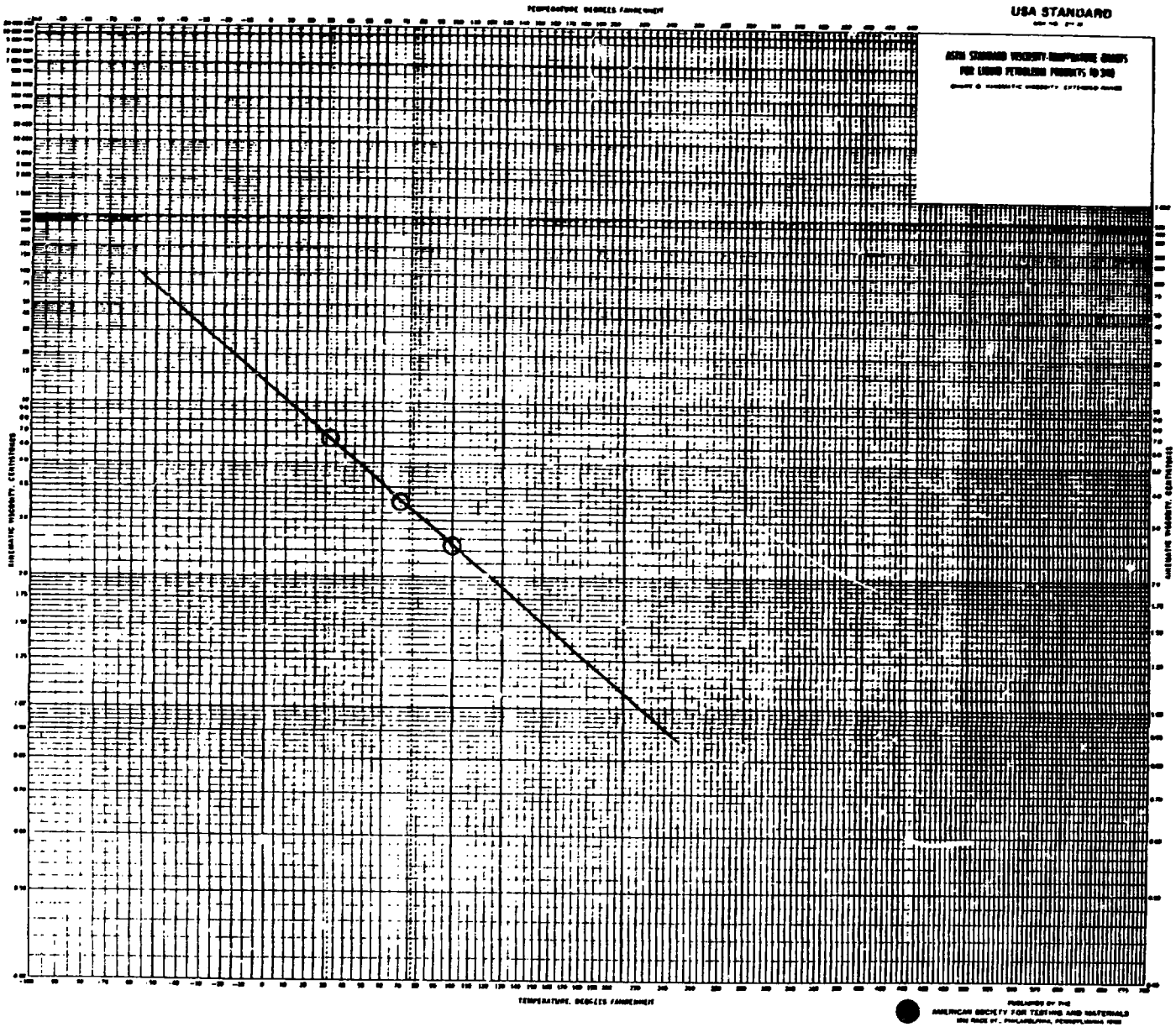

Figure 178. Viscosity/temperature plot for fuel 14C-792009.

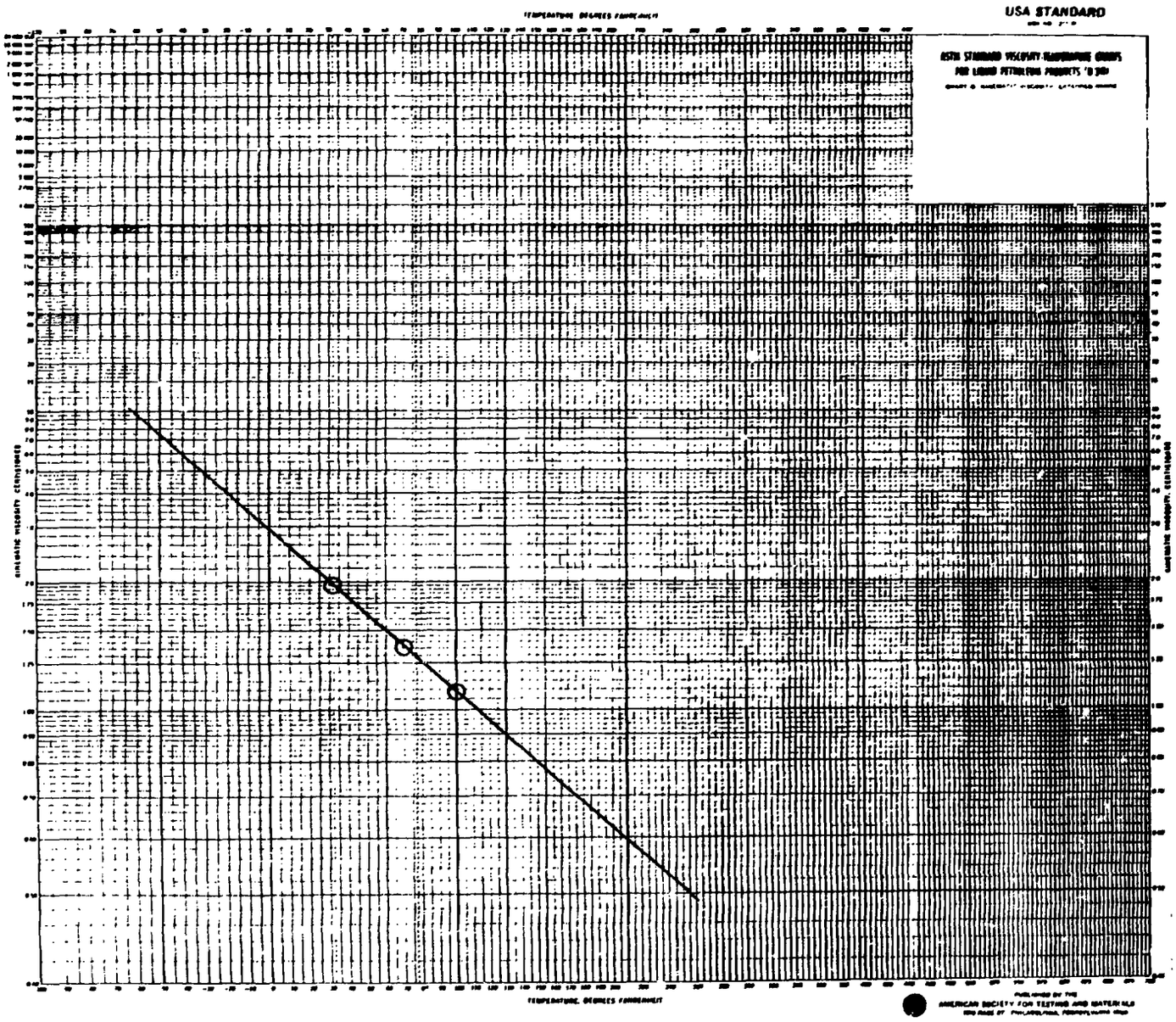

Figure 179. Viscosity/temperature plot for fuel 15C-792009.

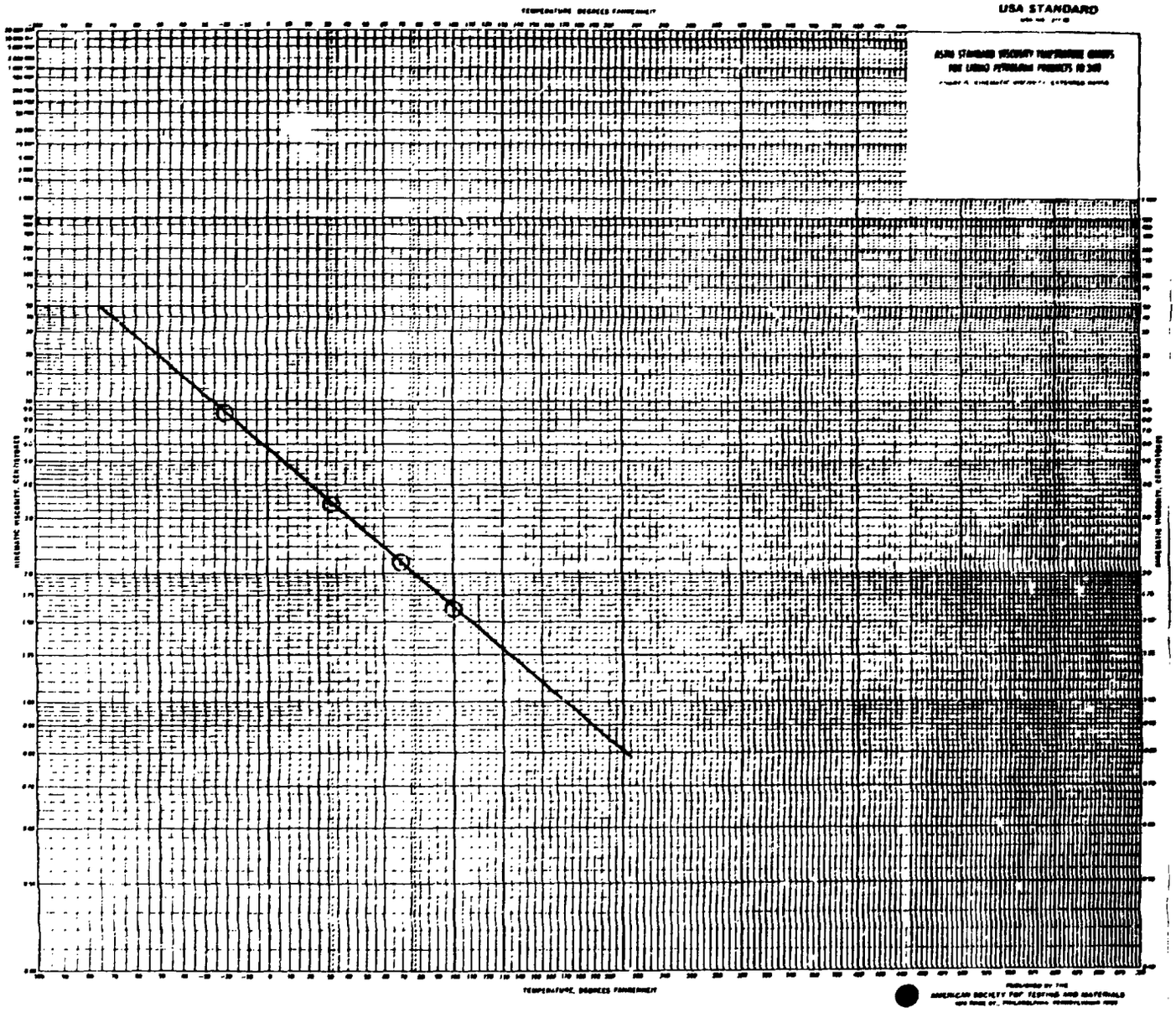

Figure 180. Viscosity/temperature plot for fuel JP-5, Tank 13.

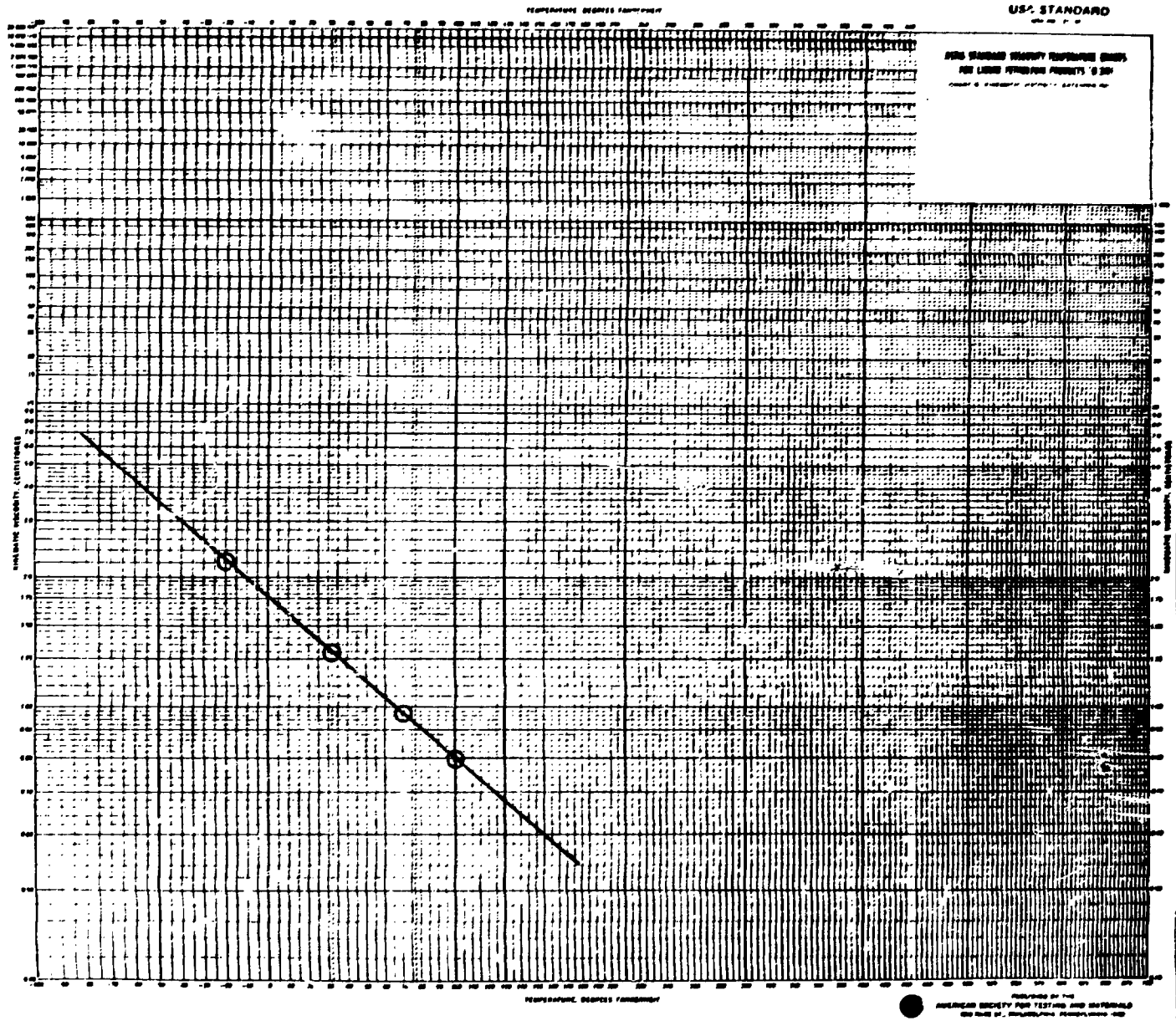

Figure 181. Viscosity/temperature plot for fuel P&W 79-C-2086, Petroleum JP-4.

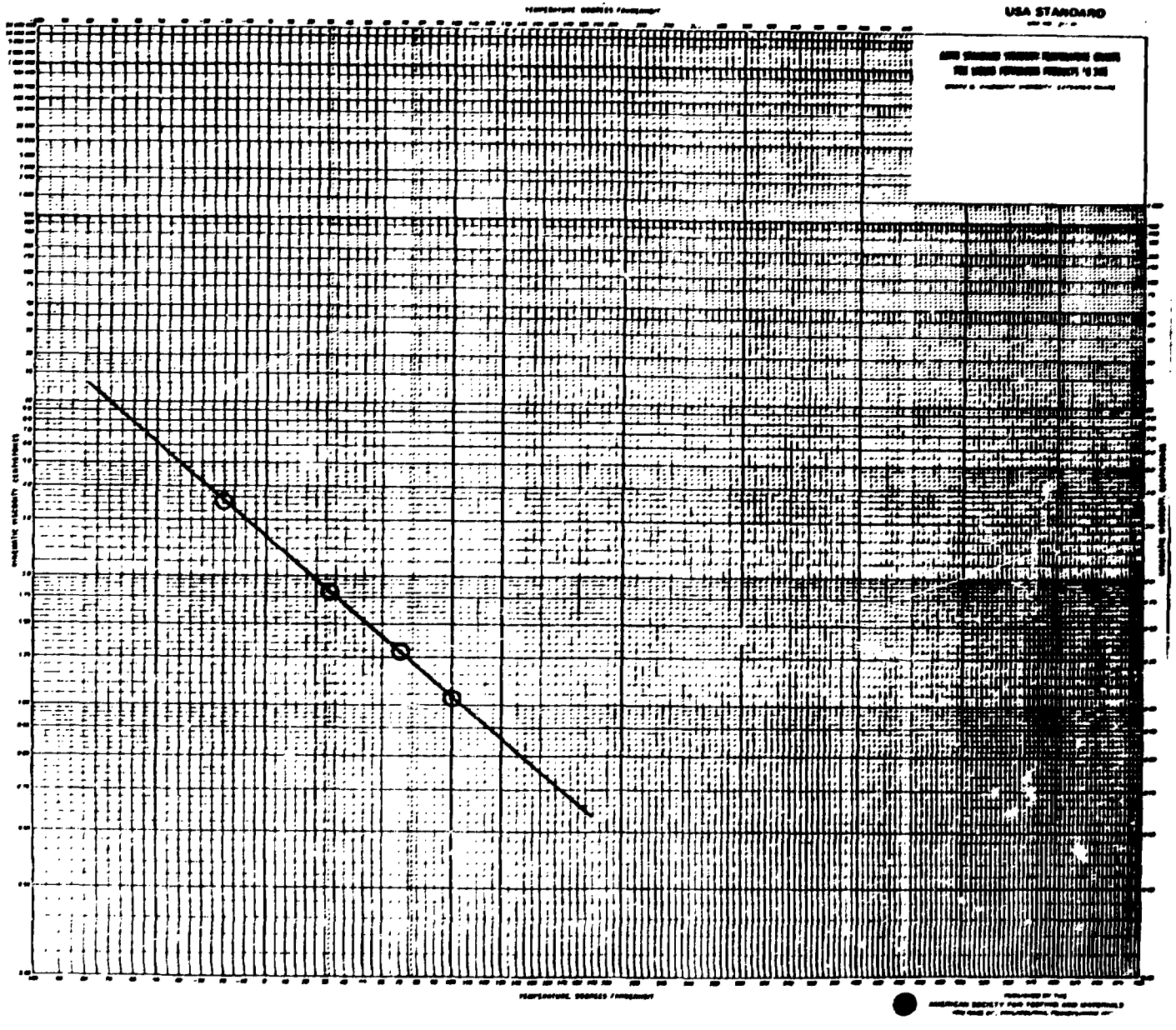

Figure 182. Viscosity/temperature plot for fuel P&W 79-C-2086, Shale JP-4.

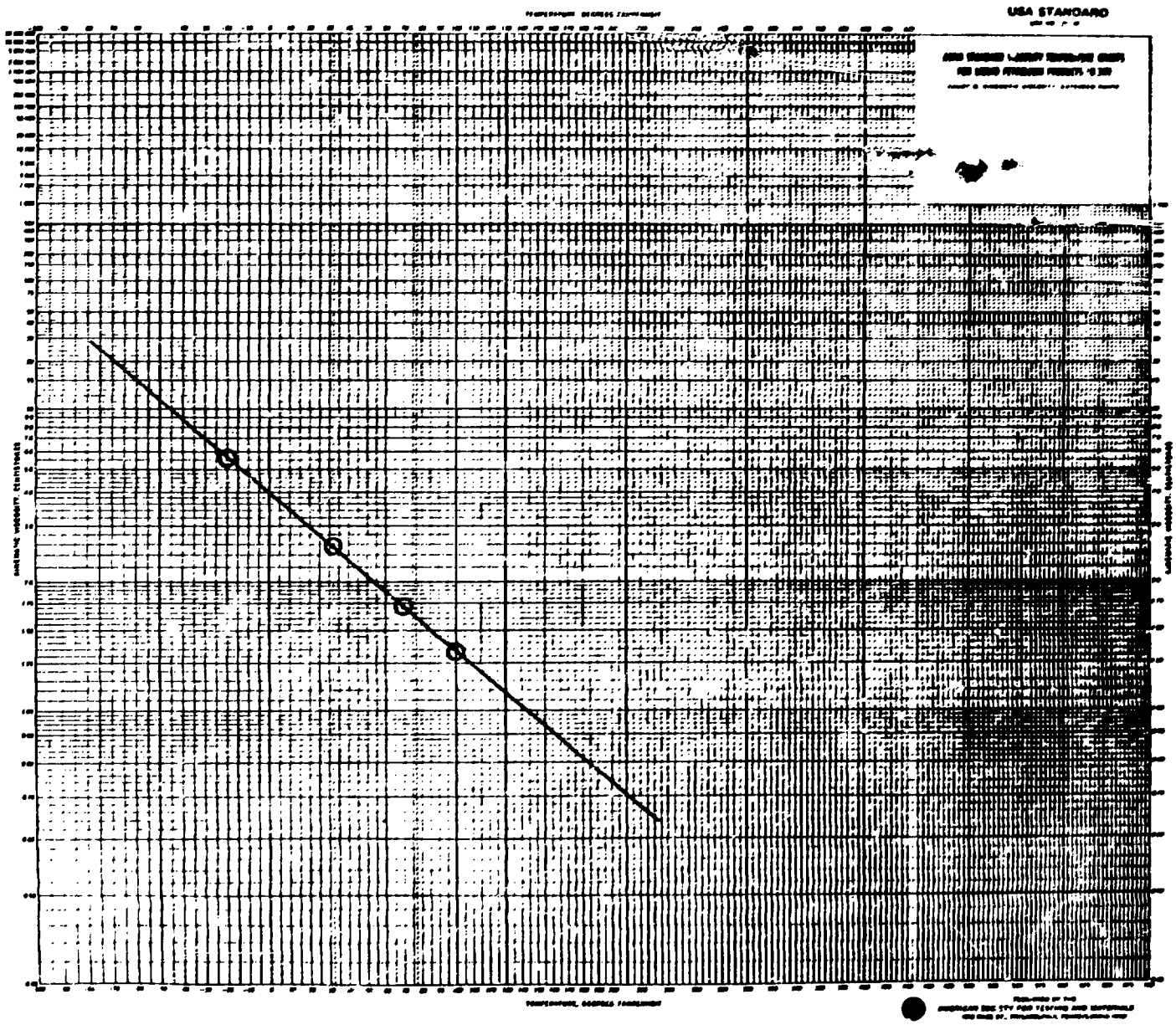

Figure 183. Viscosity/temperature plot for fuel P&W 79-C-2086, Blend #1.

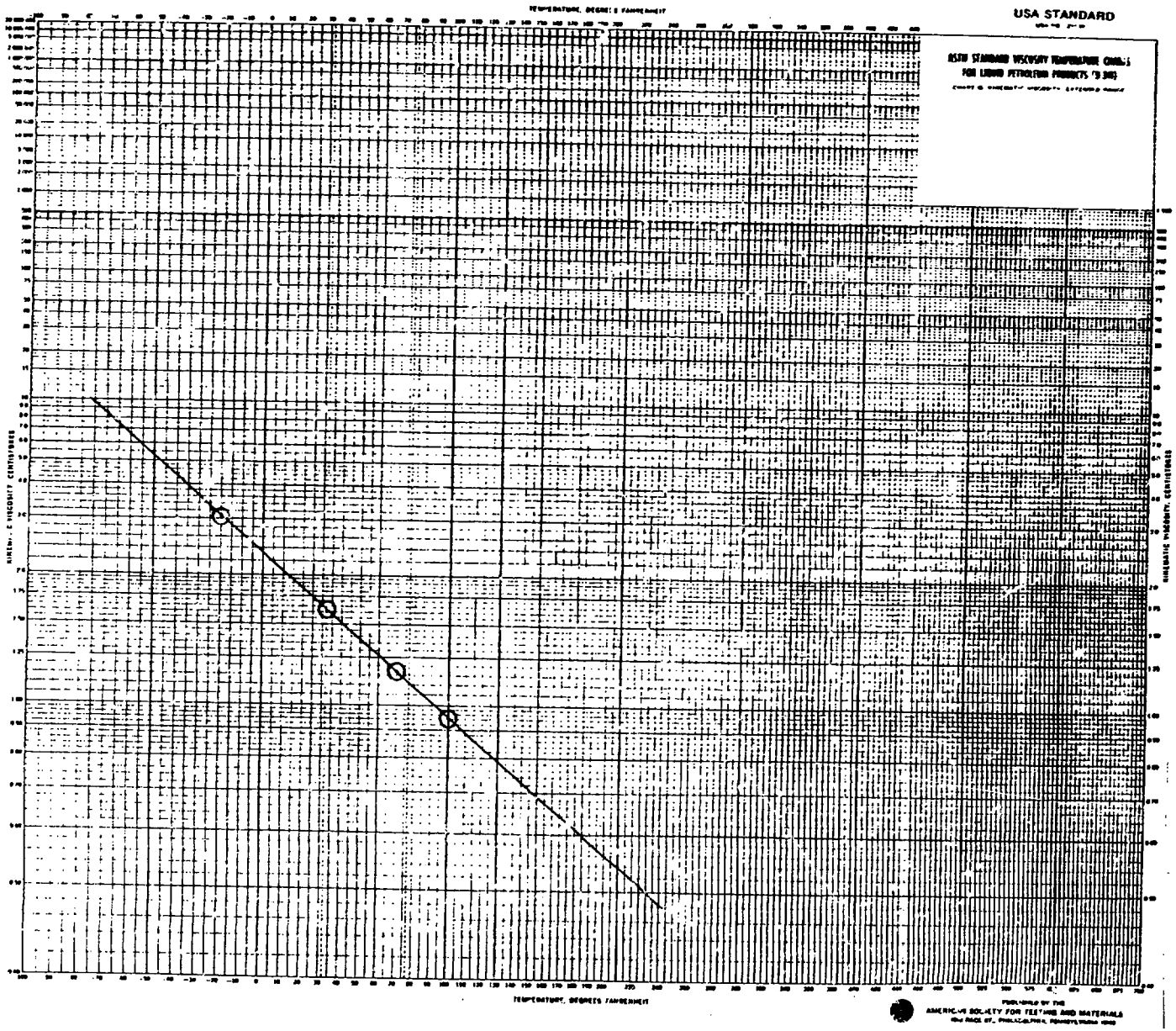

Figure 184. Viscosity/temperature plot for fuel P&W 79-C-2086, Blend #2.

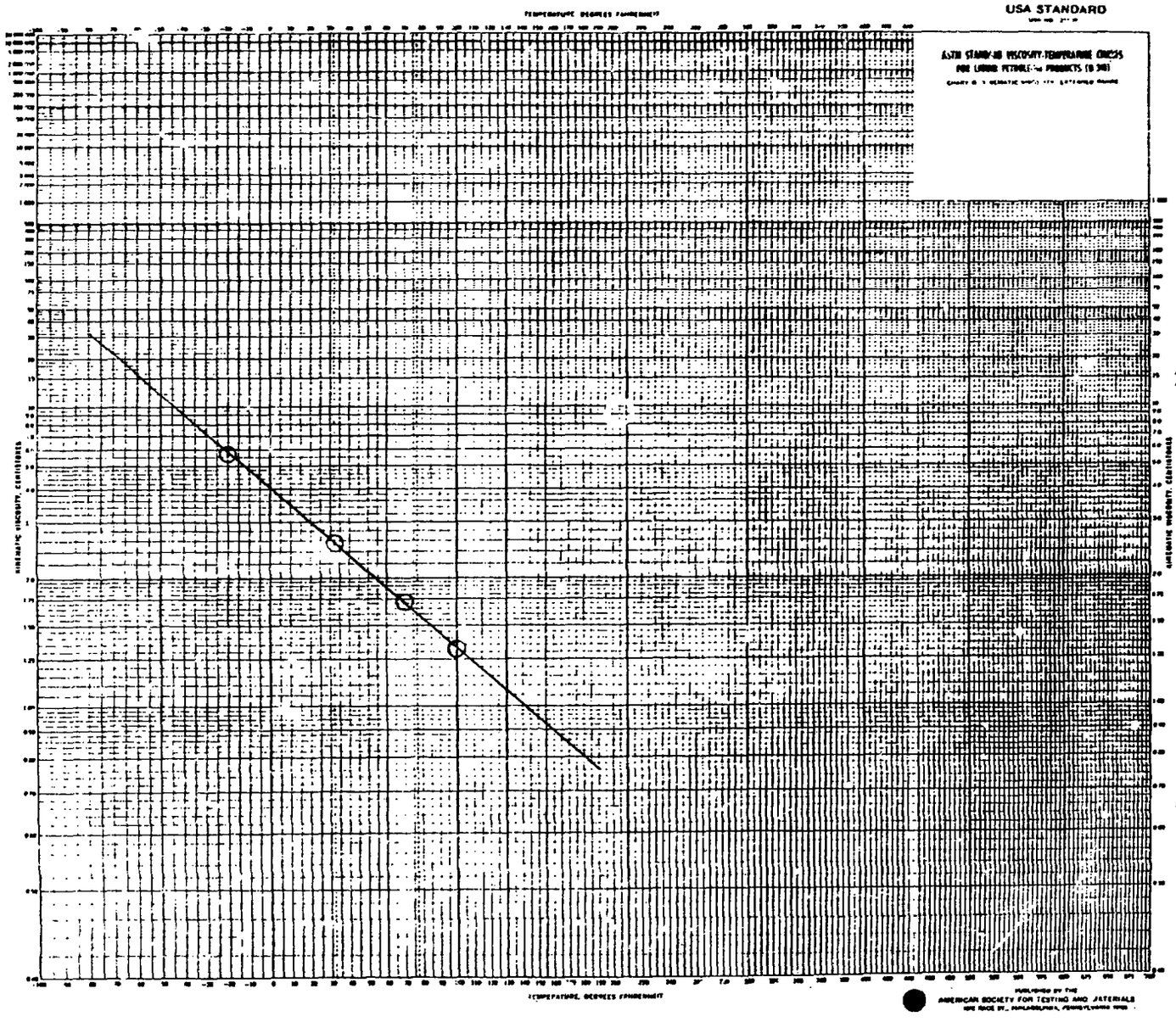

Figure 185. Viscosity/temperature plot for fuel P&W 79-C-2086, Blend #3.

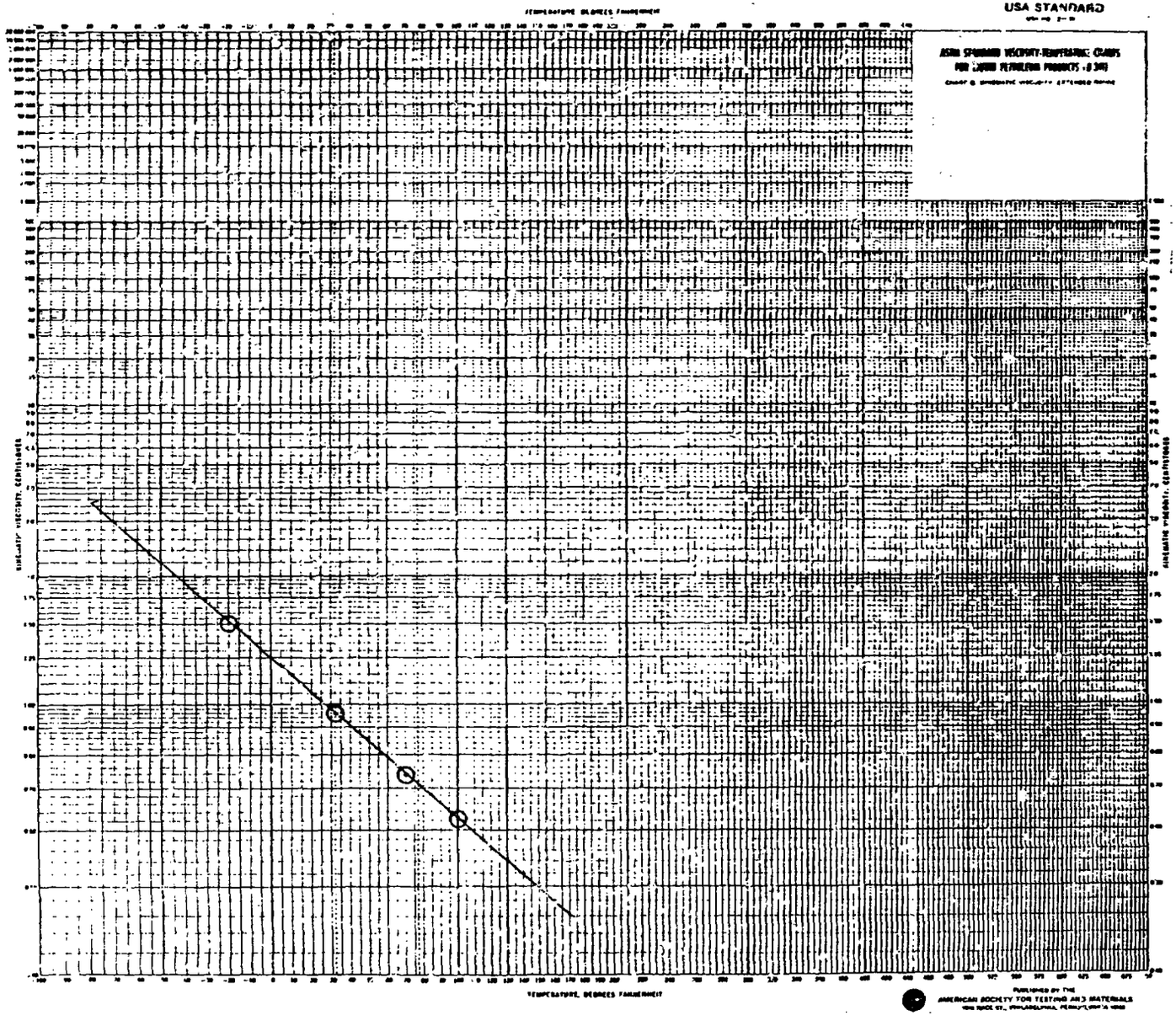

Figure 186. Viscosity/temperature plot for fuel P&W 79-C-2086, Blend #4.

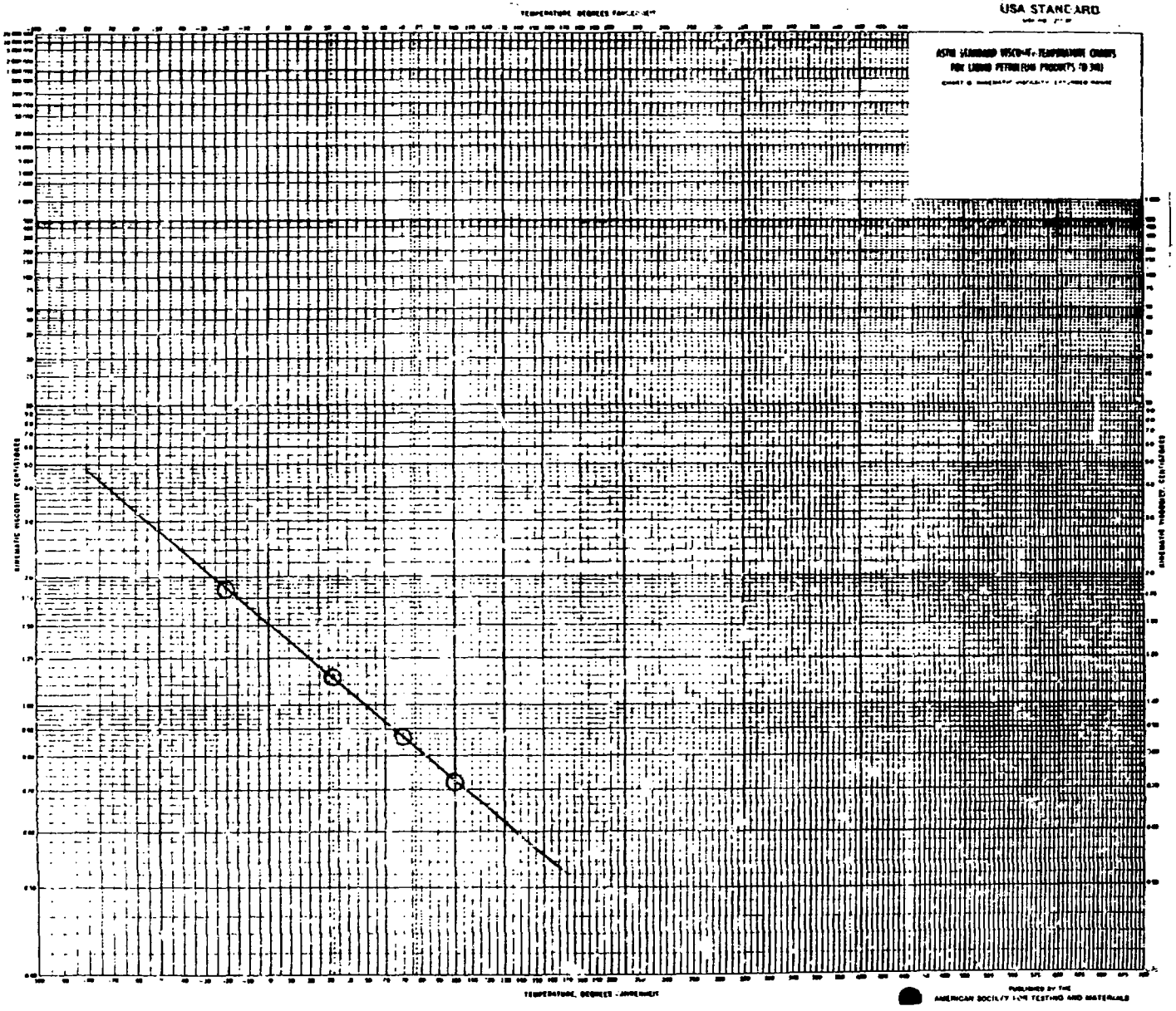

Figure 187. Viscosity/temperature plot for fuel GECS-62B-1.

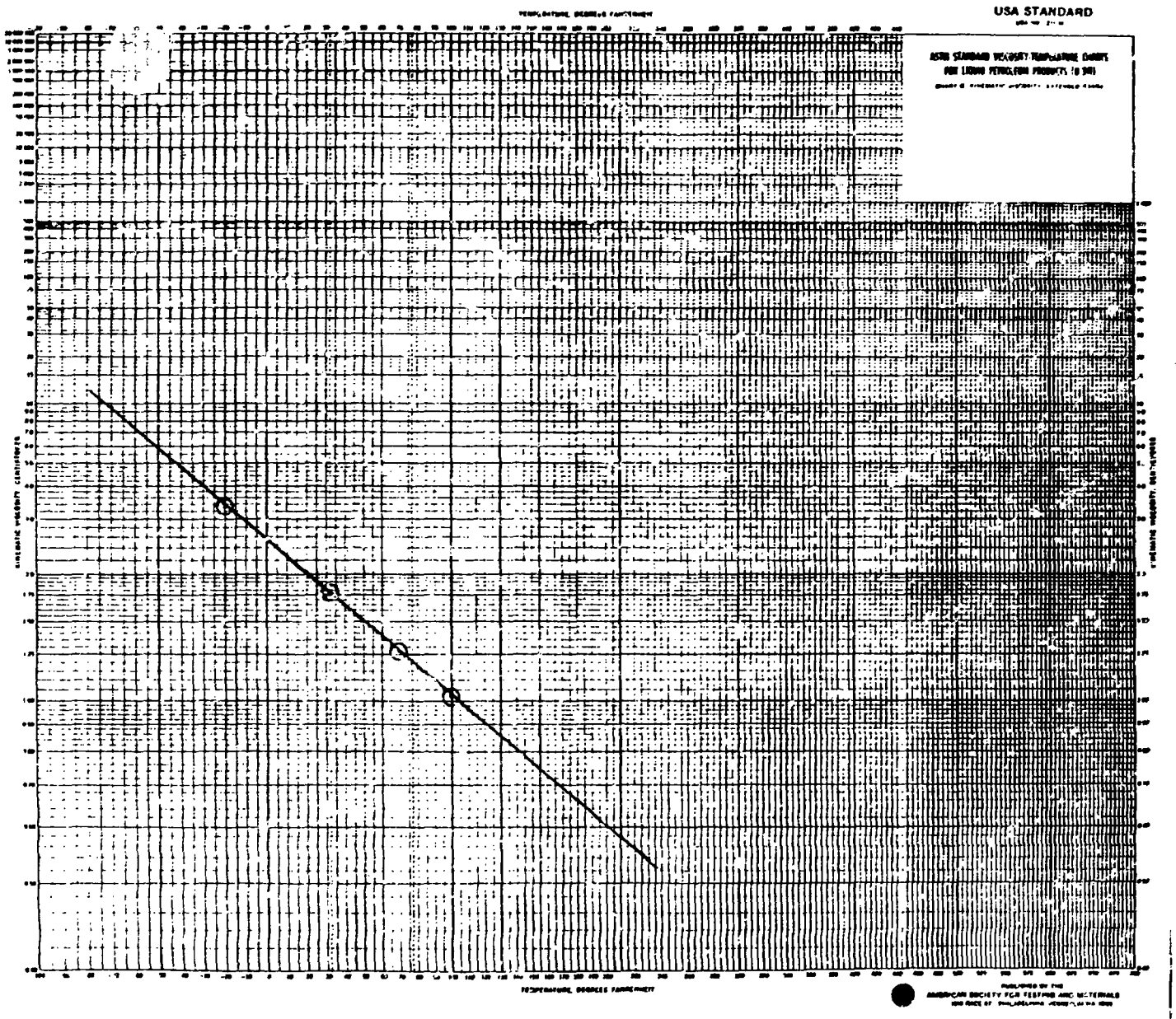

Figure 188. Viscosity/temperature plot for fuel M50001.

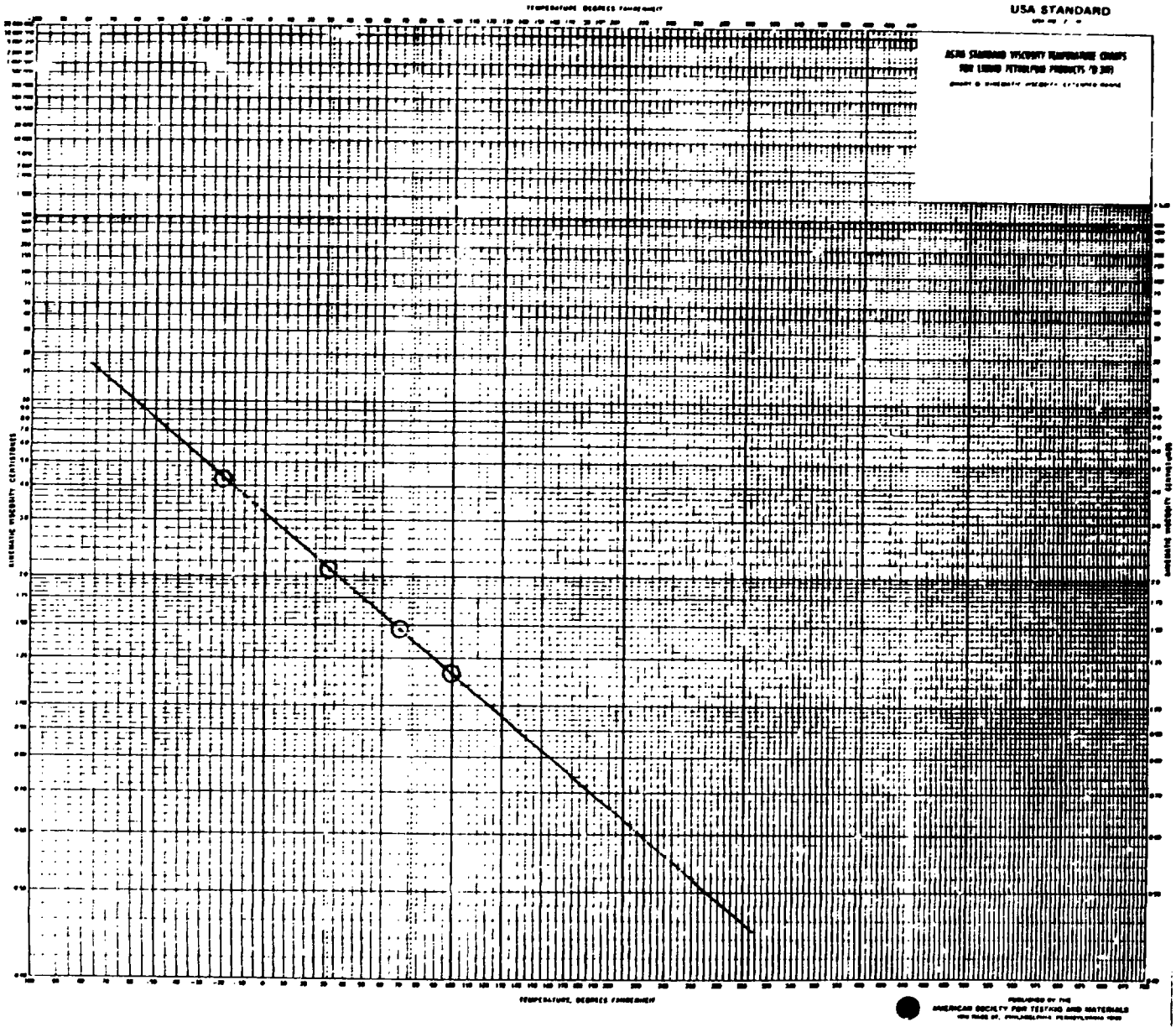

Figure 189. Viscosity/temperature plot for fuel M60001.

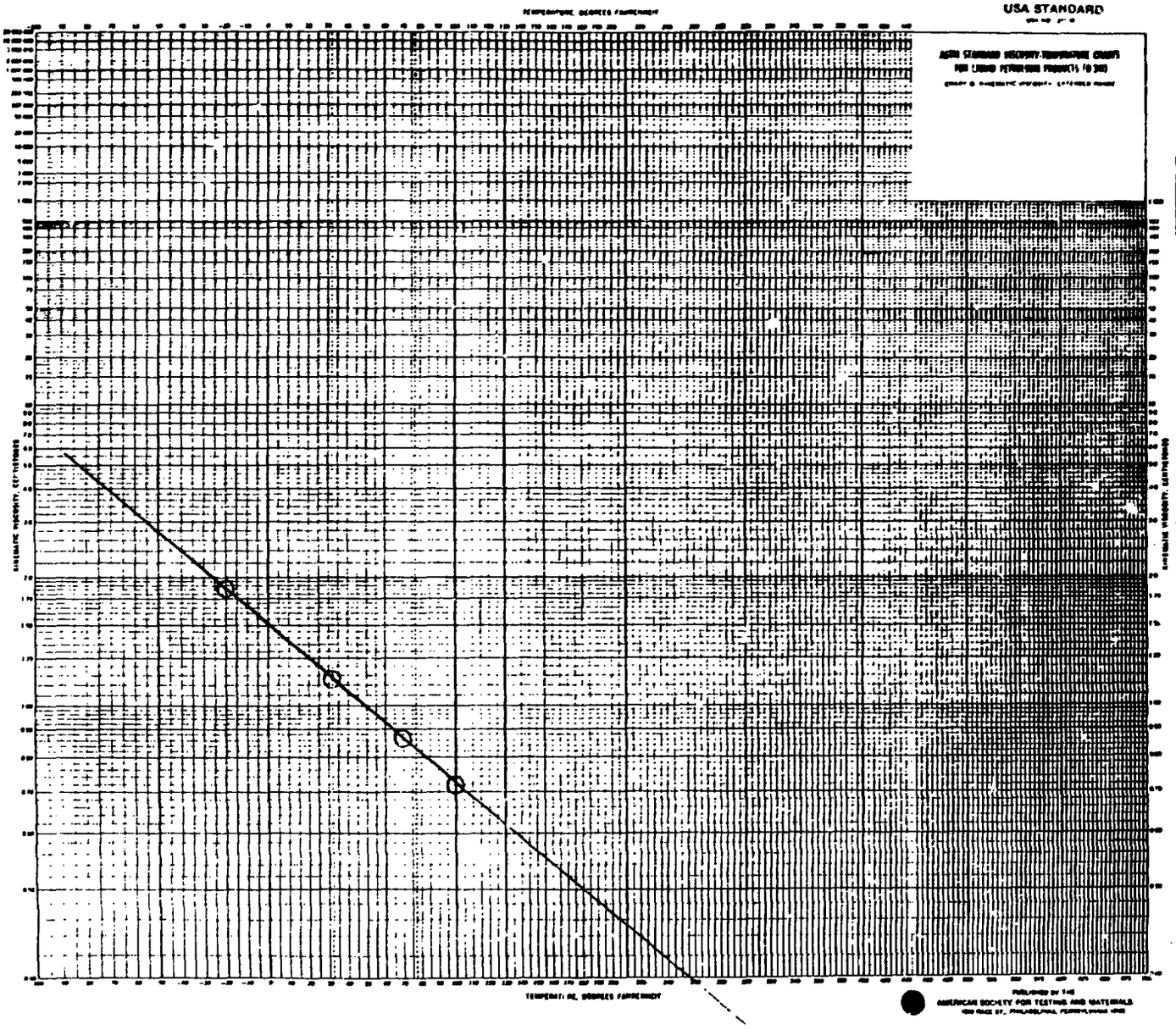

Figure 190. Viscosity/temperature plot for fuel M70001.

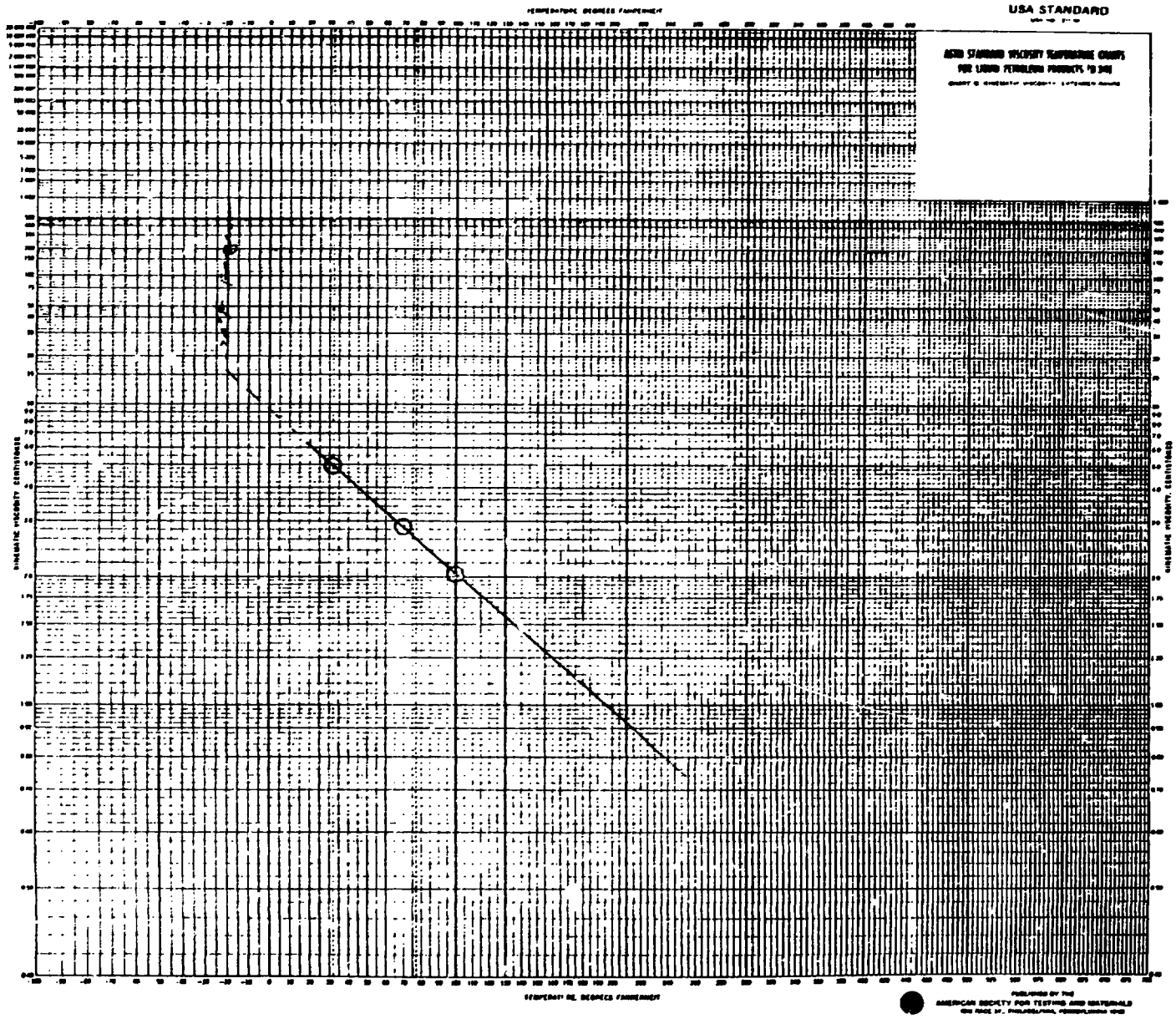

Figure 191. Viscosity/temperature plot for fuel M80001.

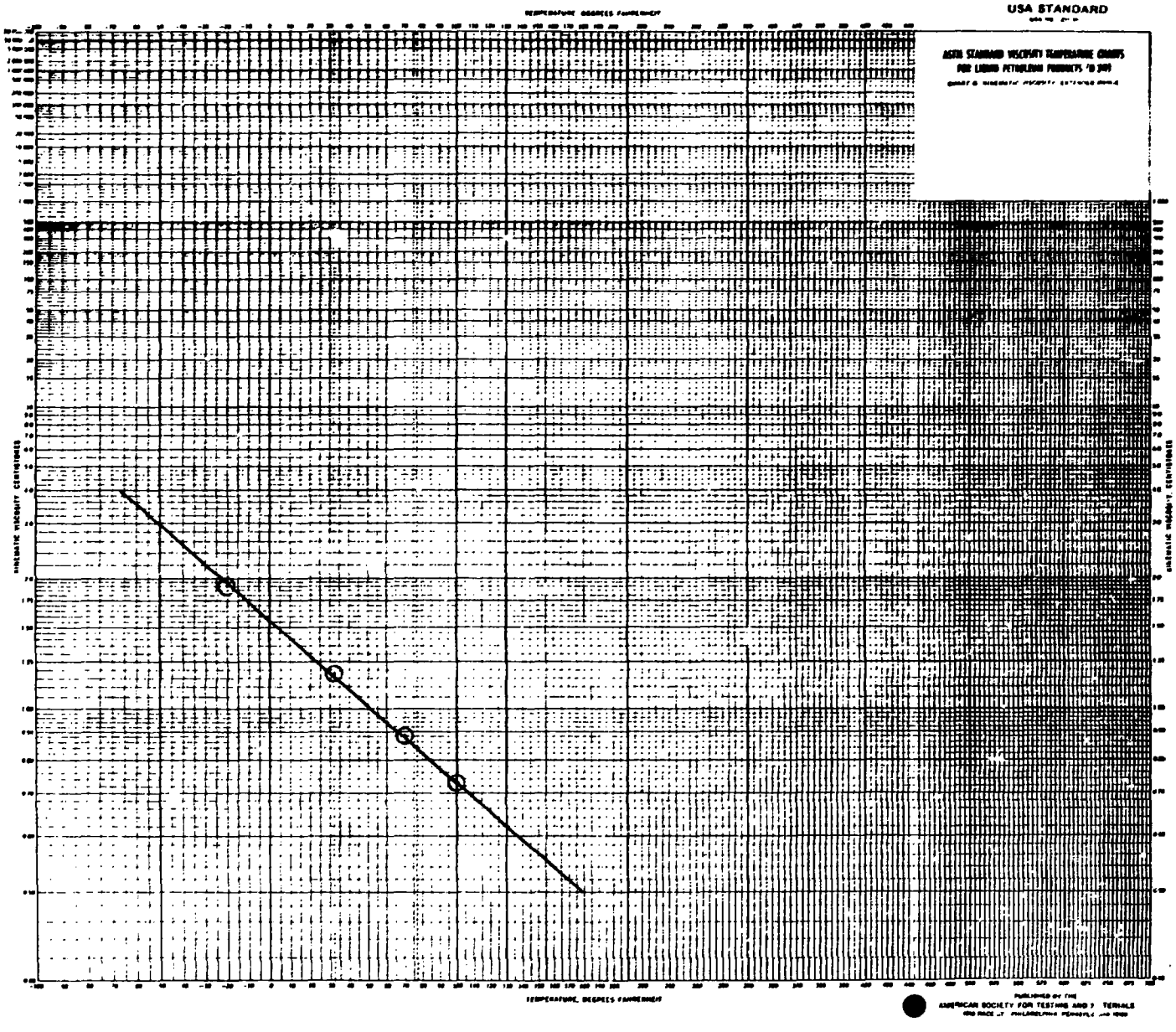

Figure 192. Viscosity/temperature plot for fuel GEC-77B-792009.

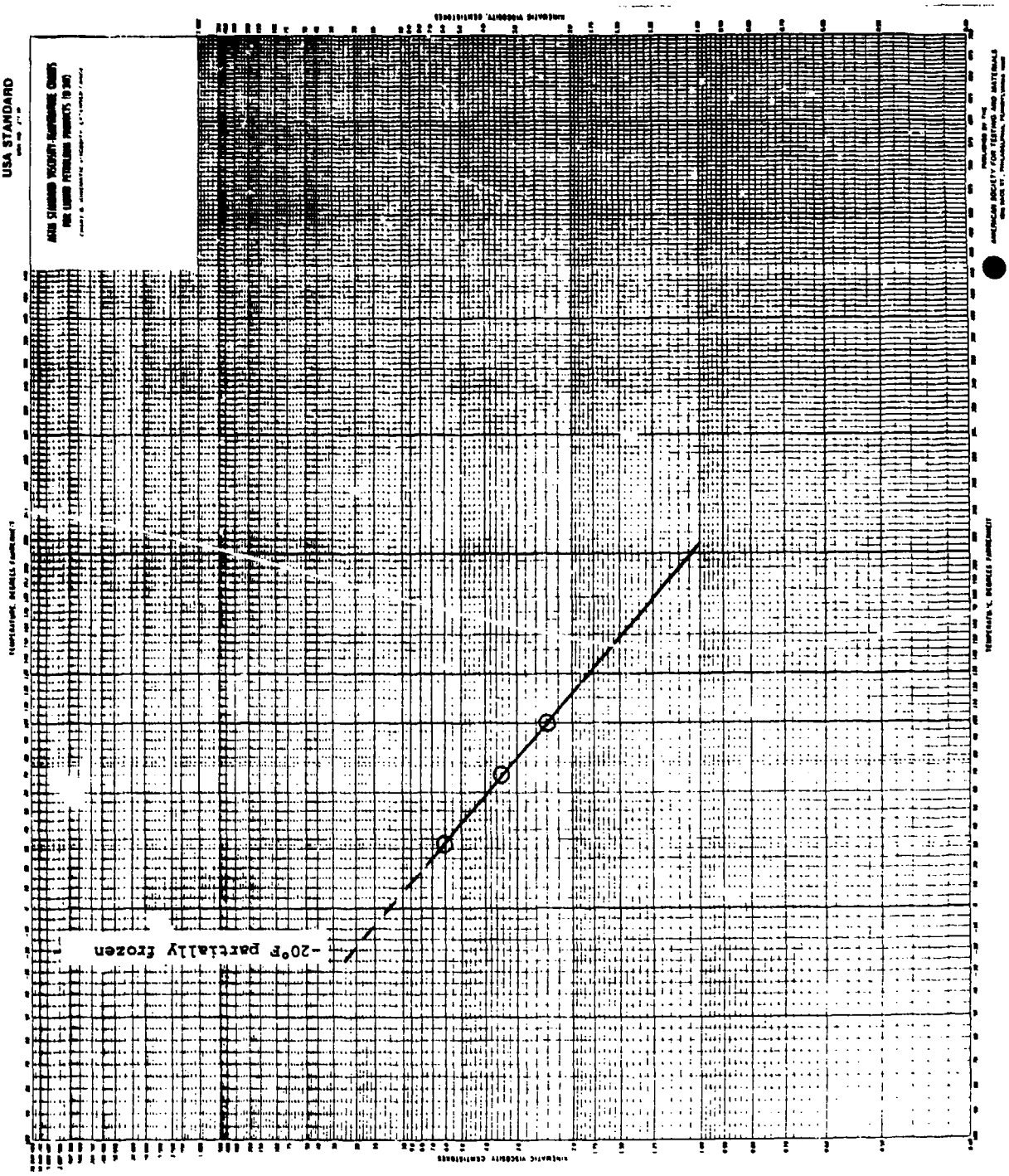

Figure 193. Viscosity/temperature plot for fuel GEC-78B-792009.

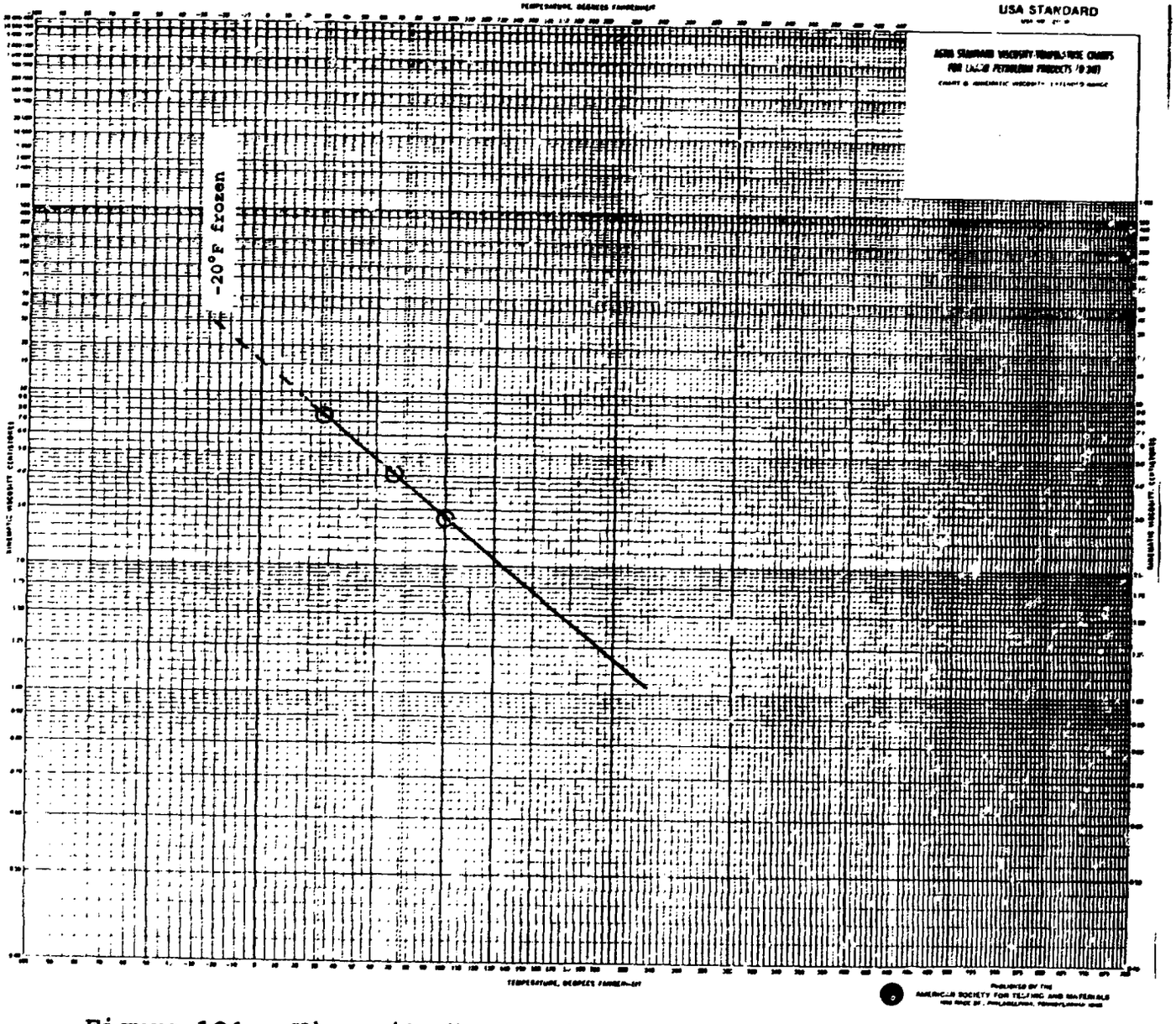

Figure 194. Viscosity/temperature plot for fuel 13C-2-792009.

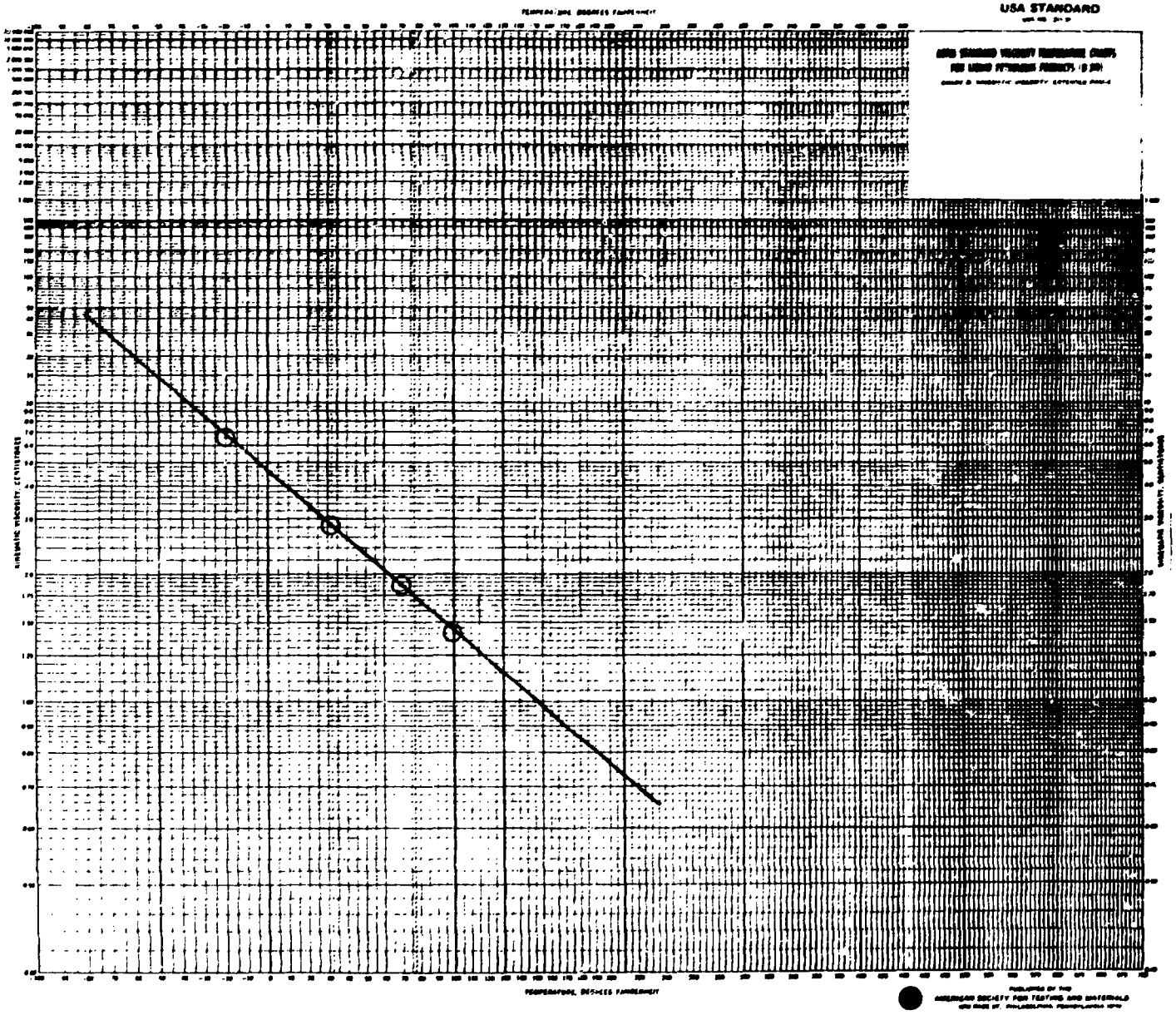

Figure 195. Viscosity/temperature plot for fuel M50014A-2.

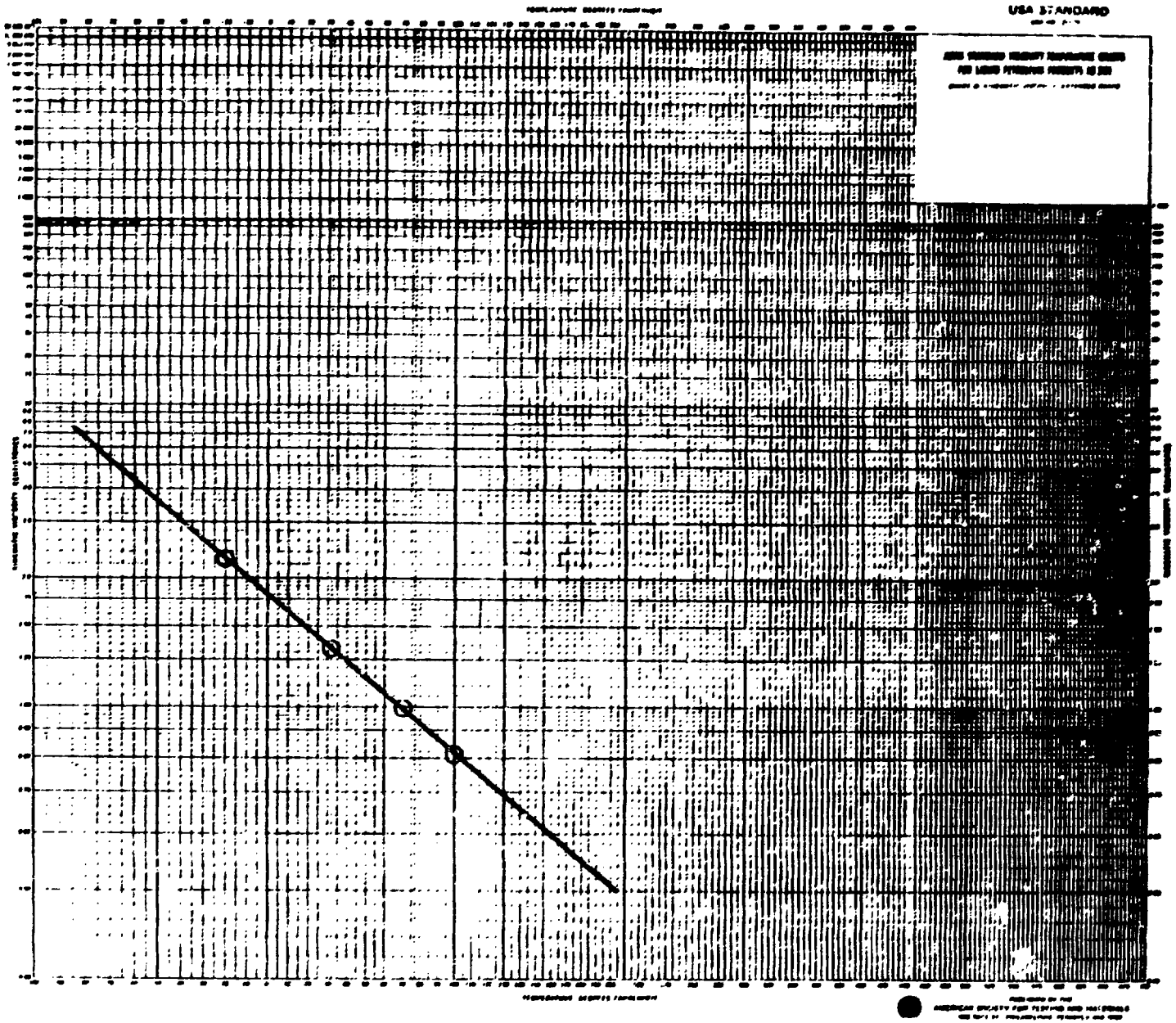

Figure 196. Viscosity/temperature plot for fuel MJ0016A.

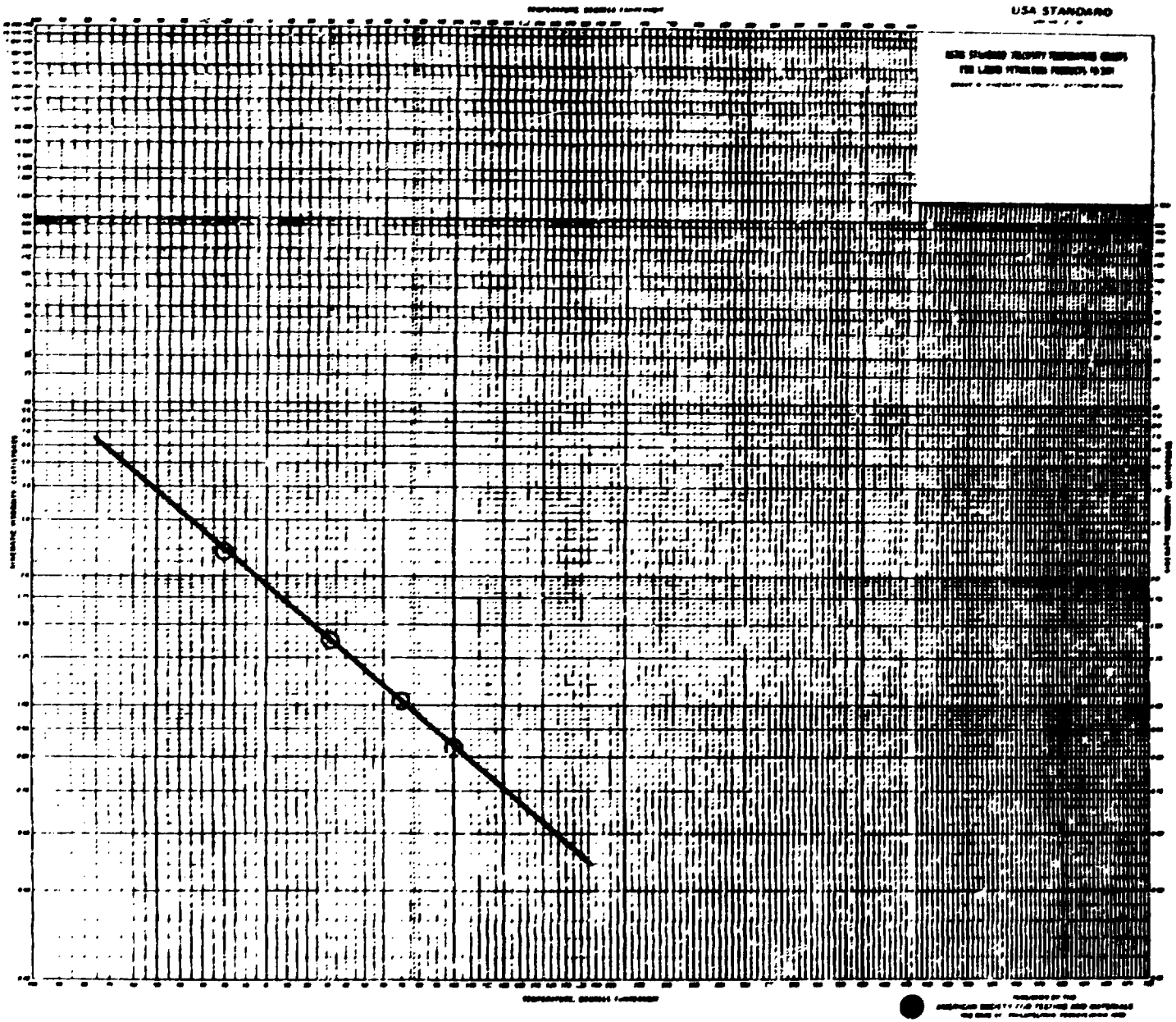

Figure 197. Viscosity/temperature plot for fuel MJ0013B.

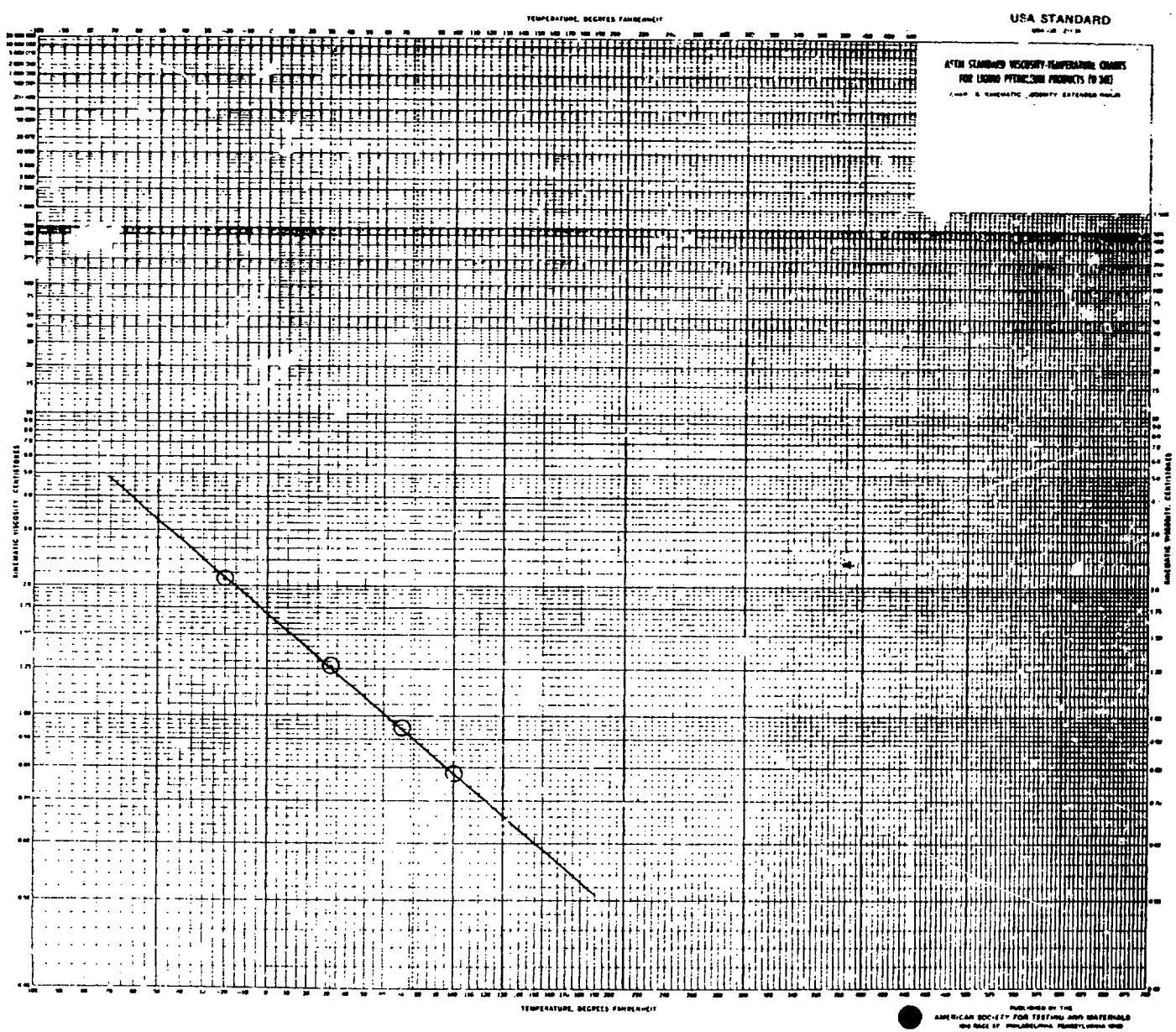

Figure 198. Viscosity/temperature plot for fuel GECF-1D, (JP-4)-043.

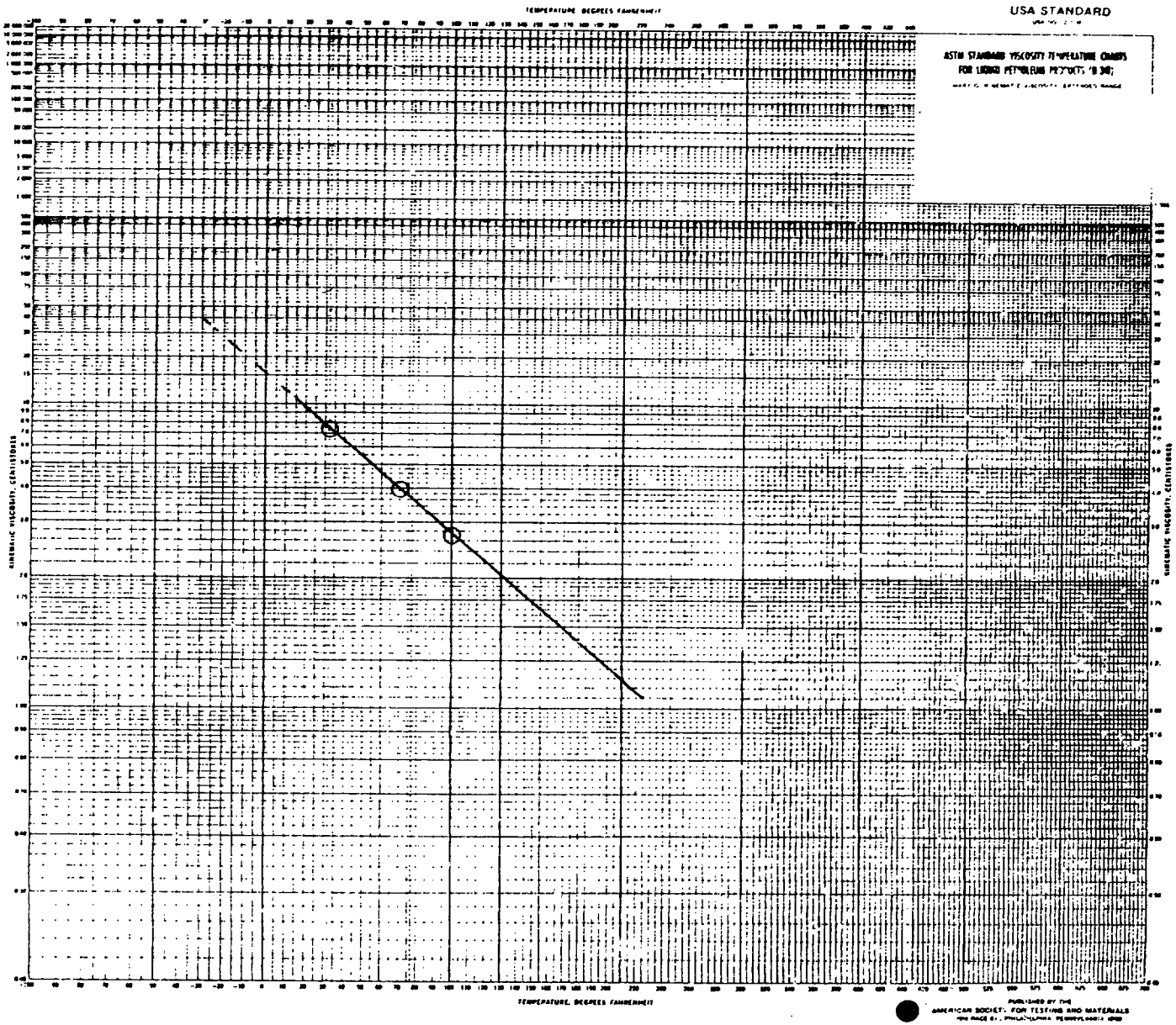

Figure 199. Viscosity/temperature plot for fuel GECF-13D, (DF-2)-044.

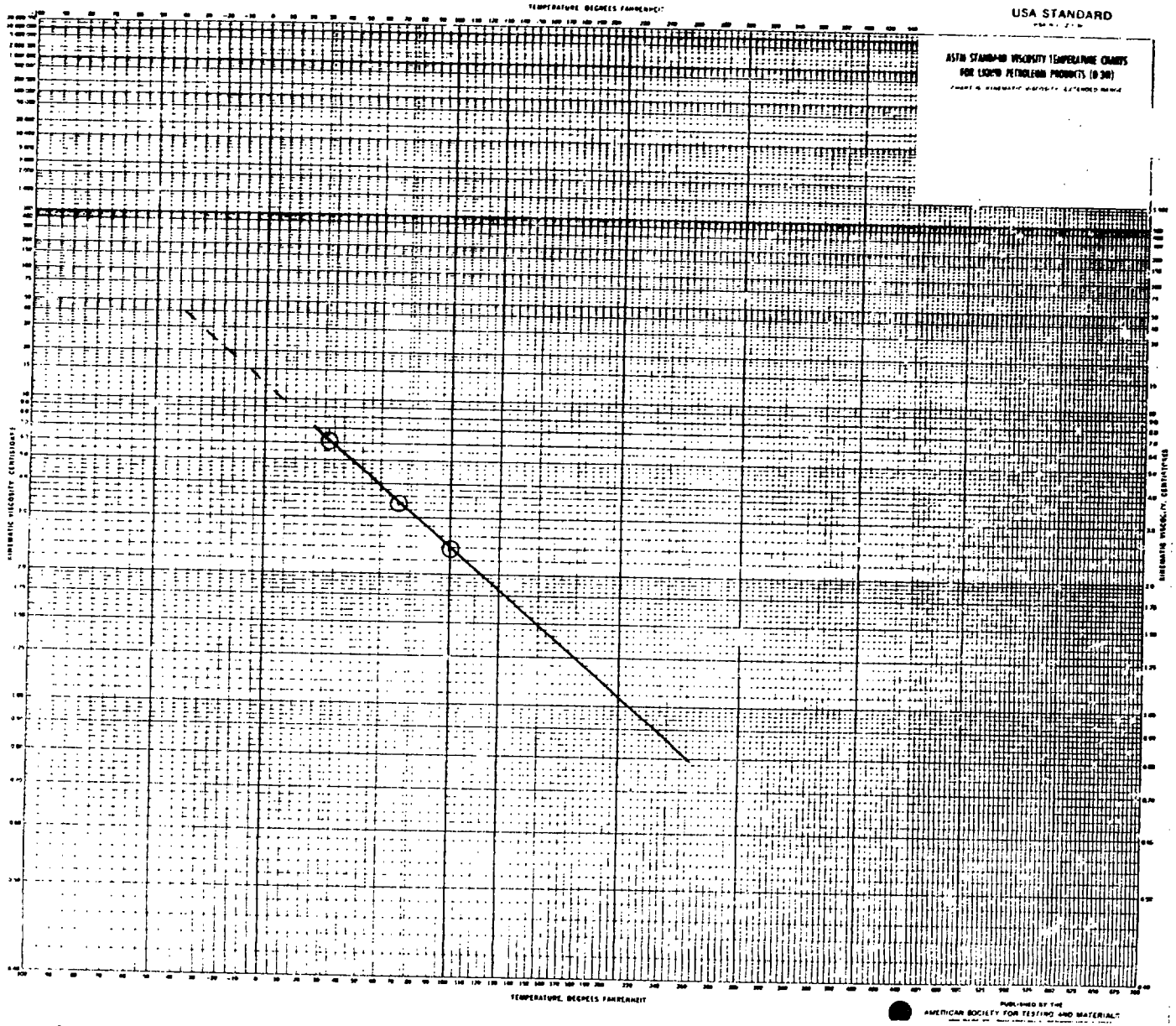

Figure 200. Viscosity/temperature plot for fuel GECF-14D POSF-D-81-042.

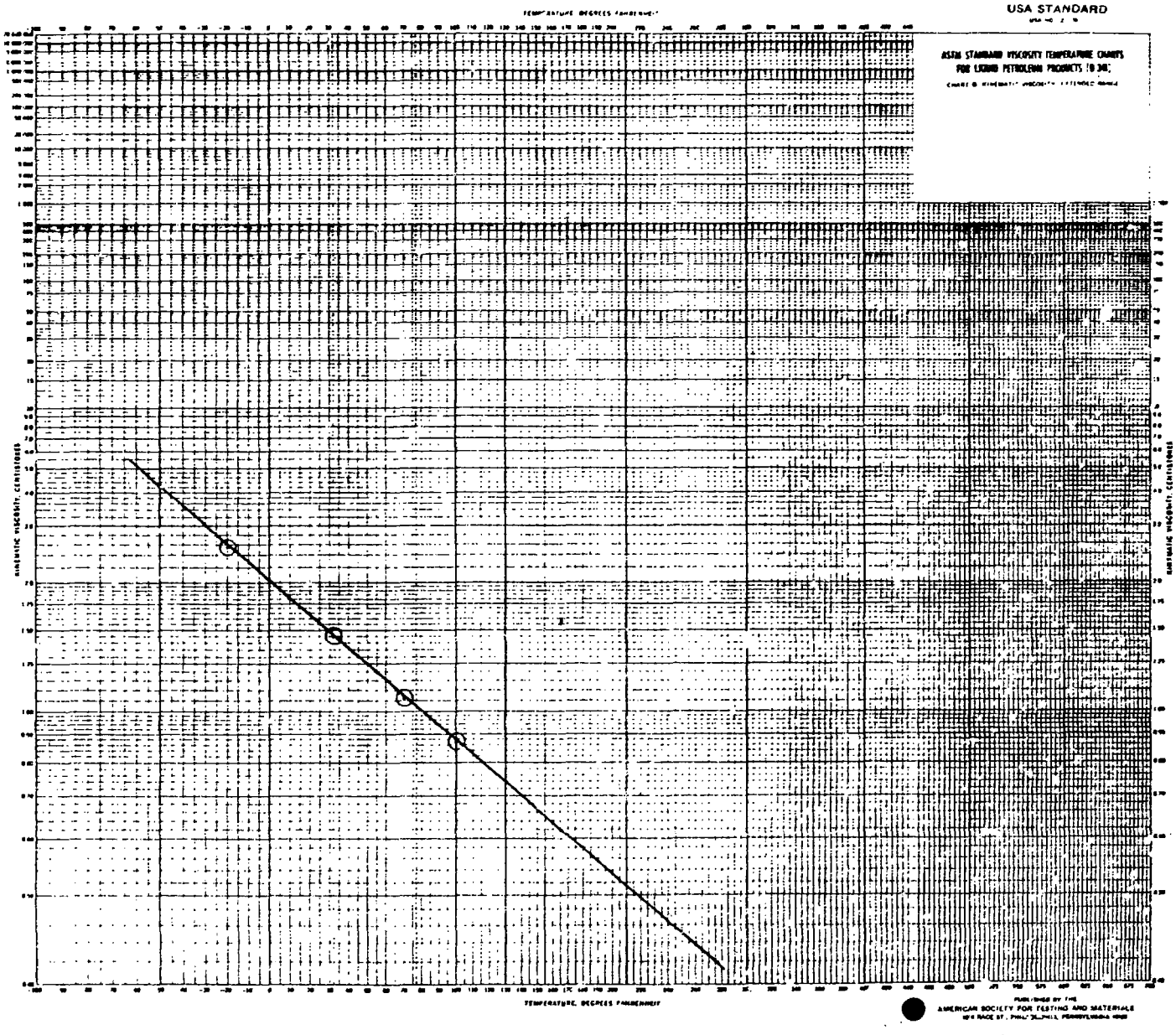

Figure 201. Viscosity/temperature plot for fuel GECF-1E, (JP-4)-046.

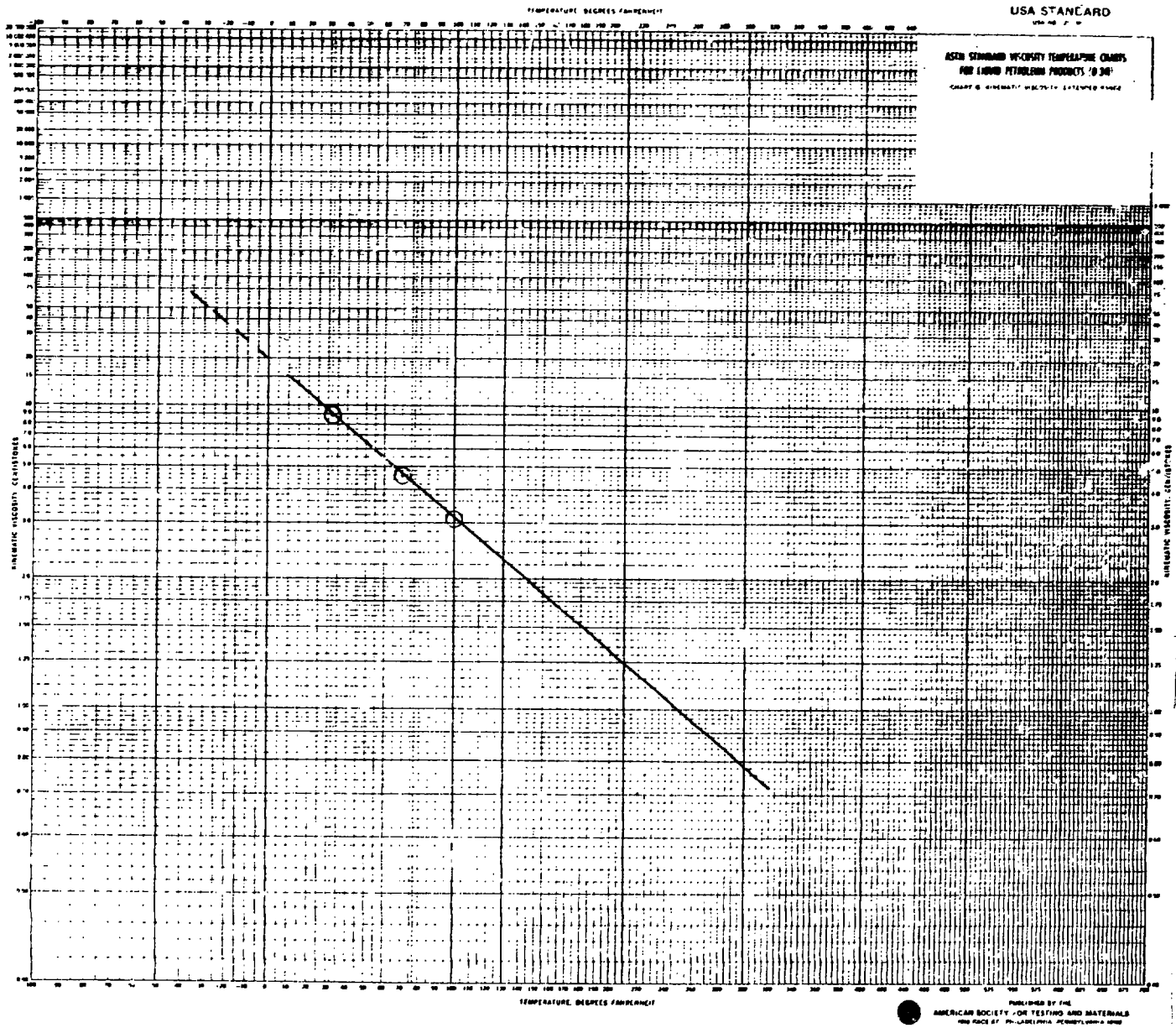

Figure 202. Viscosity/temperature plot for fuel GECF-13E, (DF-2)-045.

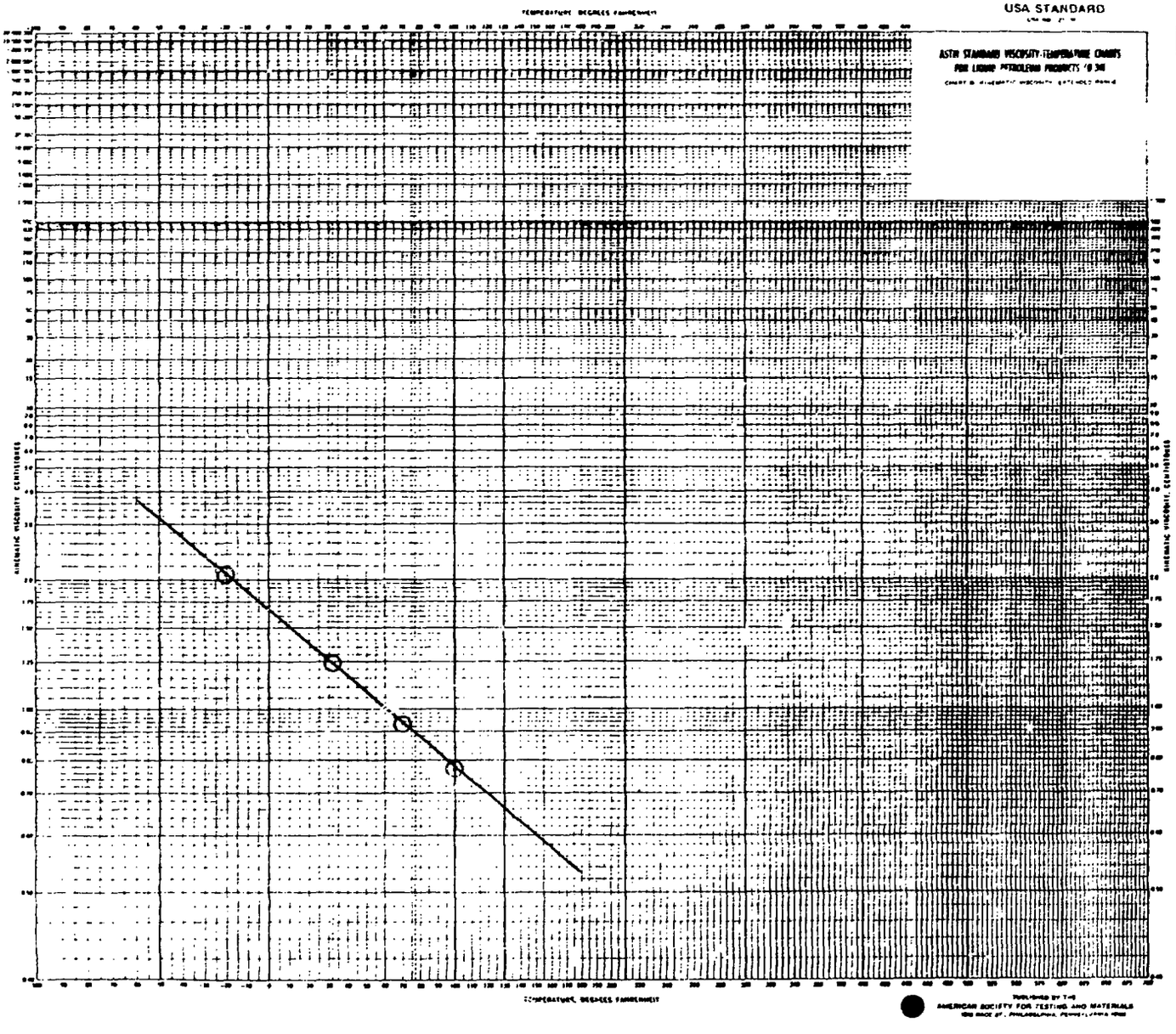

Figure 203. Viscosity/temperature plot for fuel GECS-24D.

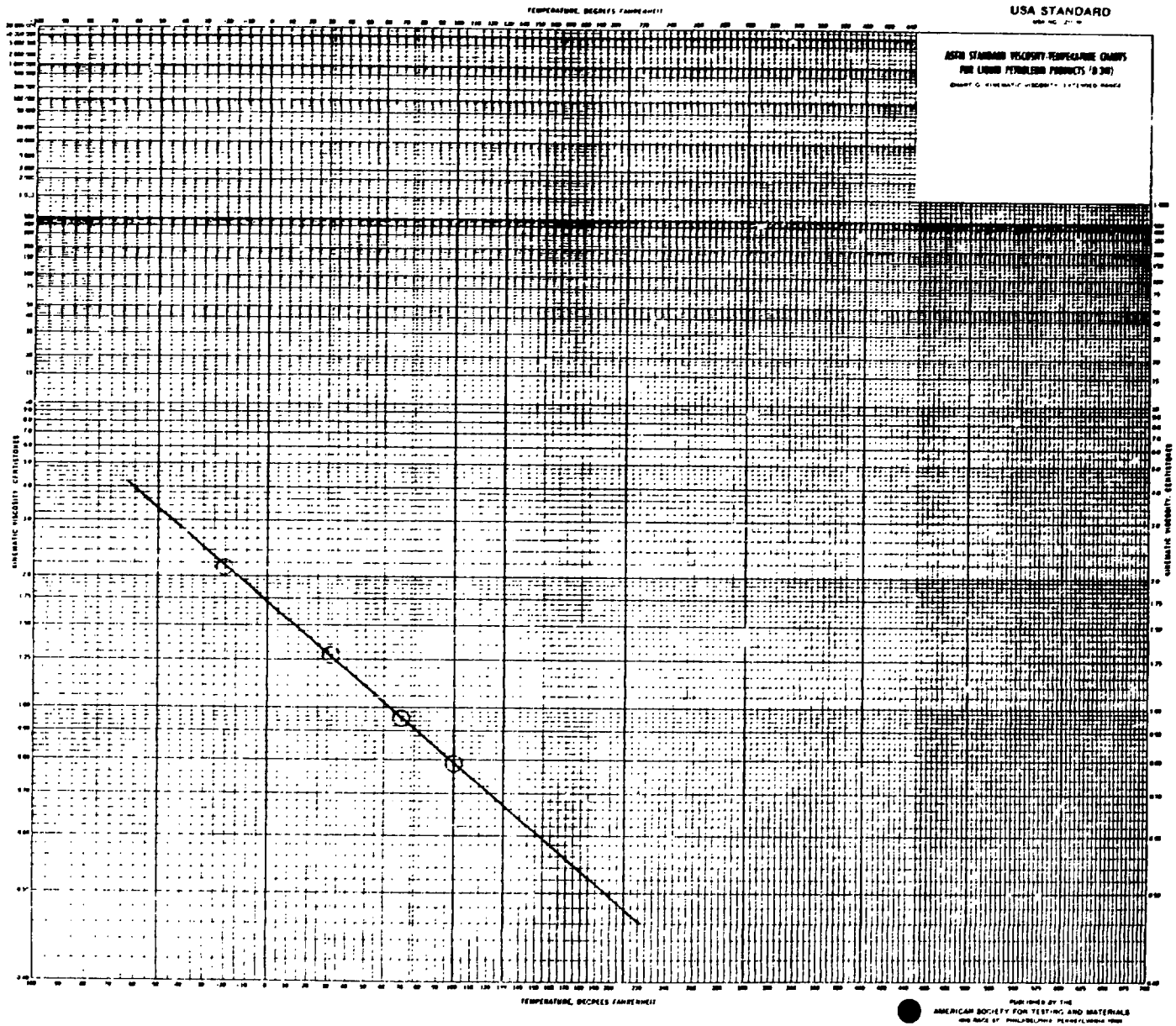

Figure 204. Viscosity/temperature plot for fuel GECS-26D.

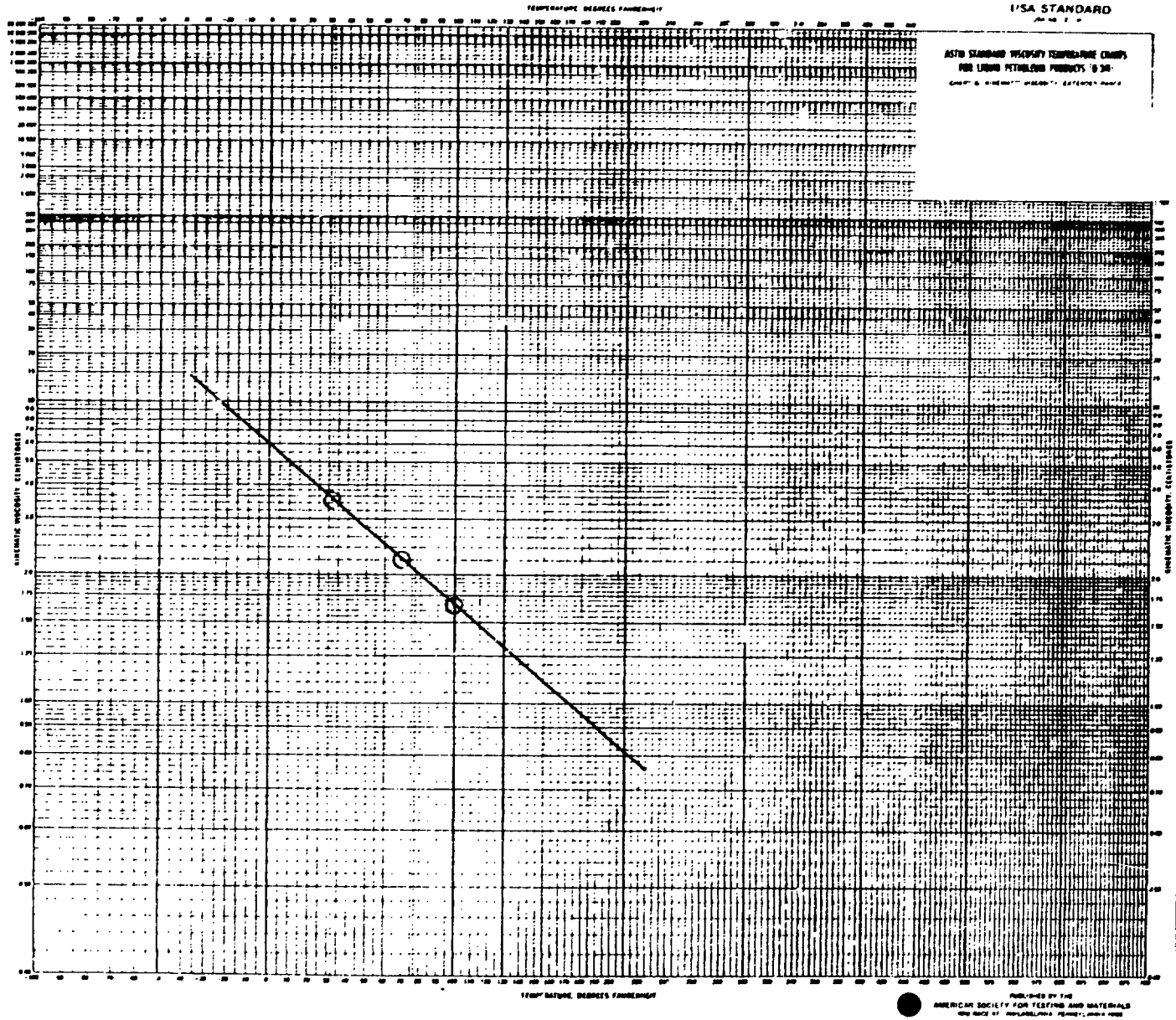

Figure 205. Viscosity/temperature plot for fuel DDP-81-08.

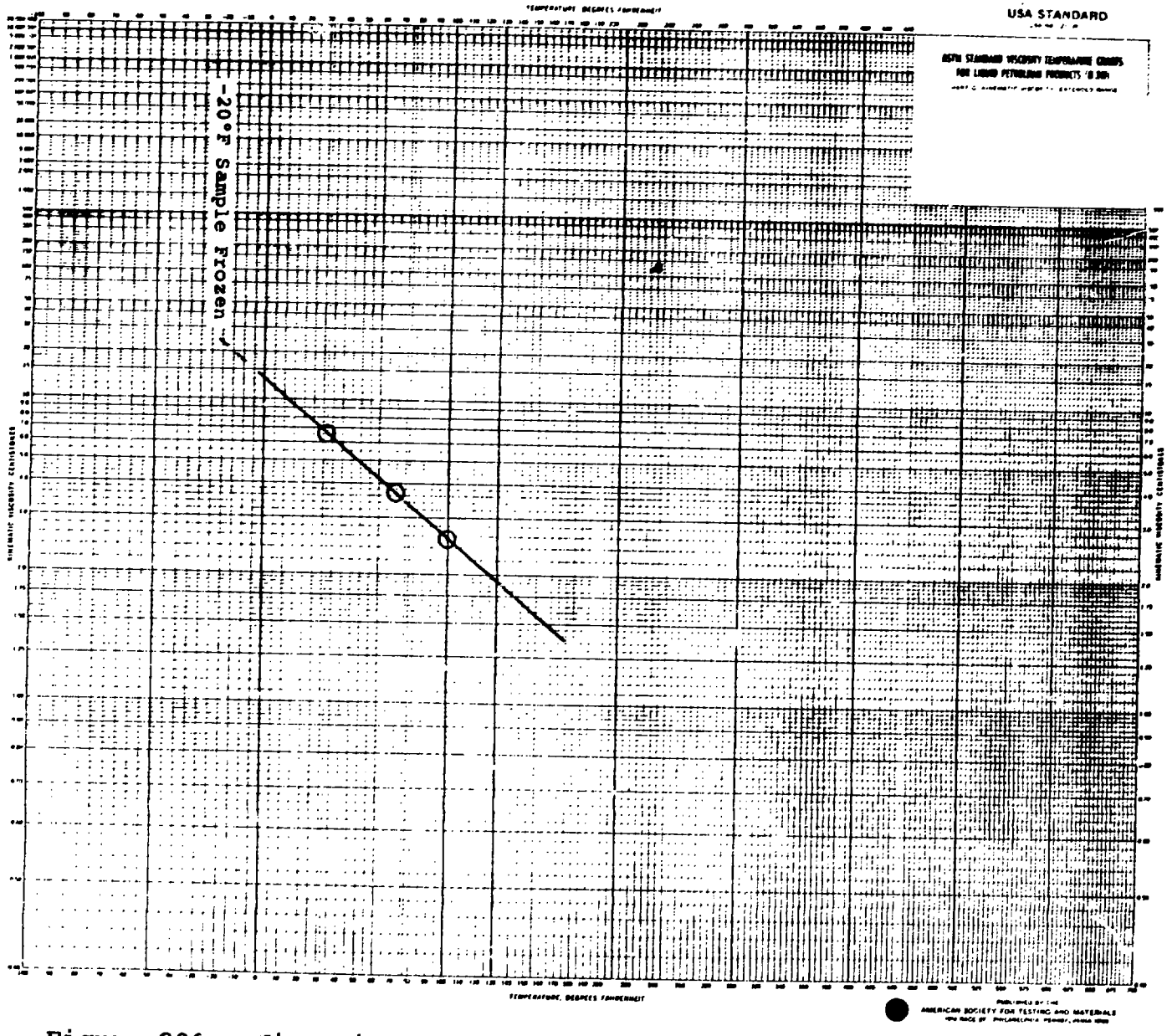

Figure 206. Viscosity/temperature plot for fuel GECS-81B-1 (DF-2).

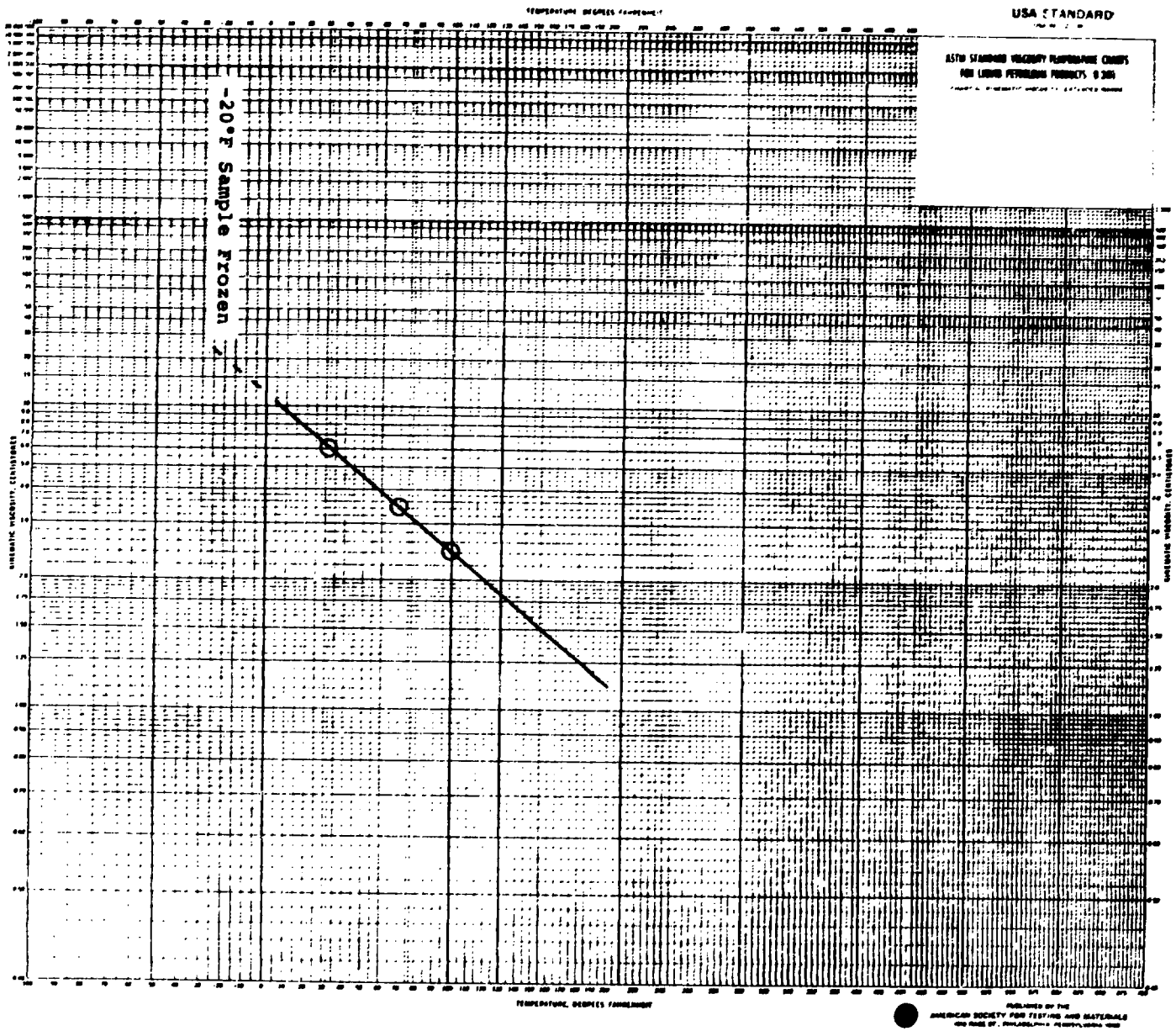

Figure 207. Viscosity/temperature plot for fuel GECS-82B (DF-2).

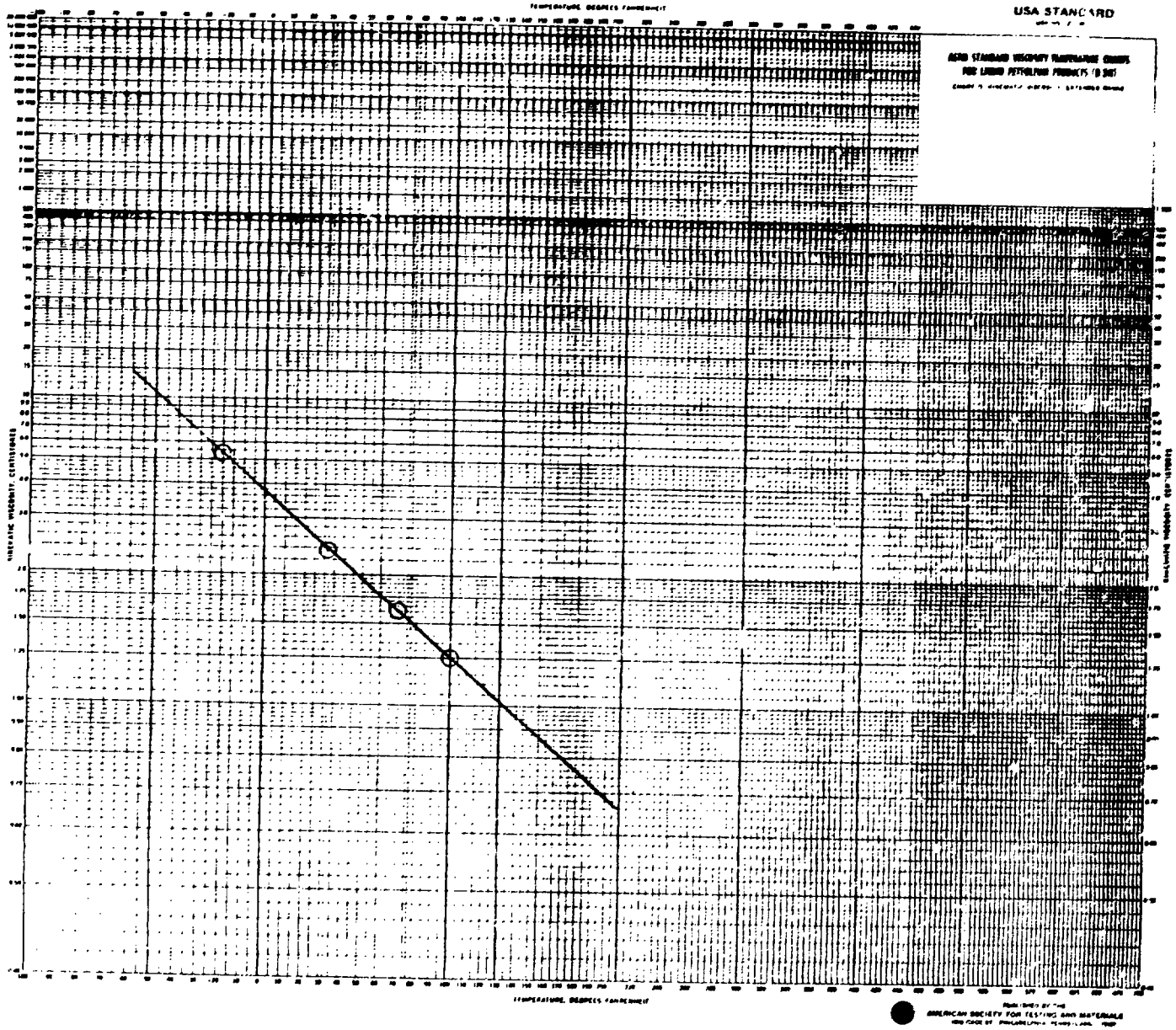

Figure 208. Viscosity/temperature plot for fuel POSF-D-81-59.

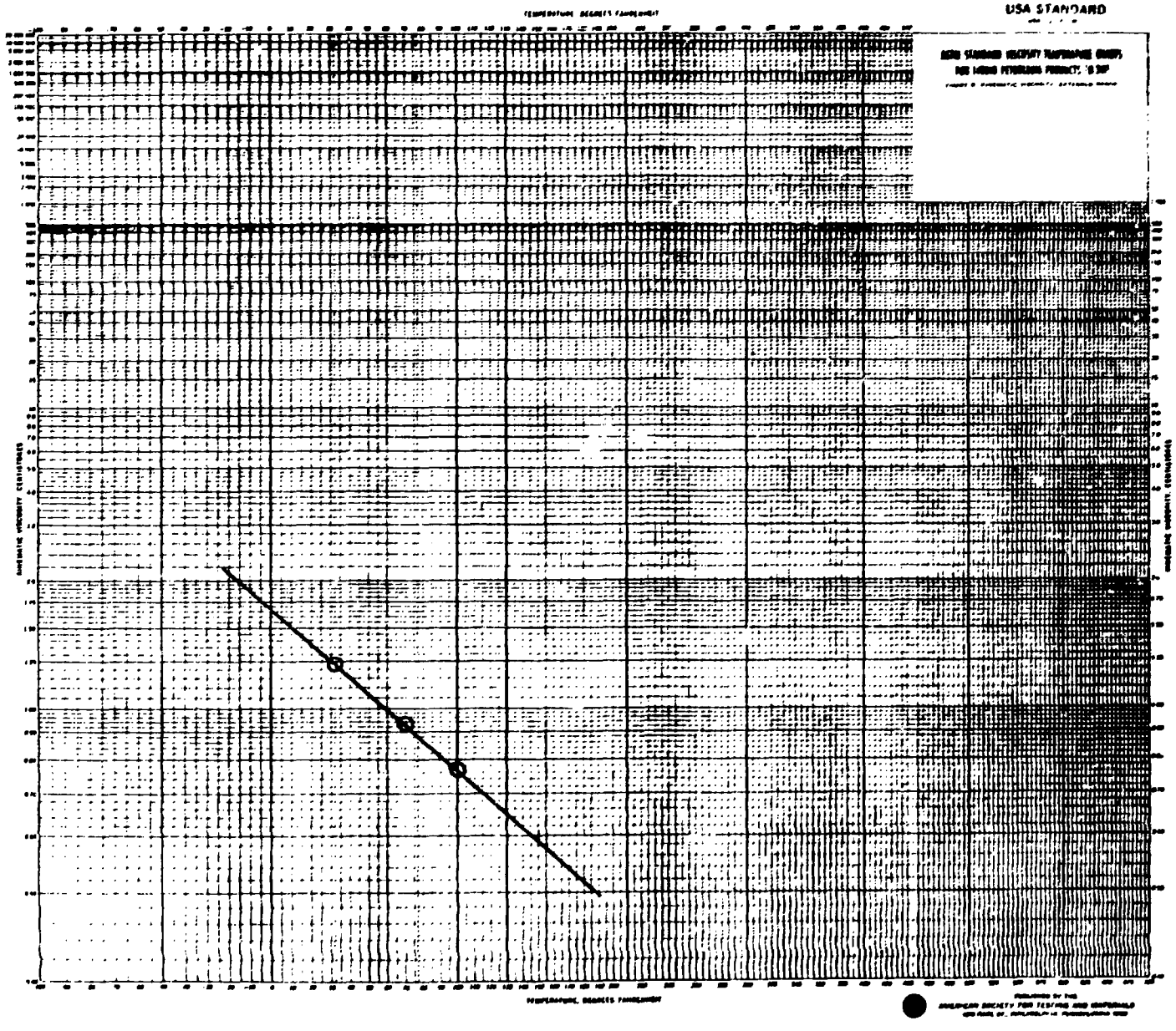

Figure 209. Viscosity/temperature plot for fuel JP-4, Tank B-11: DDP-81-22.

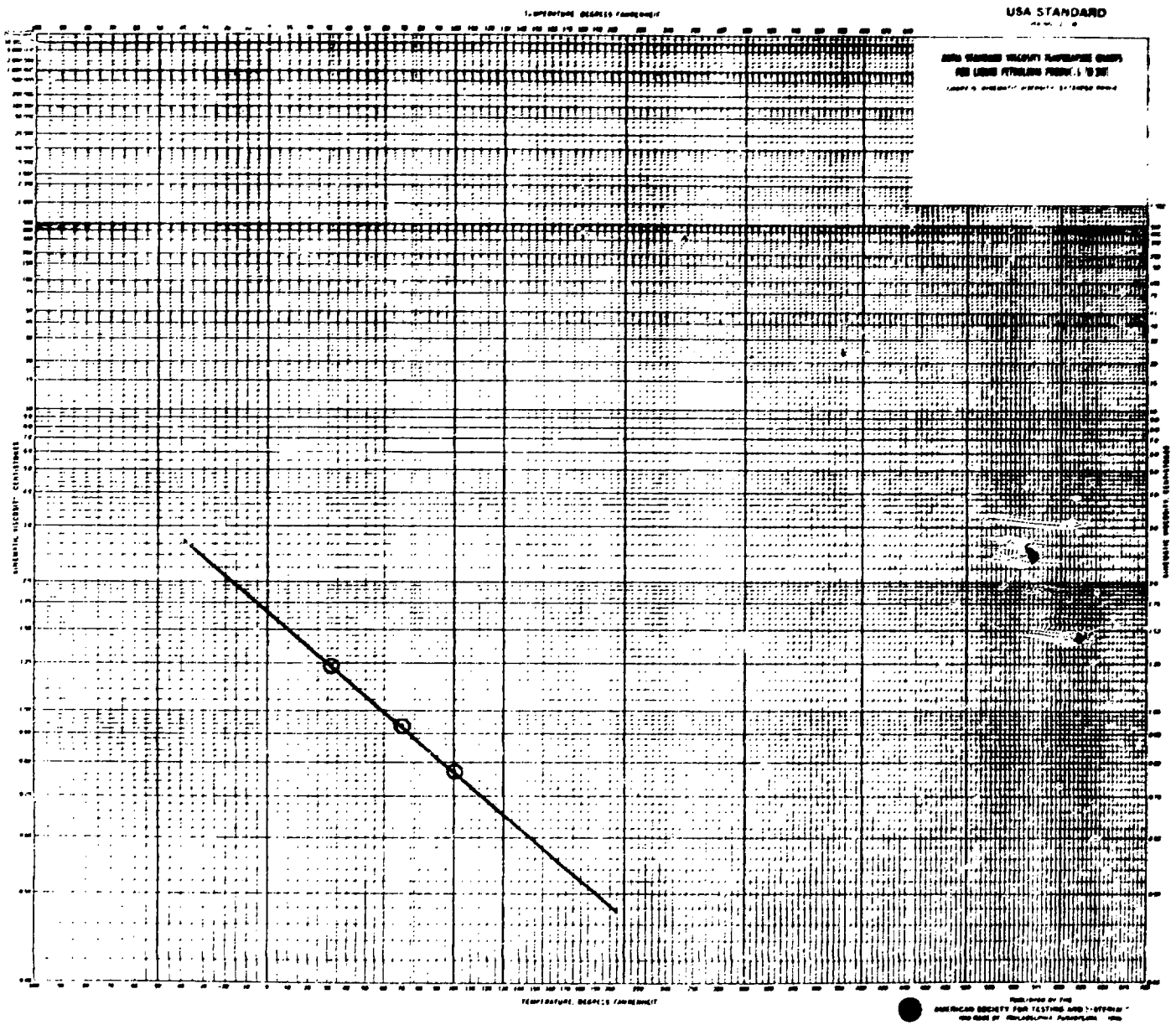

Figure 210. Viscosity/temperature plot for fuel JP-4, Tank B-12: DDP-81-23.

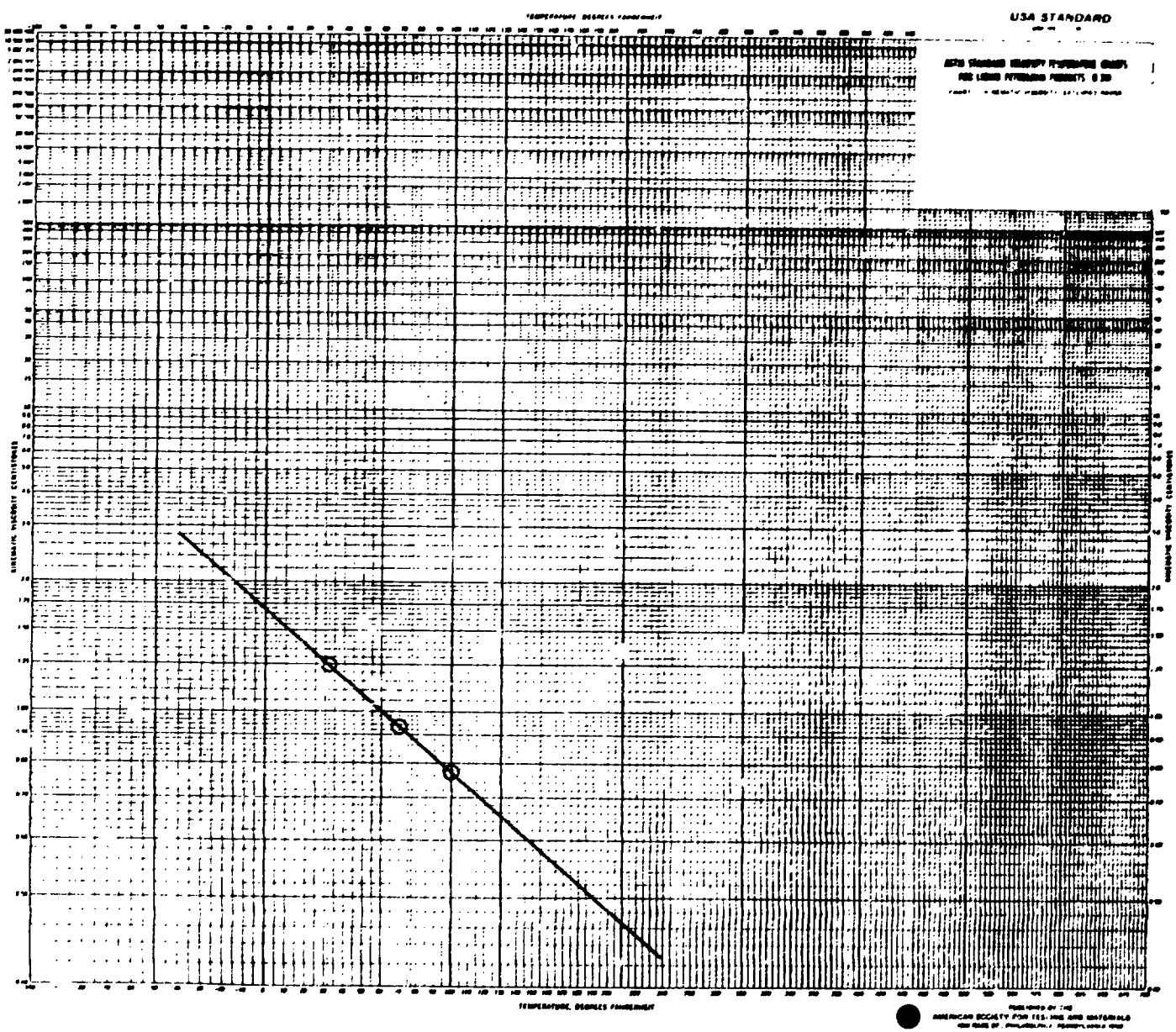

Figure 211. Viscosity/temperature plot for fuel JP-4, Tank B-13: DDP-81-24.

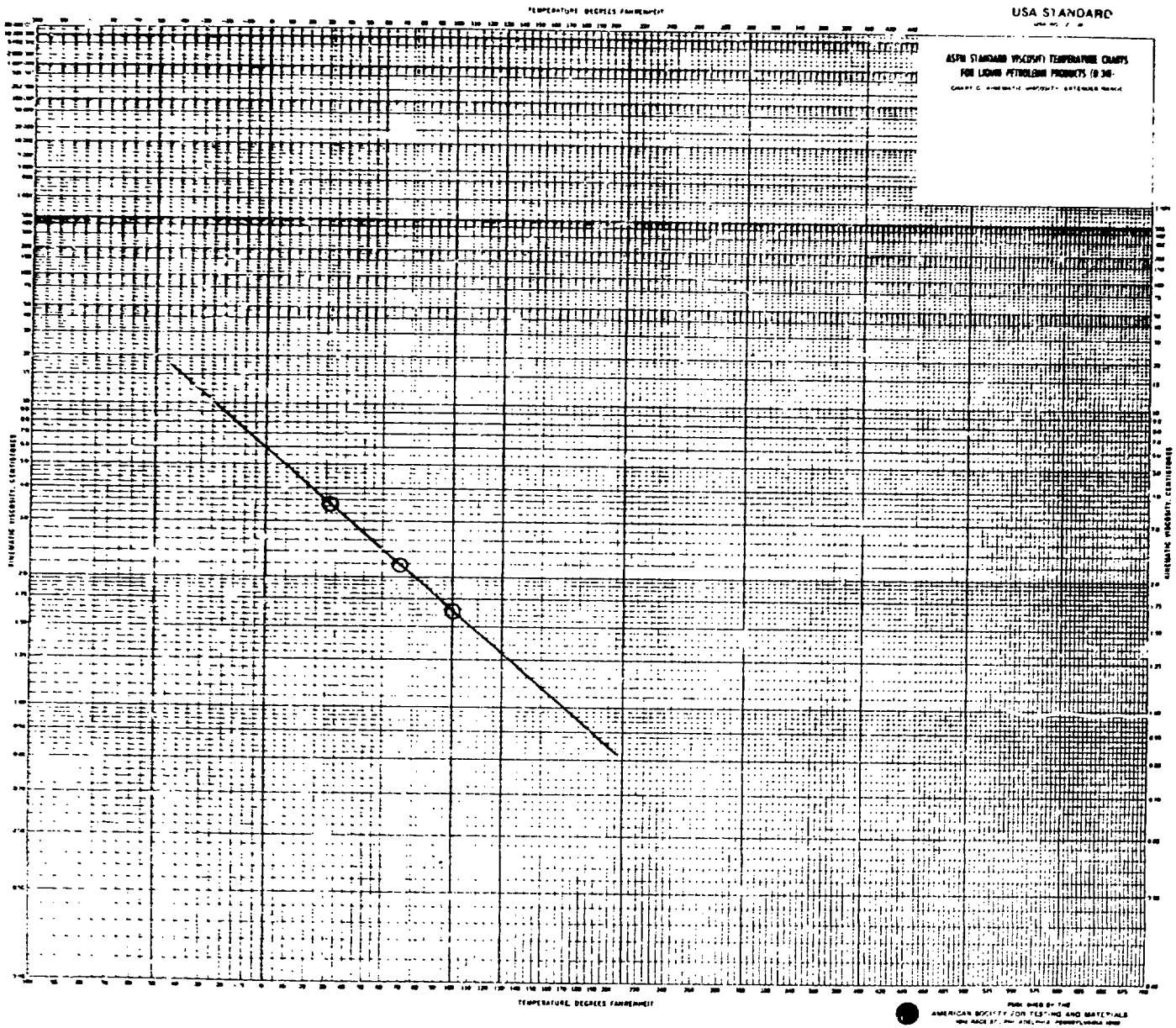

Figure 212. Viscosity/temperature plot for fuel JP-5, Tank F-6: DDP-81-20.

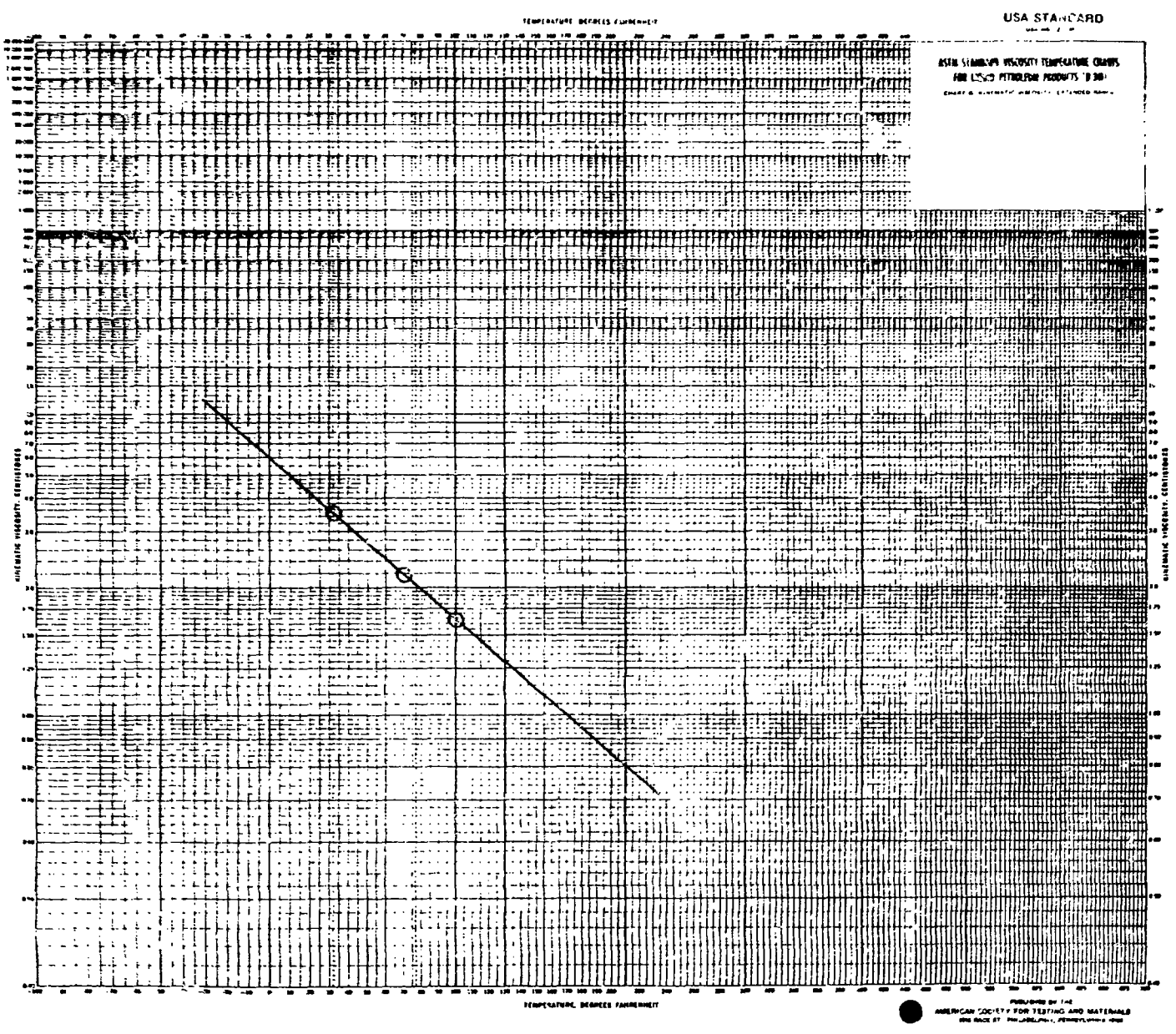

Figure 213. Viscosity/temperature plot for fuel JP-5, Tank F-7: DDP-81-21.

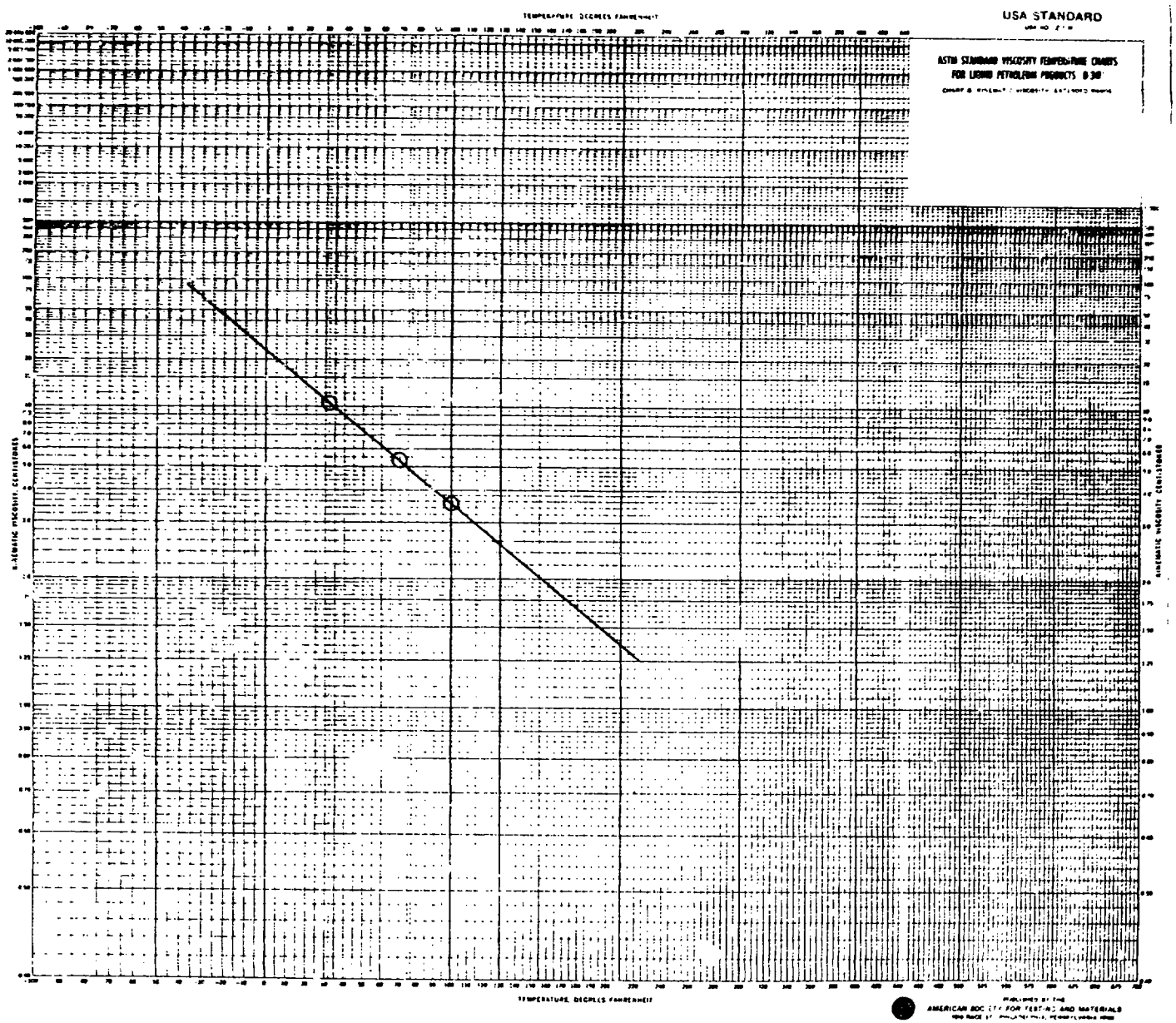

Figure 214. Viscosity/temperature plot for fuel DF-2, Tank F-9: DDP-81-17.

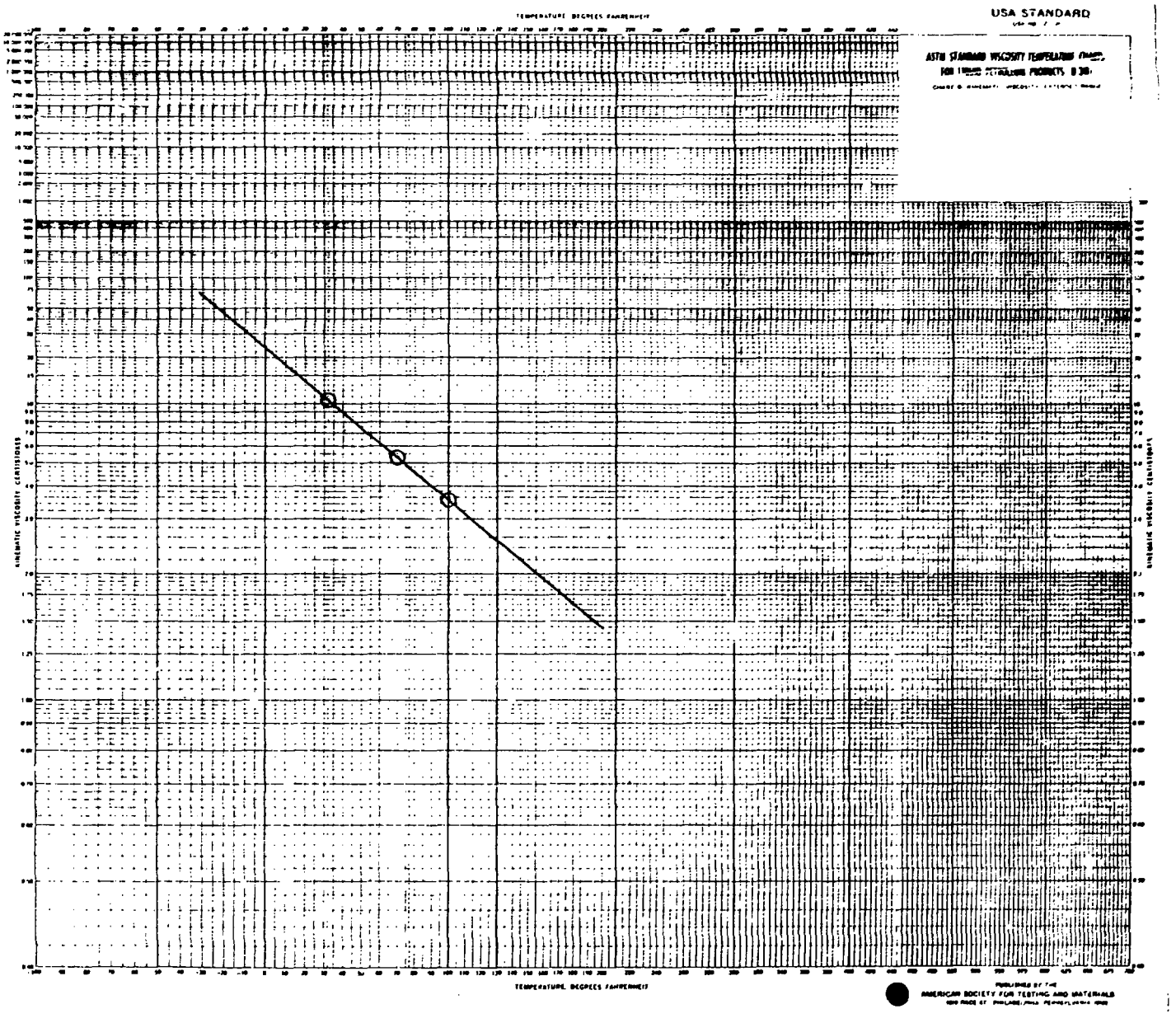

Figure 215. Viscosity/temperature plot for fuel DF-2, Tank F-10: DDP-81-18.

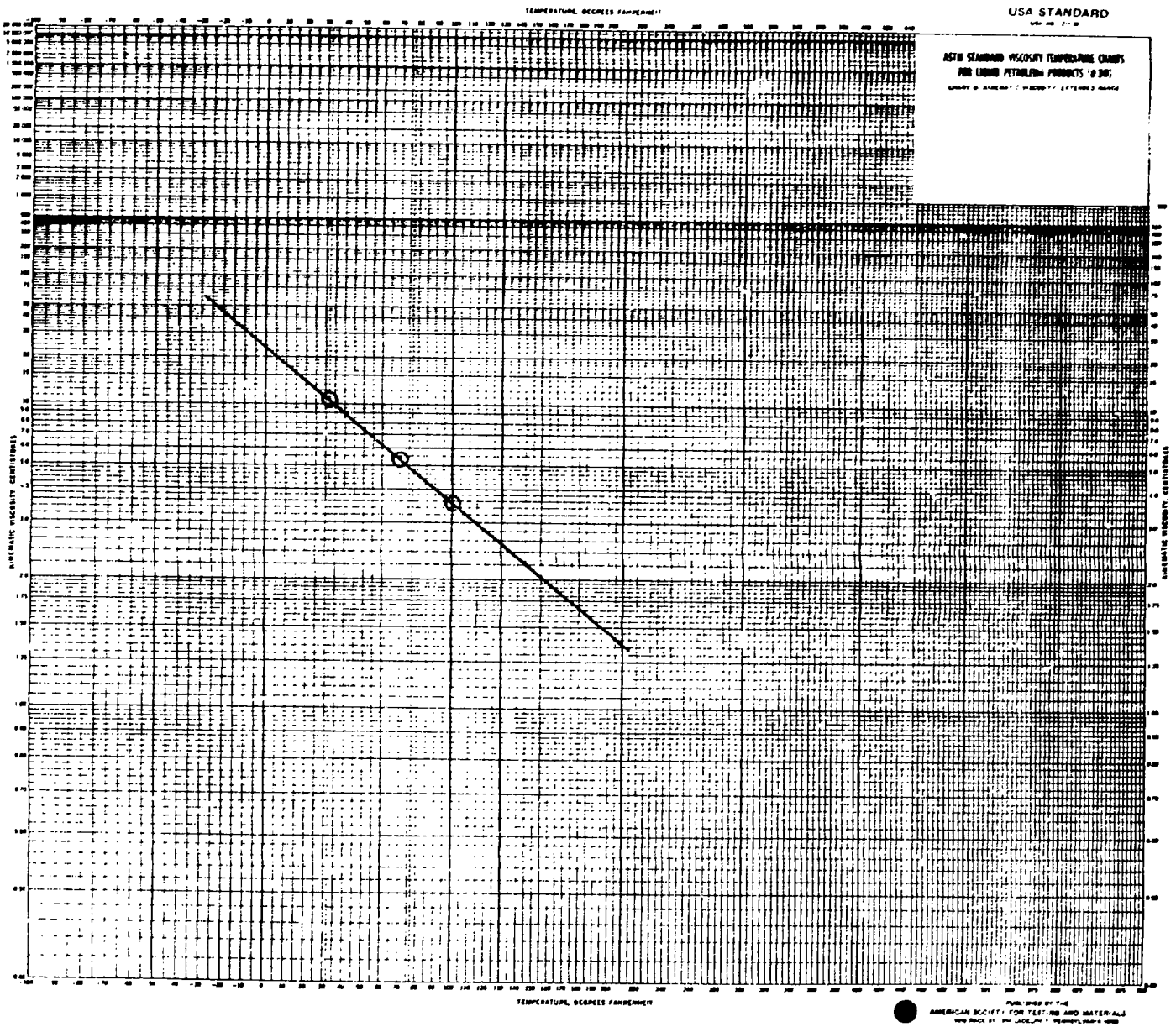

Figure 216. Viscosity/temperature plot for fuel DF-2, Tank F-11: DDP-81-19.

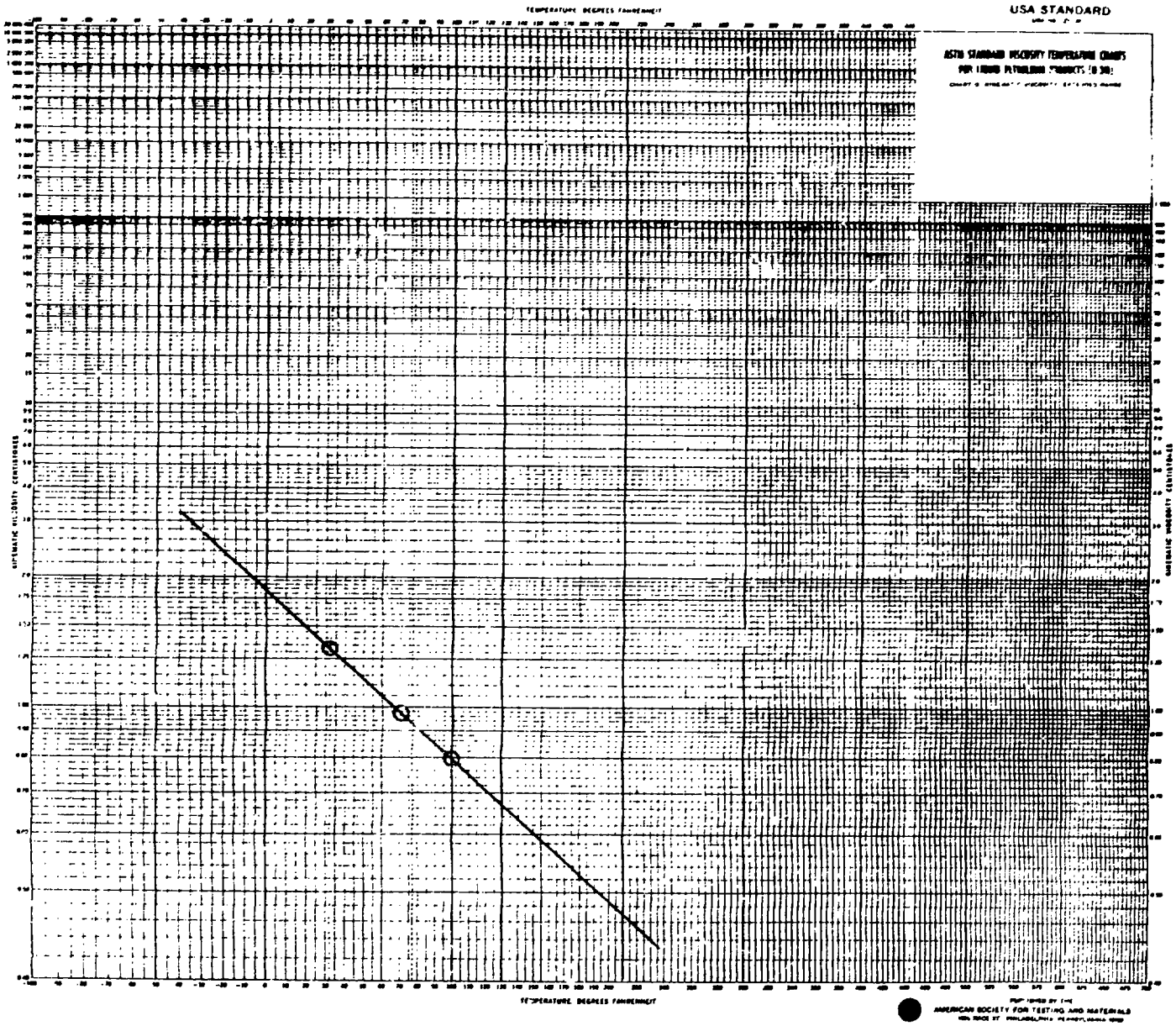

Figure 217. Viscosity/temperature plot for fuel XY-B, Tank F-8: DDP-81-12, Xylene bottoms.

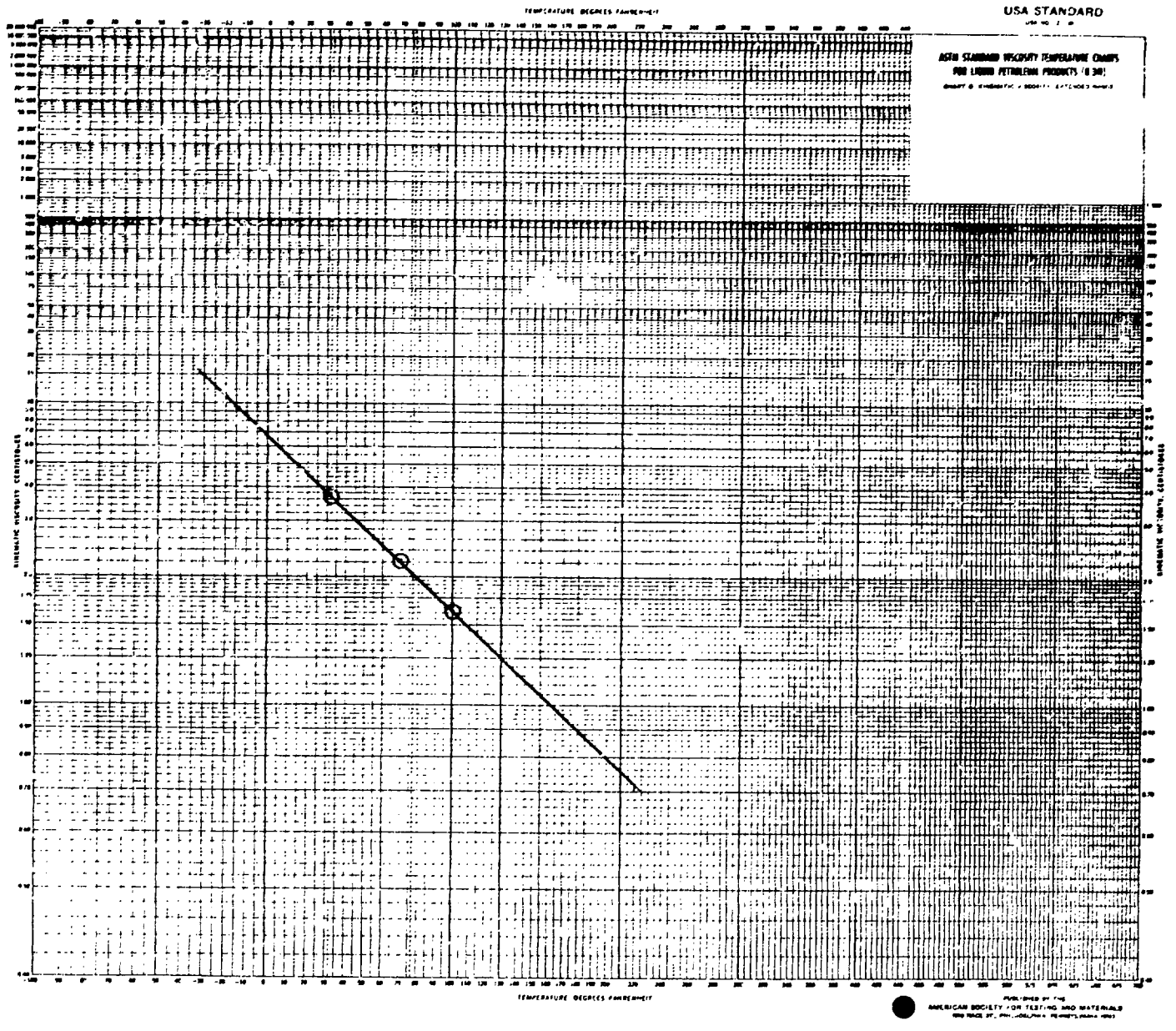

Figure 218. Viscosity/temperature plot for fuel A-400, Tank B-18: DDP-81-14, (Getty A-400).

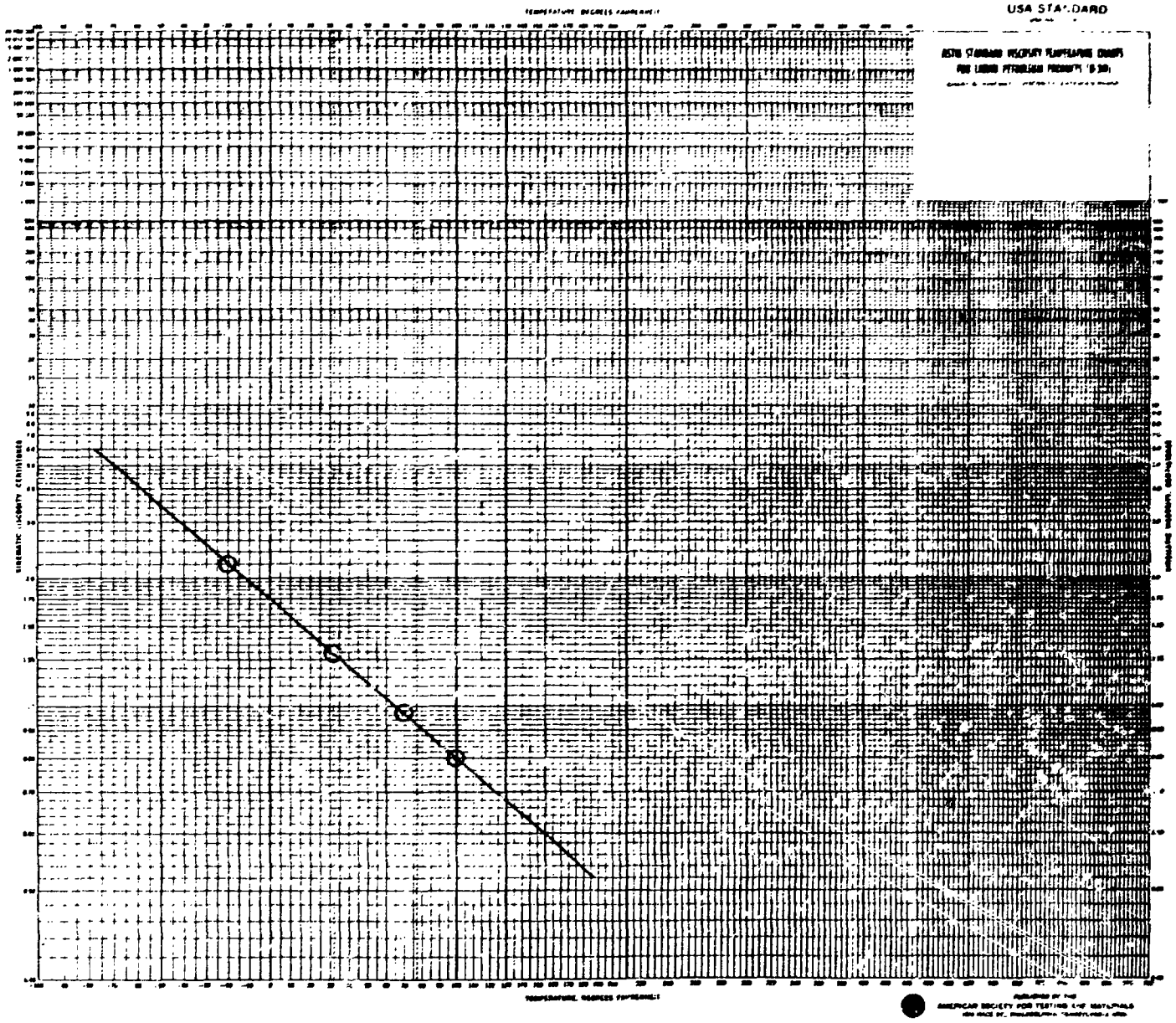

Figure 219. Viscosity/temperature plot for fuel POSF-C-81-134, AEDC JP-4, 1-A.

TABLE 177. KINEMATIC VISCOSITY VS. TEMPERATURE FOR FUELS TESTED AFTER 1 MAY 80

Sample description	Centistokes			
	-20°F	32°F	70°F	100°F
1B-792009, JP-4	1.941	1.150	0.8753	0.7262
2B-792009, JP-8	8.360	3.309	2.129	1.596
13B-792009, DF-2	gel	7.541	4.083	2.794
14B-792009, DF-2 Aromatic blend	gel	5.991	3.340	2.340
8B-792009	2.921	1.539	1.116	0.9005
9B-792009	2.345	1.324	0.9856	0.8074
15B-792009	3.242	1.730	1.241	0.9985
GEC-49B-1	1.857	1.129	0.8601	0.7172
1C-792009	2.55	1.405	1.035	0.8453
8C-792009	3.80	1.807	1.258	1.004
9C-792009	3.00	1.582	1.139	0.9225
13C-792009	--	8.946	4.614	3.109
14C-792009	--	6.537	3.568	2.472
15C-792009	4.00	1.946	1.362	1.085
JP-5, Tank 13	8.535	3.362	2.140	1.605
P&W 79-C-2086, Petroleum JP-4	2.220	1.286	0.9675	0.7956
P&W 79-C-2086, Shale JP-4	3.461	1.801	1.282	1.027
P&W 79-C-2086, Blend #1	5.564	2.554	1.713	1.331
P&W 79-C-2086, Blend #2	3.029	1.622	1.169	0.9415
P&W 79-C-2086, Blend #3	5.684	2.553	1.710	1.323
P&W 79-C-2086, Blend #4	1.503	0.9549	0.7367	0.6216
GEC 79-C-2009-62B-1, DF-2	1.848	1.137	0.8655	0.7212
P&W 792086, M50001	3.333	1.771	1.270	1.020
P&W 792086, M60001	4.246	2.086	1.460	1.159
P&W 792086, M70001	12.61	4.335	2.646	1.933
P&W 792086, M80001	frozen	4.930	2.847	2.027
GEC 792009, 77B	1.910	1.176	0.8806	0.7312
GEC 792009, 78B	~33	6.106	3.419	2.396
GEC 792009, 13C-2	frozen	7.568	4.092	2.809
P&W M50014A	6.562	2.832	1.868	1.419
P&W MJ0016A	2.301	1.332	0.9930	0.8148
P&W MJ0013B	2.382	1.371	1.015	0.8313
POSF-D-81-043, GECF-1D, JP-4	2.111	1.258	0.9428	0.7766
POSF-D-81-044, GECF-13D, DF-2	frozen	7.266	3.949	2.723
POSF-D-81-042, GECF-14D, DF-2/ARO	frozen	6.044	3.382	2.366
POSF-D-81-046, GECF-1E, JP-4	2.554	1.451	1.066	0.8700
POSF-D-81-045, GECF-13E, DF-2	frozen	8.801	4.577	3.084
GECS-24D, Reference JP-4	2.076	1.246	0.9339	0.7714
GECS-26D, Referen JP-4	2.132	1.277	0.9520	0.7855
DDP-81-08 Blending JP-5, Tank F-1, 4-23-81	5.756	3.479	2.207	1.651

TABLE 177 (continued)

Sample description	Centistokes -20°F	32°F	70°F	100°F
GECS-81B-1, DF-2	frozen	6.642	3.681	2.556
GECS-82B, DF-2	frozen	6.064	3.444	2.416
POSF-D-81-59, Blend of JP-4, DF-2, 2040 Solvent	5.438	2.355	1.604	1.252
AEDC Blending Stocks				
DDP-81-22, Tank B-11, JP-4	--	1.238	0.9357	0.7720
DDP-81-23, Tank B-12, JP-4	--	1.241	0.9339	0.7728
DDP-81-24, Tank B-13, JP-4	--	1.249	0.9366	0.7732
DDP-81-20, Tank F-6, JP-5	--	3.459	2.192	1.639
DDP-81-21, Tank F-7, JP-5	--	3.463	2.192	1.638
DDP-81-17, Tank F-9, DF-2	--	10.55	5.355	3.541
DDP-81-18, Tank F-10, DF-2	--	10.60	5.348	3.545
DDP-81-19, Tank F-11, DF-2	--	10.66	5.355	3.548
DDP-81-12, Tank F-8, Xy-B	--	1.327	0.9767	0.7978
DDP-81-14, Tank B-18, A-400	--	3.656	2.217	1.621
AEDC POSF-C-81-134, A-1 JP-4	2.209	1.293	0.9715	0.7997

TABLE 178. SURFACE TENSION VS. TEMPERATURE OF FUELS TESTED AFTER 1 MAY 80

Sample designation	Dynes per centimeter -20°F[a]	32°F	70°F	100°F
1B-79009, JP-4	27.28	24.31	22.16	20.43
2B-792009, JP-8	31.33	28.64	26.69	25.15
13B-792009, DF-2	gel	30.37	28.42	26.88
14B-792009, DF-2 Aromatic blend	gel	31.35	29.43	27.88
8B-792009	29.05	26.58	24.75	23.33
9B-792009	28.18	25.82	24.06	22.69
15B-792009	29.05	26.43	24.53	23.01
GEC-49B-1	27.53	24.68	22.53	20.89
1C-792009	27.50	24.73	22.80	21.25
8C-792009	29.58	26.99	25.09	23.61
9C-792009	28.82	26.12	24.12	22.56
13C-792009	--	30.37	28.55	27.10
14C-792009	--	31.80	29.98	28.54
15C-792009	29.10	26.60	24.78	23.34
JP-5, Tank 13	30.91	28.34	26.45	24.97

(continued)

TABLE 178 (continued)

Sample designation	Dynes per centimeter			
	-20°F[a]	32°F	70°F	100°F
P&W 79-C-2086, Petroleum JP-4	27.39	24.72	22.80	21.28
P&W 79-C-2086, Shale JP-4	29.27	26.54	24.53	22.99
P&W 79-C-2086, Blend #1	29.58	26.78	24.69	23.07
P&W 79-C-2086, Blend #2	29.94	27.07	24.94	23.30
P&W 79-C-2086, Blend #3	30.65	27.93	25.93	24.38
P&W 79-C-2086, Blend #4	28.33	25.61	23.62	22.04
GEC 79-C-2009-62B-1, DF-2	28.82	25.41	22.93	20.95
P&W 792086, M50001	29.24	26.42	24.54	22.78
P&W 792086, M60001	29.38	26.63	24.60	23.03
P&W 792086, M70001	30.21	27.36	25.36	23.66
P&W 792086, M80001	frozen	31.21	29.11	27.53
GEC 792009, 77B	26.83	24.05	22.03	20.43
GEC 792009, 78B	slushy	29.89	28.00	26.51
GEC 792009, 13C-2	frozen	29.37	27.76	26.48
P&W M50014A-2	31.98	28.92	26.68	24.93
P&W MJ0016A	27.30	24.74	22.85	21.39
P&W MJ0013B	37.32	24.74	22.84	21.38
POSF-D-81-043, GECF-1D, JP-4	27.97	25.14	23.08	21.45
POSF--D-81-044, GECF-13D, DF-2	frozen	30.54	28.58	27.12
POSF-D-81-042, GECF-14D, DF-2/ARO	frozen	31.46	29.35	27.19
POSF-D-81-046, GECF-1E, JP-4	27.66	25.03	23.11	21.61
POSF-D-81-045, GECF-13E, DF-2	frozen	30.50	28.54	26.98
GECS-24D, Reference JP-4	27.53	24.78	22.75	21.15
GECS-26D, Reference JP-4	27.63	24.89	22.86	21.27
DDP-81-08 Blending JP-5, Tank F-1, 4-23-81	30.17	28.55	26.63	25.11
GECS-81B-1, DF-2	frozen	30.07	28.09	26.53
GECS-82B, DF-2	frozen	29.73	27.73	26.23
POSF-D-81-59, Blend of JP-4, DF-2, 2040 Solvent	30.09	27.53	25.68	24.20
DDP-81-28, Tank F-12, AEDC Blend 2 (6 July 81)	--	25.37	23.52	22.06
DDP-81-29, Tank F-11, AEDC Blend 3 (6 July 81)	--	27.46	25.60	24.13
DDP-81-30, Tank F-7, AEDC Blend 5 (6 July 81)	--	29.66	27.53	25.87
DDP-81-31, Tank F-9, AEDC Blend 6 (6 July 81)	--	30.07	28.15	26.65

(continued)

TABLE 178 (continued)

Sample designation	Dynes per centimeter -20°F[a]	32°F	70°F	100°F
E314A, JP-8 Blend #3 (P&W)	30.50	27.81	25.82	24.26
M50003B, JP-4 Blend #5 (P&W)	31.88	28.90	26.72	25.00
M50008B, JP-4 Blend #5 (P&W)	31.42	28.81	26.90	25.38
MS0007A, Shale JP-4 (P&W)	29.35	26.74	24.80	23.29
MS0010A, Shale JP-4 (P&W)	29.30	26.70	24.78	23.27
MS0011A, Shale JP-4 (P&W)	30.09	27.22	25.09	23.42
EJ0020B, JP-4 (P&W)	28.14	25.35	23.28	21.67
AEDC POSF-C-81-134, A-1 JP-4	28.75	25.95	23.85	22.27

[a]Results at this temperature were extrapolated from the higher temperature data.

TABLE 179. VAPOR PRESSURE VS. TEMPERATURE OF FUELS TESTED AFTER 1 MAY 80

Sample designation	Millimeters of mercury 32°F	70°F	100°F
1B-792009, JP-4	37.5	85.0	149.0
2B-792009, JP-8	9.5	15.5	22.0
13B-792009, DF-2	9.5	14.5	19.0
14B-792009, DF-2 Aromatic blend	7.0	13.5	21.0
8B-792009	24.5	59.0	109.0
9B-792009	26.5	61.5	111.0
15B-792009	30.5	69.0	120.0
GEC-49B-1	33.5	78.0	141.0
1C-792009	35.0	81.0	145.0
8C-792009	23.5	58.0	108.0
9C-792009	29.5	71.0	131.0
13C-792009	7.0	12.0	17.0
14C-792009	6.5	11.5	17.0
15C-792009	29.5	63.0	106.0
JP-5, Tank 13	7.0	12.0	17.0
P&W ES0001, Shale JP-4	48.0	93.0	148.0
P&W 79-C-2086, Petroleum JP-4	28.5	71.0	136.0
P&W 79-C-2086, Shale JP-4	36.0	77.0	131.0

(continued)

TABLE 179 (continued)

Sample designation	Millimeters of mercury 32°F	70°F	100°F
P&W 79-C-2086, Blend #1	18.0	45.0	85.5
P&W 79-C-2086, Blend #2	13.5	34.0	66.0
P&W 79-C-2086, Blend #3	6.0	12.0	18.5
P&W 79-C-2086, Blend #4	53.0	120.0	212.0
GEC 79-C-2009-62B-1, DF-2	32.0	72.0	129.0
P&W 792086, M50001	47.0	94.0	152.0
P&W 792086, M60001	54.0	109.0	175.0
P&W 792086, M70001	8.0	15.5	24.5
P&W 792086, M80001	11.5	19.5	28.5
GEC 792009, 77B	28.0	68.5	123.0
GEC 792009, 78B	10.0	14.5	19.0
GEC 792009, 13C-2	8.5	12.5	16.0
P&W M50014A-2	6.0	11.5	18.5
P&W MJ0016A	30.0	73.0	137.5
P&W MJ0013B	32.5	77.0	140.0
POSF-D-81-043, GECF-1D, JP-4	32.0	75.0	133.0
POSF-D-81-044, GECF-13D, DF-2	7.0	12.0	16.5
POSF-D-81-042, GECF-14D, DF-2/AVO	8.0	13.5	18.5
POSF-D-81-046, GECF-1E, JP-4	35.0	83.0	154.0
POSF-D-81-045, GECF-13E, DF-2	7.0	13.5	21.0
GECS-24D, Reference JP-4	34.5	79.0	139.0
GECS-26D, Reference JP-4	42.0	91.0	156.0
DDP-81-08 Blending JP-5, Tank F-1, 4-23-81	7.5	13.0	18.0
GECS-81B-1, DF-2	7.5	13.5	19.5
GECS-82B, DF-2	10.5	20.0	32.0
POSF-D-81-59, Blend of JP-4, DF-2, 2040 Solvent	23.0	51.5	91.0
DDP-81-28, Tank F-12, AEDC Blend 2 (6 July 81)	24.5	60.0	110.0
DDP-81-29, Tank F-11, AEDC Blend 3 (6 July 81)	22.0	48.0	83.0
DDP-81-30, Tank F-7, AEDC Blend 5 (6 July 81)	7.0	12.5	18.5
DDP-81-31, Tank F-9, AEDC Blend 6 (6 July 81)	9.0	13.0	16.5
AEDC POSF-C-81-134, A-1 JP-4	26.0	62.0	111.0

TABLE 180. HEAT OF COMBUSTION OF FUELS TESTED AFTER 1 MAY 80

Sample designation	Gross values, Btu/lb			Net Btu/lb	
	Duplicates		Average	Average	% H[a]
1B-792009, JP-4	20,106	20,097	20,102	18,783	14.46
2B-792009, JP-8	19,839	19,826	19,833	18,563	13.92
13B-792009, DF-2	19,533	19,512	19,523	18,322	13.16
14B-792009, DF-2 Aromatic blend	19,144	19,095	19,120	18,033	11.92
8B-792009	19,234	19,243	19,239	18,137	12.08
9B-792009	19,622	19,611	19,617	18,418	13.14
15B-792005	19,978	19,992	19,985	18,679	14.32
GEC-49B-1	20,141	20,093	20,117	18,791	14.54
1C-792009	19,990	20,022	20,006	18,694	14.38
8C-792009	19,191	19,203	19,197	18,102	12.00
9C-792009	19,611	19,580	19,596	18,405	13.06
13C-792009	19,524	19,520	19,522	18,322	13.15
14C-792009	19,065	19,077	19,071	17,997	11.77
15C-792009	19,902	19,896	19,908	18,604	14.29
JP-5, Tank 13	19,795	19,787	19,791	18,534	13.78
P&W 79-C-2086, Petroleum JP-4	20,022	19,974	19,998	18,672	14.54
P&W 79-C-2086, Shale JP-4	20,035	19,993	20,014	18,701	14.39
P&W 79-C-2086, Blend #1	19,900	19,944	19,922	18,623	14.24
P&W 79-C-2086, Blend #2	19,708	19,743	19,726	18,500	13.44
P&W 79-C-2086, Blend #3	19,858	19,902	19,880	18,599	14.04
P&W 79-C-2086, Blend #4	19,454	19,404	19,429	18,310	12.27
GEC 79-C-2009-62B-1, DF-2	20,109	20,114	20,111	18,774	14.63
P&W 792086, M50001	19,704	19,738	19,721	18,409	14.38
P&W 792086, M60001	19,462	19,501	19,481	18,300	12.94
P&W 792086, M70001	18,811	18,759	18,785	17,730	11.56
P&W 792086, M80001	18,857	18,906	18,382	17,833	11.50
GEC 792009, 77B	20,033	19,995	20,014	18,695	14.46
GEC 792009, 78B	19,368	19,333	19,351	18,201	12.61
GEC 792009, 13C-2	19,496	19,498	19,497	18,305	13.07
P&W M50014A-2	19,667	19,627	19,647	18,421	13.44
P&W MJ0016A	20,115	20,118	20,117	18,793	14.51
P&W MJ0013B	20,094	20,140	20,117	18,796	14.48
POSF-D-81-043, GECF-1D, JP-4	20,060	20,073	20,067	18,735	14.54
POSF-D-81-044, GECF-13D, DF-2	19,193	19,204	19,199	18,100	12.04
POSF-D-81-042, GECF-14D, DF-2/ARO	19,547	19,509	19,528	18,333	13.10
POSF-D-81-046, GECF-1E, JP-4	20,048	20,075	20,062	18,750	14.38
POSF-D-81-045, GECF-13E, DF-2	19,514	19,493	19,504	18,307	13.12
GECS-24-D, Reference JP-4	20,151	20,110	20,131	18,808	14.50
GECS-26-D, Reference JP-4	20,039	20,020	20,030	18,725	14.30
DDP-81-08 Blending JP-5	19,824	19,817	19,821	18,571	--
GECS-81B-1, DF-2	19,582	19,560	19,571	18,391	--
GECS-82B, DF-2	19,530	19,562	19,546	18,373	--
POSF-D-81-59, Blend of JP-4, DF-2, 2040 Solvent	19,440	19,453	19,447	18,302	--
DDP-81-28, Tank F-12, AEDC blend 2 (6 July 81)	19,736	19,759	19,748	18,516	13.50
DDP-81-29, Tank F-11, AEDC blend 3 (6 July 81)	19,704	19,725	19,715	18,484	13.49
DDP-81-30, Tank F-7, AEDC blend 5 (6 July 81)	19,329	19,362	19,346	18,206	12.50
DDP-81-31, Tank F-9, AEDC blend 6 (6 July 81)	19,612	19,632	19,622	18,391	13.49
AEDC POSF-C-81-134, A-1 JP-4	20,137	20,121	20,129	18,817	14.27

[a]Supplied by AFWAL/POSF for net heat calculation.

TABLE 181. SIMULATED DISTILLATIONS IN °C, BY GC (ASTM D 2887)

Sample Descriptions	(IBP) 0.5	Temperatures at which the following percents were recovered (°C) 1	5	10	20	30	40	50	60	70	80	90	95	99	(FBP) 99.5
1B-792009, JP-4	21	25	58	74	89	103	118	142	174	202	223	248	266	324	337
2B-792009, JP-8	125	138	168	181	196	206	215	220	229	237	246	256	266	286	296
13B-792009, DF-2	121	141	177	196	222	240	255	271	287	302	318	340	362	400	409
14B-792009, DF-2 Aromatic blend	122	153	178	196	216	231	242	255	271	287	306	331	351	393	404
8B-792009	29	40	75	91	117	149	188	208	226	232	247	258	275	302	310
9B-792009	25	36	71	89	105	126	150	174	198	218	232	253	267	294	301
15B-792009	3	26	77	103	133	155	174	188	200	215	227	248	272	319	328
GEC-49B-1	22	25	64	84	99	116	127	143	158	172	190	219	243	278	291
1C-792009	32	41	58	68	98	152	179	195	208	221	235	250	259	286	300
8C-792009	40	53	67	90	156	189	206	218	230	234	250	264	281	322	330
9C-792009	35	46	60	74	129	176	195	207	220	231	240	254	266	292	300
13C-792009	130	150	194	211	236	254	269	282	296	308	322	342	359	399	407
14C-792009	124	152	188	204	227	232	250	262	278	295	311	332	348	381	388
15C-792009	14	35	99	119	145	167	181	196	208	219	233	256	287	336	344
GEC-S3A	139	151	184	199	219	236	251	263	276	290	305	326	344	375	380
GEC-S4A	139	151	184	199	219	236	251	263	275	289	305	328	343	373	379
GEC-SPC2A	131	144	174	186	199	210	218	225	234	244	253	265	273	290	297
GEC-S8A	21	26	64	87	106	120	140	161	182	201	219	238	254	271	279
GEC-S9A	77	92	156	178	195	206	216	223	232	240	252	263	271	286	290
GEC-S10A	74	92	140	153	162	164	169	176	200	218	236	255	270	291	300
GEC-S18A	123	137	170	184	198	208	219	222	231	238	249	260	270	286	291
GEC-S21A	129	140	170	184	198	208	217	223	231	238	248	258	267	286	296
GEC-S56A	104	127	170	184	198	209	218	225	236	242	254	266	274	295	302
GEC-S57A	98	120	167	182	197	208	217	224	233	240	253	265	273	292	299
Tank 13, JP-5	103	129	167	180	195	203	213	220	229	237	248	258	268	288	295
P&W ES0001, Shale JP-4	-1	1	81	102	134	155	173	186	198	212	225	240	259	303	313
P&W 79-C-2086, Petroleum JP-4	20	22	54	65	90	116	143	164	180	198	216	238	256	301	316
P&W 79-C-2086, Shale JP-4	0	13	82	105	134	156	172	186	198	213	222	240	260	307	320
P&W 79-C-2086, Blend #1	52	53	65	86	121	214	220	239	254	265	274	289	301	318	323
P&W 79-C-2086, Blend #2	42	53	67	92	153	165	170	181	196	210	223	240	256	300	313
P&W 79-C-2086, Blend #3	95	116	157	167	178	189	196	202	211	218	225	236	247	269	277
P&W 79-C-2086, Blend #4	-3	-1	50	67	94	111	141	161	164	167	170	183	204	279	294

(continued)

TABLE 181 (continued)

Sample Descriptions	(IBP) 0.5	Temperatures at which the following percents were recovered (°C) 1	5	10	20	30	40	50	60	70	80	90	95	99	(FBP) 99.5
SP 80-1	140	151	182	197	218	232	248	260	273	288	304	329	347	371	375
SP 80-2	145	157	188	204	226	241	255	269	283	299	315	340	360	386	391
SP 80-3	29	37	68	88	103	119	134	151	173	193	215	236	253	271	276
SP 80-4	93	111	162	178	195	205	216	222	231	240	250	263	270	279	280
SP 80-5	118	136	170	183	197	209	216	225	234	244	255	270	285	304	307
SP 80-6	116	133	160	184	197	209	218	228	236	246	251	272	285	301	305
SP 80-7	140	150	174	186	199	210	219	226	236	245	256	271	283	299	301
SP 80-8	142	151	178	190	204	216	226	236	244	259	275	303	323	350	354
SP 80-9	86	99	141	152	160	164	168	176	194	213	232	256	273	296	300
SP 80-10	38	57	89	106	135	151	161	163	168	172	189	221	247	282	289
SP 80-11	40	57	83	98	118	139	153	161	168	180	203	232	252	280	285
SP 80-12	34	42	76	92	117	133	154	171	192	216	244	288	313	344	352
SP 80-13	146	159	186	199	218	234	247	259	272	287	304	329	349	375	379
BRF-9	6	40	69	89	101	120	143	167	189	210	230	253	273	302	307
BRF-13	138	151	181	199	221	241	256	271	287	304	319	344	363	392	397
BRF-14	140	154	182	196	218	230	246	258	273	291	312	338	360	396	404
CRF-8	38	50	62	82	142	179	195	211	225	232	247	263	278	302	306
CRF-13	147	162	193	211	234	253	268	282	295	308	324	347	366	394	399
CRF-14	150	164	190	203	225	234	250	262	276	291	308	328	343	362	364
GEC 79-C-2009-62B-1, DF-2	26	29	66	88	100	118	128	141	152	162	174	190	206	253	266
P&W 792086, M50001	5	27	88	111	136	156	174	186	198	213	225	248	270	308	314
P&W 792086, M60001	10	27	63	89	120	141	172	194	216	234	256	289	320	353	376
P&W 792086, M70001	132	134	137	140	159	166	186	217	236	276	304	326	340	349	353
P&W 792086, M80001	145	157	167	181	206	224	237	251	264	280	298	329	347	373	379
GEC 792009, 77B	26	35	61	73	95	117	137	158	175	193	210	233	251	289	311
GEC 792009, 78B	122	142	184	201	221	236	250	261	271	285	301	323	343	391	405
GEC 792009, 13C-2	103	123	179	200	225	244	258	271	287	302	319	341	357	388	397
P&W M50014A-2	112	115	139	161	184	197	208	217	224	235	244	262	288	348	365
P&W MJ0016A	27	35	58	67	93	117	141	172	196	213	228	244	254	274	285
P&W MJ0013B	29	37	58	69	90	117	152	179	197	215	228	246	256	285	308
POSF-D-81-043, GECF-1D, JP-4	26	34	67	87	100	118	132	151	172	194	215	237	253	285	305
POSF-D-81-044, GECF-13D, DF-2	133	147	178	195	219	237	252	267	281	298	315	338	355	387	398
POSF-D-81-042, GECF-14D, DF-2/ARC	138	151	180	195	215	228	241	253	269	285	304	329	349	383	394

(continued)

TABLE 181 (continued)

Sample Descriptions	(IBP) 0.5	1	5	10	20	30	40	50	60	70	80	90	95	99	(FBP) 99.5
	Temperatures at which the following percents were recovered (°C)														
POSF-D-81-046, GECF-1E, JP-4	35	42	58	65	91	142	177	194	207	218	233	248	256	283	304
POSF-D-81-045, GECF-13E, DF-2	98	134	186	204	229	248	263	276	290	303	318	339	355	390	399
DDP-81-25, Blend JP-4, Tank B-1, 5 May 81	27	36	61	72	96	113	128	143	160	176	195	218	235	277	303
DDP-81-26, DF-2 Base Stock, 5 May 81	133	146	178	194	216	233	248	260	273	288	305	330	348	384	396
GECS-24D, Reference JP-4	33	40	69	87	100	118	135	157	180	201	221	243	257	300	323
GECS-26D, Reference JP-4	33	41	69	88	101	120	141	166	188	208	226	247	271	291	309
DDP-81-08, Blending JP-5 Tank F-1, 23 April 81	129	142	169	181	196	206	216	223	232	241	252	264	273	296	307
GECS-81B-1, DF-2	105	125	175	195	217	235	251	266	281	298	316	338	356	390	403
GECS-82B, DF-2	86	100	162	187	215	233	249	264	280	297	314	337	355	390	402
POSF-D-81-59, Blend of JP-4, DF-2, 2040 Solvent	39	58	88	105	147	179	203	223	236	254	277	307	330	370	383
AEDC Blending Stocks															
DDP-81-22, Tank B-11, JP-4	27	38	69	89	100	120	136	161	187	208	226	246	260	288	300
DDP-81-23, Tank B-12, JP-4	26	39	70	89	101	120	136	160	186	208	225	247	260	292	306
DDP-81-24, Tank B-13, JP-4	27	40	69	89	101	119	137	161	187	208	227	247	260	289	302
DDP-81-20, Tank F-6, JP-5	142	150	171	181	194	204	213	220	229	237	249	263	274	304	315
DDP-81-21, Tank F-7, JP-5	142	150	171	181	193	203	213	219	228	236	248	262	272	300	309
DDP-81-17, Tank F-9, DF-2	136	150	193	215	240	259	274	291	304	320	340	365	385	425	441
DDP-81-18, Tank F-10, DF-2	134	150	192	213	236	255	272	288	303	318	337	361	381	412	421
DDP-81-19, Tank F-11, DF-2	132	147	192	214	238	256	272	289	303	319	339	364	385	428	444
DDP-81-12, Tank F-8, Xy-B	157	158	167	168	173	178	180	181	183	185	187	206	273	302	312
DDP-81-14, Tank B-18, A-400	181	184	196	200	205	208	211	221	230	233	247	256	286	358	371
DDP-81-28, Tank F-12, AEDC Blend 2 (6 July 81)	25	35	67	86	98	118	139	159	168	197	215	237	254	292	315
DDP-81-29, Tank F-11, AEDC Blend 3 (6 July 81)	43	58	86	98	132	163	197	220	242	267	296	331	357	399	412
DDP-81-30, Tank F-7, AEDC Blend 5 (6 July 81)	142	145	152	159	162	171	192	203	215	227	238	255	269	301	316
DDP-81-31, Tank F-9, AEDC Blend 6 (6 July 81)	131	145	176	192	208	224	236	252	270	292	315	344	367	405	415
AEDC POSF-C-81-134, A-1, JP-4	27	34	63	82	98	117	135	153	173	196	217	238	254	277	318

TABLE 182. SIMULATED DISTILLATIONS IN °F, BY GC (ASTM D 2887)

Sample Descriptions	(IBP) 0.5	Temperatures at which the following percents were recovered (°F) 1	5	10	20	30	40	50	60	70	80	90	95	99	(FBP) 99.5
1B-792009, JP-4	70	77	136	165	192	217	244	288	345	396	433	478	511	615	639
2B-792009, JP-8	257	280	334	358	385	403	419	428	444	459	475	493	511	547	565
13B-792009, DF-2	250	286	351	385	432	464	491	520	549	576	604	644	684	752	768
14B-792009, DF-2 Aromatic blend	252	307	352	385	421	448	468	491	520	549	583	628	664	739	759
8B-792009	84	104	167	196	243	300	370	406	439	450	477	496	527	576	590
9B-792009	77	97	160	192	221	259	302	345	388	424	450	487	513	561	574
15B-792009	37	79	171	217	271	311	345	370	392	419	441	478	522	606	622
GEC-49B-1	72	77	147	183	210	241	261	289	316	342	374	426	469	532	556
1C-792009	90	106	136	154	208	306	354	383	406	430	455	482	498	547	572
8C-792009	104	127	153	194	331	372	403	424	446	453	482	507	538	612	626
9C-792009	95	115	140	165	264	349	383	405	428	448	464	489	511	558	572
13C-792009	266	302	381	412	457	489	516	540	565	586	612	648	678	750	765
14C-792009	255	306	370	399	441	450	482	504	532	563	592	630	658	718	730
15C-792009	57	95	210	246	293	333	358	385	406	426	451	493	549	637	651
GEC-S3A	282	304	363	390	426	457	484	505	529	554	581	619	651	707	716
GEC-S4A	282	304	363	390	426	457	484	505	527	552	581	622	649	703	714
GEC-SPC2A	268	291	345	367	390	410	424	437	453	471	487	509	523	554	567
GEC-S8A	70	82	147	189	223	248	284	322	360	394	426	460	489	520	534
GEC-S9A	171	198	313	352	383	403	421	433	450	464	486	505	520	547	554
GEC-S10A	165	198	284	307	324	327	336	349	392	424	457	491	518	556	572
GEC-S18A	253	279	338	363	388	406	426	432	448	460	480	500	518	547	556
GEC-S21A	264	284	338	363	388	406	423	433	448	460	478	496	513	547	565
GEC-S56A	219	261	338	363	388	408	424	437	457	468	489	511	525	563	576
GEC-S57A	208	248	333	360	387	406	423	435	451	464	487	509	523	558	570
Tank 13, JP-5	217	264	333	356	383	397	415	428	444	459	478	496	514	550	563
P&W ES0001, Shale JP-4	30	34	178	216	273	311	343	367	388	414	437	464	498	577	595
P&W 79-C-2086, Petroleum JP-4	68	72	129	149	194	241	289	327	356	388	421	460	493	574	601
P&W 79-C-2086, Shale JP-4	32	55	180	221	273	313	342	367	388	415	432	464	500	585	608
P&W 79-C-2086, Blend #1	126	127	149	187	250	417	428	462	489	509	525	552	574	604	613
P&W 79-C-2086, Blend #2	108	127	153	198	307	329	338	358	385	410	433	464	493	572	595
P&W 79-C-2086, Blend #3	203	241	315	333	352	372	385	396	412	424	437	457	477	516	531
P&W 79-C-2086, Blend #4	27	30	122	153	201	232	286	322	327	333	338	361	399	534	561

(continued)

TABLE 182 (continued)

Sample Descriptions	(IBP) 0.5	Temperatures at which the following percents were recovered (°F) 1	5	10	20	30	40	50	60	70	80	90	95	99	(FBP) 99.5
SP 80-1	284	304	360	387	424	450	478	500	523	550	579	624	657	700	707
SP 80-2	293	315	370	399	439	466	491	516	541	570	599	644	680	727	736
SP 80-3	84	99	154	190	217	246	273	304	343	379	419	457	487	520	529
SP 80-4	199	232	324	352	383	401	421	432	448	464	482	505	518	534	536
SP 80-5	244	277	338	361	387	408	421	437	452	471	491	518	545	579	585
SP 80-6	241	271	336	363	387	408	424	442	457	475	484	522	545	574	581
SP 80-7	284	302	345	367	390	410	426	439	457	473	493	520	541	570	574
SP 80-8	288	304	352	374	399	421	439	457	471	498	527	577	613	662	669
SP 80-9	187	210	286	306	320	327	334	349	381	415	450	493	523	565	572
SP 80-10	100	135	192	223	275	304	322	325	334	342	372	429	477	540	552
SP 80-11	104	135	181	208	244	262	307	322	334	356	397	450	486	536	545
SP 80-12	93	108	169	198	243	271	309	340	378	421	471	550	595	651	666
SP 80-13	295	318	367	390	424	453	477	498	522	549	579	624	660	707	714
BRF-9	43	104	156	192	214	248	289	333	372	410	446	487	523	576	585
BRF-13	280	304	358	390	430	466	493	520	549	579	606	651	685	737	747
BRF-14	284	309	360	385	424	446	475	496	523	556	594	640	680	745	759
CRF-8	100	122	144	180	288	354	383	412	437	450	477	505	532	576	583
CRF-13	297	324	379	412	453	487	514	540	563	586	615	657	691	741	750
CRF-14	302	327	374	397	437	453	482	503	529	556	586	622	649	684	687
GEC 79-C-2009-62B-1, DF-2	79	84	151	190	212	244	262	286	306	324	345	374	403	487	511
P&W 792086, M50001	41	81	190	232	277	313	345	367	388	415	437	473	518	586	597
P&W 792086, M60001	50	81	145	192	248	286	342	381	421	453	493	552	608	667	709
P&W 792086, M70001	270	273	279	284	316	331	367	423	457	529	579	619	644	660	667
P&W 792086, M80001	293	315	333	358	403	435	459	484	507	536	568	624	657	703	714
GEC 792009, 77B	79	95	142	163	203	243	279	316	347	379	410	451	484	552	592
GEC 792009, 78B	252	288	363	394	430	4[illegible]	482	502	520	545	574	613	649	736	761
GEC 792009, 13C-2	217	253	354	392	437	471	496	520	549	576	606	646	675	730	747
P&W M50014A-2	234	239	282	322	363	387	406	423	435	455	471	504	550	658	689
P&W MJ0016A	81	95	136	153	199	243	286	342	385	415	442	471	489	525	545
P&W MJ0013B	84	99	136	156	194	243	306	354	387	419	442	475	493	545	586
POSF-D-81-043, GECF-1D, JP-4	79	93	153	189	212	244	270	304	342	381	419	459	487	545	581
POSF-D-81-044, GECF-13D, DF-2	271	297	352	382	426	459	486	513	538	568	599	640	671	729	748
POSF-D-81-042, GECF-14D, DF-2/ARO	280	304	356	383	419	442	466	487	516	545	579	624	660	721	741

(continued)

TABLE 182 (continued)

Sample Descriptions	(IBP) 0.5	Temperatures at which the following percents were recovered (°F) 1	5	10	20	30	40	50	60	70	80	90	95	99	(FBP) 99.5
POSF-D-81-046, GECF-1E, JP-4	95	108	136	149	196	288	351	381	405	424	451	478	493	542	579
POSF-D-81-045, GECF-13E, DF-2	208	273	367	399	444	478	505	529	554	577	604	642	671	734	750
DDP-81-25, Blend JP-4, Tank B-1, 5 May 81	81	97	141	161	205	235	262	239	321	349	382	425	455	531	578
DDP-81-26, DF-2 Base Stock, 5 May 81	271	295	352	381	420	451	478	500	523	551	582	625	659	723	744
GECS-24D, Reference JP-4	92	105	157	189	211	244	275	315	357	395	430	469	496	572	613
GECS-26D, Reference JP-4	92	105	156	191	213	248	285	330	371	407	440	476	519	555	588
DDP-81-08, Blending JP-5, Tank F-1, 4-23-81	264	288	336	358	385	403	421	433	450	466	486	507	523	565	585
GECS-81B-1, DF-2	221	257	347	383	423	455	484	511	538	568	601	640	673	734	757
GECS-82B, DF-2	187	212	324	369	419	451	480	507	536	567	597	639	671	734	756
POSF-D-81-59, Blend of JP-4, DF-2, 2040 Solvent	102	136	190	221	297	354	397	433	457	489	531	585	626	698	721
AEDC Blending Stocks															
DDP-81-22, Tank B-11, JP-4	81	100	156	192	212	248	277	322	369	406	439	475	500	550	572
DDP-81-23, Tank B-12, JP-4	79	102	158	192	214	248	277	320	367	406	437	477	500	558	583
DDP-81-24, Tank B-13, JP-4	81	104	156	191	214	246	279	322	369	406	441	477	500	552	576
DDP-81-20, Tank F-6, JP-5	288	302	339	358	381	399	415	428	441	458	480	505	525	579	599
DDP-81-21, Tank F-7, JP-5	288	302	339	358	380	398	415	427	443	457	479	503	522	573	589
DDP-81-17, Tank F-9, DF-2	276	303	380	419	465	498	526	555	579	609	643	688	725	797	825
DDP-81-18, Tank F-10, DF-2	274	301	378	416	458	492	521	551	577	605	639	682	717	773	789
DDP-81-19, Tank F-11, DF-2	269	297	377	417	460	493	522	552	578	607	641	688	726	803	831
DDP-81-12, Tank F-8, Xy-B	315	316	333	334	343	352	356	358	361	365	369	403	523	576	594
DDP-81-14, Tank B-18, A-400	358	363	385	392	401	406	412	430	446	451	477	493	547	676	700
DDP-81-28, Tank F-12, AEDC Blend 2 (6 July 81)	77	95	153	187	208	244	282	318	334	387	419	459	489	558	599
DDP-81-29, Tank F-11, AEDC Blend 3 (6 July 81)	109	136	187	208	270	325	387	428	468	513	565	628	675	750	774
DDP-81-30, Tank F-7, AEDC Blend 5 (6 July 81)	288	293	306	318	324	340	378	397	419	441	460	491	515	574	601
DDP-81-31, Tank F-9, AEDC Blend 6 (6 July 81)	268	293	349	378	406	435	457	486	518	558	599	651	693	761	779
AEDC POSF-C-81-134, A-1, JP-4	81	93	145	180	208	243	275	307	343	385	423	460	489	531	604

TABLE 183. HYDROCARBON-TYPE ANALYSES BY MODIFIED ASTM D 2789

Sample designation	Paraffins	Monocyclo-paraffins	Dicyclo-paraffins	Alkyl benzenes	Indans/ tetralins	Naphthalenes
GEC-120-4AO-792033	37.3	23.0	0.0	12.8	4.0	22.9
GEC-120-8AO-792033	38.9	20.1	0.0	12.7	4.3	24.1
JP-8/Aro-12(772043)	30.7	28.0	2.5	11.2	5 7	21.9
JP-4/Aro-12(772043)	32.2	27.7	1.6	11.7	5.1	21.7
1B-792009, JP-4	68.8	15.3	2.4	11.9	1.6	0.0
2B-792009, JP-8	43.6	39.1	3.7	7.6	4.1	1.9
13B-792009, DF-2	45.8	32.5	2.6	8.4	5.3	5.4
14B-792009, DF-2 Aromatic blend	35.0	24.5	2.0	11.1	6.5	20.9
8B-792009	42.5	16.2	0.0	14.8	4.4	22.1
9B-792009	46.0	27.1	0.0	12.4	2.6	11.9
15B-792009	45.6	43.4	0.0	7.4	3.6	0.0
GEC-49B-1	58.5	27.9	2.8	9.1	1.0	0.7
Reanalyses of blends and stocks						
1A	61.4	23.6	5.0	8.5	1.0	0.5
2A	43.2	39.9	3.7	7.4	3.9	1.9
3A	44.0	39.7	3.5	7.2	3.8	1.8
4A	30.6	27.9	2.6	11.1	5.8	22.0
5A	34.4	31.0	3.3	28.0	1.7	1.6
6A	25.4	20.8	1.6	51.4	0.0	0.8
7A	36.8	34.0	3.2	9.3	4.8	11.9
8A	36.1	22.2	0.0	12.9	4.3	24.5
9A	44.9	27.4	0.0	11.3	2.7	13.7
10A	31.7	12.4	2.4	52.7	0.4	0.4
11A	44.0	17.2	3.5	34.3	0.6	0.4
12A	57.2	22.2	5.2	13.8	1.1	0.5
13A-1	45.7	30.4	2.3	8.1	6.0	7.5
13A-2	45.4	32.5	3.2	7.6	4.8	6.5
Xylene bottoms	1.2	0.1	0.0	98.7	0.0	0.0

(continued)

TABLE 183 (continued)

Sample designation	Paraffins	Monocyclo-paraffins	Dicyclo-paraffins	Alkyl benzenes	Indans/ tetralins	Naphthalenes
GMSO	58.2	35.0	0.0	3.5	2.5	0.8
2040 solvent	3.6	0.7	0.1	19.4	9.8	66.4
1C-792009	58.5	21.1	7.7	9.0	2.5	1.2
8C-792009	36.1	19.8	0.0	13.2	5.6	25.3
9C-792009	45.6	24.9	0.0	11.6	4.2	13.7
13C-792009	46.1	31.3	2.4	8.0	7.4	4.8
14C-792009	32.4	21.6	1.7	11.6	8.2	24.3
15C-792009	43.7	45.7	0.0	6.4	3.2	1.0
772043-F1	62.3	21.8	5.5	8.4	1.[illegible]	0.7
772043-F2	44.1	39.3	3.6	8.0	3.1	1.9
772043-F3	45.1	39.9	2.5	7.6	3.1	1.8
772043-F4	31.1	27.0	1.9	11.6	5.4	23.0
772043-F5	35.1	30.7	2.9	28.6	0.9	1.8
772043-F6	25.3	20.8	1.9	51.1	0.0	0.9
772043-F7	37.6	33.1	2.2	9.9	4.3	12.9
772043-F8	36.6	20.8	0.0	12.9	4.7	25.0
772043-F9	46.0	25.8	0.0	11.3	3.3	13.6
772043-F10	31.6	11.4	2.6	53.9	0.0	0.5
772043-F11	44.4	15.9	3.7	34.8	0.6	0.6
77-043-F12	57.5	20.9	5.4	14.3	1.2	0.7
77-043-F13	44.3	32.2	2.6	8.6	6.3	6.0
JP-5, Tank 13	43.4	35.1	4.1	10.2	4.4	2.8
P&W ES0001, Shale JP-4	44.7	45.7	0.0	6.4	3.2	0.0
P&W 79-C-2086, Petroleum JP-4	62.6	20.9	5.4	9.2	1.7	0.2
P&W 79-C-2086, Shale JP-4	44.3	45.6	0.0	6.6	3.5	0.0
P&W 79-C-2086, Blend #1	58.1	31.4	0.0	5.9	2.5	2.1
P&W 79-C-2086, Blend #2	46.0	26.2	0.3	25.4	1.4	0.7
P&W 79-C-2086, Blend #3	49.2	33.1	3.9	9.7	3.4	0.7
P&W 79-C-2086, Blend #4	40.3	4.2	0.1	52.9	2.1	0.4
GEC 79-C-2009-62B-1, DF-2	51.3	37.5	3.5	6.9	0.3	0.5

(continued)

TABLE 183 (continued)

Sample designation	Paraffins	Monocyclo-paraffins	Dicyclo-paraffins	Alkyl benzenes	Indans/ tetralins	Naphthalenes
P&W 792086, M50001	45.1	45.2	0.0	6.4	3.3	0.0
P&W 792086, M60001	46.4	18.7	0.2	28.2	2.7	3.8
P&W 792086, M70001	17.5	16.4	4.5	56.5	1.1	4.0
P&W 792086, M80001	33.5	18.7	2.3	17.6	13.0	14.9
GEC 792009, 77B	63.6	19.5	4.3	11.2	1.2	0.2
GEC 792009, 78B	42.0	30.6	3.3	7.7	6.0	10.4
GEC 792009, 13C-2	44.1	31.3	2.9	8.1	7.4	5.7
P&W M50014A-2	48.1	28.8	3.0	13.6	3.7	2.8
P&W MJ0016A	64.4	19.1	5.9	7.9	2.0	0.7
P&W MJ0013B	63.5	19.3	6.4	8.0	2.0	0.8
POSF-D-81-043, GECF-1D, JP-4	62.0	23.6	4.2	8.4	1.7	0.1
POSF-D-81-044, GECF-13D, DF-2	35.0	25.4	1.9	10.9	6.7	19.6
POSF-D-81-042, GECF-14D, DF-2/ARO	45.4	32.3	2.4	8.5	5.5	5.9
POSF-D-81-046, GECF-1E, JP-4	60.1	21.0	7.0	8.4	1.7	0.1
POSF-D-81-045, GECF-13F, DF-2	47.3	32.2	1.9	7.9	6.4	4.3
DDP-81-25 Blending JP-4, Tank B-1, 5-5-81	56.0	29.3	2.7	10.1	1.0	0.9
DDP-81-26 DF-2 Base stock, 5-5-81	41.9	32.2	3.1	8.3	6.3	8.2
GECS-24-D, Reference JP-4	63.2	22.2	3.7	9.1	1.7	0.1
GECS-26-D, Reference JP-4	61.5	20.4	4.1	12.0	1.8	0.2
DDP-81-08 Blending JP-5, Tank F-1, 4-23-81	45.4	38.9	2.8	7.5	3.0	2.4
GECS-81B-1, DF-2	44.9	32.6	2.2	8.7	5.8	5.8
GECS-82B, DF-2	45.7	32.9	1.7	8.7	5.5	5.5
POSF-D-81-59; Blend of JP-4, DF-2, 2040 Solvent	40.5	34.2	0.0	10.6	3.9	10.8

(continued)

TABLE 183 (continued)

Sample designation	Paraffins	Monocyclo-paraffins	Dicyclo-paraffins	Alkyl benzenes	Indans/ tetralins	Naphthalenes
AEDC Blending Stocks						
DDP-81-22, Tank B-11, JP-4	65.1	19.1	3.6	10.3	1.8	0.1
DDP-81-23, Tank B-12, JP-4	65.2	19.0	3.6	10.3	1.8	0.1
DDP-81-24, Tank B-13, JP-4	65.2	18.9	3.6	10.4	1.8	0.1
DDP-81-20, Tank F-6, JP-5	45.0	35.0	3.1	8.9	6.1	1.9
DDP-81-21, Tank F-7, JP-5	44.9	34.9	3.2	8.9	6.2	1.9
DDP-81-17, Tank F-9, DF-2	45.7	38.6	2.0	6.2	4.4	3.1
DDP-81-18, Tank F-10, DF-2	45.7	39.2	1.7	6.1	4.3	3.0
DDP-81-19, Tank F-11, DF-2	45.6	38.6	2.0	6.2	4.5	3.1
DDP-81-12, Tank F-8, Xy-B	1.2	1.0	0.0	96.7	0.6	0.5
DDP-81-14, Tank B-18, A-40[illegible]	2.5	0.6	0.1	22.4	23.3	51.1
DDP-81-28, Tank F-12, AEDC Blend 2 (6 July 81)	54.0	19.6	0.3	19.7	2.7	3.7
DDP-81-29, Tank F-11, AEDC Blend 3 (6 July 81)	48.8	30.6	0.0	13.2	3.6	3.8
DDP-81-30, Tank F-7, AEDC Blend 5 (6 July 81)	33.0	24.6	2.3	31.5	4.4	4.2
DDP-81-31, Tank F-9, AEDC Blend 6 (6 July 81)	44.7	36.2	2.1	7.6	5.4	4.0
E314A, JP-8 Blend #3 (P&W)	49.7	33.3	2.9	10.3	3.2	0.6
M50003P, JP-4 Blend #5 (P&W)	48.1	29.0	2.5	14.7	3.6	3.1
M50008B, JP-4 Blend #5 (P&W)	47.1	29.2	2.2	15.0	3.5	3.0
MS0007A, Shale JP-4 (P&W)	44.1	45.5	0.0	6.7	3.6	0.1
MS0010A, Shale JP-4 (P&W)	44.2	45.6	0.0	6.9	3.2	0.1
MS0011A, Shale JP-4 (P&W)	43.8	45.9	0.0	6.8	3.4	0.1
EJ0020B, JP-4 (P&W)	56.3	25.8	4.0	13.0	0.5	0.4
AEDC POSF-C-81-134, A-1 JP-4	59.8	21.6	4.5	12.3	1.5	0.3

TABLE 184. COMPARATIVE HYDROCARBON-TYPE ANALYSES BY MODIFIED ASTM D 2789 AND MONSANTO METHOD 21-PQ-38-63, IN WEIGHT PERCENTS

Components	GEC-120-[illegible]-792033		GEC-120-8A0-792033		P-8/Aro-12(772043)		JP-4/Aro-12(772043)		2B-792009, JP-8		13B-792009, DF-2	
	D 2789[a]	MONS[b]	D 2789	MONS	D 2789	MONS	D 2789	MONS	D 2789	MONS	D 2789	MONS
Paraffins	33.3	29.7	34.5	30.9	27.2	26.2	28.6	25.8	41.0	40.2	42.7	42.0
Monocycloparaffins	22.1	17.1	19.2	15.0	26.8	28.5	26.6	26.4	39.7	43.6	32.8	33.8
Dicycloparaffins	0.0	-[c]	0.0	-	2.4	-	1.5	-	3.8	-	2.6	-
Alkylbenzenes	13.3	18.3	13.1	17.9	11.5	14.4	12.0	14.2	8.3	9.8	9.1	10.5
Indans/Tetralins	4.1	3.9	4.7	4.1	6.2	4.8	5.6	4.2	4.8	4.0	6.1	4.8
Indenes/C_nH_{2n-10}	-	0.5	-	0.5	-	0.5	-	0.5	-	0.0	-	1.0
Naphthalenes	27.2	30.5	28.5	31.6	25.9	25.6	25.7	28.9	2.4	2.4	6.7	7.9

Components	14B-792009, DF-2 Aromatic Blend		8B-792009		9B-792009		15B-792009		Blend 4A		Blend 7A	
	D 2789	MONS	D 2789	MONS	D 2789	MONS	D 2789	MONS	D 2789	MONS	D 2789	MONS
Paraffins	31.1	30.5	37.9	34.5	42.3	40.7	43.2	41.4	27.1	26.2	33.6	32.9
Monocycloparaffins	23.5	24.3	15.6	9.6	26.9	19.8	44.4	44.0	26.7	28.7	33.5	36.5
Dicycloparaffins	1.9	-	0.0	-	0.0	-	0.0	-	2.5	-	3.1	-
Alkylbenzenes	11.5	13.6	15.3	21.5	13.2	19.1	8.2	10.8	11.4	14.1	9.9	11.9
Indans/Tetralins	7.2	5.5	4.9	4.3	3.0	3.0	4.2	3.8	6.3	5.0	5.4	4.4
Indenes/C_nH_{2n-10}	-	1.3	-	0.5	-	0.1	-	0.0	-	0.5	-	0.1
Naphthalenes	24.8	24.8	26.3	29.6	14.6	17.3	0.0	0.0	26.0	25.5	14.5	14.2

(continued)

TABLE 184 (continued)

Components	Blend 8A		Blend 9A		Blend 13A-1		Blend 13A-2		GMSO Stock		2040 Solvent	
	D 2789[a]	MONS[b]	D 2789	MONS	D 2789	MONS	D 2789	MONS	D 2789	MONS	D 2789	MONS
Paraffins	31.9	28.4	41.1	38.5	42.4	41.3	42.3	41.3	55.8	56.3	2.8	1.5
Monocycloparaffins	21.2	16.9	27.1	22.2	30.4	31.1	32.7	34.3	36.3	35.0	0.6	0.4
Dicycloparaffins	0.0	-[c]	0.0	-	2.3	-	3.2	-	0.0	-	0.1	-
Alkylbenzenes	13.3	18.0	12.0	16.7	8.7	10.2	8.2	9.1	3.9	4.2	17.6	22.1
Indans/Tetralins	4.7	4.1	3.1	2.9	6.9	5.6	5.5	4.5	3.0	2.5	9.5	6.9
Indenes/C_nH_{2n-10}	-	0.5	-	0.3	-	0.7	-	1.0	-	0.7	-	1.2
Naphthalenes	28.9	32.1	16.7	19.4	9.3	11.3	8.1	9.8	1.0	1.3	69.4	67.9

Components	8C-792009		9C-792009		13C-792009		14C-792009		15C-792009		POSF-C-81-134 AEDC A-1 JP-4	
	D 2789	MONS	D 2789	MONS	D 2789	MONS	D 2789	MONS	D 2789	MONS	D 2789	MONS
Paraffins	31.8	27.3	41.6	37.6	42.9	42.4	28.5	28.1	41.3	40.0	57.2	51.6
Monocycloparaffins	18.9	16.0	24.6	21.7	31.5	32.2	20.7	21.2	46.6	46.5	22.3	25.9
Dicycloparaffins	0.0	-	0.0	-	2.4	-	1.6	-	0.0	-	4.7	-
Alkylbenzenes	13.5	18.4	12.3	17.3	8.7	10.0	11.8	14.2	7.0	8.8	13.6	20.5
Indans/Tetralins	6.1	5.2	4.8	4.4	8.5	6.8	8.9	6.8	3.8	3.3	1.8	1.9
Indenes/C_nH_{2n-10}	-	0.5	-	0.2	-	1.0	-	1.2	-	0.0	-	0.0
Naphthalenes	29.7	32.6	16.7	18.8	6.0	7.6	28.5	28.5	1.3	1.4	0.4	0.1

(continued)

TABLE 184 (continued)

Components	DDP-81-29, Tank F-11 AEDC Blend 3(7-6-81)		DDP-81-30, Tank F-7 AEDC Blend 5(7-6-81)		DDP-81-31, Tank F-9 AEDC Blend 6(7-6-81)		E214A JP-8 Blend #3		M50003B JP-4 Blend #5	
	D 2789[a]	MONS[b]	D 2789	MONS	D 2789	MONS	D 2789	MONS	D 2789	MONS
Paraffins	45.7	43.6	30.1	27.7	41.9	41.0	47.1	46.0	44.7	42.3
Monocycloparaffins	31.0	28.3[c]	24.2	24.7	36.6	37.9	34.1	37.4	29.1	30.4
Dicycloparaffins	0.0	-	2.3	-	2.1	-	3.0	-	2.5	-
Alkylbenzenes	11.4	18.3	33.3	38.0	8.2	9.9	11.2	13.8	15.8	18.8
Indans/Tetralins	4.1	3.9	5.0	4.5	6.2	5.0	3.8	3.1	4.1	3.7
Indenes/C_nH_{2n-10}	-	0.3	-	0.0	-	0.6	-	0.0	-	0.0
Naphthalenes	4.8	5.6	5.1	5.1	5.0	5.6	0.8	0.7	3.8	4.8

Components	M50006B JP-4 Blend #5		M50007A Shale JP-4		M50010A Shale JP-4		M50011A Shale JP-4		EJ0020B JP-4	
	D 2789	MONS	D 2789	MONS	D 2789	MONS	D 2789	MONS	D 2789	MONS
Paraffins	44.0	42.2	41.8	41.0	41.9	40.7	41.5	40.9	53.8	44.1
Monocycloparaffins	29.6	31.0	46.5	45.8	46.6	45.9	46.9	45.8	26.6	34.6
Dicycloparaffins	2.3	-	0.0	-	0.0	-	0.0	-	4.1	-
Alkylbenzenes	16.3	18.5	7.4	9.6	7.6	9.9	7.5	9.5	14.4	21.3
Indans/Tetralins	4.1	3.7	4.2	3.4	3.8	3.3	4.0	3.5	0.6	0.0
Indenes/C_nH_{2n-10}	-	0.0	-	0.0	-	0.0	-	0.0	-	0.0
Naphthalenes	3.7	4.5	0.1	0.2	0.1	0.2	0.1	0.3	0.5	0.0

[a] Modified ASTM Method D 2789.

[b] Monsanto Method 21-PQ-38-63, which combines mono- and di-cycloparaffins into a single value.

[c] A dash indicates the compound is not detected by the method.

TABLE 185. COMPARATIVE HYDROCARBON-TYPE ANALYSES WITH THREE MASS SPECTRAL METHODS INCLUDING ASTM D 2425, IN WEIGHT PERCENTS

	POSF-D-81-044 GECF-13D, DF-2			POSF-D-81-042 GECF-14D, DF-2/ARO			DDP-81-17 Tank F-9, DF-2	
Components	D 2789[a]	D 2425[b]	MONS[c]	D 2789	D 2425	MONS	D 2789	D 2425
Paraffins	42.3	40.6	41.1	31.7	32.7	30.8	43.0	40.2
Total cycloparaffins:	34.9	29.1	33.2	26.3	22.9	24.7	41.2	36.8
Mono-	32.5	16.7	-[d]	24.5	13.3	-	39.2	25.2
Di-	2.4	9.0	-	1.8	7.0	-	2.0	9.0
Tri-	-	3.4	-	-	2.6	-	-	2.6
Alkylbenzenes	9.2	9.4	10.4	11.3	12.0	13.4	6.8	7.3
Indans/Tetralins	6.3	5.3	5.2	7.4	5.7	5.8	5.1	4.7
Indenes/C_nH_{2n-10}	-	1.9	1.1	-	2.2	1.2	-	1.9
Naphthalene	-	0.4	-	-	1.8	-	-	0.3
Total Naphthalenes[e]	7.3	8.6	9.0	23.3	21.2	24.1	3.9	5.0
Acenaphthenes	-	2.6	-	-	1.9	-	-	2.0
Acenaphthylenes	-	1.6	-	-	0.5	-	-	1.2
Tricyclic aromatics	-	0.9	-	-	0.9	-	-	0.9

	POSF-D-81-045 GECF-13E, DF-2			DDP-81-14, Tank B-18 Getty A-400			DDP-81-12, Tank F-8 Xylene Bottoms	
Components	D 2789	D 2425	MONS	D 2789	D 2425[f]	MONS	D 2789	D 2425[f]
Paraffins	44.2	41.1	43.3	2.0	0.0	0.8	1.1	0.0
Total cycloparaffins:	34.4	27.5	32.6	0.6	0.4	0.0	0.9	0.0
Mono-	32.5	16.0	-	0.5	-	-	0.9	-
Di-	1.9	8.5	-	0.1	-	-	0.0	-
Tri-	-	3.0	-	-	-	-	-	-
Alkylbenzenes	8.6	10.2	9.9	20.6	26.8	29.3	96.8	97.3
Indans/Tetralins	7.5	6.9	6.0	22.9	16.4	17.2	0.6	0.0
Indenes/C_nH_{2n-10}	-	1.9	1.1	-	0.0	0.6	-	0.0
Naphthalene	-	0.4	-	-	21.0	-	-	0.0
Total Naphthalenes	5.3	7.4	7.1	53.9	52.8	52.1	0.6	1.0
Acenaphthenes	-	2.6	-	-	1.9	-	-	1.3
Acenaphthylenes	-	1.5	-	-	1.1	-	-	0.2
Tricyclic aromatics	-	0.9	-	-	0.6	-	-	0.2

[a] Modified ASTM Method D 2789; data determined in volume percents and converted to weight percents with average density values.

[b] ASTM Method D 2425 is preceded by an ASTM D 2549 fractionation whereby fuels are separated into saturate and aromatic fractions.

[c] Monsanto mass spectral Method 21-PQ-38-63, which was developed for hydrocarbon feed stocks.

[d] A dash in a column indicates the compound can not be detected by the method.

[e] Includes naphthalene

[f] There was no ASTM D 2549 fractionation for these fuels since they were essentially all aromatic. The D 2425 analyses were conducted on the neat fuels which were considered as aromatic fractions for the calculations.

SECTION V

HIGH DENSITY FUELS

Certain advanced Air Force strategic missiles require high volumetric energy fuels because of the limited space available for the fuel. Several high density fuels have been developed based on synthetic cyclic hydrocarbons. These fuels, which include RJ-4, RJ-5, RJ-6, JP-9, and JP-10, consist of a relatively small number of chemical compounds and, thus, can be characterized by chemical composition as well as by bulk properties. The tasks described in this section pertain to defining the composition and properties of these high density fuels for engineering applications and quality control purposes, or are related to solving specific contamination problems that occur with the use of these fuels.

1. IDENTIFICATION OF CONTAMINANTS IN JP-9 TEST FUELS

JP-9 fuel specimens, which were used by an Air Force contractor in studies of fuel/elastomer compatibility, were examined to determine the kinds and amounts of contaminants present in the fuels. Four test fuels and one control fuel were involved in the evaluation. The purpose of the study was to determine whether the contamination of the fuel was due to components extracted from the elastomers, or due to oxidation or hydrolytic degradation of the fuels.

Procedure

The test fuels as received varied widely in color, and one contained a precipitate which had settled to the bottom of the container. These solids were removed by filtration before further processing. A 100-ml specimen of each fuel was passed through a short column of freshly activated 100-200 mesh silica gel. In

all cases, the fuels emerging from the silica gel columns were colorless. The columns were then carefully rinsed with hexane to remove residual fuel. Isolated material was removed from the gel by sequential rinsing with chloroform and then methanol. The two eluants were combined and the solvents were removed by evaporation in a stream of prepurified nitrogen. The recovered materials varied from a colorless oily film to a dark yellow liquid.

Infrared absorption spectra were recorded for each of the isolates from the four test fuels and the control fuel.

Results

Infrared spectra for the isolates from fuels #1 and #2, shown in Figures 220 and 221, are typical of those obtained from polysulfideformal elastomers such as the Thiokols. A reference spectrum (ref. 12) of Thiokol LP62 is shown in Figure 222. Low molecular weight elastomer species are apparently extracted by the fuel.

The infrared absorption spectrum of the material isolated from fuel #3, shown in Figure 223, closely matches the spectrum of dibutoxyethyl adipate, Figure 224 (ref. 13), and appears to be that compound or a very similar one. This material is commonly used as a plasticizer.

The silica gel isolate from fuel #4, shown in Figure 225, can be characterized as a polyethylene oxide adduct of an alcohol or phenol derivative. A typical reference spectrum (ref. 14) for a material of this type, di-t-butyl phenol-EO_{10_12} adduct, is presented in Figure 226. Fuel #4 also contained a precipitate, the spectrum of which is shown in Figure 227. The spectrum is characteristic of a carboxylic acid salt and the material is probably a metal stearate.

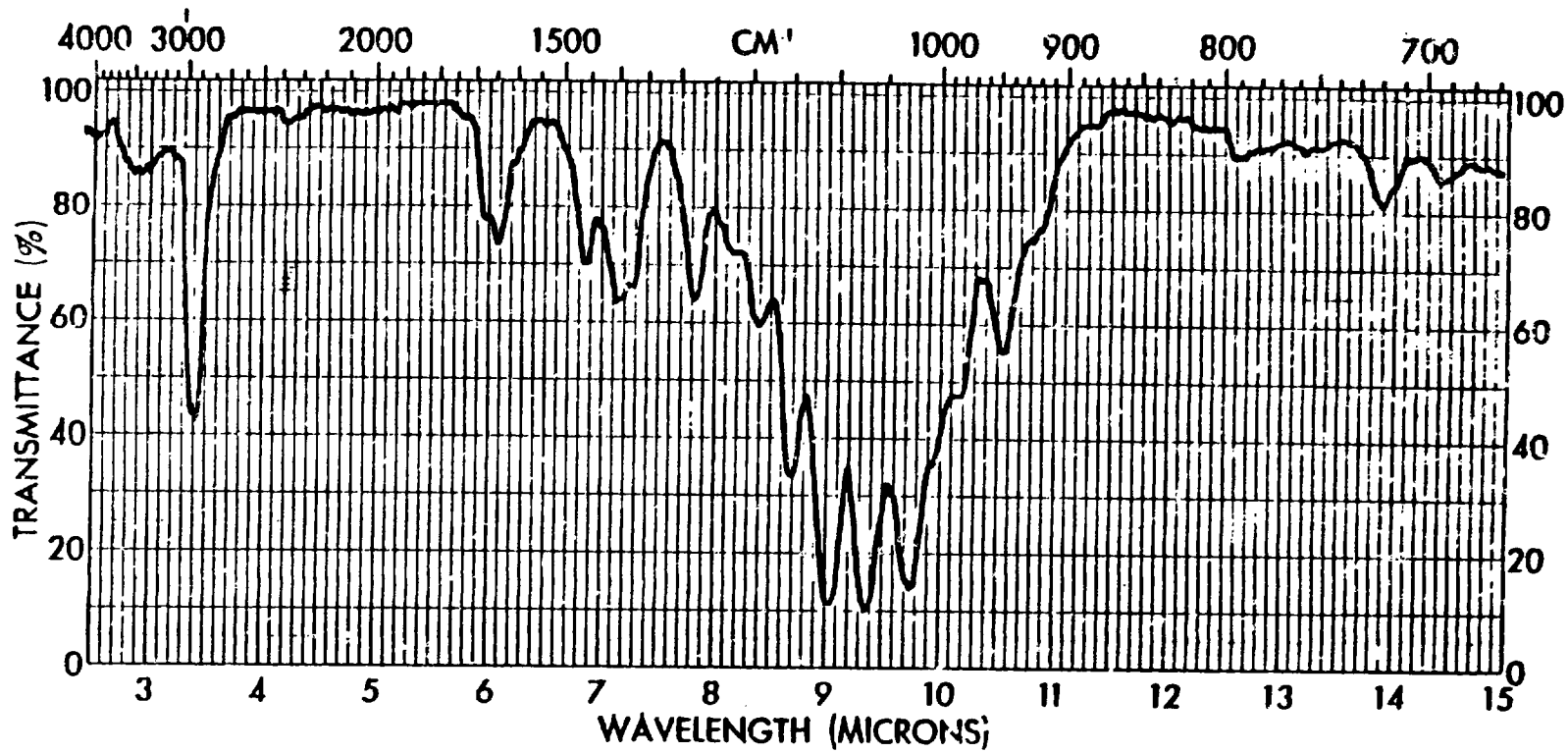

Figure 220. Infrared absorption spectrum of isolated material from JP-9 sample #1.

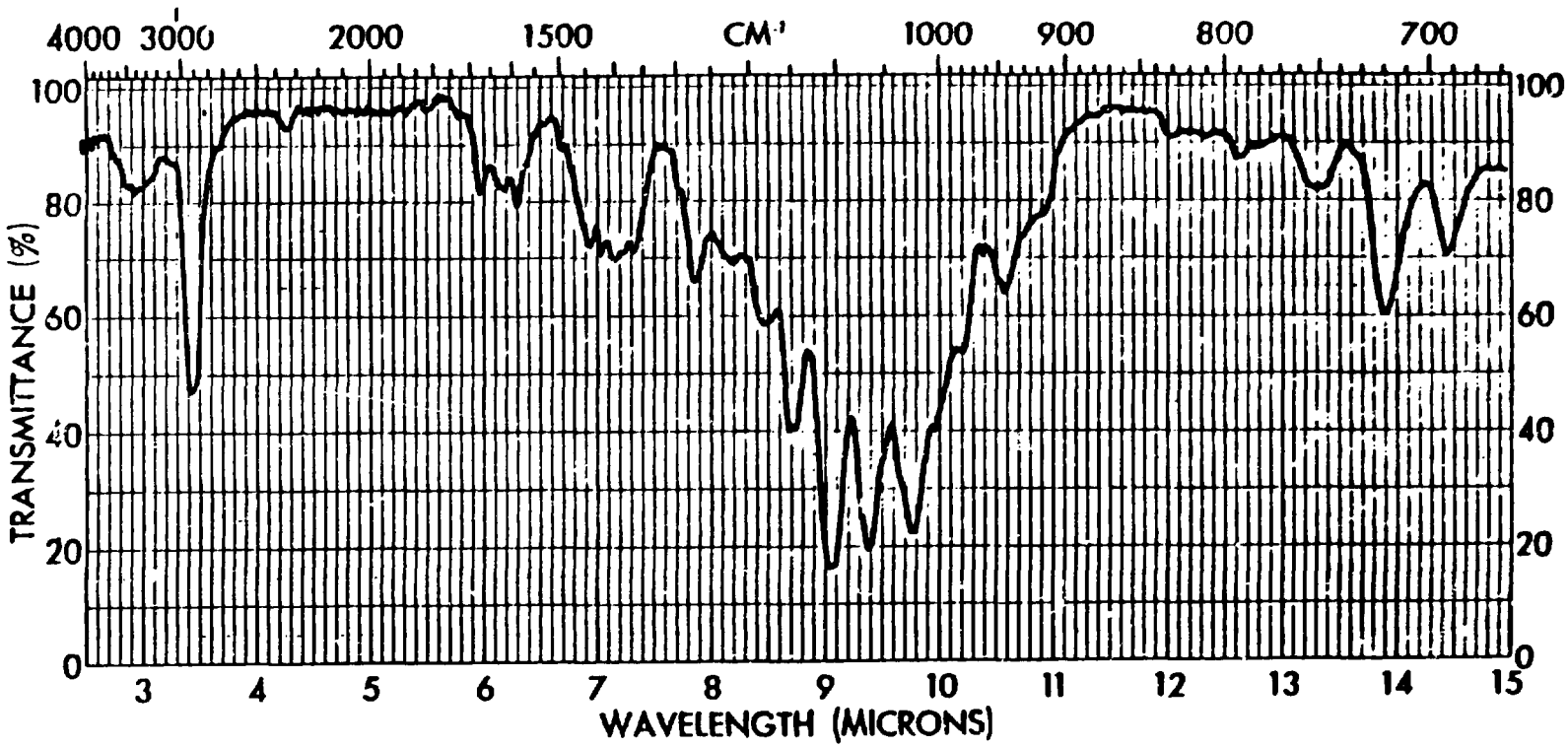

Figure 221. Infrared absorption spectrum of isolated material from JP-9 sample #2.

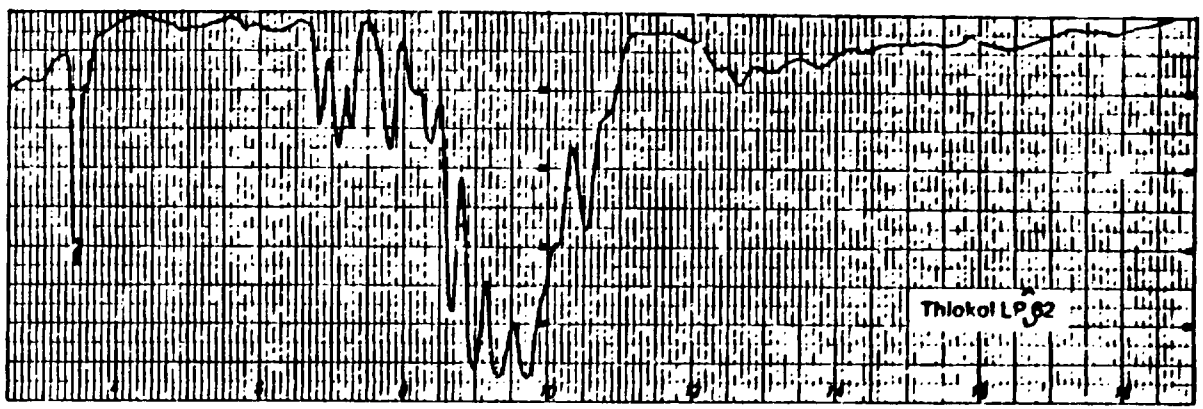

Figure 222. Infrared absorption spectrum of Thiokol LP62 polysulfide elastomer (ref. 12).

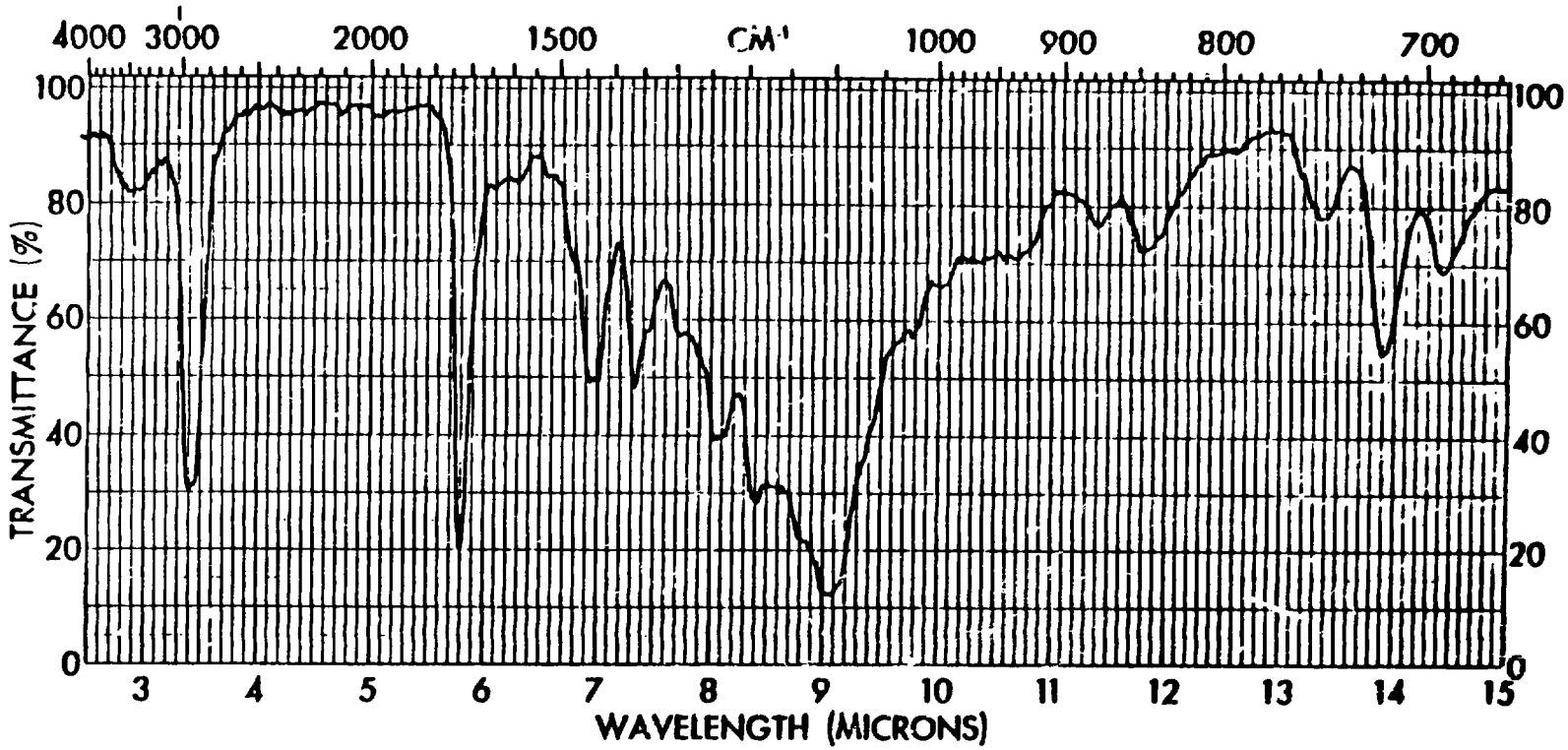

Figure 223. Infrared absorption spectrum of isolated material from JP-9 sample #3.

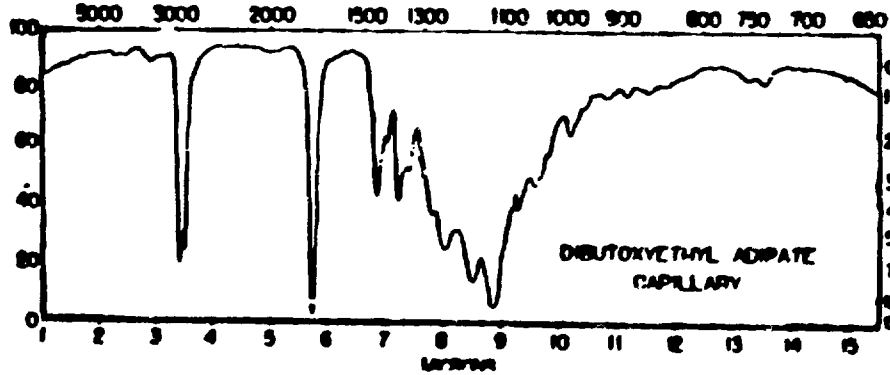

Figure 224. Infrared absorption spectrum of dibutoxyethyl adipate (ref. 13).

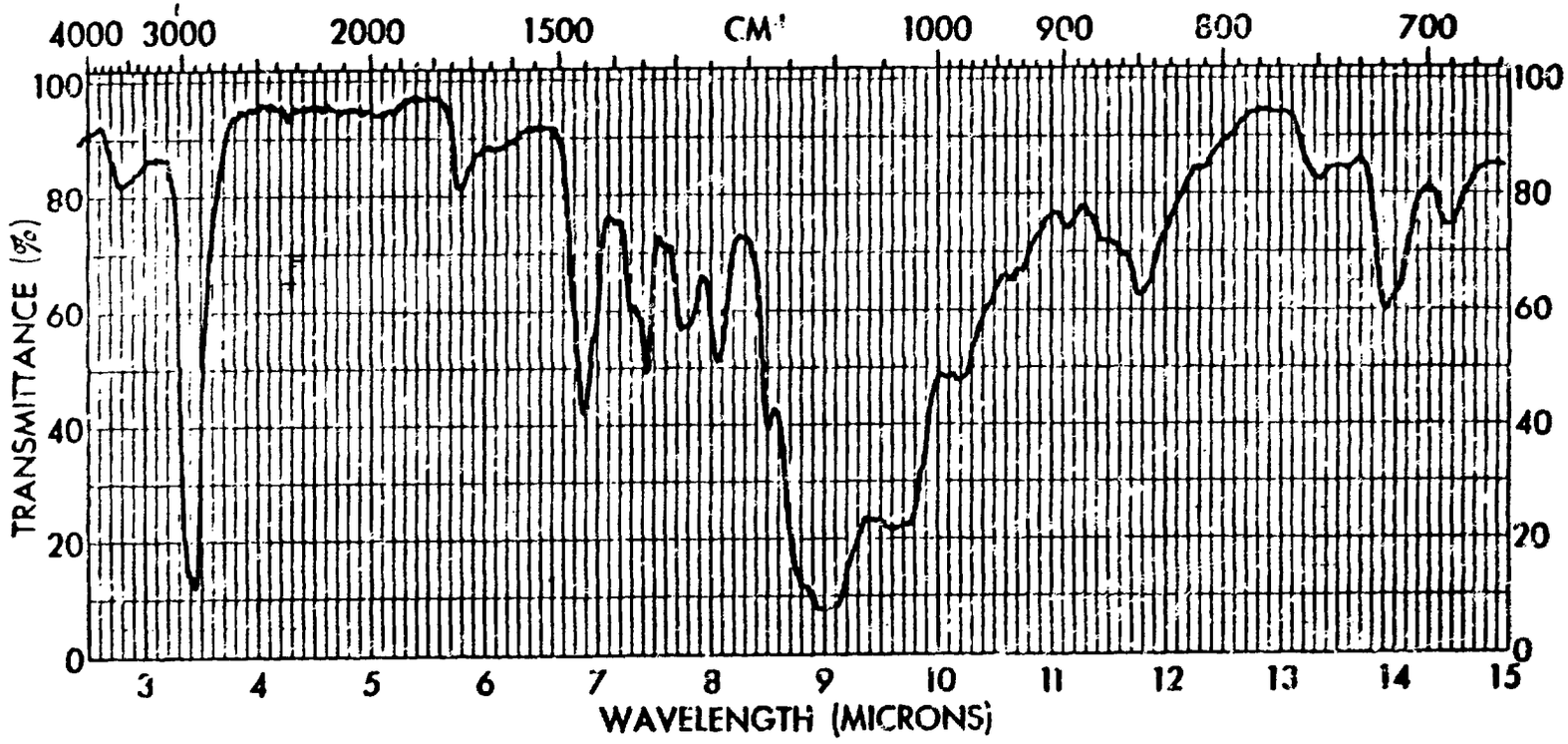

Figure 225. Infrared absorption spectrum of isolated material from JP-9 sample #4.

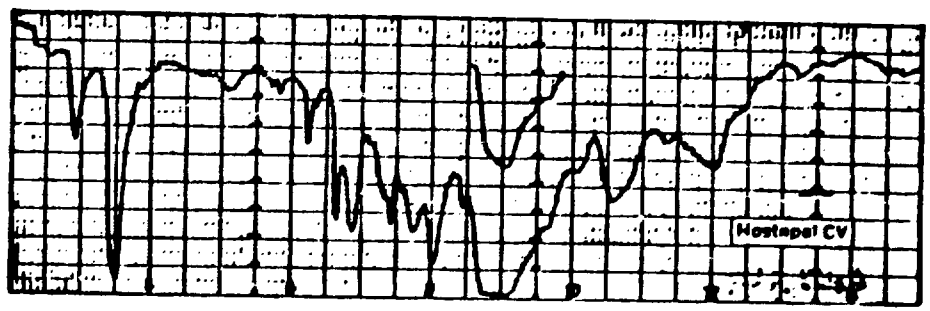

Figure 226. Infrared absorption spectrum of the ethylene oxide adduct of di-t-butyl phenol (ref. 14).

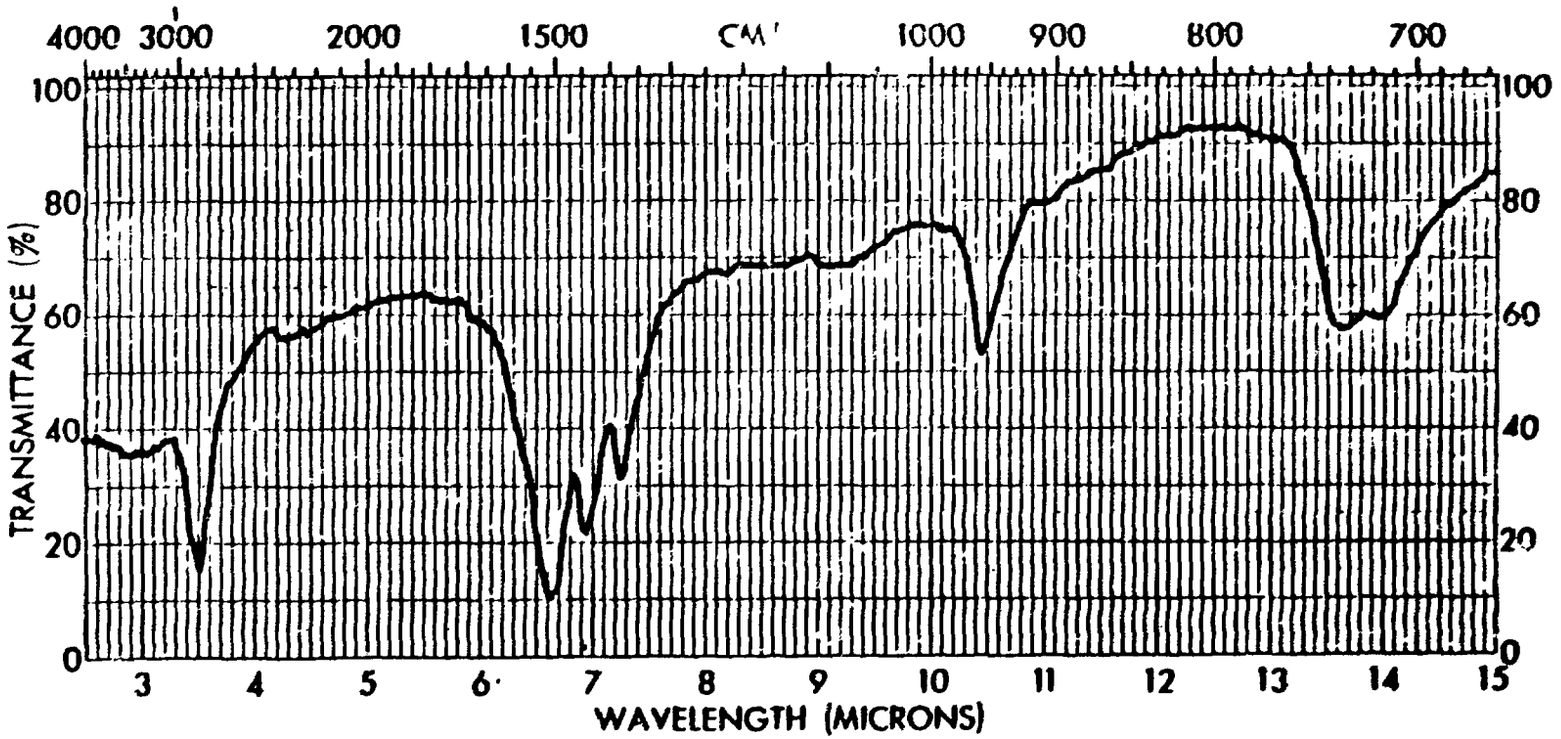

Figure 227. Infrared absorption spectrum of the precipitate present in JP-9 sample #4.

The control fuel gave very little residue, and its spectrum shows the presence of some residual fuel and has some weak bands characteristic of JP-10 oxidation products as discussed in a previous report (ref. 15).

Data for the weights and descriptions of the isolated residues are given in Table 186 along with the identification of the major constituent of each residue.

Conclusions

The major constituents of the materials isolated from the fuels were characterized and all might logically be a part of an elastomer composition. Minor components could have been present and one cannot conclusively rule out the presence of small amounts of the fuel. However, it is most unlikely that the compounds listed in Table 186 could have resulted from any reaction or degradation of the fuels themselves.

TABLE 186. MATERIALS ISOLATED FROM ONE-HUNDRED MILLILITER PORTIONS OF JP-9 FUEL SAMPLES

Fuel	Weight of isolate, grams	Color of isolate	Identity
Control	0.0251	Colorless	Fuel and its degradation products
#1	0.2540	Yellow liquid	Low molecular weight polysulfide-formal elastomer species
#2	0.1426	Colorless oil	Low molecular weight polysulfide-formal elastomer species
#3	0.1577	Dark yellow liquid	Dibutoxyethyl adipate or similar compound
#4	0.2701	Dark yellow	Ethylene oxide adduct of alcohol or phenol derivative
#4	-[a]	Yellow precipitate	Carboxylic acid salt, likely a metal stearate

[a]Precipitate taken from sample container, not associated with the 100-ml portion examined.

2. PROPERTIES OF FUELS AND FUEL BLENDS

A multitude of high density fuels and fuel blends were analyzed for specific physical and chemical properties by procedures described in the Appendix. Density and specific gravity results are shown in Table 187. Kinematic viscosity results are shown in Table 188, and viscosity/temperature relationships are shown in Figures 228 through 233. Heat of combustion values are shown in Table 189, vapor pressure in Table 190, surface tension in Table 191, flash point in Table 192, autoignition temperature in Table 193, and fuel composition data in Table 194. Gas chromatograms from the fuel composition studies are presented in Figures 234 through 244.

TABLE 187. DENSITY AND SPECIFIC GRAVITY OF HIGH DENSITY FUELS

Sample description	Test temperature, °F	Density, g/cc	Specific gravity
RJ-5 Blends			
50/50 Exo-Exo/Endo-Endo #1	60		1.0712
50/50 Exo-Exo/Endo-Endo #2	60		1.0717
50/50 Exo-Exo/Endo-Endo #3	60		1.0714
RJ-5F	60		1.0799
RJ-6 Blends			
AR 78024	-65	1.0754	
AR 78024	0	1.0469	
AR 78024	70	1.0169	
Sample 1219	60	1.0203	
Sample 1220	60	1.0223	
JP-9 Blends			
#1 (10% MCH*, 70% JP-10, 20% RJ-5	70	0.9385	
#2 (15% MCH, 55% JP-10, 30% RJ-5	70	0.9421	
Contaminated in shipment and filtered	32	1.0300	
Contaminated in shipment and filtered	70	1.0133	
Contaminated in shipment and filtered	100	0.9999	

*Methylcyclohexane.

TABLE 188. KINEMATIC VISCOSITY OF HIGH DENSITY FUELS

Sample description	Kinematic viscosity, centistokes					
	-65°F	-40°F	0°F	70°F	77°F	210°F
RJ-5 Fuel Blends						
50/50 Exo/Endo #1	9162	1231			15.97	
50/50 Exo/Endo #2	9173	1242			16.03	
50/50 Exo/Endo #3	9056	1219			15.94	
RJ-5F			189.5	22.60		3.105
RJ-6 Blends						
AR 78024	437.1		37.92	8.80		
Sample 1219	438.0					
Sample 1220	459.0					
JP-9 Blends	-30					
#1 (10% MCH*, 70% JP-10, 20% RJ-5)	43.59	17.34				
#2 (15% MCH, 55% JP-10, 30% RJ-5)	49.33	18.81				
Contaminated in shipment and filtered	893.3	150.2	51.53			

*Methylcyclohexane.

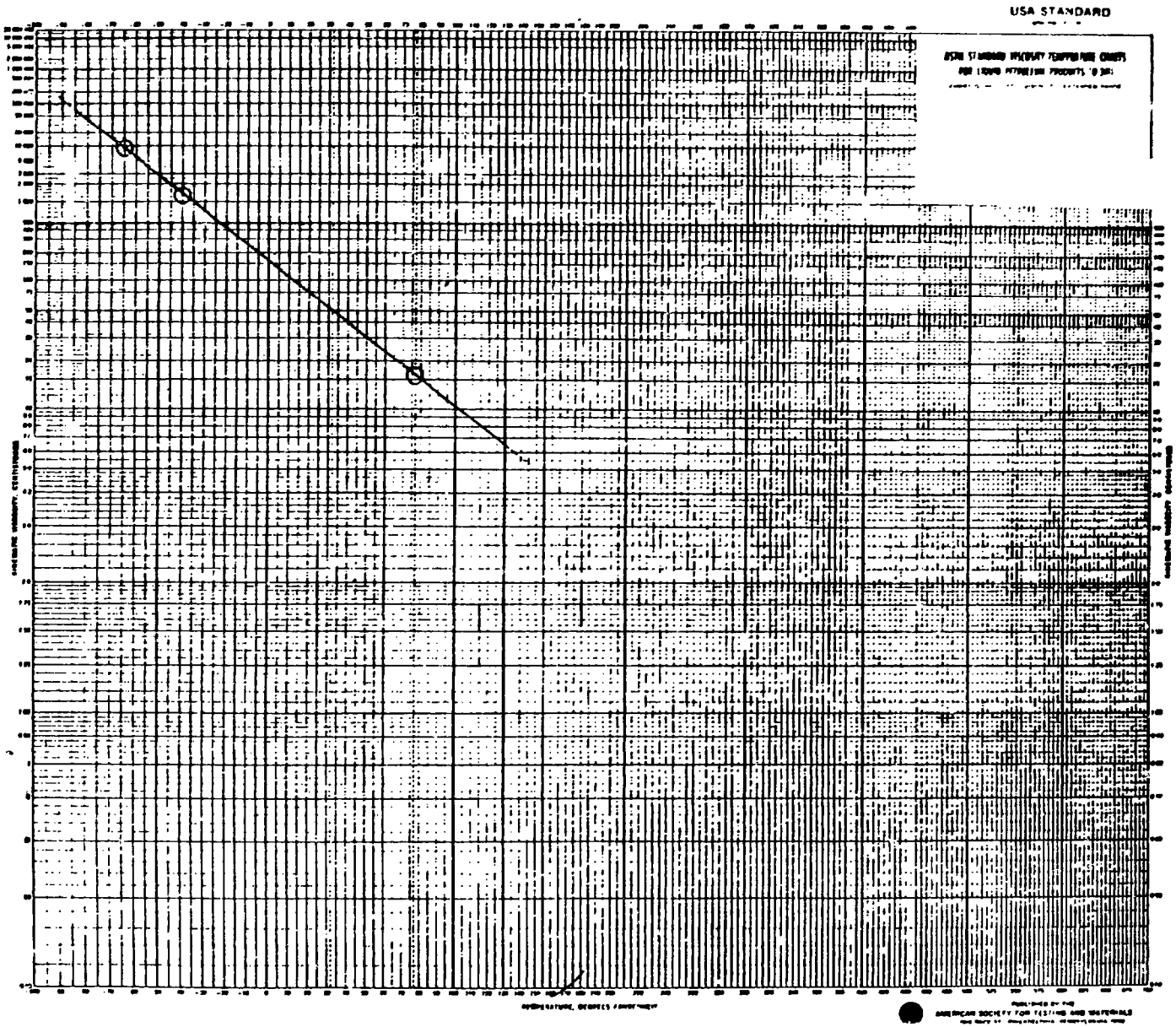

Figure 228. Viscosity/temperature plot for sample #1, 50% Exo-Exo, 50% Endo-Endo.

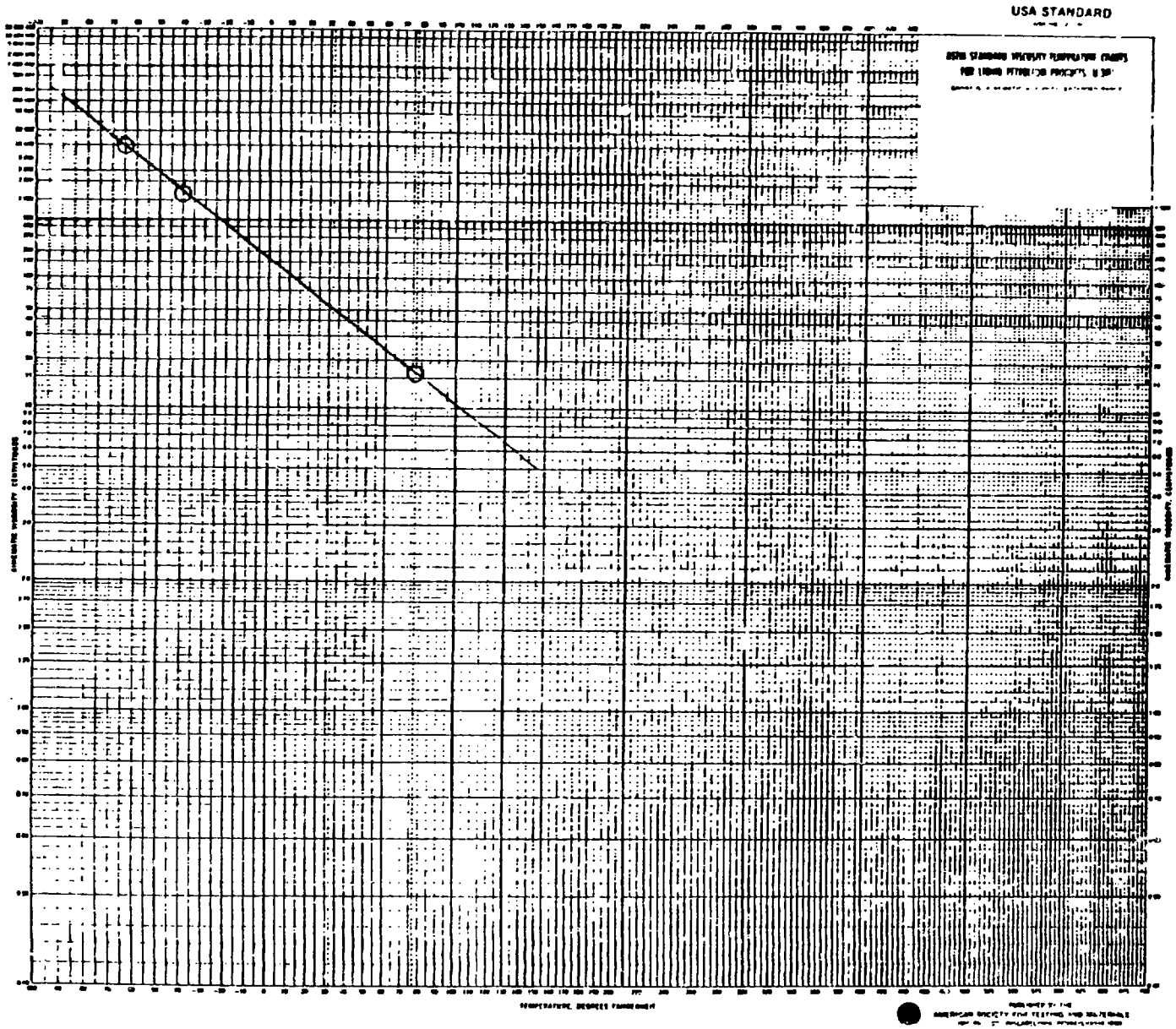

Figure 229. Viscosity/temperature plot for sample #2, 50% Exo-Exo, 50% Endo-Endo.

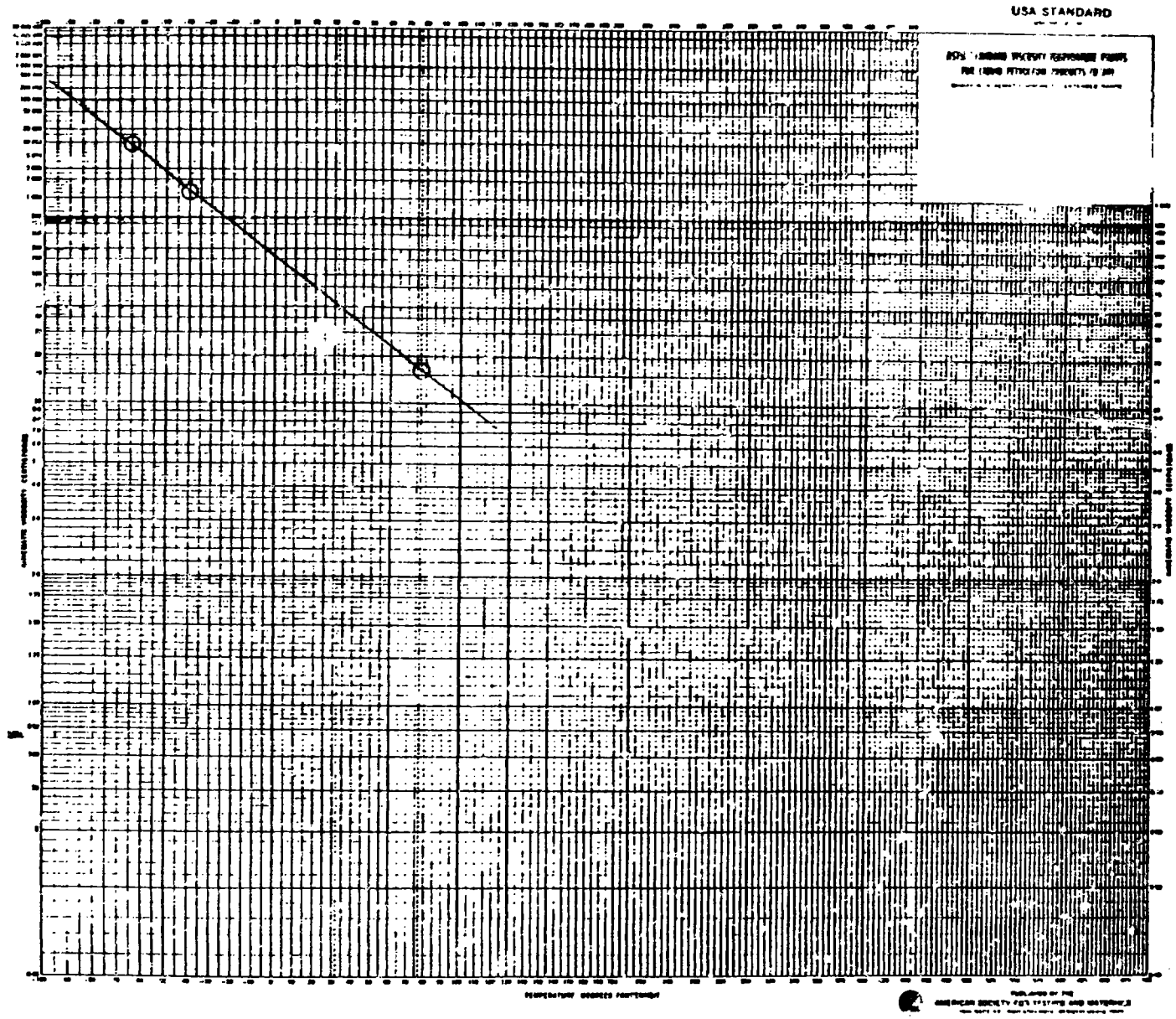

Figure 230. Viscosity/temperature plot for sample #3, 50% Exo-Ex0, 50% Endo-Endo.

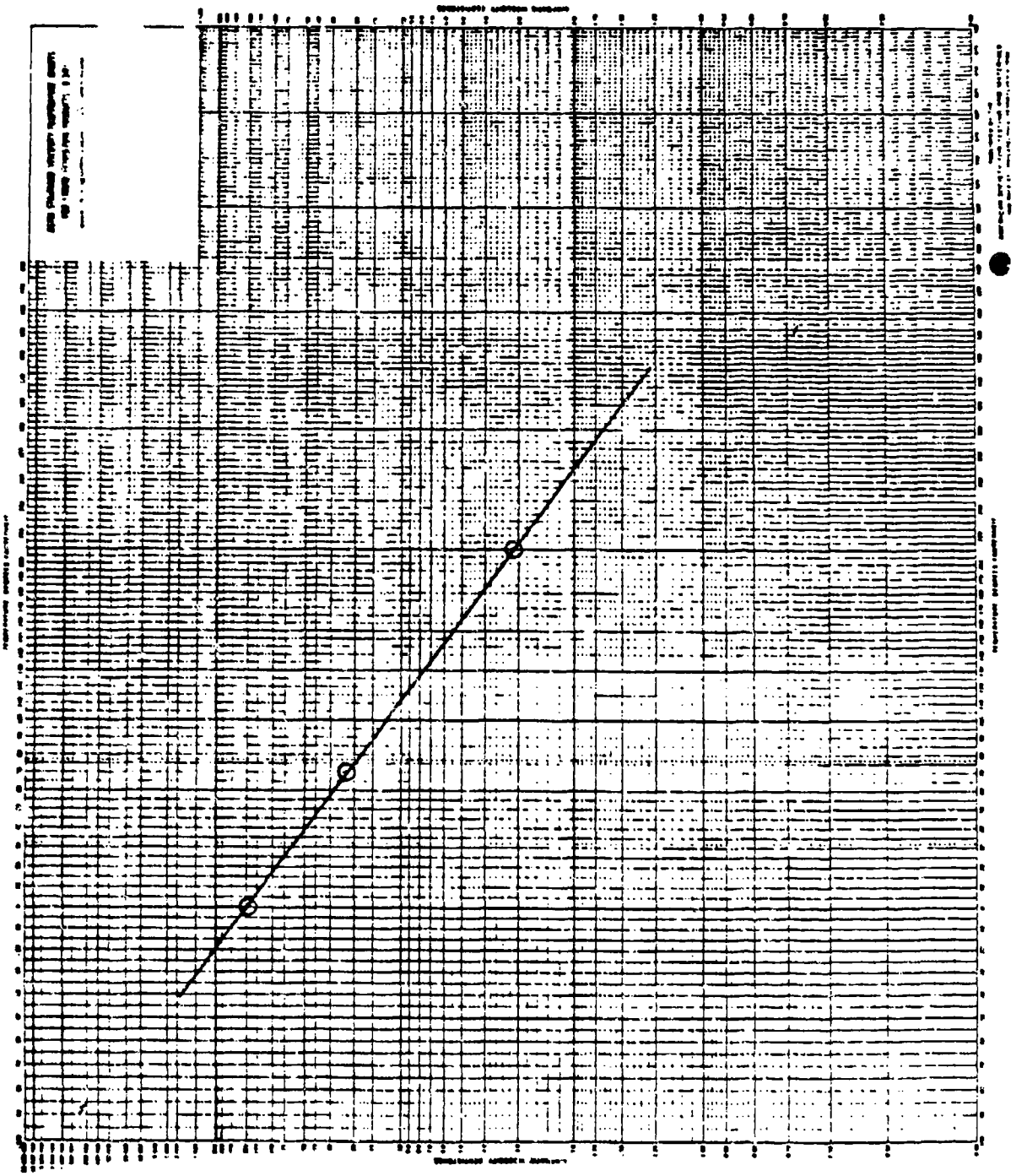

Figure 231. Viscosity/temperature plot for RJ-5F.

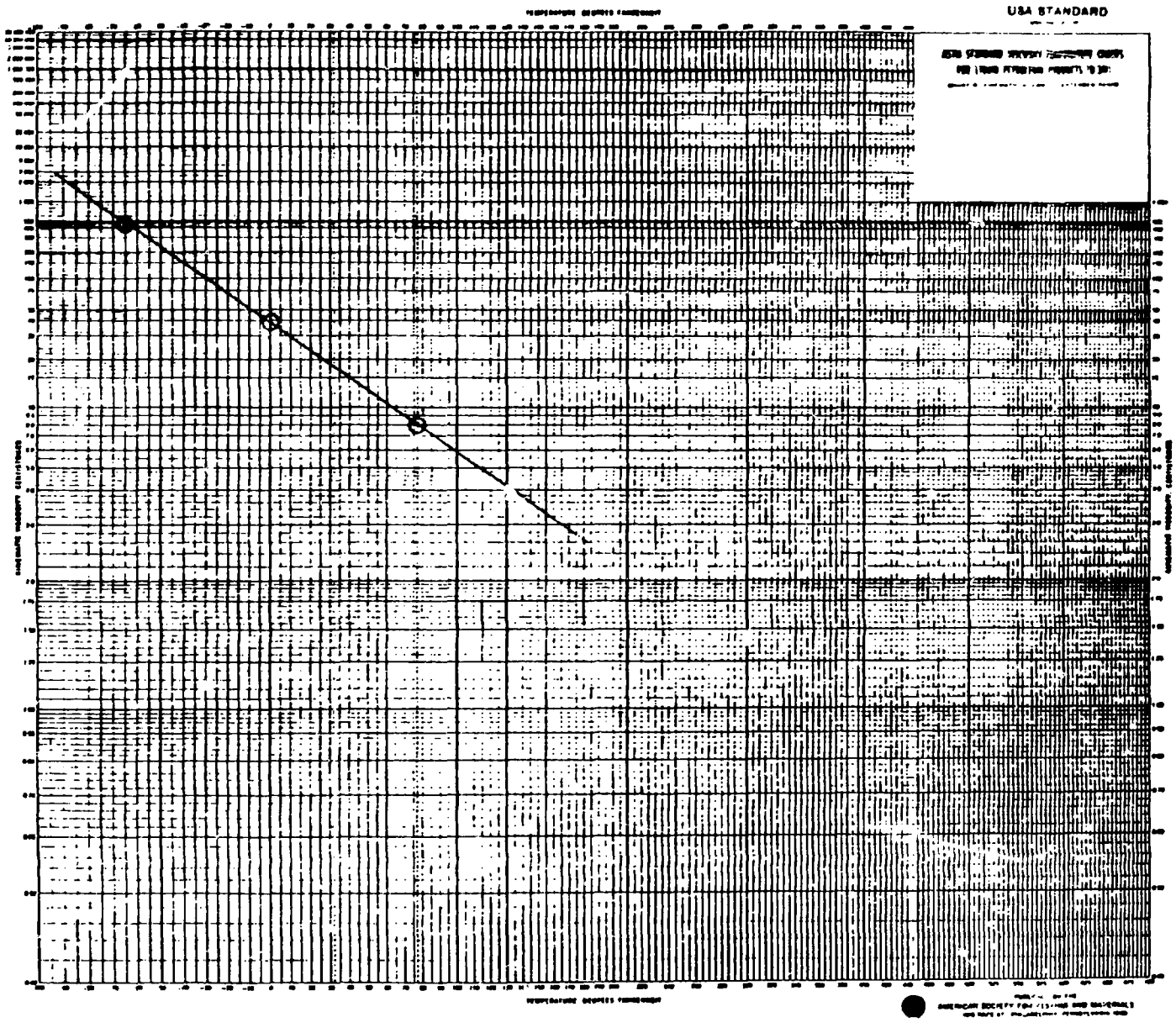

Figure 232. Viscosity/temperature plot for RJ-6.

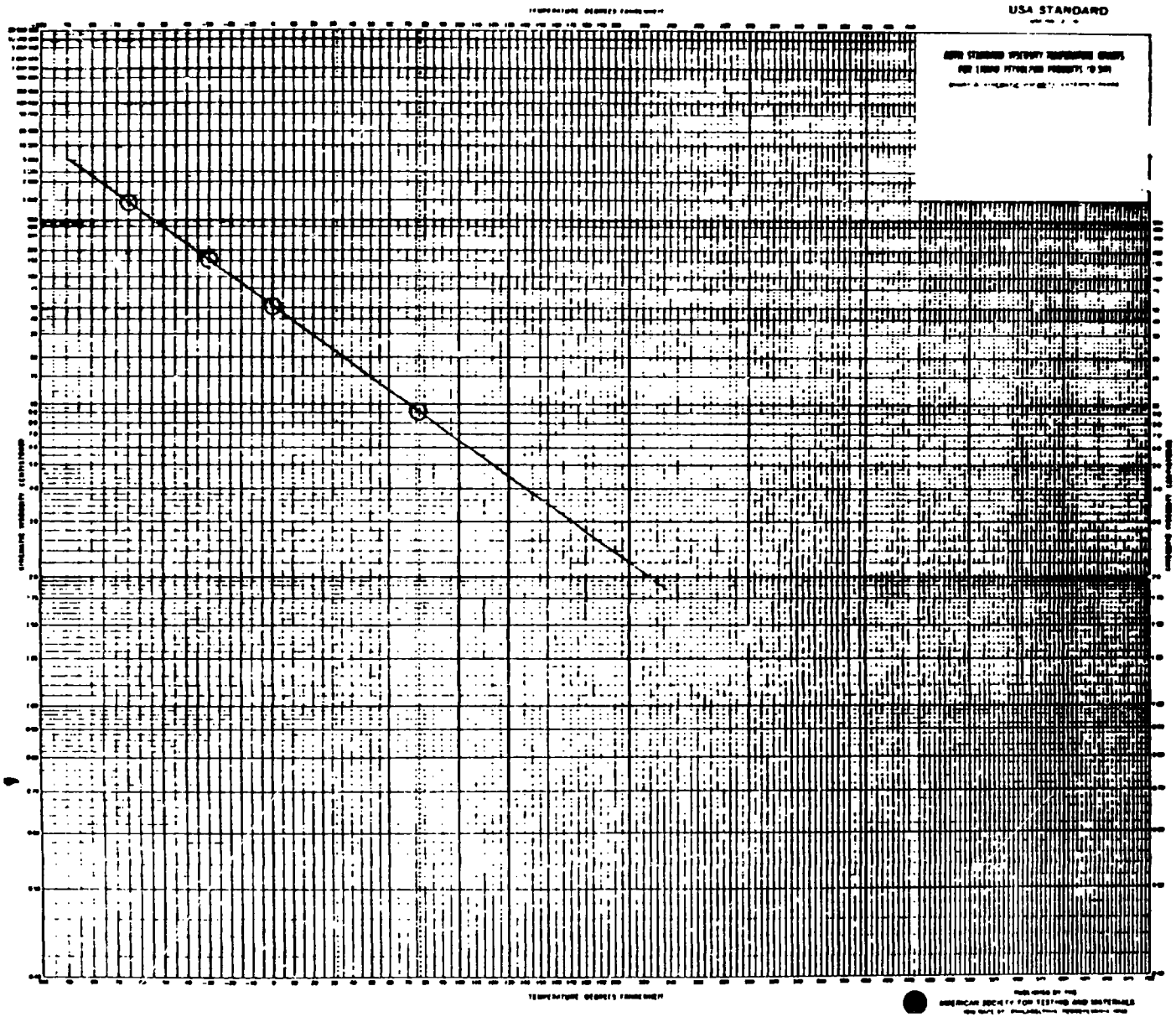

Figure 233. Viscosity/temperature plot for JP-9 (contaminated and filtered).

TABLE 189. HEAT OF COMBUSTION OF HIGH DENSITY FUELS

Sample identification	Gross values, Btu/lb Duplicates	Average	Net average, Btu/lb
RJ-5 Fuel Blends			
50/50 Exo/Endo #1	18,751; 18,745	18,748	17,845
50/50 Exo/Endo #2	18,748; 18,755	18,752	17,849
50/50 Exo/Endo #3	18,764; 18,748	18,756	17,853
RJ-5P	18,686; 18,679	18,683	17,780
RJ-6 Fuel Blends			
Sample 1219	18,913; 18,954	18,934	17,923
Sample 1220	18,886; 18,899	18,893	17,882

TABLE 190. VAPOR PRESSURE OF HIGH DENSITY FUELS

Sample identification	Temperature, °F	Pressure, torr
RJ-6 Fuel Blends		
Sample 1219	300	147.0
Sample 1220	300	138.0
JP-9 Fuels Blends		
#1 (10% MCH[a], 70% JP-10, 20% RJ-5)	70	12.0
#2 (15% MC 55% JP-10, 30% RJ-5)	70	16.5

[a]Methylcyclohexane.

TABLE 191. SURFACE TENSION OF HIGH DENSITY FUEL

Sample	Surface tension dynes/cm -65°F	0°F	70°F
RJ-6 AR78024	39.04	36.15	34.07

TABLE 192. FLASH POINT OF HIGH DENSITY FUELS

Sample description	Temperature °F	Temperature °C
RJ-5F	216	102.5
JP-9 Fuel Blends		
#1 (10% MCH,[a] 70% JP-10, 20% RJ-5)	86	29.8
#2 (15% MCH, 55% JP-10, 30% RJ-5)	66	18.8

[a]Methylcyclohexane.

TABLE 193. AUTOIGNITION TEMPERATURE OF HIGH DENSITY FUELS

Fuel	Components	Autoignition temperature °C±2.5	Autoignition temperature °F±4.5
JP-9	69.97% JP-10 20.02% RJ-5G 10.00% MCH[a]	250.1	482
JP-10	Exo-THD	245.7	474

[a]Methylcyclohexane.

TABLE 194. GAS CHROMATOGRAPHIC ANALYSIS OF TEST FUEL BLENDS

Sample	Retention Time, minutes	Area Percents of Components[a] Blend 1	Blend 2	Blend 3
Three RJ-5 fuel blends made up of 50% Exo-Exo plus 50% Endo-Endo	4.14	0.56	0.31	0.45
	6.07	0.50	0.37	0.32
	7.55	0.60	-	-
	8.54	1.17	1.14	0.93
	11.50	0.31	-	-
	12.95	0.37	0.62	0.32
	16.06	2.22	3.21	3.88
	16.25	0.71	0.80	0.97
	16.51	43.61	43.33	43.59
	16.96	0.93	0.87	0.91
	17.31	47.54	46.95	46.98
	17.65	0.50	1.31	0.62
	18.75	0.66	0.74	0.42
	19.52	0.56	0.37	0.57
RJ-5, 22 December 1978	15.51	1.260		
	15.68	8.617		
	16.00	19.208		
	16.43	0.676		
	16.91	70.235		
RJ-5F	17.24	3.548		
	17.48	25.265		
	17.51	8.234		
	17.71	13.199		
	17.77	0.932		
	17.87	1.180		
	18.15	2.567		
	18.57	44.513		
	18.90	0.561		
		Blend 1219	Blend 1220	
Two RJ-6 Fuel blends	13.45	45.111	40.577	
	14.14	1.171	1.210	
	Total JP-10	46.282	41.787	
	21.79	0.858	1.113	
	21.91	4.291	4.452	
	22.20	8.793	9.459	
	22.65	0.303	0.331	
	23.08	39.273	42.618	
	24.20	0.096	0.110	
	24.85	0.113	0.126	
	Total RJ-5	53.727	58.209	

(continued)

TABLE 194 (continued)

Sample	Retention Time, minutes	Area Percents of Components[a] Batch 3,8383-12	Batch 4,8353-13
Two RJ-6 fuel blends	13.12	37.90	38.27
	13.74	0.93	0.97
	Total JP-10	38.83	39.24
	21.24	1.57	1.59
	21.39	5.58	5.68
	21.69	9.06	9.06
	22.17	0.41	0.00
	22.59	44.53	44.44
	Total RJ-5	61.15	60.77
Contaminated JP-9 after filtering	4.24 MCH[b]	6.72	
	13.92	1.71	
	14.30	0.64	
	14.16	0.28	
	14.58	0.70	
	14.73	0.47	
	14.88	1.67	
	14.96	0.22	
	15.06	4.77	
	15.23	4.14	
	15.39	0.63	
	16.21	6.47	
	Total RJ-4	21.70	
	20.01	0.49	
	20.15	7.60	
	20.45	12.70	
	20.94	0.79	
	21.33	50.00	
	Total RJ-5	71.58	
Two JP-10 Fuels		Not distilled	Distilled
Sample distilled for DOE	11.46	98.300	99.233
	11.76	0.206	0.151
	12.02	1.118	0.615
	12.18	0.316	
Sample distilled for a standard	8.36		99.069
	8.59		0.133
	8.78		0.659
	8.90		0.139

[a]Chromatographic peak area percents are essentially the same as weight percents, since all isomers should have the same response with a flame ionization detector.

[b]Methylcyclohexane.

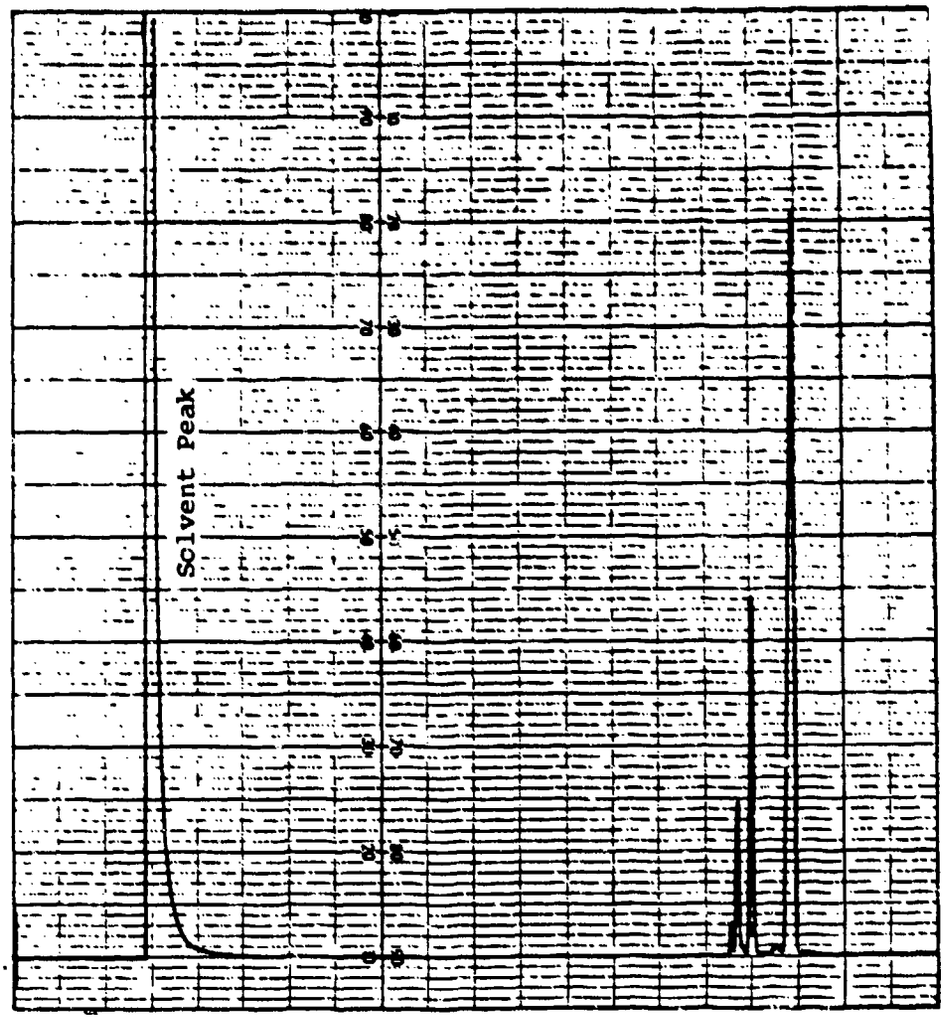

Figure 234. Gas chromatogram of RJ-5 (12-22-78).

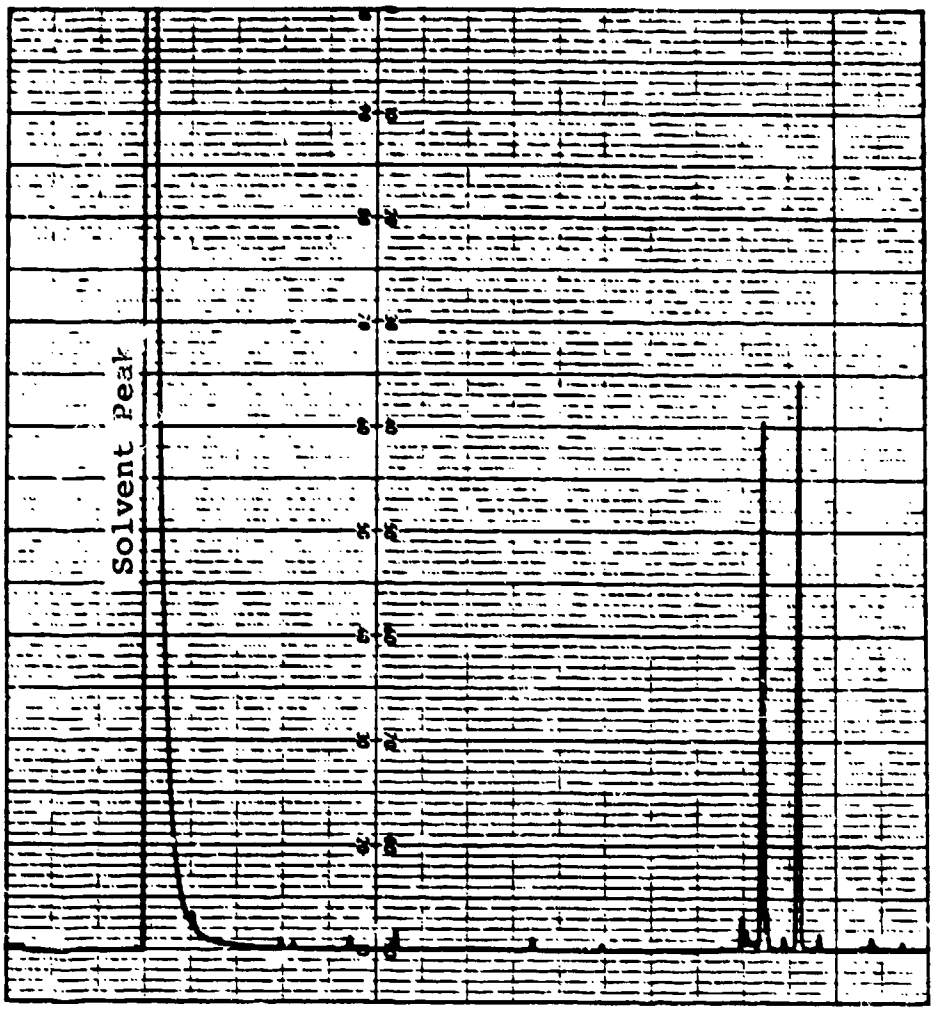

Figure 235. Gas chromatogram for 50% Exo-Exo, 50% Endo-Endo #1, RJ-5.

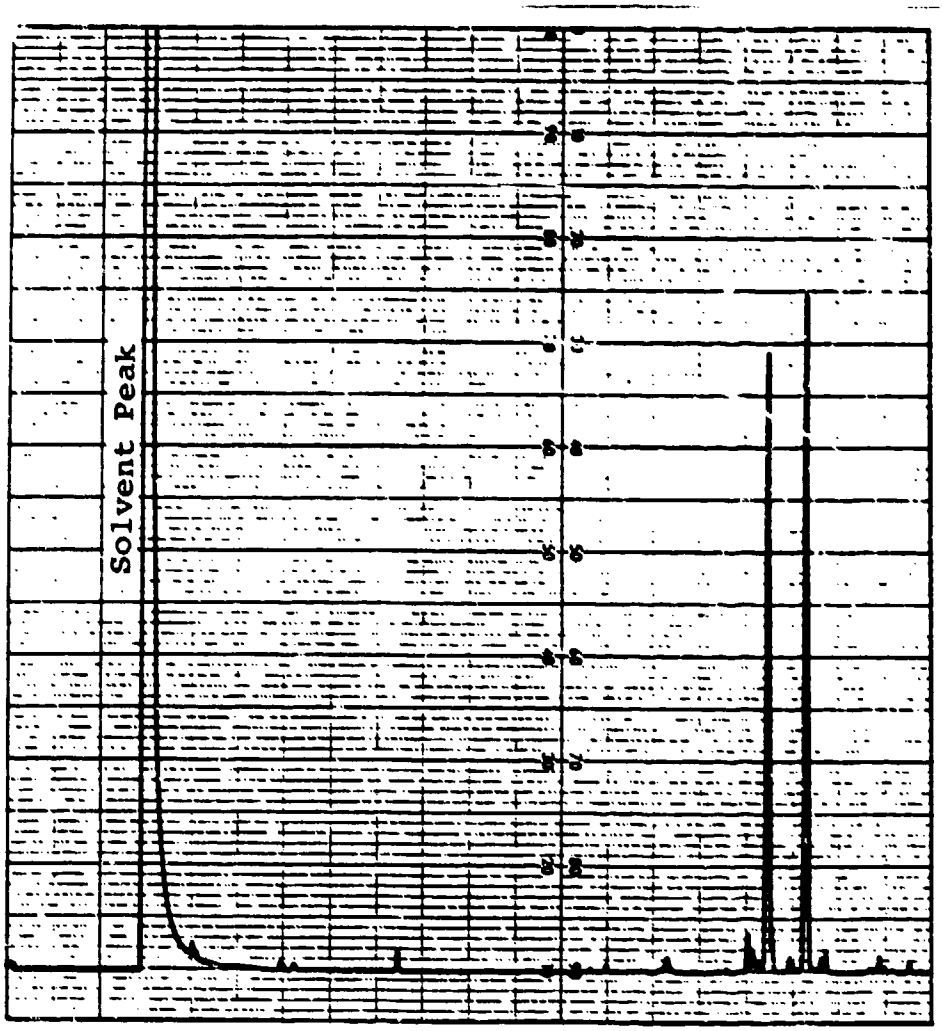

Figure 236. Gas chromatogram for 50% Exo-Exo, 50% Endo-Endo #2, RJ-5.

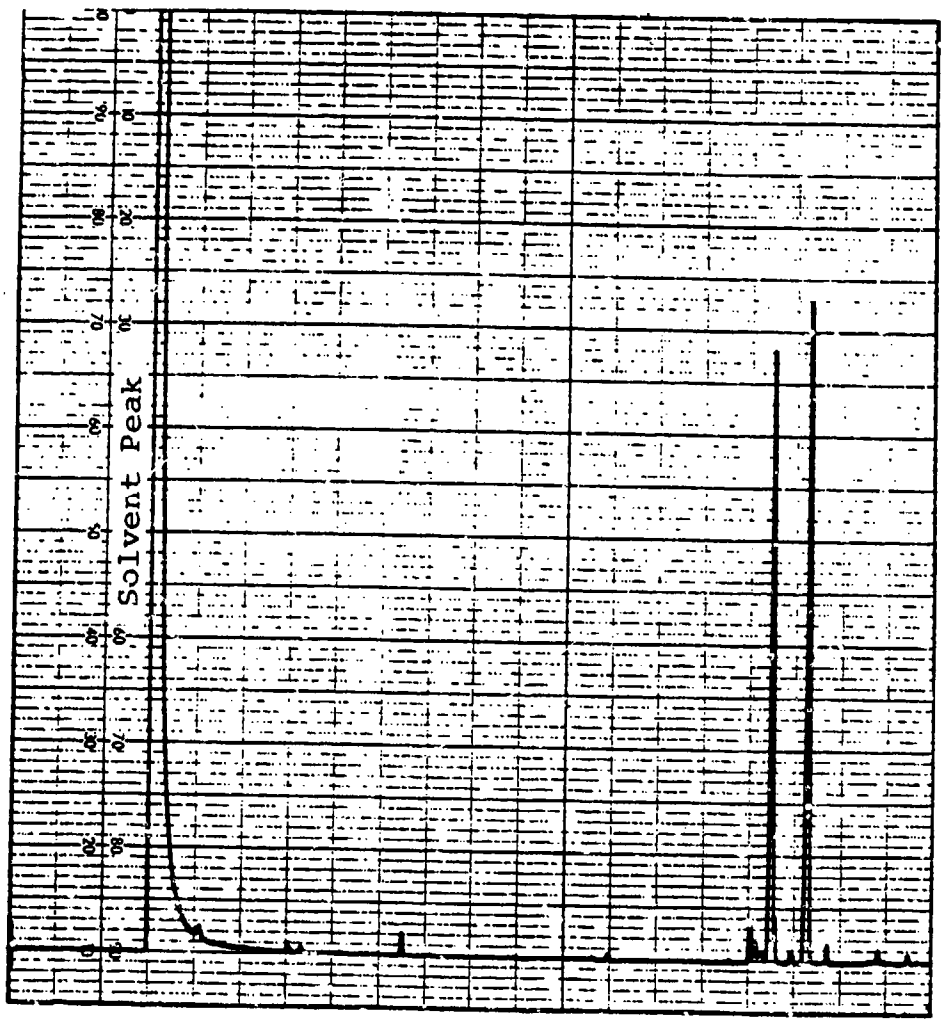

Figure 237. Gas chromatcgram for 50% Exo-Exo, 50% Endo-Endo #3, RJ-5.

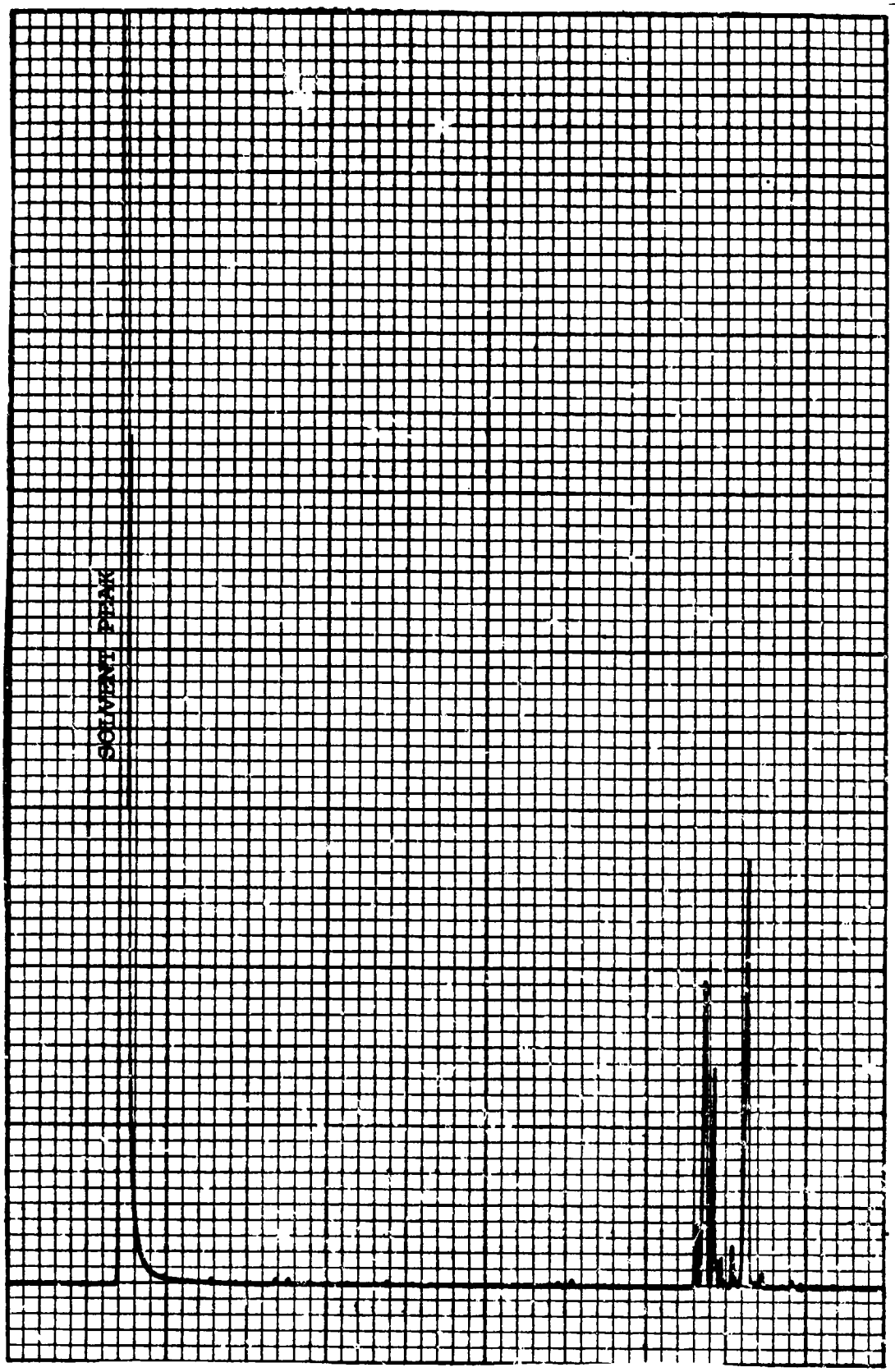

Figure 238. Gas chromatogram of RJ-5F.

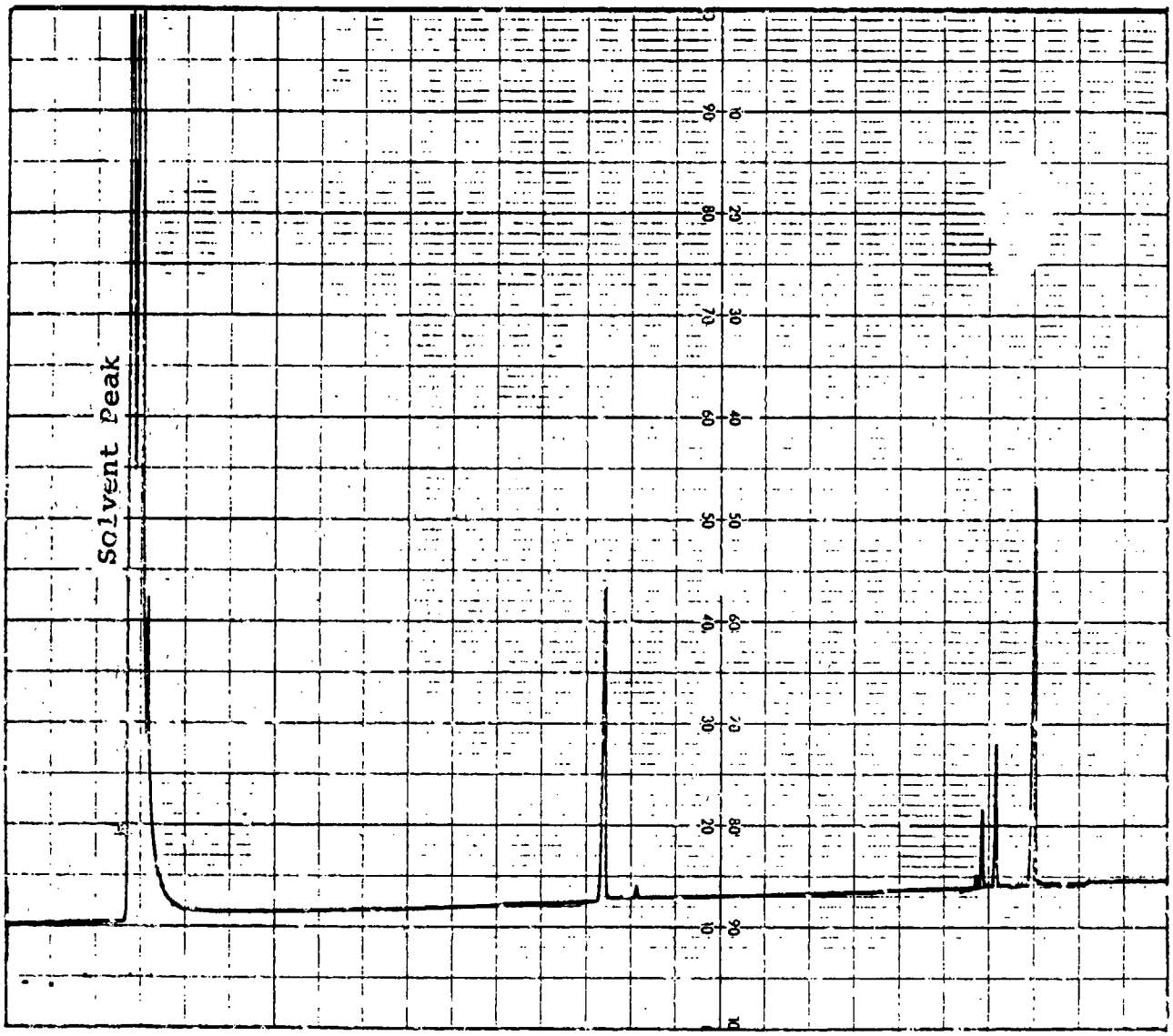

Figure 239. Gas chromatogram of RJ-6 Blend #1219.

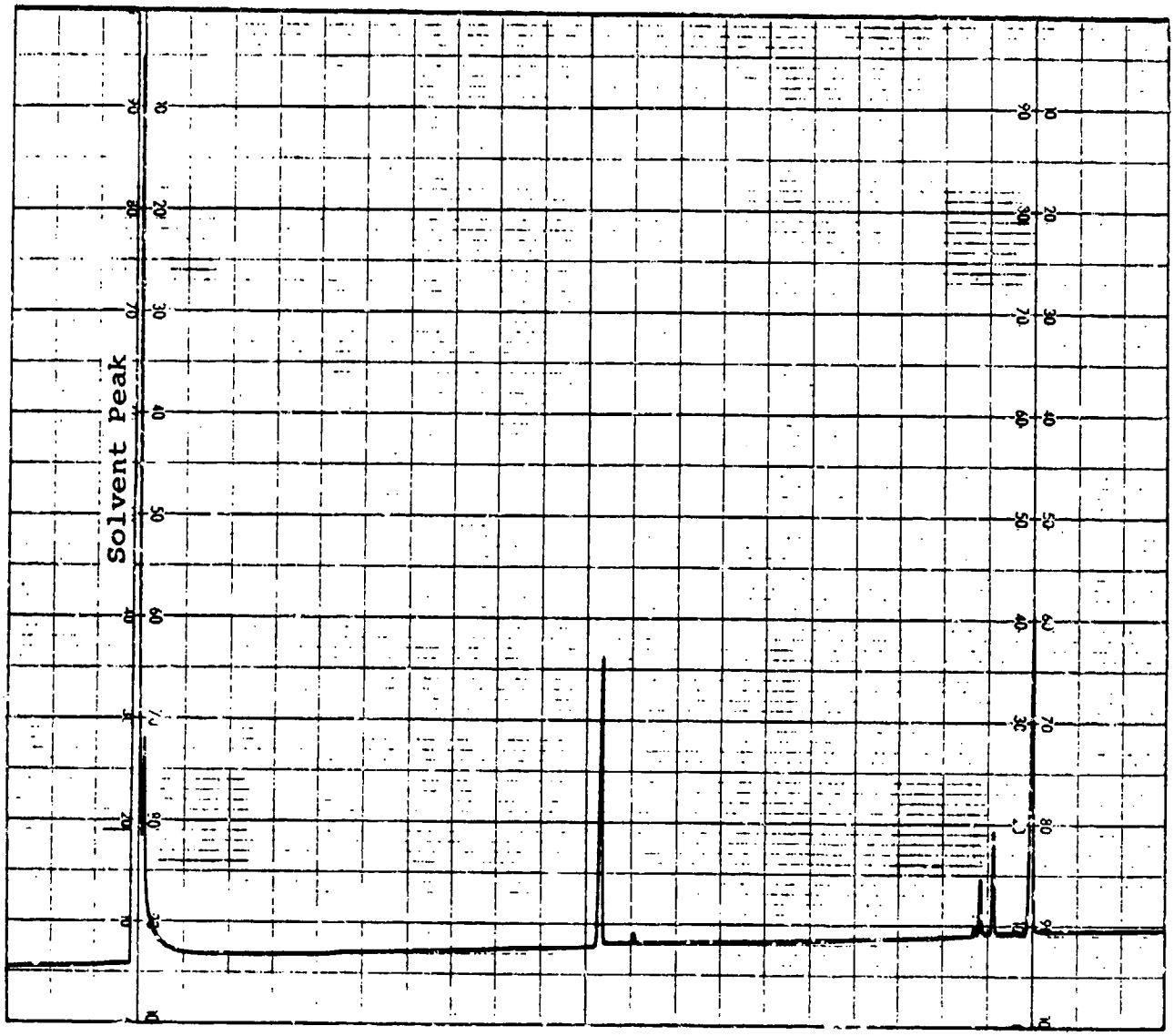

Figure 240. Gas chromatogram of RJ-6 Blend #1220.

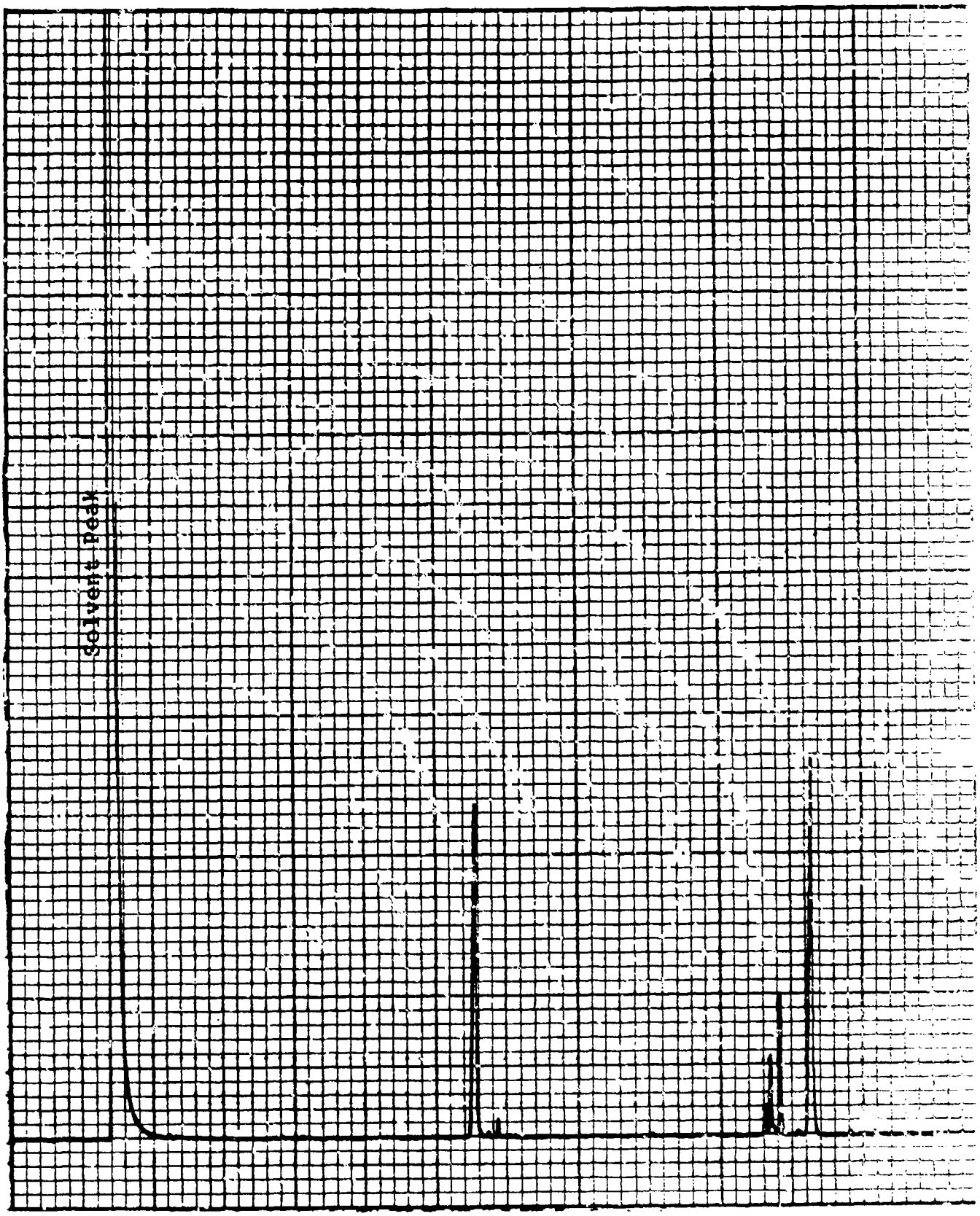

Figure 241. Gas chromatogram of RJ-6 fuel, Batch 3, 8353-12.

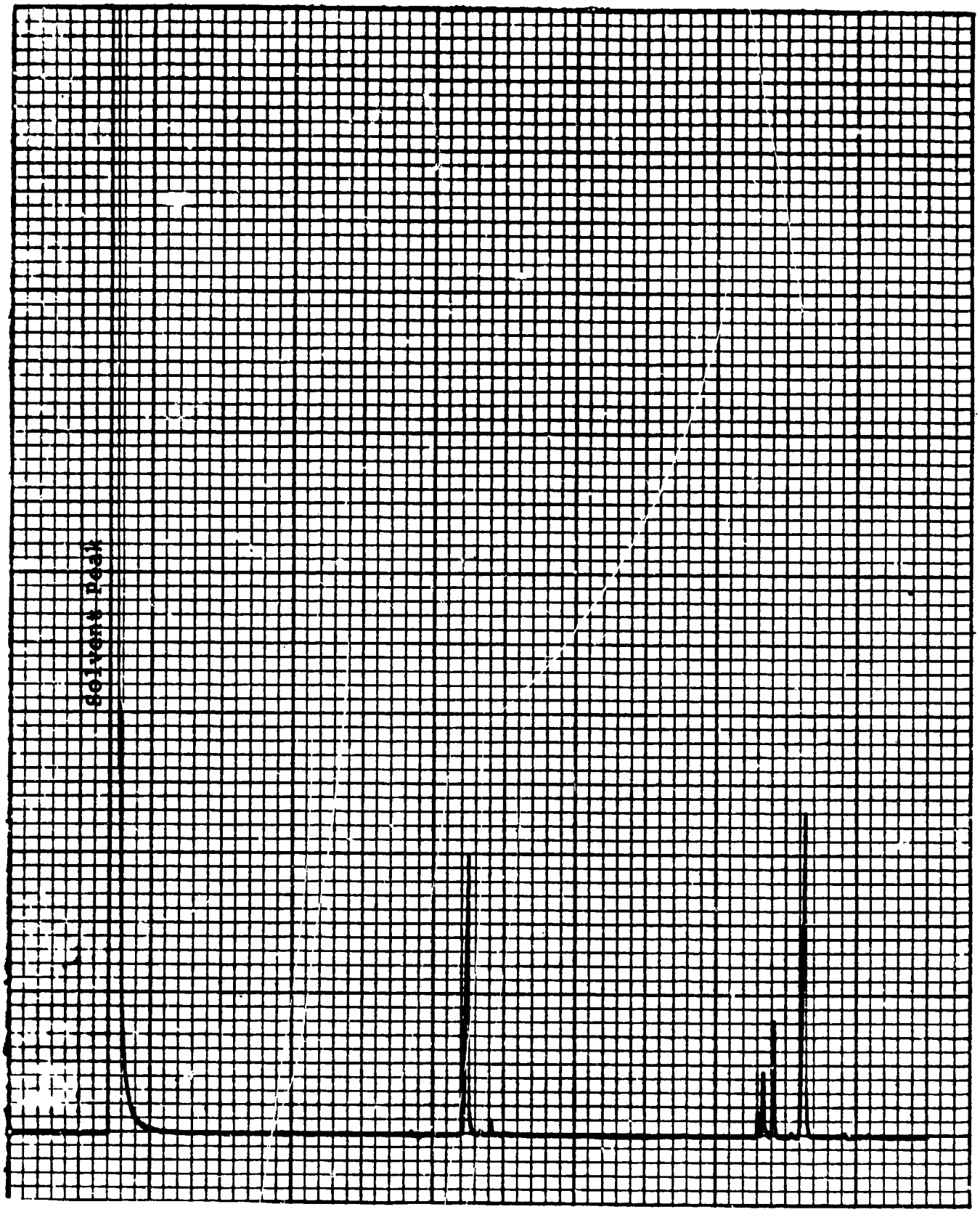

Figure 242. Gas chromatogram of RJ-6 fuel, Batch 4, 8353-13.

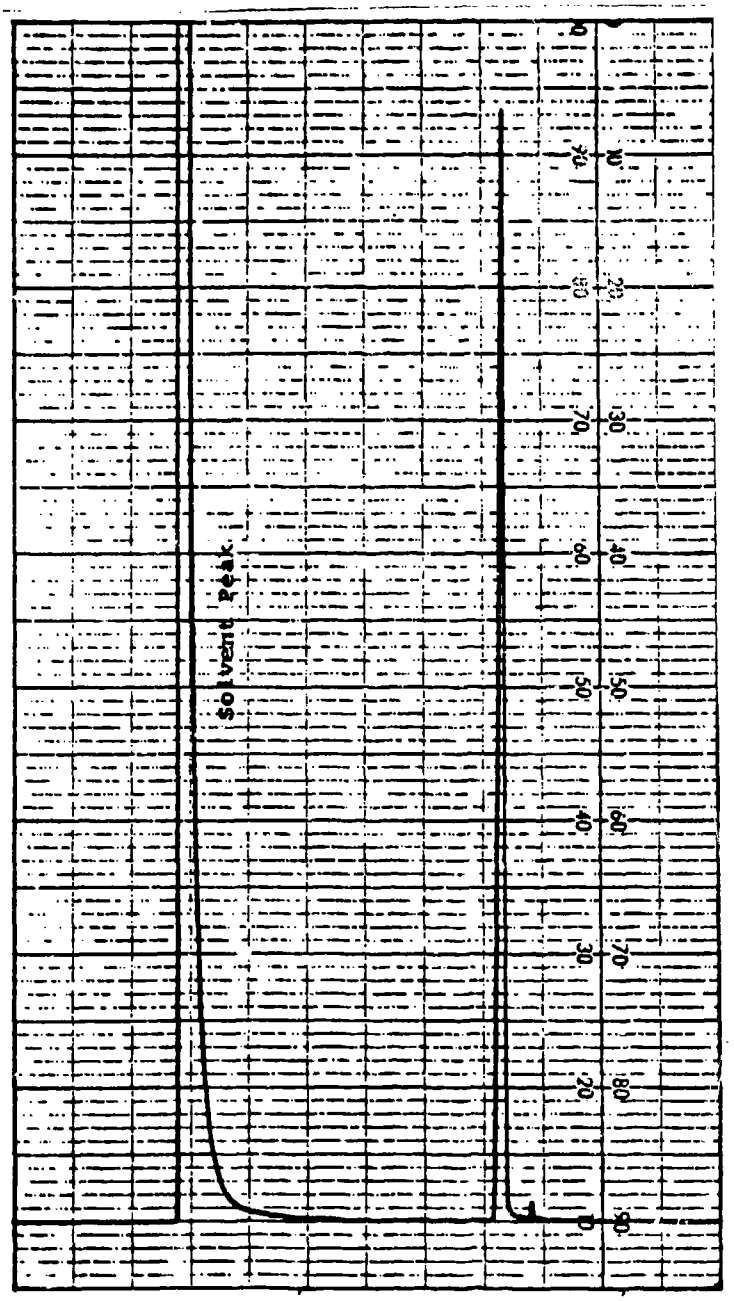

Figure 243. Gas chromatogram of JP-10 after distillation for standard preparation.

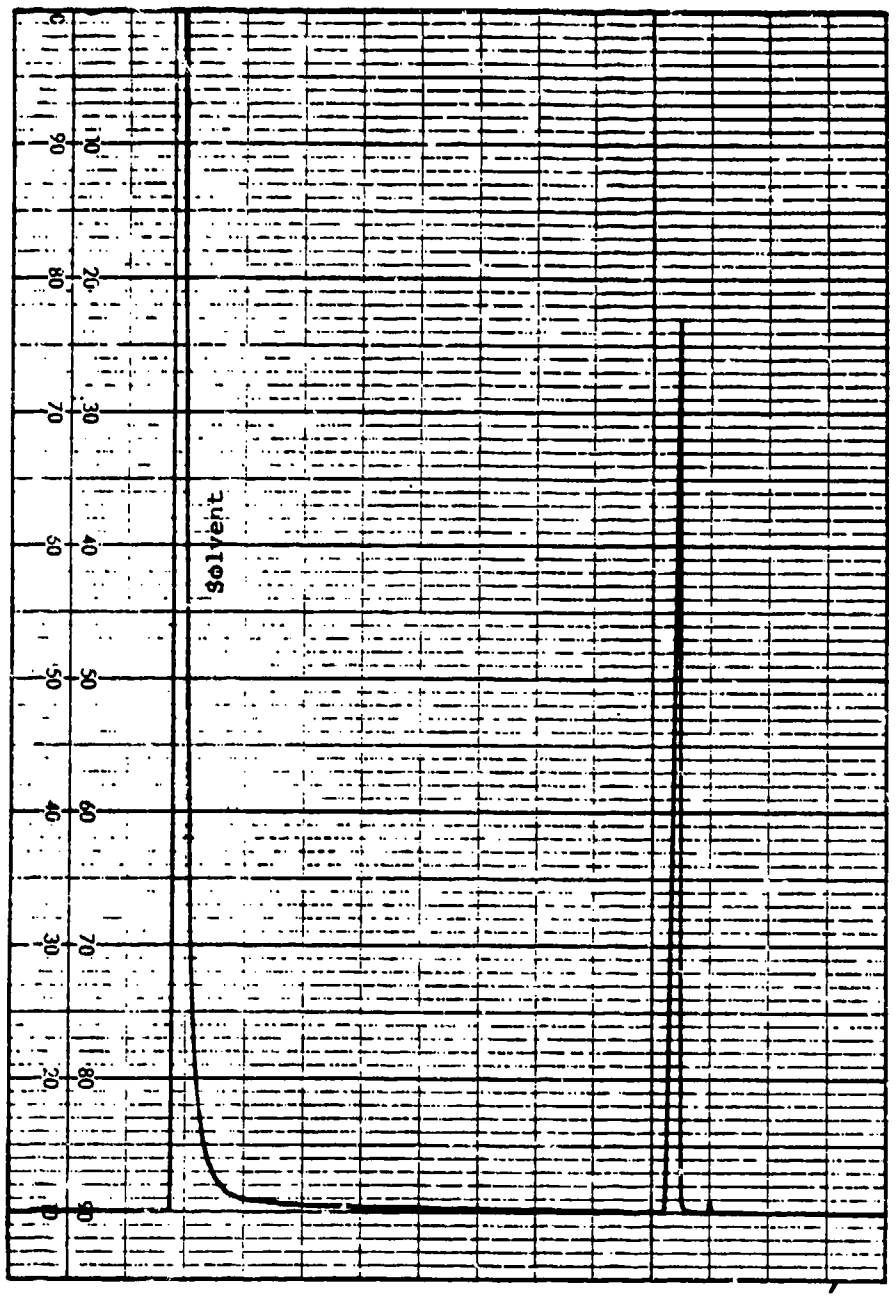

Figure 244. Gas chromatogram of JP-10 after distillation for DOE.

3. PHYSICAL PROPERTIES OF JP-10

Various physical properties of JP-10 as a function of temperature were required by ALCM design engineers. Density, surface tension, thermal conductivity, and air and water solubility were determined at temperatures between -66°F and 160°F using the analytical procedures described in the Appendix. The results are shown in Table 195.

TABLE 195. VARIOUS PROPERTIES OF JP-10

Temperature °F	Density g/cc	Surface tension dyne, cm^{-1}	Thermal conductivity Btu/ft/hr/°F	Air solubility Ostwald solubility coefficients[a]	Water solubility ppm, vol
-65	0.9926	37.850	0.07168	-	-
-60	-	-	-	0.098	-
-40	-	-	0.07055	-	-
-30	0.9772	35.928	-	-	-
14	-	-	0.06796	-	-
32	0.9500	32.926	-	-	26
68	-	-	0.06551	-	-
72	-	30.534	-	0.129	-
74	-	-	-	-	29
77	0.9303	-	-	-	-
110	-	-	-	-	47
140	-	-	-	0.140	-
151	-	-	0.06128	-	-
155	0.8960	-	-	-	-
158	-	26.097	-	-	-

Note: Dash indicates no measurement made.

[a]ml of air/ml of fuel, both volumes measured at the temperature of saturation.

4. PHYSICAL PROPERTIES OF RJ-6

Various physical properties were determined for a sample of RJ-6 fuel in support of ASALM programs. All test methodology is described in the Appendix. Surface tension, density, vapor pressure, kinematic viscosity, specific heat, thermal conductivity, dielectric constant, and water solubility were determined at -20, 32, 70, and 100°F; and these data are shown in Table 196. Air

solubility was determined at -60, -20, 70, and 140°F by mass spectrometry, and these results are shown in Table 197. Heat of combustion, flash point, and autoignition temperature data are shown in Table 198. The results of a composition analysis by gas chromatography are shown in Table 199.

TABLE 196. PHYSICAL PROPERTIES OF RJ-6 AT FOUR TEMPERATURES

	-20°F	32°F	70°F	100°F
Surface tension, dynes/cm	38.59	35.50	33.27	31.74
Density, g/cc	1.0499	1.0269	1.0106	0.9973
Vapor pressure, mm Hg	-	5.0	9.0	13.0
Kinematic viscosity, centistokes	61.30	16.110	8.160	5.315
Specific heat, cal/g/°K	0.285	0.344	0.398	0.443
Thermal conductivity, Btu/ft/hr/°F	0.0662	0.0649	0.0638	0.0630
Dielectric constant	2.395	2.354	2.319	2.297
Water solubility, ppm (vol)	-	31	52	65

TABLE 197. AIR SOLUBILITY IN RJ-6 FUEL SPECIMEN

Temperature, T °F	(°C)	Ostwald solubility coefficient[a]
-60	(-51)	0.051
-20	(-29)	0.079
70	(21)	0.089
140	(60)	0.096

[a] ml of air/ml of fuel, both at temperature, T.

TABLE 198. COMBUSTION RELATED PROPERTIES OF RJ-6

Heat of combustion, ASTM D 240-64	
Gross, Btu/lb	18,892
Net, Btu/lb	17,903
Flash point, ASTM D 93-71	62°C (144°F)
Autoignition temperature ASTM D 2155-66	241.2°C (466.2°F)

TABLE 199. GAS CHROMATOGRAPHIC ANALYSIS OF RJ-6

Retention time, min	Weight, %	
14.15	42.1	(Total JP-10)
22.07	3.4	RJ-5 Isomers (Total = 57.9%)
22.23	17.2	
22.50	12.5	
22.98	3.3	
23.31	21.5	
	100.0	

5. GC/MS ANALYSES OF JP-9/AIR SAMPLES FROM A FLAMMABILITY TEST CELL

Two vapor samples contained in glass gas bottles and taken from a test cell used to determine flammability of fuel vapors were analyzed for hydrocarbon concentration. The hydrocarbons suspected to be present were the three components of JP-9 fuel. The vapor samples were analyzed by GC/MS against a standard of JP-9 prepared in methanol. The results obtained in micrograms were converted to percent concentrations using the ideal gas law equation.

Analytical Procedure

Prior to analysis the gas bottles were warmed to ensure that all vapor components were in the gas phase. The two vapor samples were then analyzed on an HP-5982 GC/MS using the following GC conditions.

Column:	6 ft x 1/8 in. glass packed with Tenax
Column Temperature:	2 minute at -30°C, then program to 280°C at 16°C/minute
Carrier Flow:	helium at 30 ml/minute
Sample Size:	10 ml of vapor at 25°C and 760 mm

Analytical Results

The only hydrocarbons detected in the gas bottles were the components of JP-9 fuel. The weights of the components detected in ten-milliliter volumes of each gas sample are shown in Table 200.

TABLE 200. GC/MS ANALYSIS OF JP-9 COMPONENTS IN TWO GAS SAMPLES

JP-9 component	Concentration in 10-ml gas samples: Bottle 1, µg	Bottle 2, µg
Methyl cyclohexane (MCH)	300	12
Tetrahydrodicyclo pentadiene (JP-10)	100	2
Hydrogenated norbornadiene dimers (RJ-5)	50	20

The total weight of JP-9 fuel detected in the 10-ml gas specimen could be converted to volume percent using the ideal gas law:

$$PV = \frac{gRT}{m}$$

where P = pressure in atmospheres
V = volume in liters
g = weight in grams
m = molecular weight
R = 0.08202 l-atm deg $^{-1}$ mole^{-1}
T = temperature in degrees Kelvin = 302°K

The volume occupied by the JP-9 vapors could be determined by solving for V. Using this volume and the original volume of the sample analyzed (10 ml), volume percents of JP-9 vapors in the gas samples were calculated. The average molecular weight of the JP-9 vapors in each gas sample was calculated from the component molecular weights and their percentages of the total fuel. All results are shown in Table 201.

TABLE 201. DETERMINATION OF VOLUME PERCENT JP-9 IN GAS SAMPLES

Gas sample	Wt. of JP-9 in 10-ml sample, µg	Calculation average MW	Volume of JP-9, ml	Volume % JP-9
Bottle 1	450	116	0.096	1.0
Bottle 2	34	115	0.005	0.05

6. GC ANALYSES AND PHYSICAL PROPERTY MEASUREMENTS FOR THREE ASHLAND RJ-5 FUELS

Three RJ-5 fuels were analyzed for selected physical and chemical properties. The fuels, which were labeled 1, 2, and 3, were all from Ashland Lot B-9-78. The specific analyses are described below:

Specific gravity was determined by the dilatometer method in which the volume of a known weight of fuel was measured at 60°F. Results are shown in Table 202.

TABLE 202. SPECIFIC GRAVITY, 60/60°F

Fuel	Values at 60°F
B-9-78-1	1.0836
B-9-78-2	1.0833
B-9-78-3	1.0836

Kinematic viscosity was determined at four temperatures by ASTM Method D 445. The test results are presented in Table 203 and graphs illustrating viscosity as a function of temperature are presented in Figures 245 through 247.

TABLE 203. KINEMATIC VISCOSITY

Fuel	Centistokes -20°F	32°F	70°F	100°F
B-9-78-1	522.6	65.89	24.77	13.66
B-9-78-2	526.1	65.95	24.79	13.66
B-9-78-3	523.2	65.92	24.77	13.66

Gross and net heat of combustion were determined by oxygen bomb calorimetry using ASTM Method D 240 and hydrogen content data from AFWAL/POSF. The test values are shown in Table 204.

TABLE 204. HEAT OF COMBUSTION

Fuel	Gross, Btu/lb Duplicates		Average	Net, Btu/lb Average	% H[a]
B-9-78-1	18,834	18,820	18,827	17,919	9.95
B-9-78-2	18,812	18,846	18,829	17,921	9.95
B-9-78-3	18,815	18,806	18,811	17,903	9.95

[a]Percent hydrogen data from AFWAL/POSF used to calculate net heat of combustion.

Gas chromatographic analyses were conducted to determine purity and isomer ratios for the fuels. A Perkin-Elmer Model 3920B gas chromatograph fitted with a 50-meter glass capillary column coated with SF-96 stationary phase was employed for the analyses. The analytical data shown in Table 205 were obtained from a Hewlett-Packard 3350 laboratory data system. The gas chromatograms for the three fuels are reproduced in Figures 248 through 250.

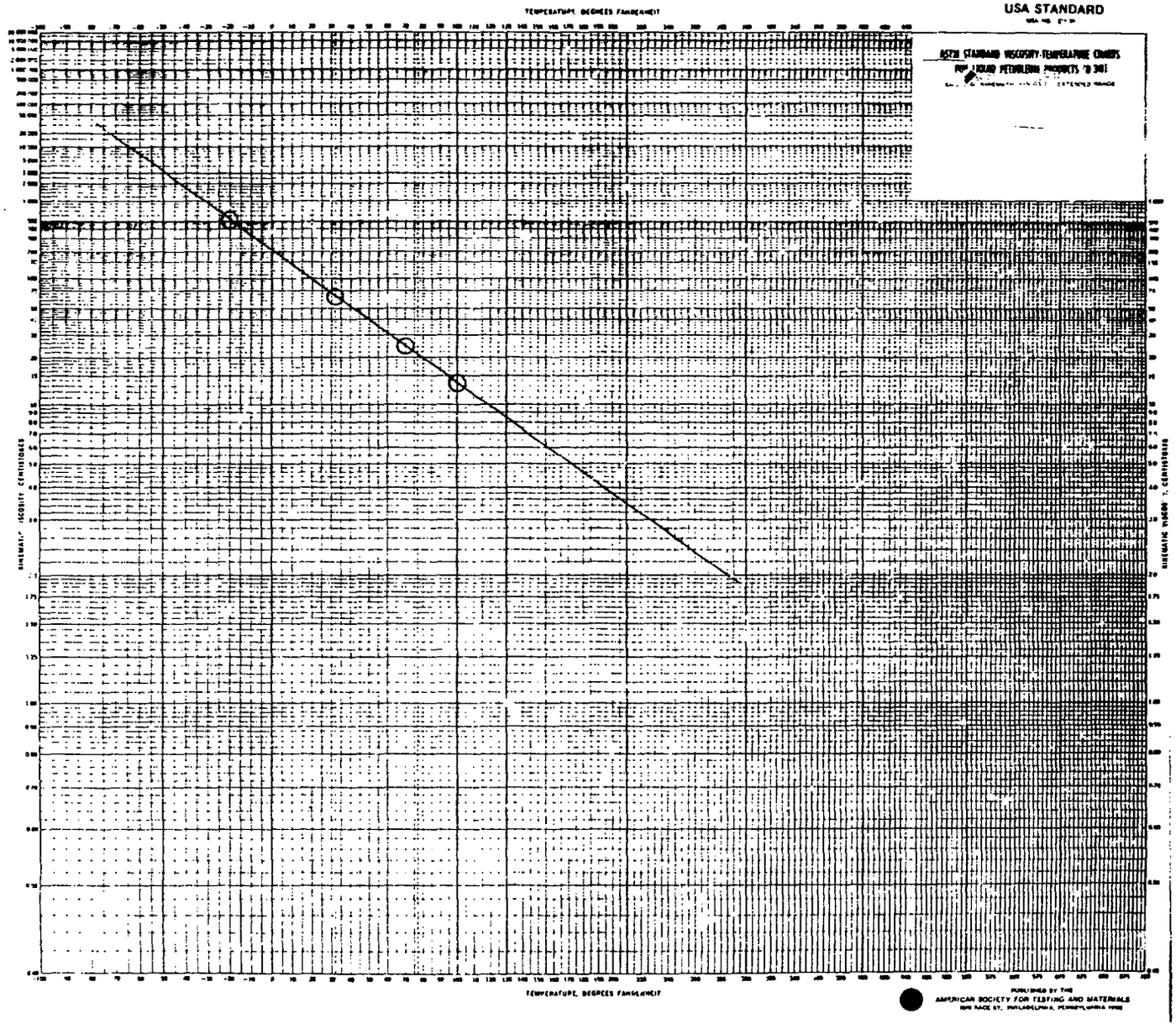

Figure 245. Viscosity/temperature plot for JP-5 fuel B-9-78-1.

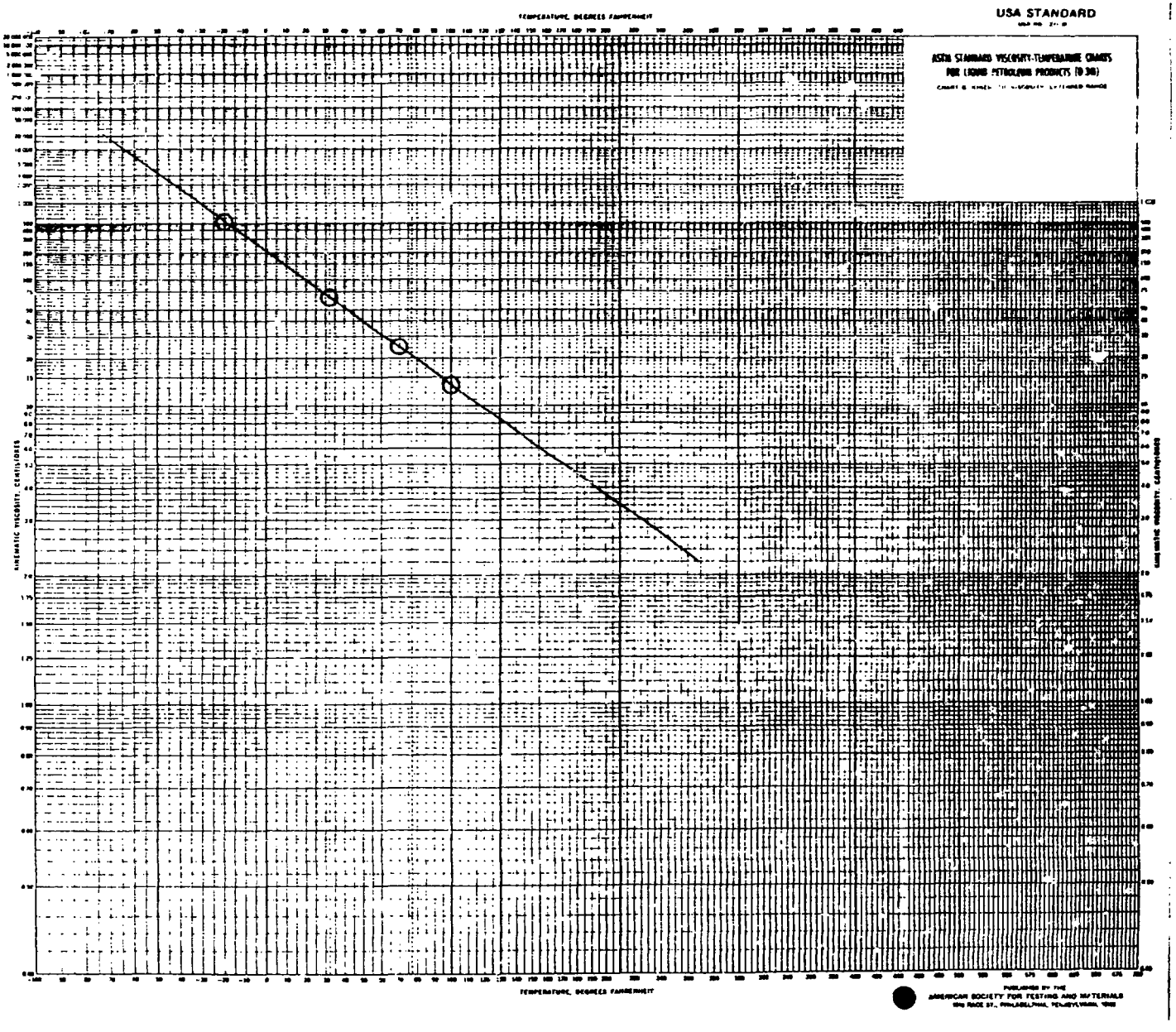

Figure 246. Viscosity/temperature plot for RJ-5 fuel B-9-78-2.

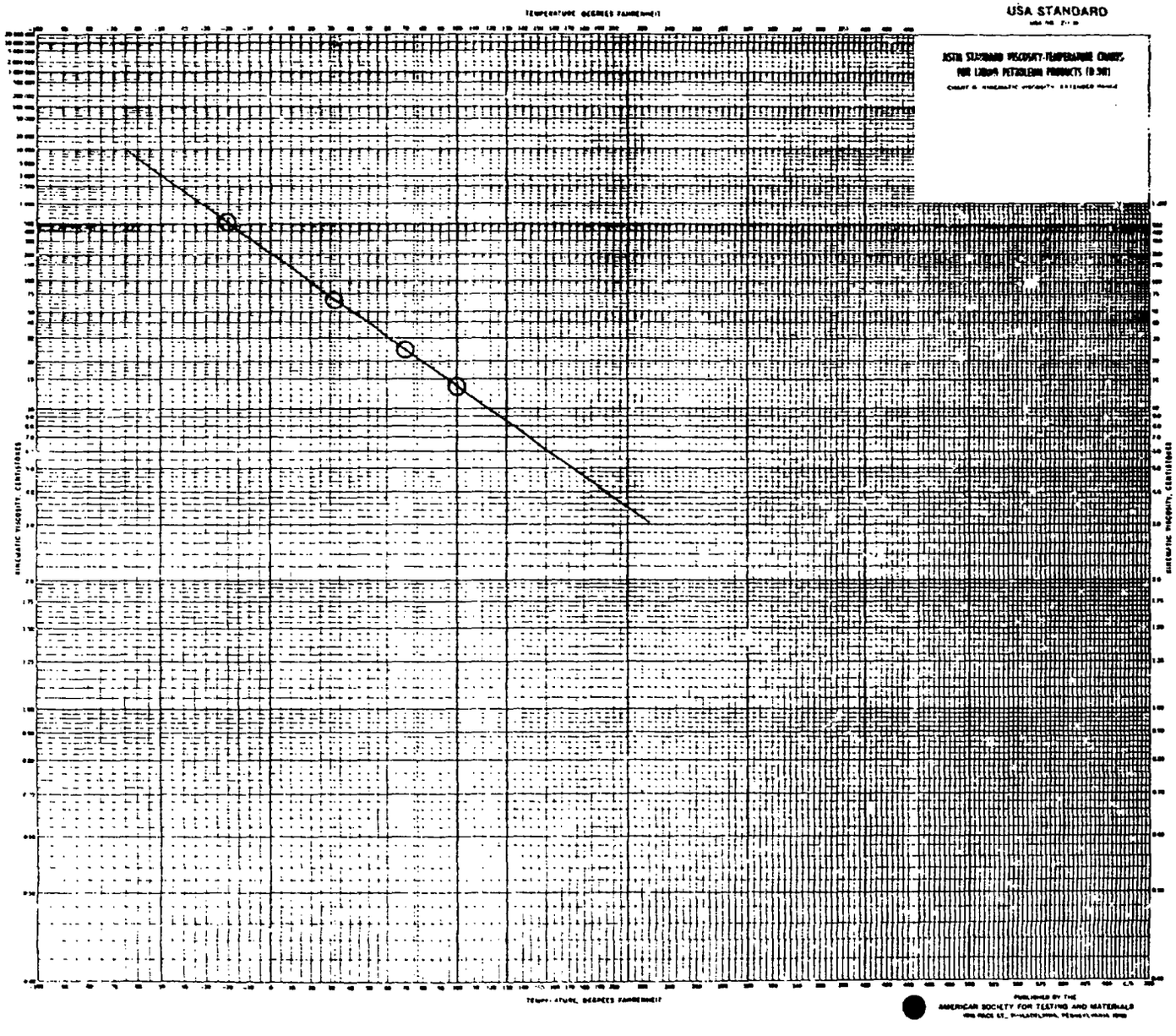

Figure 247. Viscosity/temperature plot for RJ-5 fuel B-9-78-3.

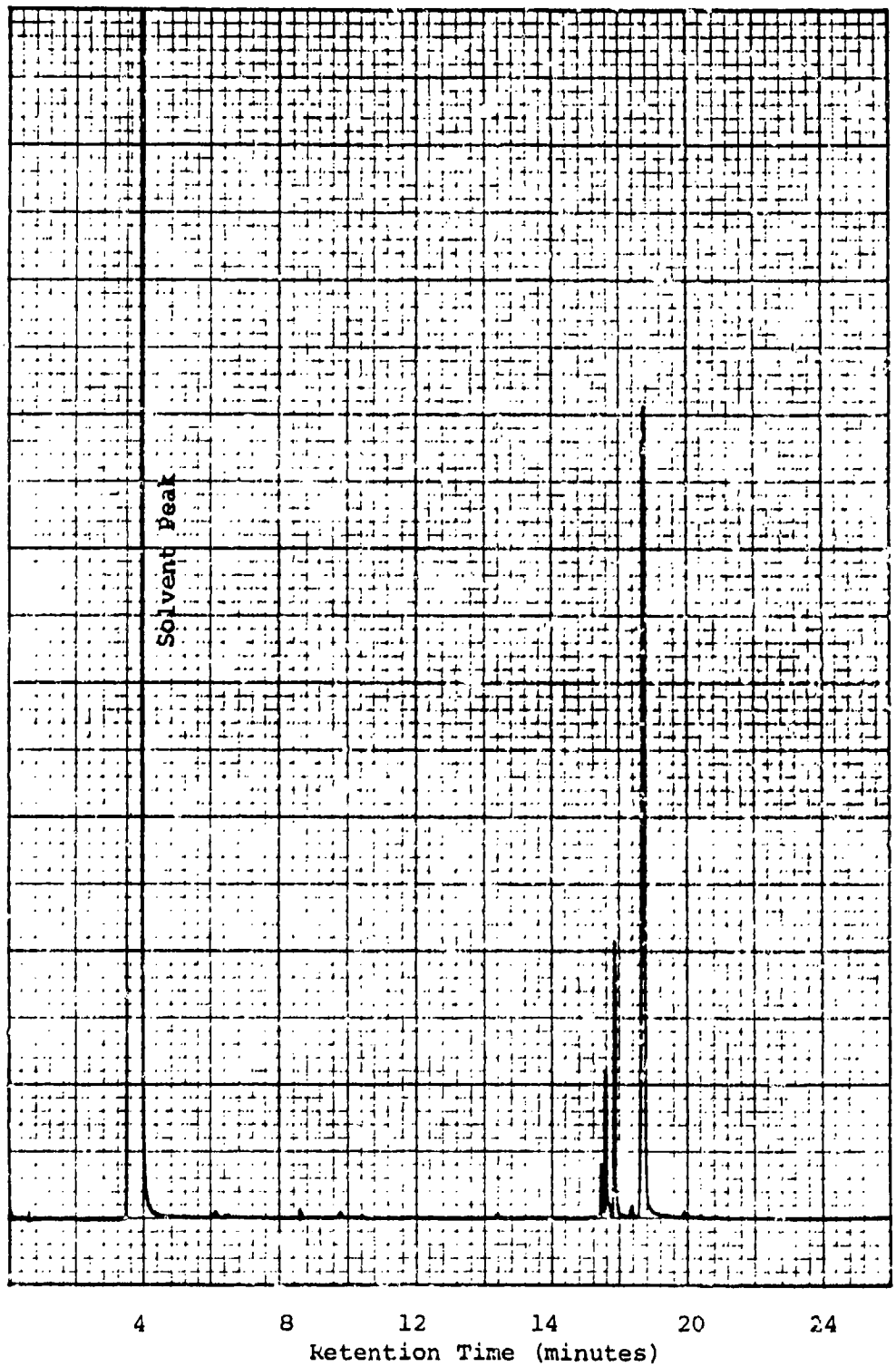

Figure 248. Gas chromatogram of RJ-5 Ashland fuel B-9-78-1.

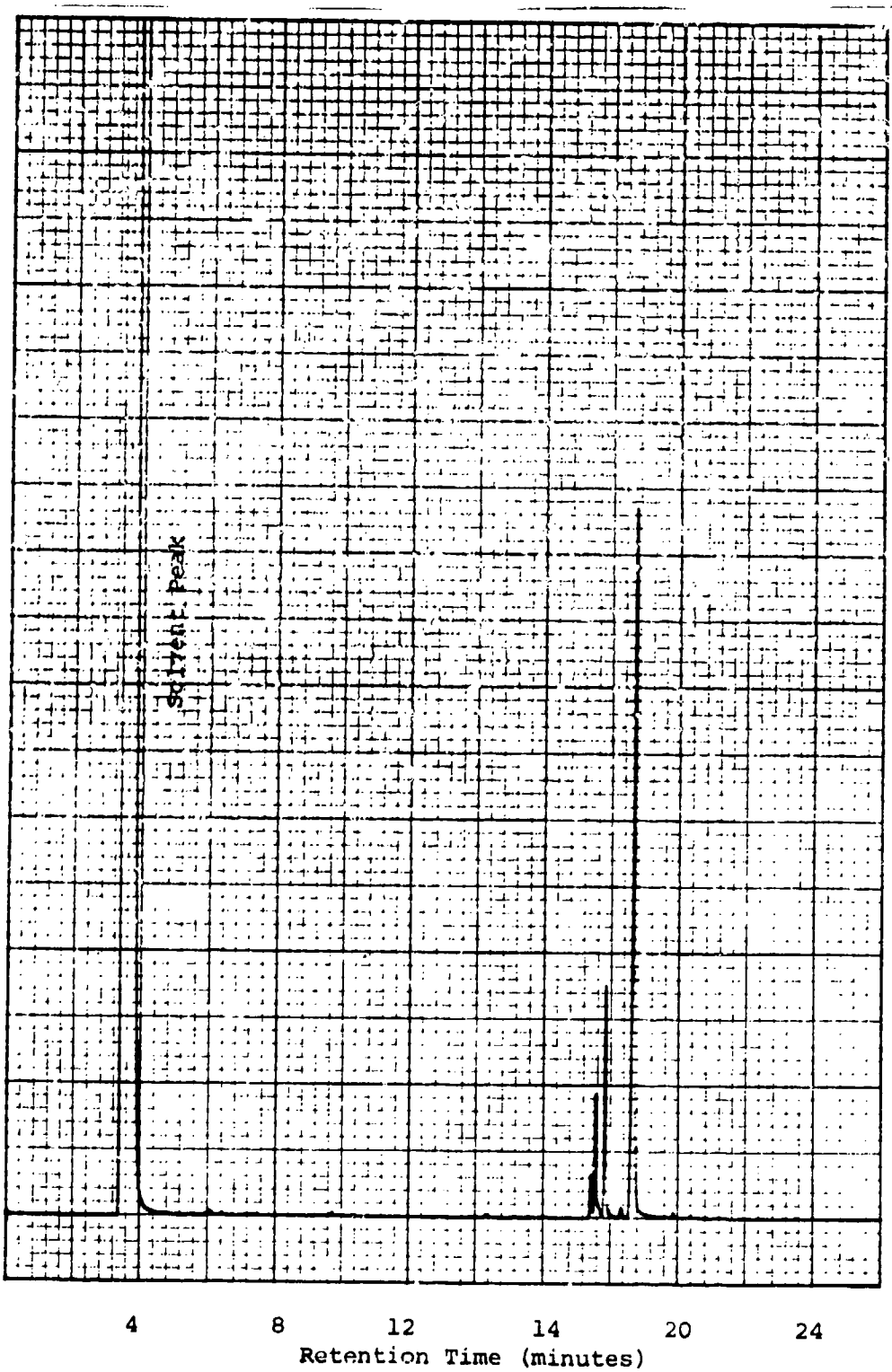

Figure 249. Gas chromatogram of RJ-5 Ashland fuel B-9-78-2.

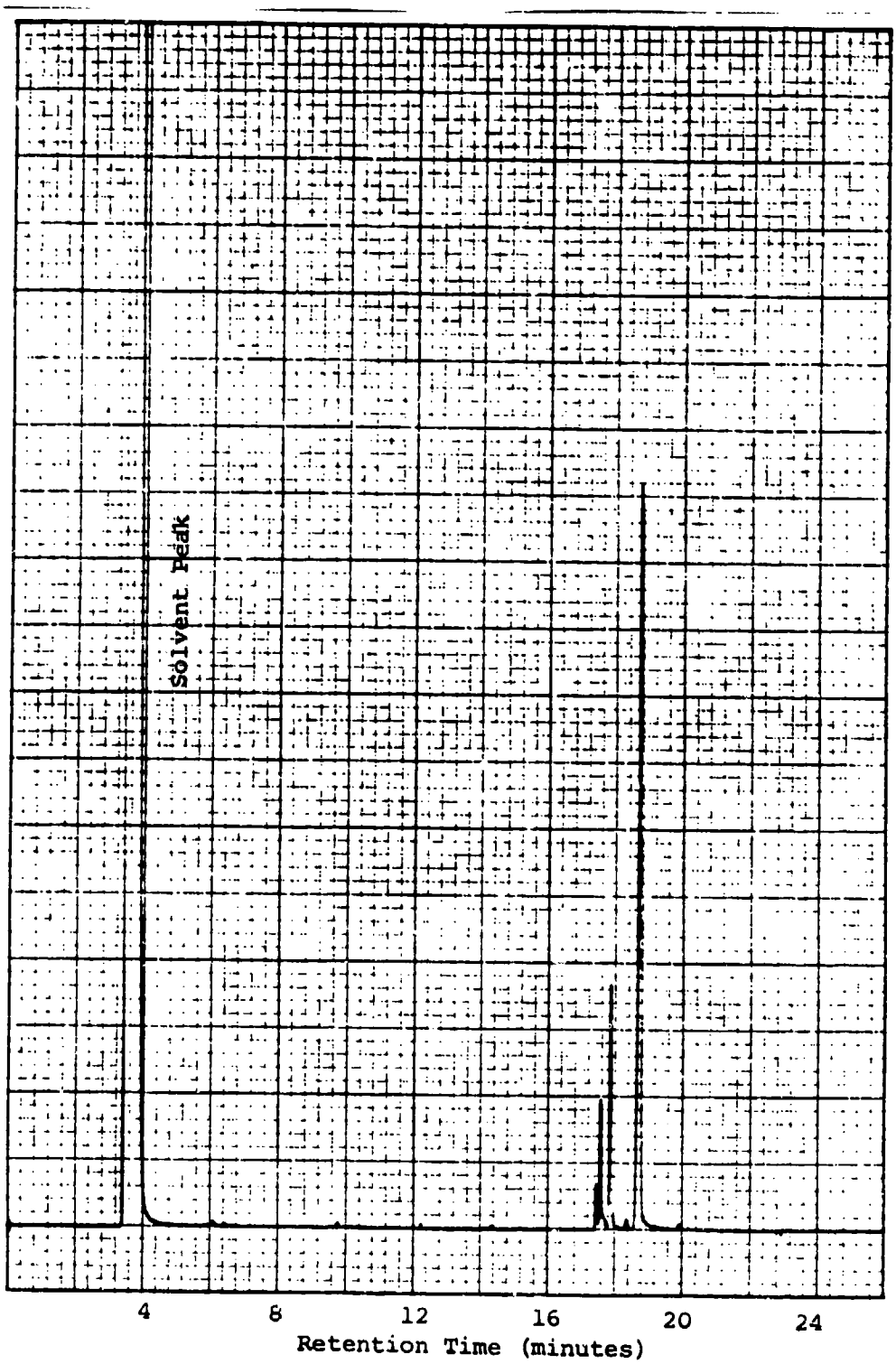

Figure 250. Gas chromatogram of RJ-5 Ashland fuel B-9-78-3.

TABLE 205. GAS CHROMATOGRAPHIC ANALYSES

Retention time, minutes		Area percents[a] of components in fuels B-9-78-1	B-9-78-2	B-9-78-3
6.10		0.40	0.33	0.32
17.49	RJ-5 Isomers	2.64	2.62	2.58
17.61		9.54	9.48	9.43
17.90		15.78	15.54	15.31
18.39		0.68	0.68	0.69
18.77		70.70	71.10	71.42
19.95		0.26	0.25	0.25

[a]Essentially the same as weight percents for these fuels.

7. VISCOSITY AND SURFACE TENSION OF RJ-4, JP-9, AND JP-10 FUELS WITH AND WITHOUT FERROCENE ADDITIVE

Kinematic viscosity and surface tension were measured at 77°F and 100°F for JP-9, JP-10, and RJ-4 jet fuels. The same measurements were then made on these fuels after addition of ferrocene at the 1,300 ppm level (400 ppm iron). The purpose of the investigation was to determine if this level of ferrocene had any effect on the physical properties. The test results are shown in Tables 206 and 207 below.

TABLE 206. KINEMATIC VISCOSITY OF FUELS WITH AND WITHOUT FERROCENE

	Centistokes					
Test fuel:	JP-9, Batch 38		JP-10, Drum 1		RJ-4	
Test temperature, °F:	77	100	77	100	77	100
Neat fuel:	3.154	2.488	2.995	2.380	4.857	3.620
Ferrocene added:	3.157	2.488	2.996	2.379	4.857	3.618

TABLE 207. SURFACE TENSION OF FUELS WITH AND WITHOUT FERROCENE

	Dynes per centimeter					
Test fuel:	JP-9, Batch 38		JP-10, Drum 1		RJ-4	
Test temperature, °F:	77	100	77	100	77	100
Neat fuel:	30.89	30.04	31.86	30.31	30.90	29.53
Ferrocene added:	31.09	29.91	32.22	30.44	31.04	29.79

The data show that the addition of ferrocene to these fuels did not have a significant effect on the physical properties in question. Examination of the surface tension data shows a slight change in surface tension values for fuels with the additive. However, the magnitude of the changes are far less than is found between various lots of RJ-5 or between various compositions within the JP-9 specification range (ref. 15, Table 8, page 14).

8. PREPARATION OF JP-10 AND RJ-5 FUEL STANDARDS BY FRACTIONATION

Highly pure JP-10 and RJ-5 fuel samples were required for use as standards in accordance with MIL-P-87107B specification. Consequently, JP-10 fuel from Drum 31 and RJ-5 fuel from Batch #3 were fractionated on a 42-inch Todd Vigreux column under vacuum. A pressure stabilizing apparatus was used to maintain the selected vacuum. After the distillations the purified fuels were placed into GC septum vials and then analyzed for purity on a capillary gas chromatographic system prior to sample distribution. Included in the following report sections are the fractionation parameters for each fuel, the GC analysis conditions and results for the determination of percent purity in each fuel, representative chromatograms, and the sample bottling procedure and distribution locations.

Distillation of JP-10

About 250 milliliters of JP-10 was distilled at a 10:1 reflux ratio under a vacuum of about 30 mm. This vacuum was selected to keep the boiling temperature below 100°C and avoid possible cracking of the hydrogenated cyclopentadiene dimer. Successive 5-milliliter fractions were collected until the refractive indices of at least three adjacent cuts agreed within ±0.0002, and then a 50 milliliter fraction was collected to be used as the standard. The boiling ranges and refractive indices of the collected fractions are shown in Table 208.

TABLE 208. DISTILLATION OF JP-10

Fraction number	Fraction size, ml	Boiling range, °C/millimeters	Refractive index, N_D^{25}	Disposition of sample
1	5	83-84/29	1.4821	Discarded
2	5	84-85.5/29	1.4848	Discarded
3	5	85/29	1.4863	Discarded
4	5	86/29	1.4868	Discarded
5	5	85.5/29	1.4867	Discarded
6	5	85/29	1.4869	Discarded
7	5	85/29	1.4868	Discarded
8	5	85/29	1.4869	Discarded
9	50	86.5-87/30-31	1.4869	Kept as standard
Residuum	~160	-	-	Discarded, still clear color

The starting fuel had a refractive index of 1.4872, which compares favorably with the value for the 50 milliliter fraction kept as a standard.

It can be observed that some of the higher numbered fractions had lower indicated boiling temperatures than lower numbered fractions. This was due to variations in the vacuum system which were too small to be recorded.

Distillation of RJ-5 Fuel

About 100 milliliters of RJ-5 was distilled at an 8:1 reflux ratio under a vacuum of about 50 milliliters. Almost the entire fuel was fractionated this time so as not to significantly change the isomer ratios present in the fuel. Successive 5-milliliter fractions were collected until only 6.9 grams of a dark yellow and viscous residuum remained. The boiling ranges and refractive indices of the collected fractions are shown in Table 209.

TABLE 209. DISTILLATION OF RJ-5

Fraction number	Fraction size, ml	Boiling range, °C at 50 mm Hg	Refractive index, N_D^{25}	Disposition of sample
1	5	165-166.5	-	Heterogeneous mixture, cloudy; discarded
2	5	166.5-167.5	1.5360	Discarded
3	5	167.5-168	1.5370	Discarded
4	5	168-168.5	1.5370	Discarded
5	5	168.5-169	1.5381	Retained
6	5	169	1.5382	Retained
7	5	169	1.5391	Retained
8	5	169	1.5395	Retained
9	5	169	1.5395	Retained
10	5	169	1.5399	Retained
11	5	169-170	1.5407	Retained
12	5	170	1.5412	Retained
13	5	170-171	1.5419	Retained
14	5	171	1.5424	Retained
15	5	171	1.5424	Retained
16	5	171	1.5429	Retained
17	5	171-171.5	1.5433	Retained
18	5	171.5-172	1.5436	Retained
19	5	172	1.5438	Retained
20	5	172	1.5439	Retained
Residuum	6.9 grams	>210		Dark yellow and viscous, discarded

Fractions 5-20 were combined to make the purified standard. This mixture had a refractive index of 1.5414 as compared to 1.5412 for the starting fuel. The fact that the two refractive indices are so close indicates that the isomer ratios were not significantly changed.

GC Analysis of Purified Fuels

Gas chromatographic analyses were conducted on the purified fuels using a Perkin-Elmer Model 3920B instrument fitted with a 50-meter by 0.01-inch glass open tubular column coated with SF-96 stationary phase. Other parameters include:

Type detector - flame ionization
Carrier gas - 1 ml/min nitrogen
Column temperature - program 50-200°C at 8°C/min
Injection port - 200°C
Detector temperature - 200°C
Recorder - 1 mV
Electrometer range - 10

The data were recorded and processed using a Hewlett-Packard 3350 laboratory system. The calculated percent purity values for the distilled fuel were 98.8 for JP-10 and 99.2 for RJ-5. In each case minor impurities which have boiling points very close to the major fuel component(s) were not removed by distillation.

The gas chromatogram for the distilled JP-10 fuel is presented in Figure 251. The gas chromatogram for distilled RJ-5 is shown in Figure 252. The gas chromatogram for the undistilled RJ-5 (not shown) was similar in shape to Figure 252, which confirmed that the distillation process did not significantly alter the isomer ratios.

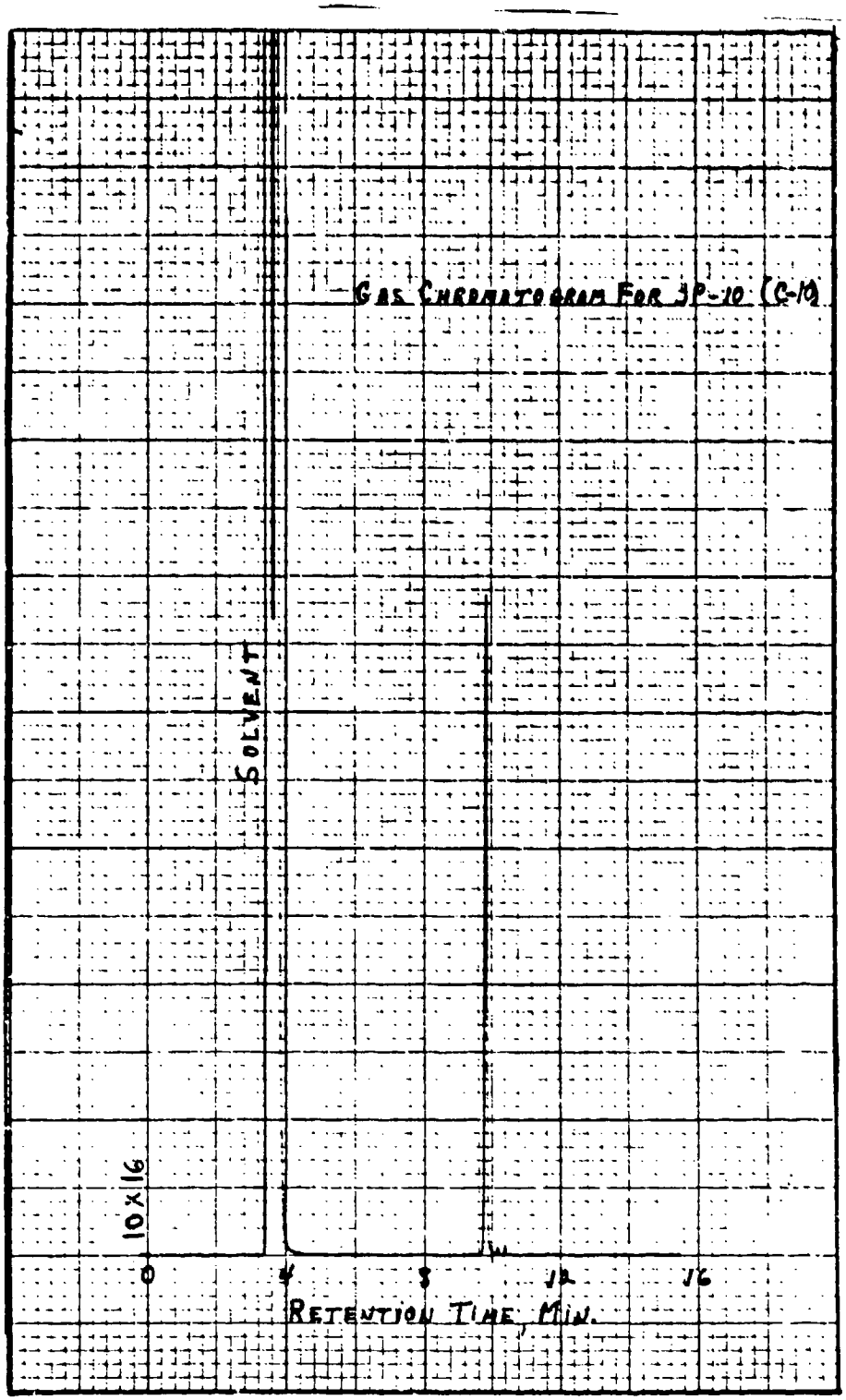

Figure 251. Gas chromatogram for distilled JP-10 fuel, labeled "C-10."

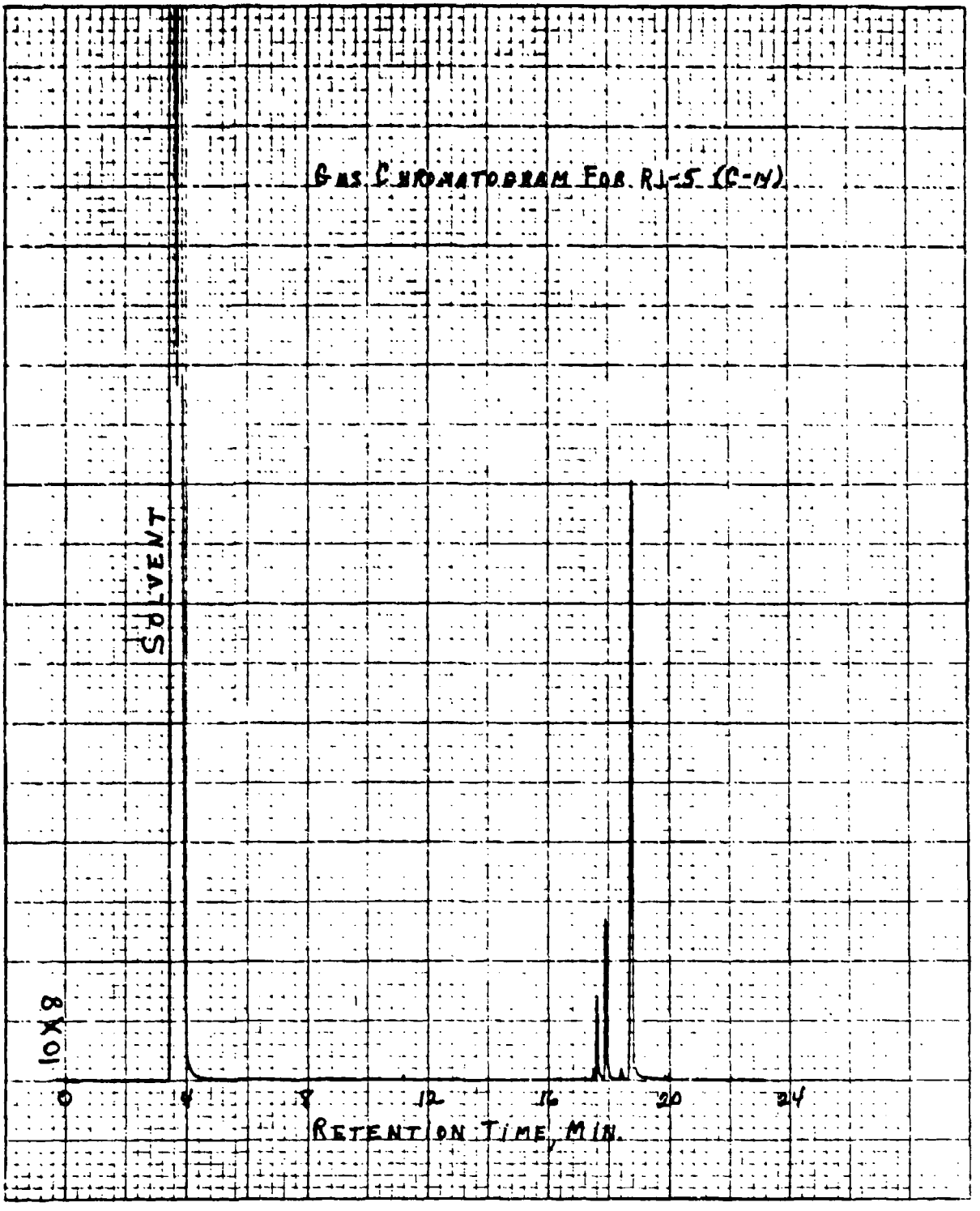

Figure 252. Gas chromatogram for distilled RJ-5 fuel, labeled "C-14."

Sample Distribution

Ten 1-milliliter septum-capped vials were prepared with each distilled fuel. Each cap contained a Teflon-lined silicone septum. The caps were crimped over the lips of the glass vials to make a seal.

The ten JP-10 vials were each labeled "C-10." The ten RJ-5 vials were each labeled "C-14." One each of the vials was then sent to Tinker AFB, Oklahoma (Attn: P. K. Meredith), along with representative chromatograms. The other 18 vials of fuel and chromatograms were sent to Mr. J. McCoy at AFWAL.

9. PHOSPHORUS ANALYSES OF JP-9 FUEL SAMPLES BY GC

Samples of JP-9 fuel required to meet ALCM fuel delivery schedules were analyzed for phosphorus content using a gas chromatograph equipped with a phosphorus-specific detector. The analyses were conducted on a Varian Model 3700 gas chromatograph equipped with a Thermionic Specific Detector (TSD), which is 10^5 times more sensitive toward phosphorus-containing compounds than hydrocarbons. The analysis conditions are recorded below.

Analytical Column:	4 ft x 1/8 in. I.D. glass containing 5% SE30 on 70/80 mesh Anakron ABS
Column Temperature:	210°C
Hydrogen:	5 ml/min at 20 psig
Air:	175 ml/min at 50 psig
Carrier Gas:	40 ml/min helium
Injection Port Temp.:	250°C
Detector Temp.:	250°C
Bias Voltage:	550 volts
Electrometer Sensitivity:	Range 10^{-12} x 256 attenuation
Recorder:	1 mV full scale with 0.5 cm/min chart speed
Minimum Detection Limit:	0.3 ppm

The analyses were conducted with triphenylphosphine (11.8% P, 99+% pure) in JP-9 standards containing 40, 20, 10, 3.2 and 0.5 ppm phosphorus. The analytical results are shown in Table 210.

TABLE 210. PHOSPHORUS IN JP-9 FUEL SAMPLES

Submitted JP-9 samples	Phosphorus, ppm
32 ppm Phosphorus from TPP[a]	32.6
16 ppm Phosphorus from TPP[a]	16.9
8 ppm Phosphorus from TPP[a]	9.8
JP-9 [Blank]	ND[b]
81-406M, 81-F-483	3.6, 3.3
81-417m, 81-F-499	10.2
81-418m, 81-F-500	ND
81-433m, 81-F-517	ND
81-438m, 81-F-421	ND
81-439m, 81-F-495	11.8, 12.2
81-440m, 81-F-496	9.9
Sun Oil, Missile AV-10, 81-464	ND
Sun Oil, Missile FTM, 14R1, 81-463M	ND
Batch 67, A/V, 443-7859	14.6
Batch 68, A/V, 443-7859	12.4
Batch 69, A/V, 443-7859	6.5
81-498-M, 81-F-588	0.5

[a]TPP - triphenylphosphine.

[b]ND - not detected, less than 0.3 ppm.

10. VISIBLE LIGHT ABSORBANCE FOR JP-9 SOLUTIONS OF OIL BLUE A DYE

Two solutions of JP-9 fuel were prepared containing 5.0 and 11.0 milligrams per liter of Oil Blue A dye. Absorbance in the visible spectral region was then measured for each solution over the wavelength range of 360 to 800 nanometers. The measurements were made on duplicate samples of each solution using a Cary Model 219 Spectrophotometer containing 1.000 centimeter sample cells and undyed JP-9 fuel as the reference fluid. Absorption spectra for the second replicate of each dye solution are presented in

Figure 253. Absorption maxima occured at wavelengths 597 and 647 (strongest) nanometers, and absorbance values at these wavelengths for the duplicate samples of each dye solution are shown in Table 211.

TABLE 211. ABSORBANCE VALUES FOR JP-9 FUEL SOLUTIONS OF OIL BLUE A DYE

Dye Concentration:	11.0 mg/Liter		9.0 mg/Liter	
Sample Replicate:	1	2	1	2
Absorbance at 646 nm:	0.580	0.582	0.485	0.474
Absorbance at 597 nm:	0.504	0.506	0.424	0.412

11. INVESTIGATION OF DYE PRECIPITATION FROM JP-9 FUEL AT -54°C

JP-9 fuel was prepared with three concentrations of Oil Blue A dye: 5 mg/liter, 10 mg/liter, and 20 mg/liter. After verifying that all dye was in solution, quart bottles of each dye solution were stored at -54°C for a period of 3 days. A visual observation of the bottles while still at -54°C was then made to determine if any of the dye had precipitated. No precipitate was detected. The dye solutions were then forwarded to AFWAL/POSF for long-term storage evaluation.

12. INVESTIGATION OF LOW TEMPERATURE TURBIDITY IN JP-10

This investigation was conducted to establish the cause of turbidity observed in JP-10 as it is cooled to a temperature of -65°F. The haze first appears at approximately -20°F. It was felt that if the turbidity is caused by the release and subsequent entrapment of dissolved air, a significant fuel system problem may be indicated. Fuel system icing inhibitor (FSII), ethylene glycol monomethylether, is used at the 0.15% level in JP-10. A preliminary experiment by the Air Force initiator of this work demonstrated that FSII has a limited solubility in JP-10 at

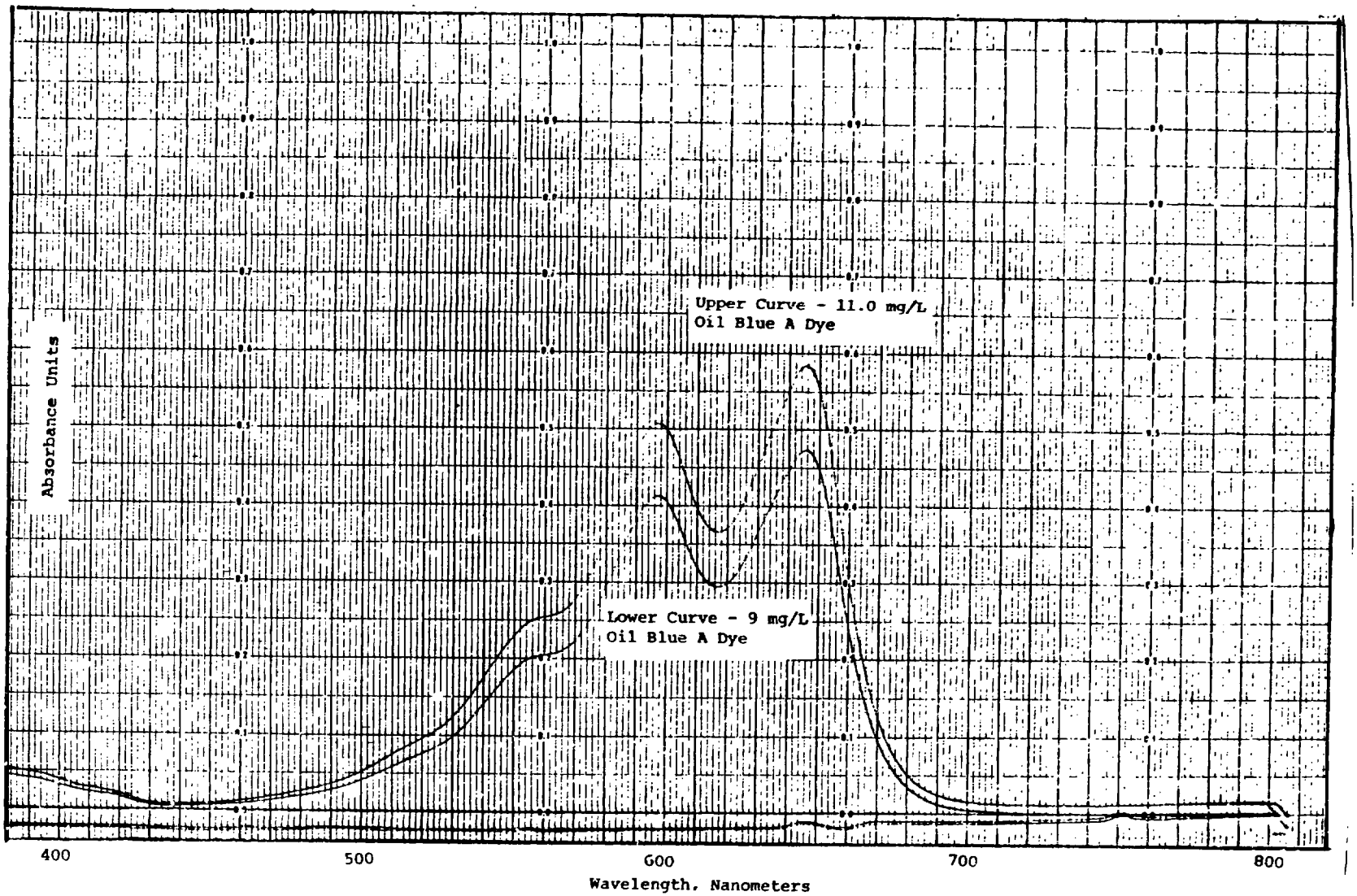

Figure 253. Absorption spectra of JP-9 dye solutions.

red temperatures. This material was thus suspected to be the cause of the turbidity.

Test Procedure

The first experiment was designed to determine the relative effects of dissolved air and FSII on low-temperature turbidity. Two two-liter specimens of JP-10 were prepared, one containing FSII at the specification level and the other containing no FSII. Both specimens were heated to 140°F and thoroughly saturated with air while at that temperature. A fritted glass gas dispersion system was used for that purpose. The samples were then sealed in separate glass containers each having 3.0% ullage. Both containers were cooled to -65°F and observed for cloudiness. The sample containing FSII was found to become very milky, while the one without FSII was less turbid but still quite hazy. Gas bubbles of approximately the size found in a carbonated beverage were observed to cling to the inner wall of each vessel, or to rise to the surface of the fuel. The specimens were withdrawn from the cooling bath and allowed to warm to room temperature. The cloudiness almost completely disappeared after 30 minutes, whereupon the unopened containers were again cooled. Exactly the same effect as before was observed except that fewer rising bubbles were noted this time.

The conclusions drawn from this experiment were that while FSII caused cloudiness at lower temperatures, another factor also contributes to the turbidity.

A second experiment was conducted to determine whether the low-temperature cloudiness in the JP-10 was due to trace amounts of dissolved water. The FSII-free JP-10 was processed through a drying column containing anhydrous sodium sulfate followed by a mixture of chromosorb-P/phosphorus pentoxide (P_2O_5). Upon cooling the dried fuel and a similar undried specimen, the cloudiness was

observed in both samples with no detectable difference in intensity. From this experiment, it was concluded that water is not a cause of haziness.

A third experiment involved comparison of two dried, FSII-free fuels, one being saturated with air at 140°F while the other was completely degassed by subjecting it to a vacuum near its vapor pressure, for a period of one hour. Cooling of these specimens resulted in both having the same degree of turbidity. The vessel containing the air-saturated specimen exhibited the macro-bubbles rising to the surface, as described above.

Summary and Conclusions

Fuel system icing inhibitor at the specification level of 0.15% was shown to be insoluble in JP-10 at -65°F. It is thus a major cause of low-temperature turbidity in this fuel. Haziness, however, appears to a smaller extent in FSII-free JP-10 and it has been shown to be unrelated to water content or to dissolved gases. It can be concluded that the turbidity is likely an endogenous phenomenon of the JP-10 itself, probably being due to a minor fuel component having limited solubility in JP-10 at temperatures approaching -65°F.

REFERENCES

1. Henry, C. P., "Electrostatic Charging in Coalescers and Reticulated Foam," PLMR 20-78, May 1978, Du Pont Petroleum Chemicals.

2. Naval Air Propulsion Center, "Aircraft Systems Fleet Support/ Organic Peroxides in JP-5 Investigation," Final Report No. NAPC-LR-78-20, 27 September 1978.

3. H. L. Alder and E. B. Reossler, Introduction to Probability and Statistics, W. H. Freeman and Company, San Francisco, 1968, pp. 333.

4. L. Parts and T. J. Bucher, "Performance Characterization of Combustible Gas Monitors Used For Military Aviation and Missile Fuels," Final Report No. AFWAL-TR-80-2089, May 1982.

5. L. S. Ettre, "Relative Molar Response of Hydrocarbons on the Ionization Detectors," in "Gas Chromatography," N. Brenner, J. E. Callen, and M. D. Weiss, Editors, Academic Press, New York, 1962, p. 307.

6. M. G. Zabetakis, "Flammability Characteristics of Combustible Gases and Vapors," Bureau of Mines Bulletin 627, 1965.

7. R. J. Scarborough and W. E. Pickett, Jr., "Industrial Hygiene Evaluation; Combustible Gas Meter Evaluation," USAF Environmental Health Laboratory Report EHL(K) 73-5, Kelly AFB, Texas, March 1973.

8. Scribner, W. G. and Gandee, G. W., "Susceptibility of Polyurethane Foam to Deterioration by Impurities or Contaminants in Ethylene Glycol Monomethyl Ether," Technical Report AFAPL-TR-70-76, October 1970.

9. A. Y. Mottlau, "Rapid, Precise Micro Vapor Pressure Method," Analytical Chemistry, 29, 1196 (1957).

10. Trump, W. N., Rev. Sci. Instrum., 48(1) No. 1, January 1977.

11. W. G. Scribner, Environmental Degradation of Fuels, Fluids, and Related Materials, Air Force Aero Propulsion Laboratory, Wright-Patterson Air Force Base, Ohio, AFAPL-TR-71-101, January 1972.

12. D. O. Hummel and F. Scholl, Infrared Analysis of Polymers, Resins and Additives: An Atlas, Wiley-Interscience, New York, 1969.

13. D. N. Kendall, R. R. Hampton, H. Hausdorff, and F. Pristera, "Catalog of Infrared Spectra of Plasticizers," Applied Spectroscopy, 7, 179-196 (1953).

14. D. Hummel, Identification and Analysis of Surface-Active Agents by Infrared and Chemical Methods, Interscience Publishers, New York, 1962.

15. F. N. Hodgson and J. D. Tobias, Analysis of Aircraft Fuels and Related Materials, Air Force Aero Propulsion Laboratory, Wright-Patterson Air Force Base, Ohio, AFAPL-TR-79-2016, March 1979.

APPENDIX

SPECIFIC TEST METHODS FOR FUEL CHARACTERIZATIONS DESCRIBED IN THIS REPORT

Many physical and chemical property tests were repeatedly conducted for a number of the projects described in this report. For the sake of conciseness and to avoid repetition, the test methods are described in this Appendix only.

DENSITY AND SPECIFIC GRAVITY

This method covers the laboratory determination, using a pyrex dilatometer, of the density of fuels normally handled as liquids. The dilatometer method is most suitable for determining the density of mobile transparent liquids ranging from 100°F to -65°F.

Summary of Method - The liquid is introduced into a clean, weighed dilatometer which is then reweighed. The sample is brought to the prescribed temperature by immersing the dilatometer in a vertical position into a constant temperature bath. After temperature equilibrium has been reached, the dilatometer scale is read by means of a cathetometer.

Definition - Density = the mass of liquid per unit volume at prescribed temperature. In this method, the unit of mass is the gram and the unit of volume, the milliliter.

Apparatus

(1) A calibrated dilatometer constructed of pyrex glass.
(2) Thermometers conforming to specifications of American Society for Testing and Materials.
(3) Constant temperature baths. Water and ethanol are suitable media for temperatures ranging from 100°F down to -65°F.
(4) Cathetometer
(5) Dilatometer holder
(6) Stopper for dilatometer
(7) Support to hold the dilatometer in approximately a vertical position while weighing, such as a small beaker.
(8) Analytical balance
(9) Hypodermic syringes and needles
(10) Laboratory detergent preparation for glassware

(11) Toluene, reagent grade
(12) Distilled water
(13) Reagent grade acetone

Preparation of Apparatus - Thoroughly clean the dilatometer with chromic acid cleaning solution, rinse well with distilled water and dry at 105 to 110°C, or rinse the dilatometer with pure dry acetone and dry by applying an aspirator to the opened end of the dilatometer. Cleaning should be performed in this manner in order to have a sharply defined miniscus during calibration of the dilatometer. Ordinarily, the dilatometer may be cleaned between test determinations by washing with a suitable solvent, such as toluene, and rinsing with pure dry acetone. Periodic cleaning with glassware detergent solution is recommended.

Calibration of Apparatus - Determine the volume held by the dilatometer when equilibrated at various test temperatures by means of a cathetometer. This is called the K value for that temperature. Freshly-boiled and cooled distilled water can be used for calibrating at 70°F and 100°F and good reagent grade solvents can be used for determining the K values at lower temperatures. Densities of the solvents at low temperature can be determined by using the International Critical Tables and the density of water at various temperatures can be found in the Handbook of Chemistry and Physics. When using the cathetometer, measure the span between two graduation marks on the dilatometer. This will be approximately 0.190 cm for a graduation interval of 0.05 ml. This should be measured at several places to assure consistency. Having determined the span of a 0.05 ml interval, the volume of the liquid can then be interpolated. It is more precise to determine the volume by the cathetometer than to estimate it by visual observation.

Procedure - Adjust a constant temperature bath to maintain the prescribed temperature. Weigh the clean, dry dilatometer and stopper to the nearest 0.1 mg and record the weight.

Fill the dilatometer to approximately the 1.5 ml graduation mark on the dilatometer by means of a hypodermic syringe. Remove any bubbles that might have been formed while transferring the sample.

Weigh the stoppered dilatometer and sample to the nearest 0.1 mg. Record the weight. Place the dilatometer in a suitable holder in the constant temperature bath adjusted to the test temperature within ±0.05°F. When the sample has reached equilibrium (about 15 minutes) take readings of the miniscus by means of a cathetometer. Read the cathetometer to the nearest 0.005 cm.

Take several readings of the miniscus until reproducible readings are obtained. After consistent readings have been made, remove the dilatometer from the bath and clean with a suitable solvent, rinse with pure dry acetone and proceed to the next test.

Calculations

$$\text{density, g/cc} = \frac{m}{K-R}$$

where m = mass of sample in grams

K = dilatometer constant at given temperature, volume of dilatometer to full mark

R = dilatometer reading at given temperature, ml below full mark

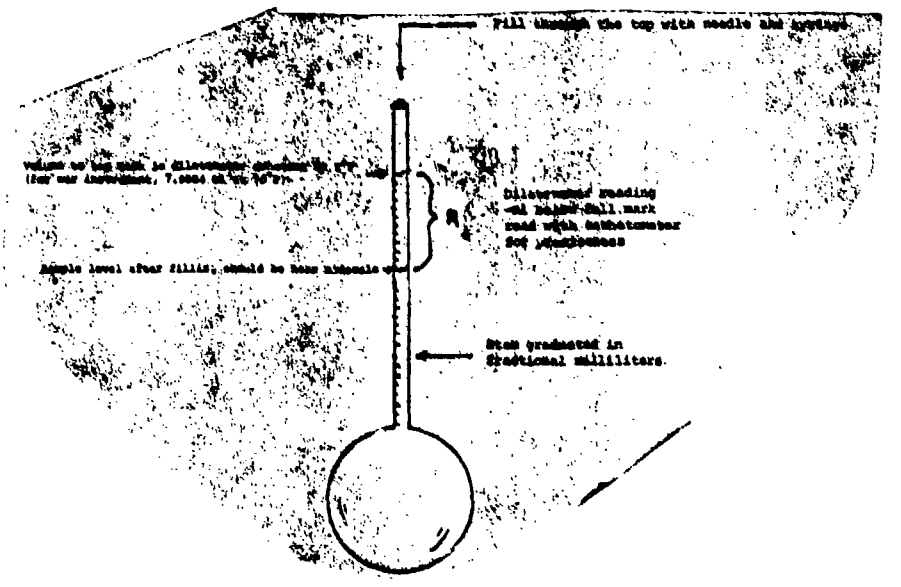

SIMULATED DISTILLATION BY GAS CHROMATOGRAPHY

Chromatographic-simulated distillations were conducted on hydrocarbon fuels using ASTM Method D 2887. Fuel components were eluted in boiling point order, and actual boiling points were assigned to retention time data by correlation with a calibration curve obtained from a standard hydrocarbon mixture. Data acquisition was accomplished with a Hewlett-Packard 3356 laboratory data system A program had been designed to record area slices of the chromatogram every ten seconds during the chromatographic analysis, and to provide cumulative area slice data as well as a running percent of the total chromatogram area at any given ten-second interval.

HYDROCARBON TYPES BY MASS SPECTROMETRY

Hydrocarbon type analyses were conducted by three separate mass spectral methods, depending on the fuel. A modification of ASTM Method D 2789 was used for JP-4 and gasoline-type fuels. ASTM Method D 2425, which first requires an ASTM D 2549 separation of the fuel into aromatic and paraffinic fractions, was utilized mainly for diesel fuels. Monsanto Method 21-PQ-38-63, developed for hydrocarbon feed stocks with an average carbon number in the range of 12 to 13, was used for JP-8 type fuels. Nonstandard fuels were sometimes analyzed by more than one mass spectral method. All of these analyses are based on the summation of characteristic mass spectral lines for each compound type. A matrix of n equations, relating each of n hydrocarbon types to the summed peak values, is constructed. A computer solution of these simultaneous equations provides a quantitative measure of each compound type present..

As noted above, ASTM D 2425 analysis must be preceded by a separation of fuel aromatics from nonaromatics using a procedure such as that described in ASTM D 2429. The D 2549 method, as currently

presented in Part 24 of the 1980 Annual Book of Standards, required a small procedural modification in order to be used for JP-8. This modification did not change the essential features of the separation, but only involved the method for removing the chromatographic solvent. The modified methodology was developed in MRC laboratories and has been employed for a number of years. An official modification of ASTM D 2549 to achieve the same effect is under study by ASTM Committee D-2 on Petroleum Products and Lubricants. By the ASTM D 2549 procedure, a steam bath is employed to evaporate solvent from the fractions obtained by elution chromatography. In the MRC modification, no heat is applied. Instead, a stream of dry nitrogen is used for desolvation. Evaporation of solvent, in fact, reduces the temperature to below ambient. After the major part of the solvent has evaporated, the weight of the fraction is carefully monitored as the final traces of solvent are removed. Complete removal of solvent is signalled by a marked decrease in the slope of the time/weight loss curve, or in some cases, by the attainment of a constant weight. MRC analysts are experienced in this procedure, which requires a short period of dedicated attention for the processing of each fraction by the analyst.

GROSS AND NET HEAT OF COMBUSTION

Heat of combustion of fuels was determined with an isothermal calorimeter according to ASTM D 240-76. A weighed sample was burned in an oxygen bomb calorimeter under controlled conditions. The heat of combustion was computed from temperature measurements before, during, and after combustion, with allowance for thermochemical and heat transfer corrections. Data were reported as Btu/lb (gravimetric).

The net heat of combustion of a fuel is the amount of heat released when liquid fuel is burned to yield gas-phase water and carbon dioxide. It is a lower value than the gross heat of

combustion which assumes liquid phase water to be the product. The difference between the net and the gross values is equivalent to the latent heat of evaporation of the water formed on burning, which depends on the amount of hydrogen in the fuel. For net heat of combustion calculation, the hydrogen content of each fuel was measured at AFWAL/POSF for use in the following relationship.

$$H_n = H_g - 91.23 \times H$$

where H_n = net heat of combustion, Btu/lb
H_g = gross heat of combustion Btu/lb
H = weight percent of hydrogen in the sample.

TRUE VAPOR PRESSURE

True vapor pressure is the maximum vapor pressure that a volatile mixture such as an aircraft fuel can exert at a given temperature. In theory, this property should be measured in the absence of sample vapor because vaporization of a portion of the sample changes the composition of the mixture and thus changes the vapor pressure. In practice, true vapor pressure must be measured at such a small vapor-to-liquid ratio that any change in the composition of the fluid produces a change in vapor pressure which is negligible, i.e., within the experimental error of the method.

For true vapor pressure measurements as a function of temperature, a micro vapor pressure apparatus as described in ASTM D 2551-80 was used. The apparatus incorporates a mercury-sealed orifice for sample introduction, and the entire unit is surrounded by a glass outer jacket through which fluid from a constant temperature bath is circulated. Using this device, a known volume of sample is introduced into an evacuated, temperature-controlled chamber of known volume.

A schematic diagram of the micromethod apparatus is shown below as it appears in the 1981 Annual Book of ASTM Standards, D 2551-80. A fuel sample is introduced through the mercury reservoir at the top of the bulb by means of a mercury displacement pipette.

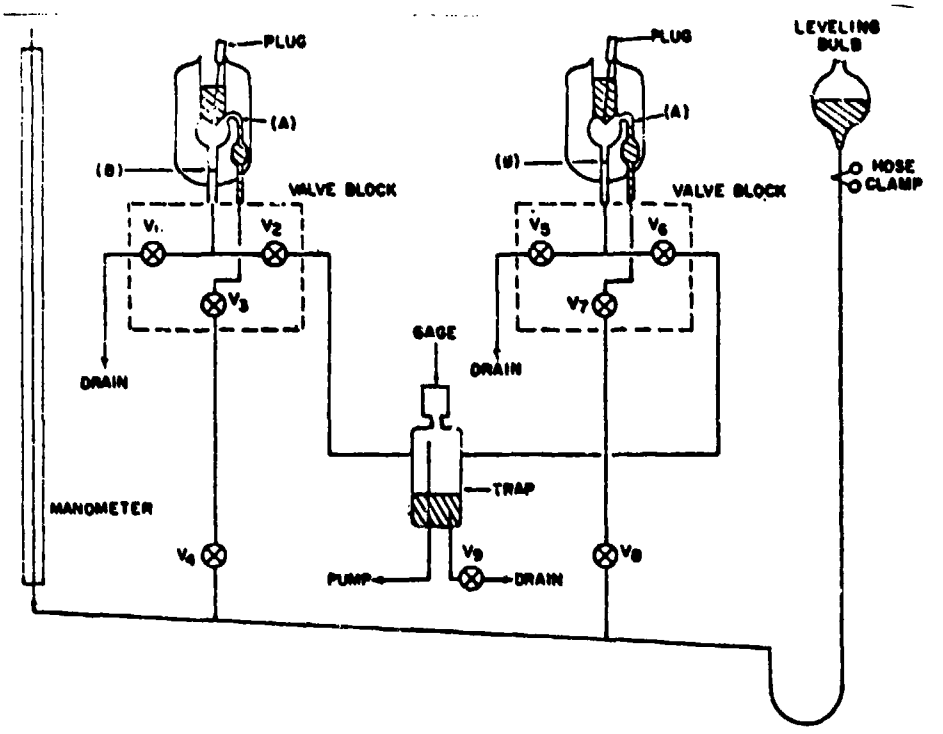

The sample enters the chamber below which has a volume of 5 ml ±0.03 ml between fiducial marks A and B. After introduction of the sample, the mercury is adjusted to the fiducial marks by means of the leveling bulb and/or drain. Vapor pressure is recorded from a mercury manometer attached to the device. The pressure measured, in actuality, is due to the sample vapor pressure and the partial pressure of any dissolved air.

The object of ASTM Method D 2551 is the determination of vapor pressure values that are comparable to those obtained by the Reid vapor pressure technique. In measurements within this laboratory, the apparatus has been employed for true vapor pressure determinations which, of course, must not include the effects of dissolved gases (atmospheric constituents). The measurements are, thus, preceded by an operation to cryogenically degas the sample, thereby

removing permanent gases while retaining even the most volatile hydrocarbons. In the cryogenic degassing procedure approximately 50 ml of fuel is placed in a glass vessel that is connected to a vacuum system through a wide-bore, greaseless stopcock. The sample vessel is submerged in liquid nitrogen until the fuel sample is frozen solid. While the fuel is still solid, the stopcock is opened and the vessel is evacuated to approximately 5 μm pressure. The stopcock is then closed and the fuel is allowed to melt. As the fuel becomes liquid, bubbles of dissolved gas are released.

The fuel is then frozen a second time and the vessel is again evacuated. By melting the fuel in the isolated vacuum vessel again, air is released but not nearly the quantity obtained the first time. This freeze/melt cycle is repeated until no increase in pressure is noted in the vessel after the fuel has been melted and refrozen. By strict adherence to this procedure, no opportunity exists for loss of sample vapors. The fuel is cooled to -70°F to recondense vapors before removal for vapor pressure testing.

The importance of removing dissolved air from the fuel can be understood by considering the solubility of air in JP-4. The Ostwald solubility coefficient (volume of dissolved gas per unit volume of liquid fuel, measured at the temperature and pressure of saturation) for air in JP-4 is approximately 0.19[a] at 75°F. Thus the 2 ml volume of JP-4 used for vapor pressure measurement can contain 0.38 ml of air. The volume of the chamber in the apparatus which is occupied by vapor is 3 ml. Sample is introduced into the vacuum of the apparatus through a mercury-pool seal. Some outgassing at this time is almost assured. Consideration of simple gas laws shows that if the entire volume of dissolved air is released, 0.38 ml at atmospheric pressure, pressures

[a]F. N. Hodgson and A. M. Kemmer, AFAPL-TR-76-26, March 1976.

up to 90 mm of mercury could result from the dissolved air. It is, thus, imperative that the bulk of the dissolved air be removed for true vapor pressure measurements.

The volume of the micro apparatus is 5 ml. By introduction of 1 ml of fuel, a vapor-to-liquid (V/L ratio) of 4:1 is obtained; 2 ml of fuel gives a V/L ratio of 3:2. Tests must be conducted at several V/L ratios to determine the point at which vapor pressure does not measurably increase with decrease in the vapor volume. Usually 2 ml of sample (V/L = 1.5) was sufficient to obtain this condition.

Classically the vapor pressure temperature relationship is expressed by:

$$\log P = A - B/T$$

where A and B are constants, P = absolute pressure and T = absolute temperature. The line resulting from a plot of this equation on semilog paper is useful over a limited range for estimating vapor pressure at temperatures intermediate to, or just beyond, those at which measurements were taken.

The repeatability and reproducibility figures provided in D 2251 should be valid for the true vapor pressure procedure. ASTM D 2551 cites the repeatability of the method (maximum difference between successive determinations by the same operator) to be 4 mm at the 95% confidence level. Reproducibility (for different operators in different laboratories) is cited as 15 mm at the 95% confidence level. In practice, differences between replicate vapor pressure measurements in this laboratory seldom exceed 2 mm and are frequently within 1 mm.

It is recommended that measurements at -20°F generally should not be conducted, but rather these values should be obtained by extrapolation of the log P versus $\frac{1}{T}$ plot which usually exhibits good linearity. In general it is recommended that vapor pressures below approximately 5 mm should not be measured directly as they are more reliably obtained by extrapolation.

SURFACE TENSION AS A FUNCTION OF TEMPERATURE

Surface tension was measured as a function of temperature using the capillary-rise method. Surface tension in dynes cm^{-1} is given by the expression:

$$\tau = \frac{rhdg}{2\cos\theta}$$

where d = density of the liquid, g/cm^3
h = height of the column of liquid, cm
g = acceleration of gravity, cm/s^2
r = radius of the capillary, cm
θ = contact angle, degrees

For most materials the contact angle (θ) was essentially zero and cos θ was equal to one. However, when the material being measured wetted the capillary walls poorly, as in the case of some high density fuels, the contact angle was measured. A Gaertner contact angle goniometer apparatus was used for this measurement. From the data generated, a linear temperature/surface tension relationship is established.

KINEMATIC VISCOSITY

Kinematic viscosity was determined as a function of the temperature for all fuels and fuel components using the procedure and equipment described in ASTM Method D 445-79. Viscosity data were plotted on standard ASTM viscosity-temperature charts which are useful for the estimation of kinematic viscosities at temperatures other than those at which measurements were conducted.

AIR AND NITROGEN SOLUBILITY AS A FUNCTION OF TEMPERATURE

The amount of air or nitrogen soluble in fuels at saturation was measured using a special degassing chamber and cold trap on the inlet of a CEC 21-103C mass spectrometer. The vacuum of the mass spectrometer inlet was used to aid in degassing the specimens. The degassing vessel was arranged so that constant agitation of the sample was possible. For viscous samples, heating was also used in the degassing process. Air and hydrocarbon vapors removed from the sample are passed through a cold trap where most of the hydrocarbons remain. The amount of air was determined in the desorbed gases as the total of the nitrogen, oxygen, argon, and carbon dioxide. For nitrogen solubility measurements, only the value for desorbed nitrogen was used.

Instrument calibration was achieved by introducing known volumes of air or nitrogen into the system. The determined value was independent of the amount of hydrocarbons in the vapor. Fuels are saturated with air in a distillation flask to which a reflux condenser was attached. The flask was placed in a constant temperature bath maintained at the desired temperature. A fritted-glass gas dispersion tube was immersed into the fuel through which CGA Grade E compressed breathing air or prepurified nitrogen was passed. Water from an ice bath was circulated through the jacket of the condenser by means of a small pump. This procedure prevents loss of volatile components during saturation of the fuel.

Solubility is expressed as an Ostwald coefficient, defined as the volume of air per unit volume of fuel, both volumes measured at the temperature of saturation.

SPECIFIC HEAT AS A FUNCTION OF TEMPERATURE

The specific heat of solids and liquids was measured with a Perkin-Elmer differential scanning calorimeter, Model DSC-1.

The calorimeter measures the rate of heat flow into a sample (which is proportional to specific heat) whose temperature is being programmed at a linear rate. The specific heat is then calculated by comparing the rate of heat flow for the weighed sample to the rate of heat flow of a weighed standard (synthetic sapphire) for which the change of specific heat with temperature is accurately known.

The specific heat can be measured anywhere between -100 and +500°C with milligram quantities of sample contained in standard cups or hermetically-sealed cups. The ultimate precision of the method is 0.3% or better, which approaches the precision of adiabatic calorimetry.

THERMAL CONDUCTIVITY AS A FUNCTION OF TEMPERATURE

Thermal conductivity was determined using a Monsanto-built transient hot wire apparatus. In this procedure a constant heating current is applied abruptly to a resistance wire immersed in the fuel. The change in temperature of the wire following application of the current is obtained from the observed change of voltage across the wire and the known resistance-temperature characteristics.

This method has been established as being among the best available for routine thermal conductivity measurements. Complete instrumentation for this measurement is located at our St. Louis laboratories where all work of this nature was conducted. Personnel from that laboratory have published the results of a detailed study on the measurement of the thermal conductivity of liquids.[b]

---

[b] "Rapid Measurement of Liquid Thermal Conductivity by the Transient Hot-Wire Method," W. N. Trump, H. W. Luebke, L. Fowler, and E. M. Emery, Rev. Sci. Instrum. 48, 47, 1977.

DIELECTRIC CONSTANT AS A FUNCTION OF TEMPERATURE

Dielectric constants were routinely measured as a function of temperature at 400 Hz for all fuels and fuel components. Measurements were made in a three terminal guarded cell relative to air at the same temperature. A General Radio 1615A capacitance bridge and guard circuit were used in the determination. Linear regression analyses were performed on the data to determine the dielectric constant as a linear function of temperature.

GAS CHROMATOGRAPHIC ANALYSES

Gas chromatographic analyses conducted on high density fuels employed the same instrument and similar analytical conditions as used for jet fuels.

A Perkin-Elmer Model 3920B gas chromatograph having a 50-meter by 0.01-inch glass open tubular column coated with SF-96 stationary phase was used as required. Other parameters were:

Detector type - flame ionization
Carrier gas - helium
Flow rate - 3 ml/min
Typical temperatures program - column initially 60°C, held for 4 min
Program rate - 8°C/min
Final temperature - 190°C
Injection port - 300°C

Data were recorded and processed using a Hewlett-Packard 3356 laboratory data system in most cases.

WATER SOLUBILITY

Water solubility, the quantity of water which will dissolve in a fuel, was determined as a function of temperature during the

course of this work. For this measurement, the fuel is saturated with water by placing a vessel containing the fuel sample, along with an excess of distilled water, into a constant temperature both. The fuel is then stirred with a small mixer for approximately 18 minutes. The water is then allowed to separate from fuel so that no turbidity remains. Samples of the fuel are then removed for analysis.

A coulometric-type Karl Fischer titrimeter was used for the determination of water. In this system, reagent is generated by an electrical current, thus no standardization is required. The end point is electronically detected. For best precision about 1,000 micrograms of water are required in the specimen. Thus to attain a 10 ppm detection limit, a sample weight of 100 grams was used.

*U.S.Government Printing Office: 1983 — 759-062/522